

**Caracterización de los
heteropolisacáridos producidos por
Lactobacillus aislados de sidra natural
y de las bacterias productoras:
Lactobacillus collinoides y
*Lactobacillus sicerae***

Ana Isabel Puertas González
San Sebastián, 2019

eman ta zabal zazu



Universidad
del País Vasco

Euskal Herriko
Unibertsitatea

Departamento de Química Aplicada
Área Microbiología



Universidad del País Vasco Euskal Herriko Unibertsitatea

**Caracterización de los heteropolisacáridos
producidos por *Lactobacillus* aislados de
sidra natural y de las bacterias productoras:
Lactobacillus collinoides y *Lactobacillus
sicerae***

TESIS DOCTORAL

Ana Isabel Puertas González

San Sebastián

2019

eman ta zabal zazu



Universidad
del País Vasco

Euskal Herriko
Unibertsitatea

Caracterización de los heteropolisacáridos
producidos por *Lactobacillus* aislados de sidra
natural y de las bacterias productoras:
Lactobacillus collinoides y *Lactobacillus sicerae*

Programa de Doctorado en Química Aplicada y Materiales
Poliméricos

Directora

Dra. María Teresa Dueñas Chasco

Profesora Titular

*A Unai y
a nuestra pequeña Izar*

AGRADECIMIENTOS

Siempre recordaré la generosidad de todas las personas que me han apoyado, ayudado, enseñado y me han hecho pasar buenos momentos durante la realización de este trabajo.

Gracias a Maite Dueñas y Ana Irastorza porque ambas me tendieron la mano y me dieron la oportunidad de iniciarme en el mundo de la investigación. Sin conocerme de nada confiaron en mi.

Especialmente le agradezco a la directora de esta tesis Maite Dueñas su apoyo y comprensión desde que comencé en el laboratorio. Siempre has tenido abierto el despacho cuando lo he necesitado, has escogido sabiamente las palabras oportunas y los silencios necesarios, me apoyaste sin condición cuando te propuse hacer la tesis y me sin mirar a otro lado me dijiste “vamos”. En ese momento yo no era muy consciente de lo que implicaría esta decisión, pero te agradezco enormemente que aceptaras. Desde entonces hemos andado un camino muy largo que no siempre ha seguido un trazo continuo, pero su recorrido me ha ayudado a crecer en diferentes aspectos de la vida, no solo en el científico. Por todo ello siempre tendré un buen recuerdo de ti. Gracias Maite de todo corazón.

A ti Idoia Ibarburu, porque estuviste presente en mis primeras andaduras en el laboratorio, siempre con un buen gesto, con una buena palabra y con toda la paciencia del mundo con la que me ibas contestando a las mil y una preguntas que te iba haciendo. Y aunque ha pasado mucho tiempo, te considero una amiga.

A Iñaki Berregi y Arantza Munduate, nunca os he tenido como profesores, pero siempre me habéis hecho un hueco cuando os he buscado con un S.O.S. Me habéis atendido de una manera amable, siempre con una sonrisa, vuestra ayuda me ha servido para crecer en esta profesión. Iñaki, siempre te he tenido como un apoyo en la facultad, alguien en que he confiado. Gracias.

A Paloma López del Centro de Investigaciones Biológicas-CSIC (Madrid), me acogiste en tu laboratorio durante un periodo corto de tiempo que me sirvió para darme cuenta de la pasión que tienes por la ciencia y eso lo logras transmitir y contagiar a la gente que se acerca a ti. Me has ayudado siempre que te lo he solicitado, siempre con un gesto amable. Gracias Paloma.

A Miguel Ángel Pardo e Iñaki Iturria, gracias por tratarme tan bien durante el tiempo que trabajé con vosotros en AZTI. Me hicisteis sentir como en casa.

A Rosa Aznar y David Ruíz Arahal profesores de la Universidad de Valencia y miembros de la CECT, gracias por permitirme colaborar con vosotros.

A Gloria del Solar del Centro de Investigaciones Biológicas-CSIC. Gracias por ser tan amable, siempre dispuesta a echarme una mano pese no haber trabajado directamente juntas.

Al profesor de Biología de la UPV/EHU, Oier Etxebeste, y al grupo de Bioquímica II, gracias chicos!!

A Virginia Gangoiti y a Giovanni Cervantes, fuisteis aire fresco para el laboratorio, transmitiendo vuestra alegría y brindándome una amistad. Gracias chicos, y como siempre hemos mantenido, no sé si en La Plata, en ciudad de Méjico o en Donostia, pero los tres nos volveremos a encontrar.

A Esther, José Antonio y Jon, porque siempre que os he necesitado habéis estado allí. Me habéis ayudado sin condiciones, sin preguntas. Gracias.

A mis padres, porque aunque estén lejos siempre se han estado pendientes de mi.

Y por último quiero dar las gracias a mi marido Unai. Todo este tiempo has estado a mi lado, en los ratos buenos y en los malos, me has dedicado tiempo y has tenido toda la paciencia del mundo conmigo. Me has apoyado y siempre has creído en mi. Llegó Izar y revolvió nuestras vidas, pero comprendías que mi deseo era terminar este trabajo y me alentabas a ello. Gracias por quitarle importancia a cosas que yo veía como montañas, me has dado luz durante este largo camino. Te quiero.

De la siguiente Tesis Doctoral se han extraído las siguientes publicaciones y comunicaciones a congresos:

Publicaciones:

- Puertas, A. I., Ibarburu, I., Elizaquivel, P., Zuriarrain, A., Berregi, I., López, P., & Dueñas, M. T. (2018). Disclosing diversity of exopolysaccharide-producing lactobacilli from Spanish natural ciders. *LWT-Food Sci. Technol.* 90, 469-474
- Puertas, A. I., Capozzi, V., Llamas, M. G., López, P., Lamontanara, A., Orrù, L., Russo, P., Spano, G., & Dueñas, M. T. (2016). Draft genome sequence of *Lactobacillus collinoides* CUPV237, an exopolysaccharide and riboflavin producer isolated from cider. *Genome Announcements*, 4(3), e00506-16.
- Puertas, A. I., Arahal, D. R., Ibarburu, I., Elizaquivel, P., Aznar, R., & Dueñas, M. T. (2014). *Lactobacillus sicerae* sp. nov., a lactic acid bacterium isolated from Spanish natural cider. *International Journal of Systematic and Evolutionary Microbiology*, 64(9), 2949-2955.

Congresos:

- A. I. Puertas, G. Caggianiello, G. Llamas, P. Russo, M. Á. Pardo, I. Iturria, A. Prieto, M. L. Mohedano, V. Jiménez, P. López, G. Spano & M. T. Dueñas. "Caracterización de lactobacilos productores de heteropolisacáridos aislados de bebidas alcohólicas." 9ª *Reunión de la Red Temática BAL*. Madrid. 2015.
- A. I. Puertas, G. Llamas, A. Zuriarrain, I. Berregi, & M.T. Dueñas. "Effect of riboflavin-producing lactic acid bacteria on the polyphenolic profile of apple juice." *Food Micro*. Nantes. 2014.
- A. I., Puertas, I. Ibarburu, G. Llamas, M.E., Muñoz, A., Prieto & M. T. Dueñas¹. "Actividad prebiótica de heteropolisacáridos producidos por *Lactobacillus* procedentes de sidra." *V Workshop Probióticos, Prebióticos y Salud. Evidencia Científica*. Valencia. 2014.
- A. I. Puertas, I. Ibarburu, M. G. Llamas, M. E. Muñoz, A. Prieto & M. T. Dueñas. "Evaluation of phenotypic characteristics of probiotic relevance in exopolysaccharide-producing *Lactobacillus* strains for Development of Functional Foods". *EFFOST Bio-based Technologies in the Context of European Food Innovation Systems*. Bolonia, Italia. 2013.

- A. I. Puertas, I. Ibarburu, M. G. Llamas, I. Berregi, M. E. Muñoz, A. Prieto & M. T. Dueñas. "Análisis del carácter probiótico en lactobacilos productores de exopolisacáridos para su uso en la elaboración de alimentos". *7ª Reunión de la Red Temática BAL. Madrid. 2013.*
- A. I. Puertas, I. Ibarburu, M. E. Muñoz, G. Cervantes, M. V. Gangoiti, A. Prieto & M. T. Dueñas. "Evaluación de características fenotípicas de relevancia probiótica para la elaboración de alimentos funcionales en cepas de *Lactobacillus* productoras de exopolisacáridos". *IV Workshop "Probióticos, Prebióticos y Salud: Evidencia Científica. Madrid. 2013.*
- A. I. Puertas, I. Ibarburu, A. Garzia, I. Berregi, A. Prieto, P. López, Ana Irastorza, & M. T. Dueñas. "Producción de heteropolisacáridos y riboflavina por cepas de *Lactobacillus* aisladas de sidra". *6ª Reunión de la Red Temática BAL. Tarragona. 2012*
- I. Ibarburu, A. I. Puertas, A. Irastorza, G. Spano, A. Prieto, P. López, & M. T. Dueñas. "Survival under simulated gastro-intestinal stresses of exopolysaccharide-producing *Lactobacillus* strains isolated from cider and prebiotic potential of these biopolymers". *International Scientific Conference Probiotics and Prebiotics – IPC2012. Kosice, Slovakia. 2012.*
- I. Ibarburu, A. I. Puertas, A. Munduate, A. Prieto, & M. T. Dueñas. "Supervivencia a estrés gástrico e intestinal de lactobacilos productores de heteropolisacáridos aislados de sidra". *III Workshop probióticos, prebióticos y salud: Evidencia científica. Castelldefels. 2011.*
- I. Ibarburu, A. I. Puertas, A. Irastorza, S. Notarariego, P. Fernández de Palencia, P. López, A. Prieto, & M. T. Dueñas. "Producción de heteropolisacáridos por cepas de *Lactobacillus* aisladas de sidra". *5ª Reunión de la Red Temática BAL. Logroño. 2011.*
- A. I. Puertas, I. Ibarburu, O. Etxebeste, A. Irastorza, & M.T. Dueñas. "Screening of EPS producer *Lactobacillus* strains isolated from cider". *10th Symposium on Lactic Acid Bacteria. Egmond aan Zee, Holanda. 2011.*
- I. Ibarburu, A. I. Puertas, A. Irastorza, & M. T. Dueñas. "Heteropolysaccharide production by two strains of *Lactobacillus*". *"Polysaccharides as source of advanced and sustainable products" 2nd EPNOE International Polysaccharide Conference. Wageningen, Holanda. 2011.*

- I. Ibarburu, A. I. Puertas, A. Prieto, A. Irastorza, & M. T. Dueñas. "Heteropolysaccharide production by two strains of *Lactobacillus suebicus*". *5th International Meeting on Biotechnology, BIOTEC 2010*. Pamplona. 2010.

Durante el periodo en el cual se ha realizado este trabajo, se ha colaborado en el desarrollo de varios trabajos de investigación, y se ha tomado parte en la siguientes publicaciones:

- Llamas-Arriba, M. G., Puertas, A. I., Prieto, A., López, P., Cobos, M., Miranda, J. I., Marieta, C., Ruas-Madiedo, P. & Dueñas, M. T. (2019). Characterization of dextrans produced by *Lactobacillus mali* CUPV271 and *Leuconostoc carnosum* CUPV411. *Food Hydrocolloids*, *89*, 613-622.
- Llamas-Arriba, M. G., Peirotén, Á., Puertas, A. I., Prieto, A., López, P., Pardo, M. Á., Rodríguez, E. & Dueñas, M. T. (2019). Heteropolysaccharide-producing bifidobacteria for the development of functional dairy products. *LWT*, *102*, 295-303
- Uranga, J., Puertas, A. I., Etxabide, A., Dueñas, M. T., Guerrero, P., & de la Caba, K. (2018). Citric acid-incorporated fish gelatin/chitosan composite films. *Food Hydrocolloids*.
- Gangoiti, M. V., Puertas, A. I., Hamet, M. F., Peruzzo, P. J., Llamas, M. G., Medrano, M., Prieto, A., Dueñas, M.T. & Abraham, A. G. (2017). *Lactobacillus plantarum* CIDCA 8327: An α -glucan producing-strain isolated from kefir grains. *Carbohydrate Polymers*, *170*, 52-59.
- Pérez-Ramos, A., Mohedano, M. L., Puertas, A. I., Lamontanara, A., Orru, L., Spano, G., Capozzi, V., Dueñas, M. T. & López, P. (2016). Draft Genome Sequence of *Pediococcus parvulus* 2.6, a Probiotic β -Glucan Producer Strain. *Genome Announcements*, *4*(6), e01381-16.
- Ibarburu, I., Puertas, A. I., Berregi, I., Rodríguez-Carvajal, M. A., Prieto, A., & Dueñas, M. T. (2015). Production and partial characterization of exopolysaccharides produced by two *Lactobacillus suebicus* strains isolated from cider. *International Journal of Food Microbiology*, *214*, 54-62.
- Zuriarrain, A., Zuriarrain, J., Puertas, A. I., Dueñas, M. T., Ostra, M., & Berregi, I. (2015). Polyphenolic profile in cider and antioxidant power. *Journal of the Science of Food and Agriculture*, *95*(14), 2931-2943.

- Zuriarrain, A., Zuriarrain, J., Puertas, A. I., Dueñas, M. T., & Berregi, I. (2015). Quantitative determination of lactic and acetic acids in cider by ^1H NMR spectrometry. *Food Control*, 52, 49-53.
- Puertas, A. I., Dueñas, M., & Marieta, C. (2014). Supramolecular structure and renaturation of a (1 \rightarrow 3)- β -D-glucan compared with curdlan and scleroglucan. *Fibers*, 2(3), 255-263.

ABREVIATURAS

ADP	adenosina difosfato
ANI	<i>Average Nucleotide Identity</i> , promedio de la identidad entre nucleótidos
Ap	área del pico
ATP	adenosina trifosfato
A _x	absorbancia a “X” nanómetros
B ₁₂	cobalamina
B ₂	riboflavina
BAL	bacterias del ácido láctico
C55-P	undecaprenil fosfato
CDD	base de datos de dominios conservados del NCBI
CDM	medio químicamente definido
CECT	Colección Española de Cultivos Tipo
CPS	polisacárido capsular
CUPV	Colección de Cultivos de la Universidad del País Vasco UPV/EHU;
DAD	detector de diodos
DDH	determinación de la hibridación DNA-DNA
DNA	ácido desoxirribonucleico
dNTP	desoxirribonucleósido trifosfato
DO _x	densidad óptica medida a “X” nanómetros.
dpf	día o días post-fecundación
DPPH [•]	radical 1,1-difenil-2-picril-hidrazilo
DSMZ	<i>German Collection of Microorganisms and Cell Cultures</i>
DSS	dextrano de sodio sulfatado
EDTA	ácido etilendiaminotetraacético
EPS	exopolisacárido
EW	solución para embriones
F-S	método del fenol-sulfúrico
FAD	flavina adenina dinucleótido
FAO/WHO	<i>Food and Agriculture Organization of the United Nations</i>
FLD	detector de fluorescencia
FML	fermentación maloláctica
FMN	flavina mononucleótido
FT-IR	espectroscopía infrarroja con transformada de Fourier
G	estrés gástrico
Gal	galactosa
GC-MS	cromatografía de gases-espectrometría de masas
GH	glicosilhidrolasa
GI	estrés gastrointestinal
Glc	glucosa
GPC	cromatografía de filtración en gel
GTF	glicosiltransferasa
GTP	guanosina 5´-trifosfato
HDO	agua semipesada
HePS	heteropolisacárido
HoPS	homopolisacárido

ABREVIATURAS

ADP	adenosina difosfato
ANI	<i>Average Nucleotide Identity</i> , promedio de la identidad entre nucleótidos
Ap	área del pico
ATP	adenosina trifosfato
A _x	absorbancia a “X” nanómetros
B ₁₂	cobalamina
B ₂	riboflavina
BAL	bacterias del ácido láctico
C55-P	undecaprenil fosfato
CDD	base de datos de dominios conservados del NCBI
CDM	medio químicamente definido
CECT	Colección Española de Cultivos Tipo
CPS	polisacárido capsular
CUPV	Colección de Cultivos de la Universidad del País Vasco UPV/EHU;
DAD	detector de diodos
DDH	determinación de la hibridación DNA-DNA
DNA	ácido desoxirribonucleico
dNTP	desoxirribonucleósido trifosfato
DO _x	densidad óptica medida a “X” nanómetros.
dpf	día o días post-fecundación
DPPH [•]	radical 1,1-difenil-2-picril-hidrazilo
DSMZ	<i>German Collection of Microorganisms and Cell Cultures</i>
DSS	dextrano de sodio sulfatado
EDTA	ácido etilendiaminotetraacético
EPS	exopolisacárido
EW	solución para embriones
F-S	método del fenol-sulfúrico
FAD	flavina adenina dinucleótido
FAO/WHO	<i>Food and Agriculture Organization of the United Nations</i>
FLD	detector de fluorescencia
FML	fermentación maloláctica
FMN	flavina mononucleótido
FT-IR	espectroscopía infrarroja con transformada de Fourier
G	estrés gástrico
Gal	galactosa
GC-MS	cromatografía de gases-espectrometría de masas
GH	glicosilhidrolasa
GI	estrés gastrointestinal
Glc	glucosa
GPC	cromatografía de filtración en gel
GTF	glicosiltransferasa
GTP	guanosina 5´-trifosfato
HDO	agua semipesada
HePS	heteropolisacárido
HoPS	homopolisacárido

TR	tiempo de retención
UFC	unidades formadoras de colonias
UPGMA	<i>Unweighted Pair Group Method with arithmetic Averages</i>
UV-Vis	ultravioleta-visible
v/v	volumen/volumen
WTA	ácido teicoico de pared celular
ΔG	energía libre
η_0	viscosidad newtoniana
λ_{em}	longitud de onda de emisión
λ_{ex}	longitud de onda de excitación
τ	cizalla o esfuerzo de corte
$\dot{\gamma}$	velocidad de deformación o velocidad de cizalla

ÍNDICE

Antecedentes y objetivos	7
Introducción general	15
1. Las bacterias del ácido láctico.....	17
1.1 Metabolismo de carbohidratos.....	18
1.2. Género <i>Lactobacillus</i>	19
1.3. Estructuras de la superficie celular de las bacterias del ácido láctico.....	21
2. Clasificación de los polisacáridos exocelulares producidos por las bacterias del ácido láctico.....	23
2.1. Homopolisacáridos.....	23
2.1.1. Alfa-glucanos y beta-glucanos.....	24
2.1.2. Beta-glucano	25
2.1.3. Poligalactanos y polimananos	25
2.2. Heteropolisacáridos	26
2.2.1. Organización génica de los <i>clusters eps/cps</i>	26
2.2.2. Proceso de síntesis del HePS	27
2.3. Biosíntesis de azúcares activados, aminoácidos y otros precursores.....	29
2.4. Aplicaciones de los exopolisacáridos	29
3. El proceso de elaboración de la sidra natural	32
3.1. Las bacterias del ácido láctico en el proceso de elaboración de la sidra	33
4. Bibliografía.....	35
Capítulo 1. Identificación de cepas de bacterias lácticas aisladas de sidra natural y descripción de la especie <i>Lactobacillus sicerae</i>.....	49
1. Introducción	51
2. Material y métodos	52
2.1 Cepas bacterianas y condiciones de cultivo	52
2.2. Caracterización fenotípica de las BAL aisladas de sidra	54
2.2.1. Características fenotípicas de los aislados.....	54
2.2.2. Cuantificación de sustratos y productos de fermentación	55
2.2.3. Composición celular de ácidos grasos	55
2.3. Microscopía electrónica de transmisión.....	56
2.4 Aislamiento y cuantificación del EPS	57
2.4.1. Producción de EPS en el medio semidefinido.....	57
2.4.2 Aislamiento de EPS a partir de biomasa	58
2.5. Determinación del tamaño de los EPS por HPSEC.....	59
2.6. Identificación y caracterización genotípica	60
2.6.1. Extracción del DNA.....	60
2.6.2. Identificación de las cepas mediante secuenciación génica	60
2.6.3. Tipificación	62
2.6.4. ANI (<i>Average Nucleotide Identity</i>).....	63
3. Resultados	65
3.1. Caracterización de los aislados del año 2009	65
3.1.1. Crecimiento y estudio del metabolismo	65

3.1.2. Producción de exopolisacárido y determinación del peso molecular	67
3.2. Identificación genotípica.....	68
3.2.1. Genotipado de cepas	70
3.3. Descripción de la especie <i>Lactobacillus sicerae</i>	73
3.3.1. Análisis de identidad nucleotídica media ANI (<i>Average Nucleotide Identity</i>) y contenido en G+C	74
3.3.2. Identificación fenotípica	74
4. Discusión	78
5. Conclusiones	81
6. Bibliografía	82

Capítulo 2. Análisis <i>in silico</i> de los genes <i>eps</i> de <i>Lactobacillus collinoides</i> y <i>Lactobacillus sicerae</i>	91
1. Introducción	96
2. Material y métodos	95
2.1. Capas bacterianas y condiciones de cultivo	95
2.2. Detección de genes implicados en la síntesis de HoPS y HePS en BAL	95
2.3. Secuenciación del genoma de <i>Lactobacillus collinoides</i> CUPV237. Análisis de las posibles secuencias proteicas de los genes <i>eps</i> en CUPV237 y CUPV261 ^T	97
2.4. Asignación de la nomenclatura	98
3. Resultados	99
3.1 Detección de genes implicados en la síntesis de EPS	99
3.2. Genes relacionados con la síntesis de heteropolisacáridos en el genoma de <i>Lactobacillus collinoides</i> CUPV237.....	100
3.2.1. Proteínas implicadas en la regulación de la síntesis de polisacárido	108
3.2.2. Proteínas implicadas en la síntesis de la unidad estructural, transporte a través de la membrana y polimerización de la cadena de EPS.....	113
3.3. Genes precursores de la síntesis de EPS en CUPV237	119
3.4. Genes relacionados con la síntesis de EPS en <i>L. sicerae</i> CUPV261 ^T	121
4. Discusión	125
5. Conclusiones	132
6. Bibliografía	133

Capítulo 3. Caracterización de los exopolisacáridos producidos por <i>Lactobacillus</i> <i>collinoides</i> y <i>Lactobacillus sicerae</i>	145
1. Introducción	147
2. Material y métodos	149
2.1. Cepas bacterianas y condiciones de cultivo	149
2.2. Microscopía electrónica de transmisión	149
2.3. Aislamiento, purificación y cuantificación de los exopolisacáridos	149
2.3.1. Determinación del contenido del EPS en el liófilo	150
2.4. Caracterización de los exopolisacáridos.....	151
2.4.1. Determinación del peso molecular, de la composición de monosacáridos y análisis de metilación	151
2.4.2. Análisis mediante espectroscopia infrarroja con transformada de Fourier (FT-IR).....	152
2.4.3. Análisis mediante Resonancia Magnética Nuclear (RMN)	152
2.4.4. Análisis de la estabilidad térmica	152

2.4.5. Reología de las fermentaciones	153
2.5. Comportamiento del EPS bajo un modelo <i>in vitro</i> de estrés gastrointestinal.....	153
2.6. Aplicación de un modelo <i>in vivo</i> de larvas de pez cebra	154
2.6.1. Obtención de los embriones	154
2.6.2. Modelo <i>in vivo</i> de enterocolitis inducida por DSS y tratamiento con EPS..	155
2.7. Análisis estadístico.....	156
3. Resultados	157
3.1. Producción de exopolisacárido	157
3.2. Análisis de los exopolisacáridos	158
3.2.1. Análisis FT-IR y RMN ¹ H.....	158
3.2.2. <i>Lactobacillus sicerae</i> CUPV261 ^T	160
3.2.3. <i>Lactobacillus collinoides</i> CUPV237	164
3.2.4. Análisis de la estabilidad térmica de los EPS.....	166
3.3. Tolerancia del EPS al estrés gastrointestinal en un modelo <i>in vitro</i>	167
3.4. Efecto de los EPS en un modelo <i>in vivo</i> de inflamación intestinal en larvas de pez cebra.....	168
4. Discusión	170
5. Conclusiones	174
6. Bibliografía	175

Capítulo 4. Caracterización biotecnológica de <i>L. collinoides</i> CUPV237 y <i>L. sicerae</i> CUPV261^T	185
1. Introducción	187
2. Material y métodos	189
2.1. Cepas bacterianas y condiciones de cultivo	189
2.2. Fermentación de matrices alimentarias	189
2.3. Características probióticas.....	190
2.3.1. Supervivencia celular bajo un modelo <i>in vitro</i> de estrés gastrointestinal ...	190
2.3.2. Autoagregación e hidrofobicidad celular.....	190
2.3.3. Actividad antioxidante	191
2.4. Transferencia del plásmido pRCR12 a las bacterias y expresión de la proteína mCherry.....	193
2.4.1. Transformación de células bacterianas con pRCR12	193
2.4.2. Detección de la expresión de la proteína fluorescente mCherry.....	195
2.5. Ensayos de colonización y visualización de <i>Lactobacillus</i> sp. [pRCR12] en el modelo de larvas gnotobióticas de <i>Danio rerio</i>	195
2.5.1. Obtención de larvas gnotobióticas de pez cebra.....	195
2.5.2. Ensayos de colonización intestinal	196
2.6. Análisis estadístico.....	197
3. Resultados	198
3.1. Fermentación de matrices alimentarias	198
3.2. Tolerancia al estrés gástrico y gastrointestinal	199
3.3. Evaluación de la actividad antioxidante	200
3.4. Capacidad de autoagregación e hidrofobicidad celular.....	201
3.5. Ensayos de colonización gastrointestinal en el modelo <i>in vivo</i> de larvas gnotobióticas de pez cebra	202
4. Discusión	206

5. Conclusiones	210
6. Bibliografía	211
Capítulo 5. Evaluación de la producción de riboflavina en bacterias lácticas aisladas de sidra y su contenido en sidra natural del País Vasco.....	219
1. Introducción	221
2. Material y métodos	226
2.1. Selección de cepas y medios de cultivo	226
2.2. Producción de riboflavina por <i>L. collinoides</i> CUPV237	229
2.3. Cuantificación de riboflavina	299
2.4. Fermentaciones de mostos de manzana.....	230
2.5. Determinación de riboflavina en sidras.....	231
2.6. Detección de genes implicados en la síntesis de riboflavina.....	232
3. Resultados	234
3.1. Producción de riboflavina por <i>L. collinoides</i> CUPV237	234
3.2. Determinación de la producción de riboflavina en cepas de la colección CUPV234	
3.3. Crecimiento y producción de riboflavina por <i>L. collinoides</i> CUPV237 y <i>L. sicerae</i> CUPV261 ^T en mostos de manzana	237
3.4. Análisis del contenido de riboflavina en sidra natural	238
3.5. Detección de genes implicados en la síntesis de riboflavina.....	239
4. Discusión	245
5. Conclusiones	249
6. Bibliografía	250
Conclusiones generales	257
ANEXO I	263
ANEXO II	269
ANEXO III	287

Antecedentes y Objetivos

La sidra natural o *sagardo* en *euskera*, es el producto resultante de la fermentación alcohólica total o parcial del mosto de manzana, y su contenido de azúcares y anhídrido carbónico es de origen endógeno, y posee un grado alcohólico igual o superior al 5 % (v/v). En el País Vasco se encuentran unas 100 sidrerías, y solo en Gipuzkoa se ubican en torno a 40 productores, que elaboran al año alrededor de 8 millones de litros de sidra natural.

En la sidra natural del País Vasco, generalmente no se lleva a cabo ningún proceso de estabilización microbiológica antes del embotellado. Las bacterias lácticas constituyen la microbiota predominante, y son las responsables de defectos organolépticos que aparecen en la bebida, incluso después del embotellado. Estas alteraciones son: la acetificación, el picado acroleínico, el “carácter Brett” y el ahilado o aceitado. Éste último es el defecto más común, y es la consecuencia de la producción de exopolisacáridos (EPS) por algunas cepas de bacterias lácticas de los géneros *Lactobacillus*, *Pediococcus* y *Oenococcus*. La síntesis de EPS ocasiona un incremento en la consistencia de la bebida por lo que es rechazada por los consumidores, y su repercusión económica es más importante cuando el producto está embotellado.

Resultados previos del grupo en el que se ha realizado esta Tesis doctoral, han mostrado que la mayoría de las estirpes de bacterias lácticas aisladas de sidra ahilada sintetizan un característico homopolisacárido, el (1,3)(1,2)- β -D-glucano, y pertenecen a las especies *P. parvulus*, *P. ethanolidurans*, *O. oeni*, *L. diolivorans* y *L. suebicus*. Algunas cepas sintetizan junto a este homopolisacárido (HoPS) otros EPS de tipo heteropolisacárido (HePS). Además, se ha encontrado que algunas cepas de *L. suebicus* sintetizan únicamente HePS, y la estirpe *L. mali* CUPV271 un HoPS de tipo dextrano. Estos antecedentes junto con la diversidad de *Lactobacillus* productores de EPS, nos sugieren que existe una gran variedad de exopolisacáridos que modifican las características organolépticas de la sidra natural del País Vasco.

Por otra parte, algunos EPS producidos por las BAL tienen efectos beneficiosos para la salud, ya que intervienen en la inmunomodulación mediada por microorganismos, son potencialmente prebióticos, poseen propiedades antioxidantes, o pueden regular los niveles de colesterol y glucosa en sangre. Otros exopolisacáridos tienen aplicaciones en la industria biotecnológica como: hidrocoloides, texturizantes, antioxidantes, agentes estabilizantes, agentes para el control de la cristalización, inhibidores de la sinéresis, y también se utilizan en procesos de encapsulación o en la formación de biopelículas. Por otro lado, ha sido probado su efecto positivo sobre las propiedades tecnofuncionales de diferentes alimentos fermentados por cepas

productoras de EPS, fundamentalmente productos lácteos, así como alimentos basados en cereales.

Teniendo en cuenta estos antecedentes, los objetivos generales de esta Tesis doctoral han sido:

- I) Identificación de una colección de *Lactobacillus* productores de EPS y responsables de la alteración del ahilado en la sidra natural del País Vasco.
- II) Caracterización fisicoquímica de los heteropolisacáridos producidos por dos estirpes seleccionadas pertenecientes a las especies *Lactobacillus collinoides* y *Lactobacillus sicerae*, y evaluación de su potencial probiótico.
- III) Evaluación de la síntesis de la vitamina riboflavina en cepas productoras de EPS, y caracterización de la cepa mutante *L. collinoides* CUPV237 con fenotipo superproductor de esta vitamina.

Para abordar estos objetivos se han llevado a cabo los siguientes estudios:

1. Identificación de cepas de *Lactobacillus* con fenotipo *ropy* que fueron aisladas de sidras ahiladas del País Vasco.
2. Identificación de forma predictiva de genes *eps* en las estirpes productoras de exopolisacárido *L. sicerae* CUPV261^T y *L. collinoides* CUPV237, mediante un análisis genómico *in silico*.
3. Caracterización parcial de los exopolisacáridos producidos por CUPV261^T y CUPV237, mediante el estudio de su composición, propiedades físico-químicas, estructura y su resistencia al estrés gastrointestinal en un modelo *in vitro*.
4. Evaluación del efecto de los EPS producidos por CUPV261^T, CUPV237, *Bifidobacterium longum* INIA P132 y *Bifidobacterium infantis* INIA P731, sobre la supervivencia de las larvas de pez cebra en un modelo *in vivo* de enfermedad inflamatoria intestinal inducida por el agente químico dextrano de sodio sulfatado (DSS).

5. Evaluación de características asociadas con el potencial probiótico en CUPV261^T y CUPV237.
6. Detección de la producción de riboflavina en bacterias lácticas productoras de exopolisacárido aisladas de sidra
7. Estudio de la síntesis de riboflavina en la cepa mutante superproductora *L. collinoides* CUPV237.

Introducción General

1. Las bacterias del ácido láctico

El término “bacterias del ácido láctico” (BAL) hace referencia a un grupo de heterogéneo de bacterias unidas por sus capacidades metabólicas, siendo el ácido láctico el producto mayoritario de la fermentación de los diferentes nutrientes (Zhang & Cai, 2014). Orla-Jensen (1919) fue el primero en clasificar a las BAL de acuerdo a sus características morfológicas y fisiológicas. Son bacterias Gram-positivas, en forma de cocos, bacilos o coco-bacilos, catalasa negativas aunque pueden contener una pseudocatalasa, ácido tolerantes, y generalmente no esporuladas. Son microorganismos muy ubicuos, asociados a ambientes ricos en nutrientes debido a sus requerimientos nutricionales (aminoácidos, vitaminas, minerales, ácidos grasos, péptidos, ácidos nucleicos y carbohidratos) (Ruíz-Rodríguez et al., 2017). Por este motivo, algunos de sus hábitats son los alimentos, como la leche, la carne, las bebidas fermentadas, los encurtidos o los vegetales. Otras BAL forman parte de la microbiota normal de boca, del intestino en animales, o de la vagina de mamíferos (Axelson, 2004).

Tradicionalmente, las relaciones filogenéticas de las BAL se han basado en la relación entre los genes ribosomales 16S (rRNA 16S). En la actualidad, el grupo de las BAL contempla especies de bacterias del filo *Firmicutes*, de la clase *Bacilli*, del orden *Lactobacillales* y de las familias: *Aerococcaceae*, *Carnobacteriaceae*, *Enterococcaceae*, *Lactobacillaceae*, *Leuconostocaceae* y *Streptococcaceae*. Dentro de estas seis familias los géneros más importantes son *Enterococcus*, *Lactobacillus*, *Lactococcus*, *Leuconostoc*, *Oenococcus*, *Pediococcus*, *Streptococcus*, *Vagococcus* y *Weisella*. El género *Bifidobacterium*, aunque pertenece a otro filo (*Actinobacteria*), ha sido tradicionalmente incluido dentro del grupo de las BAL por tener características metabólicas comunes, la más importante es la producción de ácido láctico a partir de glucosa (Aznar & Zúñiga, 2011; Liu et al., 2014). Hoy en día, la secuenciación de los genomas de las BAL junto con su fisiología, capacidades metabólicas, genes clave y la capacidad de adaptación a diferentes nichos ecológicos, está permitiendo entender mejor las características de este grupo de especies. La disponibilidad de las secuencias de los genomas permite estudiar las relaciones filogenéticas y la historia evolutiva de las BAL (Zhang & Cai, 2014).

1.1 Metabolismo de carbohidratos

Las BAL se clasifican de acuerdo a las enzimas que emplean en su metabolismo de carbohidratos. Una importante característica utilizada para la diferenciación dentro de este grupo, es el modo en que fermentan la glucosa sin factores que limiten el crecimiento, como pueden ser la falta de aminoácidos, vitaminas, precursores de ácidos nucleicos, la propia glucosa o de la disponibilidad de oxígeno (Axelson, 2004). Este grupo de bacterias ha perdido la capacidad de sintetizar citocromos y porfirinas, que son componentes de la cadena respiratoria, y por lo tanto no pueden generar ATP por la creación de un gradiente de protones. En cambio, producen energía mediante fosforilación a nivel de sustrato, siendo la oxidación de azúcares su principal fuente energética. Así, las BAL utilizan diferentes vías para la obtención de energía (von Wright & Axelsson, 2012) (Figura I.1):

- I. **Fermentación homoláctica u homofermentativa.** En este proceso se utiliza la ruta Embden-Meyerhof-Parnas (EMP) para metabolizar la glucosa. De forma teórica, la fermentación homoláctica produce 2 moles de ATP, 4 moles de NADH y dos moles de lactato por mol de glucosa. Las bacterias que exclusivamente utilizan esta ruta para la obtención de energía se denominan **homofermentativas**.
- II. **Fermentación heterofermentativa o heteroláctica.** Para la obtención de energía se utiliza la ruta de las pentosas fosfato o ruta del 6-fosfogluconato/fosfocetolasa. Las **bacterias heterofermentativas** que utilizan esta ruta, obtienen a partir de una molécula de glucosa una molécula de lactato y otra de CO₂, además de cantidades variables de etanol y acetato. Energéticamente, el rendimiento es de un ATP si el acetyl-fosfato es reducido a etanol, o de dos ATP si es transformado en acetato en presencia de aceptores de electrones alternativos.
- III. Existe otro grupo de bacterias denominadas **heterofermentativas facultativas**, que son capaces de consumir las pentosas D-xilosa, D-ribosa y L-arabinosa a través de la segunda parte de la ruta 6-fosfogluconato/fosfocetolasa. En ella se forman como productos de la fermentación cantidades equimolares de ácido láctico y acético.

1.2. Género *Lactobacillus*

El género *Lactobacillus* es uno de los géneros que más especies abarca dentro del orden *Lactobacillales*, ya que en la actualidad comprende más de 241 especies (DSMZ). La especie tipo del género es *Lactobacillus delbrueckii* (Leichmann, 1896). De forma general, son bacterias de tamaño variable, desde largos bastones hasta cocos, y algunos están dotados de movimiento por medio de flagelos peritricos; son microorganismos no esporulados, Gram-positivos, en ocasiones las células pueden exhibir polaridad o contener gránulos en su interior. Son anaerobios facultativos, ya que requieren un 5–10 % de CO₂, aunque también podemos encontrar aerotolerantes, y generalmente una anaerobiosis estricta inhibe su crecimiento. La reducción de nitratos no es habitual, tampoco licúan la gelatina, ni producen indol o H₂S; la reacción de la bencidina es negativa y la producción de pigmentos es rara (Schleifer, 2009).

Las bacterias de este género tienen requerimientos nutricionales complejos, y a menudo son específicos de la cepa en concreto. El rango de temperatura de crecimiento es de 2–53 °C, y la temperatura óptima es de 30–40 °C. Tienen preferencia por ambientes de naturaleza ácida, con pH óptimos de crecimiento entre 5,5 y 6,2 (Schleifer, 2009), y su contenido en G+C (mol %) está dentro del rango de 32–55 (Bd,Tm) (Axelsson, 2004).

Se pueden hallar lactobacilos en ambientes muy diversos, ya que participan en la elaboración de productos fermentados de origen lácteo, bebidas o encurtidos. También los podemos encontrar en suelos, agua de mar o formando parte de la microbiota normal de animales. Además, algunos son organismos alterantes, ya que afectan a las propiedades sensoriales de los alimentos a través del sabor, la textura, color, *slime*, enturbiamiento o por la formación de aminas biógenas (Vos et al., 2011).

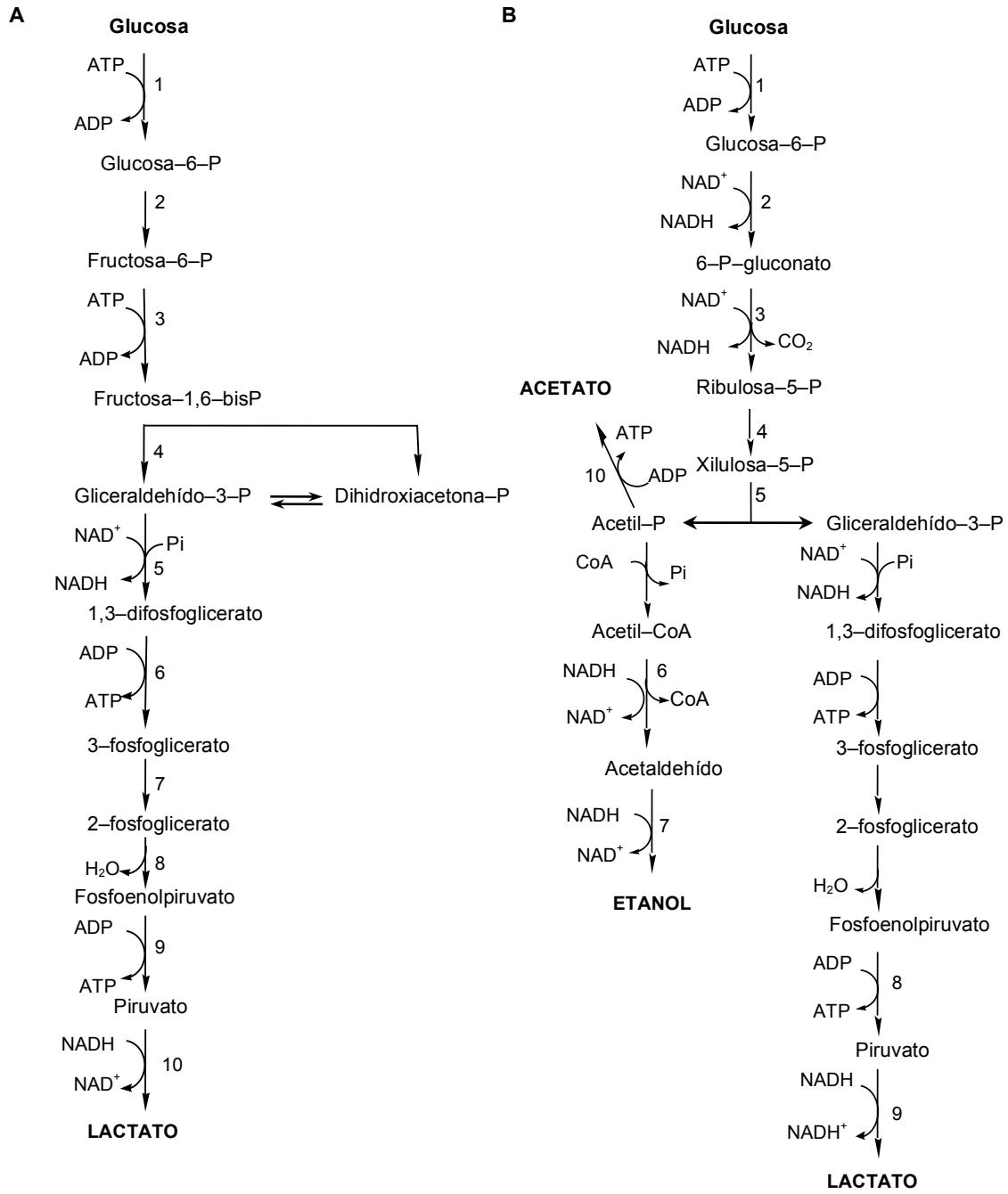


Figura 11. Metabolismo de las bacterias del ácido láctico. A, Fermentación homoláctica de la glucosa. 1, hexoquinasa; 2, glucosa-fosfato-isomerasa; 3, fosfofructoquinasa; 4, fructosa-1,6 bisfosfato aldolasa; 5, gliceralehído-3-fosfato deshidrogenasa; 6, 3-fosfo-glicerato quinasa; 7, fosfoglicerato mutasa; 8, enolasa; 9, piruvato quinasa; 10, lactato deshidrogenasa. B, Fermentación heteroláctica de la glucosa. 1, hexoquinasa; 2, glucosa-6-fosfato deshidrogenasa; 3, 6-fosfo-gluconato deshidrogenasa; 4, ribulosa-5-fosfato epimerasa; 5, fosfocetolasa; 6, acetaldehído deshidrogenasa; 7, alcohol deshidrogenasa; 8, piruvato quinasa; 9, lactato deshidrogenasa; 10, acetato quinasa.

1.3 Estructuras de la superficie celular de las bacterias del ácido láctico

La envoltura celular de las BAL es un sistema multicapa, mayoritariamente compuesto por peptidoglicano con 30–50 nm de grosor (Figura 2I). A él se anclan ácidos teicoicos, proteínas y polisacáridos, que son esenciales para mantener la forma e integridad celular. Estas moléculas de la superficie bacteriana, decoran colectivamente la envuelta de una manera cepa- o especie-específica. La envoltura celular también facilita procesos importantes para la adaptación al estrés o al medio ambiente, o relacionados con la colonización de superficies y la adhesión. En muchas especies bacterianas, los constituyentes de la pared celular pueden estar cubiertos por capas superficiales adicionales. Estas capas pueden ser la denominada capa S, formada por conjuntos cristalinos regulares de glicoproteínas, o las cápsulas de polisacárido (Leeber et al., 2008; Remus et al., 2012; Tripathi et al., 2012).

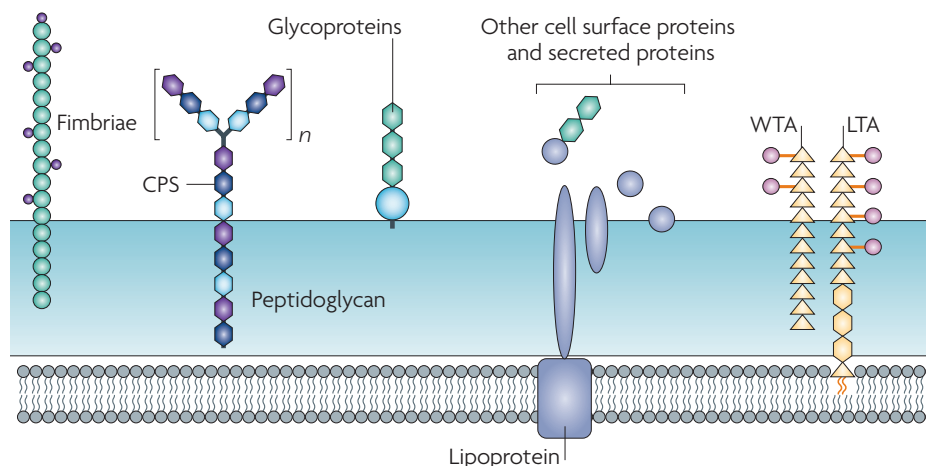


Figura 2I. Dibujo esquemático de la envoltura celular de las bacterias ácido lácticas tomado de Lebeer et al. (2010). LTA, ácido lipoteicoico (ácido teicoico anclado a la membrana plasmática); WTA, ácido teicoico de pared; CPS, polisacárido capsular.

Los polisacáridos son producidos por algunas bacterias, y se componen de pequeñas unidades repetitivas de monosacáridos, ramificadas o no, y pueden contener otros grupos funcionales de naturaleza no sacarídica (Leeber et al., 2008; Tripathi et al., 2012). Se denominan polisacáridos exocelulares (PE) a los polisacáridos capsulares (CPS) y a los polisacáridos liberados al medio extracelular o exopolisacáridos (EPS) (Figura 3I) (Zeidan et al., 2017). Los CPS forman una capa gruesa que envuelve a la célula, y a menudo está íntimamente asociada a la pared celular por uniones covalentes. Por el contrario, los EPS son los polisacáridos formados en la superficie celular que posteriormente se liberan al medio de cultivo (Vuyst et al., 2001; Korakli & Vogel, 2006; Lebeer et al., 2008).

Las BAL pueden sintetizar grandes macromoléculas de polisacáridos con pesos moleculares que llegan a alcanzar valores de $4,4 \times 10^5$ kDa (Zarour et al., 2017). Se conocen al menos 30 especies de BAL para las que se ha descrito cepas productoras de polisacáridos exocelulares. En bacterias Gram-positivas, los PE pueden ser sintetizados mediante tres mecanismos, los cuales pueden coexistir o no en una misma bacteria (Ates, 2015; Zeidan et al., 2017):

- I. Vía Wzy-dependiente. Esta vía implica la participación de diferentes enzimas codificadas por genes agrupados en *clusters*, y ejercen su función de forma secuencial para producir la cadena de polisacárido.
- II. Producción de PE mediante una proteína sintasa. En este caso, el proceso de polimerización y transporte lo lleva a cabo una única proteína transmembrana, y utiliza azúcares activados del interior celular como sustrato.
- III. Vía de producción de polisacárido mediante una enzima glicosilhidrolasa (GH). Una única enzima lleva a cabo la síntesis extracelular del polímero utilizando principalmente sacarosa como sustrato. Del disacárido obtiene el monosacárido que incorpora a la cadena y la energía necesaria para ello.

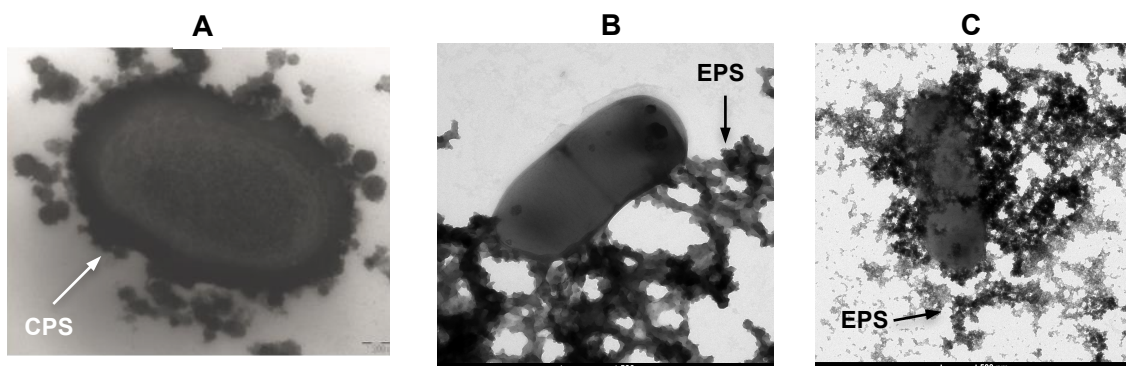


Figura 31. Microfotografías de tres lactobacilos productores de polisacáridos exocelulares, tomadas mediante microscopía electrónica de transmisión. En A, se observa la envuelta de polisacárido capsular producida por *Lactobacillus sakei* MN1 (Nácher, 2015); en B, *Lactobacillus collinoides* CUPV237 y su EPS (este trabajo); y en C, *Lactobacillus plantarum* CIDCA 8327 y su EPS (Gangoiti et al., 2017). Barra de escala, 500 nm.

La función fisiológica de los PE no está completamente entendida, aunque se piensa que podrían intervenir en la protección del microorganismo frente a las condiciones adversas de su entorno, tales como la deshidratación, el estrés ácido o temperaturas desfavorables (Baruah, Das & Goyal, 2016). Además, la presencia del polisacárido puede proteger a la bacteria frente a antibióticos o contra agentes patógenos, enzimas gástricas y pancreáticas. Los PE también pueden contribuir a la formación de biopelículas, intervenir en las interacciones hospedador-patógeno o en el

reconocimiento celular. Se ha descrito que estos polisacáridos pueden jugar un papel importante en la adhesión a la superficie de células eucariotas y en la modulación del sistema inmune del huésped (Baruah, Das & Goyal, 2016; Torino, Valdez & Mozzi, 2015). Por otro lado, se ha planteado la hipótesis de que los PE pueden desempeñar un papel de reservorio de energía extracelular, sin embargo, la mayoría de las estirpes productoras carecen de los genes relacionados con su propia degradación (Torino, Valdez & Mozzi, 2015).

2. Clasificación de los polisacáridos exocelulares producidos por las bacterias del ácido láctico

Las BAL sintetizan dos tipos de polisacáridos extracelulares:

(1) *Homopolisacáridos* (HoPS): estos polímeros están compuestos por un único tipo de monosacárido, su cadena puede estar ramificada o no, y contener uno o varios tipos de enlaces entre los monómeros.

(2) *Heteropolisacáridos* (HePS): sus cadenas están compuestas por unidades repetitivas, formadas por diferentes tipos de monosacáridos y enlaces, y además, pueden contener otros radicales de naturaleza no sacarídica.

2.1 Homopolisacáridos.

Los HoPS producidos por las BAL contienen un solo tipo de monosacárido neutro, y dependiendo de éste reciben el nombre de glucanos, cuando están compuestos por glucosa, fructanos por fructosa, poligalactanos por galactosa, o polimananos por manosa (Tabla 11). Los HoPS son polímeros de tamaño considerable, de entre 0,4 a $44,1 \times 10^5$ kDa (Badel et al., 2011; Zarour et al., 2017), y se clasifican de acuerdo a su composición y estructura. En las BAL se ha establecido una clasificación dentro de cada tipo de HoPS. Los glucanos, dependiendo del tipo de enlace pueden ser clasificados en α - y β -glucanos; y los fructanos, en levano e inulina, con configuración beta en sus enlaces (Torino, Valdez & Mozzi, 2015).

2.1.1 Alfa-glucanos y beta-fructanos

La producción de HoPS es llevada a cabo por glucosiltransferasas y fructosiltransferasas que catalizan la escisión de un residuo sacarídico de la sacarosa y lo unen a la cadena de α -glucano o β -fructano en formación, respectivamente. Además, estas enzimas pueden transferir una glucosa o fructosa a otra molécula aceptora (p. ej. maltosa o rafinosa) llevando a cabo la formación de oligosacáridos (Remaud-Simeon et al., 2000; Torino, Valdez & Mozzi, 2015). Estas reacciones ocurren cuando las concentraciones del sustrato y de los glicosil-aceptores alternativos son altas (Gänzle, 2009).

Tabla 11. Estructura de los homopolisacáridos producidos por bacterias del ácido láctico.

Especies productoras	Enlaces mayoritarios	Enlaces minoritarios	Tipo	Procedencia	Referencia
Glucano					
α-D-glucosa					
<i>L. curvatus</i> ; <i>Leuc. lactis</i>	(1,6)		dextrano	-	Palomba et al., 2012
<i>Leuc. mesenteroides</i>	(1,6)	(1 \rightarrow 4,6)		-	Leemhuis et al., 2013
<i>L. sakei</i>	(1,6)	(1 \rightarrow 3,6)		embutido	Nácher, 2015
<i>L. diolivorans</i>	(1,6)	(1 \rightarrow 2,6)		sidra alterada	Dueñas et al., 1998
<i>Leuc. mesenteroides</i>	(1,6) y (1,3)	(1 \rightarrow 3,6)	alternano	-	Patel et al., 2012; Leemhuis et al., 2013
<i>Leuc. mesenteroides</i> ; <i>L. reuteri</i> ; <i>S. downei</i> ; <i>S. mutans</i> ; <i>S. salivarius</i> y <i>S. sobrinus</i>	(1,3)	(1,6) y (1 \rightarrow 3,6)	mutano	-	Leemhuis et al., 2013
<i>L. reuteri</i>	(1,4) y (1,6)	(1 \rightarrow 4,6)	reuterano	-	van Hijum et al., 2006 Leemhuis et al., 2013
<i>L. plantarum</i>	(1,4)	(1 \rightarrow 3,4)	-	kéfir	Gangoiti et al., 2015
β-D-glucosa					
<i>P. parvulus</i> , <i>O. oeni</i> , <i>L. suebicus</i> y <i>L. diolivorans</i> .	(1,3)	(1 \rightarrow 3,2)	-	sidra alterada y vino	Werning et al., 2006 Lonvaud-Funel et al., 1993
<i>L. brevis</i> <i>L. fermentum</i>			-	cerveza queso	Fraunhofer et al., 2018 Vitlic et al., 2019
Fructano					
β-D-fructosa					
<i>L. reuteri</i> ; <i>Leuc. mesenteroides</i> <i>W. confusa</i>	(2,6)		levano	masa madre leche fermentada	Ni et al., 2018a Malang et al., 2015
<i>L. gasserii</i> <i>L. johnsonii</i> <i>L. reuteri</i> , <i>Leuc. citreum</i> , <i>S. mutans</i>	(2,1)		inulina	origen humano -	Ni et al., 2018b
Manano					
α-D-manosa					
<i>L. crispatus</i>	(1,2)	(1,6), (1,3) y (1 \rightarrow 2,6)	-	secreción vaginal	Donnarumma et al., 2014
Galactano					
galactosa					
<i>L. plantarum</i>	α -D-(1,4)-Gal y β -D-(1,4)-Gal	α -D-(1,6), β -D-(1,6) y β -D-(1 \rightarrow 2,3)	-	vegetales encurtidos	Wang et al., 2014
<i>Lc lactis</i> subsp. <i>cremoris</i>	β -D-(1,4)-Gal y β -D-(1,3)-Gal	α -D-(1,3)	-	-	Gruter et al., 1992

L., *Lactobacillus*; *Lc.*, *Lactococcus*; *Leuc.*, *Leuconostoc*; *S.*, *Streptococcus*; y *W.*, *Weissella*.

Las glucosiltransferasas, también denominadas glucansucrasas, son glicosilhidrolasas (GH) que pertenecen a la familia 70, Estas enzimas catalizan la síntesis de una gran variedad de α -glucanos, y la proporción entre los tipos de enlaces α -glucosídicos, la frecuencia y la longitud de las ramificaciones, ocasiona una amplia

variedad de polímeros diferentes (Leemhuis et al., 2013, Malang et al., 2015; Torino, Valdez & Mozzi, 2015) (Tabla 1I). Se ha descrito la producción de α -glucano en los siguientes géneros de BAL: *Leuconostoc*, *Lactobacillus*, *Streptococcus*, *Pediococcus*, *Weissella* y *Oenococcus* (Leemhuis et al., 2013; Torino, Valdez & Mozzi, 2015; Dimopoulou et al., 2016).

Las fructansacararas o fructosiltransferasas son GH de la familia 68 (Torino, Valdez & Mozzi, 2015). La producción de β -fructano se ha descrito en cepas pertenecientes a los géneros *Leuconostoc*, *Lactobacillus*, *Streptococcus*, *Weissella*; y *Oenococcus* (Tabla 1I) (Hugenholtz & Smid, 2002; Tieking et al., 2005; Di Cagno et al., 2006; Malang et al., 2015; Dimopoulou et al., 2016).

2.1.2 Beta-glucano

Una única proteína glicosiltransferasa (GTF) es la responsable de la producción del (1,3)(1,2)- β -D-glucano. Este polisacárido es sintetizado por cepas de las especies *P. parvulus*, *P. ethanolidurans*, *O. oeni*, *L. diolivorans*, *L. suebicus* y *L. brevis*, ligadas a la producción de sidra, vino o cerveza (Dueñas et al. 1997; Werning et al., 2006, Dols-Lafargue et al., 2008, Garai-Ibabe et al., 2010, Fraunhofer et al., 2018, Llamas-Arriba et al., 2018), y *L. fermentum* aislada de queso (Vitlic et al., 2019) (Tabla 1I). La enzima GTF es una proteína transmembrana que pertenece a la familia COG1215. A diferencia de otras sintasas productoras de glucano, no tiene función glicosil-hidrolasa (Werning et al., 2006) sino que utiliza UDP-glucosa de origen intracelular para sintetizar el polímero (Dols-Lafargue et al., 2008; Velasco et al., 2007). El resultado es un β -glucano con un peso molecular del orden de 4×10^3 kDa (Lambo-Fodje et al., 2007; Velasco et al., 2007; Garai-Ibabe et al., 2010; Werning et al., 2012).

2.1.3 Poligalactanos y polimananos

Es poco frecuente encontrarnos con especies de BAL productoras de polimananos o poligalactanos, y por el momento se desconocen los mecanismos para su producción (Torino, Valdez & Mozzi, 2015). Los poligalactanos contienen unidades pentaméricas de galactosa, y se han observado en dos cepas de *Lactobacillus plantarum* y *Lactococcus lactis* subsp. *cremoris* (Wang et al., 2014; Gruter et al., 1992). En el caso de los polimananos, sólo se ha descrito un único polímero producido por

una cepa de *Lactobacillus crispatus*, al cual se le atribuyen efectos beneficiosos contra patógenos vaginales (Donnarumma et al., 2014).

2.2 Heteropolisacáridos

Los HePS contienen combinaciones de monosacáridos formando una unidad estructural, la cual se repetirá a lo largo de la cadena para formar la molécula de polisacárido. Los distintos HePS producidos por las BAL, muestran gran variabilidad en su estructura y en las proporciones de sus monómeros (Patten & Laws, 2015). En su composición encontramos unidades de D-glucosa, D-galactosa y L-ramnosa, aunque también se han observado residuos de D-fructosa, D-manosa o L-fucosa, y aminoazúcares acetilados (*N*-acetil-D-glucosamina y *N*-acetil-D-galactosamina). De manera menos frecuente, en las cadenas de HePS se han observado unidades de naturaleza no sacarídica, como son el ácido glucurónico, el *sn*-glicerol-3-fosfato, grupos fosfato, acetilo o piruvato. Estos polímeros muestran tamaños moleculares de 10 a 6×10^3 kDa (Vuyst et al., 2001; Polak-Berecka et al., 2015; Patten & Laws, 2015).

2.2.1 Organización genética de los *clusters eps/cps*

Las proteínas implicadas en la síntesis de HePS están codificadas por genes contenidos en los *clusters eps/cps*, localizados tanto en plásmidos como en el cromosoma bacteriano (Cagganiello et al., 2016). Los *clusters* frecuentemente muestran un alto nivel de conservación, e incluso, los genes *eps/cps* se orientan en la misma dirección y son transcritos en un único mRNA (Vuyst & Degeest, 1999; Jolly and Stinglele, 2001; Lebeer et al., 2008; Cagganiello et al., 2016). Estos *clusters* incluyen genes que codifican tanto factores reguladores, como enzimas implicadas en la biosíntesis de EPS, en la polimerización y en la secreción, incluyendo glicosiltransferasas responsables del ensamblaje de la unidad estructural característica de cada exopolisacárido (Figura 4I) (Zeidan et al., 2017).

2.2.2 Proceso de síntesis del HePS.

Previamente al proceso de inicio de la síntesis, se debe producir el transporte de carbohidratos al interior de la célula y la activación de las unidades sacarídicas (NDP-azúcares) en el citoplasma (Figura 5I). En este paso intervienen proteínas del metabolismo central de carbohidratos, además de otras que están codificadas por genes localizados dentro de los *clusters eps/cps* (frecuentemente colocados en uno de los extremos del operón, Figura 4I). Un ejemplo son los genes *rml*, que intervienen en la formación de dTDP-Ram. (Stingele et al., 1996; Laws et al., 2001).

El proceso de síntesis de los HePS por la vía dependiente de Wzy puede dividirse en cinco etapas (Figura 4I):

- I. Activación del lípido de membrana undecaprenil-P (C55-P) cuando una glicosiltransferasa de membrana (WelE, EpsE o CpsE) le añade el primer azúcar activado mediante un enlace fosfodiéster (Zeidan et al., 2017).
- II. Diferentes enzimas glicosiltransferasas (desde WelF/EpsF/CpsF en adelante, p. ej., WelG, WelH) se coordinan para formar la unidad repetitiva del polisacárido. Son proteínas altamente específicas que incorporan cada componente de la unidad estructural, y liberan una molécula de UDP o TDP al espacio intracelular. Generalmente, los genes que codifican estas enzimas se sitúan en la parte central del operón, habiendo tantos genes de glicosiltransferasas como residuos diferentes incorporados en la unidad repetitiva (Stingele et al., 1996; Laws et al., 2001; Zeidan et al., 2017).
- III. Una vez formada la unidad repetitiva y todavía unida al C55-P, es transportada a través de la membrana por una proteína flipasa (Wzx). En la cara externa de la membrana celular, cada unidad estructural se añadirá al polisacárido exocelular en formación mediante un enlace O-glicosídico catalizado por una polimerasa (Wzy), quedando libre el C55-P (Zeidan et al., 2017). Tanto el gen de la flipasa como el gen de la polimerasa son genes poco conservados, y generalmente se sitúan dentro del *cluster eps/cps*, en el lado opuesto a los genes de las proteínas moduladoras del proceso (Stingele et al., 1996; Laws et al., 2001).
- IV. Después de completarse la polimerización, el polisacárido puede unirse al peptidoglicano de la pared celular por la acción de la proteína Wzr (CpsA, EpsA

o LytR-CpsA-Psr), o puede ser liberado al espacio extracelular (Toniolo et al., 2015; Zeidan et al., 2017).

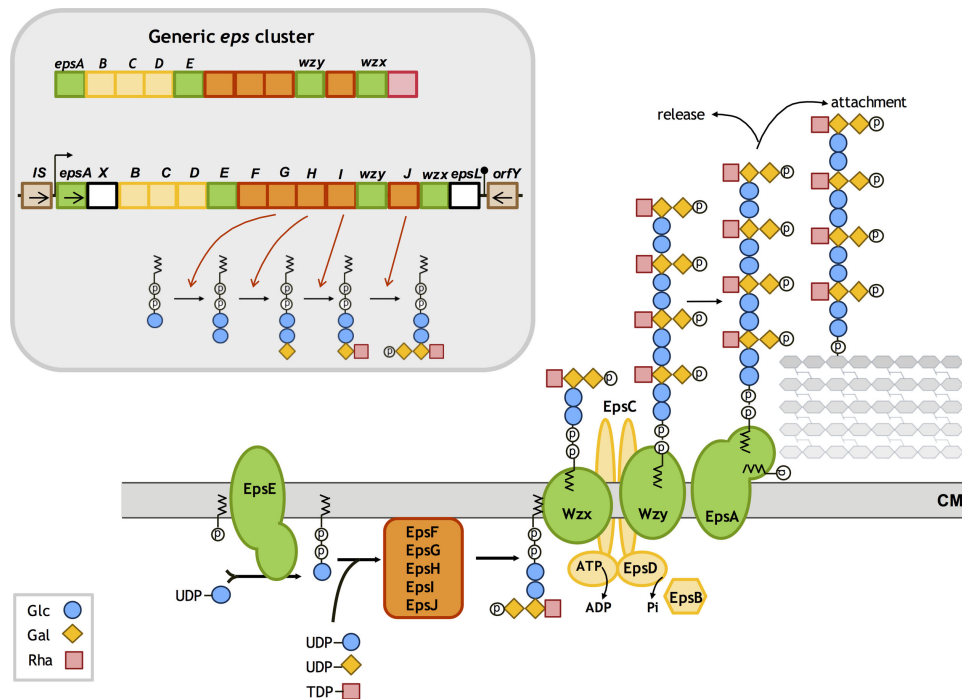


Figura 41. Ruta Wzy-dependiente para la biosíntesis de heteropolisacáridos en bacterias lácticas (Zeidan et al., 2017). El locus genético muestra los genes involucrados en la síntesis y exportación de polisacárido exocelular. Como ejemplo se muestra el ensamblaje y polimerización del polisacárido de *L. lactis* subsp. *cremoris* NIZO B40. **Arriba a la izquierda**, se representa un *cluster eps/cps* genérico y abajo el *cluster eps* de la estirpe B40; cada cuadrado representa un gen: en verde, genes de polimerización y transporte; en amarillo, genes del sistema fosforegulador; en naranja, genes de glicosiltransferasa; y en rosa, genes relacionados con la formación de NTP-azúcares. **Abajo y a la derecha**, las proteínas de la ruta Wzy-dependiente están representadas en el esquema-dibujo. Las reacciones catalizadas por las proteínas correspondientes a cada gen glicosiltransferasa se indican en el recuadro gris de la izquierda. Estas reacciones ocurren en el citoplasma y en la membrana citoplasmática.

Las proteínas moduladoras Wzd (también denominadas EpsC o CpsC) y Wze (EpsD o CpsD) constituyen una "tirosina kinasa activa (BY)" que podría ser la responsable de determinar la longitud de la cadena del polisacárido en formación. La proteína Wzd posee dos hélices transmembrana y ejerce una labor de andamio para la maquinaria de síntesis, manteniendo unidas las proteínas WeIE, la flipasa, la polimerasa y Wzr (EpsA o CpsA). Este modelo de síntesis de PE propone que el ciclo entre la forma fosforilada y no fosforilada de la kinasa BY es requerido para la adecuada síntesis y exportación del polisacárido; y que la desfosforilación está catalizada por la proteína fosfotirosina fosfatasa metalodependiente Wzb (CpsB, EpsB) (Zeidan et al., 2017).

2.3 Biosíntesis de azúcares activados, aminoazúcares y otros precursores.

Para la síntesis de los EPS o CPS son necesarias moléculas precursoras proporcionadas por diferentes rutas metabólicas de la célula bacteriana (Figura 5I). Estas rutas son llevadas a cabo por enzimas *housekeeping* necesarias para el mantenimiento de la vida celular, y por tanto, las bacterias deben asegurarse la perdurabilidad de sus genes (Boels et al., 2001). A excepción de la síntesis de polisacárido por las glicosilhidrolasas, para la producción de polisacárido son necesarios azúcares activados (UDP/UTP-azúcar o azúcares-nucleótido), sintetizados mediante reacciones de interconversión de los azúcares: epimerización, descarboxilación o deshidrogenación. Estos azúcares activados se encuentran en el citoplasma y son captados por las glicosiltransferasas para su incorporación a la cadena de polisacárido en formación (de Vuyst et al., 2001). En ocasiones, aparecen genes que codifican enzimas que intervienen en la conversión de azúcares a azúcares activados dentro del *cluster eps/cps* o cerca de ellos (Lebeer et al., 2009; Remus et al., 2012).

Otras rutas metabólicas también proporcionan moléculas no sacarídicas como el acetil-CoA, CDP-glicerol y piruvato presentes en determinados PE y que son indispensables para la confección de los componentes de la pared celular: peptidoglicano, ácidos teicoicos, lipopolisacáridos y antígenos de membrana en Gram-negativas. Cabe destacar la situación del C55-P, este lípido está comprometido en otros procesos para la formación de los componentes de la pared celular y puede limitar la producción de EPS/CPS (van Heijenoort, 2001).

2.4 Aplicaciones de los exopolisacáridos

Los beneficios de los exopolisacáridos en el área de los alimentos fermentados son detectables a concentraciones bajas (<1 %). La presencia de EPS en un producto puede hacer que sea más atractivo para el consumidor, aportando brillo, y generando una textura cremosa o firmeza a la matriz en la que se encuentra (Jolly & Stingele, 2001). La masa molecular de los EPS tiene especial relevancia en las características tecnológicas y funcionales de estos polímeros, influyendo en la viscosidad y en la textura de la matriz alimentaria (Badel et al., 2011; Torino, Valdez & Mozzi, 2015). En el caso de los productos fermentados lácteos, los EPS tienen la capacidad de unirse al agua, interactuar con las proteínas y aumentar la viscosidad de la fase sérica de la

leche. De esta manera, suavizan la textura y aportan cremosidad en los productos lácteos bajos en grasa y azúcares (Badel et al., 2011). Los EPS producidos por BAL no tienen un sabor intrínseco, pero pueden aumentar el tiempo de contacto de los alimentos que lo contienen con el paladar y con los receptores gustativos. Por lo tanto, el sabor del producto puede cambiar significativamente tras la texturización por el EPS (Jolly et al., 2002). En quesos, la presencia de los HePS liberados al medio promueven la retención de agua y mejoran la textura general del queso evitando la alteración de su estructura.

Con respecto a las aplicaciones de los HoPS, se utilizan dextranos industriales en la fabricación de productos de filtración en gel, así como extensores de volumen sanguíneo y mejoradores del flujo. También se emplean en los procesos de recubrimiento de papel y metales. En la industria alimentaria, el dextrano se utiliza actualmente como espesante para la elaboración de mermeladas y helados, o como estabilizador de jarabes alimentarios. Evita la cristalización del azúcar, mejora la retención de humedad y mantiene el sabor y la apariencia de diversos alimentos. Los levanos se utilizan en alimentación como biotexturizantes (Vuyst & Degeest, 1999; Zannini et al., 2016). Así mismo, se ha descrito el uso de bacterias productoras de dextrano en la elaboración de masa ácida de panadería (Tiekling et al., 2003; Galle et al., 2012) y de bacterias productoras de (1,3)(1,2)- β -D-glucano para la elaboración de productos basados en avena (Mårtensson et al., 2005; Pérez-Ramos et al. 2017).

Por otro lado, se ha descrito que algunos EPS tienen carácter prebiótico, que se define como: sustrato que es utilizado selectivamente por los microorganismos y que le confieren salud al huésped (Gibson et al., 2017). De esta manera, algunos EPS estimulan selectivamente el crecimiento de las bacterias en el tracto gastrointestinal para beneficiar la salud del huésped (Mårtensson et al., 2005; Parra, 2010; Baruah et al., 2016). La degradación de los EPS por la microbiota intestinal genera ácidos grasos de cadena corta (SCFA). Los SCFA proporcionan energía a las células epiteliales, y algunos podrían desempeñar un papel en la prevención del cáncer de colon (Jolly et al., 2002). Por lo tanto, el uso de bacterias probióticas que producen EPS beneficiosos para la salud *in situ*, es un enfoque muy prometedor para una nueva generación de alimentos funcionales (Jolly et al., 2002).

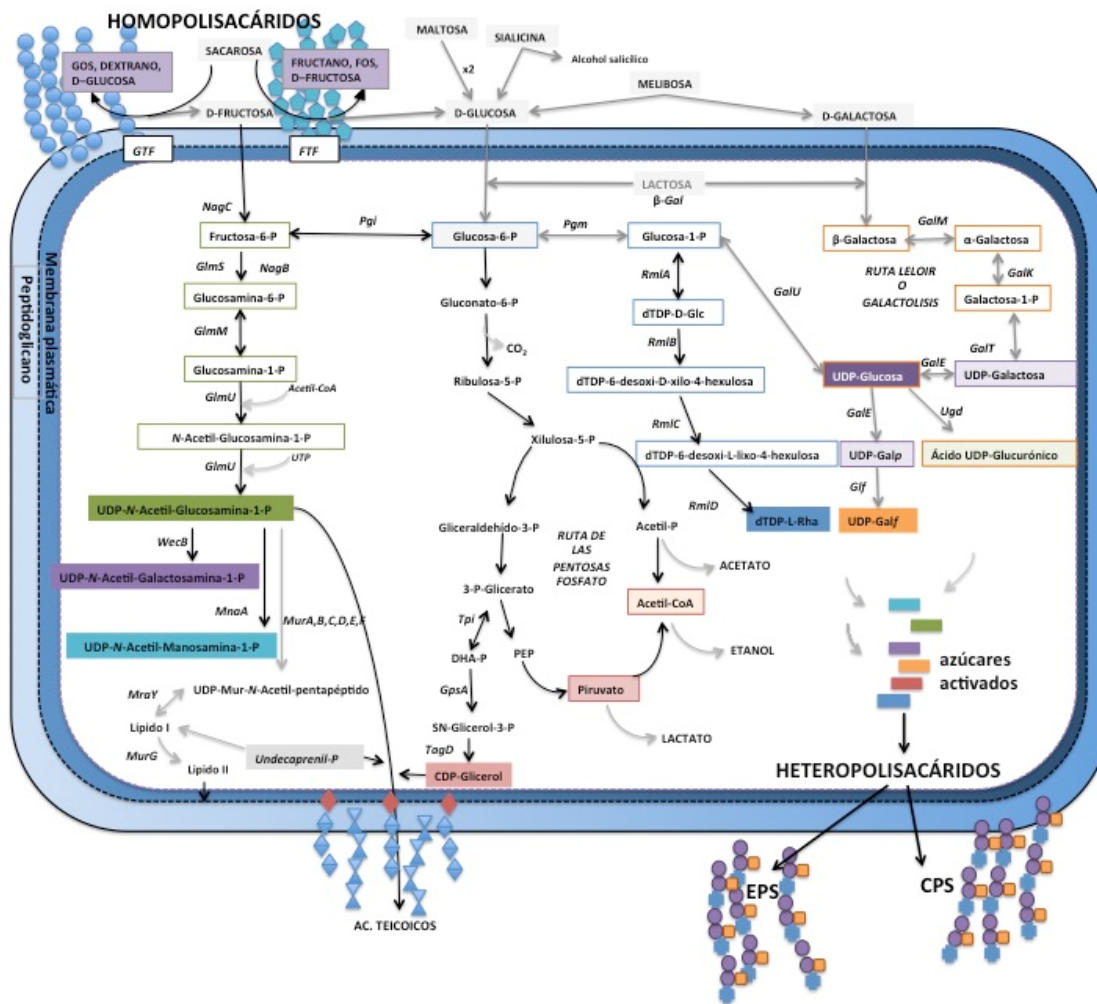


Figura 5I. Rutas metabólicas para la formación de los precursores necesarios para la síntesis de los polisacáridos exocelulares bacterianos y de los componentes de la pared celular. β -Gal, β -galactosidasa; NagB, glucosamina-6-P-epimerasa; NagC, fructokinasa; GlmS, Glucosamina-fructosa 6-P-aminotransferasa; GlmM, fosfoglucosamina mutasa; GlmU, enzima bifuncional N-acetil-glucosamina-1-P-uridililtransferasa/glucosamina 1-P-acetiltransferasa; WecB, UDP-N-acetil-glucosamina-2-epimerasa; MnaA, UDP-N-acetilglucosamina-2-epimerasa; Pgi, glucosa-6-P-isomerasa; GikA, glucokinasa; Pgm, fosfoglucomutasa; RmlA, glucosa-1-P timidililtransferasa; RmlB, dTDP-D-glucosa-4,6 deshidratasa; RmlC, dTDP-4-ceto-6-deoxiglucosa epimerasa; RmlD, dTDP-6-desoxi-L-lixo-4-hexulosa reductasa; GalU, UTP-glucosa-1-P-uridililtransferasa; GalE, UDP-glucosa-4-epimerasa; Gif, UDP-galactopyranoside mutasa; GalT, galactosa-1-P-uridililtransferasa; GalK, galactokinasa; GalM, galactosa mutarotasa, MurA, UDP-N-acetilglucosamina 1-carboxiviniltransferasa; MurB, UDP-N-acetilenolpiruvoylglucosamina reductasa; MurC, UDP-N-acetilmuramato-L-alanina ligasa; MurD, UDP-N-acetilmuramoilalanina-D-glutamato ligasa; MurE, UDP-N-acetilmuramoilalanil-D-glutamato-2,6 diaminopimelato ligasa; MurF, UDP-N-acetilmuramoil-tripéptido-D-alani-D-alanina ligasa; MraY, fosfo-N-acetilmuramoilpentapéptido transferasa; undecaprenil-difosfomuramoilpentapéptido beta-N-acetilglucosaminiltransferasa; Tpi, triosafato isomerasa; Gpsa, glicerol-3-P-deshidrogenasa; TagD, glicerol-3-P-citidililtransferasa. GTF, glucosiltransferasa; FTF, fructosiltransferasa; GOS, glucooligosacáridos; FOS, fructooligosacáridos (Boels et al., 2001; Degeest et al., 2001; van Heijenoort, 2001; Korakli & Vogel, 2006; Swoboda et al., 2010; González-Rodríguez et al., 2013; Dimopoulou, 2013).

3. El proceso de elaboración de la sidra natural

La producción de sidra en España se concentra sobre todo en las regiones de Asturias y País Vasco. En *Euskadi* la producción de sidra natural es una actividad culturalmente muy arraigada, sobre todo en Gipuzkoa. La sidra natural se define como el producto resultante de la fermentación del mosto natural de manzana, cuyo contenido en gas carbónico y azúcares tiene origen endógeno exclusivamente. Su grado alcohólico volumétrico adquirido será igual o superior a 5 % (v/v) y su presión relativa en el interior de la botella será superior a 0,5 bares a 20 °C (Código de la Sidra, actualización del 8 de abril de 2019).

En el proceso de producción de la sidra la selección de las variedades de manzana y las proporciones en que éstas se van a emplear es de suma importancia (Figura 6I). Tanto la variedad de manzana como el punto de maduración de ésta, influyen en la composición del mosto. Una vez recogidos los frutos, éstos se lavan, se mezclan, se trituran y se dejan macerando entre 2 y 4 días. Posteriormente, la pasta obtenida se prensa para la obtención del mosto, que se deposita en depósitos o *kupelas*. En ellas se lleva a cabo la fermentación alcohólica (por levaduras) y maloláctica (bacterias lácticas) por la microbiota indígena del fruto y de los útiles empleados en el proceso (Laplace et al., 1998; Herrero et al., 2010; Irastorza & Dueñas, 2010; Cousin et al., 2017). Además de los diferentes procesos físico-químicos y biológicos que conlleva la elaboración de la sidra, es en su maduración donde se redondean los sabores amargos y se conjugan los atributos sensoriales. El caldo ya hecho sidra se trasiega para separarlo de las borras de fermentación. Durante la permanencia de la sidra en el depósito, se incrementará la acidez volátil debido a la actividad de las BAL y las bacterias acéticas. Una vez que se alcanza la densidad adecuada, las cualidades aromático-gustativas y la turbidez del producto lo aconsejen, se procede al embotellado de la sidra (www.euskadi.eus/contenidos/informacion/calidad_diferenciada_dopigp/es_def/adjuntos/PLIEGO%20DE%20CONDICIONES_euskalsagardoa.pdf; [://www.serida.org/pdfs/772.pdf](http://www.serida.org/pdfs/772.pdf)).

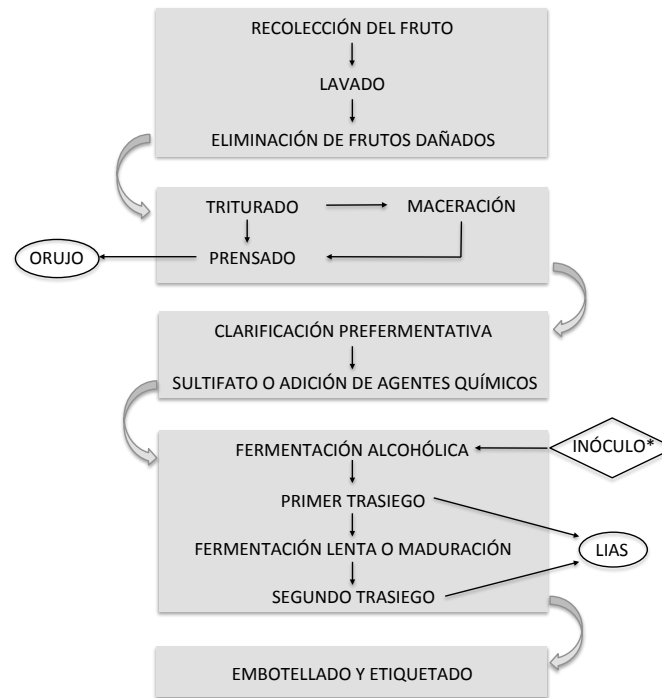


Figura 6I. Diagrama de flujo del proceso de elaboración de la sidra natural. (*) opcional (Herrero et al., 2010).

3.1 Las bacterias del ácido láctico en el proceso de elaboración de la sidra

En el proceso de producción de la sidra natural del País Vasco, la población de bacterias lácticas en mostos está influida fundamentalmente por la tecnología del prensado y el estado sanitario de la manzana. Tras el prensado, es habitual la presencia en los mostos de niveles elevados de BAL, del orden de 10^5 – 10^7 unidades formadoras de colonias por mL (UFC mL⁻¹). Incluso, en algunos casos se ha detectado que esta población es superior a la de las levaduras (Irastorza & Dueñas, 2010). Los microorganismos mejor adaptados a las condiciones posfermentativas son las BAL, mientras que las bacterias acéticas, al ser microorganismos aerófilos, tienen mayor dificultad para su desarrollo en este ambiente (<http://www.serida.org/pdfs/772.pdf>). Los géneros *Lactobacillus*, *Leuconostoc*, *Oenococcus* y *Pediococcus* son de especial interés por ser capaces de habitar en el ambiente de la sidra, caracterizado por un pH bajo (en torno a 3,7), una concentración alta de etanol (aprox. 6,5 % vol.) y bajo contenido de nutrientes (Suarez et al., 2007; Cousin et al., 2017).

La Tabla 2I muestra las especies de BAL aisladas de mostos y sidras del País Vasco y de diferentes países. Las especies más abundantes son heterofermentativas

y pertenecen a los géneros *Lactobacillus* y *Oenococcus*. También se han aislado especies homofermentativas obligadas del género *Pediococcus*.

Las bacterias lácticas llevan a cabo la fermentación maloláctica (FML), que consiste en una descarboxilación del ácido L-málico para producir ácido L-láctico. La FML conlleva una disminución de la sensación de astringencia y un aumento del pH de la sidra. Esta transformación la realizan principalmente las especies de los géneros *O. oeni* y *P. parvulus*, además de algunas especies del género *Lactobacillus* (Sánchez et al., 2010; Irastorza & Dueñas, 2010; Dueñas et al., 1994).

Tabla 21. Especies de bacterias lácticas encontradas en sidra.

Espece	Metabolismo	Referencia
	Homofermentativo	
<i>L. mali</i>		Carr & Davies, 1970; Buron et al., 2011; Llamas-Arriba et al., 2019a.
<i>L. delbrueckii</i> subsp. <i>lactis</i>		Marshall & Walkley, 1951; Weiss et al., 1983.
<i>L. acidophilus</i>		Laplace et al., 2001.
<i>L. sicerae</i>		Puertas et al., 2014.
<i>P. parvulus</i>		Garai-Ibabe et al., 2010a
<i>P. ethanolidurans</i>		Llamas-Arriba et al., 2018
	Heterofermentativo facultativo	
<i>L. plantarum</i>		Kleynmans et al., 1989.
	Heterofermentativo	
<i>L. collinoides</i>		Carr & Davies, 1972; Claisse & Lonvaud-Funel, 2000; Sauvageot et al., 2000; Garai et al., 2007; Buron et al., 2011; Puertas et al., 2016.
<i>L. paracollinoides</i>		Whiting & Carr, 1957.
<i>L. fermentum</i>		Carr & Davies, 1972; Dellaglio et al., 2004
<i>L. viridescens</i>		Carr & Davies, 1972
<i>L. hilgardii</i>		
<i>L. buchneri</i>		
<i>L. diolivorans</i>		Garai-Ibabe et al., 2008
<i>L. brevis</i>		Buron et al., 2011
<i>L. suebicus</i>		Marieta et al., 2009; Ibarburu et al., 2015.
<i>O. oeni</i>		Ibarburu et al., 2007; Buron et al., 2011.
<i>Leuc. mesenteroides</i>		Buron et al., 2011
<i>L.</i> , <i>Lactobacillus</i> ; <i>Lc.</i> , <i>Lactococcus</i> ; <i>Leuc.</i> , <i>Leuconostoc</i> ; y <i>O.</i> , <i>Oenococcus</i> .		

4. BIBLIOGRAFÍA

- Ates, O. (2015). Systems biology of microbial exopolysaccharides production. *Frontiers in Bioengineering and Biotechnology*, 3.
- Axelsson L.T. (2004). Lactic acid bacteria: classification y physiology. pp. 1-66. En: S. Salminen, A. von Wright & A. Ouwehand (Eds.), Lactic acid bacteria. Microbiological and functional aspects. Third Edition, revised and expanded. Marcel Dekker, Inc, New York.
- Aznar, R., & Zúñiga, M. (2011). ¿Qué son las bacterias lácticas? <http://redbal.iata.csic.es/documentos/sabiasque/Que%20son%20las%20bacterias%20lacticas.pdf>
- Badel, S., Bernardi, T., & Michaud, P. (2011). New perspectives for Lactobacilli exopolysaccharides. *Biotechnology Advances*, 29(1), 54-66.
- Baruah, R., Das, D., & Goyal, A. (2016). Heteropolysaccharides from lactic acid bacteria: Current trends and applications. *Journal of Probiotics and Health*, 4(141), 2.
- Boels, I. C., Ramos, A., Kleerebezem, M., & de Vos, W. M. (2001). Functional analysis of the *Lactococcus lactis galU* and *galE* genes and their impact on sugar nucleotide and exopolysaccharide biosynthesis. *Applied and Environmental Microbiology*, 67(7), 3033-3040.
- Buron, N., Coton, M., Desmarais, C., Ledauphin, J., Guichard, H., Barillier, D., & Coton, E. (2011). Screening of representative cider yeasts and bacteria for volatile phenol-production ability. *Food Microbiology*, 28(7), 1243-1251.
- Caggianiello, G., Kleerebezem, M., & Spano, G. (2016). Exopolysaccharides produced by lactic acid bacteria: from health-promoting benefits to stress tolerance mechanisms. *Applied Microbiology and Biotechnology*, 100(9), 3877-3886.
- Claisse, O., & Lonvaud-Funel, A. (2000). Assimilation of glycerol by a strain of *Lactobacillus collinoides* isolated from cider. *Food Microbiology*, 17(5), 513-519.
- Carr, J. G., & Davies, P. A. (1970). Homofermentative lactobacilli of ciders including *Lactobacillus mali* nov. spec. *Journal of Applied Microbiology*, 33(4), 768-774.
- Carr, J. G., & Davies, P. A. (1972). The ecology and classification of strains of *Lactobacillus collinoides* nov. spec.: A bacterium commonly found in fermenting apple juice. *Journal of Applied Microbiology*, 35(3), 463-471.

- Cousin, F. J., Le Guellec, R., Schlüsselhuber, M., Dalmaso, M., Laplace, J. M., & Cretenet, M. (2017). Microorganisms in fermented apple beverages: current knowledge and future directions. *Microorganisms*, 5(3), 39.
- Degeest, B., Vaningelgem, F., Laws, A. P., & De Vuyst, L. (2001). UDP-N-acetylglucosamine 4-epimerase activity indicates the presence of N-acetylgalactosamine in exopolysaccharides of *Streptococcus thermophilus* strains. *Applied and Environmental Microbiology*, 67(9), 3976-3984.
- Dellaglio, F., Torriani, S., & Felis, G. E. (2004). Reclassification of *Lactobacillus cellobiosus* Rogosa et al. 1953 as a later synonym of *Lactobacillus fermentum* Beijerinck 1901. *International Journal of Systematic and Evolutionary Microbiology*, 54(3), 809-812.
- Di Cagno, R., De Angelis, M., Limitone, A., Minervini, F., Carnevali, P., Corsetti, A., Gaenzle, M., Ciatì, R., & Gobbetti, M. (2006). Glucan and fructan production by sourdough *Weissella cibaria* and *Lactobacillus plantarum*. *Journal of Agricultural and Food Chemistry*, 54(26), 9873-9881.
- Dimopoulou, M. (2013). Les polysaccharides de la bactérie lactique *Oenococcus oeni*, de l'élucidation de leurs structures et voies de biosynthèse à leur valorisation technologique (Doctoral dissertation, Bordeaux 2).
- Dimopoulou, M., Bardeau, T., Ramonet, P. Y., Miot-Certier, C., Claisse, O., Doco, T., Petrel, M., Lucas, P., & Dols-Lafargue, M. (2016). Exopolysaccharides produced by *Oenococcus oeni*: from genomic and phenotypic analysis to technological valorization. *Food Microbiology*, 53, 10-17.
- Dols-Lafargue, M., Lee, H. Y., Le Marrec, C., Heyraud, A., Chambat, G., & Lonvaud-Funel, A. (2008). Characterization of *gtf*, a glucosyltransferase gene in the genomes of *Pediococcus parvulus* and *Oenococcus oeni*, two bacterial species commonly found in wine. *Applied and Environmental Microbiology*, 74(13), 4079-4090.
- Donnarumma, G., Molinaro, A., Cimini, D., De Castro, C., Valli, V., De Gregorio, V., De Rosa, M., & Schiraldi, C. (2014). *Lactobacillus crispatus* L1: high cell density cultivation and exopolysaccharide structure characterization to highlight potentially beneficial effects against vaginal pathogens. *BMC Microbiology*, 14(1), 137.
- DSMZ. https://github.com/CSB5/atminter/blob/master/data/DSMZ_bactnames0315.csv
- Dueñas, M., Irastorza, A., Fernandez, K., Bilbao, A., & Huerta, A. (1994). Microbial populations and malolactic fermentation of apple cider using traditional and modified methods. *Journal of Food Science*, 59(5), 1060-1064.

- Dueñas-Chasco, M. T., Rodríguez-Carvajal, M. A., Mateo, P. T., Franco-Rodríguez, G., Espartero, J., Irastorza-Iribas, A., & Gil-Serrano, A. M. (1997). Structural analysis of the exopolysaccharide produced by *Pediococcus damnosus* 2.6. *Carbohydrate Research*, 303(4), 453-458.
- Dueñas-Chasco, M. T., Rodríguez-Carvajal, M. A., Tejero-Mateo, P., Espartero, J. L., Irastorza-Iribas, A., & Gil-Serrano, A. M. (1998). Structural analysis of the exopolysaccharides produced by *Lactobacillus spp.* G-77. *Carbohydrate Research*, 307(1), 125-133.
- Fraunhofer, M. E., Geissler, A. J., Wefers, D., Bunzel, M., Jakob, F., & Vogel, R. F. (2018). Characterization of β -glucan formation by *Lactobacillus brevis* TMW 1.2112 isolated from slimy spoiled beer. *International Journal of Biological Macromolecules*, 107, 874-881.
- Galle, S., Schwab, C., Dal Bello, F., Coffey, A., Gänzle, M., & Arendt, E. (2012). Comparison of the impact of dextran and reuteran on the quality of wheat sourdough bread. *Journal of Cereal Science*, 56(3), 531-537
- Gangoiti, M. V., Puertas, A. I., Hamet, M. F., Peruzzo, P. J., Llamas, M. G., Medrano, M., Prieto, A., Dueñas, M.T., & Abraham, A. G. (2017). *Lactobacillus plantarum* CIDCA 8327: An α -glucan producing-strain isolated from kefir grains. *Carbohydrate Polymers*, 170, 52-59.
- Gänzle, M. G. (2009). From gene to function: metabolic traits of starter cultures for improved quality of cereal foods. *International Journal of Food Microbiology*, 134(1-2), 29-36.
- Garai-Ibabe, G., Ibarburu, I., Berregi, I., Claisse, O., Lonvaud-Funel, A., Irastorza, A., & Dueñas, M. T. (2008). Glycerol metabolism and bitterness producing lactic acid bacteria in cidermaking. *International Journal of Food Microbiology*, 121(3), 253-261.
- Garai-Ibabe, G., Areizaga, J., Aznar, R., Elizaquivel, P., Prieto, A., Irastorza, A. & Dueñas, M. T. (2010). Screening and selection of 2-branched (1, 3)- β -D-glucan producing lactic acid bacteria and exopolysaccharide characterization. *Journal of Agricultural and Food Chemistry*, 58(10), 6149-6156.
- Gibson, G. R., Hutkins, R., Sanders, M. E., Prescott, S. L., Reimer, R. A., Salminen, S.J., Scott, K., Stanton, C., Swanson, K.S., Cani, P.D., & Verbeke, K. (2017). The International Scientific Association for Probiotics and Prebiotics (ISAPP) consensus

- statement on the definition and scope of prebiotics. *Nat Rev Gastroenterol Hepatol*, 14(8), 491-502.
- González-Rodríguez, I., Gaspar, P., Sánchez, B., Gueimonde, M., Margolles, A., & Neves, A. R. (2013). Catabolism of glucose and lactose in *Bifidobacterium animalis* subsp. *lactis*, studied by ¹³C nuclear magnetic resonance. *Applied and Environmental Microbiology*, 79(24), 7628-7638.
- Gruter, M., Leeftang, B. R., Kuiper, J., Kamerling, J. P., & Vliegthart, J. F. (1992). Structure of the exopolysaccharide produced by *Lactococcus lactis* subspecies *cremoris* H414 grown in a defined medium or skimmed milk. *Carbohydrate Research*, 231, 273-291.
- van Heijenoort, J. (2001). Recent advances in the formation of the bacterial peptidoglycan monomer unit. *Natural Product Reports*, 18(5), 503-519.
- van Hijum, S. A., Kralj, S., Ozimek, L. K., Dijkhuizen, L., & van Geel-Schutten, I. G. (2006). Structure-function relationships of glucansucrase and fructansucrase enzymes from lactic acid bacteria. *Microbiology and Molecular Biology Reviews*, 70(1), 157-176.
- Herrero, M., Gonzalo, A., & García, L. A. (2010). 7. Tecnología de la producción de sidra. Equipamiento industrial. pp. 197-220. En: Blanco, D. & Mangas, J. J. (Eds.), La manzana y la sidra: bioprocesos, tecnologías de elaboración y control. Astugraf, Oviedo, España.
- Hughenoltz, J., & Smid, E. J. (2002). Nutraceutical production with food-grade microorganisms. *Current Opinion in Biotechnology*, 13(5), 497-507.
- Ibarburu, I., Soria-Díaz, M. E., Rodríguez-Carvajal, M. A., Velasco, S. E., Tejero-Mateo, P., Gil-Serrano, A. M., Irastorza, A., & Dueñas, M. T. (2007). Growth and exopolysaccharide (EPS) production by *Oenococcus oeni* I4 and structural characterization of their EPSs. *Journal of Applied Microbiology*, 103(2), 477-486.
- Ibarburu, I., Puertas, A. I., Berregi, I., Rodríguez-Carvajal, M. A., Prieto, A., & Dueñas, M. T. (2015). Production and partial characterization of exopolysaccharides produced by two *Lactobacillus suebicus* strains isolated from cider. *International Journal of Food Microbiology*, 214, 54-62.
- Irastorza, A., & Dueñas, M. T. (2010). 4. Microbiología de la sidra. pp. 115-135. En: Blanco, D. & Mangas, J. J. (Eds.), La manzana y la sidra: bioprocesos, tecnologías de elaboración y control. Astugraf, Oviedo, España.

- Jolly, L., & Stingele, F. (2001). Molecular organization and functionality of exopolysaccharide gene clusters in lactic acid bacteria. *International Dairy Journal*, 11(9), 733-745.
- Jolly, L., Vincent, S. J., Duboc, P., & Neeser, J. R. (2002). Exploiting exopolysaccharides from lactic acid bacteria. *Antonie Van Leeuwenhoek*, 82(1-4), 367-374.
- Khalid, K. (2011) An Overview of Lactic Acid Bacteria. *International Journal of Biosciences*, 1, 1-13.
- Kleynmans, U., Heinzl, H., & Hammes, W. P. (1989). *Lactobacillus suebicus* sp. nov., an obligately heterofermentative *Lactobacillus* species isolated from fruit mashes. *Syst Appl Microbiol* 11, 267–271.
- Korakli, M., & Vogel, R. F. (2006). Structure/function relationship of homopolysaccharide producing glycosyltransferases and therapeutic potential of their synthesised glycans. *Applied Microbiology and Biotechnology*, 71(6), 790-803.
- Lambo-Fodje, A. M., Leeman, M., Wahlund, K. G., Nyman, M., Öste, R., & Larsson, H. (2007). Molar mass and rheological characterisation of an exopolysaccharide from *Pediococcus damnosus* 2.6. *Carbohydrate Polymers*, 68(3), 577-586.
- Laplace, J. M., Apery, S., Frere, J., & Ray, Y. A. (1998). Incidence of indigenous microbial flora from utensils and surrounding air in traditional french cider making. *Journal of the Institute of Brewing*, 104(2), 71-74.
- Laplace, J. M., Jacquet, A., Travers, I., Simon, J. P., & Auffray, Y. (2001). Incidence of land and physicochemical composition of apples on the qualitative and quantitative development of microbial flora during cider fermentations. *Journal of the Institute of Brewing*, 107, 227–233.
- Laws, A., Gu, Y. & Marshall, V. (2001). Biosynthesis, characterisation, and design of bacterial exopolysaccharides from lactic acid bacteria. *Biotechnology Advances*, 19(8), 597-625.
- Lebeer, S., Vanderleyden, J., & De Keersmaecker, S. C. (2008). Genes and molecules of lactobacilli supporting probiotic action. *Microbiology and Molecular Biology Reviews*, 72(4), 728-764.
- Lebeer, S., Verhoeven, T. L., Francius, G., Schoofs, G., Lambrichts, I., Dufrêne, Y., Vanderleyden, J., & De Keersmaecker, S. C. (2009). Identification of a gene cluster for the biosynthesis of a long, galactose-rich exopolysaccharide in *Lactobacillus*

- rhamnosus* GG and functional analysis of the priming glycosyltransferase. *Applied and Environmental Microbiology*, 75(11), 3554-3563.
- Lebeer, S., Vanderleyden, J., & De Keersmaecker, S. C. (2010). Host interactions of probiotic bacterial surface molecules: comparison with commensals and pathogens. *Nature Reviews Microbiology*, 8(3), 171.
- Leemhuis, H., Pijning, T., Dobruchowska, J. M., van Leeuwen, S. S., Kralj, S., Dijkstra, B. W., & Dijkhuizen, L. (2013). Glucansucrases: three-dimensional structures, reactions, mechanism, α -glucan analysis and their implications in biotechnology and food applications. *Journal of Biotechnology*, 163(2), 250-272.
- Leichmann, G. (1896). Über die im Brennereiprozess bei der Bereitung der Kunsthefe auftretende spontane Milchsäuregärung. *Zentralbl Bakteriol II*, 2, 281–285.
- Liu, W., Pang, H., Zhang, H., & Cai, Y. (2014) Biodiversity of Lactic Acid Bacteria. pp. 103-203. En: Zhang H., Cai Y. (Eds), Lactic Acid Bacteria. Springer, Dordrecht, Holanda.
- Llamas-Arriba, M. G., Pérez-Ramos, A., Puertas, A. I., López, P., Prieto, A., & Dueñas, M. T. (2018). Characterization of *Pediococcus ethanolidurans* CUPV141: A β -D-glucan and heteropolysaccharide-producing bacterium. *Frontiers in Microbiology*, 9, 2041.
- Llamas-Arriba, M. G., Peirotén, A., Puertas, A. I., Prieto, A., López, P., Pardo, M. A., Rodríguez, E., & Dueñas, M. T. (2019). Heteropolysaccharide-producing bifidobacteria for the development of functional dairy products. *LWT-Food Science and Technology*, 102, 295-303.
- Lonvaud-Funel, A., Guilloux, Y., & Joyeux, A. (1993). Isolation of a DNA probe for identification of glucan-producing *Pediococcus damnosus* in wines. *Journal of Applied Bacteriology*, 74(1), 41-47.
- Makarova, K. S., & Koonin, E. V. (2007). Evolutionary genomics of lactic acid bacteria. *Journal of Bacteriology*, 189(4), 1199-1208.
- Malang, S. K., Maina, N. H., Schwab, C., Tenkanen, M., & Lacroix, C. (2015). Characterization of exopolysaccharide and rpy capsular polysaccharide formation by *Weissella*. *Food Microbiology*, 46, 418-427.
- Marieta, C., Ibarburu, I., Dueñas, M., & Irastorza, A. (2009). Supramolecular structure and conformation of a (1→3)(1→2)- β -D-glucan from *Lactobacillus suebicus* CUPV

- 221 as observed by tapping mode atomic force microscopy. *Journal of Agricultural and Food Chemistry*, 57(14), 6183–6188.
- Marshall, C. R., & Walkley, V. T. (1951). Some aspects of microbiology applied to commercial apple juice production. I. Distribution of microorganisms on the fruit. *Journal of Food Science*, 16(1-6), 448–456.
- Mårtensson, O., Biörklund, M., Lambo, A. M., Dueñas-Chasco, M., Irastorza, A., Holst, O., Norin, E., Welling, G., Öste, R., & Önning, G. (2005). Fermented, rory, oat-based products reduce cholesterol levels and stimulate the bifidobacteria flora in humans. *Nutrition Research*, 25(5), 429-442.
- Nácher, M. (2015). Dextranos de bacterias lácticas aisladas de productos cárnicos: caracterización y aplicaciones (Tesis doctoral, Universitat de València).
- Ni, D., Xu, W., Bai, Y., Zhang, W., Zhang, T., & Mu, W. (2018a). Biosynthesis of levan from sucrose using a thermostable levansucrase from *Lactobacillus reuteri* LTH5448. *International Journal of Biological Macromolecules*, 113, 29-37.
- Ni, D., Zhu, Y., Xu, W., Bai, Y., Zhang, T., & Mu, W. (2018b). Biosynthesis of inulin from sucrose using inulosucrase from *Lactobacillus gasseri* DSM 20604. *International Journal of Biological Macromolecules*, 109, 1209-1218.
- Palomba, S., Cavella, S., Torrieri, E., Piccolo, A., Mazzei, P., Blaiotta, G., Ventorino, V. & Pepe, O. (2012). Wheat sourdough from *Leuconostoc lactis* and *Lactobacillus curvatus* exopolysaccharide-producing starter culture: polyphasic screening, homopolysaccharide composition and viscoelastic behavior. *Applied and Environmental Microbiology*, AEM-07302.
- Parra, R. A. (2010). Review. Bacterias ácido lácticas: papel funcional en los alimentos. *Facultad de Ciencias Agropecuarias*. 8(1) Enero-Junio 2010.
- Patel, S., Majumder, A., & Goyal, A. (2012). Potentials of exopolysaccharides from lactic acid bacteria. *Indian Journal of Microbiology*, 52(1), 3-12.
- Patten, D. A. & Laws, A. P. (2015). *Lactobacillus*-produced exopolysaccharides and their potential health benefits: a review. *Beneficial Microbes*, 6(4), 457-471.
- Pérez-Ramos, A., Mohedano, M.L., López, P., Spano, G., Fiocco, D., Russo, P., & Capozzi, V. (2017). In Situ β -Glucan fortification of cereal-based matrices by *Pediococcus parvulus* 2.6: Technological aspects and prebiotic potential. *International Journal of Molecular Sciences*, 18, 1588.

- Polak-Berecka, M., Choma, A., Waško, A., Górska, S., Gamian, A. & Cybulska, J. (2015). Physicochemical characterization of exopolysaccharides produced by *Lactobacillus rhamnosus* on various carbon sources. *Carbohydrate Polymers*, 117, 501-509.
- Puertas, A. I., Arahál, D. R., Ibarburu, I., Elizaquível, P., Aznar, R., & Dueñas, M. T. (2014). *Lactobacillus sicerae* sp. nov., a lactic acid bacterium isolated from Spanish natural cider. *International Journal of Systematic and Evolutionary Microbiology*, 64(9), 2949-2955.
- Puertas, A. I., Capozzi, V., Llamas, M. G., López, P., Lamontanara, A., Orrù, L., Russo, P., Spano G., & Dueñas, M. T. (2016). Draft genome sequence of *Lactobacillus collinoides* CUPV237, an exopolysaccharide and riboflavin producer isolated from cider. *Genome Announcements*, 4(3), e00506-16.
- Remaud-Simeon, M., Willemot, R. M., Sarçabal, P., de Montalk, G. P., & Monsan, P. (2000). Glucansucrases: molecular engineering and oligosaccharide synthesis. *Journal of Molecular Catalysis B: Enzymatic*, 10(1-3), 117-128.
- Remus, D. M., van Kranenburg, R., van Swam, I. I., Taverne, N., Bongers, R. S., Wels, M., Bron, P.A., & Kleerebezem, M. (2012). Impact of 4 *Lactobacillus plantarum* capsular polysaccharide clusters on surface glycan composition and host cell signaling. *Microbial Cell Factories*, 11(1), 149.
- Ruíz-Rodríguez, L., Bleckwedel, J., Eugenia Ortiz, M., Pescuma, M., & Mozzi, F. (2017). Lactic acid bacteria. pp. 395-451. En: Wittman, C. & Liao, J.C. (Eds). *Industrial Biotechnology: Microorganisms*, Wiley VCH, Verlag GmbH & Co. KGaA, Weinheim, Alemania.
- Sánchez, A., Rodríguez, R., Coton, M., Coton, E., Herrero, M., García, L. A., & Díaz, M. (2010). Population dynamics of lactic acid bacteria during spontaneous malolactic fermentation in industrial cider. *Food Research International*, 43(8), 2101-2107.
- Schleifer, K. H. (2009). Phylum XIII. Firmicutes Gibbons and Murray 1978, 5 (Firmacutes [sic] Gibbons and Murray 1978, 5). pp. 19-1317. En: *Bergey's Manual® of Systematic Bacteriology*, Springer, New York.
- Shiratori-Takano, H., Akita, K., Yamada, K., Itoh, T., Sugihara, T., Beppu, T., & Ueda, K. (2014). Description of *Symbiobacterium ostreiconchae* sp. nov., *Symbiobacterium turbinis* sp. nov. and *Symbiobacterium terraclitae* sp. nov., isolated from shellfish, emended description of the genus *Symbiobacterium* and

- proposal of *Symbiobacteriaceae* fam. nov. *International Journal of Systematic and Evolutionary Microbiology*, 64(10), 3375-3383.
- Stinglele, F., Neeser, J. R., & Mollet, B. (1996). Identification and characterization of the *eps* (exopolysaccharide) gene cluster from *Streptococcus thermophilus* Sfi6. *Journal of Bacteriology*, 178(6), 1680-1690.
- Suárez, B., Bedriñana, R., Tascón, N., Simón, A., & Madrera, R. (2007). Yeast species associated with the spontaneous fermentation of cider. *Food Microbiology*, 24(1), 25-31.
- Swoboda, J. G., Campbell, J., Meredith, T. C., & Walker, S. (2010). Wall teichoic acid function, biosynthesis, and inhibition. *ChemBiochem*, 11(1), 35-45.
- Tieking, M., Korakli, M., Ehrmann, M. A., Gänzle, M. G., & Vogel, R. F. (2003). *In situ* production of exopolysaccharides during sourdough fermentation by cereal and intestinal isolates of lactic acid bacteria. *Appl. Environ. Microbiol.*, 69(2), 945-952.
- Tieking, M., Kaditzky, S., Valcheva, R., Korakli, M., Vogel, R. F., & Gänzle, M. G. (2005). Extracellular homopolysaccharides and oligosaccharides from intestinal lactobacilli. *Journal of Applied Microbiology*, 99(3), 692-702.
- Toniolo, C., Balducci, E., Romano, M. R., Proietti, D., Ferlenghi, I., Grandi, G., Berti, F., Margarit, I., & Janulczyk, R. (2015). *Streptococcus agalactiae* capsule polymer length and attachment is determined by the proteins CpsABCD. *Journal of Biological Chemistry*, jbc-M114.
- Torino, M. I., de Valdez, G. F., & Mozzi, F. (2015). Biopolymers from lactic acid bacteria. Novel applications in foods and beverages. *Frontiers in Microbiology*, 6, 834.
- Tripathi, P., Beaussart, A., Andre, G., Rolain, T., Lebeer, S., Vanderleyden, J., Hols, P., & Dufrêne, Y. F. (2012). Towards a nanoscale view of lactic acid bacteria. *Micron*, 43(12), 1323-1330.
- Velasco, S. E., Yebra, M. J., Monedero, V., Ibarburu, I., Dueñas, M. T., & Irastorza, A. (2007). Influence of the carbohydrate source on β -glucan production and enzyme activities involved in sugar metabolism in *Pediococcus parvulus* 2.6. *International Journal of Food Microbiology*, 115(3), 325-334.
- Vitlic, A., Sadiq, S., Ahmed, H. I., Ale, E. C., Binetti, A. G., Collett, A., Humpreys, P.N., & Laws, A. P. (2019). Isolation and characterization of a high molecular mass β -glucan from *Lactobacillus fermentum* Lf2 and evaluation of its immunomodulatory activity. *Carbohydrate Research*, 476, 44-52.

- Von Wright, A., & Axelsson, L. (2012). Lactic acid bacteria: an introduction. pp. 1-17. En: Lahtinen, S., Ouwehand, A. C., Salminen, S. & von Wright, A. (Eds.), *Lactic Acid Bacteria, Microbiological and functional aspects*. CRC Press, Taylor & Francis Group, Parma, Italia.
- Vos, P., Garrity, G., Jones, D., Krieg, N. R., Ludwig, W., Rainey, F. A., Schleifer, K.H., & Whitman, W. (Eds.). (2011). *Bergey's Manual of Systematic Bacteriology: The Firmicutes*. pp. 474. (Vol. 3). Springer Science & Business Media, Athens, USA.
- De Vuyst, L., & Degeest, B. (1999). Heteropolysaccharides from lactic acid bacteria. *FEMS Microbiology Reviews*, 23(2), 153-177.
- De Vuyst, L., De Vin, F., Vanielingem, F., & Degeest, B. (2001). Recent developments in the biosynthesis and applications of heteropolysaccharides from lactic acid bacteria. *International Dairy Journal*, 11(9), 687-707.
- Wang, K., Li, W., Rui, X., Chen, X., Jiang, M., & Dong, M. (2014). Characterization of a novel exopolysaccharide with antitumor activity from *Lactobacillus plantarum* 70810. *International Journal of Biological Macromolecules*, 63, 133-139.
- Weiss, N., Schillinger, U., & Kandler, O. (1983). *Lactobacillus lactis*, *Lactobacillus leichmannii* and *Lactobacillus bulgaricus*, subjective synonyms of *Lactobacillus delbrueckii*, and description of *Lactobacillus delbrueckii* subsp. *lactis* comb. nov. and *Lactobacillus delbrueckii* subsp. *bulgaricus* comb. nov. *Systematic and Applied Microbiology*, 4(4), 552–557.
- Werning, M. L., Ibarburu, I., Dueñas, M. T., Irastorza, A., Navas, J., & López, P. (2006). *Pediococcus parvulus* *gtf* gene encoding the GTF glycosyltransferase and its application for specific PCR detection of β -D-glucan-producing bacteria in foods and beverages. *Journal of Food Protection*, 69(1), 161-169.
- Werning, M. L., Notararigo, S., Nácher, M., de Palencia, P. F., Aznar, R., & López, P. (2012). Biosynthesis, purification and biotechnological use of exopolysaccharides produced by lactic acid bacteria. Capítulo 5 en: *Food Additive*, pp. 83-114. Ed. El-Samragi, I. Intech-Open Science.
- Whiting, G. C., & Carr, J. G. (1957). Chlorogenic acid metabolism in cider fermentation. *Nature*, 180, 1479.
- Zannini, E., Waters, D. M., Coffey, A., & Arendt, E. K. (2016). Production, properties, and industrial food application of lactic acid bacteria-derived exopolysaccharides. *Applied Microbiology and Biotechnology*, 100(3), 1121-1135.

- Zarour, K., Llamas, M. G., Prieto, A., Rúas-Madiedo, P., Dueñas, M. T., Fernández de Palencia, P., Aznar, R., Kihal, M., & López, P. (2017). Rheology and bioactivity of high molecular weight dextrans synthesised by lactic acid bacteria. *Carbohydrate Polymers*.
- Zeidan, A. A., Poulsen, V. K., Janzen, T., Buldo, P., Derkx, P. M., Øregaard, G., & Neves, A. R. (2017). Polysaccharide production by lactic acid bacteria: from genes to industrial applications. *FEMS Microbiology Reviews*, fux017.
- Zhang, H., & Cai, Y. (Eds.)(2014). Lactic acid bacteria, fundamentals and practice. Springer Berlin Heidelberg, Nueva York, EEUU.

1. Identificación de cepas de bacterias lácticas aisladas de sidra natural y descripción de la especie *Lactobacillus sicerae*

1. INTRODUCCIÓN

La fermentación del mosto de manzana es un complejo proceso microbiológico donde actúan levaduras, bacterias lácticas y bacterias acéticas. En la sidra natural del País Vasco, después de la fermentación maloláctica no se lleva a cabo ningún proceso de estabilización antes del embotellado, salvo si el enólogo o el productor detectan alguna alteración organoléptica.

Las BAL constituyen la microbiota predominante de la sidra madura, y en ocasiones son responsables de producir defectos organolépticos en el producto, como son: (i) el “carácter Brett”, que es consecuencia de la alteración del contenido polifenólico y de la aparición de fenoles volátiles que ocasionan olores desagradables en la bebida (Buron et al., 2012); (ii) el amargor o picado acroleínico, causado por la presencia de acroleína, que proviene directamente del 3-hidroxiacetaldehído, compuesto producido durante el metabolismo del glicerol (Garai-Ibabe et al., 2008); (iii) la producción de aminas biógenas (Garai-Ibabe et al., 2007); y (iv) la alteración más común en sidra es el ahilado, que es la consecuencia de la producción de exopolisacáridos (EPS) por algunas especies de bacterias del género *Lactobacillus* (Dueñas et al., 1995; Dueñas et al., 1998), *Pediococcus parvulus* (Dueñas-Chasco et al., 1997) y *Oenococcus oeni* (Ibarburu et al., 2007). La síntesis de EPS ocasiona un incremento de la consistencia de la bebida, por lo que es rechazada por los consumidores.

El objetivo de este capítulo fue el estudio de los *Lactobacillus* productores de EPS aislados de sidra natural ahilada del País Vasco, y pertenecientes a la colección CUPV. Se abordó la identificación y la diferenciación genotípica de 41 aislados recogidos entre los años 1992 y 2009, que permitió realizar el seguimiento de la incidencia de sus especies como organismos alterantes en la bebida. Los resultados obtenidos permitieron la descripción de la nueva especie *Lactobacillus sicerae* y se asignó como cepa tipo el aislado CUPV261^T(=CECT8227^T). Los resultados de este capítulo se recogen en las publicaciones Puertas et al., (2014) y Puertas et al., (2018).

2. MATERIAL Y MÉTODOS

2.1 Cepas bacterianas y condiciones de cultivo.

En este trabajo se han utilizado 41 cepas de *Lactobacillus sp.* aislados de sidra natural guipuzcoana alterada (Puertas et al., 2018). Sus nombres, origen y año del aislamiento se recogen en la Tabla 1.1. Algunas de estas estirpes fueron previamente caracterizadas, y son: *L. diolivorans* G77 (CUPV218) (Dueñas et al., 1998); *L. suebicus* (CUPV221, CUPV225 y CUPV226) (Garai-Ibabe et al., 2010b; Notararigo et al., 2013; Ibarburu et al., 2015); y *L. sicerae* (CUPV261^T y CUPV262) (Puertas et al., 2014, este trabajo de tesis). Además, con fines comparativos se incluyeron 12 cepas de referencia de 11 especies diferentes de *Lactobacillus sp.* (a parte de *L. sicerae*).

Los aislamientos se realizaron entre los años 1992 y 2009 a partir de sidra ahilada procedente de diferentes sidrerías. Los lactobacilos incluidos en este estudio fueron seleccionados en base a su fenotipo *ropy*, mostrando la formación de largos hilos o filamentos al tocar la colonia con el asa de siembra, y una apariencia viscosa al ser cultivados en caldo MRS (Figura 1.1). Las bacterias se cultivaron en medio MRS (Anexo I), durante 48 h y a 28 °C, en una estufa de incubación de CO₂ 5 % (v/v) y se conservaron congeladas a -80 °C en el mismo medio de cultivo suplementado con glicerol 20 % (v/v).

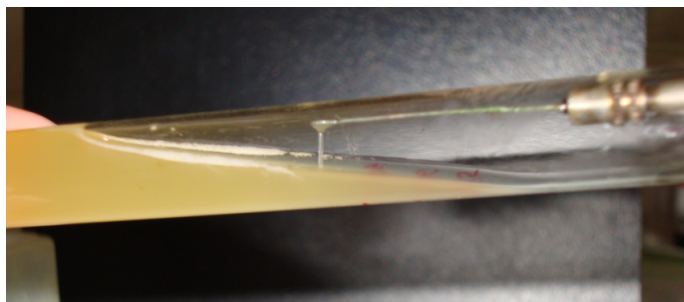


Figura 1.1. Imagen de un cultivo con fenotipo *ropy*.

Tabla 1.1. Cepas utilizadas en este estudio.

Especie	Colección	Origen	Sidrería de procedencia	Año de aislamiento
<i>Lactobacillus brevis</i> CECT 4121 ^T	CECT	Heces humanas		
<i>L. collinoides</i>				
CECT 922 ^T	CECT	Zumo de manzana fermentado		
CUPV238, CUPV239, CUPV2311, CUPV2312, CUPV2371	EE	Sidra ahilada	D	2009
CUPV236	CUPV	Sidra	K	2003
CUPV231, CUPV232, CUPV234, CUPV235, CUPV2119, CUPV2328	CUPV	Sidra alterada	G	2000
CUPV2313, CUPV2315	EE	Sidra ahilada	H	2009
CUPV2317, CUPV2320, CUPV2322, CUPV2323, CUPV2324	EE	Sidra ahilada	I	2009
<i>L. diolivorans</i>				
LMG19667 ^T	LMG	Ensilado de maíz		
CUPV213	CUPV	Sidra ahilada	A	1992
CUPV211, CUPV219, CUPV2112	CUPV	Sidra	B	1992
CUPV212, CUPV214, CUPV215, CUPV216, CUPV217, CUPV218= ^a G77, CUPV2110, CUPV2111, CUPV2113	CUPV	Sidra ahilada	C	1992
CUPV2117, CUPV2118	CUPV	Sidra alterada	E	2003
CUPV2114, CUPV2115	CUPV	Sidra	K	2003
<i>L. hilgardii</i> CECT 4786 ^T	CECT	Vino		
<i>L. mali</i> CECT 4149	CECT	Mosto de uva		
<i>L. paracollinoides</i> CECT 5926, DSM15502 ^T	CECT DSMZ	Industria cervecera		
<i>L. satsumensis</i> CECT 7371 ^T	CECT	Mosto de uva		
<i>L. sicerae</i> ^a CUPV 261 ^T =CECT 8227 ^T , ^d CUPV 262	EE	Sidra ahilada	F	2009
<i>L. suebicus</i>				
CECT 5917 ^T	CECT	Manzana triturada		
^c CUPV225	CUPV	Sidra ahilada	E	2003
^b CUPV221	CUPV	Sidra ahilada	F	2003
^c CUPV226	CUPV	Sidra ahilada	J	2003
<i>L. uvarum</i> CECT 7335 ^T	CECT	Mosto de uva		
<i>L. vini</i> CECT 5924 ^T	CECT	Mosto de uva fermentado		

CUPV, Colección de cultivos de la Universidad del País Vasco UPV/EHU; CECT, Colección Española de Cultivos Tipo (Universidad de Valencia, Burjassot); DSMZ, Leibniz Institute DSMZ-German Collection of Microorganisms and Cell Cultures (Braunschweig, Alemania); LMG, BCCM/LMG Belgian Coordinated Collection of Microorganism (Bruselas, Bélgica). EE (=Este estudio), cepas estudiadas durante este trabajo y procedentes de la colección CUPV. (a) Dueñas-Chasco et al., 1998; (b) Garai-Ibabe et al., 2010b; (c) Ibarburu et al., 2015; (d) Puertas et al., 2014.

2.2 Caracterización fenotípica de las BAL aisladas de sidra

Para realizar una caracterización fenotípica de los aislados, se utilizaron diferentes pruebas de acuerdo a los criterios establecidos en el *Bergey's Manual of Systematics of Archaea and Bacteria* (Whitman, 2015).

2.2.1 Características fenotípicas de los aislados

Para elaborar una descripción de la morfología de las colonias, cada bacteria se creció en el medio MRS-agar (Anexo I) a 28 °C, en una atmósfera con el 5 % (v/v) de CO₂ y durante 48 h.

Para la determinación de la actividad catalasa, se depositó una gota de una solución de H₂O₂ al 10 % (v/v) sobre una colonia crecida en el medio MRS-agar. Se observó la formación de burbujas (O₂), que indicaría un resultado positivo.

La producción de gas carbónico a partir de glucosa y gluconato se determinó mediante el cultivo de los aislados en caldo MRS, sin extracto de carne y suplementado con un 2 % (p/v) del carbohidrato. Para observar la formación de gas, se introdujeron campanas Durham en los cultivos y se incubaron a 28 °C, durante 7-10 días (Mañes-Lázaro et al., 2008).

Para las pruebas de fermentación de diferentes carbohidratos, se utilizó el test comercial API 50CH (bioMérieux). A partir de un cultivo realizado en el medio MRS e incubado durante 24 h, se recogieron las células por centrifugación (15.680 × g, 2 min) y se lavaron dos veces con solución Ringer®. Se preparó un inóculo con una densidad óptica a 600 nm (DO₆₀₀) de 0,6 en el medio API 50CHL (Anexo I) para ser introducido en cada galería. Los cultivos se cubrieron con una gota de aceite de vaselina estéril y se incubaron a 28 °C durante 48 h. Una vez finalizado el tiempo de incubación se anotaron los cambios de color.

Para detectar la capacidad de producir fenotipo *ropy* a partir de glucosa, fructosa, sacarosa, lactosa, galactosa, maltosa, rafinosa, manitol, sorbitol, trehalosa, xilosa o ramnosa, las bacterias se cultivaron en 5 mL del medio MRS suplementado con el indicador de pH rojo de clorofenol (Anexo I). Los medios fueron inoculados a una DO₆₀₀ del orden de 0,6, y se incubaron durante 7 días a 28 °C. Diariamente se anotaron los cambios de color. Para la detectar la capacidad de producción de

dextrano a partir de sacarosa, se realizaron cultivos en MRS-agar donde la glucosa fue reemplazada por un 5 % (p/v) de sacarosa.

2.2.2 Cuantificación de sustratos y productos de fermentación

Para realizar el estudio del metabolismo de carbohidratos, los diferentes aislados fueron cultivados en el medio semidefinido MSD (Anexo I). El medio fresco se inoculó con células procedentes de un cultivo en el medio MRS y lavadas dos veces con solución Ringer® (15.680 × g, 10 min), para obtener una DO₆₀₀ inicial de 0,2. Los cultivos se incubaron durante 65 h, a 28 °C y en atmósfera con un 5 % (v/v) de CO₂. Posteriormente, se centrifugaron (15.680 × g, 30 min y 20 °C), y los sobrenadantes se filtraron en un filtro de acetato de celulosa, con un diámetro de poro de 0,2 µm. Las concentraciones de glucosa, ácido láctico, ácido L-málico, etanol y ácido acético, se determinaron mediante un sistema de HPLC, con 20 µL de volumen de inyección. Este sistema estaba compuesto por dos columnas de intercambio iónico Aminex HPX-87H (Bio-Rad) y termostalizadas a 65 °C. Como fase móvil se empleó una solución de H₂SO₄ 5 mM, a una velocidad de flujo de 0,6 mL min⁻¹ (Palmfeldt et al., 2004). El equipo estaba dotado de un detector de índice de refracción (IR) y otro de ultravioleta-visible (UV-Vis) a una longitud de onda de 210 nm.

Para la determinación del ácido L-láctico se utilizó el kit enzimático *L-LACTATE ACID* (Biosystems), siguiendo las instrucciones indicadas por el fabricante.

2.2.3 Composición celular de ácidos grasos

Los análisis de la composición celular de ácidos grasos se llevaron a cabo mediante el protocolo descrito por Lucena et al. (2012b), y se realizaron bajo la dirección del profesor David R. Arahal de la Universidad de Valencia, en la Colección Española de Cultivos Tipo.

2.3 Microscopía electrónica de transmisión

La preparación de la muestra y las fotografías se realizaron en los servicios generales de la UPV/EHU, SGIKER, y su visualización se realizó mediante las siguientes técnicas:

Tinción negativa

Para la preparación de la muestra, se utilizó un rejilla de cobre recubierta de carbono (AGAR S-160-3) y sometida a una descarga eléctrica en vacío (*glow discharge*) que provoca una conversión hidrófila temporal. En la rejilla se depositaron 10 μ L de cultivo y se mantuvieron a temperatura ambiente durante 1 min. A continuación, se retiró el exceso de muestra con papel Whatman, y se depositaron 10 μ L de una solución de acetato de uranilo 2 %. Transcurridos 30 s, se retiró el exceso de acetato de uranilo con papel de filtro y se dejó secar a temperatura ambiente. Las muestras se visualizaron en un microscopio electrónico de transmisión Philips CM120 BioTwin. Las imágenes se capturaron con una cámara digital (Modelo Morada, Olympus SIS).

Crio-Microscopía electrónica de transmisión

Las bacterias fueron vitrificadas y visualizadas mediante crio-microscopía electrónica de transmisión. Para ello, una gota de un cultivo bacteriano crecido en el medio MRS durante 48 h, fue vitrificada por congelación rápida en etano líquido mediante un dispositivo Vitrobot Markt IV (FEI) y automatizado para la vitrificación (congelación por inmersión) de muestras acuosas. La muestra se transfirió a través de una bomba 655 Turbo Pumping Station (Gatan) a un 626 DH Single Tilt Liquid Nitrogen Cryo-holder (Gatan), donde se mantuvo en torno a -180 °C. La rejilla de cobre (300 mesh Quantifoils) se hidrofilió mediante un tratamiento de *glow discharge*. La muestra se examinó en un microscopio electrónico de transmisión, TECNAI G2 20 TWIN (FEI), bajo un voltaje de 200 KeV en el modo de imagen de campo luminoso y de dosis baja.

2.4 Aislamiento y cuantificación del EPS

2.4.1 Producción de EPS en el medio semidefinido

Para el aislamiento y la cuantificación del EPS producido en el medio semidefinido MSD (Anexo I), las bacterias se cultivaron tal y como se describe en el apartado 2.2.2. El EPS contenido en el sobrenadante se precipitó con 3 volúmenes de etanol frío, a 4 °C y durante 2 días. El EPS se recuperó por centrifugación (15.680 × g, 4 °C, 10 min) y se realizaron dos lavados con etanol al 70 %. Posteriormente, el EPS se recolectó por centrifugación, se resuspendió en agua ultrapura y se dializó en una membrana de un diámetro de poro de 3,5 kDa (Medicell, International, Ltd.). La membrana permaneció en agitación durante 72 h, y se realizaron dos cambios diarios de agua. El contenido de la membrana se congeló a –80 °C y se liofilizó.

La cuantificación del EPS en el medio de cultivo se llevó a cabo en 0,5 mL del sobrenadante libre de células y por triplicado. El EPS se precipitó añadiendo tres volúmenes de etanol frío al 99 % (v/v), y se mantuvo a 4 °C durante toda la noche. Posteriormente, las muestras se centrifugaron (32.967 × g, 15 min y 4 °C) y el precipitado se resuspendió en agua destilada, para volver a ser precipitado con 3 volúmenes de etanol frío. Este proceso se repitió tres veces, y el precipitado final se secó en una estufa a 40 °C para eliminar los restos de etanol. Finalmente, el EPS desecado se resuspendió en 0,6 mL de agua ultrapura. Para la cuantificación del EPS se utilizó el método del fenol-sulfúrico (F-S) descrito por Dubois et al. (1956), utilizando la D-glucosa como estándar (Figura 1.2). Aplicando este método, el azúcar se transforma fundamentalmente en hidroximetilfurfural o furfural, y la solución adopta una coloración anaranjada. La reacción se llevó a cabo en un tubo de vidrio al cual se añadió 0,5 mL de la suspensión de EPS y 0,5 mL de fenol 5 % (v/v), se mezcló mediante vórtex y se añadieron 2,5 mL de ácido sulfúrico 95,5 % (v/v). La mezcla se agitó y se incubó en un baño a 100 °C durante 5 min. Finalizado este tiempo, los tubos se enfriaron en un baño de hielo antes de medir la absorbancia a 490 nm (A_{490}). Para obtener la concentración del EPS de las muestras, los datos de absorbancia obtenidos se compararon con la curva de calibrado que se muestra en la Figura 1.2, y se multiplicaron por el factor de dilución 1,2.

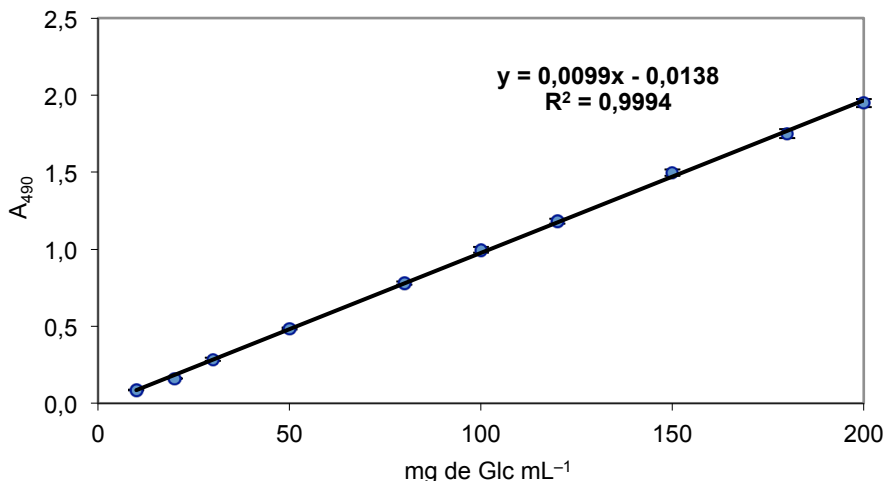


Figura 1.2. Curva de calibrado para la cuantificación de la concentración de EPS utilizando glucosa como estándar. Esta curva fue realizada mediante el método espectrofotométrico del fenol-sulfúrico descrito por Dubois et al. (1956).

2.4.2 Aislamiento del EPS a partir de biomasa

Las bacterias se cultivaron en placas de MRS-agar inoculadas con 10^7 - 10^8 UFC mL⁻¹, y se incubaron durante 6 días, a 28 °C y en una atmósfera con un 5 % (v/v) de CO₂. Las colonias se recogieron con un asa de siembra y se depositaron en un matraz que contenía agua ultrapura estéril. La suspensión se homogeneizó y se añadió un volumen de NaOH 2 M, permaneciendo en agitación suave durante toda la noche. Posteriormente, el contenido del matraz se centrifugó ($15.680 \times g$, 5 min), y el EPS contenido en el sobrenadante se precipitó con 2 volúmenes de etanol frío (99,9 %, v/v), a 4 °C y durante 2 días. El EPS se recogió por centrifugación ($15.680 \times g$, 4 °C, 10 min) y se resuspendió en agua ultrapura. Para eliminar las proteínas y los restos celulares se añadió ácido tricloroacético 80 % (v/v) hasta alcanzar una concentración final del 12 % (v/v), y se mantuvo en agitación suave a 4 °C durante 30 min. La muestra se centrifugó ($15.680 \times g$, 4 °C, 10 min) y posteriormente se descartó el precipitado. El EPS en suspensión se precipitó con dos volúmenes de etanol frío y se centrifugó. Finalmente, la muestra se dializó con una membrana de un diámetro de poro de 3,5 kDa (Medicell, International, Ltd.), con dos cambios diarios de agua y durante 72 h. Finalizada la diálisis, el contenido de la membrana se congeló y se liofilizó.

2.5 Determinación del tamaño de los EPS por HPSEC

Se determinó el peso molecular (M_w), la polidispersidad (IP, parámetro que refleja cómo es la distribución de pesos moleculares de cada fracción, $IP = M_w/M_n$), el número de fracciones que componen el EPS y el porcentaje relativo de cada una. Para ello, se suspendieron 1,5 mg de EPS (apartados 2.4.1 y 2.4.2) en 2 mL de eluyente (NaNO_3 0,1 M y NaN_3 0,02 % (p/v), pH 7), se centrifugó ($15.680 \times g$, 2 min) y el sobrenadante se filtró ($0,2 \mu\text{m}$) para su análisis mediante HPLC. Se analizaron 100 μL de muestra en un equipo Agilent 1100 Series (Hewlett-Packard, Germany), equipado con un detector de índice de refracción. Para la separación de las fracciones se utilizaron 3 columnas de cromatografía de exclusión molecular PL-aquagel-OH 40, 50 y 60 ($15 \mu\text{m}$, Agilent Technologies) más una columna de guarda PL-aquagel-OH ($8 \mu\text{m}$, Agilent Technologies), termostalizadas a 35°C . El flujo utilizado en el ensayo fue de $0,8 \text{ mL min}^{-1}$ y con una duración del método de 50 min. Los resultados obtenidos se compararon con la curva de calibrado mostrada en la Figura 1.3, que fue elaborada utilizando patrones de dextrano comercial con los siguientes pesos moleculares (Sigma-Aldrich): 1, 5, 12, 50, 80, 150, 270, 410, 670, 1400 y 2000 kDa. Para el tratamiento de los datos se utilizó el programa informático ChemStation (for LC 3D systems, Rev. B.04.03 [16], Agilent), en combinación con ChemStation GPC (Rev. B.01.01). Para la detección de contaminantes (proteínas) se utilizó un detector DAD a una longitud de onda de 280 nm.

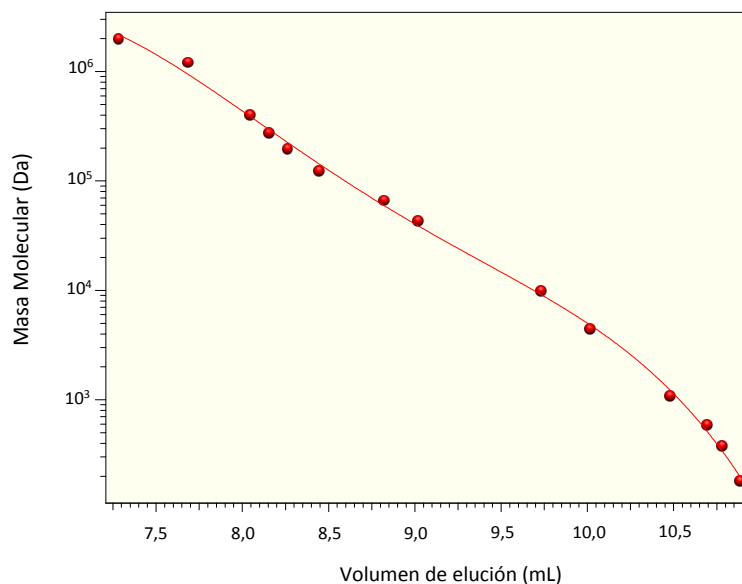


Figura 1.3. Curva de calibrado construida con patrones de dextrano comercial. $R^2 = 0.999$.

2.6 Identificación y caracterización genotípica

2.6.1 Extracción del DNA

La purificación del DNA cromosómico se realizó mediante el kit comercial DNeasy[®] Blood & Tissue (Qiagen) utilizando el protocolo descrito para bacterias Gram-positivas. Para ello, las células de 1 mL de cultivo bacteriano se recogieron por centrifugación ($17.159 \times g$, 10 min), y se suspendieron en 180 μL de solución de lisis enzimática suplementada con lisozima 30 mg mL^{-1} y mutanolisina $2 \text{ U } \mu\text{L}^{-1}$ (Anexo I). La mezcla de lisis se mantuvo a 37°C durante 30 min, y se continuó siguiendo las instrucciones descritas en el manual del fabricante.

La concentración del DNA se determinó mediante electroforesis en un gel teñido con bromuro de etidio, comparando las intensidades de las bandas obtenidas en las muestras con las halladas en el marcador λ DNA Hind III (Promega). Para ello, 1 μL de la muestra del DNA se mezcló con 2 μL de tampón de carga (Anexo I) y 8 μL de agua ultrapura. La mezcla se introdujo en un pocillo del gel (agarosa 0,8 % (p/v) en tampón TAE (Anexo I), y bromuro de etidio $0,2 \mu\text{g mL}^{-1}$), el cual fue sometido a un voltaje de 100 V, durante 60 min. Tras la migración del DNA, las bandas se visualizaron por exposición a luz ultravioleta, y se analizaron en un dispositivo GelDoc (BioRad) utilizando el programa informático Image Lab[™] 3.0.1 (Beta 2). Finalmente, las muestras del DNA se ajustaron a una concentración de $40 \text{ ng } \mu\text{L}^{-1}$ con agua ultrapura.

2.6.2 Identificación de las cepas mediante secuenciación génica

La identificación de las BAL aisladas de sidra de la campaña del 2009 se realizó mediante la amplificación parcial del gen rRNA 16S por PCR. Se emplearon los oligonucleótidos 616V ($5' \text{-AGA GTT TGA TYM TGG CTC AG-3'}$, T_m $55,3^\circ\text{C}$) y 699R ($5' \text{-RGG GTT GCG CTC GTT-3'}$, T_m $51,9^\circ\text{C}$) (Arahal et al., 2008; Ehrman et al., 2003) y se obtuvieron fragmentos del orden de 1000 pb. La mezcla de reacción se preparó en 50 μL y contenía: 1x del tampón de PCR, 100 μM de cada dNTP (dATP, dCTP, dTTP y dGTP), MgCl_2 0,5 mM, 2 μM de cada cebador, 1 U de DNA polimerasa de alta fidelidad Phusion[®] (Thermo Scientific[™]) y 200 ng de DNA diana. Se utilizaron las siguientes condiciones: una etapa de desnaturalización de 5 min a 95°C ; 35 ciclos de 1 min a 95°C , 1 min a 55°C y 30 s a 72°C ; y una extensión final de 10 min a 72°C .

Cuando fue necesario la amplificación completa del gen, se utilizaron los cebadores 616V y 630R (5'-CAK AAA GGA GGT GAT CC-3'), y el cebador interno 699R (Ehrman et al., 2003).

La identificación de las cepas aisladas en los años 1992, 2000 y 2003 había sido llevada a cabo previamente por el personal del laboratorio. Para ello, se amplificó un fragmento de 530 pb del gen rRNA 16S mediante PCR, con los cebadores PA (5'-AGA GTT TGA TCC TGG CTC AG-3') y UP1R (5'-TAC CGC GGC TGC TGG CAC-3'). La mezcla de reacción se preparó en 50 μ L, y estaba compuesta por: 1x del tampón de PCR, 200 μ M de cada dNTP, $MgCl_2$ 1,5 mM, 0,5 μ M de cada cebador, 2,5 U de Taq DNA polimerasa (Sigma) y 5 μ L de DNA diana. Se utilizaron las siguientes condiciones: una primera etapa de desnaturalización de 5 min a 94 °C, 25 ciclos de 1 min a 94 °C, 1 min a 55 °C y 2 min a 72 °C y una etapa final de 10 min a 72 °C.

Los productos de la PCR se visualizaron mediante una electroforesis en un gel de agarosa 0,8 % (p/v) en tampón TAE (Anexo I) y teñido con bromuro de etidio 0,2 μ g mL⁻¹, al cual se le aplicó un voltaje de 100 V durante 40 min. Las bandas de DNA se documentaron en un equipo GelDoc (Bio-Rad) y se analizaron con el programa Image LabTM 3.0.1 (Beta 2), utilizando para la estimación del peso molecular el marcador 1 Kb Plus DNA (Invitrogen).

La banda con el peso molecular esperado se extrajo del gel y se purificó utilizando el kit comercial QIAquick Gel Extraction (Qiagen), para su posterior secuenciación en la Unidad de Secuenciación y Genotipado (SGIKER, Universidad del País Vasco UPV/EHU).

Las secuencias de los amplímeros se compararon con las secuencias de rRNA 16S depositadas en las bases de datos del NCBI (National Center for Biotechnology Information) mediante el algoritmo BLASTn (<https://BLAST.ncbi.nlm.nih.gov/BLAST.cgi>), y con la base de datos EzBioCloud mediante EzTaxon (<http://www.ezbiocloud.net/eztaxon>) (Kim et al., 2012). Las secuencias correspondientes a *L. sicerae* CUPV261^T se analizaron adicionalmente utilizando el paquete de programas de ARB (Ludwig et al., 2004; <http://www.arb-home.de>) con métodos de árbol alternativos (matriz de máxima parsimonia, máxima verosimilitud y distancia) y subconjuntos de datos. Los alineamientos automatizados de las secuencias se corrigieron manualmente utilizando el editor de secuencias ARB_EDIT, y también se usaron como referencias los alineamientos recuperados de SILVA y las últimas actualizaciones de LTP (Pruesse et al., 2007; Yarza et al., 2010).

La secuencia del gen rRNA 16S de CUPV261^T fue depositada en la base de datos del NCBI con el número de acceso (*Reference Sequence*, RS) HG794492. Los datos de la secuencia cruda del genoma generados en este estudio para esta cepa, están disponibles públicamente en el depósito de lectura de secuencia de archivo (SRA) bajo el número de acceso del estudio PRJEB5073 y del ejercicio ERR385820.

2.6.3 Tipificación

Para el genotipado de los aislados, se combinaron 4 perfiles RAPD-PCR (*Random Amplified Polymorphic DNA-PCR*) con los cebadores M13 (5'-GAA ACA GCT ATG ACC ATG-3') (Pinto et al., 2005), M13V (5'-GTT TTC CCA GTC ACG AC-3') (Ehrman et al., 2003), P1 (5'-ACG CGC CCT-3') y P2 (5'-ATG TAA CGC C-3') (Simpson et al., 2002). Además, en este análisis también se tuvo en cuenta la amplificación de la región ISR 16S-23S, obtenida con la pareja de cebadores LA2-ITSMR (5'-GTT CTC GGC TTA ATT ACT G-3') y LA2-16S1F (5'-CAC CCA AAG TCG GTT CGG-3') para diferenciar entre *L. collinoides* y *L. paracollinoides* (Suzuki et al., 2004). Las amplificaciones y electroforesis se realizaron por duplicado.

La mezcla de reacción se preparó en 50 μ L, y estaba compuesta por: 1x del tampón de PCR, 200 μ M de cada dNTP (Takara Bio), $MgCl_2$ 5 mM, 1 U de DNA polimerasa KAPA (KapaBiosystems), 200 ng de DNA diana, y un cebador por reacción a una concentración de: 5 μ M de M13, 2 μ M de M13V, 1 μ M de P1 o de P2. Las condiciones para la amplificación con cada cebador fueron las siguientes:

- M13: un ciclo de 5 min a 94 °C, 5 min a 40 °C y 5 min a 72 °C; 33 ciclos de 20 s a 94 °C, 30 s a 45 °C, y 45 s a 72 °C.
- P1 o P2: 5 min a 94 °C, 5 min a 40 °C y 5 min a 72 °C; 33 ciclos de 1 min a 94 °C, 1 min a 40 °C y 1 min a 72 °C.
- M13V: 3 ciclos de 3 min a 94 °C, 3 min a 40 °C y 5 min a 72 °C; 35 ciclos de 1 min a 94 °C, 1,5 min a 55 °C y 3 min a 72 °C.

Para la obtención del perfil de bandas RAPD-PCR, las electroforesis se realizaron con 20 μ L de cada amplificado y 2 μ L de tampón de carga (Anexo I), en un gel de agarosa 1,9 % (p/v) en tampón TAE y con bromuro de etidio (0,2 μ g mL⁻¹). Se

aplicó un voltaje de 80 V durante 90 min, y en el caso de M13V de 90 V durante 75 min.

En la amplificación con la pareja de cebadores LA2-16S1F & LA2-ITSMR, se utilizó una mezcla de PCR compuesta por: 1x tampón de PCR, 200 μM de cada dNTP, 0,2 μM de cada cebador, 1 U de Ex Taq polimerasa (Takara) y 200 ng de DNA muestra. Las condiciones para la amplificación fueron las siguientes: una etapa de desnaturalización de 2,5 min a 94 °C; seguida de 35 ciclos de 54 s a 94 °C, 1,5 min a 52 °C, y 2 min a 72 °C. Los productos de la PCR se visualizaron mediante una electroforesis en un gel de agarosa 1,5 % (p/v) en tampón TAE y con bromuro de etidio 0,2 $\mu\text{g mL}^{-1}$, al cual se le aplicó un voltaje de 90 V durante 60 min.

Para facilitar el análisis y la asignación del peso molecular a las bandas obtenidas en cada carril y para cada aislado, los geles de electroforesis se prepararon intercalando cada cinco pocillos con muestra, un pocillo con el marcador 1 Kb Plus DNA Ladder (Invitrogen). Éstos se visualizaron y se digitalizaron utilizando un equipo GelDoc y el programa Image LabTM 3.0.1 (Beta 2) (Bio-Rad), y se almacenaron como archivos Tiff. Para el análisis de genotipado se empleó el programa informático Bionumerics 2.5 (Applied Maths), mediante el cual se combinaron y se compararon los diferentes perfiles de bandas obtenidos a partir de los diferentes aislados de sidra y de las cepas de referencia (Tabla 1.1). Para ello, se utilizó el coeficiente de Pearson y se realizó un análisis de agrupamiento con el algoritmo UPGMA (*Unweighted Pair Group Method With Arithmetic Averages* (Sneath & Sokal, 1973).

2.6.4 ANI (Average Nucleotide Identity)

El análisis ANI se realizó a partir de una pirosecuenciación parcial al azar del genoma de CUPV261^T (Lucena et al., 2012a) utilizando un secuenciador GS-Junior (Roche) en el Servicio Central de Soporte a la investigación Experimental (SCSIE) de la Universidad de Valencia. Para ello se utilizó DNA extraído con el kit comercial Real Pure kit (Durviz S.L., Roche) con el fin de incrementar el rendimiento total de las lecturas. Se obtuvieron 1,73 Mb (978 *contigs*), que representan un 66 % del tamaño estimado genoma. El cálculo del ANI de acuerdo al MUMmer (ANIm) y a BLAST (ANIB) entre *Lactobacillus vini* DSM 20605^T (AHYZ01000001-AHYZ01000220) y los datos ensamblados de CUPV261^T, se llevó a cabo en JSpecies tal y como se describe en Richter & Rosselló-Móra (2009) y en las referencias citadas en él.

El valor predictivo de hibridación DNA-DNA (DDH) se obtuvo a partir de BLAST+ y la fórmula recomendada (identidades/máxima puntuación de la longitud de las secuencias apareadas) del programa “genome-to-genome distance” (GGDC2.0). Se considera que dos cepas pertenecen a la misma especie si este valor es igual o superior al 70 % (Meier-Kolthoff et al., 2013).

3. RESULTADOS

Los 41 aislados con fenotipo *ropy* incluidos en este estudio forman parte de la colección de la Universidad del País Vasco UPV/EHU (CUPV), y fueron aislados de sidra natural guipuzcoana con la alteración del ahilado (Tabla 1.1). De todas las estirpes, 6 habían sido previamente identificadas y 35 corresponden con aislados de las campañas 1992, 2000, 2003 y 2009.

3.1 Caracterización de los aislados del año 2009

A partir de 4 botellas de sidra alterada procedentes de la campaña de 2009 se seleccionaron 14 aislados y se incluyeron en este estudio. Todos ellos presentaron morfología bacilar, con células dispuestas en cadenas, formando parejas o en solitario. Doce mostraron un metabolismo heterofermentativo, y los aislados CUPV261^T y CUPV262 un metabolismo homofermentativo estricto (no forman gas a partir de glucosa y no utilizan el gluconato de sodio). Las enzimas lactato deshidrogenasa (LDH) de las cepas homofermentativas producen una mezcla racémica de D:L-lactato con un ratio de 1:0,85 para CUPV261^T y 1:0,78 en el caso de CUPV262. Además, se estudió la capacidad de cada cepa para utilizar diferentes azúcares mediante el kit comercial API® CH (bioMérieux), y los resultados obtenidos se muestran en la Tabla 1.2.

3.1.1 Crecimiento y estudio del metabolismo

Los 14 aislados se cultivaron en el medio MSD suplementado con ácido L-málico (Tabla 1.3). Finalizadas las fermentaciones, las cepas CUPV261^T, CUPV262 y CUPV2371 mostraron los valores de DO₆₀₀ más altos, y en el resto se observaron dificultades para su crecimiento en este medio semidefinido. Las cepas CUPV261^T y CUPV262 presentaron un metabolismo homoláctico con una transformación de la glucosa a lactato. En los demás aislados se observó un metabolismo heteroláctico con una producción mayoritaria de lactato y acetato. Por otro lado, las 14 estirpes realizaron la fermentación maloláctica (transformación del ácido L-málico a L-láctico), y solo en las fermentaciones de tres aislados se consumieron más de 4 g L⁻¹ de este compuesto.

Tabla 1.2. Resultados de las pruebas API® CH (bioMérieux).

Cepa	L-Arabinosa	D-Ribosa	D-Xilosa	Metil-β-D-Xilopiranosido	D-Galactosa	D-Glucosa	D-Fructosa	D-Manosa	Metil-α-D-manopiranosido	Metil-α-D- glucopiranosido	N-Acetilglucosamina	Arbutina	Salicina	D-Maltosa	D-Lactosa	D-Melibiosa	D-Sacarosa	D-Trehalosa	D-Turanosa	D-Tagatosa	D-Arabitól	D-Rafinosa	2-ceto-gluconato potásico	5-ceto-gluconato potásico	LDH
CUPV261 ¹					+	+	+	+	+			+	+	w	+		+	w		+					DL
262					+	+	+	+	+			+	+	w			+	+		+					DL
238	+	+	+		+	+	+	+	+	+	w	+	+	+	+	+	+		w	+			+		
239	+	+	+		+	+	+	+		+	+		+	+		+	+		w				+		
2311	+	+	+		+	+	+	+	+	+	+	+	+	+		+	+		w	+			+		
2312	+	+	+		+	+	+			+	w			+		+							+		
2371	+	+	+		+	+	+				w		+	+		+							+		
2313	+	+	+		+	+				+	+	w		+		+	w		w				+	w	
2315	+	+	+		+	+				+	+			+		+	w		w				w		
2317	+	+	+		+	+	+			+	+	w		+		+	+		+				+		
2320	+	+	+		+	+				+	+			+		+	w		w				+		
2322	+	+	+	+	+	+	+			+	+			+		+	+		+				+	+	
2323	+	+	+		+	+				+	+			+		+	w		w				+		
2324	+	+	+		+	+				+	+			+		+	w		w				+		
<i>L. collinoides</i>	+	+	+		w	+	+				w			w		w								w	
<i>L. suebicus</i>	+	+	+	+		+															+				
<i>L. diolivorans</i>	+	+	+	+	+	+	+							+		+					+	+		+	

(+) fermentan; (w) viraje débil; (LDH) lactato deshidrogenasa. Los resultados de *L. collinoides*, *L. suebicus* y *L. diolivorans* corresponden al perfil fermentativo representativo de cada grupo de cepas previamente identificadas para cada especie de la colección CUPV.

3.1.2 Producción de exopolisacárido y determinación del peso molecular

Los 14 aislados se cultivaron en el medio MRS-agar, y sus colonias presentaron fenotipo *ropy* ya que formaron largos hilos o se desprendían completamente quedando adheridas al asa de siembra. Estas características indicaron una posible producción de exopolisacárido. Se descartó aislar el EPS a partir de cultivos realizados en caldo MRS, dado que algunos de sus componentes tales como el extracto de levadura presentan polisacáridos en su composición. Tras aplicar el protocolo de aislamiento del EPS a este medio fresco, se obtuvo un líofilo cuyo análisis mediante HPSEC mostró un pico de un peso molecular de 12,9 kDa con un índice de polidispersidad de 4,89.

Teniendo en cuenta estos resultados, las cepas se cultivaron en el medio semidefinido MSD. En éste solo manifestaron el fenotipo *ropy* los aislados CUPV261^T, CUPV262 y CUPV2371, y en sus sobrenadantes se cuantificaron entre 38 y 68 mg L⁻¹ de EPS (Tabla 1.3). Por este motivo las cepas se cultivaron en MRS-agar, y el EPS se aisló a partir de la biomasa, a excepción de CUPV262 (Tabla 1.3). El análisis de los EPS mediante HPSEC reveló la presencia de tres picos con diferente peso molecular, a excepción del producido por CUPV262: i) una fracción de alto peso molecular superior a 10³ kDa, ii) otra de peso molecular intermedio en torno a 10 kDa, y iii) una tercera de menor peso molecular cercana a 1 kDa. Las proporciones entre las fracciones variaron según la cepa, y en la mayoría de los EPS la fracción más abundante fue la de peso molecular intermedio, a excepción de los EPS procedentes de CUPV261^T y CUPV2311. Sin embargo, el EPS producido por CUPV262 estaba compuesto mayoritariamente por una fracción en torno a 10 kDa, y en él no se detectó la fracción de peso molecular superior.

Tabla 1.3. Estudio del perfil de fermentación de los aislados del año 2009 y peso molecular de los EPS.

Cepa	^a DO ₆₀₀	^a Glucosa (g L ⁻¹)	^a Malato (g L ⁻¹)	^a Lactato (g L ⁻¹)	^a Acetato (g L ⁻¹)	^a Etanol (g L ⁻¹)	^a pH _{final}	^a EPS (mg mL ⁻¹)	^b Mw (kDa)			Ratio
									×10 ³	×10	×1	
<i>L. siceræ</i>												
CUPV261 ^T	1,36±0,06	8,46±0,02	1,01±0,01	14,04±0,00	3,75±0,00	0,00±0,00	4,48	64,11±4,66	>2	1,69	4,99	4,9: 3,0: 2,0
262	1,72±0,06	10,42±0,01	1,63±0,03	10,67±0,03	3,82±0,00	0,00±0,00	4,21	68,69±3,65		^c 2,77	^c 4,1	^c 0,0: 3,0: 2,0
<i>L. collinoides</i>												
CUPV2371	1,13±0,07	10,47±0,01	0,00±0,00	6,33±0,01	5,14±0,00	1,70±0,01	4,88	37,98±2,75	1,07	1,95	4,35	1,6: 6,5: 1,8
238	0,37±0,01	17,02±0,02	1,04±0,00	2,89±0,01	4,88±0,00	0,03±0,01	5,44	7,91±3,97	1,22	1,93	4,85	3,6: 4,7: 1,6
239	0,33±0,01	17,85±0,02	1,33±0,60	2,75±0,01	4,83±0,01	0,02±0,00	5,52	7,14±1,95	>2	2,1	4,79	4,5: 4,6: 0,8
2311	0,28±0,01	17,76±0,08	2,90±0,03	2,44±0,01	4,39±0,01	0,09±0,13	5,66	8,28±3,83	1,76	2,07	4,93	5,0: 4,0: 1,0
2312	0,51±0,01	16,59±0,17	1,93±0,01	2,98±0,03	4,56±0,05	0,05±0,00	5,59	7,91±2,28	>2	2,05	5,13	3,6: 4,8: 1,6
2313	0,26±0,07	16,61±0,01	4,09±0,03	2,45±0,00	4,34±0,00	0,00±0,00	5,55	11,65±3,57	1,41	2,26	5,03	2,5: 6,5: 0,9
2315	0,45±0,03	17,78±0,02	3,08±0,01	3,03±0,06	4,76±0,00	0,01±0,01	5,60	10,84±3,08	1,58	2,01	4,74	2,1: 6,9: 1,0
2317	0,76±0,01	17,17±0,03	0,31±0,01	3,04±0,00	5,02±0,00	0,12±0,17	5,54	10,77±2,00	1,65	2,02	4,86	2,5: 6,3: 1,2
2320	0,44±0,05	16,31±0,05	0,36±0,04	3,03±0,00	4,83±0,00	0,07±0,01	5,43	10,91±3,12	1,21	2,02	4,96	3,2: 5,8: 1,0
2322	0,45±0,01	17,12±0,046	1,50±0,03	2,83±0,00	4,83±0,14	0,04±0,00	5,39	9,36±5,44	1,29	2,05	4,75	4,0: 5,0: 1,0
2323	0,49±0,05	16,08±0,01	2,69±0,01	2,85±0,00	4,43±0,01	0,07±0,00	5,56	8,72±2,28	1,36	2,02	4,81	3,8: 5,2: 1,0
2324	0,32±0,05	16,22±0,06	3,83±0,01	2,60±0,00	4,49±0,00	0,00±0,01	5,51	8,62±2,25	1,89	2	4,48	2,7: 6,5: 0,8
Medio MSD	-	20,85±0,03	4,46±0,03	0,00±0,00	3,70±0,00	0,00±0,00	5,50	2,77±2,43	-	-	-	-

(a) Datos procedentes de fermentaciones en el medio MSD durante 65 h. Los cultivos se realizaron por duplicado. Los resultados representan la media aritmética ± desviación estándar.

(b) EPS aislados a partir de biomasa.

(c) EPS aislado del sobrenadante de un cultivo en el medio MSD.

3.2 Identificación genotípica

Este estudio abarca 41 aislados (Tabla 1.1), de los cuales 4 fueron identificados previamente por nuestro grupo de investigación como *Lactobacillus diolivorans* CUPV218=G77, y *Lactobacillus suebicus* CUPV221, CUPV225 y CUPV226. Para la identificación de los 14 aislados procedentes del año 2009 se amplificó y se secuenció un fragmento del gen rRNA 16S de aproximadamente 1000 pb; el resto de las cepas (23) fueron identificadas de manera preliminar a partir del análisis de una secuencia parcial de unas 500 pb. Una vez comparada cada secuencia en la base de datos del NCBI, se observó que 35 aislados compartían una similitud superior al 98 % con las especies *L. diolivorans* (RS: HM218248.1) 16 aislados de los años 1992 y 2003) y *L. collinoides/paracollinoides* (19 de 2000, 2003 y 2009).

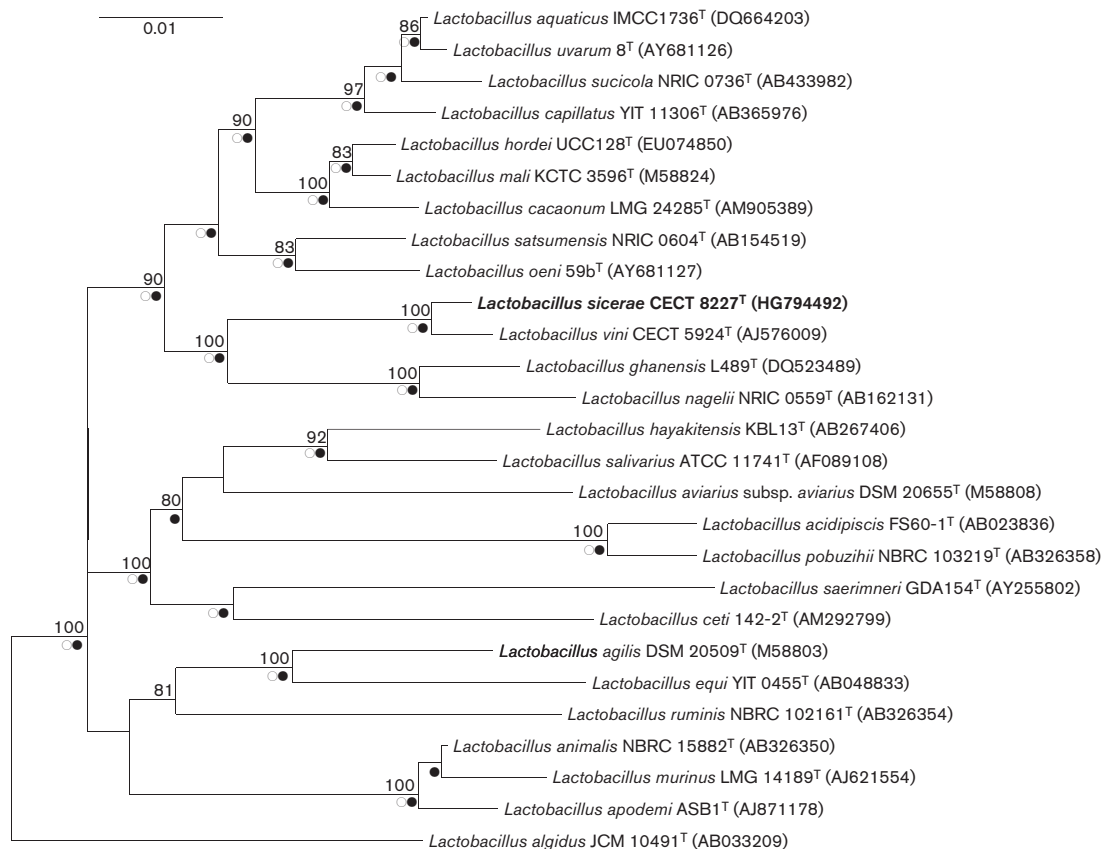


Figura 1.5. Árbol filogenético realizado a partir de la secuencia casi completa del gen rRNA 16S de la cepa CUPV261^T y con las especies estrechamente relacionadas. Las secuencias de referencia del NCBI o números de acceso del *GenBank* están indicados entre paréntesis. Los valores de confianza de *Bootstrap* >70 % se muestran en las ramificaciones (1000 re-muestrados). Los círculos blancos y los círculos negros indican nodos coincidentes en los árboles de máxima verosimilitud y máxima parsimonia, respectivamente. Barra de escala, 0,01 sustituciones por posición.

Para las estirpes CUPV261^T y CUPV262 aisladas en 2009, se obtuvo una secuencia parcial del gen rRNA 16S con una longitud de 1466 pb y fueron idénticas entre sí, por lo que para los resultados que se muestran a continuación nos referimos a la secuencia de la cepa CUPV261^T (RS: HG794492.1). El análisis comparativo realizado en Ez-Taxon mostró una similitud del 99,1 % con el gen rRNA 16S de *Lactobacillus vini* CECT 5924^T (NR_042196.1), del 96,4 % con el de *Lactobacillus satsumensis* NRIC 0604^T (NR_028658.1) y del 96,2 % con el de *Lactobacillus oeni* 59b (NR_043095.1). Además, la secuencia del gen rRNA 16S de CUPV261^T formó un par muy estable con la secuencia de *Lactobacillus vini* CECT 5924^T, y ambos con el par formado por las cepas tipo de *Lactobacillus ghaenensis* y *Lactobacillus nagelii* (Figura 1.5, Anexo II.I y II.II). Otras especies que aparecieron próximas con un alto nivel de confianza son: *Lactobacillus satsumensis*, *Lactobacillus oeni*, *Lactobacillus cacaonum*, *Lactobacillus mali*, *Lactobacillus hordei*, *Lactobacillus capillatus*, *Lactobacillus sucicola*, *Lactobacillus aquaticus* y *Lactobacillus uvarum*.

3.2.1 Genotipado de cepas

Muchas especies de BAL presentan similitudes elevadas entre sus genes rRNA 16S, p. ej., *L. collinoides* y *L. paracollinoides*, y por tanto una adecuada identificación requiere de otras pruebas adicionales.

Respecto a las estirpes CUPV261^T y CUPV262, el análisis comparativo de los perfiles RAPD realizados con los cebadores M13, P1 y P2, reveló un 83,17 % de similitud entre ellas (Figura 1.6 A), sugiriendo que pertenecen a la misma especie sin ser clones. Además, estos dos aislados se unieron a algunas cepas de referencia pertenecientes a las especies *Lactobacillus satsumensis*, *Lactobacillus nagelii*, *Lactobacillus vini* y *Lactobacillus uvarum* con un 20,51 % de similitud. Este valor confirmó que CUPV261^T y CUPV262 pertenecen a una especie diferente. El valor de correlación cofenética global calculado para el análisis general fue 92, indicando un buen nivel de fiabilidad.

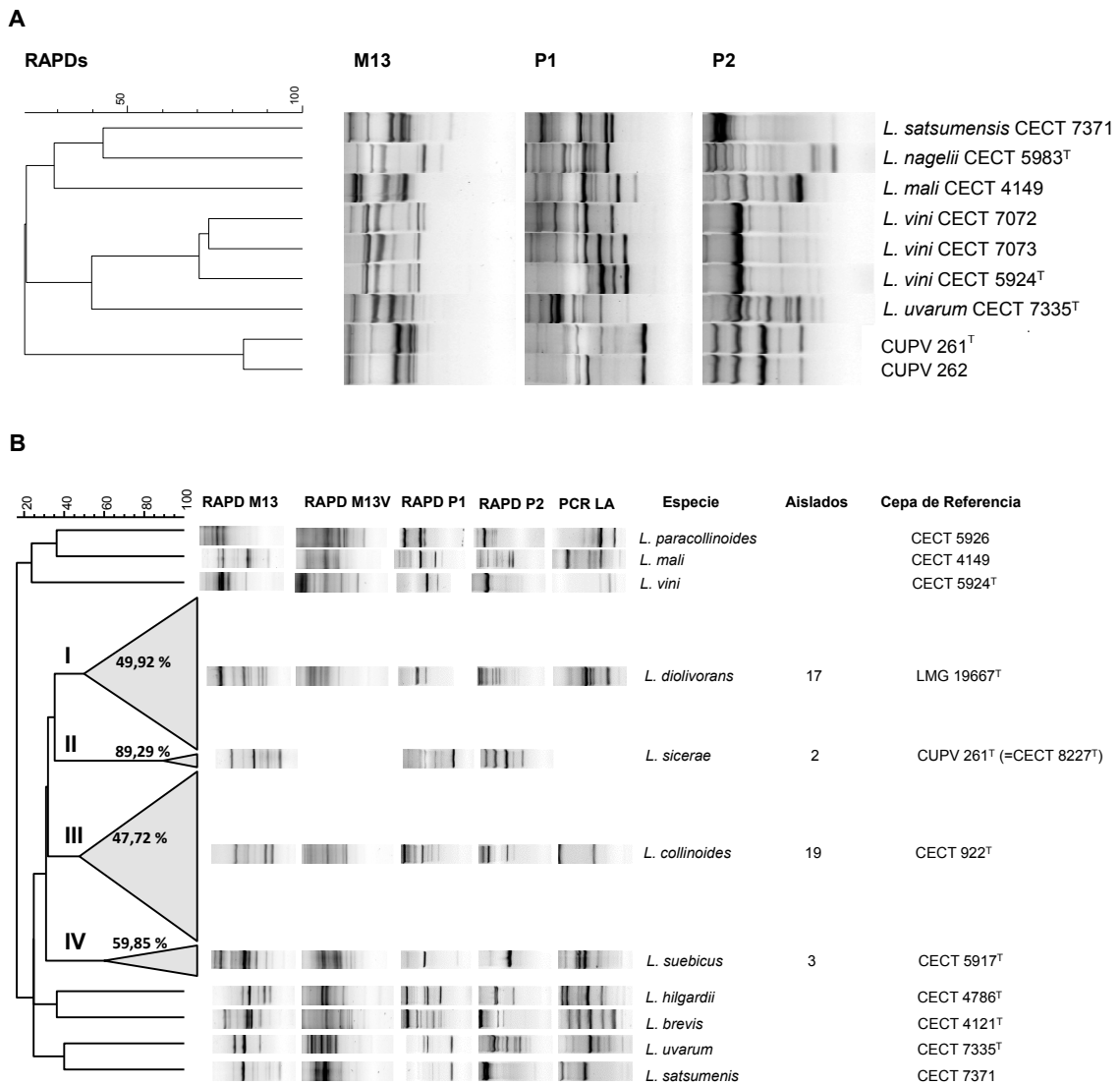


Figura 1.6. Dendrograma derivado del análisis de agrupamiento de UPGMA. A, dendrograma basado en la matriz de similitud combinada obtenida de los perfiles digitalizados RAPD M13, P1 y P2. Se muestran los patrones de banda procesados correspondientes a RAPD M13, P1 y P2 después de la conversión, normalización y sustracción del *background* (Puertas et al., 2014). **B**, dendrograma basado en la matriz de similitud combinada, obtenida a partir de los perfiles de la amplificación de la región ISR 16S-23S, los RAPD-PCR M13, P1, P2, M13V y los resultados API® CH (bioMérieux) de las cepas de *Lactobacillus sp.* estudiadas de la colección CUPV junto con las cepas de referencia. La escala indica el porcentaje de similitud. Los perfiles muestran las bandas representativas para cada *cluster* o especie. Los *clusters* están numerados.

Para el genotipado de los 41 aislados se tuvo en cuenta la combinación de los perfiles de la amplificación de la región ISR 16S-23S y los RAPD-PCR utilizando cuatro cebadores universales (M13, P1, P2, M13V), así como la sidrería de procedencia, el año de aislamiento y los resultados obtenidos en las pruebas bioquímicas API (Figura 1.6 B y Anexo II.III). Como se muestra en la Figura 1.6 B, la mayor diferenciación intraespecífica fue obtenida combinando los RAPD, ISR-PCR y

los perfiles API. En este análisis los aislados de sidra se diferenciaron en 4 grupos o *clusters* a un nivel de similitud del 50 %:

- El *cluster* I incluye 17 aislados junto con la cepa tipo *L. diolivorans* LMG19667^T, y este resultado confirma la identificación realizada mediante el análisis de la secuencia del gen rRNA 16S (99 % de similitud).
- El *cluster* II incluye las 2 cepas de *L. sicerae*.
- El *cluster* III agrupa 19 aislados junto con la cepa tipo *L. collinoides* CECT 922^T. Este resultado corrobora su pertenencia a esta especie, y además los perfiles ISR-PCR permitieron su diferenciación de la especie *L. paracollinoides*.
- El *cluster* IV agrupa a tres aislados junto con la cepa de referencia *L. suebicus* CECT 5917^T. Estas estirpes habían sido previamente identificadas como *L. suebicus*, y además CUPV225 y CUPV226 como productoras de heteropolisacárido, y CUPV221 como productora de β -glucano (Tabla 1.1)

El análisis de la diversidad intraespecífica realizada mediante RAPD mostró diferencias entre los aislados de *L. suebicus*, que fueron recogidos en diferentes sidrerías (Figura 1.7). Los aislados de *L. collinoides* se agruparon en tres grupos y separados de la cepa de referencia. Uno de ellos incluye dos cepas aisladas en el año 2000 y una en 2003, un segundo grupo compuesto por 11 cepas recogidas en el 2009, y un tercer grupo con 4 cepas del 2000 y una del 2009.

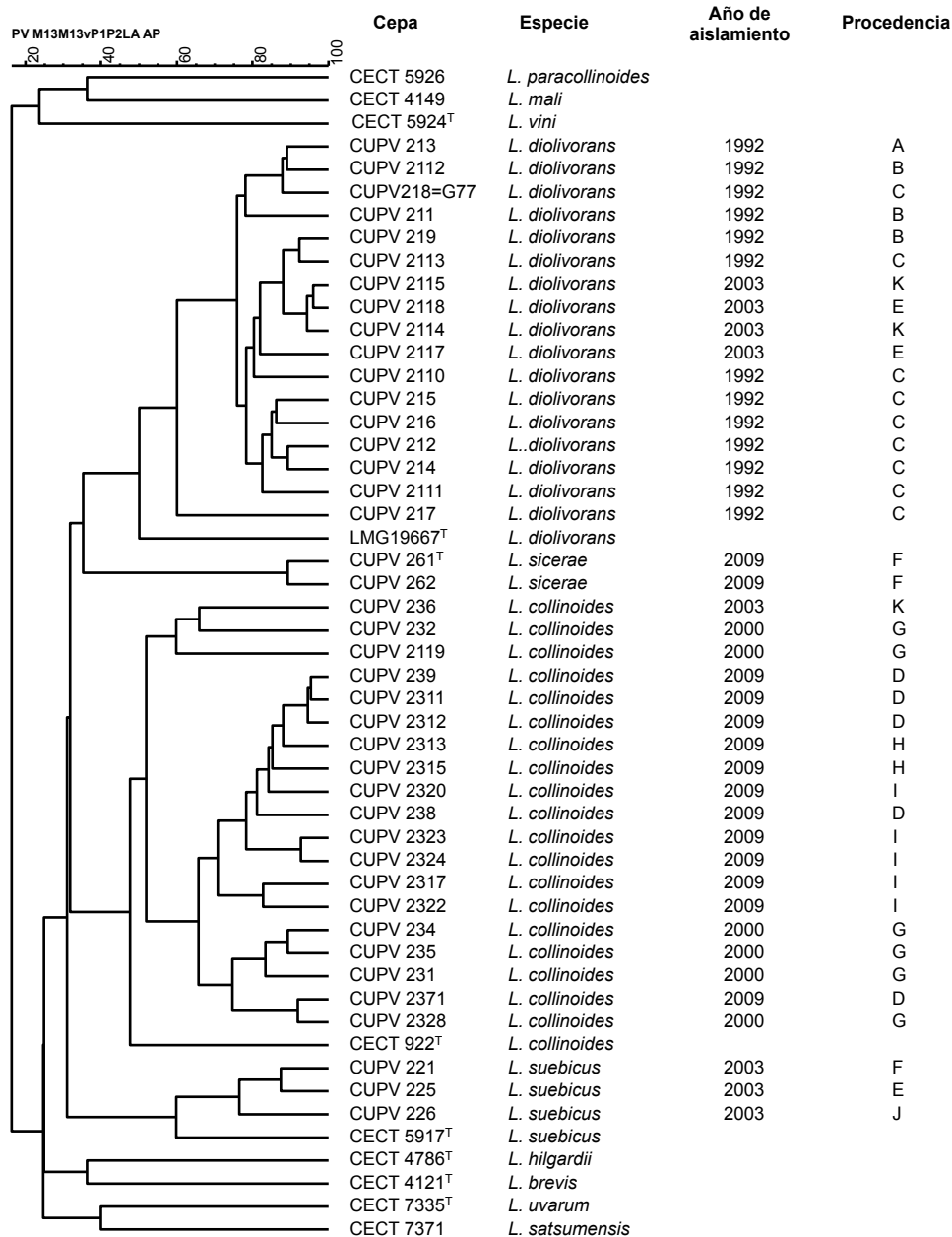


Figura 1.7. Dendrograma derivado del análisis de agrupamiento de UPGMA, basado en la matriz de similitud combinada, obtenida a partir de los perfiles de amplificación 16S-23S ISR y los resultados RAPD-PCR utilizando los 4 cebadores universales (M13, M13V, P1 y P2), junto con los resultados API® CH (bioMérieux), correspondientes con las cepas de *Lactobacillus sp.* productoras de EPS y de las cepas de referencia. Los perfiles con las bandas no se muestran. La escala mide el porcentaje de similitud. El dendrograma también incluye el año de aislamiento y la sidrería de donde fueron aislados.

3.3 Descripción de la especie *Lactobacillus sicerae*

Aunque los resultados de la huella genética RAPD fueron claros y situaron a las dos cepas CUPV261^T y CUPV262 alejadas genéticamente del resto de especies próximas, se quiso reforzar la evidencia genética de que la cepa CUPV261^T y la cepa tipo de *L. vini* pertenecen a especies diferentes, a pesar de compartir el 99,12 % de

similitud entre la secuencia de sus genes rRNA 16S. Para confirmar este resultado, se realizaron los siguientes ensayos adicionales, que dieron lugar a la descripción de la nueva especie *Lactobacillus sicerae* en el manuscrito de Puertas et al. (2014).

3.3.1 Análisis de identidad nucleotídica media ANI (*Average Nucleotide Identity*) y contenido en G+C

La determinación de la hibridación DNA-DNA (DDH) utilizada durante años para clasificar a una cepa dentro de un taxón determinado en especies procariontas, puede ser sustituida por una comparación entre genomas secuenciados de las cepas estudiadas, utilizando el promedio de la identidad entre nucleótidos (ANI) aplicado a un mínimo del 20 % del genoma secuenciado al azar (Richter & Roselló-Mora, 2009).

El cálculo de los parámetros del ensayo ANI se llevó a cabo utilizando las secuencias genómicas de CUPV261^T (66 % del tamaño estimado del genoma) y el genoma de *Lactobacillus vini* CECT 5924^T (AHYZ01000001–AHYZ01000220). Se obtuvieron los valores de 87,50-87,65 % para el índice ANI_b, y de 88,69-88,71 % para ANI_m. Se considera que dos cepas pertenecen a la misma especie si el valor del ANI es igual o superior al 95 %. Por lo tanto, ambos valores están muy por debajo del límite propuesto para la definición genómica de especies, permitiendo la diferenciación en dos especies diferentes. La misma conclusión se obtuvo a partir del valor predictivo de DDH, que fue del 37,7 %, muy por debajo del valor umbral del 70 %.

La secuencia parcial del genoma de CUPV261^T, también permitió la determinación de su contenido en G+C, el cual fue del 37,5 mol %.

3.3.2 Identificación fenotípica

Los cultivos de CUPV261^T y CUPV262 en caldo MRS presentaron una apariencia viscosa, y sus colonias crecidas en el medio MRS-agar mostraron el fenotipo *ropy*. Estas colonias presentaron una textura gomosa, de aspecto brillante, ligeramente convexas, a veces rodeadas por un halo, y con un diámetro de poco más de 1 mm (Figura 1.8 A). Mediante microscopía se observaron bacilos con unas dimensiones de $0,52 \pm 0,10 \times 2,71 \pm 0,72 \mu\text{m}$ (Figura 1.8 B), no esporulados, solitarios,

en parejas o en cadenas cortas, con un flagelo apical (Figura 1.8 D), y envueltos en una red de EPS (Figura 1.8 C).

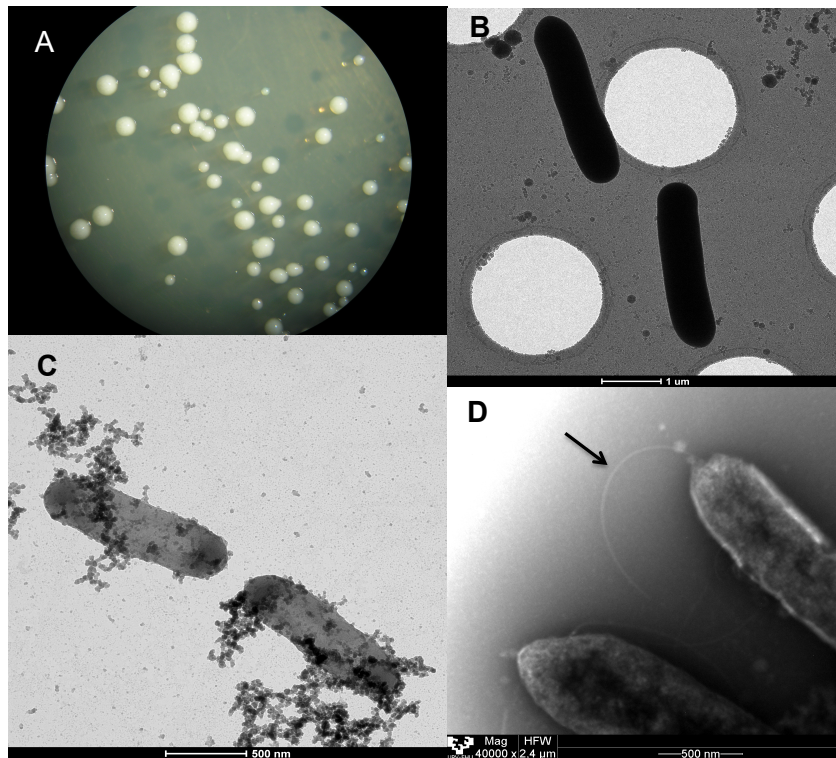


Figura 1.8. Microfotografías de la cepa CUPV261^T realizadas mediante diferentes técnicas: A, fotografía de colonias cultivadas en MRS-agar; **B,** microfotografía tomada mediante crio-TEM (barra de escala, 1 µm); **C y D,** microfotografía tomada mediante TEM a partir de una muestra sometida a una tinción con acetato de uranilo 2 % (barra de escala, 500 nm). La flecha indica el flagelo apical.

Para complementar el análisis genómico y diferenciar las cepas CUPV261^T y CUPV262 de las especies filogenéticamente cercanas, se realizaron las pruebas fenotípicas que se muestran en la Tabla 1.4. Las colonias cultivadas en MRS-sacarosa mostraron el fenotipo *ropy*, aunque no se observó un cambio en su apariencia respecto a las cultivadas en MRS-glucosa, lo que indicaría que no sintetizan dextrano.

Las cepas CUPV261^T y CUPV262 crecieron en el medio MRS a los valores de pH de 3,7, 4,5 y 8 (28 °C) y a las temperaturas de 15-45 °C, pero no a 5 °C (pH 5,5). Las células pudieron crecer y en el medio suplementado con un 10 % (v/v) de etanol, pero no lo hicieron con un 5 % (v/v) de NaCl. Así mismo, se cultivaron en el medio MSD, y los sobrenadantes se analizaron mediante HPLC. Estos aislados poseen un metabolismo homofermentativo estricto, con una producción exclusiva de ácido DL-láctico a partir de la glucosa, y además no utilizaron el gluconato de sodio. Son capaces de realizar la fermentación maloláctica, transformando el ácido L-málico en ácido L-láctico, y pueden consumir citrato.

Tabla 1.4. Características diferenciales de la cepa CUPV261^T y las cepas de las especies estrechamente relacionadas. 1, CUPV261^T; 2, *Lactobacillus vini* CECT 5924^T; 3, *Lactobacillus ghanensis* L489^T; 4, *Lactobacillus nagelii* CECT 5983^T; 5, *Lactobacillus satsumensis* CECT 7371; 6, *Lactobacillus oeni* CECT 7334^T; 7, *Lactobacillus uvarum* CECT 7335^T; y 8, *Lactobacillus mali* CECT 4149. Todos los datos proceden de este estudio, a excepción de los indicados. Todas las cepas son móviles, catalasa-negativa y producen ácido a partir de D-manosa. La cepa CUPV262 mostró el mismo resultado que CUPV261^T, a diferencia de la fermentación de la lactosa (negativo para CUPV262). +, positivo; -, negativo; w, débilmente positivo; ND, dato no disponible.

Característica	1	2	3 [†]	4	5	6	7	8
EPS a partir de sacarosa	+	-	-	+	+	+	+	+
Isómero del ácido láctico	DL	DL*	DL	DL [‡]	L [§]	L	L [¶]	L [#]
Crecimiento con/a:								
NaCl 5 %	-	+	ND	+	+	+	+	-
15 °C	+	-	w	+	+	+	ND	+
45 °C	+	+	+	+	+	+	ND	-
Producción de ácido a partir de:								
L-Arabinosa	-	+	-	-	-	-	-	-
D-Ribosa	-	+	-	+	-	-	-	-
D-Galactosa	+	-	+	+	+	-	-	-
L-Sorbosa	-	-	+	+	-	+	-	-
L-Ramnosa	-	-	+	+	-	-	-	-
D-Manitol	-	-	+	+	+	+	+	+
D-Sorbitol	-	-	-	+	+	+	-	+
Metil α-D-manopiranosido	+	-	ND	-	-	-	-	-
Metil α-D-glucopiranosido	-	-	-	+	+	+	+	-
N-Acetilglucosamina	-	+	+	+	w	+	w	+
Amigdalina	-	+	+	+	+	-	+	+
Citrato férrico de esculina	-	+	+	+	+	-	+	+
Celobiosa	-	+	+	+	+	-	+	+
Maltosa	w	+	-	+	-	-	-	+
Lactosa	+	-	-	-	-	-	-	+
Melibiosa	-	-	-	+	-	-	-	-
Melezitosa	-	-	-	-	-	-	-	+
β-Gentiobiosa	-	+	-	+	+	-	+	+
Turanosa	-	-	-	-	+	-	+	-
D-Tagatosa	+	-	-	+	+	-	-	-
D-Arabitol	-	+	ND	-	-	-	-	-
Contenido de G+C en el DNA (mol %)	37,5	39,4*	37,8	37,7 [†]	40,0 [§]	37,2	36,1 [¶]	32,5 [#]

Datos procedentes de: (*) Rodas et al. (2006); (†) Nielsen et al. (2007); (‡) Edwards et al. (2000); (§) Endo & Okada (2005); (||) Mañes-Lázaro et al. (2009); (¶) Mañes-Lázaro et al. (2008); (#) Kaneuchi et al. (1988).

Además, en las cepas CUPV261^T y CUPV262 y en las cepas tipo de las especies próximas filogenéticamente, se valoró la capacidad de fermentar diversos carbohidratos mediante la utilización de las galerías API® 50CH (Tabla 1.4). A diferencia de *L. vini* (la especie filogenéticamente más próxima), no fueron capaces de fermentar las pentosas. El crecimiento en el medio MRS-rojo de clorofenol provocó un aumento de la viscosidad en los medios suplementados con glucosa, trehalosa, fructosa y sacarosa, pero no con galactosa, maltosa o lactosa.

Los perfiles de ácidos grasos de las cepas CUPV261^T y *Lactobacillus vini* CECT 5924^T contenían los mismos ácidos grasos, pero con diferente abundancia relativa, permitiendo su diferenciación (Tabla 1.5). Las diferencias fueron más

acusadas para los ácidos grasos C_{16:0}, C_{19:1}^{ω7c}/C_{19:1}^{ω6c}, C_{18:1}^{ω9c} y C_{14:0}. Así mismo, la cepa CECT 5924^T contiene una fracción mayor de ácidos grasos saturados que CUPV261^T.

Tabla 1.6. Comparación del contenido de ácidos grasos celulares (%) de la cepa CUPV261^T y *Lactobacillus vini* CECT 5924^T (células crecidas en el medio MA, durante 48 h y a 28 °C).

Ácido graso celular	<i>Lactobacillus sicerae</i> CUPV261 ^T	<i>Lactobacillus vini</i> CECT 5924 ^T
<i>Saturados</i>		
C _{12:0}	1,1	1,0
C _{14:0}	5,3	10,0
C _{16:0}	12,4	26,4
C _{18:0}	2,8	2,0
<i>Insaturados</i>		
C _{18:1} ^{ω9c}	40,0	30,7
C _{16:1} ^{ω7c} /C _{16:1} ^{ω6c}	3,9	5,1
C _{19:1} ^{ω7c} /C _{19:1} ^{ω6c}	29,9	17,2
C _{18:1} ^{ω7c} /C _{18:1} ^{ω6c}	4,6	7,6

4. DISCUSIÓN

Los lactobacilos son microorganismos nutricionalmente muy exigentes y requieren medios complejos como el MRS para su cultivo. Algunas bacterias lácticas son capaces de producir exopolisacárido durante su crecimiento, lo que está relacionado con el fenotipo *ropy*. Su producción está influida por varios factores, tales como el pH, la temperatura y el contenido de compuestos nitrogenados en el medio de cultivo (Kimmel et al., 1998). Las 41 cepas incluidas en este estudio presentan el carácter *ropy* y pertenecen a la colección de la Universidad del País Vasco (CUPV). Todas ellas fueron aisladas de sidra natural ahilada, y producida en el País Vasco entre los años 1992 y 2009. Esta alteración está ocasionada por la presencia de exopolisacárido de origen bacteriano en la bebida (Dueñas et al., 1995).

La identificación de los aislados se realizó mediante la secuenciación parcial del gen rRNA 16S, y se apoyó en los resultados obtenidos en los agrupamientos realizados a partir de los perfiles de amplificación RAPD e ISR 16S-23S, debido a la elevada identidad encontrada entre los genes ribosomales 16S de especies próximas p. ej., *L. collinoides* y *L. paracollinoides* (Figura 1.6 B). Se concluyó que 19 de ellos pertenecen a la especie *Lactobacillus collinoides*; 17 cepas, a la especie *Lactobacillus diolivorans*, entre las que se encuentra la cepa G77, identificada como productora de α y β -glucano (Dueñas et al., 1998); y las 3 cepas ya identificadas como *L. suebicus* se agruparon con su cepa de referencia. *L. suebicus* CUPV225 y CUPV226 son estirpes productoras de heteropolisacárido (Ibarburu et al., 2015), y CUPV221 produce el homopolisacárido (1,3)(1,2)- β -D-glucano (Garai-Ibabe et al., 2010b). Los aislados CUPV261^T y CUPV262 con un metabolismo homofermentativo, se situaron en un mismo *cluster* y no se asociaron a una cepa de referencia, aunque su análisis filogenético basado en las secuencias del gen rRNA 16S mostró una similitud muy elevada con las cepas tipo de *Lactobacillus vini* (99,12%), seguida de *Lactobacillus satsumensis* (96,4 %) y *Lactobacillus oeni* (96,2 %). Además, se llevó a cabo una pirosecuenciación parcial del genoma la cepa CUPV261^T con el fin de compararlo con el genoma de *Lactobacillus vini* CECT 5924^T y calcular los índices ANI entre ellos. Estos resultados permitieron llegar a la conclusión de que las cepas CUPV261^T y CUPV262 representan una nueva especie del género *Lactobacillus*, y se propuso el nombre *Lactobacillus sicerae* sp. nov. La cepa tipo es CUPV261^T (=CECT 8227^T=KCTC 21012^T). Por otro lado, el análisis combinado de RAPD-PCR, ISR-PCR, el perfil de fermentación de carbohidratos, la sidrería de procedencia y el año de producción de la bebida, permitió la diferenciación intraespecífica de los aislados (Figura 1.7 y Anexo II.I).

Con respecto a la incidencia de las especies responsables de la alteración del ahilado en la sidra, se observó que en el año 1992 la especie alterante fue *Lactobacillus diolivorans*; en el 2000, *L. collinoides*; en 2003, *L. diolivorans*, *L. collinoides* y *L. suebicus*; y en 2009, *L. collinoides* y *L. sicerae*. Los aislados analizados fueron recogidos de sidras ahiladas bajo petición de las sidrerías, y únicamente la sidrería F fue muestreada en 2003 y 2009, y en este último año se recogieron los aislados de la nueva especie *Lactobacillus sicerae*. Por lo tanto, no hay posibilidad de conocer la incidencia de las especies de lactobacilos alterantes en cada sidrería. Sin embargo, *L. collinoides* y *L. diolivorans* fueron los aislados mayoritarios que se recogieron en tres y dos años, respectivamente. Estas dos especies frecuentemente se asocian con defectos organolépticos en la sidra, como es el amargor (Garai-Ibabe et al., 2008). Además, la especie *L. collinoides* se relaciona con la producción de fenoles volátiles (4-etilfenol, 4-etilguayacol y 4-etilcatecol) causantes del “carácter Brett” (Buron et al., 2012), y la producción de aminas biógenas en sidras (Coton et al., 2010; Garai-Ibabe et al., 2007).

Con respecto a las cepas aisladas en el año 2009, tanto las cepas heterofermentativas de la especie *L. collinoides*, como las estirpes homofermentativas obligadas de *L. sicerae*, realizaron la fermentación maloláctica. Esta transformación del ácido L-málico a ácido L-láctico es habitual en la sidra natural del País Vasco (Dueñas-Chasco et al., 1994; del Campo et al., 2008).

Los 14 aislados fueron seleccionadas debido a que presentaron fenotipo *ropy* cuando fueron cultivadas en el medio MRS. Debido a la interferencia de algunos componentes de este medio para la cuantificación y aislamiento de polisacárido, los aislados se cultivaron en el medio de cultivo semidefinido MSD, que fue utilizado previamente por nuestro grupo para determinar la producción de EPS por otros aislados de sidra (Dueñas-Chasco et al., 1997; Dueñas-Chasco, et al., 1998; Ibarburu et al., 2007; Ibarburu et al., 2015). Sin embargo, en este medio solo crecieron las estirpes *L. sicerae* CUPV261^T y CUPV262, y *L. collinoides* CUPV2371. La concentración del EPS encontrada en sus sobrenadantes fue de entre 35-70 mg L⁻¹ (Tabla 1.3), del orden de las producciones descritas para bacterias lácticas aisladas de vino (Dimopoulou, 2013), aunque inferiores a las observadas en estirpes aisladas de sidra de las especies *L. suebicus* (heteropolisacárido, 130 mg L⁻¹; Ibarburu et al., 2015) *Pediococcus parvulus* (β-D-glucano, 233 mg L⁻¹; Garai-Ibabe et al., 2010a) y *Lactobacillus mali* (dextrano, 11 g L⁻¹; Llamas-Arriba et al., 2019).

Por otro lado, los EPS producidos por las BAL presentan pesos moleculares de hasta 6×10^3 kDa (Vuyst & Degeest, 1999, Ruas-Madiedo et al., 2002), e incluso se han descrito homopolisacáridos que alcanzan los $4,4 \times 10^5$ kDa (Zarour et al., 2017). En el presente estudio, el análisis de las muestras del EPS aislado a partir de la biomasa de cultivos en medio MRS-agar de las cepas de *L. collinoides* y *L. sicerae*, reveló que estaban compuestos por tres fracciones con pesos moleculares del orden de 1, 10 y otra mayor de 10^3 kDa (Tabla 1.3). En general, la más abundante fue la fracción de peso molecular intermedio, y las proporciones entre unas y otras variaron dependiendo de la cepa. La presencia de varios polímeros en los EPS han sido también descrita en otros lactobacilos (Baruah et al., 2016; Ibarburu et al., 2015). Es también el caso de los aislados de sidra *L. diolivorans* G77 y *O. oeni* I₄, los cuales además de β -glucano, sintetizan (1,6)(1,2)- α -D-glucano (Dueñas et al. 1998), y dos heteropolisacáridos (Ibarburu et al., 2007), respectivamente. En vino, la producción de HePS y β -glucano ha sido descrita para estirpes de *O. oeni*, así como la síntesis de HoPS a partir de sacarosa (dextranos o levanos) (Dimopoulou et al., 2014; Dimopoulou et al., 2016). Estos autores mostraron que los EPS (HePS o dextranos) unidos a la célula ejercen un efecto protector durante la liofilización en cultivos iniciadores malolácticos de cepas de *O. oeni*, y sugirieron que estos EPS podrían ayudar a mejorar su supervivencia durante la producción y conservación.

5. CONCLUSIONES

En este estudio se ha realizado un profundo análisis del conjunto de *Lactobacillus* con fenotipo *ropy*, que fueron aislados de sidra natural ahilada del País Vasco, y pertenecientes a la colección de la Universidad del País Vasco. Se incluyeron un total de 41 aislados recogidos entre los años 1992 y 2009, y procedentes de diferentes sidrerías.

La identificación mediante el análisis combinado de la secuenciación parcial del gen ribosomal 16S, las características bioquímicas (API), RAPD-PCR utilizando cuatro cebadores universales (M13, M13V, P1 y P2) y los perfiles de amplificación ISR-PCR, reveló que las especies alterantes fueron *L. collinoides* (19), *L. diolivorans* (17), *L. suebicus* (3) y *L. sicerae* (2). La incidencia de estas especies varió en función del año de aislamiento, identificándose *L. diolivorans* como responsable de la alteración en el año 1992, *L. collinoides* en el 2000; éstas dos especies junto con *L. suebicus* en 2003; y *L. collinoides* y *L. sicerae* en 2009.

Los resultados de los análisis fenotípicos y genotípicos llevados a cabo en las cepas homofermentativas CUPV261^T y CUPV262, permitieron la descripción de una nueva especie del género *Lactobacillus*, y se propuso el nombre *Lactobacillus sicerae* sp. nov., cuya cepa tipo es CUPV261^T (=CECT 8227^T=KCTC 21012^T).

El estudio fenotípico de los 14 cepas de *Lactobacillus collinoides* y *Lactobacillus sicerae* procedentes del año 2009, mostró que son capaces de realizar la fermentación maloláctica. El análisis de sus EPS aislados a partir de la biomasa, reveló que estaban compuestos por tres fracciones con pesos moleculares del orden de 1, 10 y mayor de 10³ kDa. Finalmente, las estirpes *L. sicerae* CUPV261^T y CUPV262, y *L. collinoides* CUPV2371 fueron seleccionadas por presentar una producción de EPS superior al resto de cepas en el medio semidefinido MSD.

6. BIBLIOGRAFÍA

- Arahal, D. R., Sánchez, E., Macián, M. C., & Garay, E. (2008). Value of *recN* sequences for species identification and as a phylogenetic marker within the family “*Leuconostocaceae*”. *International Microbiology*, 11(1), 33–39.
- Baruah, R., Das, D., & Goyal, A. (2016). Heteropolysaccharides from lactic acid bacteria: current trends and applications. *Probiotics & Health*, 4(141), 2.
- Buron, N., Coton, M., Legendre, P., Ledauphin, J., Kientz-Bouchart, V., Guichard, H., Barillier, D. & Coton, E. (2012). Implications of *Lactobacillus collinoides* and *Brettanomyces/Dekkera anomala* in phenolic off-flavour defects of ciders. *International Journal of Food Microbiology*, 153(1), 159-165.
- del Campo, G., Berregi, I., Santos, J. I., Dueñas, M., & Irastorza, A. (2008). Development of alcoholic and malolactic fermentations in highly acidic and phenolic apple musts. *Bioresource Technology*, 99(8), 2857-2863.
- Coton, M., Romano, A., Spano, G., Ziegler, K., Vetrana, C., Desmarais, C., Lonvaud-Funel, A, Lucas, P., & Coton, E. (2010). Occurrence of biogenic amine-forming lactic acid bacteria in wine and cider. *Food Microbiology*, 27(8), 1078-1085.
- Cousin, F. J., Le Guellec, R., Schlusshuber, M., Dalmaso, M., Laplace, J. M., & Cretenet, M. (2017). Microorganisms in Fermented Apple Beverages: Current Knowledge and Future Directions. *Microorganisms*, 5(3), 39.
- Dimopoulou, M. (2013). *Les polysaccharides de la bactérie lactique Oenococcus oeni, de l'élucidation de leurs structures et voies de biosynthèse à leur valorisation technologique* (Doctoral dissertation, Bordeaux 2).
- Dimopoulou, M., Vuillemin, M., Campbell-Sills, H., Lucas, P.M., Ballestra, P., Miot-Sertier, C., Favier, M., Coulon, J., Moine, V., Doco, T., Roques, M., Williams, P., Petrel, M., Gontier, E., Moulis, C., Remaud-Simeon, M., & Dols-Lafargue, M., 2014. Exopolysaccharide (EPS) synthesis by *Oenococcus oeni*: from genes to phenotypes. *PLOS ONE* 9 (6) Article number e98898.
- Dimopoulou, M., Bardeau, T., Ramonet, P. Y., Miot-Certier, C., Claisse, O., Doco, T., Petrel, M., Lucas, P., & Dols-Lafargue, M. (2016). Exopolysaccharides produced by *Oenococcus oeni*: from genomic and phenotypic analysis to technological valorization. *Food Microbiology*, 53, 10-17.

- Dubois, M., Gilles, K. A., Hamilton, J. K., Rebers, P. A. T., & Smith, F. (1956). Colorimetric method for determination of sugars and related substances. *Analytical Chemistry*, 28(3), 350-356.
- Dueñas, M., Irastorza, A., Fernández, K., Bilbao, A., & Huerta, A. (1994). Microbial populations and malolactic fermentation of apple cider using traditional and modified methods. *Journal of Food Science*, 59(5), 1060–1064.
- Dueñas, M., Irastorza, A., Fernandez, K., & Bilbao, A. (1995). Heterofermentative lactobacilli causing ropiness in Basque Country ciders. *Journal of Food Protection*, 58(1), 76–80.
- Dueñas-Chasco, M. T., Rodríguez-Carvajal, M. A., Tejero Mateo, P., Franco-Rodríguez, G., Espartero, J. L., Irastorza-Iribas, A., & Gil-Serrano, A. M. (1997). Structural analysis of the exopolysaccharide produced by *Pediococcus damnosus* 2.6. *Carbohydrate Research*, 303(4), 453-458.
- Dueñas-Chasco, M. T., Rodríguez-Carvajal, M. A., Tejero-Mateo, P., Espartero, J. L., Irastorza-Iribas, A., & Gil-Serrano, A. M. (1998). Structural analysis of the exopolysaccharides produced by *Lactobacillus* spp. G-77. *Carbohydrate Research*, 307(1-2), 125–133.
- Edwards, C. G., Collins, M. D., Lawson, P. A., & Rodriguez, A. V. (2000). *Lactobacillus nagelii* sp. nov., an organism isolated from a partially fermented wine. *International Journal of Systematic Bacteriology*, 50(2), 699–702.
- Ehrmann, M. A., Müller, M. R., & Vogel, R. F. (2003). Molecular analysis of sourdough reveals *Lactobacillus mindensis* sp. nov. *International Journal of Systematic and Evolutionary Microbiology*, 53(1), 7-13.
- Endo, A., & Okada, S. (2005). *Lactobacillus satsumensis* sp. nov., isolated from mashes of shochu, a traditional Japanese distilled spirit made from fermented rice and other starchy materials. *International Journal of Systematic Bacteriology*, 55(1), 83-85.
- Garai, G., Dueñas, M. T., Irastorza, A. & Moreno-Arribas, M. V. (2007). Biogenic amine production by lactic acid bacteria isolated from cider. *Letters in Applied Microbiology*, 45(5), 473–478.
- Garai-Ibabe, G., Ibarburu, I., Berregi, I., Claisse, O., Lonvaud-Funel, A., Irastorza, A., & Dueñas, M. T. (2008). Glycerol metabolism and bitterness producing lactic acid bacteria in cidermaking. *International Journal of Food Microbiology*, 121(3), 253-261.

- Garai-Ibabe, G., Areizaga, J., Aznar, R., Elizaquivel, P., Prieto, A., Irastorza, A., & Dueñas, M. T. (2010a). Screening and selection of 2-branched (1, 3)- β -D-glucan producing lactic acid bacteria and exopolysaccharide characterization. *Journal of Agricultural and Food Chemistry*, *58*(10), 6149-6156.
- Garai-Ibabe, G., Dueñas, M. T., Irastorza, A., Sierra-Filardi, E., Werning, M. L., López, P., Corví, A. L., & De Palencia, P. F. (2010b). Naturally occurring 2-substituted (1, 3)- β -D-glucan producing *Lactobacillus suebicus* and *Pediococcus parvulus* strains with potential utility in the production of functional foods. *Bioresource Technology*, *101*(23), 9254-9263.
- Ibarburu, I., Soria-Díaz, M. E., Rodríguez-Carvajal, M. A., Velasco, S. E., Tejero-Mateo, P., Gil-Serrano, A. M., Irastorza, A., & Dueñas, M. T. (2007). Growth and exopolysaccharide (EPS) production by *Oenococcus oeni* I4 and structural characterization of their EPSs. *Journal of Applied Microbiology*, *103*(2), 477-486.
- Ibarburu, I., Puertas, A. I., Berregi, I., Rodríguez-Carvajal, M. A., Prieto, A., & Dueñas, M. T. (2015). Production and partial characterization of exopolysaccharides produced by two *Lactobacillus suebicus* strains isolated from cider. *International Journal of Food Microbiology*, *214*, 54-62.
- Kaneuchi, C., Seki, M., & Komagata, K. (1988). Taxonomic study of *Lactobacillus mali* Carr and Davis 1970 and related strains: validation of *Lactobacillus mali* Carr and Davis 1970 over *Lactobacillus yamanashiensis* Nomomura 1983. *International of Journal Systematic Bacteriology*, *38*(3), 269-272.
- Kim, O. S., Cho, Y. J., Lee, K., Yoon, S. H., Kim, M., Na, H., Park, S. C., Jeon, Y. S., Lee, J. H., Yi, H., Won, S., & Chun, J. (2012). Introducing EzTaxon-e: a prokaryotic 16S rRNA gene sequence database with phylotypes that represent uncultured species. *International Journal of Systematic and Evolutionary Microbiology*, *62*(3), 716-721.
- Kimmel, S. A., Roberts, R. F., & Ziegler, G. R. (1998). Optimization of exopolysaccharide production by *Lactobacillus delbrueckii* subsp. *bulgaricus* RR grown in a semidefined medium. *Applied and Environmental Microbiology*, *64*(2), 659-664.
- Llamas-Arriba, M. G., Puertas, A. I., Prieto, A., López, P., Cobos, M., Miranda, J. I., Marieta, C., Ruas-Madiedo, P., & Dueñas, M. T. (2019). Characterization of dextrans produced by *Lactobacillus mali* CUPV271 and *Leuconostoc carnosum* CUPV411. *Food Hydrocolloids*, *89*, 613-622.

- Lucena, T., Ruvira, M. A., Arahal, D. R., Macián, M. C., & Pujalte, M. J. (2012a). *Vibrio aestivus* sp. nov. and *Vibrio quintilis* sp. nov., related to Marisflavi and Gazogenes clades, respectively. *Systematic and Applied Microbiology*, 35(7), 427-431.
- Lucena, T., Pujalte, M. J., Ruvira, M. A., Garay, E., Macián, M. C., & Arahal, D. R. (2012b). *Tropicibacter multivorans* sp. nov., an aerobic alphaproteobacterium isolated from surface seawater. *International Journal of Systematic and Evolutionary Microbiology*, 62(4), 844-848.
- Ludwig, W., Strunk, O., Westram, R., Richter, L., Meier, H., Yadhukumar, Buchner, A., Lai, T., Steppi, S., Jobb, G., & other authors (2004). ARB: a software environment for sequence data. *Nucl Acids Res* 32(4), 1363-1371.
- Mañes-Lázaro, R., Ferrer, S., Roselló-Mora, R., & Pardo, I. (2008). *Lactobacillus uvarum* sp. nov. a new lactic acid bacterium isolated from a Spanish bobal grape must. *Systematic and Applied Microbiology*, 31(6-8), 425-433.
- Mañes-Lázaro, R., Ferrer, S., Roselló-Mora, R. & Pardo, I. (2009). *Lactobacillus oeni* sp. nov., from wine. *International Journal of Systematic and Evolutionary Microbiology*, 59(8), 2010–2014.
- Meier-Kolthoff, J. P., Auch, A. F., Klenk, H. P., & Göker, M. (2013). Genome sequence-based species delimitation with confidence intervals and improved distance functions. *BMC Bioinformatics*, 14(1), 60.
- Nielsen, D. S., Schillinger, U., Franz, C. M., Bresciani, J., Amoa-Awua, W., Holzapfel, W. H., & Jakobsen, M. (2007). *Lactobacillus ghanensis* sp. nov., a motile lactic acid bacterium isolated from Ghanaian cocoa fermentations. *International Journal of Systematic and Evolutionary Microbiology*, 57(7), 1468-1472.
- Notararigo, S., Náchter-Vázquez, M., Ibarburu, I., Werning, M. L., de Palencia, P. F., Dueñas, M. T., Aznar, R., López, P. & Prieto, A. (2013). Comparative analysis of production and purification of homo-and hetero-polysaccharides produced by lactic acid bacteria. *Carbohydrate Polymers*, 93(1), 57-64.
- Palmfeldt, J., Paese, M., Hahn-Hägerdal, B., & Van Niel, E. W. (2004). The pool of ADP and ATP regulates anaerobic product formation in resting cells of *Lactococcus lactis*. *Applied and Environmental Microbiology*, 70(9), 5477-5484.
- Pinto, B., Chenoll, E., & Aznar, R. (2005). Identification and typing of food-borne *Staphylococcus aureus* by PCR-based techniques. *Systematic and Applied Microbiology*, 28(4), 340-352.

- Pruesse, E., Quast, C., Knittel, K., Fuchs, B., Ludwig, W., Peplies, J., & Glöckner, F. O. (2007). SILVA: a comprehensive online resource for quality checked and aligned ribosomal RNA sequence data compatible with ARB. *Nucleic Acids Research*, 35(21), 7188-7196.
- Puertas, A. I., Arahál, D. R., Ibarburu, I., Elizaquível, P., Aznar, R., & Dueñas, M. T. (2014). *Lactobacillus sicerae* sp. nov., a lactic acid bacterium isolated from Spanish natural cider. *International Journal of Systematic and Evolutionary Microbiology*, 64(9), 2949-2955.
- Puertas, A. I., Ibarburu, I., Elizaquível, P., Zuriarrain, A., Berregi, I., López, P., Prieto, A., Aznar, R., & Dueñas, M. T. (2018). Disclosing diversity of exopolysaccharide-producing lactobacilli from Spanish natural ciders. *LWT*, 90, 469-474.
- Richter, M., & Rosselló-Móra, R. (2009). Shifting the genomic gold standard for the prokaryotic species definition. *Proceedings of the National Academy of Sciences*, 106(45), 19126-19131.
- Rodas, A. M., Chenoll, E., Macian, M. C., Ferrer, S., Pardo, I. & Aznar, R. (2006). *Lactobacillus vini* sp. nov., a wine lactic acid bacterium homofermentative for pentoses. *International Journal of Systematic and Evolutionary Microbiology*, 56(3), 513-517.
- Ruas-Madiedo, P., Hugenholtz, J., & Zoon, P. (2002). An overview of the functionality of exopolysaccharides produced by lactic acid bacteria. *International Dairy Journal*, 12(2-3), 163-171.
- Simpson, P. J., Stanton, C., Fitzgerald, G. F., & Ross, R. P. (2002). Genomic diversity within the genus *Pediococcus* as revealed by randomly amplified polymorphic DNA PCR and pulsed-field gel electrophoresis. *Applied and Environmental Microbiology*, 68(2), 765-771.
- Sneath, P. H. A., & Sokal, R. R. (1973). The principles and practice of numerical classification. *Numerical Taxonomy*, pp. 573.
- Suzuki, K., Funahashi, W., Koyanagi, M., & Yamashita, H. (2004). *Lactobacillus paracollinoides* sp. nov., isolated from brewery environments. *International Journal of Systematic and Evolutionary Microbiology*, 54(1), 115-117.
- Vuyst, L., & Degeest, B. (1999). Heteropolysaccharides from lactic acid bacteria. *FEMS Microbiology Reviews*, 23(2), 153-177.
- Whitman, W. B. (Ed.). (2015). *Bergey's manual of systematics of Archaea and Bacteria*. Wiley.

- Yarza, P., Ludwig, W., Euzéby, J., Amann, R., Schleifer, K. H., Glöckner, F. O., & Rossello-Mora, R. (2010). Update of the All-Species Living Tree Project based on 16S and 23S rRNA sequence analyses. *Systematic and Applied Microbiology*, 33(6), 291-299.
- Zarour, K., Llamas, M. G., Prieto, A., Rúas-Madiedo, P., Dueñas, M. T., de Palencia, P. F., & López, P. (2017). Rheology and bioactivity of high molecular weight dextrans synthesised by lactic acid bacteria. *Carbohydrate Polymers*, 174, 646-657.

2. Análisis *in silico* de los genes *eps* de *Lactobacillus collinoides* y
Lactobacillus sicerae

1. INTRODUCCIÓN

En el presente capítulo se describe el estudio realizado sobre la detección de genes implicados en la síntesis de exopolisacárido (HoPS y HePS) en las cepas de *L. collinoides* y *L. sicerae* procedentes de los aislamientos de 2009, y estudiadas en el capítulo 1. Los resultados obtenidos nos sugirieron que las cepas de *L. collinoides* y *L. sicerae* aisladas en la campaña 2009 sintetizan heteropolisacáridos. Así mismo, durante el desarrollo del presente trabajo, se aisló la cepa *L. collinoides* CUPV237 productora de exopolisacárido, que es un mutante espontáneo superproductor de riboflavina de la cepa *L. collinoides* CUPV2371 (ver detalles en capítulo 5). Con estos antecedentes, se seleccionaron las cepas *L. collinoides* CUPV237 *L. sicerae* CUPV261^T para realizar mediante un análisis genómico *in silico*, una identificación de forma predictiva de sus genes *eps*. Los resultados de este capítulo se recogen parcialmente en las publicaciones Puertas et al., (2016, y 2018).

Para la síntesis de HePS se requieren proteínas localizadas en la membrana o en el espacio periplásmico, y son codificadas por los *clusters eps/cps* (Jolly & Stinglee, 2001). En el apartado 2.2.1 de la introducción general se ha descrito la organización genética de los *clusters eps*, así como el proceso de síntesis de HePS. En resumen, estos *clusters* incluyen genes que codifican factores reguladores y enzimas involucradas en la síntesis de la unidad repetitiva, polimerización y secreción de los HePS, incluidas las glicosiltransferasas (GT), que son responsables del ensamblaje de la unidad de repetición característica de estos polímeros (Caggianiello et al., 2016). La biosíntesis de disacáridos, oligosacáridos y EPS/CPS implica la acción de múltiples GT, y su composición es cepa específica. Estas enzimas, catalizan la transferencia de azúcares activados desde moléculas donadoras específicas a moléculasceptoras, formando enlaces glicosídicos (Campbell et al., 1997), y dan lugar a diferentes combinaciones de monosacáridos y enlaces que componen la unidad estructural. La elongación de la cadena se lleva a cabo en la cara extracelular de la membrana plasmática. Para ello, son necesarias las proteínas flipasas que exportan la unidad repetitiva al exterior, y las polimerasas que las unen al polisacárido en formación (Jolly & Stinglee, 2001; Ruas-Madiedo et al., 2002; Lebeer et al., 2009).

Los resultados mostrados en este capítulo, junto con la caracterización de los HePS sintetizados por *L. collinoides* CUPV237 y *L. sicerae* CUPV261^T (capítulo 3), contribuyen al conocimiento de los *Lactobacillus* productores de EPS implicados en la

elaboración de la sidra natural del País Vasco, y en la modificación de la características organolépticas de la bebida.

2. MATERIAL Y MÉTODOS

2.1 Cepas bacterianas y condiciones de cultivo

Las cepas analizadas proceden de los aislamientos del año 20019 (capítulo 1) y fueron las siguientes: 12 pertenecientes a la especie *L. collinoides* (CUPV238, CUPV239, CUPV2311, CUPV2312, CUPV2371, CUPV2313, CUPV2315, CUPV2317, CUPV2320, CUPV2322, CUPV2323, CUPV2324), 2 de la especie *L. sicerae* (CECT 8227^T=CUPV261^T y CUPV 262), además de *P. parvulus* 2.6 y *L. diolivorans* G-77 como controles positivos del gen *gtf* (apartado 2.2). La cepa *Lactobacillus collinoides* CUPV237 productora de exopolisacárido es un mutante espontáneo superproductor de riboflavina de la cepa CUPV2371. En el capítulo 5 se describe como fue aislado, así como el cambio ocurrido en su genoma que explicaría su fenotipo superproductor.

Los cultivos se llevaron a cabo de forma rutinaria en el medio MRS (pH 5,5) con un 2 % de inóculo, a 28 °C y hasta que alcanzaron la mitad de la fase exponencial de crecimiento.

2.2 Detección de genes implicados en la síntesis de HoPS y HePS en BAL

Para detectar la presencia de genes relacionados con la síntesis de homopolisacárido (genes *gtf*, *deg* y *lev*) y de heteropolisacárido (*epsD/E*, *epsA*, *epsB* y *epsE-G*), se realizaron PCR dirigidas utilizando los cebadores descritos en la Tabla 2.1. Para ello, se utilizaron las extracciones de DNA de dos cultivos independientes realizadas según lo descrito en el capítulo 1 (apartado 2.6.1).

La mezcla de reacción se preparó en un volumen final de 20 μL , y que contenía: 0,075 U μL^{-1} de la DNA polimerasa ExTaq (Takara), 1x del tampón de PCR (Takara), 2,5 mM de MgCl_2 ó 4,5 mM para las parejas de cebadores de los genes *deg* y *lev*; 6,25 μM de cada uno de los oligonucleótidos, 100 μM de cada uno de los cuatro dNTP, y 200 ng de DNA molde por reacción. Por cada cepa se realizaron dos PCR independientes con cada pareja de cebadores. La reacción de amplificación se realizó en un equipo 7300 Real Time PCR System (Applied Biosystem Inc.) y se utilizaron las siguientes condiciones según la pareja de cebadores empleada:

- GTFF/GTFR: 1 ciclo de desnaturalización de 5 min a 95 °C; 30 ciclos de 95 °C durante 1 min, 55 °C durante 1 min y 72 °C durante 30 s; y una extensión de 72 °C durante 10 min.
- PG-F/PG-R: 1 ciclo de desnaturalización a 94 °C; 5 ciclos de 94 °C durante 30 s, 62 °C durante 31 s y 72 °C durante 32 s; seguido de 40 ciclos de 94 °C durante 30 s, 52 °C durante 31 s; y una extensión final de 72 °C durante 10 min.
- eps A-F/eps A-R: 1 ciclo de desnaturalización de 5 min a 94 °C; 35 ciclos de 94 °C durante 15 s, 40 °C durante 31 s y 72 °C durante 1,5 min; y una extensión final de 72 °C durante 10 min.
- eps B-F/eps B-R: 1 ciclo de desnaturalización de 5 min a 94 °C; 35 ciclos de 94 °C durante 45 s, 46 °C durante 1 min y 72 °C durante 1 min; y una extensión final de 72 °C durante 10 min.
- epsEFG-F/epsEFG-R: 1 ciclo de desnaturalización de 5 minutos a 94 °C; 40 ciclos de 94 °C durante 30 s, 49 °C durante 45 s y 72 °C durante 90 s; y una extensión final de 72 °C durante 10 minutos.
- GSF/GSR y FS-F/FS-R: 1 ciclo de desnaturalización de 5 min a 95 °C; 35 ciclos de 95 °C durante 30 s, 42 °C durante 45 s y 72 °C durante 1 min; y una extensión final de 72 °C durante 2 min.

Tabla 2.1. Cebadores empleados para la amplificación de genes implicados en la síntesis de exopolisacárido.

Cebador	Secuencia (5'→3')	Tamaño amplicón (pb)	Gen diana	Referencia
PGF PGR	TCATTTTATTCGTAAAACCTCAATTGAYGARYTNCC AATATTATTACGACCTSWNAYYTGCCA	189	<i>epsD/E</i>	Provencher et al., 2003 Mozzi et al., 2006
epsA-F epsA-R	TAGTGACAACGGTTGTA CTG GATCATTATGGACTGT CAC	784	<i>epsA</i>	Low et al., 1998 Mozzi et al., 2006
epsB-F epsB-R	CGTACGATTTCGTACGACCAT TGACCAGTGACACTTGAAGC	1150	<i>epsB</i>	Deveau et al., 2003
EpsEFG-F Eps EFG-R	GAYGARYTNCCNCARYTNWKNAAYGT TGCAGCYTCWGCCACATG	1600	<i>epsE-G</i>	Mozzi et al., 2006
GTFF GTTR	CGGTAATGAAGCGTTTCCTG GCTAGTACGGTAGACTTG	417	<i>gtf</i>	Werning et al., 2006
GSF GSR	GAYAAYWSNAAYCCNRYNGTNC ADRTCNCRTARTANAVNYKNG	660	<i>deg</i>	Krajl et al., 2003
FSF FSR	GAYGTITGGGAYWSITGGC TCITYYTCRTCISWIRMCAT	800	<i>lev</i>	Tieking et al., 2005

Los productos de PCR se visualizaron mediante electroforesis (100 V, 50 min) a partir de 10 µL de producto, con 1,5 µL de tampón de carga (Anexo I), en un gel de agarosa al 1 %, ó 2 % para la amplificación parcial del gen *epsE* (100 V, 70 min). Los geles fueron teñidos con 0,2 µg mL⁻¹ de bromuro de etidio y visualizados por

exposición a luz ultravioleta. La comparación y normalización de los geles se realizó de acuerdo al marcador 1 Kb Plus DNA (Invitrogen), utilizando el equipo GelDoc para documentar los geles.

2.3 Secuenciación del genoma de *Lactobacillus collinoides* CUPV237. Análisis de las posibles secuencias proteicas de los genes *eps* en CUPV237 y CUPV261^T

La secuenciación del genoma completo de CUPV237 se realizó utilizando la plataforma Illumina GALx en el CREA Genomics Research Centre, (Fiorenzuola d'Arda, Italia). Para la preparación de la biblioteca se partió de una muestra de 2 µL de DNA extraída con el kit TruSeq FC-121-1001, y se siguieron las instrucciones del fabricante. El análisis de la librería fue realizado en colaboración con los Drs. Giuseppe Spano (Universidad de Foggia, Italia) y Luigi Orrú (Agricultural Research and Economics (CREA)-Genomics Research Centre, Fiorenzuola d'Arda, Italia) (Puertas et al., 2016).

Se obtuvieron un total de 8.107.203 lecturas pareadas (*paired-ends*), de una longitud de entre 90 y 115 pb, las cuales se ensamblaron *de novo* utilizando CLC Genomics Workbench v 7.0. Esto dio como resultado 127 *contigs* con una longitud N_{50} de 70.285 pb. El *contig* más pequeño contenía 203 pb y el mayor 243.224 pb. El genoma consta de 3.707.616 pb y fue anotado utilizando NCBI Prokariotic Genome Annotation Pipeline (http://www.ncbi.nlm.nih.gov/genome/annotation_prok). La secuencia fue depositada en la base de datos GenBank con el número de acceso JYDC00000000.

Por otro lado, en este ensayo se tuvo en cuenta la información obtenida de la secuenciación parcial del genoma de *L. sicerae* CUPV261^T (ensayo ANI, capítulo 1, apartado), la cual contiene 978 lecturas o *contigs* que abarcan una porción del genoma de 1.727.988 pb.

Las secuencias de cada *contig* se depositaron en la plataforma RAST para una anotación rápida (*Rapid Annotation using Subsystem Technology*, <http://rast.nmpdr.org/rast.cgi>; Aziz et al., 2008; Overbeek et al., 2014; Brettin et al., 2015). Para determinar la función posible de los genes relacionados con la síntesis de HePS, éstos se compararon con secuencias depositadas en las bases de datos del NCBI mediante el algoritmo BlastX (<https://blast.ncbi.nlm.nih.gov/Blast.cgi>). Para la

predicción de segmentos o hélices transmembrana (HTM) y su orientación, se utilizaron los programas TopCons (<http://topcons.cbr.su.se/pred/>; Tsirigos et al., 2015), TMPred (http://embnet.vital-it.ch/software/TMPRED_form.html), y SACS MEMSAT 2 (<http://www.sacs.ucsf.edu/cgi-bin/memsat.py>; Jones et al., 1994). Para la localización de aminoácidos (serina, tirosina y treonina) susceptibles de ser fosforilados por kinasas, se utilizó el programa NetPhos 3.1 server (<http://www.cbs.dtu.dk/services/NetPhos/>; Blom et al., 2004) y annie (<http://annie.bii.a-star.edu.sg/annie/home.do>; Ooi et al., 2009). Los alineamientos entre las secuencias de las proteínas con la misma función posible y codificadas por los genes *eps*, se realizaron mediante ClustalW (<https://www.genome.jp/tools-bin/clustalw>), y T-Coffee (<http://tcoffee.crg.cat>) para alinear las secuencias de las proteínas transmembrana. Finalmente, el programa mfold (<http://unafold.rna.alany.edu/?q=mfold/RNA-Folding-Form>; Zuker, 2003) se utilizó para detectar y modelar las secuencias de mRNA que pudieran corresponderse con terminadores de la transcripción en los transcritos de RNA.

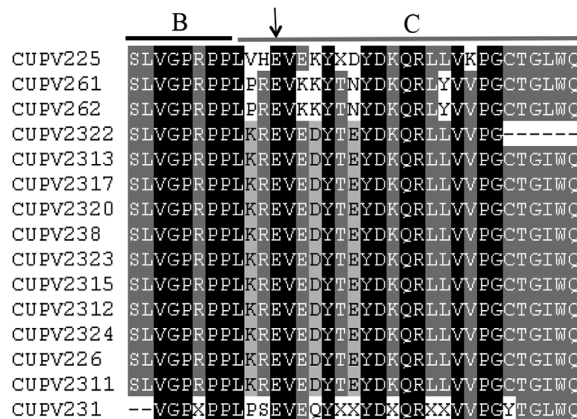
2.4 Asignación de la nomenclatura

En este trabajo se utilizó el sistema de nomenclatura indicado por *Bacterial Polysaccharide Gene Nomenclature* (BPGN) (www.microbio.usyd.edu.au/BPGD/default.htm) y utilizado por otros autores (Reeves et al., 1996; Pèant et al., 2005; Dimopoulou et al., 2014). Es un sistema aplicable a todas las especies, el cual distingue diferentes clases de genes y aporta un único nombre para todos los genes con una misma función. Así, con el prefijo “we-“ se referenciaron los genes de exopolisacárido y “weI-“ los descritos en el género *Lactobacillus*. El prefijo “wz-“ se asignó en genes homólogos cuya función predicha fue la de regular la síntesis del EPS, y se acompañó de “-r” en los genes identificados como regulador transcripcional, o de “-b, -e o -d”, cuando son genes del sistema fosfo-regulador; de “-y” en los genes de polimerasa; y de “-x” en los de transporte transmembrana o flipasa. Finalmente, los genes implicados en la biosíntesis de los precursores azúcares-nucleótido se nombraron de acuerdo a la ruta a la que pertenecen. Además, para distinguir el *cluster* de procedencia se añadió una última cifra del 1 al 4.

3. RESULTADOS

3.1 Detección de genes implicados en la síntesis de EPS.

Las cepas procedentes de los aislamientos del 2009 pertenecientes a las especies *L. collinoides* y *L. sicerae* sintetizan EPS (Tabla 1.2). La detección de genes específicos para la síntesis de HoPS y HePS se realizó mediante PCR. En ninguna de las cepas estudiadas se detectaron los genes implicados en la síntesis de HoPS: β -glucano (*gtf*), dextrano (*deg*) o levano (*lev*), y tampoco para los genes relacionados con la síntesis de HePS: *epsA* (o según la nomenclatura que hemos utilizado en este trabajo, *wzr*), *epsB* (*wzb*) o *epsEFG* (*weI-E-G*).



(a) Identidad máxima de la secuencia respecto a la ORF de referencia.

Figura 2.1. Detección del gen de la glicosiltransferasa iniciadora relacionada con la síntesis de HePS. Panel superior, alineación de las secuencias de aminoácidos deducidas a partir de la secuenciación de los productos de PCR con los cebadores PG de Provencher et al. (2003). La letra X indica un aminoácido indeterminado; sombreado oscuro, aminoácidos idénticos; sombreado claro, aminoácidos conservados (solo dos aminoácidos diferentes entre distintas cepas); flecha negra, indica un residuo catalítico posible; las líneas oscura y clara sitúan dos de los bloques en los que se divide la enzima (van Kranenburg et al., 1999). **Panel inferior**, tabla resultante de la comparación de las secuencias de DNA obtenidas en las amplificaciones, con las secuencias de proteínas contenidas en las bases de datos mediante BlastP.

Sin embargo, en las 14 cepas se obtuvo el amplicón esperado para el gen de la glicosiltransferasa iniciadora (pGT). Los fragmentos se secuenciaron y se compararon mediante el algoritmo BlastP (Tabla de la Figura 2.1).

Las secuencias de aminoácidos de las pGT posibles de *L. sicerae* CUPV261^T y CUPV262 mostraron similitud con la secuencia de la proteína EpsE de la cepa productora de HePS *L. helveticus* CRL1176 (RS: ABB59702.1, Mozzi et al., 2006). Mientras que las secuencias de *L. collinoides* presentaron similitud con la secuencia de la proteína EpsF de la cepa productora de EPS *L. fermentum* TDS030603 (BAI67356.1, Dan et al., 2009). Mediante el análisis de los dominios conservados, se observó que estas secuencias pertenecerían a proteínas de la familia Bac_transf (pfam02397), la cual se compone de proteínas azúcar-transferasas bacterianas, y se incluyen en la superfamilia cl27431.

3.2 Genes relacionados con la síntesis de heteropolisacárido en el genoma de *Lactobacillus collinoides* CUPV237

Mediante la secuenciación del genoma de la cepa CUPV237 se obtuvieron 116 *contigs*, cuyas secuencias se depositaron en la plataforma bioinformática RAST. En la lista de genes previamente anotados por RAST se realizó una búsqueda *in silico* de genes que pudieran estar relacionados con la síntesis de polisacárido. Se encontraron 38 *orf* predichas distribuidas en 4 *clusters*, de las cuales 8 se relacionan con la síntesis de precursores (Tabla 2.2 y Figura 2.2).

En los *clusters eps*-1, -2 y -3, predictivamente se encontraron genes relacionados con funciones de regulación, de síntesis de la unidad repetitiva, de exportación y polimerización. Se observó un cuarto *cluster (eps4)*, que además, podría estar relacionado con la formación de dNDP-azúcares.

De forma general, los posibles genes *eps* encontrados en el genoma de CUPV237 codificarían las siguientes proteínas necesarias para la síntesis de HePS: tirosina kinasas (5 genes), fosfatasa (2), glicosiltransferasas iniciadoras de la síntesis (3), glicosiltransferasas (12), flipasas (2), polimerasas (2) y reguladores transcripcionales (3) (Tabla 2.2). Así mismo, se buscaron secuencias relacionadas con enzimas implicadas en la síntesis de HoPS, glicosil-hidrolasas (dextranos y levanos) y la sintasa responsable de la producción de (1,3)(1,2)-β-D-glucano, pero no se detectó

ninguna de ellas. Para la descripción de los *clusters eps* de CUPV237, se comienza por el extremo próximo a los genes fosforeguladores (Figura 2.2 y Tabla 2.2).

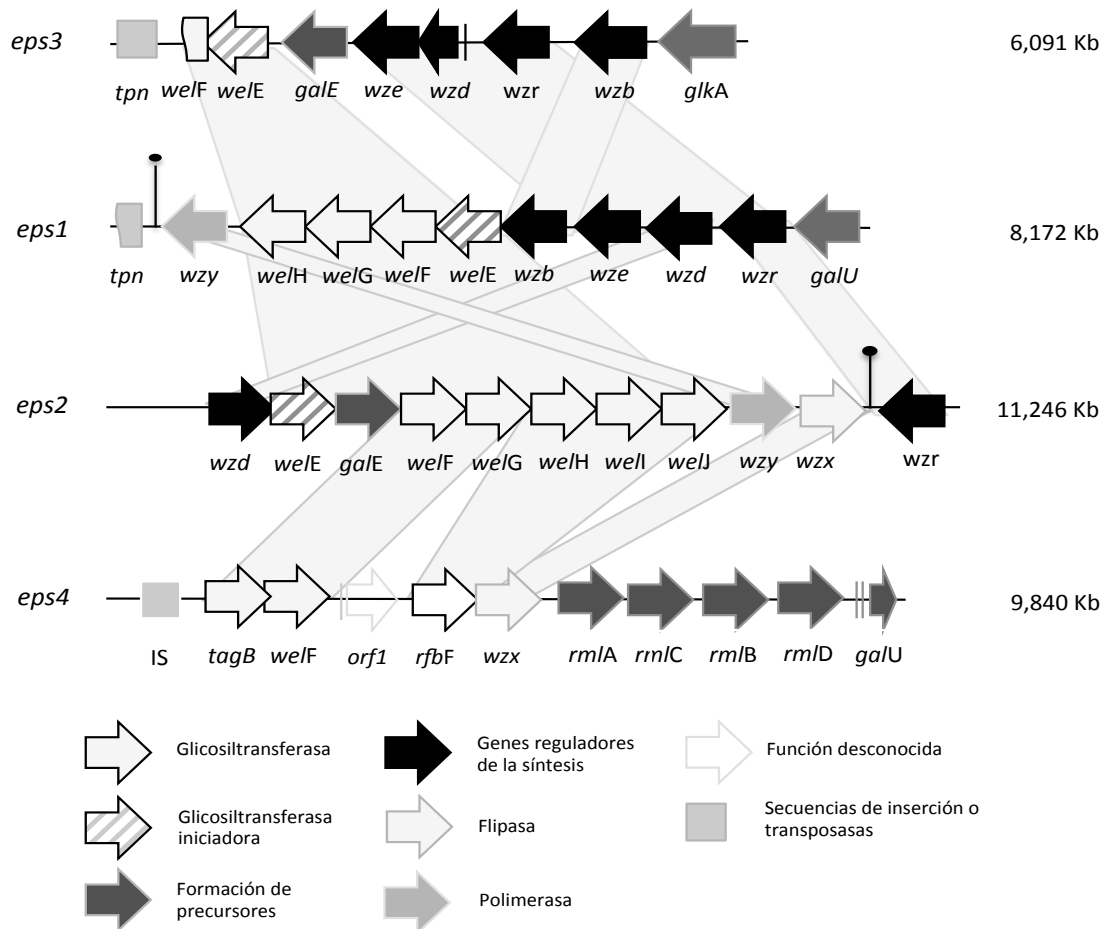


Figura 2.2. Representación esquemática de los posibles *clusters eps* localizados en el genoma de *L. collinoides* CUPV237. Las flechas representan los genes, y su color o trama indica la función posible de las proteínas codificadas. Las bandas de color gris claro conectan genes que codificarían proteínas con una actividad similar, y las líneas negras terminadas en círculo sitúan a los posibles terminadores de la transcripción.

Cluster *eps1*

Este *cluster* está codificado por la hebra complementaria, tiene un tamaño de 8,172 pb y predictivamente contiene 10 *orf*. Está flanqueado en el extremo 5' por un gen incompleto relacionado con la transposasa *tnp_IS153* de *Streptococcus thermophilus* eps X tipo 0 (RS: AAN63776.1). En el extremo 3', se sitúa el gen *galU* relacionado con la síntesis de precursores para la biosíntesis de EPS. Corriente arriba, se detectaron cuatro genes reguladores *wzr*, *wzd*, *wze* y *wzb*, seguidos de los genes implicados en la formación de la unidad repetitiva: *welE*, *welF*, *welG* y *welH*. Corriente arriba del *cluster*, se identificó un gen codificante de una polimerasa (*wzy*), además de

un posible terminador transcripcional ρ -independiente (5' AGGAGGCUGUUUAUGUUUUUU 3').

El análisis de las secuencias del *cluster eps1* realizados con BlastX mostró identidades del 100 % entre las GT de este *cluster* con GT de *L. parabuchneri*, entre el 75 y el 91 % con las proteínas reguladoras de las especies *L. brevis*, *L. buchneri* y *L. paracollinoides*, y un 63 % con la polimerasa de *L. plantarum* (Tabla 2.2). Por otro lado, en RAST se observó que corriente arriba del gen *galU1* se situarían los genes *znuA* (COG0803, pfam01297), *znuC* (COG1121, pfam00005) y *znuB* (COG1108, pfam00950) que codificarían una permeasa de membrana tipo ABC.

Cluster eps2

El *cluster eps2* se compone predictivamente de 11 *orf* codificadas en la hebra sentido que comprenden una secuencia de 11.246 pb (Tabla 2.2). Se encontraron dos genes reguladores, *wzd* y *wzr*, localizados en el extremo 5' y 3', respectivamente. Este *cluster* también contiene el gen *galE* relacionado con la formación de azúcares activados, situado entre el gen *we/E* (ρ GT) y un grupo con 5 genes consecutivos de GT (*we/F*, *we/G*, *we/H*, *we/I* y *we/J*). Corriente abajo se observó un gen *wzy* de polimerasa, seguido de un gen *wzx* de flipasa (transportador de membrana). Cercano al extremo 3' entre los genes *wzx* y *wzr*, apareció una secuencia que podría corresponderse con un terminador transcripcional ρ -independiente (5'AGCUGAUGUGCUGAGUCAGUU 3').

Los análisis de las secuencias del *cluster eps2* realizadas con BlastX mostraron identidades entre el 99 y el 100 % con proteínas de la cepa *L. collinoides* DSM20515 (Tabla 2.2).

Tabla 2.2. Organización génica predicha de los *clusters eps* en la estirpe *Lactobacillus collinoides* CUPV237.

Cluster y genes	Tamaño (aa)	^a Función predicha, secuencia de referencia (RS)	^b Número de HTM	^c Dom. cons.(valor-e)/ S-Fam	^d Bacteria / Proteína con la mayor identidad, RS (valor-e)	^e Identidad de los aminoácidos (%)
Cluster eps1						
<i>wzy</i>	379	Polimerasa WP_063285235.1	11	-/-	<i>L. plantarum</i> WP_076632965.1 (4e ⁻¹⁶⁴)	63
<i>welH</i>	251	Glicosiltransferasa KZL42808.1	0	Gly_Tranf_sug pfam04488 (3,2e ⁻⁷)/ Gly_trans_sug cl19952	<i>L. parabuchneri</i> WP_084975616.1 (2e ⁻¹⁴¹)	77
<i>welG</i>	163	Glicosiltransferasa KZL42809.1	0	COG5017 (6,63e ⁻¹⁵)/ Glycosyltransferase_GTB cl10013	<i>L. parabuchneri</i> WP_063285224.1 (4e ⁻¹¹⁶)	100
<i>welF</i>	150	Glicosiltransferasa KZL42810.1	0	Alg14 pfam08660 (3,76 e ⁻¹⁴)/ Glycosyltransferase_GTB cl10013	<i>L. parabuchneri</i> WP_063285225.1 (1e ⁻¹⁰⁶)	100
^c <i>welE</i>	234	Glicosiltransferasa iniciadora KZL42819.1	1	Bac_trans pfam02397 (1,26e ⁻⁵⁶)/ Bac_trans cl27431	<i>L. buchneri</i> CD034 AFS01453.1 (1e ⁻¹³⁸)	100
<i>wzb</i>	255	Tirosina fosfatasa KZL42811.1	0	YwqE COG4464 (9,75e ⁻⁶⁶)/ PHP cl23724	<i>L. buchneri</i> CD034 AFS01452.1 (3e ⁻¹⁷³)	91
<i>wze</i>	243	Tirosina kinasa autokinasa KZL42812.1	1	eps_fam TIGR1007 (1,40e ⁻⁴⁴)/ P_loop_NTPase cl21455	<i>L. brevis</i> ARQ94399.1 (1e ⁻¹⁶⁶)	97
<i>wzd</i>	286	Determinación de la longitud de la cadena KZL42813.1	2	Yvek COG3944 (9,28e ⁻²⁵)/ GNVR cl26080	<i>L. paracollinoides</i> WP_054711923.1 (3e ⁻¹²⁸)	70
<i>wzr</i>	325	Regulador transcripcional KZL42814.1	1	LytR PKK09379 (6,66e ⁻⁵³)/ LytR_CpsA_psr cl00581	<i>L. paracollinoides</i> ANZ65373.1 (3e ⁻¹⁶⁶)	75
<i>galU</i>	309	UTP-glucosa-1-fosfato uridiltransferasa KZL42815.1	0	GalU COG1210 (7,55e ⁻¹¹¹)/ Glyco_tranf_GTA cl11394	<i>L. collinoides</i> DSM20515 KRM74556.1 (0,0)	89
Cluster eps 2						
<i>wzd</i>	251	Determinación de la longitud de la cadena WP_063285778.1	2	Yvek COG3944 (4,93e ⁻⁰⁹)/ GNVR cl26080	<i>L. collinoides</i> DSM20515 KRM77917.1 (2e ⁻¹⁴⁷)	99
<i>welE</i>	216	Glicosiltransferasa iniciadora KZL35798.1	1	Bac_transf pfam02397 (2,55e ⁻⁴⁶)/ Bac_transf cl27431	<i>L. collinoides</i> KRM77916.1 (1e ⁻¹⁵⁵)	99

Cluster y genes	Tamaño (aa)	^aFunción predicha, secuencia de referencia	^bNúmero de HTM	^cDom. cons.(valor-e)/ S-Fam	^dBacteria / Proteína con la mayor identidad, RS (valor-e)	^eIdentidad de los aminoácidos (%)
galE	328	Epimerasa–deshidratasa NAD– dependiente WP_056995942.1	3	UDP_AE_SDR_e cd05256 (3,81e ⁻⁷²)/ Epimerase superfamily cl25660	<i>L. collinoides</i> DSM20515 KRM77915.1 (0,0)	100
welF	256	Glicosiltransferasa KZL35799.1	0	Glycos_transf_2 pfam00535 (2,14e ⁻¹⁹)/ Glyco_tranf_GTA cl11394	<i>L. collinoides</i> DSM20515 KRM77914.1 (0,0)	100
welG	246	Glicosiltransferasa KZL35800.1	0	OCH1 COG3774 (9,42e-11)/ Caps_synth cl26275	<i>L. collinoides</i> DSM20515 KRM77913.1 (0,0)	100
welH	376	Glicosiltransferasa KZL35801.1	0	GT1_WabH_like cd03811 (2,06e ⁻³²)/ glycosyltransferase_GTB_type cl10013	<i>L. collinoides</i> DSM20515 KRM77912.1 (0,0)	100
welI	326	Glicosiltransferasa KZL35802.1	0	Stelth_CR2 pfam11380 (2,71e ⁻²⁴)/ Stealth_CR2 cl15596	<i>L. collinoides</i> DSM20515 KRM77911.1 (0,0)	100
welJ	328	Glicosiltransferasa WP_056995931.1	0	Glyco_tranf_GTA_type cd00761 (4,05e ⁻¹⁴)/ Glyco_tranf_GTA_Type cl11394	<i>L. collinoides</i> DSM20515 KRM77910.1 (0,0)	100
wzy	409	Polimerasa KZL35803.1	12	-/-	<i>L. collinoides</i> DSM20515 KRM77909.1 (0,0)	100
wzx	511	Flipasa WP_056995929	12	MATE_WZX_like cd13128 (1,35e ⁻¹²)/ MATE_like cl09326	<i>L. collinoides</i> DSM20515 KRM77908.1 (0,0)	100
wzr	405	Regulador transcripcional KZL35804.1	1	LytR PKK09379 (4,66e ⁻⁵⁹)/ LytR_CpsA_psr cl00581	<i>L. collinoides</i> DSM20515 KRM77907.1 (0,0)	99
Cluster eps3						
welF*	131	Glicosiltransferasa WP_063285809.1	0	GT2_AmsE_like cd4195 (1,70e ⁻²⁷)/ Glyco_tranf_GTA cl11394	<i>L. rennini</i> SFZ87057.1 (1e ⁻⁴⁰)	61
welE	169	Glicosiltransferasa iniciadora KZL35613.1	1	Bac_trans pfam02397 (1,33e ⁻⁵⁰)/ Bac_transf cl27431	<i>L. collinoides</i> WP_082620226.1 (2e ⁻¹⁴¹)	100
galE	284	Epimerasa–deshidratasa NAD– dependiente KZL35614.1	0	UDP_AE_SDR_e cd05256 (1,44e ⁻⁵⁶)/ SDR cl25409	<i>L. collinoides</i> WP_056996466.1 (0,0)	100

Cluster y genes	Tamaño (aa)	^a Función predicha, secuencia de referencia	^b Número de HTM	^c Dom. cons.(valor-e)/ S-Fam	^d Bacteria / Proteína con la mayor identidad, RS (valor-e)	^e Identidad de los aminoácidos (%)
<i>wze</i>	244	Tirosina kinasa autokinasa KZL35615.1	0	Eps_fam TIGR01007 (1,80e ⁻³²)/ P_loop_NTPase cl21455	<i>L. collinoides</i> WP_054762722.1 (3e ⁻¹⁷²)	99
<i>wzd*</i>	287	^e Determinación de la longitud de la cadena	2	Yvek COG3944 (1,29e ⁻¹³)/ GNVR cl26080	<i>L. similis</i> DSM 23365 KRN23810.1 (2e ⁻⁹⁰)	72
<i>wzr</i>	338	Regulador transcripcional KZL35622.1	1	LytR PRK09379 (2,46e ⁻⁶⁰)/ LytR_cpsA_psr cl00581	<i>L. collinoides</i> DSM20515 KRM76450.1 (0,0)	100
<i>wzb</i>	260	Tirosina fosfatasa KZL35616.1	0	YwqE COG4464 (5,08e ⁻⁶⁷)/ PHP cl23724	<i>L. collinoides</i> DSM20515 KRM76451.1 (0,0)	100
<i>glkA</i>	327	Glucokinasa KZL35617.1	0	ROK_glcA_fam TIGR00744 (6,23e ⁻⁵⁵)/ NDB sugarkinase HSP70_actin cl17037	<i>L. collinoides</i> DSM20515 KRM76452.1 (0,0)	100
Cluster eps4						
<i>tagB</i>	300	Glicosiltransferasa WP_082820869.1	1	TagB COG1887 (3,15e ⁻²¹)/ GlyTranf_GTB cl10013	<i>L. collinoides</i> KRM76464.1 (0,0)	99
<i>welF</i>	333	Glicosiltransferasa KZL41392.1	0	GT2 COG1216 (5,32e ⁻⁵)/ Glyco_tranf_2_3 cl26112	<i>L. collinoides</i> KRM76465.1 (2e ⁻¹³⁴)	99
<i>orf1*</i>	374	^e Proteína hipotética	9	EpsG pfam14897 (4,89e ⁻⁹)/ EpsG cl22544	<i>L. collinoides</i> DSM20515 KRM75026.1 (2e ⁻¹⁷⁹)	100
<i>rfbF</i>	287	Glicosiltransferasa KZL41393.1	0	GT2_RfbF_like cd02526 (2,06e ⁻²⁸)/ Glyco_tranf_GTA cl11394	<i>Lactobacillus brevis</i> WP_024526586.1 (6e ⁻¹¹⁴)	57
<i>wzx</i>	515	Flipasa KZL41497.1	12	RfbX COG2244 (4,24e ⁻⁸)/ MATE_like cl09326	<i>L. pentosus</i> WP_120768212.1 (0,0)	71
<i>rmlA</i>	290	Glucosa-1-fosfato-timidilil-transferasa KZL41394.1	0	rmlA TIGR01207 (1,49e ⁻¹⁴²)/ Glyco_tranf_GTA cl11394	<i>L. collinoides</i> DSM20515 KRM74284.1 (0,0)	100
<i>rmlC</i>	193	dTDP-4-deshidroramnosa-3,5-epimerasa KZL41395.1	0	rmlC TIGR01221 (4,43e ⁻⁵⁸)/ cupin_like cl21464	<i>L. collinoides</i> DSM20515 KRM74283.1 (4e ⁻¹⁴¹)	100
<i>rmlB</i>	345	dTDP-D-glucosa-4,6-deshidratasa KZL41396.1	1	RfbB COG1088 (5,91e ⁻¹⁰⁴)/ SDR cl25409	<i>L. collinoides</i> DSM20515 KRM74282.1 (0,0)	100
<i>rmlD</i>	286	dTDP-4-deshidroramnosa-reductasa KZL41397.1	0	RfbD COG1091 (3,43e ⁻⁶³)/ NADB_Rossmann cl21454	<i>L. collinoides</i> DSM20515 KRM74281.1 (0,0)	100

Cluster y genes	Tamaño (aa)	^aFunción predicha, secuencia de referencia	^bNúmero de HTM	^cDom. cons.(valor-e)/ S-Fam	^dBacteria / Proteína con la mayor identidad, RS (valor-e)	^eIdentidad de los aminoácidos (%)
<i>galU</i> *	251	^e UTP–glucosa–1–fosfato–uridililtransferasa	0	UGPasa prokariotic cd02541 (0,0)/ Glyco_tranf_GTA cl11394	<i>Lactobacillus sp.</i> WP_005688890.1(1e ⁻⁶⁶)	75

- (a) Función predicha en base a los resultados obtenidos en las comparaciones de los genes *eps* en la base de datos NCBI con la función BlastX y el análisis de los dominios conservados, además de la información derivada por la anotación de RAST.
- (b) HTM, indica el número de hélices transmembrana predichas en los modelos bioinformáticos obtenidos en los programas TopCons, TMPred, TMHMM y SACs MEMSAT.
- (c) La secuencia de WelE1 depositada en NCBI está incompleta en el extremo NH₃-terminal, la secuencia de WelE3 correcta es "MQTERRSGGDPKYGHP + KZL42819.1".
- (d) Resultados obtenidos utilizando la función BlastX.
- (*) Secuencias incompletas o con la pauta de lectura alterada.
- (aa) aminoácidos.

Cluster *eps3*

El *cluster eps3* está localizado en la hebra complementaria, tiene una longitud total de 6.091 pb y se compone predictivamente de 7 genes *eps* posibles. En este *cluster* encontramos dos genes relacionados con la formación de precursores de la síntesis de EPS, uno es el gen de la glucokinasa (*glkA*) en el extremo 3' y el segundo es *galE*, situado en la porción media del *cluster*. Corriente arriba de *glkA* se sitúa un grupo de 4 genes reguladores: *wzb*, *wzr*, *wzd* (con la pauta de lectura alterada) y el gen *wze*. En este *cluster* solo se detectaron dos genes que podrían corresponderse con GT, uno es el gen de la pGT (*welE*) y el otro un gen de GT incompleto (*welF*). Por último, en el extremo 3' se observó una secuencia parcial de la integrasa ISLp11 de *Lactobacillus kefiranofaciens* ZW3 (RS: CP002764.1).

Los análisis de las secuencias del *cluster eps3* realizados con BlastX, mostraron similitudes del 100 % con proteínas reguladoras de *L. collinoides* DSM20515, a excepción de *Wzd* y *WelF* cuyas pautas de lectura aparecen predictivamente alteradas (Tabla 2.2).

Cluster *eps4*

El *cluster eps4* está codificado en la hebra molde, se compone predictivamente de 10 *orf* que abarcarían 9.840 pb. En él se encontraron genes relacionados con la síntesis de precursores, *galU* (con varias interrupciones en su marco de lectura), además de los cuatro genes necesarios para la biosíntesis de dTDP-L-ramnosa (*rmlA*, *rmlC*, *rmlB* y *rmlD*). En este *cluster* no se detectaron genes reguladores, pero sí tres genes de GT (*tagB*, *welF* y *rfbF*), además de *orf1* que podría estar relacionado con una GT de membrana. También se localizó en el extremo 5' del *cluster*, un gen de flipasa (*wzx*) y parte de un gen relacionado con la transposasa 1187 de *L. fermentum* IFO3956 (RS: AP008937).

Los análisis de las secuencias del *cluster eps4* realizadas con BlastX mostraron identidades de entre el 99-100 % con las proteínas *TagB*, *WelF*, *Orf1* y *RmlA*, -C, -B y -D de *L. collinoides* DSM20515, y entre 57-75 % de similitud con proteínas *GalU*, *Wzx* y *RfbF* de otras especies de lactobacilos (Tabla 2.2).

3.2.1 Proteínas implicadas en la regulación de la síntesis de polisacárido

Los genes *eps* que codifican las proteínas reguladoras Wzr, Wzd, Wzb y Wze, están altamente conservados, probablemente debido a que juegan un papel fundamental y necesario para llevar a cabo la síntesis de polisacárido exocelular. Estos genes se relacionan con la producción, procesado y regulación de su biosíntesis (Bender & Yother, 2001).

Wzr

Estas proteínas son miembros de la familia Lytr_CpsA_Psr (LCP) y están relacionadas con el mantenimiento de la envoltura celular (Hübscher et al., 2008; Lebeer et al., 2009). En el genoma de la cepa CUPV237 se localizaron tres posibles genes *wzr* distribuidos en los *clusters eps* 1, -2 y -3. En el estudio predictivo del perfil de hidrofobicidad de sus secuencias de aminoácidos, se observó que podrían contener: una hélice transmembrana compuesta por 18 ó 20 aminoácidos, una porción corta de entre 21-34 residuos en el citosol, y el resto de la proteína quedaría expuesta al espacio extracelular (Figura 2.3). Y es en esta porción extracelular donde encontramos predictivamente un mayor número de residuos y de regiones conservadas entre sí. La proteína Wzr1 tiene una similitud con Wzr2 y Wzr3 del 42 % (valor-e de $2e^{-80}$) y del 72 % ($1e^{-163}$) respectivamente, y entre Wzr2 y Wzr3 del 45 % ($7e^{-81}$). Además, Wzr1 y Wzr3 presentaron similitudes con reguladores transcripcionales de *L. paracollinoides* (RS: ANZ65373.1) y *L. pentosiphilus* (WP_089088798.1) superiores al 70 %, y Wzr2 con otros de *L. paracollinoides* (WP_065901133.1) del 92 %.

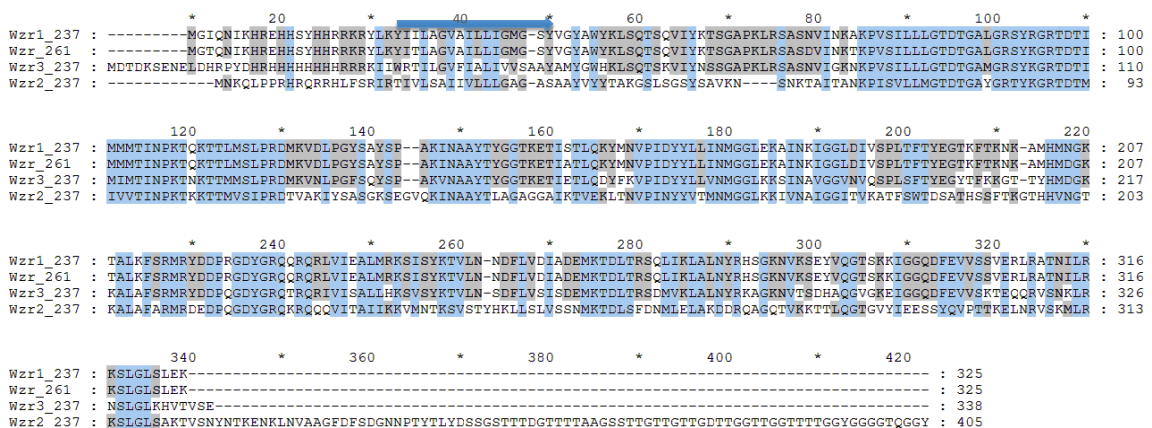


Figura 2.3. Estudio predictivo de las secuencias de aminoácidos de las proteínas reguladoras transcripcionales Wzr, encontradas en los *clusters eps* de *L. collinoides* CUPV237 (Wzr_237) y *L. sicerae* CUPV261^T (Wzr_261). Los residuos sombreados de azul están altamente conservados, y los sombreados en gris, aquellos residuos conservados en el 80 % de las secuencias. La flecha azul indica predictivamente la posición de las hélices transmembrana predichas en las secuencias Wzr de CUPV237, situando la punta de la flecha hacia el espacio extracelular.

Wzd

Las proteínas Wzd realizan la función de tirosina quinasa, y se encargan de determinar la longitud de la cadena del polisacárido que se está sintetizando en una acción conjunta con Wze (Péant et al., 2005, Lebeer et al., 2009). En el genoma de la cepa CUPV237, se encontraron dos genes posibles *wzd* localizados en los *clusters eps1* y *eps2*. Se identificó un tercer gen *wzd3*, cuya pauta de lectura aparece interrumpida en una región rica en adeninas. Esta mutación altera el marco de lectura generando una proteína truncada.

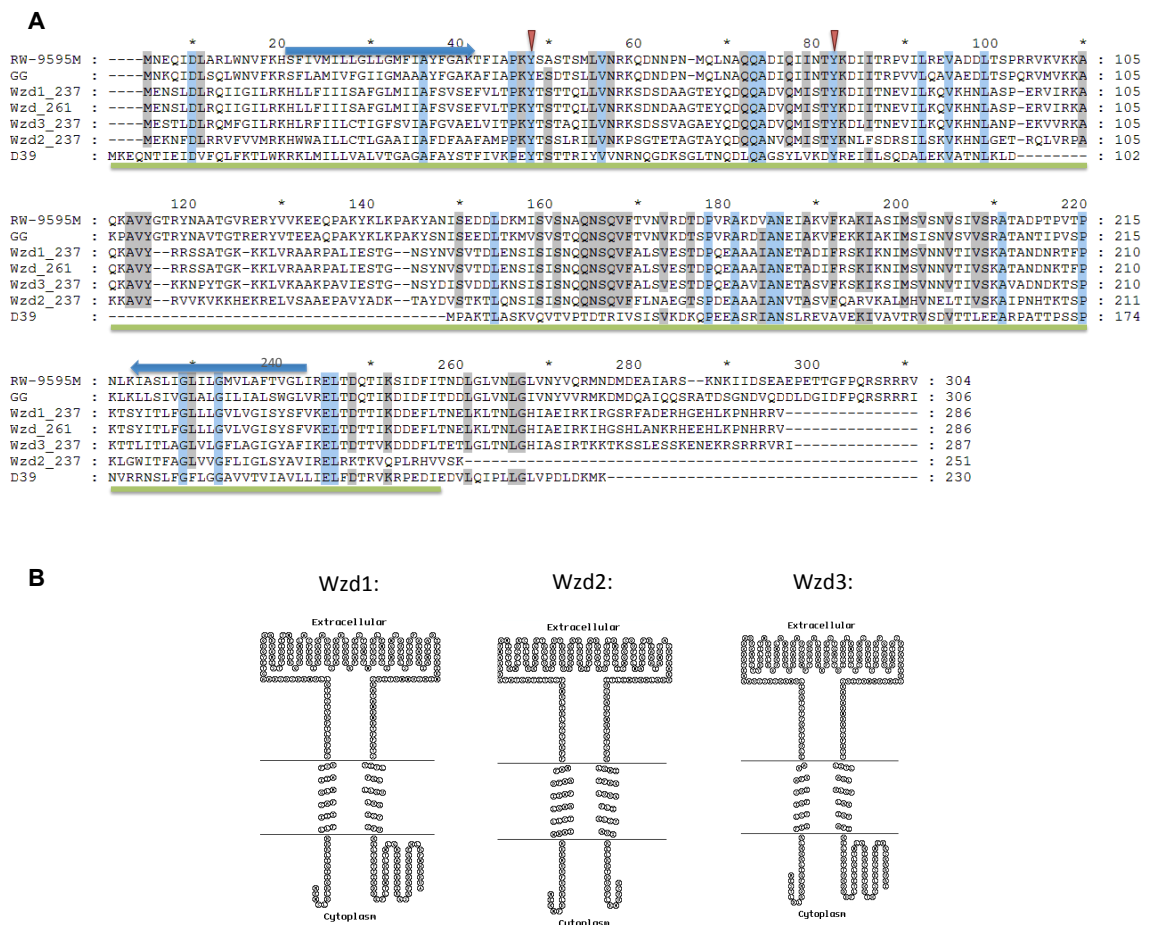


Figura 2.4. Estudio predictivo de las secuencias de aminoácidos de las proteínas tirosina kinasa Wzd, encontradas en los clusters eps de *L. collinoides* CUPV237 y *L. sicerae* CUPV261^T. **A**, Alineamiento de las secuencias (CLUSTALW) de: Wzd237 (CUPV237), Wzd261, (CUPV261); RW-9595M, (*Lactobacillus rhamnosus* RW-9595M, RS: AAW22487.1; Kang et al., 2015); GG (*L. rhamnosus* GG, CAR87948.1; Lebeer et al., 2009); y D39 (*Streptococcus pneumoniae* D39, ABJ55335.1; Morona et al., 2006). Sombreados en azul se muestran los residuos altamente conservados, y en gris los residuos que comparten al menos el 80 % de las secuencias. De manera predictiva: la flecha azul indica la posición de las hélices transmembrana predichas en las secuencias Wzd de CUPV237, situando la punta de la flecha hacia el espacio extracelular; los triángulos rojos muestran dos tirosinas conservadas fundamentales para la función tirosina kinasa (Kang et al., 2015); y la línea verde sitúa el dominio Yvek. **B**, Modelado de las secuencias de aminoácidos de las proteínas Wzd1, Wzd2 y Wzd3 mediante SACS MEMSAT para la detección de posibles fragmentos transmembrana.

La comparación entre sí de las secuencias de las proteínas Wzd halladas en el genoma de CUPV237 mediante BlastP, indicó que Wzd1 y Wzd2 tienen una similitud entre sí del 49 %, entre Wzd1 y Wzd3 de 72 %, y entre Wzd2 y Wzd3 de 55 %. Además, Wzd1 y Wzd3 parecen contener una región citosólica cercana al extremo carboxílico más extensa que Wzd2 (55, 54 y 17 aminoácidos respectivamente, Figura 2.4 A). Estas proteínas también mostraron una identidad del orden de 70 % con proteínas de otras especies, Wzd1 y Wzd2 con *L. paracollinoides* (RS: WP_054711923.1), y Wzd3 con *L. hokkaidonensis* (WP_041092315.1).

La predicción del perfil de hidrofobicidad predicho a partir de la secuencia de aminoácidos, mostró que estas proteínas Wzd podrían contener dos HTM (Figura 2.4 B). El alineamiento de las tres posibles proteínas sugirió que el dominio conservado Yvek presente en este tipo de enzimas, predictivamente se sitúa en la región que está orientada hacia el entorno extracelular (Figura 2.4 A).

Wze

Aparecen dos posibles genes *wze* localizados en los *clusters eps1* y *eps3* (Tabla 2.2). Estos genes suelen estar altamente conservados y codificarían proteínas implicadas en la regulación de la producción de EPS junto con Wzd (Zeidan et al., 2017). Los análisis predictivos realizados mediante BlastX de los genes *wze*, indican que podrían codificar proteínas tirosina kinasas pertenecientes a la superfamilia P-loopNTPasa, y que contienen un posible dominio autokinasa PRK09841 (valor-e de $1,75e^{-37}$) en el extremo carboxilo.

La identidad entre las secuencias de proteínas Wze1 y Wze3 fue del 66 % (valor-e de $2e^{-112}$). Wze1 presentó similitudes por encima del 95 % con proteínas implicadas en la biosíntesis de exopolisacárido de especies como *L. brevis*, *L. buchneri*, *P. damnosus*, *L. kisonensis*, *L. parabuchneri* y *L. sunkii*. Sin embargo, cuando se analizó la secuencia de Wze3, se encontró una identidad del 99 % con proteínas de cepas de *L. collinoides*, y desciende al 80 % con las de *L. paracollinoides*, y al 74 % con las de *L. similis*.

Por otro lado, no se detectaron HTM ni péptido señal en las secuencias de Wze1 y Wze3, indicando que estas proteínas podrían situarse en el citosol. En ambas secuencias de aminoácidos se observó una región poli-Glu-Tyr localizada en el extremo carboxilo de la proteína (Figura 2.5, en amarillo). El residuo de lisina (K)

coloreado en gris (K66 de Wze1, y K65 de Wze3) se relaciona con un motivo de unión del ATP denominado Walker A. Este motivo confiere la capacidad auto-fosforilativa a Wze, por la cual se auto-adicionaría fosfatos en las tirosinas de su región C-terminal de manera dependiente de Mg^{2+} . El recuadro azul muestra el motivo de unión del Mg^{2+} o Walker B (Walker et al., 1982, Péant et al., 2005). Dicha región estaría implicada en la coordinación del Mg^{2+} en el lugar de unión a nucleótidos, y se cree que es esencial para la actividad ATPasa (Figura 2.5, banda verde) situada a 21 residuos de Walker A (Horn et al., 2013).

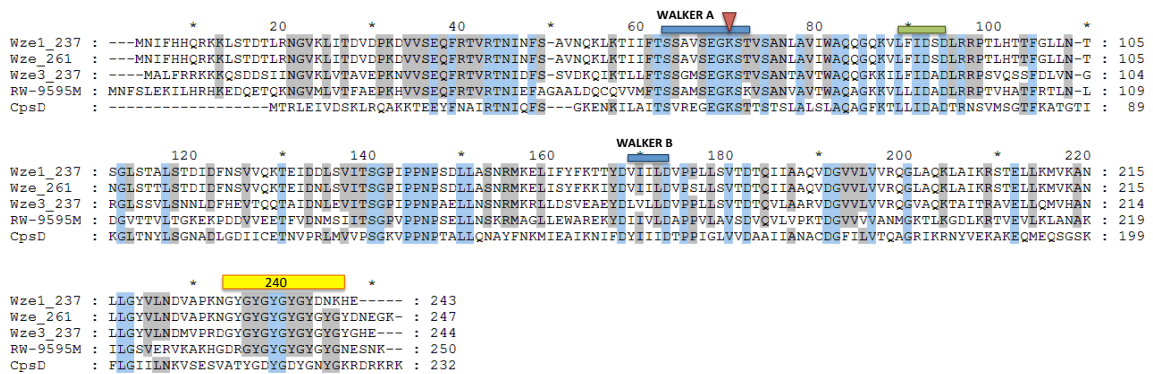


Figura 2.5. Estudio predictivo de las secuencias de las proteínas tirosina autokinasas Wze encontradas en los clusters eps de *L. collinoides* CUPV237 y *L. sicerae* CUPV261^T. Se realizó un alineamiento (CLUSTALW) de las secuencias de: Wze_237 (CUPV237); Wze_261 (CUPV261^T); CpsD (*Streptococcus agalactiae* A909, RS: Q3K0T0); y RW-9595M (*L. rhamnosus* RW-9595M, AAW22488.1). Sombreados en azul se muestran los residuos altamente conservados, y en gris los residuos que comparten al menos el 80 % de las secuencias. El triángulo rojo indica un residuo catalítico de Lys (K); en amarillo, la región fosfo-aceptora C-terminal (GY)_x (Toniolo et al., 2015); las bandas azules señalan la posición del motivo de unión del ATP, Walker A [(AG)_xGK(ST)], y el motivo de unión del Mg^{2+} , Walker B (hhhD, donde “h” representa aminoácidos de naturaleza hidrófoba) (Walker et al., 1982, Péant et al., 2005); y la banda verde muestra el motivo hhhDxD relacionado con la actividad ATPasa (Horn et al., 2013).

Wzb

Wzb es una proteína tirosina fosfatasa implicada en la síntesis de exopolisacárido mediante el mecanismo Wzy-dependiente (Kang et al., 2015). En este estudio se encontraron dos tirosinas fosfatasas en los clusters *eps*1 y -3, las cuales comparten un 67 % de identidad (valor-e de $8e^{-130}$). La secuencia de Wzb1 mostró identidades del 90 % o superiores con proteínas de las especies *L. buchneri*, *L. parabuchneri*, *L. parafarraginis* o *P. damnosus*. Sin embargo la proteína posible Wzb3, presentó identidades del 85 % con cepas de *L. paracollinoides* (RS: WP_054711925.1), del 77 % con *L. similis* (WP_054735993.1), o del 74 % con *L. wasatchensis* (WP_044009825.1).

En el alineamiento de la secuencia de aminoácidos predicha, se localizaron de manera predictiva los siguientes motivos y residuos destacados en la bibliografía (Figura 2.6). Kim et al., (2011) describe los bucles flexibles loop I y loop II alrededor del sitio activo, y que en este tipo de proteínas (YwqE) son responsables de la conformación abierta o cerrada de la misma (Figura 2.6, recuadros negros). El loop I se situaría entre los residuos M43 y H51 de Wzb1, y M46 y H54 de Wzd3. Éste es un sitio activo que contiene el motivo conservado [(G/P)X(Y/F)], donde la tirosina Y es la encargada de controlar el acceso al sitio catalítico (Figura 2.6, β). El loop II podría situarse desde V169 a K175 en Wzb1, y desde V172 a K178 en Wzb3. Este motivo contiene la secuencia [(G/P)X₁₋₂FG₀₋₁(K/R)] con el residuo conservado F (Figura 2.6, β), que también podría tener funciones de control de acceso al sitio catalítico. Las secuencias de Wzb contienen los residuos necesarios para coordinar iones metálicos (dos hierros y un magnesio), necesarios para realizar la actividad fosfatasa (Kim et al., 2011) y están marcados en azul. La arginina (R) del motivo III corresponde con el residuo R139 de la proteína CpsB de *Streptococcus pneumoniae*, esencial para la actividad catalítica de esta proteína (Kim et al., 2011), y también observada en las Wzd de CUPV237 (Figura 2.6, α).

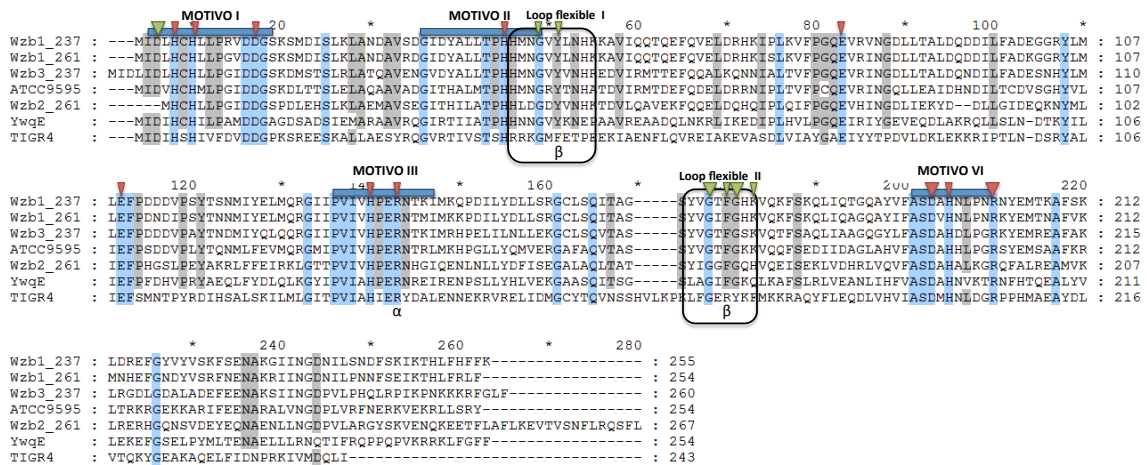


Figura 2.6. Estudio predictivo de las secuencias de las proteínas tirosinas fosfatasas Wzb encontradas en los clusters eps de *L. collinoides* CUPV237 y *L. sicerae* CUPV261^T. En la figura se muestra el alineamiento (CLUSTALW) de: Wzb_237 (CUPV237); Wzb_261 (CUPV261^T); ATCC9595 (*L. rhamnosus* ATCC9595, RS: AAW22448.1); YwqE (*Bacillus subtilis*, P96717); TIGR4 (Cps4B de *Streptococcus pneumoniae* TIGR4, AAK74520.1). Se representa con sombreado azul los residuos altamente conservados, y en sombreado gris los residuos conservados en el 80 % de las secuencias; las bandas azules localizan los cuatro motivos conservados en las proteínas histidinol fosfatasas (PHP) (Lapointe et al., 2008); los triángulos rojos indican los residuos que predicativamente coordinan los iones metálicos; los rectángulos negros enmarcan los motivos descritos para los loops I y II; α, indica un residuo catalítico de arginina; y β, los aminoácidos que podrían ser responsables de la configuración “abierto” o “cerrado” de la proteína (Kim et al., 2011).

3.2.2 Proteínas implicadas en la síntesis de la unidad estructural, transporte a través de la membrana y polimerización de la cadena de EPS

Glicosiltransferasas iniciadoras

Las pGT se caracterizan por ser proteínas incluidas en la membrana celular y tienen función de glicosiltransferasa. Se encargan de catalizar la unión del primer monosacárido de la unidad estructural del EPS al lípido de membrana C55-P mediante un enlace fosfodiéster (van Kranenburg et al., 1999; Videira et al., 2005; Provencher et al., 2003; Lebeer et al., 2009). En el genoma de CUPV237, predictivamente se localizaron tres genes posibles de pGT distribuidos en los *clusters eps1*, -2 y -3. Predictivamente, las tres proteínas pertenecen a la familia pfam02397, de la superfamilia Bac_trans cl27431 (Dimopoulou et al., 2017; Horn et al., 2013). La homología obtenida a partir del alineamiento entre las secuencias de aminoácidos de Wel1E con Wel2E y Wel3E, fue del 33 % (valor-e de $1e^{-33}$) y del 38 % ($5e^{-36}$), respectivamente, mientras que entre estas dos la homología fue del 58 % ($4e^{-82}$).

Por otro lado, se compararon las secuencias predichas de las proteínas WelE de CUPV237 con algunas de las pGT caracterizadas en la bibliografía (Provencher et al., 2003; Dan et al., 2005; Remus et al., 2012; Horn et al., 2013; Dimopoulou, 2013). En este análisis se encontró una identidad del 63 % (valor-e de $2e^{-100}$) entre Wel1E y la proteína undecaprenil-fosfato galactosafosfotransferasa (RS: WP_012846316.1) de *L. johnsonii* FI9785; un 53 % de identidad de Wel2E ($4e^{-56}$) y Wel3E ($1e^{-75}$) con la proteína Cps1E (CCC78588.1) de *L. plantarum* WCFS1. El análisis filogenético de las pGT de CUPV237 mostró a Wel1E con un alto grado de conservación (pequeñas distancias de evolución) con las proteínas de *L. sicerae*, *L. helveticus*, *L. fermentum* y *L. johnsonii* FI9785 (Figura 2.7 A). Mientras que las Wel2E y -3E fueron próximas a la pGT de WCFS1.

Las predicciones realizadas en base a los perfiles de hidrofobicidad de las tres WelE mostraron una HTM próxima al extremo N-terminal, además de una segunda región hidrófoba en Wel1E y Wel3E. En el gráfico de la representación de la predicción del incremento de la energía libre de Gibbs podemos observar la posición de las HTM (Figura 2.7 B).

Además, se estudió mediante NetPhos qué residuos (serina, treonina o tirosina) tienen una mayor probabilidad de ser fosforilados (Anexo II.IV), y se encontraron los siguientes:

- WelE1: T3, S7, Y13, S138, S154 y Y169.
- WelE2: Y15, T17, T27, S166, T205 y T211.
- WelE3: T39, T95, 145T Y154, T157, Y167 y T184.

Sin embargo, el servidor annie solo encontró un motivo de fosforilación de tirosina kinasa ([RK]-x(2,3)-[DE]-x(2,3)-Y) en las posiciones 164-172 de WelE1.

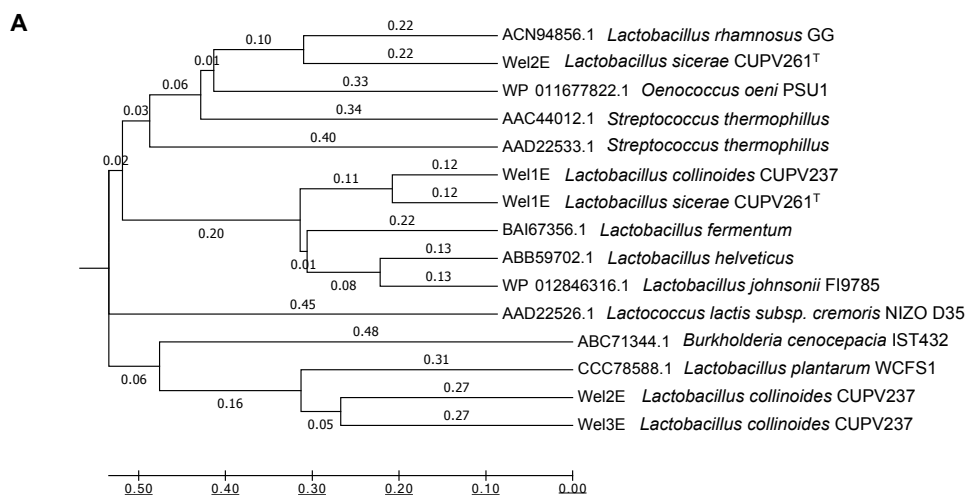


Figura 2.7. Estudio predictivo de la secuencia de la glicosiltransferasa iniciadora WelE. **A**, análisis filogenético deducido mediante el método UPGMA (Sneath, 1973) y elaborado con MEGA a partir de los alineamientos realizados con CLUSTALW. Las distancias filogenéticas (en unidades de número de aminoácidos sustituidos por sitio Kumar et al., 2006) fueron obtenidas con el método de correlación de Poisson (Zuckerland & Pauling, 1965). **B**, predicciones de la energía libre de Gibbs (ΔG) de las secuencias de WelE obtenidas con el programa TopCons. Las flechas indican la localización de las HTM.

Búsqueda in silico de los motivos catalíticos de las pGT

Para identificar y analizar de una manera más exhaustiva las proteínas pGT, hemos analizado sus secuencias de acuerdo a lo descrito por otros autores (Figura 2.8). En las secuencias de WelE se pueden diferenciar tres bloques, de los cuales A y B podrían estar implicados en la interacción con el lípido *carrier* C-55P, y el C estar relacionado con labores de tipo transferasa (Wang et al., 1996; van Kranenburg et al., 1999). Para este tipo de proteínas, van Kranenburg et al. (1999) propusieron 4 aspartatos (D) y 2 glutamatos como residuos conservados en bacterias Gram-positivas. De estos 4 aspartatos, dos podrían formar un motivo catalítico DxD encontrado en diversas GT (Jolly & Stingle, 2001; Provencher et al., 2003; van Kranenburg et al., 1999). Estos aminoácidos son esenciales para la actividad

priming-glicosiltransferasa (Videira et al., 2005), y se localizaron en el bloque B (Figura 2.8, línea roja). Además, las pGT poseen un aspartato y un glutamato ambos conservados, consecutivos y con carga negativa (Figura 2.8, α), los cuales están implicados en la coordinación del catión divalente (Mg^{2+}) necesario para la adición del primer residuo al lípido C55-P (Patel et al., 2010). Por otro lado, se ha descrito que en las enzimas galactosiltransferasas iniciadoras aparece de manera conservada en el bloque C un residuo de tirosina (Y), y localizado en la posición Y214 en la estirpe NIZO D35 (van Kranenburg et al., 1999), el cual no se detectó en las WelE de CUPV237. Sin embargo, próximo al extremo C-terminal aparece una tirosina altamente conservada implicada en la fosforilación y en la regulación de la síntesis del EPS (Figura 2.8, triángulo amarillo) (Minic et al., 2007). En el alineamiento mostrado en la Figura 2.8, se observó que estos residuos no fueron propuestos como sitios de fosforilación en los análisis de NetPhos. Aunque, en el análisis con annie se localizó un motivo de fosforilación de tirosina kinasa ([RK]-x(2,3)-[DE]-x(2,3)-Y) en la proteína Wel1E entre las posiciones R164-Y172.

Glicosiltransferasas

Las glicosiltransferasas forman la región variable de los *clusters eps*. En los *clusters eps* de CUPV237 encontramos un total de 12 GT posibles (Tabla 2.2). Cuatro GT pertenecen a la superfamilia GTB (cl10013) y otras cuatro a la superfamilia GTA (cl11394). Una de las proteínas GTA es WelF3, cuyo gen parece estar incompleto. El resto de GT pertenecen a las superfamilias Gly_tranf_sug (cl19952), Stealth_CR2 (cl15596), Caps_synth (cl26275) y Glyco_tranf_2_3 (cl26112).

Las proteínas GTA y -B catalizan la transferencia de un residuo de azúcar a una molécula aceptora (lípido, proteína, u otro carbohidrato) formando un enlace O-glicosídico (<https://www.ncbi.nlm.nih.gov/Structure/cdd/cddsrv.cgi?uid=cl11394>). El resto de GT pertenecerían a las superfamilias Gly_tranf_sug (cl19952), Stealth_CR2 (cl15596), Caps_synth (cl26275) y Glyco_tranf_2_3 (cl26112). La Gly_tranf_sug (cl19952), contiene un dominio conservado con el motivo Dx D, relacionado con la adición de carbohidratos a otros carbohidratos, grupos fosfato u otras proteínas (<https://www.ncbi.nlm.nih.gov/Structure/cdd/cddsrv.cgi?uid=cl19952>). Las proteínas Stealth_CR2 (cl15596) se vinculan a la existencia de grupos fosfato en los polisacáridos, principalmente de bacterias patógenas debido a que son D-hexosa-1-fosforil transferasas, y también catalizan enlaces fosfodiéster

interglucosídicos (Sperisen et al., 2005). Las proteínas de la superfamilia Caps_synth (https://www.ncbi.nlm.nih.gov/Structure/cdd/cddsrv.cgi?uid=cl26275) y Glyco_tranf_2_3 (https://www.ncbi.nlm.nih.gov/Structure/cdd/cddsrv.cgi?uid=cl26112) están relacionadas con polisacáridos capsulares.

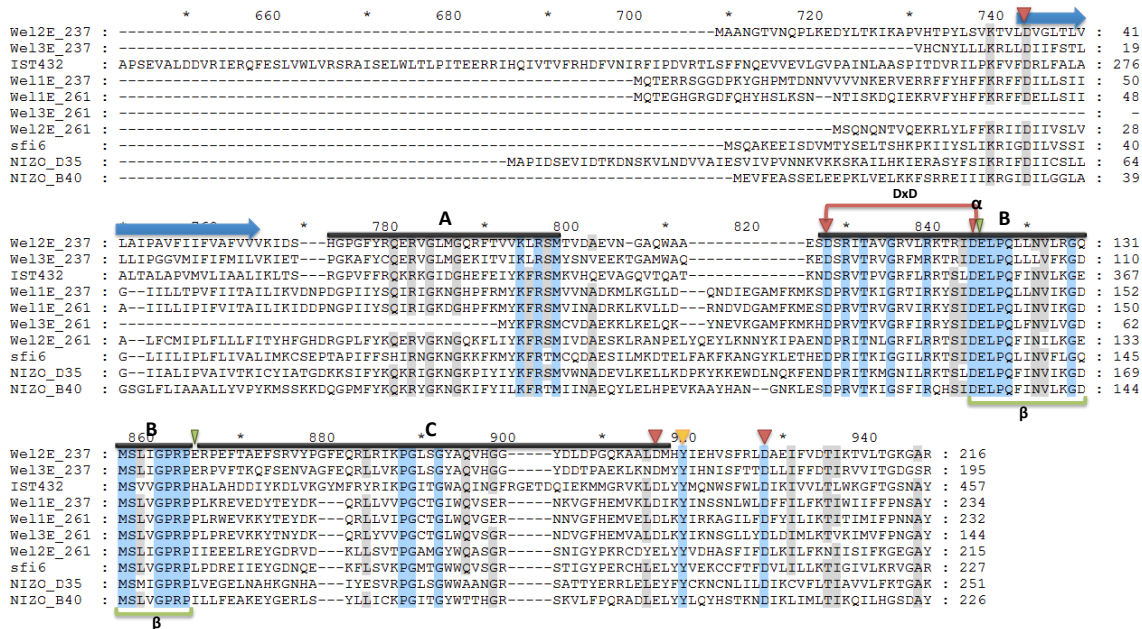


Figura 2.8. Estudio predictivo de las secuencias de las proteínas glicosiltransferasas iniciadoras WelE encontradas en los clusters eps de *L. collinoides* CUPV237 y *L. sicerae* CUPV261^T. Se muestra el alineamiento de las pGT (CLUSTALW) de: We1E_237 (CUPV237); We1E_261 (CUPV261^T); NIZO_D35, (EpsD de *Lactococcus lactis* subsp. *cremoris* NIZO D35, RS: AAD22526.1); NIZO_B40, (EpsD de *Lactococcus lactis* subsp. *cremoris* NIZO B40, NP_053030.1); sfi6 (EpsE de *Streptococcus thermophilus* sfi6, AAC44012.1); IST432, (BceB de *Burkholderia cenocepacia* IST432, ABC71344.1). Con una franja negra están marcados los tres bloques funcionales (A, B y C) (van Kranenburg et al., 1999); la flecha azul indica la posición aproximada de las hélices transmembrana predichas en las secuencias WelE de CUPV237, situando la punta de la flecha hacia el espacio extracelular; α, indica el sitio de interacción con el catión divalente Mg²⁺ (Patel et al., 2010); β, enmarca a la región conservada del bloque B; los triángulos rojos indican los residuos conservados de aspartato (D), los verdes los de glutamato (E), y el amarillo, una tirosina conservada y sitio de fosforilación (Minic et al., 2006); DxD corresponde con un motivo catalítico (Videira et al., 2005).

Wzx

Se encontraron dos posibles genes *wzx* en los clusters *eps2* y *eps4*, que podrían codificar proteínas flipasas con una función de transporte de la unidad repetitiva a través de la membrana. Actualmente, se conoce que Wzx es una proteína multitransmembrana con una enorme diversidad en su secuencia, y exporta oligosacáridos con diferentes grados de preferencia (Hong et al., 2018).

La comparación entre las secuencias de Wzx mostró un 32 % de identidad entre ellas (valor-e de 1e⁻⁶⁵). Según el programa informático utilizado para realizar las

predicciones en base a la hidrofobicidad de sus secuencias de aminoácidos predichos, cada una podría contener de 12 a 14 HTM (Figura 2.9).

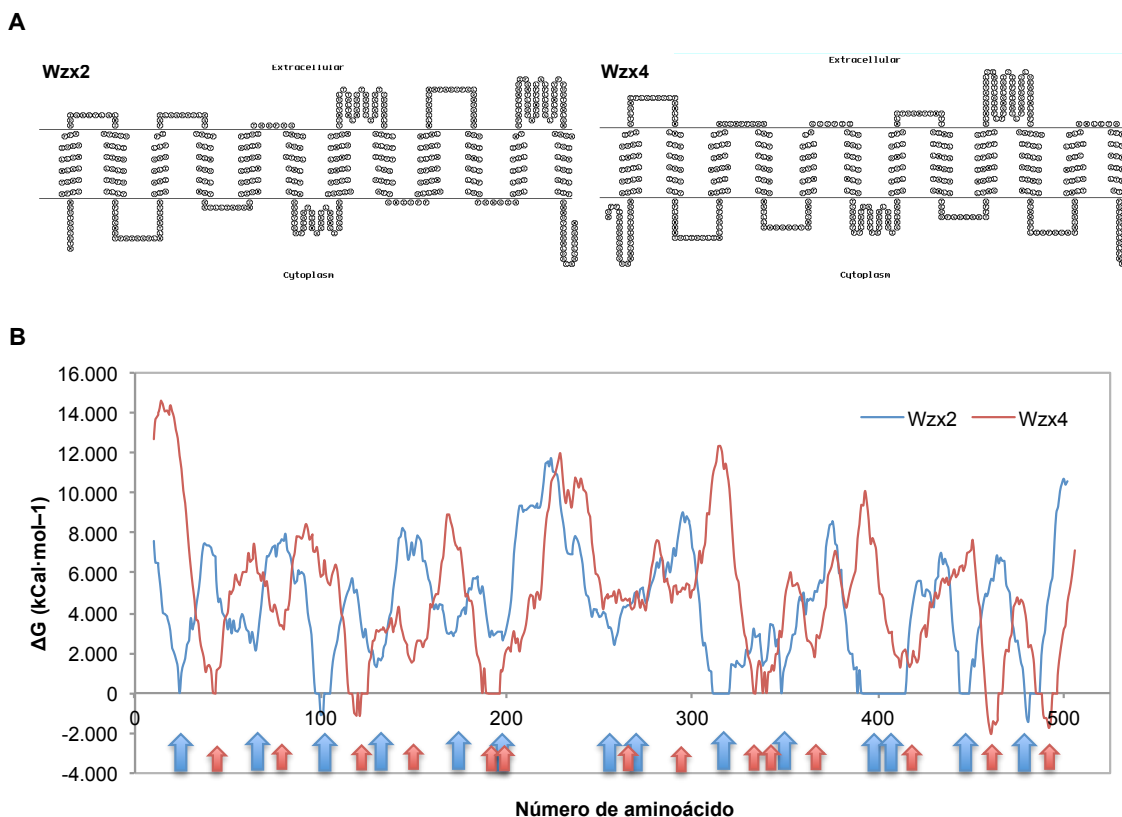


Figura 2.9. Estudio predictivo de las secuencias de la proteína flipasa Wzx. A, modelado de las posibles proteínas Wzx2 y Wzx4 de *L. collinoides* CUPV237, mediante SACs MEMSAT; **B**, perfil de las energías libres de Gibbs (ΔG) de la secuencia de aminoácidos obtenidas con TopCons, las flechas indican la predicción de la posición de la hélice transmembrana.

Wzy

La proteína de membrana Wzy se encarga de polimerizar la unidad repetitiva en la cadena naciente de EPS y se sitúa en la cara externa de la membrana (Wang et al., 1996). El genoma de CUPV237 contiene dos posibles genes relacionados con proteínas polimerasas. Estos genes están localizados en los *clusters eps1* y *-2*, y no se detectaron en ellos dominios conservados (Tabla 2.2).

Los resultados obtenidos en BlastP, mostraron que Wzy1 presenta una identidad en torno al 63 % con proteínas polimerasas de las especies *L. plantarum*, *L. helveticus*, *L. kefiranofaciens* o *L. sakei* entre otras. El mismo análisis en Wzy2 mostró una similitud del 100 % con *L. collinoides* DSM20515, además del 38 % con la proteína hipotética de *L. hokkaidonensis* (RS: WP_041092334.1), y del 24 % con una

polimerasa de *Streptococcus pneumoniae* (WP_061388839.1). Por otro lado, los modelos de predicción del perfil hidrofóbico de la proteína predicha Wzy1, exhibieron hasta 11 posibles HTM (Figura 2.10), además de un péptido señal en el extremo amino, mientras que en la secuencia de Wzy2 se identificaron hasta 12 HTM.

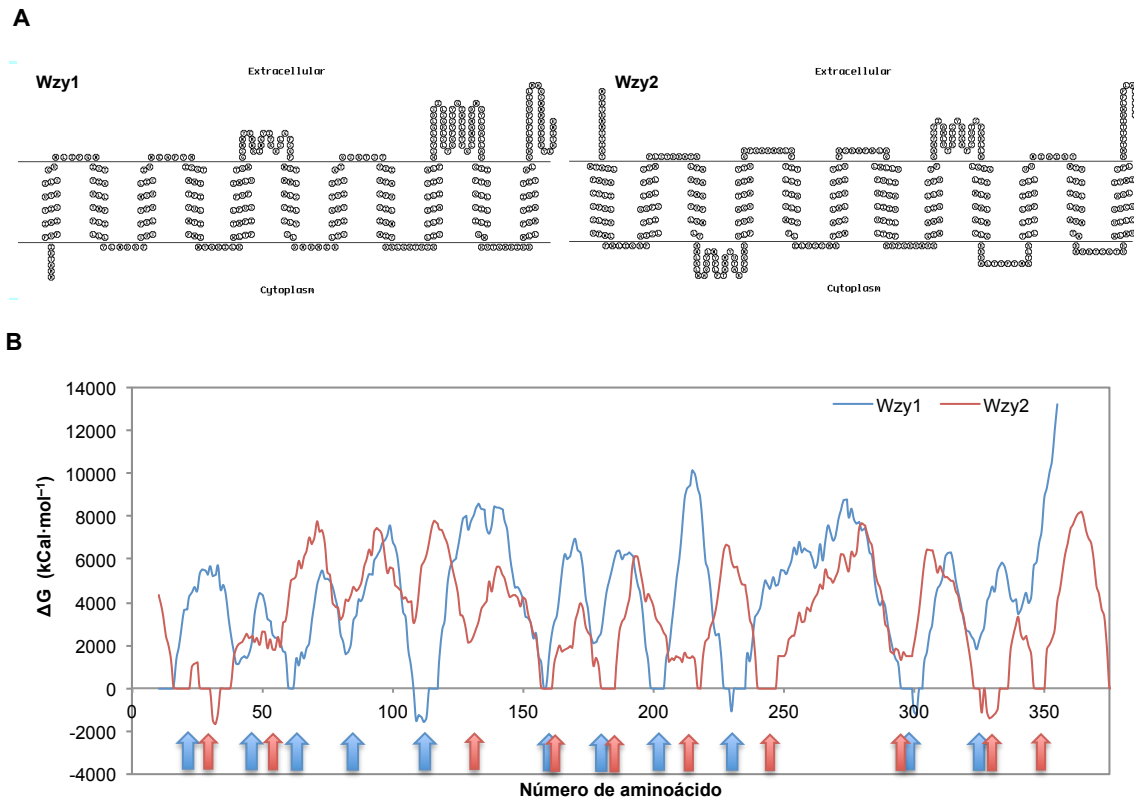


Figura 2.10. Estudio predictivo de las proteínas Wzy1 y -2, basada en sus perfiles de hidrofobicidad. A, modelado de las posibles proteínas Wzy de *L. collinoides* CUPV237, mediante SACs MEMSAT; **B,** representación gráfica del perfil de las energías libres de Gibbs (ΔG) de la secuencia de aminoácidos obtenidas con TopCons, las flechas indican la predicción de la posición de la hélice transmembrana.

ORF desconocida

Encontramos un posible gen de función desconocida en el *cluster eps4* con la pauta de lectura alterada. Esta ORF1 podría contener entre 9 y 11 HTM, mostrándola como una proteína de membrana (Figura 2.11). Además, su secuencia presenta una identidad de entre el 56 y el 60 % con proteínas hipotéticas sin función anotada de *L. pentosus*, *L. brevis* o *L. plantarum*. El análisis de los dominios conservados la relacionó con proteínas de la familia EpsG (pfam14897), identificadas como glicosiltransferasas de membrana.

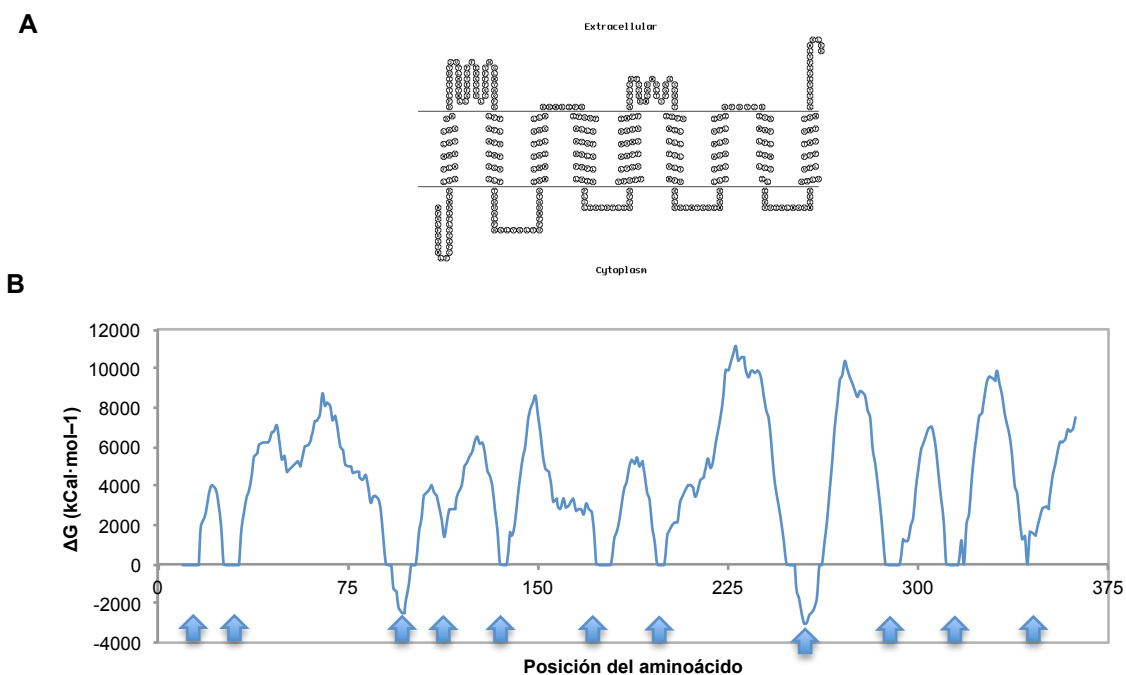


Figura 2.11. Estudio predictivo de la proteína ORF1 del *cluster eps4* basada en su perfil de hidrofobicidad. A, modelado de la secuencia de aminoácidos de ORF1 de *L. collinoides* CUPV237, mediante SACs MEMSAT; **B**, representación gráfica del perfil de las energías libres de Gibbs (ΔG) de la secuencia de aminoácidos obtenidas con TopCons, las flechas indican la predicción de la posición de la hélice transmembrana.

3.3 Genes precursores de la síntesis de EPS en CUPV237

Con respecto a los precursores de la síntesis de EPS, encontramos compuestos de diferente naturaleza entre los que se encuentran: UDP-Glc, UDP-Gal, dTDP-L-Rha, UDP-*N*-acetilglucosamina, UDP-*N*-acetilgalactosamina y UDP-*N*-acetilmanosamina, así como el ácido UDP-galacturónico, acetil-CoA, piruvato, CDP-glicerol o el lípido C55-P (Figura 2.12). *L. collinoides* CUPV237 utiliza para su crecimiento los azúcares arabinosa, ribosa, xilosa, galactosa, glucosa, fructosa, salicina, maltosa, melibiosa y gluconato (Tabla 1.2). Probablemente, a partir de todos estos carbohidratos, CUPV237 no sintetiza azúcares nucleótido para la biosíntesis del EPS, sino que pueden destinarse a la biosíntesis de componentes de membrana, y son considerados esenciales para el crecimiento de la bacteria (Boels et al., 2001). Predictivamente, en el genoma de *L. collinoides* se encontraron diferentes genes que corresponderían con proteínas implicadas en la formación de UDP-azúcares y que se indican a continuación:

Se encontraron dos copias del gen posible de la glucosa-6-fosfato mutasa Pgm (EC 5.3.1.9), la cual cataliza la transformación reversible de Glc-6-P a Glc-1-P (Figura 2.12). También se detectaron los genes necesarios para completar la ruta

metabólica de las pentosas fosfato. En esta la ruta se produce entre otras moléculas acetil-CoA, que es el donador del grupo acetilo utilizado en la formación de los UDP-acetil aminoazúcares.

Por otro lado, la glucosa-6-fosfato isomerasa Pgi (EC 5.3.1.9), convierte la Glc-6-P en Fru-6-P (Figura 2.12). Se encontraron dos genes *pgi* con una identidad del 87 % entre sí. En la formación de UDP-*N*-acetil-glucosamina intervienen las enzimas GlmS (EC 2.6.1.16), GlmM (EC 5.4.2.10), GlmU (EC 2.7.7.23 y EC 2.3.1.157), cuyos genes se encontraron en el genoma de CUPV237, y además se necesita Acetil-CoA. Esta UDP-*N*-acetilglucosamina puede ser utilizada para producir tanto polisacáridos exocelulares, como componentes de la pared celular, ácidos teicóicos o peptidoglicano. En el genoma encontramos una copia del gen que codificaría la UDP-*N*-acetilglucosamina 4-epimerasa NagE (EC 5.1.3.14) para la conversión a UDP-*N*-acetilgalactosamina y la UDP-*N*-acetilglucosamina 2-epimerasa MnaA, (EC 5.1.3.14) para producir UDP-*N*-acetilmanosamina.

También se localizaron los genes relacionados con el metabolismo de la galactosa, la ruta Leloir o galactogénesis, y que codifican las proteínas GalT (EC 2.7.7.10), GalK (EC 2.7.1.6) y (GalE EC 5.1.3.2) (Figura 2.12). Estos genes se agruparían en un mismo *cluster*, con una copia en el genoma de *L. collinoides*. Además, se hallaron cuatro genes homólogos de GalU (EC 2.7.7.9), dos de estos se encontraron en el *eps4* muy próximos entre sí, aunque una de las secuencias contiene varias interrupciones en su marco de lectura. Por otro lado, también se encontró tres copias de los genes necesarios para la formación de UDP-Galp a partir de UDP-Glc (GalE, EC 5.1.3.2), y para la formación de UDP-Galf a partir de UDP-Galp (Glf, EC 5.4.99.9).

En el genoma de CUPV237 se detectó una copia de cada gen posible necesario para la formación de CDP-glicerol a partir del 3-fosfoglicerato (GAP) (Figura 2.12). En esta ruta, la actividad secuencial de las proteínas Tpi (EC 5.3.1.1), GpsA (EC 1.1.1.94) y TagD (EC 2.7.7.39) da lugar a CDP-glicerol.

Por último, para la formación del intermediario dTDP-L-Rha interviene la transferasa RmlA (EC 2.7.7.24), la deshidratasa RmlB (EC 4.2.1.46), la epimerasa RmlC (EC 5.1.3.13) y la reductasa RmlD (EC 1.1.1.133) (Graninger et al., 1999). En el genoma de CUPV237 se observó una copia de cada posible gen relacionado con cada una de estas enzimas localizadas en el cluster *eps4*.

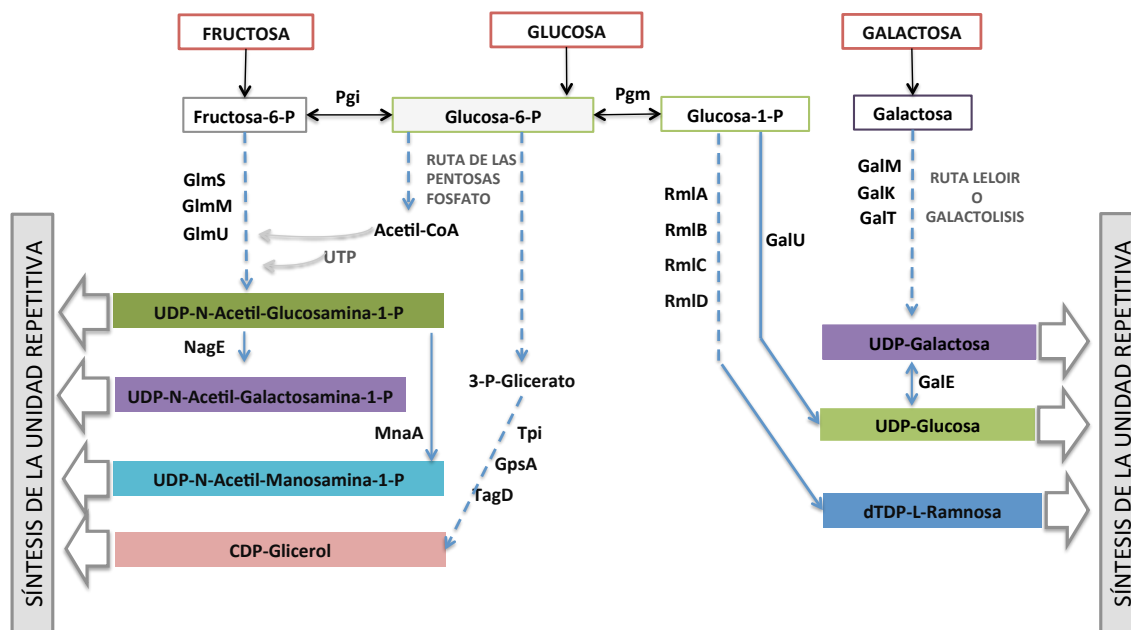


Figura 2.12. Rutas para la formación de los precursores necesarios en la síntesis de EPS, deducidas a partir del análisis genómico de *Lactobacillus collinoides* CUPV237. Pgi (RS: KZL38943.1, KZL40223.1); Pgm (KZL35972.1); GlmS (KZL39182.1), GlmM (KZL39183.1), GlmU (KZL41703.); GalT (KZL35969.1), GalK (KZL35971.1), GalE (KZL35970.1; KZL35614.1 (WP_056995942.1); GalU (WP_082820862.1, KZL41498.1, KZL42815.1; KRL79635.1); GalM (KZL41063.1, KZL43334.1, KZL37607.1); Gif (KZL41075.1); NagE; MnaA (KZL41455.1); RmlA (KZL41394.1); RmlB (KZL41396.1); RmlC (KZL41395.1); RmlD (KZL41397.1); Tpi (KZL41520.1); GpsA (KZL41535.1); TagD (KZL41459.1).

3.4 Genes relacionados con la síntesis de EPS en *L. sicerae* CUPV261^T

Para el análisis *in silico* de los genes *eps* en CUPV261^T se utilizaron los *contigs* de DNA obtenidos a partir de la secuenciación parcial del genoma, realizada para el ensayo ANI descrito en el capítulo 1. Predictivamente, se detectaron genes *eps* en 8 de los *contigs* (Tabla 2.3), los cuales codificarían las proteínas: regulador transcripcional (1), tirosina quinasa (4), tirosina fosfatasa (2), glicosiltransferasa iniciadora de la síntesis (3), glicosiltransferasa (9), flipasa (1) y precursores de la síntesis (1), además de genes de transposasa (3). No se detectaron genes *eps* de polimerasas (*wzy*), aunque podrían situarse en la porción no secuenciada del genoma. En la anotación rápida del genoma parcial realizada por RAST, tampoco se encontraron genes correspondientes con enzimas sintasas o glicosil-hidrolasas.

El análisis mediante Blast de las secuencias de las proteínas predichas de los posibles genes *eps* encontrados en CUPV261^T (Tabla 2.3), mostró proteínas relacionadas con genes reguladores en los *contigs* 3 y 225, con identidades de entre

el 70 y el 98 % con proteínas de *L. collinoides*, *L. paracollinoides*, *L. buchneri* y *L. sunkii*, y *L. vini*, respectivamente. Se encontraron posibles genes de pGT en tres *contigs* diferentes, una de ellas relacionada con una proteína de *L. sunkii* (99 % de identidad), y dos con *L. vini* (93 %). Por otro lado, se encontraron identidades superiores al 87 % entre las GT predichas y GT de las especies *L. plantarum* y *L. nuruki* (*contig* 6), *L. buchneri* (*contig* 52), *L. vini* (*contigs* 189 y 229), e inferiores al 55 % de identidad con *L. satsumensis* y *L. murinus* (*contig* 232). También se localizó un gen *wzy* con un 99 % de identidad con una flipasa de *Pediococcus damnosus*, y un gen *galU* con un 99 % con una proteína de *L. nuruki*. Además, se detectaron tres transposasas en tres *contigs* (6, 52 y 146), con identidades superiores al 95 % con proteínas de *L. sakei*, *L. hordei* y *L. plantarum*.

Las secuencias de las proteínas correspondientes con los posibles genes *eps* encontrados en CUPV261^T, se compararon con las proteínas posibles de los *clusters eps1*, -2, -3 y -4 de *L. collinoides* CUPV237 (Tabla 2.3). Se observó una identidad entre el 99,5 y el 70 % con las secuencias del *contig* 3 de *L. sicerae* y las posibles proteínas del *cluster eps1* de *L. collinoides*. Además, en RAST se observó que aguas arriba del gen *galU1* se situarían los genes *znuB* (COG1108, pfam00950), *znuC* (COG1121, pfam00005), *tpn* ISL3 (COG3464, pfam13542) y *znuA* (COG0803, pfam01297), y que estarían relacionados con una permeasa de membrana tipo ABC y una transposasa. Los tres genes *znu* mostraron una identidad superior al 99 % con los genes *znu* encontrados aguas arriba del *cluster eps1* de CUPV237.

Tabla 2.3. Relación de genes encontrados en la secuenciación parcial y no ensamblada del genoma de *L. sicerae* CUPV261^T.

Contig y genes	Longitud proteína (aa)	^a Función predicha	^b Número de HTM	Dominio conservado (valor-e) / Superfamilia	Bacteria / Proteína con la mayor identidad, RS (valor-e)	Identidad de los aminoácidos (%)	^c Identidad con CUPV237 (%)
3							
<i>galU</i>	310	UTP–glucosa–1–fosfato uridiltransferasa	0	GalU (4,13e ⁻¹⁶⁹) COG1210/ Glyco_tranf_GTA_Type cl11394	<i>L. collinoides</i> DSM20515 KRM74556.1 (0,0)	89	GalU1 (99,03)
<i>wzr</i>	325	Regulador transcripcional	1	LytR (3,10e ⁻⁷⁶) PRK09379/ LytR_CpsA_psr cl00581	<i>L. paracollinoides</i> WP_083224292.1 (2e ⁻¹⁶⁵)	75	Wzr1 (97,85)
<i>wzd</i>	286	Determinación de la longitud de la cadena	2	Yvek (2,96e ⁻⁴⁰) COG3944/ GNVR cl26080	<i>L. paracollinoides</i> WP_054711923.1 (6e ⁻¹⁴⁵)	70	Wzd1 (97,20)
<i>wze</i>	247	Tirosina kinasa autokinasa	0	eps_fam (6,61e ⁻⁶¹) TIGR01007/ P_loop_NTPasa cl21455	<i>L. buchneri</i> WP_003561315 (3e ⁻¹⁷⁴)	98	Wze1 (96,93)
<i>wzb</i>	254	Tirosina fosfatasa	0	YwqE (9,27e ⁻⁷¹) COG4464/ PHP cl23724	<i>L. sunkii</i> WP_070368065 (5e ⁻¹⁷⁵)	92	Wzb1 (87,29)
<i>welE</i>	232	Glicosiltransferasa iniciadora	1	Bac_transf (4,12e ⁻⁸⁴) pfam02397/ Bac_Transf cl27431	<i>L. sunkii</i> WP_070368066 (1e ⁻¹⁶⁷)	99	WelE1 (71,37)
6							
<i>welF</i>	358	Glicosiltransferasa	0	GT1_cap1E_like (6,36e ⁻⁶¹) cd03808/ Glycosyltransferase_GTB_type cl10013	<i>L. plantarum</i> WP_105316413.1 (0,0)	99	-
<i>welG</i>	371	Glicosiltransferasa	0	GT1_cap1E_like (1,62e ⁻¹¹⁷) cd03808/ Glycosyltransferase_GTB_type cl10013	<i>L. plantarum</i> WP_103851980.1 (0,0)	99	-
<i>welH</i>	361	Glicosiltransferasa	0	GT1_capH_like (3,61e ⁻¹¹⁰) cd03812/ Glycosyltransferase_GTB_type cl10013	<i>L. nuruki</i> WP_102197015.1 (0,0)	99	-
<i>orf1</i>	384	-	7	-	<i>L. nuruki</i> WP_102197010.1 (0,0)	98	-
<i>welI</i>	335	Glicosiltransferasa	0	Glycos_transf_2 (2,17e ⁻³²) pfam00535/ Glyco_transf_GTA cl11394	<i>L. nuruki</i> WP_102197009.1 (0,0)	98	-
<i>Tpn</i>	251	Transposasa	0	Transposase_mut (2,08e ⁻⁷⁵) pfam00872/ Transposase_mut cl27632	<i>L. plantarum</i> WHE 92 EYR70495.1(2e ⁻¹⁷⁵)	98	-
52							
<i>welF</i>	327	Glicosiltransferasa	0	Stealth_CR2 (5,92e ⁻⁴⁸) pfam11380/ Stealth CR2 cl15596	<i>L. buchneri</i> WP_003561329.1 (0,0)	99	-
<i>tpn</i>	93	Transposasa IS30	0	Tra8 (4,27e ⁻²⁶) COG2826/ Tra8 cl28104	<i>L. sakei</i> WP_004271217 (2e ⁻⁶³)	99	-

Contig y genes	Longitud proteína (aa)	^a Función potencial	^b Número de HTM	Dominio conservado (valor-e) / Superfamilia	Bacteria / Proteína con la mayor identidad, RS (valor-e)	Identidad de los aminoácidos (%)	^c Identidad con CUPV237 (%)
<i>wzx</i>	516	Flipasa	12	MATE_Wzx_like (8,86e ⁻⁰⁸) cd13128/ MATE_like cl09326	<i>Pediococcus damnosus</i> WP_100078227.1 (0,0)	99	Wzx4 (40,97)
146							
<i>welF</i>	290	Glicosiltransferasa	0	Glycos_transf_2 (1,16e ⁻²³) pfam00535/ Glyco_transf_GTA cl11394	<i>L. vini</i> WP_034992479.1 (2e ⁻¹⁶²)	74	-
<i>tpn</i>	456	Transposasa familia IS4	0	DDE_5 (3,70 ⁻¹⁰) pfam13546/ DDE_5 cl17874	<i>L. hordei</i> DSM19519 KRL03996.1 (0,0)	95	-
189							
<i>welF*</i>	122	Glicosiltransferasa	0	DUF4422 (4,01e ⁻⁴⁹) pfam14393/ DUF4422 cl16851	<i>L. vini</i> WP_034992922.1 (1e ⁻⁶⁶)	88	-
<i>welE</i>	215	Glicosiltransferasa iniciadora	1	Bac_transf (6,11e ⁻⁸³) pfam02397/ Bac_Transf cl27431	<i>L. vini</i> WP_010581115.1 (1e ⁻¹⁴⁷)	93	-
225							
<i>wzd*</i>	57	Determinación de la longitud de la cadena	-	-	<i>L. vini</i> WP_034994003.1 (6e ⁻²⁶)	89	Wzd3 (39,62)
<i>wze*</i>	253	Tirosina kinasa autokinasa	0	eps_fam (3,88e ⁻⁵⁸) TIGR01007/ P_loop_NTPasa (cl21455)	<i>L. vini</i> WP_034994000.1 (6e ⁻¹⁷⁸)	95	Wze3 (50,86)
<i>wzb</i>	267	Tirosina fosfatasa	0	YwqE (2,50e ⁻⁶⁰) COG4464/ PHP cl23724	<i>L. vini</i> WP_010579464.1 (1e ⁻¹⁸⁰)	92	Wzb3 (46,06)
229							
<i>welF</i>	233	Glicosiltransferasa	0	GT1_amsD_like (1,23e ⁻²⁶) cd03820/ GTB cl10013	<i>L. vini</i> WP_010579590.1 (7e ⁻¹⁴⁸)	87	-
232							
<i>welG</i>	284	Glicosiltransferasa	0	Glycos_transf_2_4 (2,60e ⁻¹⁷) pfam13704/ Glyco_transf_GTA cl11394	<i>L. satsumensis</i> WP_056960644.1 (9e ⁻⁷⁸)	47	-
<i>welF</i>	254	Glicosiltransferasa	0	DUF4422 (1,66e ⁻⁹⁷) pfam14393/ DUF4422 cl16851	<i>L. murinus</i> WP_112194069.1 (5e ⁻⁹⁵)	55	-
<i>welE*</i>	216	Glicosiltransferasa iniciadora	-	Bac_transf (1,28e ⁻⁷²) pfam02397/ Bac_transf cl27431	<i>L. vini</i> WP_057870782 (1e ⁻¹⁴⁷)	93	-

(a) Función predicha en base a los resultados obtenidos en las comparaciones de los genes *eps* en la base de datos NCBI con la función BlastX y el análisis de los dominios conservados, además de la información derivada por la anotación de RAST.

(b) HTM, indica el número de hélices transmembrana predichas en los modelos bioinformáticos obtenidos en los programas TMPred, TMHMM y SACs MEMSAT.

(c) Comparación entre las secuencias de las proteínas predichas de CUPV237 y CUPV261^T mediante RAST.

(*) Secuencias incompletas o con la pauta de lectura alterada.

4. DISCUSIÓN

Los exopolisacáridos producidos por las bacterias lácticas muestran una gran variedad en su composición (HoPS o HePS), que está directamente relacionada con su mecanismo de producción (Zeidan et al., 2017). La presencia de genes *eps* en las cepas de *L. sicerae* (2) y *L. collinoides* (12) procedentes de los aislamientos del 2009, fue estudiada mediante PCR. A partir de los resultados obtenidos, se descartó la presencia de los genes de HoPS relacionados con la glicosiltransferasa GTF responsable de la síntesis de (1,3)(1,2)- β -D-glucano (Werning et al., 2006), con dextranacarasas (*deg*) o levansacarasas (*lev*) (Puertas et al., 2018).

La detección de la presencia de genes implicados en la síntesis de HePS, se llevó a cabo utilizando varias parejas de cebadores (*epsD/E*, *epsA*, *epsB*, *epsEFG*, *epsF*) previamente descritos (Ibarburu et al., 2015). Se obtuvo una banda de 200 pb aproximadamente, que corresponde con una porción del gen de la pGT (Provencher et al., 2003) (Figura 2.1, panel inferior). Esta enzima es fundamental en el inicio de la biosíntesis del oligosacárido estructural de la cadena de EPS, anclando el primer residuo de la unidad repetitiva al lípido C55-P en la cara citoplásmica de la membrana (Lebeer et al., 2009). Las secuencias parciales de la proteína WeIE presentaron identidades entre el 83 y el 66 % con secuencias parciales de proteínas pGT descritas por los autores Mozzi et al. (2006) y Dan et al. (2009). Las secuencias de las proteínas pGT se caracterizan por diferenciarse en bloques funcionales, donde los bloques A y B participan en la interacción con el lípido *carrier* C55-P, y el bloque C con labores de glicosiltransferasa en *Salmonella entérica* (Wang et al., 1996). Las secuencias de aminoácidos predichas a partir de los productos de PCR, mostraron parte de los bloques conservados B y C (Figura 2.1), que se localizan en el extremo carboxilo de la pGT, similar a lo descrito en bacterias productoras de HePS de los géneros *Lactobacillus* y *Bifidobacterium* (Provencher et al., 2003; Ruas-Madiedo et al., 2007).

Los resultados anteriores sugieren que las cepas de *L. collinoides* y *L. sicerae* aisladas en la campaña 2009 sintetizan heteropolisacáridos. Con estos antecedentes, se realizó posteriormente un estudio *in silico* de los genomas de *L. collinoides* CUPV237 y *L. sicerae* CUPV261^T para la detección de genes *eps* y la descripción de sus secuencias predichas de proteína, implicadas en la síntesis de HePS.

La capacidad de formación de HePS está habitualmente mediada por *clusters* genéticos cuya organización está muy conservada (Zeidan et al., 2017). En el genoma no ensamblado de *Lactobacillus collinoides* CUPV237 se describieron predictivamente

cuatro posibles *clusters* relacionados con la síntesis de polisacárido. Estos *clusters* albergarían enzimas relacionadas con la síntesis de HePS características de una ruta biosintética Wzy-dependiente. En ellos se encontraron genes relacionados con funciones de regulación, de síntesis de la unidad repetitiva, de exportación y polimerización, además, de genes relacionados con la formación de dNDP-azúcares, todos ellos son fundamentales para la biosíntesis de HePS en las BAL (Stingele et al., 1996; Laws et al., 2001; Berger et al., 2007; Lebeer et al., 2009; Horn et al., 2013; Zivkovik et al., 2015; Hidalgo-Cantabrana et al., 2015; Caggianiello et al., 2016; Zeidan et al. 2017).

Los *clusters eps2* y -3 contienen genes que codificarían proteínas con una identidad cercana al 100 % con proteínas de *L. collinoides* DSM20515 y que incluso mantienen el mismo orden génico, aunque no se ha descrito la producción de HePS en esta bacteria. Por otro lado, los *clusters eps1* y -4 mostraron una similitud elevada con proteínas relacionadas con la síntesis de HePS de lactobacilos heterofermentativos (*L. parabuchneri*, *L. buchneri*, *L. paracollinoides*, *L. plantarum* o *L. pentosus*). En vista de lo encontrado en CUPV237 y DSM20515, estas proteínas parecen estar altamente conservadas entre cepas de la misma especie o próximas filogenéticamente, como se observó en la especie *Lactobacillus paracasei* (Noda et al., 2018).

Los *clusters eps* de CUPV237 por separado no contienen todos los genes necesarios para la síntesis de polisacárido exocelular. Sólo los *clusters eps1* y -3 poseen todos los genes reguladores (*wzr*, *wzd*, *wze* y *wzb*, Figura 2.2), y solo en los *eps1*, -2 ó -4 se encontraron los genes predichos de flipasa o polimerasa. La producción de EPS podría explicarse entonces, si aparece una función cooperativa entre estos *clusters eps*, tal y como se ha sugerido para los *clusters* responsables de la síntesis de HePS de *L. paracasei* IJH-SONE68 (Noda et al., 2018) y de *Lactobacillus plantarum* TMW 1.1478 (Prechtel et al., 2018). Además, es habitual encontrar secuencias de inserción o transposasas formando parte de los *clusters eps* de CUPV237 (Tabla 2.2) o en las proximidades de ellos, como ha sido descrito por otros autores (Bentley et al., 2006; Berger et al., 2007; Lebeer et al., 2009; Remus et al., 2012; Noda et al., 2018). La presencia de estas secuencias nos sugiere una posible fragmentación de estos *clusters* a causa de fenómenos de transposición.

Por otro lado, predictivamente se han podido identificar y relacionar los *genes eps* posibles de CUPV237 con las proteínas predichas que corresponden, no solo por

la identificación realizada en Blast o RAST, sino también por contener los motivos catalíticos o característicos de dichas proteínas que han sido descritos en otros trabajos. El gen *wzr* es ortólogo del gen *epsA*, el cual funciona como un regulador positivo o activador de la síntesis de HePS (Dertli et al., 2013; Cieslewicz et al., 2001), y codifica proteínas pertenecientes a la familia LytR-Cps2A-Psr (Eberhardt et al., 2012). En *Streptococcus aureus*, a estas proteínas se les ha atribuido una función de anclaje de un glicopolímero a la pared celular (Chan et al., 2014; Schaefer et al., 2017), sin encontrar evidencias de que funcione como un regulador transcripcional en *Streptococcus agalatae* (Toniolo et al., 2015). En las posibles proteínas Wzr2 y -3 predictivamente se encontró una HTM próxima al extremo N-terminal, situándolas en la membrana celular al igual que ocurre en la proteína Cps2A de *Streptococcus pneumoniae* (Morona et al., 2000; Eberhardt et al., 2012). Las dos proteínas Wzr de CUPV237 mostraron una identidad elevada (en torno al 70 %) con reguladores transcripcionales de otras especies de *Lactobacillus*. El efecto de la proteína Wzr en la biosíntesis del EPS de CUPV237 no está claro, ya que su proteína ortóloga CpsA de *Streptococcus pneumoniae* tiene una implicación directa en la formación de cápsula mediante la unión del EPS al peptidoglicano (Eberhardt et al., 2012). Sin embargo, en CUPV237 no se observó la formación de cápsula como se aprecia en la microfotografía de la Figura 3I B.

Con respecto a las proteínas fosforreguladoras, se han descrito en *L. rhamnosus* tres proteínas que desempeñan un papel de control de la producción de HePS: Wzb (tirosina fosfatasa), Wzd (modulador transmembrana de la tirosina proteína quinasa) y Wze (fosfotirosina quinasa) (Kang et al., 2015). Predictivamente, en el caso de CUPV237, los genes que las codifican se han localizado en los *clusters eps1* (Wzd, -e y -b), *eps2* (Wzd) y *eps3* (Wzb, -d y -e). Encontramos identidades elevadas (>70 %) entre sus secuencias predichas de aminoácidos y las de otras especies de *Lactobacillus*. Tal y como han descrito otros autores, los genes reguladores permanecen muy conservados en diferentes especies de BAL (Zeidan et al., 2017, Prechtel et al., 2018). En las dos posibles proteínas Wze de CUPV237 se han podido localizar predictivamente los motivos Walker A y B, así como una región C-terminal rica en glicinas y tirosinas (GY)₇ (Figura 2.5). Estas tres regiones se han observado en la proteína CpsD de *St. pneumoniae* (Morona et al., 2000), y son necesarias para una actividad autokinasa (Mijakovik et al., 2003). Las proteínas Wzd de CUPV237 contienen predictivamente 2 HTM (Figura 2.6), y son identificadas en Blast y RAST como tirosinas kinasas implicadas en la determinación de la longitud de la cadena, al igual que se ha descrito en la Wzd de *L. rhamnosus* (Lebeer et al., 2009).

Sin embargo, en las secuencias de Wzd1, -2 y -3, no encontramos correspondencia con la tirosina conservada Y266 del extremo C-terminal de *L. rhamnosus* RW-9595M, importante para la fosforilación de Wzd (Kang et al., 2015). Se ha sugerido que parece estar implicada más de una tirosina en la función asignada a esta proteína (Kang et al., 2015). En las secuencias predichas de Wzd de CUPV237 se encontraron los residuos de tirosina que corresponden con Y33 e Y77 de *Streptococcus pneumoniae*, cuya mutación provocó una disminución de la cantidad de CPS total producido por la bacteria (Morona et al., 2006).

Por último, en CUPV237 se observaron dos posibles tirosinas fosfatasas Wzb1 y -3 pertenecientes a la superfamilia de las histidinol fosfatasas-2 (PHP), en cuyas secuencias predichas se localizaron los motivos que darían funcionalidad a la misma y que han sido descritos por otros autores (Lapointe et al., 2008; Kim et al., 2011). Estas proteínas, fueron identificadas en los análisis de Blast como proteínas kinasas fosfatasas con una identidad superior al 85 % con fosfatasas de otras especies de lactobacilos (Wzb1: *Lactobacillus buchneri*, *Lactobacillus parabuchneri* y *Lactobacillus parafarraginis*; Wzb3: *Lactobacillus paracollinoides*). Mediante el alineamiento de Wzd1 y -3 con la proteína de *B. subtilis* YwqE se reconocieron predictivamente (Figura 2.6): (i) los residuos de arginina (R) correspondientes con la actividad catalítica (Kim et al., 2011; Hagelueken et al., 2009), (ii) los cuatro motivos presentes en las proteínas de la superfamilia PHP, (iii) las histidinas necesarias para la actividad fosfatasa localizadas en los motivos I y III (Lapointe et al., 2008) y (iv) se localizaron los bucles flexibles loop I y loop II alrededor del sitio activo, que en este tipo de proteínas (YwqE) son responsables de la conformación abierta o cerrada de la misma (Kim et al., 2011).

La producción de la unidad estructural del HePS se lleva a cabo en el interior de la célula debido a la disponibilidad de precursores y de GT (Wang et al., 1996). El análisis de los dominios conservados de las posibles proteínas Wel1E, -2E y -3E de CUPV237 permitió clasificarlas como proteínas pfam02397, al igual que las pGT de *Oenococcus oeni* y de otras bacterias, que han sido catalogadas como poliisoprenil-fosfato-hexosa-1-fosfato transferasas (PHPTs) (Dimopoulou et al., 2017). Como se ha descrito en las pGT de *Oenococcus oeni*, estas WelE son proteínas de menor tamaño (169-234 aminoácidos) que las encontradas en las especies patógenas *Streptococcus pneumoniae*, *Salmonella enterica* o *Escherichia coli* (>400) (Dimopoulou et al., 2017). En el estudio de las secuencias predichas de aminoácidos de las tres WelE, se localizaron los tres bloques funcionales (A, B y C) conservados,

descritos en *Salmonella enterica* (Wang et al., 1996) (Figura 2.8). El análisis de los perfiles de hidrofobicidad indicó la presencia de una HTM próxima al extremo N-terminal, y que sitúa a las pGT de CUPV237 en la membrana plasmática, tal y como se ha descrito en cepas de *L. rhamnosus* (Lebeer et al., 2009) u *Oenococcus oeni* (Dimopoulou et al., 2017). Además, en el extremo C-terminal de Wel1E y -2E, se identificó una segunda región de carácter hidrófobo observada en WbaP de *Salmonella enterica* (Wang et al., 1996). Las WelE de CUPV237 poseen el motivo catalítico DxD esencial para la actividad *priming*-glicosiltransferasa (Videira et al., 2005), además de un aspartato y un glutamato consecutivos relacionados con la coordinación del ion divalente, que es necesario para la adición del primer residuo de azúcar activado al lípido *carrier* C55-P (Patel et al., 2010) (Figura 2.8). Por otro lado, el trabajo de Minic et al. (2007) propone que el inicio de la síntesis puede implicar la activación de la pGT mediante la fosforilación de una tirosina conservada, cuyos residuos corresponden predictivamente con las tirosinas Y180, Y189 e Y168 de Wel1E, Wel2E y Wel3E, respectivamente.

La pGT inicia la construcción de la unidad repetitiva y le siguen de manera secuencial y ordenada las GT para añadir el resto de residuos que la constituyen. En los *clusters eps* de CUPV237 se localizaron predictivamente 12 GT. Se ha observado de manera habitual dentro de los *clusters eps* de diferentes cepas de *Lactobacillus*, e incluso de *Pseudomonas aeruginosa*, genes relacionados con GT de las superfamilias GTA y GTB como ocurre en CUPV237 (Friedman & Kolter, 2004; Lebeer et al., 2009; Horn et al., 2013; Zivkovic et al., 2015). Además, se encontró una glicosiltransferasa Stelth_CR2, estas enzimas están implicadas en la síntesis de polisacárido y se han descrito en bacterias con la función D-hexosa-1-fosforil transferasa. Estas GT también se han detectado en algunas BAL productoras de HePS: *Lactobacillus plantarum* WCFS1 (Cps2G), *Oenococcus oeni* PSU-1 o *Streptococcus thermophilus* NCFB 2393 (Cps5J) (Sperisen et al., 2005). Por otro lado, Wel1H y Wel2G de CUPV237 pertenecen a las superfamilias de glicosiltransferasas Gly_trans_sug y Caps_synth, que no han sido relacionadas hasta el momento por otros autores con la producción de EPS en bacterias. Aunque, Wel1H contiene el motivo DxD encontrado en múltiples GT de procariontes y de eucariotes (Wiggins & Munro, 1998; Jolly & Stingle, 2001).

Por otro lado, se han identificado en el genoma de CUPV237 posibles genes que codificarían enzimas relacionadas con funciones de exportación y polimerización. Entre ellas están dos polimerasas (Wzy1 y -2) que muestran identidades del 63 % o inferiores con otras Wzy de *Lactobacillus* depositadas en la base de datos del NCBI.

En ellas no se han detectado dominios conservados y las predicciones indican que poseen 11 ó 12 HTM. El alto número de dominios transmembrana es típico de proteínas Wzy (Jolly & Stinglele, 2001), y pese a la falta de una clara similitud, se asume que actúan como polisacárido polimerasas y que pertenecen a una familia aún desconocida de Wzy homólogos (Prechtel et al., 2018). Aún menos conservadas se encuentran las proteínas flipasas de CUPV237, con un 53 % de identidad con flipasas de *L. hokkaidonensis*. Estas proteínas de CUPV237 contienen el dominio MATE-Wzx-like característico de estos transportadores transmembrana y que se ha observado en la flipasa EpsN de *L. kefiranofaciens* (Wang et al., 2016).

En algunas BAL se han descrito los genes responsables de las rutas metabólicas para la producción de los precursores necesarios para la síntesis de HePS (Dimopoulou et al., 2014, Zeidan et al., 2017). En ocasiones, estos genes se localizan alejados de los *clusters eps*, pero en otros casos se han visto asociados a ellos (Dimopoulou et al., 2014; Zeidan et al., 2017; Prechtel et al., 2018). Esto último ocurre con los genes GalU, GalE y RmlA, -B, -C y D de *L. collinoides* CUPV237, que fueron encontrados en los *clusters eps1*, -3 y -4. Además, también localizamos los genes necesarios para la producción de UDP-galactosa, UDP-glucosa, dTDP-ramnosa, UDP-N-acetil-glucosamina, UDP-N-acetil-galactosamina, UDP-N-acetil-manosamina y CDP-glicerol.

Con respecto al trabajo *in silico* realizado en *Lactobacillus sicerae* CUPV261^T, en el análisis de la parte del genoma secuenciado (1.727.988 pb) se encontraron posibles genes relacionados con la producción de EPS en 8 de los *contigs*. Estos genes *eps* codificarían proteínas típicas de un mecanismo de producción de EPS Wzy-dependiente, entre las que encontramos proteínas reguladoras, GT y proteínas de exportación, además de otros genes relacionados con transposasas. Sin embargo, no se detectaron genes de polimerasa que son necesarios para la producción del HePS, y que podrían encontrarse en la porción no secuenciada del genoma. Las posibles proteínas codificadas por los genes *eps* detectados en *L. sicerae* y *L. collinoides* CUPV237, predictivamente comparten los dominios conservados, la superfamilia y además poseen las mismas HTM. Cabe destacar, que las posibles proteínas codificadas en el *contig* 3 de CUPV261^T, comparten unas identidades superiores al 71 % con las proteínas ortólogas reguladoras, GalU y WeE del *cluster eps1* de CUPV237. También RAST mostró similitud entre las posibles proteínas codificadas en el *contig* 225 y las posibles proteínas del *cluster eps3* de CUPV237, aunque con unos porcentajes de identidad que no superaron el 62 % (Wzd, Wze y

Wzb). Estas coincidencias podrían explicarse por ser dos cepas que comparten nicho ecológico (sidra natural), ya que pertenecen a especies separadas filogenéticamente dentro del género *Lactobacillus sp.* Por otro lado, las posibles proteínas codificadas en el *contig* 6 presentaron unas similitudes muy elevadas (próximas al 100 %) con *Lactobacillus plantarum* y *Lactobacillus murinus*. Además, las proteínas codificadas en cuatro de los *contigs* con genes *eps*, mostraron identidades superiores al 74 % con proteínas ortólogas de *L. vini*, especie muy próxima a *L. sicerae*, y en la que no se ha descrito hasta el momento la producción de HePS.

5. CONCLUSIONES

En este trabajo se ha abordado la localización de genes *eps* en las cepas productoras de exopolisacárido pertenecientes a las especies *L. collinoides* y *L. sicerae* aisladas en la campaña 2009. La detección mediante PCR de genes *eps* sugiere que todas las cepas sintetizan heteropolisacáridos.

El análisis *in silico* del genoma completo de *L. collinoides* CUPV237 mostró 4 posibles *clusters eps*; y en *L. sicerae* CUPV 261^T, se identificaron genes *eps* en 8 de los *contigs* obtenidos de la secuenciación parcial del su genoma. En ambas cepas, estos genes codificarían proteínas propias de la ruta biosintética Wzy-dependiente para la producción de HePS en BAL: proteínas relacionadas con funciones de regulación, de síntesis de la unidad repetitiva, de exportación y polimerización, además de otras relacionadas con la formación de dNDP-azúcares. Sin embargo, no se detectó el gen de proteína GTF implicada en la síntesis de (1,3)(1,2)- β -D-glucano, ni genes de dextran- o levansacarosas, todas ellas relacionadas con la biosíntesis de homopolisacáridos.

6. BIBLIOGRAFÍA

- Aziz, R. K., Bartels, D., Best, A. A., DeJongh, M., Disz, T., Edwards, R. A., Formsma K., Gerdes S., Glass E.M., Kubal M., Meyer F., Olsen G.J., Olson R., Osterman A.L., Overbeek R.A., McNeil L.K., Paarmann D., Paczian T., Parrello B., Pusch G.D., Reich C., Stevens R., Vassieva O., Vonstein V., Wilke A., & Zagnitko O. (2008). The RAST Server: rapid annotations using subsystems technology. *BMC Genomics*, 9(1), 75.
- Bender, M. H., & Yother, J. (2001). CpsB is a modulator of capsule-associated tyrosine kinase activity in *Streptococcus pneumoniae*. *Journal of Biological Chemistry*, 276(51), 47966-47974.
- Berger, B., Pridmore, R. D., Barretto, C., Delmas-Julien, F., Schreiber, K., Arigoni, F., & Brüßow, H. (2007). Similarity and differences in the *Lactobacillus acidophilus* group identified by polyphasic analysis and comparative genomics. *Journal of Bacteriology*, 189(4), 1311-1321.
- Bentley, S. D., Aanensen, D. M., Mavroidi, A., Saunders, D., Rabinowitsch, E., Collins, M., Donohoe, K., Harris, D., Murphy L., Quail, M. A., Samuel, G., Skovsted, I. C., Kalltoft, M.S., Barrell,B., Reeves, P. R., Parkhill, J., & Samuel, G. (2006). Genetic analysis of the capsular biosynthetic locus from all 90 pneumococcal serotypes. *PLoS Genet*, 2(3), e31.
- Blom, N., Sicheritz-Pontén, T., Gupta, R., Gammeltoft, S., & Brunak, S. (2004). Prediction of post-translational glycosylation and phosphorylation of proteins from the amino acid sequence. *Proteomics*, 4(6), 1633-1649.
- Boels, I. C., Ramos, A., Kleerebezem, M., & de Vos, W. M. (2001). Functional analysis of the *Lactococcus lactis galU* and *galE* genes and their impact on sugar nucleotide and exopolysaccharide biosynthesis. *Applied and Environmental Microbiology*, 67(7), 3033-3040.
- Brettin T., Davis J. J., Disz T., Edwards R. A., Gerdes S., Olsen G. J., Olson R., Overbeek R., Parrello B., Pusch G. D., Shukla M., Thomason J. A., Stevens R., Vonstein V., Wattam, A. R., & Xia F. (2015). RASTtk: a modular and extensible implementation of the RAST algorithm for building custom annotation pipelines and annotating batches of genomes. *Scientific Reports*, 5, 8365.

- Caggianiello, G., Kleerebezem, M., & Spano, G. (2016). Exopolysaccharides produced by lactic acid bacteria: from health-promoting benefits to stress tolerance mechanisms. *Applied Microbiology and Biotechnology*, 100(9), 3877-3886.
- Campbell, J. A., Davies, G. J., Bulone, V., & Henrissat, B. (1997). A classification of nucleotide-diphospho-sugar glycosyltransferases based on amino acid sequence similarities. *The Biochemical Journal*, 326(Pt 3), 929.
- Chan, Y. G. Y., Kim, H. K., Schneewind, O., & Missiakas, D. (2014). The capsular polysaccharide of *Staphylococcus aureus* is attached to peptidoglycan by the LytR-CpsA-Psr (LCP) family of enzymes. *Journal of Biological Chemistry*, 289(22), 15680-15690.
- Cieslewicz, M. J., Kasper, D. L., Wang, Y., & Wessels, M. R. (2001). Functional analysis in type Ia group B *Streptococcus* of a cluster of genes involved in extracellular polysaccharide production by diverse species of streptococci. *Journal of Biological Chemistry*, 276(1), 139-146.
- Dan, T., Fukuda, K., Sugai-Bannai, M., Takakuwa, N., Motoshima, H., & Urashima, T. (2009). Characterization and expression analysis of the exopolysaccharide gene cluster in *Lactobacillus fermentum* TDS030603. *Bioscience, Biotechnology and Biochemistry*, 73(12), 2656-2664.
- Dertli, E., Colquhoun, I. J., Gunning, A. P., Bongaerts, R. J., Le Gall, G., Bonev, B. B., Meyer, M. J., & Narbad, A. (2013). Structure and biosynthesis of two exopolysaccharides produced by *Lactobacillus johnsonii* F19785. *Journal of Biological Chemistry*, 288(44), 31938-31951.
- Deveau, H., & Moineau, S. (2003). Technical note: use of RFLP to characterize *Lactococcus lactis* strains producing exopolysaccharides. *Journal of Dairy Science*, 86(4), 1472-1475.
- Dimopoulou, M. (2013). Les polysaccharides de la bactérie lactique *Oenococcus oeni*, de l'élucidation de leurs structures et voies de biosynthèse à leur valorisation technologique (Tesis doctoral : Université Bordeaux II, Francia).
- Dimopoulou, M., Vuillemin, M., Campbell-Sills, H., Lucas, P. M., Ballestra, P., Miot-Sertier, C., Favier, M., Coulon, J., Moine, V., Doco, T., Roques, M., Williams, P., Petrel, M., Gontier, E., Moulis, C., Remaud-Simeon, M., & Roques, M. (2014). Exopolysaccharide (EPS) synthesis by *Oenococcus oeni*: from genes to phenotypes. *PLoS one*, 9(6), e98898.

- Dimopoulou, M., Claisse, O., Dutilh, L., Miot-Sertier, C., Ballestra, P., Lucas, P. M., & Dols-Lafargue, M. (2017). Molecular cloning, expression and characterization of *Oenococcus oeni* priming glycosyltransferases. *Molecular Biotechnology*, 59(8), 323-333.
- Eberhardt, A., Hoyland, C. N., Vollmer, D., Bisle, S., Cleverley, R. M., Johnsborg, O., Havarstein, L., ,2 Richard J. Lewis, R. J., & Vollmer, W. (2012). Attachment of capsular polysaccharide to the cell wall in *Streptococcus pneumoniae*. *Microbial Drug Resistance*, 18(3), 240-255.
- Friedman, L., & Kolter, R. (2004). Two genetic loci produce distinct carbohydrate-rich structural components of the *Pseudomonas aeruginosa* biofilm matrix. *Journal of Bacteriology*, 186(14), 4457-4465.
- Graninger, M., Nidetzky, B., Heinrichs, D. E., Whitfield, C. & Messner, P. (1999). Characterization of dTDP-4-dehydrorhamnose 3, 5-epimerase and dTDP-4-dehydrorhamnose reductase, required for dTDP-L-rhamnose biosynthesis in *Salmonella enterica* serovar Typhimurium LT2. *Journal of Biological Chemistry*, 274(35), 25069-25077.
- Hagelueken, G., Huang, H., Mainprize, I. L., Whitfield, C., & Naismith, J. H. (2009). Crystal structures of Wzb of *Escherichia coli* and CpsB of *Streptococcus pneumoniae*, representatives of two families of tyrosine phosphatases that regulate capsule assembly. *Journal of Molecular Biology*, 392(3), 678-688.
- Hidalgo-Cantabrana, C., Sánchez, B., Álvarez-Martín, P., López, P., Martínez-Álvarez, N., Delley, M., Martí, M., Varela, E., Suárez, A., Antolín, M., Guarner, F., Berger, B., Ruas-Madiedo, P., & Margolles, A. (2015). A single mutation in the gene responsible for the mucoid phenotype of *Bifidobacterium animalis* subsp. *lactis* confers surface and functional characteristics. *Applied and Environmental Microbiology*, AEM-02095.
- Hong, Y., Liu, M. A., & Reeves, P. R. (2018). Progress in our understanding of Wzx flippase for translocation of bacterial membrane lipid-linked oligosaccharide. *Journal of Bacteriology*, 200(1), e00154-17.
- Horn, N., Wegmann, U., Dertli, E., Mulholland, F., Collins, S. R., Waldron, K. W., Bongaerts, R. J., Mayer M. J., & Narbad, A. (2013). Spontaneous mutation reveals influence of exopolysaccharide on *Lactobacillus johnsonii* surface characteristics. *PloS one*, 8(3), e59957.

- Hübscher, J., Lüthy, L., Berger-Bächli, B., & Meier, P. S. (2008). Phylogenetic distribution and membrane topology of the LytR-CpsA-Psr protein family. *BMC Genomics*, 9(1), 617.
- Ibarburu, I., Puertas, A. I., Berregi, I., Rodríguez-Carvajal, M. A., Prieto, A., & Dueñas, M. T. (2015). Production and partial characterization of exopolysaccharides produced by two *Lactobacillus suebicus* strains isolated from cider. *International Journal of Food Microbiology*, 214, 54-62.
- Jolly, L., & Stingele, F. (2001). Molecular organization and functionality of exopolysaccharide gene clusters in lactic acid bacteria. *International Dairy Journal*, 11(9), 733-745.
- Jones, D. T., Taylor, W. R., & Thornton, J. M. (1994). A model recognition approach to the prediction of all-helical membrane protein structure and topology. *Biochemistry*, 33(10), 3038-3049.
- Kang, H. J., GiLert, C., Badeaux, F., Atlan, D., & LaPointe, G. (2015). A tyrosine phosphorylation switch controls the interaction between the transmembrane modulator protein Wzd and the tyrosine kinase Wze of *Lactobacillus rhamnosus*. *BMC Microbiology*, 15(1), 40.
- Kim, H. S., Lee, S. J., Yoon, H. J., An, D. R., Kim, S. J., & Suh, S. W. (2011). Crystal structures of YwqE from *Bacillus subtilis* and CpsB from *Streptococcus pneumoniae*, unique metal-dependent tyrosine phosphatases. *Journal of Structural Biology*, 175(3), 442-450.
- Kumar, S., Stecher, G., & Tamura, K. (2016). MEGA7: molecular evolutionary genetics analysis version 7.0 for bigger datasets. *Molecular Biology and Evolution*, 33(7), 1870-1874.
- van Kranenburg, R., Vos, H. R., Van Swam, I. I., Kleerebezem, M., & De Vos, W. M. (1999). Functional analysis of glycosyltransferase genes from *Lactococcus lactis* and other gram-positive cocci: complementation, expression, and diversity. *Journal of Bacteriology*, 181(20), 6347-6353.
- Krajl, S., van Geel-Schutten, G. H., Van Der Maarel, M. J. E. C., & Dijkhuizen, L. (2003). Efficient screening methods for glucosyltransferase genes in *Lactobacillus* strains. *Biocatalysis and Biotransformation*, 21(4-5), 181-187.
- LaPointe, G., Atlan, D., & Gilbert, C. (2008). Characterization and site-directed mutagenesis of Wzb, an O-phosphatase from *Lactobacillus rhamnosus*. *BMC Biochemistry*, 9(1), 10.

- Laws, A., Gu, Y., & Marshall, V. (2001). Biosynthesis, characterisation, and design of bacterial exopolysaccharides from lactic acid bacteria. *Biotechnology Advances*, 19(8), 597-625.
- Lebeer, S., Verhoeven, T. L., Francius, G., Schoofs, G., Lambrichts, I., Dufrêne, Y., Vanderleyden, J., & De Keersmaecker, S. C. (2009). Identification of a gene cluster for the biosynthesis of a long, galactose-rich exopolysaccharide in *Lactobacillus rhamnosus* GG and functional analysis of the priming glycosyltransferase. *Applied and Environmental Microbiology*, 75(11), 3554-3563.
- Looijesteijn P.J., Boels I.C., Kleerebezem M., & Hugenholtz J. (1999). Regulation of exopolysaccharide production by *Lactococcus lactis* subsp. *cremoris* by the sugar source. *Applied and Environmental Microbiology*, 65(11), 5003-5008.
- Low, D., Ahlgren, J. A., Horne, D., McMahon, D. J., Oberg, C. J., & Broadbent, J. R. (1998). Role of *Streptococcus thermophilus* MR-1C capsular exopolysaccharide in cheese moisture retention. *Applied and Environmental Microbiology*, 64(6), 2147-2151.
- Minic, Z., Marie, C., Delorme, C., Faurie, J. M., Mercier, G., Ehrlich, D., & Renault, P. (2007). Control of EpsE, the phosphoglycosyltransferase initiating exopolysaccharide synthesis in *Streptococcus thermophilus*, by EpsD tyrosine kinase. *Journal of Bacteriology*, 189(4), 1351-1357.
- Mijakovic, I., Poncet, S., Boël, G., Mazé, A., Gillet, S., Jamet, E., Decottignies, P., Grangeasse, C., Doublet, P., Le Maréchal, P., & Deutscher, J. (2003). Transmembrane modulator-dependent bacterial tyrosine kinase activates UDP-glucose dehydrogenases. *The EMBO Journal*, 22(18), 4709-4718.
- Morona, J. K., Paton, J. C., Miller, D. C., & Morona, R. (2000). Tyrosine phosphorylation of CpsD negatively regulates capsular polysaccharide biosynthesis in *Streptococcus pneumoniae*. *Molecular Microbiology*, 35(6), 1431-1442.
- Morona, J. K., Morona, R., & Paton, J. C. (2006). Attachment of capsular polysaccharide to the cell wall of *Streptococcus pneumoniae* type 2 is required for invasive disease. *Proceedings of the National Academy of Sciences*, 103(22), 8505-8510.
- Mozzi, F., Vanningelgem, F., Hébert, E. M., Van der Meulen, R., Moreno, M. R. F., de Valdez, G. F., & De Vuyst, L. (2006). Diversity of heteropolysaccharide-producing lactic acid bacterium strains and their biopolymers. *Applied and Environmental Microbiology*, 72(6), 4431-4435.

- Noda, M., Sugimoto, S., Hayashi, I., Danshiitsoodol, N., Fukamachi, M., & Sugiyama, M. (2018). A novel structure of exopolysaccharide produced by a plant-derived lactic acid bacterium *Lactobacillus paracasei* IJH-SONE68. *The Journal of Biochemistry*, 164(2), 87-92.
- Ooi, H. S., Kwo, C. Y., Wildpaner, M., Sirota, F. L., Eisenhaber, B., Maurer-Stroh, S., Wong, W. C., Schleiffer, A., Eisenhaber, F., & Schneider, G. (2009). ANNIE: integrated de novo protein sequence annotation. *Nucleic Acids Research*, 37(suppl_2), W435-W440.
- Overbeek, R., Olson, R., Pusch, G. D., Olsen, G. J., Davis, J. J., Disz, T., Edwards R. A., Gerdes S., Parrello B., Shukla M., Vonstein V., Wattam A. R., Xia F., & Stevens R. (2014). The SEED and the Rapid Annotation of microbial genomes using Subsystems Technology (RAST). *Nucleic Acids Research*, 42(D1), D206-D214.
- Patel, K. B., Furlong, S. E., & Valvano, M. A. (2010). Functional analysis of the C-terminal domain of the WbaP protein that mediates initiation of O-antigen synthesis in *Salmonella enterica*. *Glycobiology*, 20(11), 1389-1401.
- Péant, B., LaPointe, G., GiLert, C., Atlan, D., Ward, P., & Roy, D. (2005). Comparative analysis of the exopolysaccharide biosynthesis gene clusters from four strains of *Lactobacillus rhamnosus*. *Microbiology*, 151(6), 1839-1851.
- Prechtel, R. M., Wefers, D., Jakob, F., & Vogel, R. F. (2018). Structural characterization of the surface-associated heteropolysaccharide of *Lactobacillus plantarum* TMW 1.1478 and genetic analysis of its putative biosynthesis cluster. *Carbohydrate Polymers*, 202, 236-245.
- Provencher, C., LaPointe, G., Sirois, S., Van Calsteren, M. R., & Roy, D. (2003). Consensus-degenerate hybrid oligonucleotide primers for amplification of priming glycosyltransferase genes of the exopolysaccharide locus in strains of the *Lactobacillus casei* group. *Applied and Environmental Microbiology*, 69(6), 3299-3307.
- Puertas, A. I., Capozzi, V., Llamas, M. G., López, P., Lamontanara, A., Orrù, L., Russo, P., Spano G., & Dueñas, M. T. (2016). Draft genome sequence of *Lactobacillus collinoides* CUPV237, an exopolysaccharide and riboflavin producer isolated from cider. *Genome Announcements*, 4(3), e00506-16.
- Puertas, A. I., Ibarburu, I., Elizaquivel, P., Zuriarrain, A., Berregi, I., López, P., Prieto, A., Aznar, R., & Dueñas, M. T. (2018). Disclosing diversity of exopolysaccharide-

- producing lactobacilli from Spanish natural ciders. *LWT-Food Science and Technology*, 90, 469-474.
- Reeves, P. R., Hobbs, M., Valvano, M. A., Skurnik, M., Whitfield, C., Coplin, D., Kido, N., Klena, J., Maskell D., Raetz, C. R. H., & Rick, P. D. (1996). Bacterial polysaccharide synthesis and gene nomenclature. *Trends in Microbiology*, 4(12), 495-503.
- Remus, D. M., van Kranenburg, R., van Swam, I. I., Taverne, N., Bongers, R. S., Wels, M., Bron, P.A., & Kleerebezem, M. (2012). Impact of 4 *Lactobacillus plantarum* capsular polysaccharide clusters on surface glycan composition and host cell signaling. *Microbial Cell Factories*, 11(1), 149.
- Ruas-Madiedo, P., Hugenholtz, J., & Zoon, P. (2002). An overview of the functionality of exopolysaccharides produced by lactic acid bacteria. *International Dairy Journal*, 12(2-3), 163-171.
- Ruas-Madiedo, P., Moreno, J. A., Salazar, N., Delgado, S., Mayo, B., Margolles, A., & Clara, G. (2007). Screening of exopolysaccharide-producing *Lactobacillus* and *Bifidobacterium* strains isolated from the human intestinal microbiota. *Applied and Environmental Microbiology*, 73(13), 4385-4388.
- Schaefer, K., Matano, L. M., Qiao, Y., Kahne, D., & Walker, S. (2017). In vitro reconstitution demonstrates the cell wall ligase activity of LCP proteins. *Nature Chemical Biology*, 13(4), 396.
- Sneath, P. H. A. (1973). The principles and practice of numerical classification. *Numerical Taxonomy*, 573.
- Sperisen, P., Schmid, C. D., Bucher, P., & Zilian, O. (2005). Stealth proteins: *in silico* identification of a novel protein family rendering bacterial pathogens invisible to host immune defense. *PLoS Comput Biol*, 1(6), e63.
- Stingle, F., Neeser, J. R., & Mollet, B. (1996). Identification and characterization of the *eps* (Exopolysaccharide) gene cluster from *Streptococcus thermophilus* Sfi6. *Journal of Bacteriology*, 178(6), 1680-1690.
- Tieking, M., Kaditzky, S., Valcheva, R., Korakli, M., Vogel, R. F., & Gänzle, M. G. (2005). Extracellular homopolysaccharides and oligosaccharides from intestinal lactobacilli. *Journal of Applied Microbiology*, 99(3), 692-702.
- Toniolo, C., Balducci, E., Romano, M. R., Proietti, D., Ferlenghi, I., Grandi, G., Berti, F., Margarit, I., Ros, Y., & Janulczyk, R. (2015). *Streptococcus agalactiae* capsule

- polymer length and attachment is determined by the proteins CpsABCD. *Journal of Biological Chemistry*, 290(15), 9521-9532.
- Tsirigos, K. D., Peters, C., Shu, N., Käll, L., & Elofsson, A. (2015). The TOPCONS web server for consensus prediction of membrane protein topology and signal peptides. *Nucleic Acids Research*, 43(W1), W401-W407.
- Videira, P. A., Garcia, A. P., & Sá-Correia, I. (2005). Functional and topological analysis of the *Burkholderia cenocepacia* priming glucosyltransferase BceB, involved in the biosynthesis of the cepacian exopolysaccharide. *Journal of Bacteriology*, 187(14), 5013-5018.
- Walker, J. E., Saraste, M., Runswick, M., J. & Gay, N. J. (1982). Distantly related sequences in the alpha-and beta-subunits of ATP synthase, myosin, kinases and other ATP-requiring enzymes and a common nucleotide binding fold. *The EMBO Journal*, 1(8), 945.
- Wang, L., Liu, D., & Reeves, P. R. (1996). C-terminal half of *Salmonella enterica* WbaP (RfbP) is the galactosyl-1-phosphate transferase domain catalyzing the first step of O-antigen synthesis. *Journal of Bacteriology*, 178(9), 2598-2604.
- Werning, M. L., Ibarburu, I., Dueñas, M. T., Irastorza, A., Navas, J., & López, P. (2006). *Pediococcus parvulus* *gtf* gene encoding the GTF glycosyltransferase and its application for specific PCR detection of β -D-glucan-producing bacteria in foods and beverages. *Journal of Food Protection*, 69(1), 161-169.
- Wiggins, C. A., & Munro, S. (1998). Activity of the yeast MNN1 α -(1,3)-mannosyltransferase requires a motif conserved in many other families of glycosyltransferases. *Proceedings of the National Academy of Sciences*, 95(14), 7945-7950.
- Yother, J. (2011). Capsules of *Streptococcus pneumoniae* and other bacteria: paradigms for polysaccharide biosynthesis and regulation. *Annual Review of Microbiology*, 65, 563-581.
- Zeidan, A. A., Poulsen, V. K., Janzen, T., Buldo, P., Derkx, P. M., Øregaard, G., & Neves, A. R. (2017). Polysaccharide production by lactic acid bacteria: from genes to industrial applications. *FEMS Microbiology Reviews*, 41(Supp_1), S168-S200.
- Zivkovic, M., Miljkovic, M., Ruas-Madiedo, P., Strahinic, I., Tolinacki, M., Golic, N., & Kojic, M. (2015). Exopolysaccharide production and ropy phenotype are determined by two gene clusters in putative probiotic strain *Lactobacillus paraplantarum* BGCG11. *Appl. Environ. Microbiol.*, 81(4), 1387-1396.

Zuckerandl, E., & Pauling, L. (1965). Evolutionary divergence and convergence in proteins. En: *Evolving genes and proteins* (pp. 97-166). Academic Press.

Zuker, M. (2003). Mfold web server for nucleic acid folding and hybridization prediction. *Nucleic Acids Research*, 31(13), 3406-3415.

3. Caracterización de los exopolisacáridos producidos por
Lactobacillus collinoides y *Lactobacillus sicerae*

1. INTRODUCCIÓN

En sidras ahiladas del País Vasco se han aislado con frecuencia bacterias lácticas productoras de EPS. La mayoría de las cepas sintetizan el característico homopolisacárido (1,3)(1,2)- β -D-glucano, este biopolímero es sintetizado por cepas de las especies *P. parvulus*, *P. ethanolidurans*, *O. oeni*, *L. diolivorans* y *L. suebicus* (Dueñas-Chasco et al., 1997; Dueñas-Chasco et al., 1998; Ibarburu et al., 2007; Garai-Ibabe et al., 2010; Llamas-Arriba et al., 2018). Algunas estirpes aisladas de sidra sintetizan junto a este HoPS otros heteropolisacáridos. Además, se ha encontrado que algunas cepas de *L. suebicus* sintetizan únicamente HePS (Ibarburu et al., 2015), e incluso la estirpe de *L. mali* CUPV271 sintetiza un HoPS de tipo dextrano (Llamas-Arriba et al., 2019). Estos antecedentes, junto con la diversidad de *Lactobacillus* productores de EPS (capítulo 1), nos sugieren que existe una gran variedad de exopolisacáridos producidos por estirpes de BAL aisladas de sidra, que contribuyen a la modificación de las características organolépticas de la sidra natural del País Vasco y a la alteración del ahilado.

A partir de los resultados obtenidos en el capítulo 1 y 2 se seleccionaron el par de cepas *L. collinoides* CUPV237 y *L. sicerae* CUPV261^T para el estudio de la estructura y de las características físico-químicas de sus EPS, debido a que presentaron una mayor producción y que en sus genomas se encontraron genes relacionados con la síntesis de HePS.

Algunos EPS producidos por bacterias son un importante componente biológico de interacción entre los microorganismos y el hospedador a través de su capacidad mediadora en la adhesión a superficies y de reconocimiento celular (Laiño et al., 2016). Por otro lado, se han descrito sus efectos beneficiosos sobre la salud de los consumidores, ya que algunos EPS pueden regular en la sangre los niveles de colesterol (Nakajima, Suzuki & Hirota, 1992; Lindström et al., 2012) y de glucosa (Maeda et al., 2004), inhibir la adipogénesis (Zhang et al., 2016), actuar como agentes anticancerígenos (Liu et al., 2011; Deepak et al., 2016), poseer un carácter antiinflamatorio (Notararigo et al., 2014) o actividad antiviral (Nácher-Vázquez et al., 2015). A ciertos EPS se les atribuyen efectos inmunomoduladores, particularmente en el ambiente intestinal, los cuales han sido observados tanto en ensayos *in vivo* como *in vitro* (Liu et al., 2011; Murofushi et al., 2015; Castro-Bravo et al., 2018).

En los últimos años el modelo animal del pez cebrá está siendo una herramienta muy útil para realizar estudios en la biología del desarrollo de los

órganos o sistemas del pez, o como un modelo animal para estudiar los mecanismos implicados en la evolución de enfermedades. Se debe a su elevada fecundidad, a la transparencia de sus larvas y a que éstas poseen un tiempo de desarrollo corto (Fleming et al., 2010). En el contexto del estudio de enfermedades intestinales, dado que el pez cebra tiene un tracto digestivo homólogo al de mamíferos (Marjoram & Bagnat, 2015), se ha propuesto como un buen modelo para el estudio de la enfermedad de inflamación intestinal (IBD, *Inflammation Bowel Disease*) (Sartor, 2006).

El trabajo mostrado en este capítulo tuvo como objetivo la caracterización parcial de los exopolisacáridos producidos por *Lactobacillus sicerae* CUPV261^T y *Lactobacillus collinoides* CUPV237, mediante el estudio de su composición, propiedades físico-químicas, estructura y resistencia al estrés gastrointestinal en un modelo *in vitro*. Además, se evaluó el efecto de los EPS producidos por CUPV261^T, CUPV237, *Bifidobacterium longum* INIA P132 y *Bifidobacterium infantis* INIA P731, sobre la supervivencia de las larvas de pez cebra en un modelo *in vivo* de enfermedad inflamatoria intestinal inducida por el agente químico dextrano de sodio sulfatado (DSS).

2. MATERIAL Y MÉTODOS

2.1 Cepas bacterianas y condiciones de cultivo

Las cepas *L. collinoides* CUPV237 y *L. sicerae* CUPV261^T fueron cultivadas de forma rutinaria en el medio MRS. Además, se incluyeron las cepas *Bifidobacterium longum* INIA P132 y *Bifidobacterium infantis* INIA P731 (origen humano) procedentes del Instituto Nacional de Investigación Agroalimentaria (INIA), que fueron cultivadas en el medio RCA-agar (Difco).

2.2 Microscopía electrónica de transmisión

La observación de las bacterias y de los exopolisacáridos. se realizó con tinción negativa mediante microscopía electrónica de transmisión (TEM), aplicando el protocolo descrito en el capítulo 1 (apartado 2.3).

2.3 Aislamiento, purificación y cuantificación de los exopolisacáridos

La producción y el aislamiento del EPS a partir de las cepas de *L. collinoides* y de *L. sicerae* se realizó en el medio MSD, y se aplicó el protocolo descrito en el capítulo 1 (apartado 2.4.1), mediante el cual se obtuvo el EPS en forma de líofilo (EPS crudo).

Para la cuantificación del EPS en el medio de cultivo se utilizó el sobrenadante libre de células. El contenido en azúcares neutros se analizó mediante el método del fenol-sulfúrico descrito del capítulo 1 (apartado 2.4.1).

Con el fin de reducir la contaminación de proteínas, DNA y RNA en el EPS, la solución acuosa obtenida tras la diálisis se concentró (con fuerte agitación, 50 °C, 5 h) y se le aplicó el tratamiento enzimático descrito por López et al., (2012): El EPS fue suspendido en una solución tampón (Tris-HCl 0,05 M, MgSO₄·7H₂O 0,1 M a pH 7), con 0,25 µg mL⁻¹ de DNasa I de páncreas bovino (Sigma) y 0,2 µg mL⁻¹ de RNasa (Sigma), y se incubó durante 6 h (150 rpm, 37 °C). Posteriormente, se añadieron 50 µg mL⁻¹ de Pronasa E de *Streptomyces griseus* (Sigma), preparada previamente en una solución de Tris-HCl 50 mM y EDTA 2 % (p/v; pH 7,5), y se incubó a 37 °C durante 18 h. Las proteínas y péptidos de la mezcla se precipitaron

con ácido tricloroacético (TCA) a una concentración final del 12 % (p/v), con agitación suave, a temperatura ambiente y durante 30 min. El pH de la suspensión se ajustó a 5,5 con NaOH y se centrifugó ($15.680 \times g$, $4 \text{ }^\circ\text{C}$, 10 min) para descartar el precipitado. Finalmente, el EPS se dializó y liofilizó.

La cuantificación de los contaminantes en el liófilo (proteínas, DNA y RNA) se realizó utilizando los kits fluorescentes específicos para el fluorímetro Qubit® 2.0 (Invitrogen), siguiendo las indicaciones aportadas por el fabricante.

2.3.1 Determinación del contenido del EPS en el liófilo

La cuantificación del EPS se llevó a cabo en una suspensión de $0,5 \text{ mg mL}^{-1}$ de liófilo mediante cromatografía de exclusión molecular (HPSEC), y aplicando el protocolo descrito en el capítulo 1 (apartado 2.5). Para el análisis cromatográfico, se empleó una columna PL-aquagel-OH MIXED-H ($8 \text{ }\mu\text{m}$, Agilent Technologies) y una columna de guarda PL-aquagel-OH ($8 \text{ }\mu\text{m}$, Agilent Technologies), termostatzadas a $35 \text{ }^\circ\text{C}$. La duración del método fue de 20 min, con un flujo de 1 mL min^{-1} . Los resultados correspondientes a las áreas de los picos (A_p) se sustituyeron en la ecuación: $\text{mg de EPS mL}^{-1} = (A_p + 12.586) / 3 \times 10^5$. Esta ecuación se obtuvo a partir de la curva de calibrado mostrada en la Figura 3.1, que fue elaborada con un patrón de dextrano de peso molecular 12 kDa (Sigma).

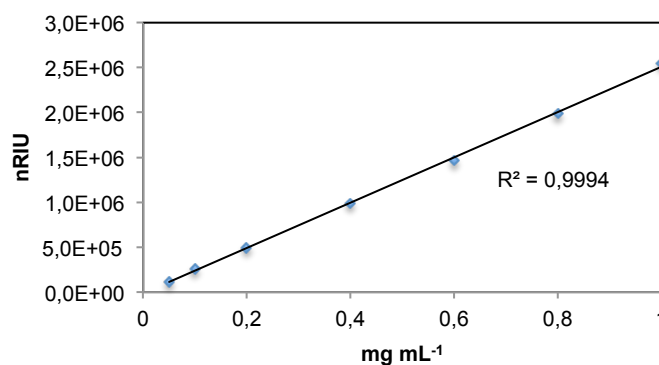


Figura 3.1. Curva de calibrado para la cuantificación del EPS en el liófilo. nRIU, unidades aportadas por el detector índice de refracción.

2.4 Caracterización de los exopolisacáridos

2.4.1 Determinación del peso molecular, de la composición de monosacáridos y análisis de metilación

Para la determinación del peso molecular del EPS y visualización de las fracciones que lo componen, se aplicó el protocolo descrito en el capítulo 1 (apartado 2.5).

El EPS crudo fue separado en dos fracciones mediante un sistema Amicon® (diámetro de poro de 50 kDa). Las muestras se disolvieron en una solución de NaOH 0,2 M, se centrifugaron ($15.680 \times g$, 15 min) y el sobrenadante se filtró por centrifugación de acuerdo a las indicaciones del fabricante. La fracción eluída y la retenida fueron dializadas con una membrana de un diámetro de poro de 14 kDa (Medicell International, Ltd.), y liofilizadas.

Para la determinación de la composición de monosacáridos, los EPS fueron hidrolizados con ácido trifluoroacético (TFA) 3 M y convertidos en sus correspondientes acetatos de alditol, mediante su reducción con NaBH₄ y posterior acetilación, de acuerdo al método descrito por Notararigo et al. (2013). La identificación y la cuantificación de los monosacáridos se realizó mediante cromatografía de gases.

Con el fin de determinar el tipo de sustitución de los monosacáridos, los EPS se permetilaron siguiendo el método descrito por Ciucanu & Kerek (1984). Posteriormente, las muestras se hidrolizaron con TFA 3 M (120 °C, durante 1 h), se redujeron y se acetilaron para su conversión en acetatos de alditol (Laine et al., 1972). Finalmente, los polisacáridos se analizaron mediante cromatografía de gases-espectrometría de masas (GC-MS), en un equipo Agilent, 6890A/5975C (Hewlett-Packard), utilizando helio como fase móvil. El inyector *split/splitless* se programó a 250 °C, y se analizó 1 µL de muestra con una relación de *split* de 1:50. La columna utilizada fue una Agilent J&W HP-5ms (30 m x 0,25 mm I.D. x 0,2 µm de espesor de película). El método comenzó a 160 °C durante 1 min, y después se aplicó un incremento de temperatura de 2 °C min⁻¹ hasta alcanzar los 200 °C. Se utilizó un rango de *m/z* entre 40 y 450 amu. La identificación se realizó en base a los tiempos de retención y al espectro de masas, y la cuantificación teniendo en cuenta las áreas de los picos. Tanto este análisis como la determinación de la composición

del EPS, fueron realizados por la doctora Alicia Prieto en el Centro de Investigaciones Biológicas (Madrid).

2.4.2 Análisis mediante espectroscopía infrarroja con transformada de Fourier (FT-IR)

Para detectar la presencia de grupos N-acetilo, carboxilo, fosfato o sulfato, así como la configuración α - o β - del carbono anomérico de los monosacáridos, los EPS se analizaron mediante espectroscopía FT-IR. Los espectros de infrarrojos se obtuvieron en un espectrómetro de infrarrojos con transformada de Fourier Nicolet 6700 (Thermo Scientific), a partir de 64 barridos, con una resolución de 4 cm^{-1} y en el rango de $4000\text{-}400\text{ cm}^{-1}$. La preparación de las muestras se llevo a cabo mediante la técnica del KBr, por la cual las pastillas se prepararon con 1-3 mg de EPS.

2.4.3 Análisis mediante Resonancia Magnética Nuclear (RMN)

Los espectros de RMN ^1H se obtuvieron a partir de una suspensión de 1 mg mL^{-1} de EPS en agua deuterada (óxido de deuterio, 99 atom % D, Sigma). Los análisis se realizaron a 500,13 MHz en un espectrómetro Bruker DRX-500, registrando los espectros a 303 K. Los desplazamientos químicos son dados en partes por millón utilizando como referencia la señal del agua semipesada (HDO) a 4,23 ppm. El tratamiento de datos se realizó con el programa MestReNova (versión 10.0.2-15465, © Mestrelab Research S.L.).

2.4.4 Análisis de la estabilidad térmica

La degradación térmica de los EPS se estudió en un analizador termogravimétrico (TGA) Q500 (TA instruments). Para ello, 10 mg de EPS se sometieron a un rango de temperatura de $40\text{-}600\text{ }^\circ\text{C}$ en presencia de oxígeno, con una velocidad de calentamiento de $10\text{ }^\circ\text{C min}^{-1}$, y se determinó la correspondiente pérdida de peso. También, se obtuvo la curva elaborada a partir de la primera derivada de la curva de la pérdida de peso obtenida en el análisis TGA (DGT).

Por otro lado, se analizó el efecto que produce un proceso de esterilización en un autoclave sobre el EPS. Para ello, una suspensión de $0,75 \text{ mg mL}^{-1}$ del EPS disuelto en el eluyente (NaNO_3 0,1 M y NaN_3 0,02 % (p/v), pH 7) se calentó hasta $120 \text{ }^\circ\text{C}$, permaneciendo a esta temperatura durante 20 min, y posteriormente se enfrió a temperatura ambiente. El EPS se analizó mediante HPSEC (capítulo 1, apartado 2.5), y se comparó el peso molecular y la polidispersidad de las fracciones.

2.4.5 Reología de las fermentaciones

La viscosidad de los cultivos realizados en el medio MSD (capítulo 1, apartado 2.2.2), y de sus sobrenadantes libres de células, se midió en un reómetro Physica Rheolab MC 100 (Anton Paar). El equipo estaba dotado con una geometría de cilindros concéntricos de diámetro interior de 27,00 mm y exterior de 28,92 mm. Además, este equipo tiene un dispositivo de control de temperatura Peltier, que estabilizó la muestra a $4 \text{ }^\circ\text{C}$ desde los 5 min previos al comienzo de la toma de datos. Se aplicó una velocidad de cizalla creciente desde $1,01$ a 1000 s^{-1} , durante 5 min. Las medidas se realizaron por duplicado y en dos cultivos independientes.

Los resultados obtenidos se ajustaron al modelo Newtoniano, en el cual el esfuerzo de cizalla aplicado (τ) es directamente proporcional a la velocidad de deformación ($\dot{\gamma}$), y η_0 es la viscosidad newtoniana. La siguiente ecuación relaciona estos parámetros:

$$\tau = \eta_0 \dot{\gamma}$$

2.5 Comportamiento del EPS bajo un modelo *in vitro* de estrés gastrointestinal

Para el análisis del comportamiento de los EPS bacterianos bajo el estrés gástrico (G) y el estrés gastrointestinal (GI), se utilizaron 7,5 mg del EPS suspendidos en 10 mL de la solución electrolítica estéril ($6,2 \text{ g L}^{-1}$ de NaCl , $2,2 \text{ g L}^{-1}$ de KCl , $0,22 \text{ g L}^{-1}$ de CaCl_2 , y $1,2 \text{ g L}^{-1}$ de NaHCO_3). Para simular el estrés gástrico se añadieron las enzimas lisozima y pepsina, y para el ensayo gastrointestinal se añadieron además, sales biliares y pancreatina (Figura 3.2). La incubación se realizó en un incubador-agitador orbital (150 rpm, $37 \text{ }^\circ\text{C}$). Se tomaron 2 mL de muestra en los tratamientos G1, G5, G6, y GI5, y se centrifugaron a $15.680 \times g$ durante 10 min.

Para recuperar el EPS se añadió al sobrenadante 3 volúmenes de etanol frío, manteniéndose a $-20\text{ }^{\circ}\text{C}$ durante 48 h. El precipitado se recogió por centrifugación, se dializó en una membrana con un diámetro de poro de 3,5 kDa (Medicell International, Ltd.) y se liofilizó. Finalmente, se analizó la variación del peso molecular y la polidispersidad mediante HPSEC (capítulo 1, apartado 2.5).

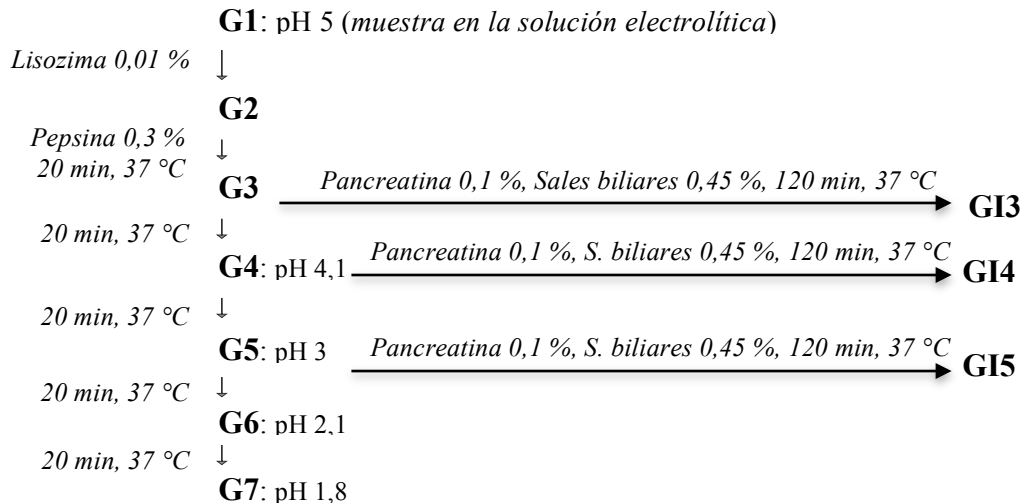


Figura 3.2. Representación del modelo *in vitro* del estrés gástrico y del estrés gastrointestinal (Fernández de Palencia et al., 2009).

2.6 Aplicación de un modelo *in vivo* de larvas de pez cebra

2.6.1 Obtención de los embriones

Los embriones de pez cebra se obtuvieron por fecundación natural a partir de individuos adultos de una estirpe salvaje (*Danio rerio*, Hamilton 1822), en las instalaciones de AZTI (REGA nº ES489010006105; Derio, Bizkaia). Los peces adultos se criaron a $27\text{ }^{\circ}\text{C}$ en tanques de 60 L de agua dulce, con aireación, y se mantuvieron bajo protocolos estándar. Los tanques disponían de tres sistemas de filtración (biológico, químico y físico), además de una lámpara de luz ultravioleta, y se iluminaron en ciclos de 12 h de luz y 12 h de oscuridad. Los peces se alimentaron diariamente con una cantidad aproximada del 5 % del peso del animal, con un alimento comercial en escamas (Gemma Micro 300, Skretting) (Russo et al., 2015). Además, para mejorar la eficiencia reproductiva, se les suministró *Artemia sp.* tres veces a la semana. Los embriones se recogieron a primera hora de la mañana, se lavaron con solución para embriones (EW: 294 mg mL^{-1} de CaCl_2 , $123,3\text{ mg mL}^{-1}$ de $\text{MgSO}_4 \cdot 7\text{H}_2\text{O}$, 63 mg mL^{-1} de NaHCO_3 , $5,5\text{ mg mL}^{-1}$ de KCl), y permanecieron hasta su utilización en EW suplementada con azul de metileno 0,01 % (p/v) a $27\text{ }^{\circ}\text{C}$.

2.6.2 Modelo *in vivo* de enterocolitis inducida por DSS y tratamiento con EPS

Los EPS fueron producidos por *L. sicerae* CUPV261^T (EPS-CUPV261^T), *L. collinoides* CUPV237 (EPS-CUPV237), *B. longum* INIA P132 (EPS-P132) y *B. infantis* INIA P731 (EPS-P731) (Llamas-Arriba et al., 2019), y se suspendieron en EW a una concentración de 150 µg mL⁻¹ (37 °C, 30 min, agitación fuerte) (Figura 3.3). Grupos de 20-30 huevos de pez cebra de 1 día posfecundación (dpf) se transfirieron a microplacas de 12 pocillos (Corning), y fueron expuestos por inmersión en las suspensiones de EPS hasta los 4 dpf, a 27 °C y con ciclos de 12 h de luz-oscuridad. Para la inducción química de la enterocolitis (larvas IBD), las soluciones de EPS se suplementaron con dextrano de sodio sulfatado 0,8 % (p/v) (DSS) (Mw 6,5-10 kDa, Across Organics) desde los 4 dpf hasta el final del ensayo (Marjoram & Bagnat (2015) y Oehlers et al. (2012), con modificaciones). Los tratamientos se renovaron diariamente, y se contabilizaron las larvas que iban muriendo hasta los 7 dpf. Además, se incluyeron grupos de larvas no tratadas (larvas EW), y como control positivo, larvas tratadas exclusivamente con DSS desde los 4 dpf. Los ensayos se realizaron por triplicado.

Para determinar el efecto dosis-dependiente de los EPS sobre la atenuación de la mortalidad de las larvas IBD, se utilizó el protocolo anterior, con las concentraciones de 50, 100 y 150 µg mL⁻¹ (Oyarbide, Rainieri & Pardo, 2012), y con un tratamiento simultáneo de 0,8 % (p/v) de DSS (Figura 3.3).

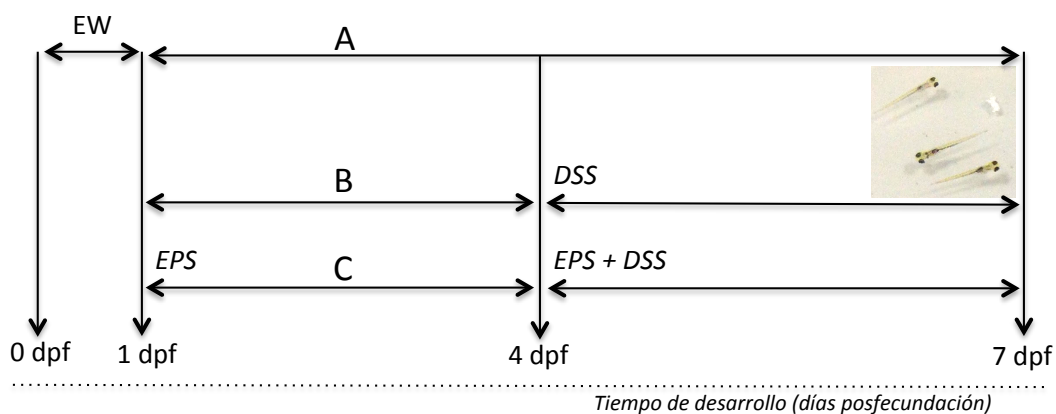


Figura 3.3. Esquema de los diferentes tratamientos utilizados en el modelo *in vivo* de larvas IBD de pez cebra. EW, huevos conservados en solución para embriones con azul de metileno; A, individuos conservados en EW; B, larvas tratadas con DSS 0,8 % (p/v); y C, embriones expuestos al EPS, y larvas tratadas con EPS más DSS a partir de los 4 dpf.

2.7 Análisis estadístico

Los datos se expresan como la media \pm desviación estándar. Los análisis estadísticos se realizaron utilizando el programa informático SPSS (Versión 24.0). Para detectar las diferencias significativas, se aplicó un análisis de la varianza (ANOVA) de un factor, seguido de un test de Dunnett T3.

3. RESULTADOS

Las cepas *L. sicerae* CUPV261^T y *L. collinoides* CUPV237 fueron seleccionadas en este estudio por manifestar fenotipo *ropy*, presentar un mayor rendimiento en la producción de EPS y por pertenecer a especies no descritas anteriormente como productoras de EPS (capítulo 1). Las colonias de estas estirpes forman hilos largos cuando son tocadas con el asa bacteriológica, y los cultivos en medio líquido adoptan una apariencia viscosa (Figura 1.1).

Los cultivos de las bacterias en el medio líquido MRS fueron observados a nivel celular mediante microscopía electrónica de transmisión (TEM) (Figura 3.4). En las microfotografías se observa el EPS distribuido alrededor de las células en forma de red.

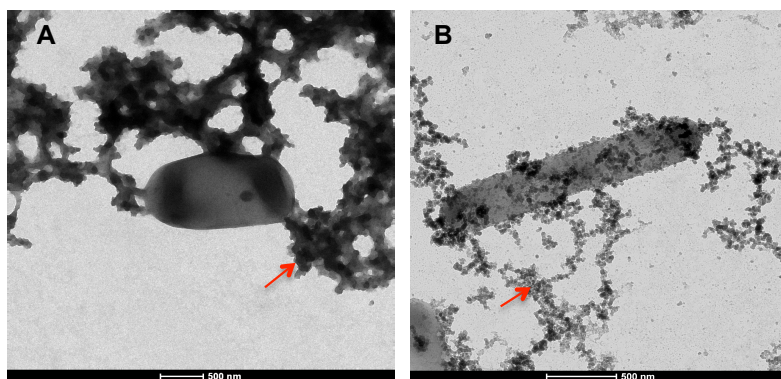


Figura 3.4. Microfotografías de *L. collinoides* CUPV237 (A) y *L. sicerae* CUPV261^T (B) en cultivo líquido, tomadas mediante TEM. La flecha roja indica el EPS. Barra de escala, 500 nm.

3.1 Producción de exopolisacárido

La producción de EPS se ensayó mediante el cultivo de las bacterias en el medio líquido semidefinido MSD durante 48 h (Tabla 3.1). Tras la fermentación, el crecimiento de CUPV261^T fue 3,75 veces inferior al observado en CUPV237, y aunque el rendimiento de EPS fue superior en *L. sicerae*, en ningún caso se alcanzaron los 100 mg L⁻¹. Las diferencias observadas en la cuantificación del EPS por los dos métodos (fenol-sulfúrico y HPSEC) podrían deberse a que los furfurales e hidroxifurfurales de los monosacáridos obtenidos por el método del F-S, presentan diferencias en su absorbancia a 490 nm (Dubois et al., 1956; Masuko et al., 2005; Le & Stuckey, 2016).

Además, se determinó la viscosidad de los cultivos y de los sobrenadantes libres de células (Tabla 3.1). En todas las muestras, la viscosidad se mantuvo

constante independientemente del aumento de la velocidad de cizalla (datos no mostrados); por lo tanto, los cultivos y sobrenadantes presentaron un comportamiento reológico de tipo newtoniano. Los valores de la viscosidad fueron ligeramente superiores en la estirpe CUPV237 que en CUPV261^T.

Tabla 3.1. Cultivo de *L. collinoides* CUPV237 y *L. sicerae* CUPV261^T en el medio MSD.

	DO ₆₀₀	^a EPS F-S (mg L ⁻¹)	^b EPS (mg L ⁻¹)	Viscosidad η_0 [mPa s]	
				Cultivo	Sobrenadante
CUPV261 ^T	0,893 ± 0,071	57,11 ± 7,45	86,65 ± 7,52	2,248	2,215
CUPV237	3,022 ± 0,096	30,26 ± 6,57	49,67 ± 13,13	2,956	2,474
Medio MSD	-	-	-	-	1,799

(η_0) Viscosidad newtoniana.

(a) Concentración de exopolisacárido en el sobrenadante, obtenida mediante el método fenol-sulfúrico.

(b) Producción del EPS teniendo en cuenta la cantidad de líofilo aislado en los cultivos (EPS crudo), y posterior análisis del contenido de polisacárido mediante HPSEC.

Se analizó la pureza de los EPS que iban a ser posteriormente utilizados en el ensayo del modelo *in vivo* de inflamación intestinal en larvas de pez cebra (apartado 3.5). El EPS crudo de *L. sicerae* presentaba un 6,55 ± 0,05 % de proteína, un 0,03 ± 0,02 % de DNA y un 0,14 ± 0,06 % de RNA; y el de *L. collinoides* un 7,38 ± 1,87 % de proteína, un 0,03 ± 0,01 % de DNA y un 0,07 ± 0,02 % de RNA. Las muestras se trataron enzimáticamente y se redujo su contenido a valores inferiores al límite de detección del método.

3.2 Análisis de los exopolisacáridos

Los EPS fueron sometidos a diferentes análisis. Para la determinación de la estructura se utilizó la espectrometría infrarroja de la transformada de Fourier (FT-IR), la resonancia magnética nuclear RMN ¹H, análisis de metilación y cromatografía de gases-espectrometría de masas. Además, se analizó el peso molecular mediante cromatografía de exclusión por tamaño de alta resolución (HPSEC).

3.2.1 Análisis FT-IR y RMN ¹H

Los EPS crudos de *L. sicerae* CUPV261^T y *L. collinoides* CUPV237 fueron analizados mediante FT-IR para obtener información acerca de sus principales grupos estructurales. Ambos EPS presentaron unos espectros típicos de carbohidratos (Figura 3.5 A). Aparecieron bandas estrechas entre 1200 y 950 cm⁻¹

que corresponden a enlaces C–O–C (O–glicosídico), C–O (Xu et al., 2011), C–C y vibraciones de deformación de la estructura CH₂OH del anillo (Grube et al., 2006). La banda en la región de 1080–1030 cm⁻¹ indicó un estiramiento del polisacárido o de compuestos similares a polisacáridos (Grube et al., 2006). El espectro comprendido entre 950–700 cm⁻¹ pertenece a la región anomérica (Xu et al., 2011), y en este intervalo solo se observó una banda a 860 cm⁻¹ que no indicó claramente la configuración del carbono anomérico (α -anomérica: 915 y 850 cm⁻¹; β -anomérica: 890 cm⁻¹) (Notararigo et al., 2013). Las bandas en la región 3600–3200 cm⁻¹ se deben a las vibraciones de estiramiento de los grupos –OH del polisacárido (Xu et al., 2011). Apareció un pico de absorción en torno a 2944 cm⁻¹ provocado por las vibraciones de flexión del grupo C–H (Xu et al., 2011; Shao et al., 2014) o –CH₂– (Ibarburu et al., 2015). La banda a 1450 cm⁻¹ corresponde con la deformación asimétrica de los grupos –CH₃ y CH₂ de las proteínas contenidas en las muestras (Wang et al., 2010), y una banda a 1379 cm⁻¹ provocada por la vibración de flexión del grupo C–H (Shao et al., 2014). La banda de absorción a 1551 cm⁻¹ corresponde a la amida I, ya que está ocasionada por la vibración de estiramiento del grupo C=O. Además, se observó a 1655 cm⁻¹ la banda de la amida II, debida a la flexión del enlace N–H y a la vibración de estiramiento del enlace C–N. Estas dos últimas bandas, indicarían la presencia de aminoazúcares en las muestras (De Giacomo et al., 2008; Ibarburu et al., 2015).

El espectro de RMN ¹H de los EPS de ambas cepas presenta un conjunto de señales en la región entre 4,5–5,5 ppm que están relacionadas con el C1, e indican la presencia de configuraciones α - y β -anomérica (Figura 3.5 B). En el caso de *L. collinoides* aparece una señal en torno a 2 ppm que corresponde con la presencia de grupos acetilo.

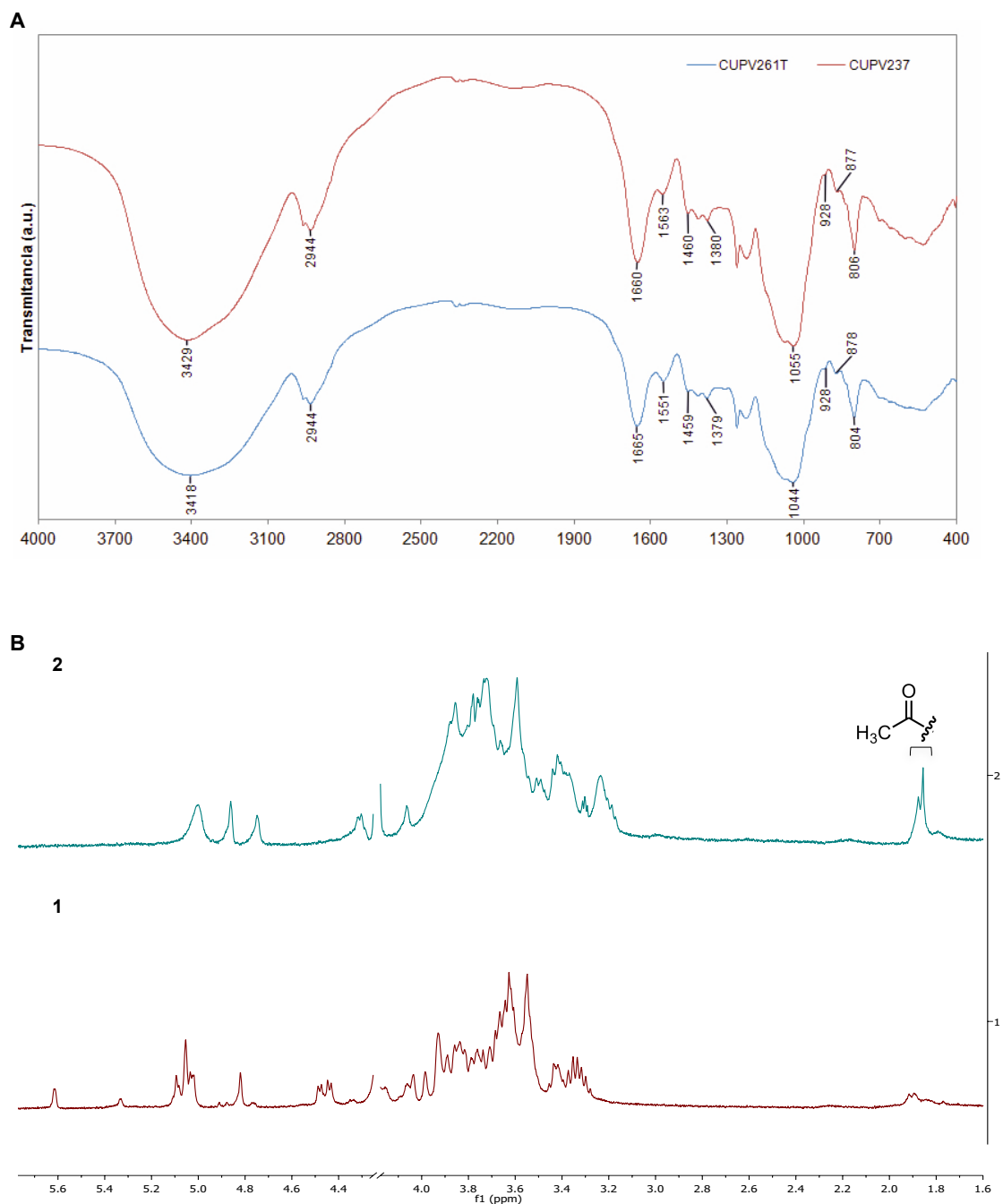


Figura 3.5 Análisis de los EPS mediante técnicas espectrométricas. **A**, espectros FT-IR; **B**, espectros de RMN ^1H del EPS producido por (1) *L. sicerae* CUPV261^T y (2) *L. collinoides* CUPV237. En el cromatograma se omitió la señal producida por el agua semipesada (//).

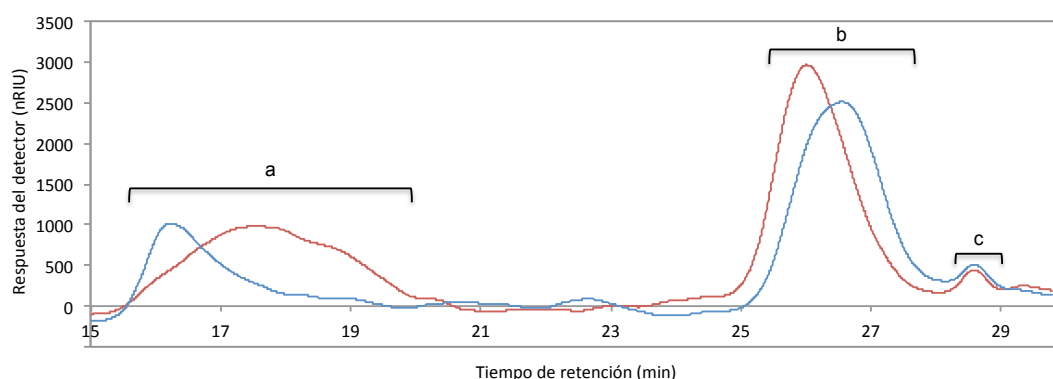
3.2.2 *Lactobacillus sicerae* CUPV261^T

Para determinar el peso molecular del EPS, el líofo fue analizado mediante HPSEC (Figura 3.6). Los cromatogramas obtenidos mostraron que el EPS estaba compuesto por 3 fracciones: (i) una de alto peso molecular, superior a 2,000 kDa

(límite del calibrado); (ii) otra del orden de 20 kDa (la más abundante); (iii) y una fracción de inferior peso molecular, del orden de 4 kDa.

El análisis de la composición de azúcares neutros se realizó a partir de una hidrólisis ácida del EPS y derivatización a acetatos de alditol. El posterior análisis mediante CG reveló la presencia de glucosa, galactosa y ramnosa (Figura 3.7 A).

El EPS crudo fue tratado con una solución alcalina (NaOH 0,2 M) para favorecer su disolución. Se obtuvo una porción insoluble correspondiente al 41 % de la muestra cruda, y el resto fue separado mediante un sistema Amicon®. Se obtuvieron dos fracciones, una >50 kDa y otra <50 kDa, que representaron el 14 y 44 % del EPS crudo, respectivamente. Con el fin de investigar el tipo de enlaces O-glicosídicos presentes, las diferentes fracciones fueron sometidas a un análisis de metilación (Figura 3.7 B y Tabla 3.7 C).

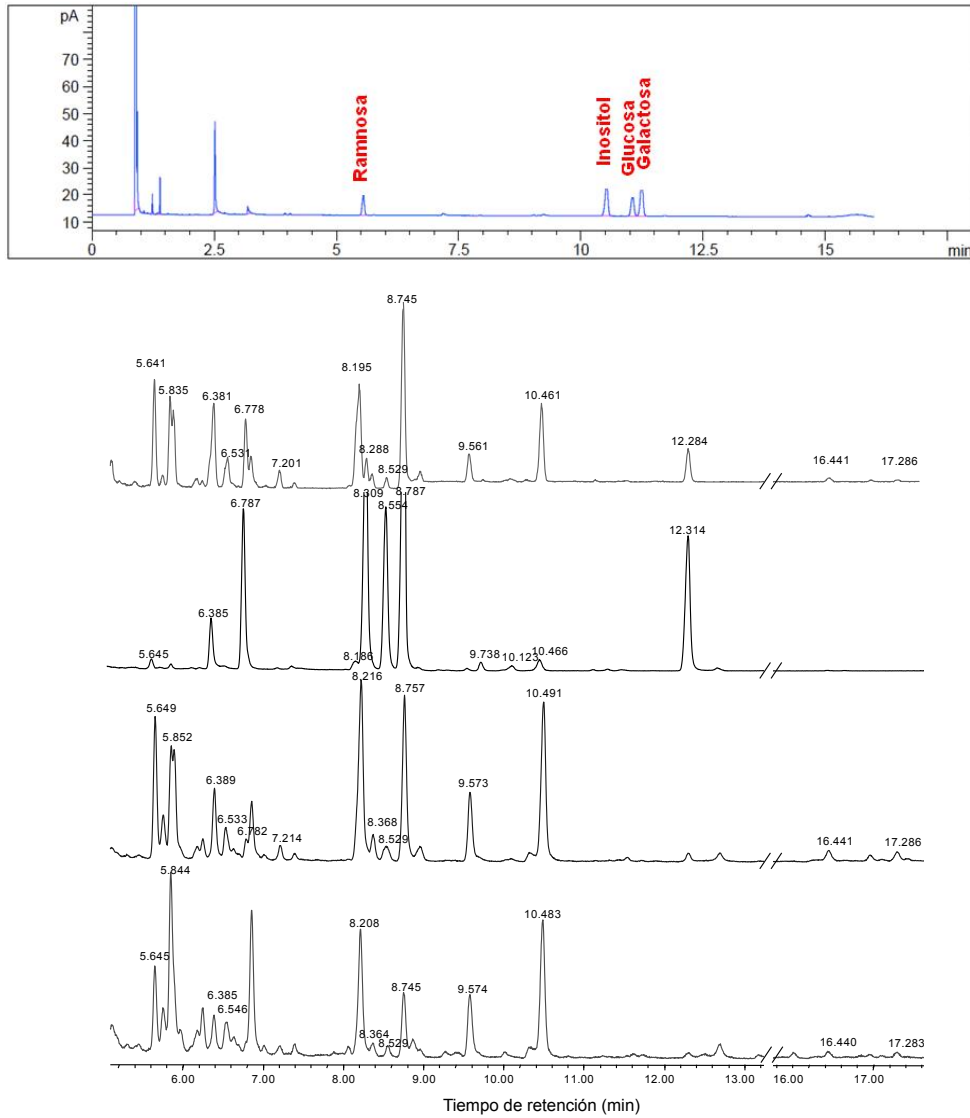


Fracción	<i>L. sicerae</i> CUPV261 ^T		<i>L. collinoides</i> CUPV237	
	EPS	EPS (autoclave)	EPS	EPS (autoclave)
a: 10³ kDa	>2	>2	>2	>2
Polidispersidad	1,57	1,45	1,74	1,60
b: 10 kDa	2,23	1,97	3,12	2,59
Polidispersidad	1,18	1,18	1,29	1,17
c: 1 kDa	4,84	5,06	5,61	5,69
Polidispersidad	1,08	1,04	1,03	1,03
Ratio 10⁶:10⁴:10³	3,8: 7,4: 1,0	3,6: 7,2: 1,0	5,5: 8,0: 1,0	5,2: 6,6: 1,0

Figura 3.6. Análisis del EPS mediante cromatografía de exclusión molecular (HPSEC). A, cromatogramas de los EPS sintetizados por *L. sicerae* CUPV261^T (línea azul) y *L. collinoides* CUPV237 (línea roja); a, b y c marcan la posición de las fracciones. B, valores de los pesos moleculares e índice polidispersidad (Mw/Mn) de cada fracción observada en el EPS y en el EPS sometido a 120 °C durante 20 min en un autoclave.

El análisis del EPS crudo mostró la complejidad de esta muestra, en la que se detectaron todos los tipos de enlace encontrados en las tres fracciones obtenidas a

partir de ella. La porción insoluble en sosa se compone principalmente de restos de galactosa y glucosa, en una proporción aproximada de 2:1, respectivamente. Estructuralmente, la presencia del 15 % de unidades de 3,6)-Galp-(1 y de 11 % de galactopiranosas terminal indican la existencia de una cadena ramificada. Los restantes componentes de esta fracción son unidades lineales de glucopiranosas enlazadas en (1→3) y (1→4), y una gran cantidad (34 %) de (1→3) galactopiranosas. Estos componentes difieren notablemente de los encontrados en las dos fracciones solubles obtenidas a partir de la muestra inicial, que muestran muchas similitudes entre sí. Ambas contienen importantes cantidades de unidades de ramnosa unidas en cadena lineal mediante enlaces (1→3) y (1→4), siendo particularmente relevante la presencia de un 18 % de (1→3) ramnosa en la fracción <50 kDa. En cuanto a la galactosa contenida en ellas, hay que destacar su abundancia en unidades lineales de (1→3) galactofuranosa (19 %). La identificación de unidades de galactosa sustituidas en sus posiciones 2 y 3 sugiere que el esqueleto de (1→3) galactofuranosa se ramifica parcialmente en sus posiciones 2, aunque existen otras posibilidades estructurales que expliquen estos datos. Otros componentes de estas fracciones son unidades de (1→3) y (1→6) galactopiranosas, que aparecen representadas en las dos muestras en diferente proporción, y cantidades muy bajas de glucosamina y galactosamina unidas mediante enlaces (1→4).



TR ^a (min)	Enlace deducido	Fragmentos característicos (m/z)	Proporción relativa de EPS (%)			
			Crudo	Insoluble	> 50 kDa	< 50 kDa
5,64	→2)-Ramp-(1→	89, 115, 131, 190	10,2	0,6	10,5	9,2
5,91	→3)-Ramp-(1→	89, 101, 118, 131, 202, 234	8,1	0,0	7,1	18,4
6,38	Glc _p -(1→	87, 88, 102, 118, 129, 161, 205	11,7	3,7	5,2	4,3
6,53	Gal _f -(1→	89, 102, 118, 162, 205, 278	0,0	0,0	2,4	4,0
6,78	Gal _p -(1→	87, 88, 102, 118, 129, 161, 205	7,3	11,6	1,2	0,7
7,21	→2,3)-Ramp-(1→	89, 131, 202, 262	2,0	0,0	1,3	0,0
8,19	→2)-Gal _p -(1→	87, 88, 101, 129, 130, 161, 190	0,0	0,8	0,0	0,0
8,19	→3)-Gal _f -(1→	118, 306	16,8	0,0	19,8	19,4
8,28	→3)-Glc _p -(1→	101, 118, 129, 161, 234	2,9	19,7	2,1	1,4
8,55	→4)-Glc _p -(1→	87, 102, 113, 118, 129, 131, 162, 173, 233	0,0	13,2	0,0	1,7
8,75	→3)-Gal _p -(1→	101, 118, 129, 161, 234	21,8	34,8	15,6	9,1
9,56	→6)-Gal _f -(1→	88, 101, 102, 117, 118, 127, 159, 233	3,5	tr. ^b	6,8	10,3
10,46	→2,3)-Gal _p /f-(1→	101, 129, 161, 202, 262	10,3	tr. ^b	16,6	20,4
12,28	→3,6)-Gal _p -(1→	118, 129, 189, 174, 234	4,4	15,1	0,9	0,0
16,43	→4)-Glc _p NH ₂ -(1→	117, 159, 233	0,7	0,0	1,0	1,0
17,27	→4)-Gal _p NH ₂ -(1→	117, 159, 233	tr. ^b	0,0	1,0	0,8

^aTiempo de retención

^bMenos de 0,2 %

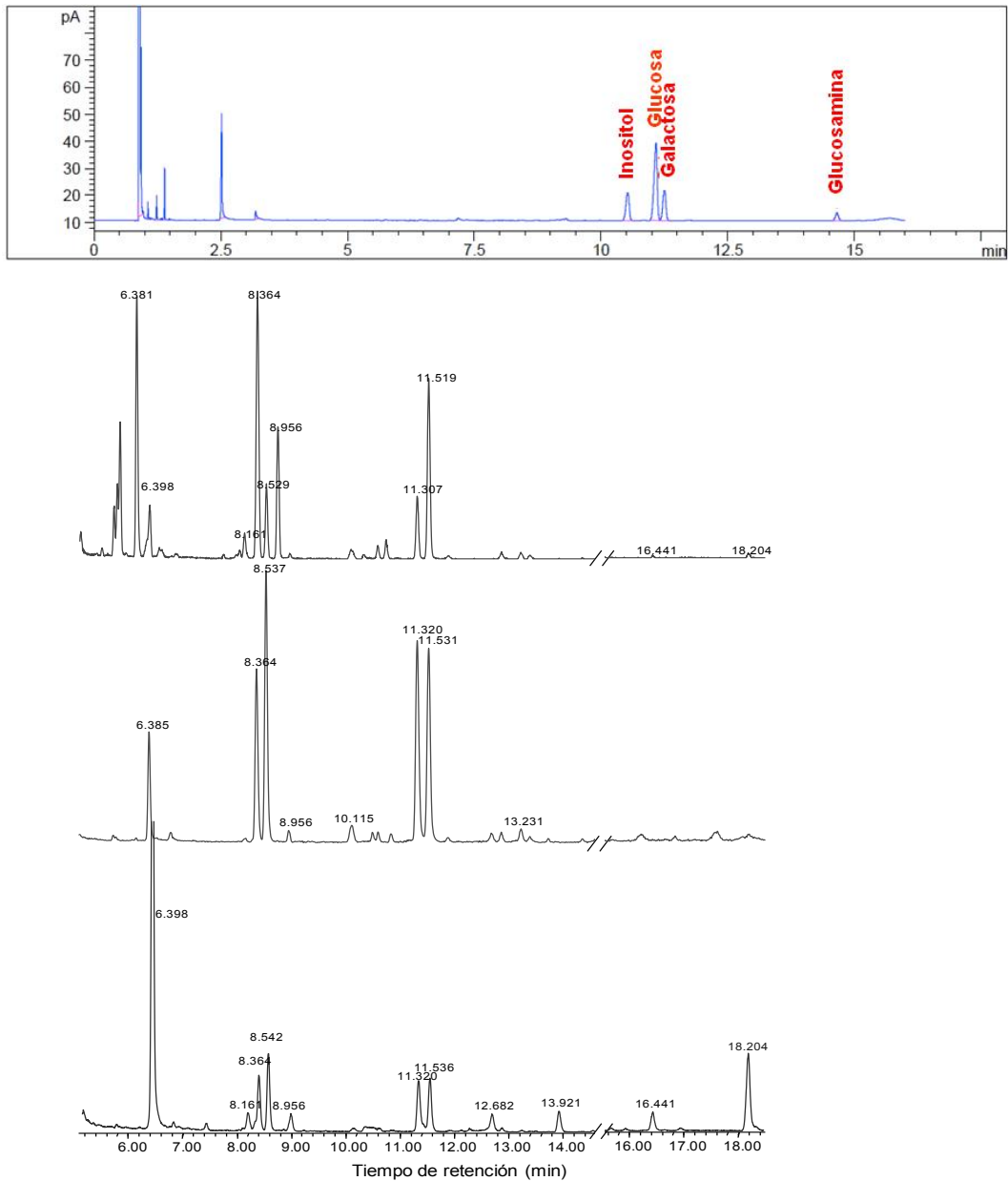
Figura 3.7. Cromatogramas resultado del análisis de monosacáridos (A) y de metilación (B) del EPS sintetizado por *L. sicerae* CUPV261^T. La tabla refleja el tipo de unión entre monosacáridos y sus porcentajes relativos, deducidos del análisis de metilación.

3.2.3 *Lactobacillus collinoides* CUPV237

Para determinar el peso molecular del EPS crudo, el líofilo fue analizado mediante HPSEC (Figura 3.6 B). Los cromatogramas mostraron que el EPS estaba compuesto por 3 fracciones: (i) fracción de alto peso molecular, superior a 2,000 kDa (límite del calibrado); (ii) fracción del orden de 30 kDa (la más abundante); (iii) y una fracción en torno a 5 kDa (en una proporción de 6 y 5 veces inferior a las otras dos, respectivamente).

El análisis de la composición de azúcares neutros reveló la presencia de glucosa, galactosa y glucosamina (Figura 3.8 A). Posteriormente, el EPS crudo fue solubilizado completamente en una solución alcalina y fue separado mediante un sistema Amicon® en dos fracciones de >50 kDa (58,5 %) y <50 kDa (41,5 %). Con el fin de investigar el tipo de enlaces O-glicosídicos presentes en la muestra, las diferentes fracciones fueron sometidas a un análisis de metilación (Figuras 3.8 B y Tabla).

Al igual que en el caso anterior, el EPS crudo mostró una mezcla de los tipos de enlace detectados en las dos fracciones solubles separadas. Los resultados del análisis del polímero de mayor masa molecular (>50 kDa) indican que se trata de una molécula ramificada. El esqueleto principal parece estar formado por unidades lineales de glucosa y unidas mediante enlaces (1→4) y/o tal vez (1→5) en el caso de la galactosa. Presumiblemente, algunas de estas unidades se ramifican en sus posiciones 6, tal y como se deduce de la presencia de dos tipos diferentes de hexosas unidas en (1→4,6). Sin embargo, en esta muestra, la proporción registrada para el total de puntos de ramificación es muy superior a la de residuos terminales. Esto puede deberse bien a una metilación deficiente del polímero analizado, asunto que no pudo resolverse tras sucesivas metilaciones del producto, o bien a la presencia en este EPS de sustituyentes no detectados en el análisis realizado. El polímero de menor masa molecular contiene, además de los mismos componentes encontrados en la fracción >50 kDa (en proporciones mucho menores), una cantidad relevante de glucosamina, principalmente con uniones (1→4,6), es decir, en puntos de ramificación de la cadena. Otros componentes de estas fracciones son unidades de (1→3) y (1→6) galactopiranosas, que aparecen representadas en las dos muestras en diferente proporción, y pequeñas cantidades de glucosamina y galactosamina unidas mediante enlaces (1→4). Es también reseñable la alta cantidad de unidades terminales de glucopiranosas detectadas en esta fracción.



TR ^a (min)	Enlace deducido	Fragmentos característicos (m/z)	Proporción relativa de EPS (%)		
			Crudo	>50 kDa	< 50 kDa
6,38	Glc _p -(1→	87, 88, 102, 118, 129, 161, 205	8,2	9,0	51,1
6,78	Gal _f -(1→	89, 102, 118, 162, 205, 278	0,0	1,2	0,0
8,16	→2)-Man _p -(1→	87, 88, 101, 129, 130, 161, 190	2,4	0,0	1,8
8,36	→4 ó 5)-Gal-(1→	87, 102, 113, 118, 129, 131, 162, 173, 233	40,3	17,9	5,5
8,53	→4)-Glc _p -(1→	87, 102, 113, 118, 129, 131, 162, 173, 233	9,1	25,8	8,0
8,96	→6)-Glc _p -(1→	87, 88, 102, 118, 129, 162, 189	tr. ^b	0,0	2,1
10,11	→3,4)-Glc _p -(1→	118, 129, 305	1,55	2,5	0,0
11,32	→4,6)-Hex _p -(1→	118, 201, 261	8,0	22,4	6,9
11,53	→4,6)-Hex _p -(1→	118, 201, 261	28,2	22,1	6,2
13,92	Glc _p NH ₂ -(1→	117, 129, 145, 159, 161, 203, 205	tr. ^b	0,0	2,6
16,43	→4)-Glc _p NH ₂ -(1→	117, 159, 233	tr. ^b	0,0	2,4
18,20	→4,6)-Glc _p NH ₂ -(1→	117, 159, 189, 233	1,0	0,0	11,0

^aTiempo de retención

^bMenos de 0,2 %

Figura 3.8. Cromatogramas resultado del análisis de monosacáridos (A) y de metilación (B) del EPS sintetizado por *L. collinoides* CUPV237. La tabla refleja el tipo de unión entre monosacáridos y sus porcentajes relativos, deducidos del análisis de metilación.

3.2.4 Análisis de la estabilidad térmica de los EPS

El análisis termogravimétrico es un análisis simple y preciso para el estudio del patrón de descomposición y estabilidad térmica de los polímeros. En él se registra la pérdida de peso del EPS al aplicarle un aumento progresivo de temperatura. La degradación termogravimétrica de los EPS crudos de *L. collinoides* y *L. sicerae* ocurrió en tres fases (Figura 3.9): La primera se localiza entre los 45-120 °C, en la cual se observa una disminución del peso inferior al 10 %; la segunda entre los 170-400 °C, donde los dos EPS pierden en torno al 50 %; y una tercera etapa hasta los 600 °C, con una disminución del peso de entre el 5-14 %.

Las curvas obtenidas en el análisis TGA del EPS de *L. sicerae* muestran una temperatura de inicio de la descomposición (T_o) a 237 °C; y dos temperaturas a las que se degrada la mayoría de la muestra (T_{max}), una de ellas a 252 °C y otra menos intensa a 308 °C. En la última fase de degradación hay una pérdida de peso del 5 %, y permanece el 34 % del residuo carbonáceo al alcanzar los 600 °C. Sin embargo, en el análisis termogravimétrico del EPS de *L. collinoides* se observa una T_o a 244 °C y una T_{max} a 284 °C, notablemente más alta que en el EPS de CUPV261^T (Figura 3.9). Por último, la pérdida de peso en la última fase de degradación es del 14 %, y el residuo carbonáceo final es menor que el encontrado en el análisis del EPS de *L. sicerae*.

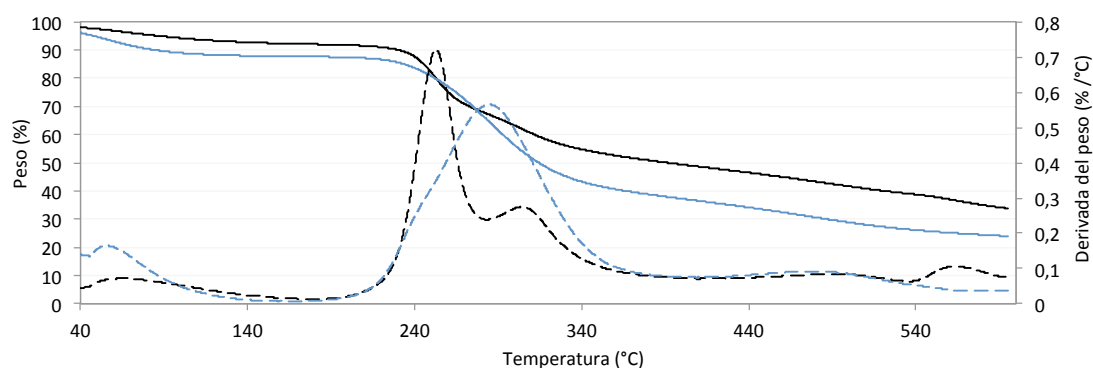


Figura 3.9. Análisis termogravimétrico de los EPS. Curvas de termodegradación del EPS de *L. sicerae* CUPV261^T (en negro) y *L. collinoides* CUPV237 (en azul), donde la línea continua representa el % del peso restante, y la línea discontinua la primera derivada de la curva del peso (DTG).

Los EPS fueron también sometidos a 120 °C durante 20 min mediante un autoclave, y el posterior análisis por HPSEC no reveló cambios importantes en el peso molecular de las fracciones (Figura 3.6). Los perfiles cromatográficos fueron similares a los obtenidos en los EPS que no recibieron el tratamiento térmico.

3.3 Tolerancia del EPS al estrés gastrointestinal en un modelo *in vitro*

Los EPS producidos por *L. sicerae* CUPV261^T y *L. collinoides* CUPV237 fueron sometidos a tratamientos enzimáticos junto con una disminución progresiva del pH, siguiendo un modelo *in vitro* de estrés gástrico y gastrointestinal (Figura 3.2). La tolerancia de los EPS al estrés fue evaluada en las fracciones de >2000 kDa y de peso molecular intermedio (en torno a 10 kDa). Para ello, se tomaron muestras en los tratamientos G1 (control, pH 5), G6 (pH 2,1), G7 (pH 1,8) y GI5 (pH 3,0), y se determinó el peso molecular de las fracciones mediante HPSEC (Figura 3.10). Se estudió la variación del área del pico en G1 y después del tratamiento (cantidad relativa), así como el índice de polidispersidad (IP).

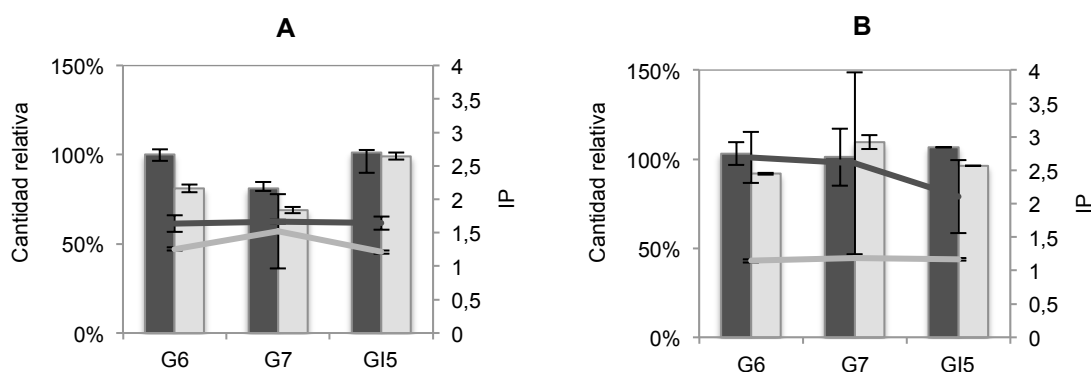


Figura 3.10. Tolerancia al estrés gástrico (G) y gastrointestinal (GI) de los EPS producidos por *L. sicerae* CUPV261^T (A) y *L. collinoides* CUPV237 (B). Las barras representan la cantidad relativa; las líneas indican el valor del índice de polidispersidad (IP) de cada fracción. De color gris oscuro se muestra la fracción de un peso molecular >2000 kDa, y de gris claro la fracción próxima a 10 kDa. Los resultados representan la media aritmética ± desviación estándar. No se han encontrado diferencias significativas para un nivel de significación p<0,05.

Con respecto al efecto del estrés gastrointestinal sobre el EPS de CUPV261^T (Figura 3.10 A), después del tratamiento G6 (pH 2,1) se recuperó el 100 % de la fracción de alto peso molecular, mientras que tras el G7 (pH 1,8), se detectó una disminución del 19 % en su cantidad relativa. El índice de polidispersidad se mantuvo constante durante todo el ensayo. Sin embargo, el área de la fracción de inferior peso molecular se redujo un 19 % en G6 y un 31 % en G7. En ningún caso se detectaron cambios en ambas fracciones después del tratamiento gastrointestinal (GI5, pH 3).

En el caso del EPS de CUPV237 (Figura 3.10 B), las dos fracciones sufrieron cambios en su cantidad relativa, que fueron inferiores al 10 % tras los tratamientos de estrés G y GI. El IP de la fracción de peso molecular intermedio se mantuvo constante durante todo el ensayo.

3.4 Efecto de los EPS en un modelo *in vivo* de inflamación intestinal en larvas de pez cebra

Se analizó el efecto de los EPS producidos por *L. sicerae* CUPV261^T, *L. collinoides* CUPV237, *B. longum* INIA P132 y *B. infantis* INIA P731, sobre la mortalidad de las larvas tratadas con el agente químico DSS (larvas IBD) para inducir la enfermedad inflamatoria intestinal (Figura 3.3).

Los embriones se trataron exclusivamente con 150 µg mL⁻¹ de EPS hasta los 4 días posfecundación (dpf) (Figura 3.11 A). Durante este periodo no se observaron efectos negativos de los polisacáridos sobre la supervivencia de los embriones ($p < 0,05$). La exposición de las larvas IBD a los EPS produjo un efecto paliativo en la mortalidad, en comparación al grupo tratado exclusivamente con DSS ($p < 0,05$ y $p < 0,01$). Además, a los 6 dpf no se detectaron diferencias significativas entre las mortalidades de las larvas no tratadas (EW) y las co-tratadas con DSS-EPS ($p < 0,05$). Este comportamiento se mantuvo hasta los 7 dpf en el grupo co-tratado con el EPS de CUPV261^T.

Además, se evaluó el efecto dosis-dependiente de los EPS producidos por *L. sicerae* CUPV261^T, *L. collinoides* CUPV237 y *B. infantis* INIA P731. Para ello, se utilizaron las concentraciones de 50, 100 y 150 µg mL⁻¹, y se siguieron las condiciones del ensayo anterior (Figura 3.11 B). De nuevo, los resultados mostraron que la presencia del EPS favoreció la supervivencia de los individuos respecto al control positivo (DSS). La mortalidad se redujo significativamente ($p < 0,05$) en las larvas de 6 dpf co-tratadas con los EPS producidos por las cepas de *Lactobacillus*, y fue inferior en las expuestas a 150 µg mL⁻¹ con el EPS de *L. sicerae*, y a 100 µg mL⁻¹ con el de *L. collinoides*. A los 7 dpf, se mantuvieron las diferencias significativas entre el grupo de larvas tratadas exclusivamente con DSS y el de las co-tratadas EPS-DSS, para las tres concentraciones y EPS ($p < 0,01$ y $p < 0,05$). La dosis más efectiva en los EPS producidos por los lactobacilos fue de 100 µg mL⁻¹, y de 150 µg mL⁻¹ con el EPS de la bifidobacteria INIA P731.

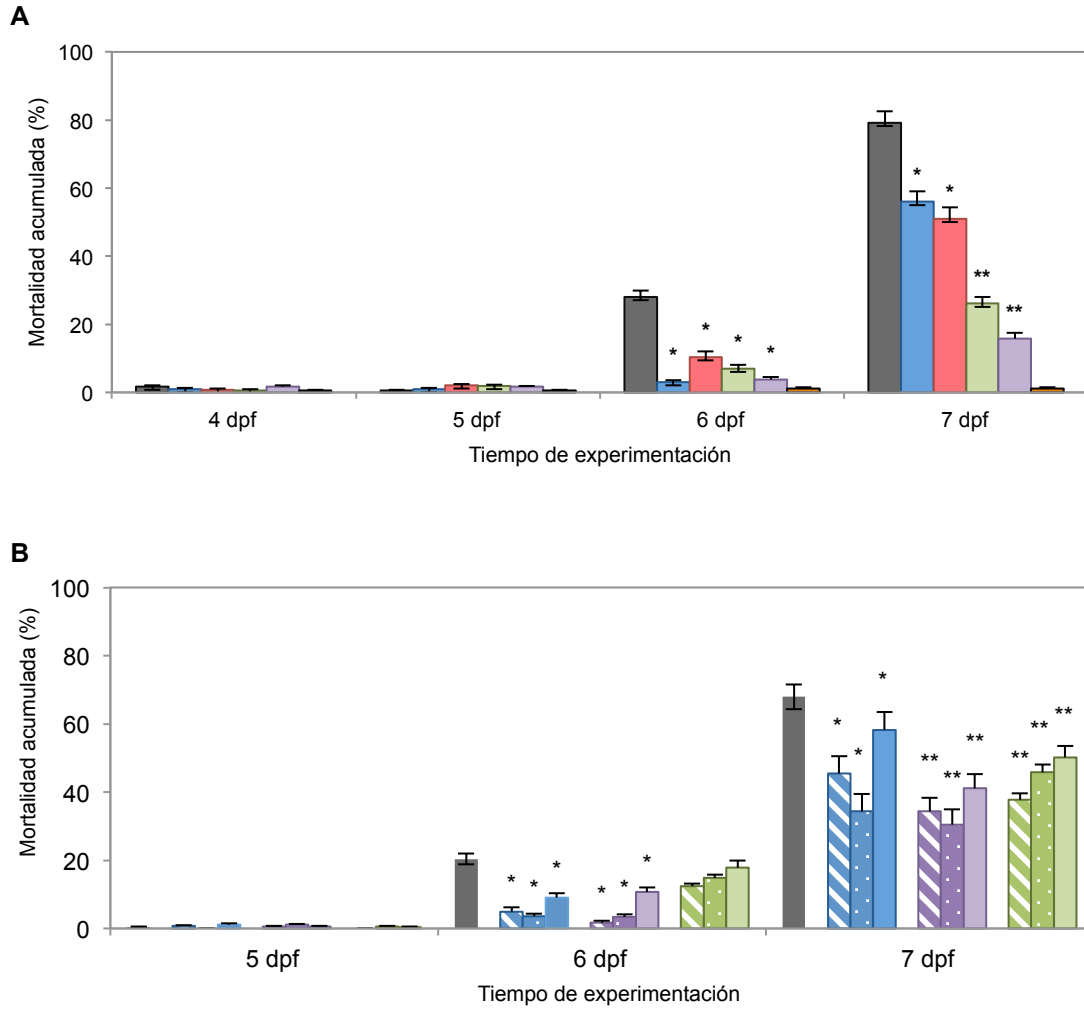


Figura 3.11. Efecto de los exopolisacáridos en el modelo de enterocolitis de larvas de pez cebra. El gráfico muestra la mortalidad (%) observada en los grupos de larvas expuestas a: 0,8 % (p/v) de DSS (■); y co-tratadas con DSS más el EPS producido por *L. sicerae* CUPV261^T (■), *L. collinoides* CUPV237 (■), *B. infantis* INIA P731 (■), *B. longum* INIA P132 (■); y sin tratamiento (■). En **A**, se muestra el ensayo realizado con las larvas tratadas con 150 µg mL⁻¹ de EPS; y en **B**, el efecto dosis-dependiente de los diferentes EPS, donde no se observó ninguna muerte en el grupo sin tratamiento (control negativo). La textura de las barras indica la concentración utilizada: líneas inclinadas, 50 µg mL⁻¹; puntos, 100 µg mL⁻¹; y barra sólida, 150 µg mL⁻¹. Los resultados representan la media aritmética ± desviación estándar; y las diferencias significativas entre el grupo DSS y el resto de tratamientos se indican como ** (p<0,01) y * (p<0,05).

4. DISCUSIÓN

Las aplicaciones de los exopolisacáridos en diferentes áreas industriales se deben principalmente a sus propiedades reológicas, que permiten la formación de soluciones viscosas a bajas concentraciones (0,05–1 %), y además, presentan estabilidad en un amplio rango de temperatura, pH y fuerza iónica (Baruah, Das & Goyal, 2016). Las diferentes características de los polisacáridos, tales como su unión a la célula (CPS vs. EPS), composición y peso molecular, conformación y tamaño, rigidez, grado de ramificación y existencia de grupos funcionales cargados, pueden influir en sus propiedades reológicas (Zeidan et al., 2017). Las cepas *L. sicerae* CUPV261^T y *L. collinoides* CUPV237 estudiadas en este trabajo mostraron un fenotipo *ropy*, y un incremento de la viscosidad (newtoniana, η_0) de los cultivos líquidos y de los sobrenadantes libres de células.

Los polisacáridos bacterianos pueden quedar adheridos a la superficie celular formando una cápsula o ser liberados al medio en forma de exopolisacáridos, como ocurre con los EPS producidos por *L. sicerae* CUPV261^T y *L. collinoides* CUPV237 (Figura 3.3), y en otras especies de *Lactobacillus* aisladas de sidra pertenecientes a las especies *L. diolivorans* y *L. suebicus* (Dueñas et al., 1998; Ibarburu et al., 2015). En las bacterias lácticas, la producción de polisacárido y su rendimiento, dependen de varios factores, tales como las condiciones de cultivo, la composición del medio, el tipo de polímero (HoPS o HePS) y de la cepa en sí (de Vuyst & Degeest, 1999; Dueñas et al., 2003). Algunas bacterias productoras del HoPS dextrano, pueden alcanzar rendimientos de hasta 14 g L⁻¹ en presencia de 50 g L⁻¹ de sacarosa (Korakli et al., 2001); sin embargo, la producción de HePS por BAL es sensiblemente menor (Patten & Laws, 2015). En este estudio, las bacterias CUPV261^T y CUPV237 en el medio de cultivo semidefinido MSD han producido en torno a los 90 y 50 mg mL⁻¹ de EPS, respectivamente, similar a los niveles de producción descritos en otras estirpes aisladas de sidra de la especie *L. suebicus* (Ibarburu et al., 2015).

Por otro lado, el peso molecular de los exopolisacáridos tiene una gran influencia sobre las propiedades físico-químicas y biológicas de estos polímeros (Hidalgo-Cantabrana et al., 2012; Laiño et al., 2016; Zhou, Cui & Qu, 2019). El análisis mediante cromatografía de exclusión por tamaño HPSEC de los EPS producidos por las dos cepas estudiadas puso de manifiesto que están compuestos por tres fracciones, una de elevado peso molecular (>2000 kDa, límite de exclusión de la columna), otra de 20-30 kDa y una tercera en torno a los 5 kDa, siendo mayoritaria la fracción de peso molecular intermedio. Al igual que ocurre con estas

estirpes de *Lactobacillus*, es frecuente encontrar especies de BAL que producen más de un exopolisacárido con diferente peso molecular y composición (Mozzi et al., 2009; Garai-Ibabe, 2010; Leivers et al., 2011; Ibarburu et al., 2015; Llamas-Arriba et al., 2018; Llamas-Arriba et al. 2019). Así mismo, se ha descrito que las proporciones de las diferentes fracciones dependen de la composición del medio de cultivo, en concreto del ratio carbono/nitrógeno (Degeest & De Vuyst, 1999), y del tipo de azúcar disponible en el medio (Ibarburu et al., 2015).

Con respecto a los EPS producidos por *Lactobacillus*, algunas estirpes pertenecientes a las especies *L. reuteri* o *L. sakei* sintetizan HoPS del tipo dextrano y levano (van Hijum et al., 2001; Nácher-Vázquez et al., 2015). Otros lactobacilos como *L. plantarum* o *L. casei* entre otros, sintetizan HePS, que están la mayoría constituidos por glucosa y galactosa, y de forma menos frecuente aparecen otros componentes (*N*-acetilglucosamina, *N*-acetilgalactosamina, ramnosa, manosa o grupos acetilo) (Baruah, Das & Goyal, 2016; Zhou, Cui & Qu, 2019). También se ha descrito en aislados de sidra la producción simultánea del HoPS β -glucano y HePS en *L. suebicus* CUPV221 (Garai-Ibabe, 2010), así como β -glucano y un dextrano en *L. diolivorans* G-77 (Dueñas et al. 1998).

La caracterización estructural de los EPS producidos por *L. collinoides* y *L. sicerae* se llevó a cabo mediante análisis de metilación, cromatografía de gases, espectroscopía infrarroja (FTIR) y RMN ^1H . Con respecto al EPS producido por *L. collinoides*, los análisis de la composición de azúcares y de metilación, mostraron que las diferentes fracciones analizadas (EPS crudo, >50 kDa o <50 kDa), estaban compuestas por glucosa, galactosa y glucosamina (Figura 3.8). Los tres monosacáridos se hallaron en diferentes proporciones según la fracción analizada y sustituidos en distintas posiciones. El espectro RMN ^1H del EPS crudo indicó la presencia de grupos acetilo, que podrían estar unidos al grupo amino en forma de *N*-acetil-azúcares (*N*-acetil-glucosamina), como se ha sido descrito en los EPS de *L. acidophilus* 5e2 (Laws et al., 2008) y en las estirpes *L. suebicus* CUPV225 y CUPV226 aisladas de sidra (Ibarburu et al., 2015), cuyos EPS tienen la misma composición que el de *L. collinoides* (Glc:Gal:NAcGlc).

En el caso de *L. sicerae* CUPV261^T, los análisis de la composición de azúcares y de metilación de su EPS (Figura 3.7), mostraron que las diferentes fracciones (EPS crudo, > 50 Da, <50 kDa, e insoluble) están compuestas por glucosa, galactosa y ramnosa, y en menor proporción glucosamina y galactosamina. El análisis RMN ^1H del EPS crudo, mostró una muy señal débil para el grupo acetilo.

Esta es la primera vez que se describe la presencia de ramnosa en exopolisacáridos producidos por aislados de sidra, aunque es muy común encontrar EPS de *Lactobacillus* compuestos por glucosa, galactosa y ramnosa, como en *L. delbrueckii* subsp. *bulgaricus*, *L. rhamnosus*, *L. helveticus*, *L. fermentum* o *L. plantarum* (De Vuyst & Degeest, 1999; De Vuyst et al., 2001; Badel, Bernardi & Michaud, 2011).

En cuanto a la caracterización físico-química de los EPS, una importante característica para ser utilizados en la sector alimentario es su estabilidad térmica, un ejemplo de ello es la temperatura para el procesado de la leche en la industria láctea, que raramente sobrepasa los 150 °C (Ahmed et al., 2013). Los análisis termogravimétricos y el estudio del perfil cromatográfico de los pesos moleculares de los HePS sometidos a un tratamiento térmico (120 °C, 20 min) revelaron una estabilidad térmica de los polímeros sintetizados por las dos cepas estudiadas (Figura 3.9). El estudio termogravimétrico mostró que la degradación de los polisacáridos se llevó a cabo en tres fases, tal y como ha sido descrito en el (1,3)(1,2)- β -D-glucano de *P. parvulus* 2.6 (Zamora et al. 2002). La temperatura (T_o) a la cual comienza la descomposición fue similar en ambos EPS (próxima a 240 °C). Sin embargo, la mayor parte del EPS-CUPV237 se degradó a 284 °C (T_{max}), mientras que en el EPS-CUPV261^T se observaron dos T_{max} , a 252 y 308 °C. Los valores de las T_{max} observadas fueron similares a las descritas para los EPS producidos por *L. plantarum* KF5 (T_{max} de 278 °C, Wang et al., 2010), *L. plantarum* DM5 (292 °C, Das, Baruah & Goyal, 2014) y *Bacillus* sp. I-471 (307 °C, Kumar et al., 2004), cuyas variaciones pueden ser debidas a las diferencias en la composición y estructura de los EPS (Botelho et al., 2014).

Por otro lado, la síntesis de EPS por las bacterias podría suponer una ventaja frente a las células desnudas, ya que se ha observado un efecto beneficioso del exopolisacárido en la supervivencia celular durante su paso por el tracto gastrointestinal, y en condiciones *in vitro* (Boke, Alp & Aslim, 2010; Alp & Aslim, 2010; Hongpattarakere et al., 2012, Darilmaz, 2013; Cagganiello et al., 2016). El análisis de la respuesta al estrés gástrico (pH 2,1) y gastrointestinal (pH 3, pancreatina y sales biliares) de los HePS de CUPV261^T y CUPV237 reveló que la tolerancia de exopolisacárido de *L. collinoides* fue elevada, así como la del producido por *L. sicerae* al ser sometido al estrés gastrointestinal (Figura 3.10). Sin embargo, el EPS de *L. sicerae* se vio afectado durante el tratamiento de estrés gástrico. Este resultado fue similar a lo descrito por Mozzi et al. (2009), que observaron una degradación parcial de los HePS producidos por *Streptococcus thermophilus* CRL

1190 y por *L. casei* CRL 87 cuando fueron sometidos a las condiciones de estrés gástrico en un modelo *in vitro*. La tolerancia de los HePS al estrés gástrico y gastrointestinal nos sugiere que pueden tener un efecto beneficioso en la supervivencia de las bacterias productoras a su paso por el tracto gastrointestinal, tal y como se ha observado en la cepa productora de HePS *B. animalis* subsp. *lactis* (Hidalgo-Cantabrana et al., 2015) o de (1,3)(1,2)- β -D-glucano por *L. casei* (Stack et al., 2010). Los HePS producidos por CUPV261^T y por CUPV237 podrían tener un efecto prebiótico dada su resistencia a las condiciones gastrointestinales, y ser potencialmente utilizados por la microbiota intestinal (Corzo et al., 2015).

En relación a la actividad biológica de los EPS y de las bacterias productoras, Şengül et al., (2006) sugirieron que el efecto antiinflamatorio de bacterias probióticas productoras de exopolisacáridos y de los propios EPS, pueden suponer una prometedora terapia para la enfermedad inflamatoria intestinal. La producción de HePS por bacterias lácticas puede constituir una ventaja, ya que podrían ser utilizadas en la elaboración de productos fermentados y así tratar de una forma amable este tipo de enfermedades intestinales. En el presente estudio se analizó el efecto de los HePS producidos por *L. sicerae*, *L. collinoides*, y por las bifidobacterias INIA P132 e INIA P731, en el modelo *in vivo* de enterocolitis inducida por el agente químico DSS en larvas de pez cebra (larvas IBD) (Oehlers et al., 2012). Los resultados obtenidos mostraron que los tratamientos con los EPS atenuaron significativamente la mortalidad de las larvas IBD. Además, se observó un efecto dosis-dependiente de los HePS. Así, la concentración más efectiva para disminuir la mortalidad de las larvas IBD fue de 100 $\mu\text{g mL}^{-1}$ con los HePS los producidos por las cepas de *Lactobacillus*, y de 150 $\mu\text{g mL}^{-1}$ con el EPS producido por INIA P731. No se han encontrado trabajos similares en la bibliografía, pero sí ensayos *in vivo* con el modelo murino de enterocolitis inducida por DSS o por la administración de ácido acético en el colon (Şengül et al. 2006; Hidalgo-Cantabrana et al., 2016). Estos trabajos describieron una atenuación de la colitis experimental con el tratamiento de las bacterias probióticas *Bifidobacterium animalis* subsp. *lactis* y *Lactobacillus delbrueckii* subsp. *bulgaricus*, además de un efecto dosis-dependiente del EPS que producen. La cepa *ropy B. animalis* subsp. *lactis* Balat_1410^{S89L} posee una alta capacidad inmunomoduladora de las células T procedentes de los nodos linfoides mesentéricos, confiriéndole un efecto antiinflamatorio a nivel de la mucosa intestinal (Hidalgo-Cantabrana et al., 2016).

5. CONCLUSIONES

En el presente trabajo se han caracterizado los EPS producidos por las bacterias *Lactobacillus sicerae* CUPV261^T y *Lactobacillus collinoides* CUPV237. Ambas cepas presentan un fenotipo *ropy* e incrementan la viscosidad del medio de cultivo provocado por la presencia de exopolisacárido. Las microfotografías de CUPV261^T y CUPV237 tomadas mediante microscopía electrónica muestran la presencia de EPS alrededor de las bacterias

Los EPS de *L. sicerae* y de *L. collinoides* son una combinación de tres fracciones cuyos pesos moleculares están en torno a 1, 10 y superiores a 10³ kDa. Son heteropolisacáridos y están compuestos mayoritariamente por glucosa y galactosa, además de ramnosa en el EPS de CUPV261^T, o glucosamina y grupos acetilo en el EPS de CUPV237. Ambos presentan estabilidad térmica hasta los 244 °C.

Estos heteropolisacáridos resisten las condiciones de estrés gástrico y gastrointestinal ensayadas en un modelo *in vitro*. Además, los HePS producidos por *L. sicerae* CUPV261^T, *L. collinoides* CUPV237, *B. longum* INIA P132 y *B. infantis* INIA P731 poseen la capacidad de atenuar la mortalidad de las larvas de pez cebra, en el modelo *in vivo* de enfermedad inflamatoria intestinal inducido por el agente químico DSS. Este efecto es dosis-dependiente, y la concentración más efectiva es de 100 µg mL⁻¹ con los HePS producidos por las dos estirpes de *Lactobacillus*, y de 150 µg mL⁻¹ con el EPS de INIA P731.

6. BIBLIOGRAFÍA

- Ahmed, Z., Wang, Y., Anjum, N., Ahmad, A., & Khan, S. T. (2013). Characterization of exopolysaccharide produced by *Lactobacillus kefiranofaciens* ZW3 isolated from Tibet kefir—Part II. *Food Hydrocolloids*, 30(1), 343-350.
- Alp, G., & Aslim, B. (2010). Relationship between the resistance to bile salts and low pH with exopolysaccharide (EPS) production of *Bifidobacterium spp.* isolated from infants feces and breast milk. *Anaerobe*, 16(2), 101-105.
- Badel, S., Bernardi, T., & Michaud, P. (2011). New perspectives for *Lactobacilli* exopolysaccharides. *Biotechnology Advances*, 29(1), 54-66.
- Baruah, R., Das, D., & Goyal, A. (2016). Heteropolysaccharides from lactic acid bacteria: current trends and applications. *Probiotics & Health*, 4(141), 2.
- Boke, H., Aslim, B., & Alp, G. (2010). The role of resistance to bile salts and acid tolerance of exopolysaccharides (EPSs) produced by yogurt starter bacteria. *Arch. Biol. Sci*, 62(2), 323-328.
- Botelho, P. S., Maciel, M. I., Bueno, L. A., Marques, M. F., Marques, D. N. & Silva, T. M. S. (2014). Characterisation of a new exopolysaccharide obtained from of fermented kefir grains in soymilk. *Carbohydrate Polymers*, 107, 1-6.
- Caggianiello, G., Kleerebezem, M., & Spano, G. (2016). Exopolysaccharides produced by lactic acid bacteria: from health-promoting benefits to stress tolerance mechanisms. *Applied Microbiology and Biotechnology*, 100(9), 3877-3886.
- Castro-Bravo, N., Wells, J. M., Margolles, A., & Ruas-Madiedo, P. (2018). Interactions of surface exopolysaccharides from *Bifidobacterium* and *Lactobacillus* within the intestinal environment. *Frontiers in Microbiology*, 9.
- Ciucanu, I., & Kerek, F. (1984). A simple and rapid method for the permethylation of carbohydrates. *Carbohydrate Research*, 131(2), 209-217.
- Corzo, N., González, A., Luis, J., Azpiroz, F., Calvo, M. A., Cirici, Leis, M., R., Lombó, F., Mateos-Aparicio, I., Plou, F. J., Ruas-Madiedo, P., Rúperez, P., Redondo-Cuenca, A., Sanz, M. L. & Clemente, A. (2015). Prebiotics: Concept, properties and beneficial effects= Prebióticos; Concepto, propiedades y efectos beneficiosos. *Nutrición Hospitalaria*, 31(Supl.1), 99-118.
- Darilmaz, D. O. (2013). Relationship between gastrointestinal tolerance and exopolysaccharide production of propionibacteria strains under different pH and bile conditions. *International Journal of Dairy Technology*, 66(2), 194-201.

- Das, D., Baruah, R., & Goyal, A. (2014). A food additive with prebiotic properties of an α -D-glucan from *Lactobacillus plantarum* DM5. *International Journal of Biological Macromolecules*, 69, 20-26.
- Deepak, V., Ramachandran, S., Balahmar, R. M., Pandian, S. R. K., Sivasubramaniam, S. D., Nellaiah, H., & Sundar, K. (2016). In vitro evaluation of anticancer properties of exopolysaccharides from *Lactobacillus acidophilus* in colon cancer cell lines. *In Vitro Cellular & Developmental Biology-Animal*, 52(2), 163-173.
- Degeest, B., & De Vuyst, L. (1999). Indication that the nitrogen source influences both amount and size of exopolysaccharides produced by *Streptococcus thermophilus* LY03 and modelling of the bacterial growth and exopolysaccharide production in a complex medium. *Appl. Environ. Microbiol.*, 65(7), 2863-2870.
- Dueñas-Chasco, M. T., Rodríguez-Carvajal, M. A., Mateo, P. T., Franco-Rodríguez, G., Espartero, J., Irastorza-Iribas, A., & Gil-Serrano, A. M. (1997). Structural analysis of the exopolysaccharide produced by *Pediococcus damnosus* 2.6. *Carbohydrate Research*, 303(4), 453-458.
- Dueñas-Chasco, M. T., Rodríguez-Carvajal, M. A., Tejero-Mateo, P., Espartero, J. L., Irastorza-Iribas, A., & Gil-Serrano, A. M. (1998). Structural analysis of the exopolysaccharides produced by *Lactobacillus* spp. G-77. *Carbohydrate Research*, 307(1), 125-133.
- Dueñas, M., Munduate, A., Perea, A., & Irastorza, A. (2003). Exopolysaccharide production by *Pediococcus damnosus* 2.6 in a semidefined medium under different growth conditions. *International Journal of Food Microbiology*, 87(1-2), 113-120.
- Dubois, M., Gilles, K. A., Hamilton, J. K., Rebers, P. T., & Smith, F. (1956). Colorimetric method for determination of sugars and related substances. *Analytical Chemistry*, 28(3), 350-356.
- Fernández de Palencia, P., Werning, M. L., Sierra-Filardi, E., Dueñas, M. T., Irastorza, A., Corbí, A. L., & López, P. (2009). Probiotic properties of the 2-substituted (1, 3)- β -D-glucan-producing bacterium *Pediococcus parvulus* 2.6. *Applied and Environmental Microbiology*, 75(14), 4887-4891.
- Fleming, A., Jankowski, J., & Goldsmith, P. (2010). In vivo analysis of gut function and disease changes in a zebrafish larvae model of inflammatory bowel disease: a feasibility study. *Inflammatory Bowel Diseases*, 16(7), 1162-1172.

- Garai-Ibabe, G. (2010). Bacterias lácticas de sidra natural: implicación en alteraciones y potencial probiótico de cepas productoras de (1, 3)(1, 2)- β -D-glucanos (Tesis doctoral, Universidad del País Vasco-Euskal Herriko Unibertsitatea).
- Garai-Ibabe, G., Areizaga, J., Aznar, R., Elizaquivel, P., Prieto, A., Irastorza, A., & Dueñas, M. T. (2010). Screening and selection of 2-branched (1, 3)- β -D-glucan producing lactic acid bacteria and exopolysaccharide characterization. *Journal of Agricultural and Food Chemistry*, 58(10), 6149-6156.
- De Giacomo, O., Cesàro, A. & Quaroni, L. (2008). Synchrotron based FTIR spectromicroscopy of biopolymer blends undergoing phase separation. *Food Biophysics*, 3(1), 77-86.
- Grube, M., Lin, J. G., Lee, P. H., & Kokorevicha, S. (2006). Evaluation of sewage sludge-based compost by FT-IR spectroscopy. *Geoderma*, 130(3), 324-333.
- Hidalgo-Cantabrana, C., López, P., Gueimonde, M., Clara, G., Suárez, A., Margolles, A., & Ruas-Madiedo, P. (2012). Immune modulation capability of exopolysaccharides synthesised by lactic acid bacteria and bifidobacteria. *Probiotics and Antimicrobial Proteins*, 4(4), 227-237.
- Hidalgo-Cantabrana, C., Sánchez, B., Álvarez-Martín, P., López, P., Martínez-Álvarez, N., Delley, M., Martí, M., Varela, E., Suárez, A., Antolín, M., Guarner, F., Berger, B., Ruás-Madiedo, P. & Margolles, A. (2015). A single mutation in the gene responsible for the mucoid phenotype of *Bifidobacterium animalis* subsp. *lactis* confers surface and functional characteristics. *Applied and Environmental Microbiology*, 81(23), 7960-7968.
- Hidalgo-Cantabrana, C., Algieri, F., Rodriguez-Nogales, A., Vezza, T., Martínez-Cambor, P., Margolles, A., Ruas-Madiedo, P. & Gálvez, J. (2016). Effect of a Ropy Exopolysaccharide-Producing *Bifidobacterium animalis* subsp. *lactis* strain orally administered on DSS-induced colitis mice model. *Frontiers in Microbiology*, 7.
- van Hijum, S. A., Bonting, K., van der Maarel, M. J. & Dijkhuizen, L. (2001). Purification of a novel fructosyltransferase from *Lactobacillus reuteri* strain 121 and characterization of the levan produced. *FEMS Microbiology Letters*, 205(2), 323-328.
- Hongpattarakere, T., Cherntong, N., Wichienchot, S., Kolida, S., & Rastall, R. A. (2012). *In vitro* prebiotic evaluation of exopolysaccharides produced by marine isolated lactic acid bacteria. *Carbohydrate Polymers*, 87(1), 846-852.

- Ibarburu, I., Soria-Díaz, M. E., Rodríguez-Carvajal, M. A., Velasco, S. E., Tejero-Mateo, P., Gil-Serrano, A. M., Irastorza, A. & Dueñas, M. T. (2007). Growth and exopolysaccharide (EPS) production by *Oenococcus oeni* I4 and structural characterization of their EPSs. *Journal of Applied Microbiology*, 103(2), 477-486.
- Ibarburu, I., Puertas, A. I., Berregi, I., Rodríguez-Carvajal, M. A., Prieto, A., & Dueñas, M. T. (2015). Production and partial characterization of exopolysaccharides produced by two *Lactobacillus suebicus* strains isolated from cider. *International Journal of Food Microbiology*, 214, 54-62.
- Korakli, M., Rossmann, A., Gänzle, M. G., & Vogel, R. F. (2001). Sucrose metabolism and exopolysaccharide production in wheat and rye sourdoughs by *Lactobacillus sanfranciscensis*. *Journal of Agricultural and Food Chemistry*, 49(11), 5194-5200.
- Kumar, C. G., Joo, H. S., Kavali, R., Choi, J. W., & Chang, C. S. (2004). Characterization of an extracellular biopolymer flocculant from a haloalkalophilic *Bacillus* isolate. *World Journal of Microbiology and Biotechnology*, 20 (8), 837-843
- Laine, R., Sweeley, C. C., Li, Y. T., Kistic, A., & Rapport, M. M. (1972). On the structure of cytolipin R, a ceramide tetrahexoside hapten from rat lymphosarcoma. *Journal of Lipid Research*, 13, 519-524.
- Laiño, J., Villena, J., Kanmani, P., & Kitazawa, H. (2016). Immunoregulatory Effects Triggered by Lactic Acid Bacteria Exopolysaccharides: New Insights into Molecular Interactions with Host Cells. *Microorganisms*, 4(3), 27.
- Laws, A. P., Chadha, M. J., Chacon-Romero, M., Marshall, V. M., & Maqsood, M. (2008). Determination of the structure and molecular weights of the exopolysaccharide produced by *Lactobacillus acidophilus* 5e2 when grown on different carbon feeds. *Carbohydrate Research*, 343(2), 301-307.
- Le, C. & Stuckey, D. C. (2016). Colorimetric measurement of carbohydrates in biological wastewater treatment systems: A critical evaluation. *Water Research*, 94, 280-287.
- Leivers, S., Hidalgo-Cantabrana, C., Robinson, G., Margolles, A., Ruas-Madiedo, P., & Laws, A. P. (2011). Structure of the high molecular weight exopolysaccharide produced by *Bifidobacterium animalis* subsp. *lactis* IPLA-R1 and sequence analysis of its putative eps cluster. *Carbohydrate Research*, 346(17), 2710-2717
- Lindström, C., Holst, O., Nilsson, L., Öste, R., & Andersson, K. E. (2012). Effects of *Pediococcus parvulus* 2.6 and its exopolysaccharide on plasma cholesterol levels and inflammatory markers in mice. *AMB Express*, 2(1), 1.

- Liu, C. F., Tseng, K. C., Chiang, S. S., Lee, B. H., Hsu, W. H., & Pan, T. M. (2011). Immunomodulatory and antioxidant potential of *Lactobacillus* exopolysaccharides. *Journal of the Science of Food and Agriculture*, 91(12), 2284-2291.
- Llamas-Arriba, M. G., Pérez-Ramos, A., Puertas, A. I., López, P., Prieto, A. & Dueñas, M. T. (2018). Characterization of *Pediococcus ethanolidurans* CUPV141: A β -D-glucan and heteropolysaccharide-producing bacterium. *Frontiers in Microbiology*, 9, 2041.
- Llamas-Arriba, M. G., Peirotén, A., Puertas, A. I., Prieto, A., López, P., Pardo, M. A., Rodríguez, E. & Dueñas, M. T. (2019). Heteropolysaccharide-producing bifidobacteria for the development of functional dairy products. *LWT*, 102, 295-303.
- López, P., Monteserin, D. C., Gueimonde, M., Clara, G., Margolles, A., Suarez, A., & Ruas-Madiedo, P. (2012). Exopolysaccharide-producing *Bifidobacterium* strains elicit different *in vitro* responses upon interaction with human cells. *Food Research International*, 46(1), 99-107.
- Maeda, H., Zhu, X., & Mitsuoka, T. (2004). Effects of an exopolysaccharide (kefiran) from *Lactobacillus kefiranofaciens* on blood glucose in KKAY mice and constipation in SD rats induced by a low-fiber diet. *Bioscience and Microflora*, 23(4), 149-153.
- Marjoram, L. & Bagnat, M. (2015). Infection, Inflammation and Healing in Zebrafish: Intestinal Inflammation. *Current Pathobiology Reports*, 3(2), 147-153.
- Masuko, T., Minami, A., Iwasaki, N., Majima, T., Nishimura, S. I., & Lee, Y. C. (2005). Carbohydrate analysis by a phenol-sulfuric acid method in microplate format. *Analytical Biochemistry*, 339(1), 69-72.
- Mozzi, F., Gerbino, E., Font de Valdez, G., & Torino, M. I. (2009). Functionality of exopolysaccharides produced by lactic acid bacteria in an *in vitro* gastric system. *Journal of Applied Microbiology*, 107(1), 56-64.
- Murofushi, Y., Villena, J., Morie, K., Kanmani, P., Tohno, M., Shimazu, T., Aso, H., Suda, Y., Hashiguchi, K., Saito, T. & Kitazawa, H. (2015). The toll-like receptor family protein RP105/MD1 complex is involved in the immunoregulatory effect of exopolysaccharides from *Lactobacillus plantarum* N14. *Molecular Immunology*, 64(1), 63-75.
- Nácher-Vázquez, M., Ballesteros, N., Canales, Á., Saint-Jean, S. R., Pérez-Prieto, S. I., Prieto, A., Aznar, R. & López, P. (2015). Dextrans produced by lactic acid bacteria exhibit antiviral and immunomodulatory activity against salmonid viruses. *Carbohydrate Polymers*, 124, 292-301.

- Nakajima, H., Suzuki, Y., & HIROTA, T. (1992). Cholesterol lowering activity of ropy fermented milk. *Journal of Food Science*, 57(6), 1327-1329.
- Notararigo, S., Náchter-Vázquez, M., Ibarburu, I., Werning, M. L., de Palencia, P. F., Dueñas, M. T., Aznar, R., López, P. & Prieto, A. (2013). Comparative analysis of production and purification of homo-and hetero-polysaccharides produced by lactic acid bacteria. *Carbohydrate Polymers*, 93(1), 57-64.
- Notararigo, S., de las Casas-Engel, M., de Palencia, P. F., Corbí, A. L., & López, P. (2014). Immunomodulation of human macrophages and myeloid cells by 2-substituted (1–3)- β -D-glucan from *P. parvulus* 2.6. *Carbohydrate Polymers*, 112, 109-113.
- Oehlers, S. H., Flores, M. V., Hall, C. J., Crosier, K. E., & Crosier, P. S. (2012). Retinoic acid suppresses intestinal mucus production and exacerbates experimental enterocolitis. *Disease Models and Mechanisms*, 5(4), 457-467.
- Oyarbide, U., Rainieri, S., & Pardo, M. A. (2012). Zebrafish (*Danio rerio*) larvae as a system to test the efficacy of polysaccharides as immunostimulants. *Zebrafish*, 9(2), 74-84.
- Patten, D. A. & Laws, A. P. (2015). *Lactobacillus*-produced exopolysaccharides and their potential health benefits: a review. *Beneficial Microbes*, 6(4), 457-471.
- Russo, P., Iturria, I., Mohedano, M. L., Caggianiello, G., Rainieri, S., Fiocco, D., Pardo, M. A., López, P. & Spano, G. (2015). Zebrafish gut colonization by mCherry-labelled lactic acid bacteria. *Applied Microbiology and Biotechnology*, 99(8), 3479-3490.
- Sartor, R. B. (2006). Mechanisms of disease: pathogenesis of Crohn's disease and ulcerative colitis. *Nature Clinical Practice Gastroenterology & Hepatology*, 3(7), 390-407.
- Şengül, N., Aslím, B., Uçar, G., Yücel, N., Işık, S., Bozkurt, H., Sakaogullari, Z. & Atalay, F. (2006). Effects of exopolysaccharide-producing probiotic strains on experimental colitis in rats. *Diseases of the Colon & Rectum*, 49(2), 250-258.
- Shao, L. I., Wu, Z., Zhang, H., Chen, W., Ai, L., & Guo, B. (2014). Partial characterization and immunostimulatory activity of exopolysaccharides from *Lactobacillus rhamnosus* KF5. *Carbohydrate Polymers*, 107, 51-56.
- Stack, H. M., Kearney, N., Stanton, C., Fitzgerald, G. F., & Ross, R. P. (2010). Association of beta-glucan endogenous production with increased stress tolerance of intestinal lactobacilli. *Applied and Environmental Microbiology*, 76(2), 500-507.

- De Vuyst, L., & Degeest, B. (1999). Heteropolysaccharides from lactic acid bacteria. *FEMS Microbiology Reviews*, 23(2), 153-177.
- De Vuyst, L., De Vin, F., Vaningelgem, F., & Degeest, B. (2001). Recent developments in the biosynthesis and applications of heteropolysaccharides from lactic acid bacteria. *International Dairy Journal*, 11(9), 687-707.
- Wang, Y., Li, C., Liu, P., Ahmed, Z., Xiao, P., & Bai, X. (2010). Physical characterization of exopolysaccharide produced by *Lactobacillus plantarum* KF5 isolated from Tibet Kefir. *Carbohydrate Polymers*, 82(3), 895-903.
- Xu, R., Shen, Q., Ding, X., Gao, W., & Li, P. (2011). Chemical characterization and antioxidant activity of an exopolysaccharide fraction isolated from *Bifidobacterium animalis* RH. *European Food Research and Technology*, 232(2), 231-240.
- Zamora, F., González, M. C., Duenas, M. T., Irastorza, A., Velasco, S., & Ibarburu, I. (2002). Thermodegradation and thermal transitions of an exopolysaccharide produced by *Pediococcus damnosus* 2.6. *Journal of Macromolecular Science, Part B*, 41(3), 473-486.
- Zhang, Z., Zhou, Z., Li, Y., Zhou, L., Ding, Q., & Xu, L. (2016). Isolated exopolysaccharides from *Lactobacillus rhamnosus* GG alleviated adipogenesis mediated by TLR2 in mice. *Scientific Reports*, 6, 36083.
- Zeidan, A. A., Poulsen, V. K., Janzen, T., Buldo, P., Derkx, P. M., Øregaard, G., & Neves, A. R. (2017). Polysaccharide production by lactic acid bacteria: from genes to industrial applications. *FEMS Microbiology Reviews*, 41(1), S168-S200.
- Zhou, Y., Cui, Y., & Qu, X. (2019). Exopolysaccharides of lactic acid bacteria: Structure, bioactivity and associations: A review. *Carbohydrate Polymers*, 207, 317-332.

4. Caracterización biotecnológica de *L. collinoides* CUPV237 y
L. sicerae CUPV261^T

1. INTRODUCCIÓN

Los alimentos fermentados forman parte de la dieta de los humanos debido a su gran interés nutricional. Estos alimentos, así como las bebidas fermentadas portan microorganismos vivos que ejercen un efecto beneficioso sobre la salud de los consumidores. La *Food and Agriculture Organization of the United Nations* y la Organización Mundial de la Salud definieron el concepto probiótico como: "Microorganismos vivos que administrados en adecuadas cantidades confieren efectos beneficiosos en la salud del hospedador" (FAO, 2001). Posteriormente, un nuevo comité de expertos reunidos por la *International Scientific Association for Probiotics and Prebiotics* revisó la definición de la FAO/WHO aceptándola con un pequeño cambio gramatical (Hill et al. 2014; Calatayud, Marcos & Margolles, 2016). Para ello, un microorganismo probiótico debe: (i) estar debidamente identificado y tipificado, (ii) no debe de poseer factores de patogenicidad, (iii) ser resistente a la acidez gástrica y a las sales biliares, (iv) poseer la habilidad de adherirse al epitelio intestinal, (v) y de colonizar el colon, (vi) aportar clínicamente efectos beneficiosos en la salud del hospedador, y (vii) debe ser seguro (Fric, 2007). Entre los microorganismos que se utilizan como probióticos encontramos cepas de las especies *Lactobacillus rhamnosus*, *Lactobacillus reuteri*, *Lactobacillus casei*, *Lactobacillus acidophilus*, ciertas bifidobacterias, *Bacillus coagulans*, algunos enterococos, especialmente *Enterococcus faecium* SF68, así como la estirpe *Escherichia coli* Nissle 1917, y la levadura *Saccharomyces boulardii*. Estos probióticos se añaden a los alimentos, particularmente a los productos lácteos, ya sea individualmente o en combinación de varios (Pandey et al., 2015).

Los efectos beneficiosos más importantes y documentados de los microorganismos probióticos sobre la salud del consumidor incluyen: la prevención de la diarrea, el estreñimiento, cambios en la conjugación de las sales biliares, actividad antibacteriana contra patógenos o actividad antiinflamatoria. Además, también contribuyen a la síntesis de nutrientes y mejoran su biodisponibilidad (Harish & Varghese, 2006). Algunas estirpes de bacterias son capaces de producir vitaminas en el alimento fermentado, como las del grupo B, y resisten las condiciones del tracto gastrointestinal (TGI) de los mamíferos llegando a colonizarlo (Capozzi et al., 2012; Bhushan et al. 2017; Panda et al., 2018; Chikmath et al., 2018). En el TGI conviven bacterias, arqueas, hongos, protozoos y virus, que interactúan mutuamente, con el epitelio y con las células inmunes del propio hospedador (Sánchez et al., 2017). Algunos probióticos poseen actividad antioxidante en forma de células intactas o

lisados. Ciertas estirpes han mostrado efectos en el alivio de los síntomas de alergia, cáncer, SIDA, infecciones respiratorias o urinarias. También existen trabajos que evalúan el efecto beneficioso de los probióticos sobre el envejecimiento, la fatiga, el autismo, la osteoporosis, la obesidad y diabetes tipo 2 (Harish & Varghese, 2006).

Por otro lado, entre los ingredientes de los alimentos funcionales se incluyen cepas probióticas, prebióticos, vitaminas y minerales entre otros. En conjunto, son utilizados en la elaboración de alimentos como la leche fermentada y yogur, bebidas deportivas, comida infantil, fórmulas libres de azúcares, e incluso chicles. La funcionalidad de este tipo de alimentos está basada en sus componentes bioactivos, a menudo contenidos naturalmente en el producto, y en ocasiones son añadidos como ingredientes específicos con el objetivo de optimizar sus propiedades beneficiosas. Los microorganismos probióticos, así como los compuestos prebióticos son ingredientes fundamentales de la leches fermentadas y el yogur, que representan la fracción más importante del mercado global de alimentos funcionales (Figueroa-González et al., 2011).

La participación de *L. collinoides* CUPV237 y *Lactobacillus sicerae* CUPV261^T podría tener un interés potencial para la elaboración de alimentos fermentados. Ambas cepas poseen la capacidad de producir heteropolisacáridos que incrementan la viscosidad del medio de cultivo MSD. Además, los resultados obtenidos en el capítulo 3 han demostrado que estos EPS tienen efectos paliativos sobre la mortalidad larvaria en el modelo IBD de larvas pez cebra inducido por agente químico DSS. Por otro lado, la estirpe CUPV237 fue seleccionada debido a que es una cepa superproductora de vitamina B₂ (capítulo 5). Con estos antecedentes, este capítulo está dedicado a la evaluación en estas dos cepas de algunas características asociadas con el potencial probiótico, y al estudio de su comportamiento cuando son añadidas como cultivos iniciadores a un alimento.

2. MATERIAL Y MÉTODOS

2.1 Cepas bacterianas y condiciones de cultivo

Las cepas estudiadas en este capítulo son *L. sicerae* CUPV261^T y *L. collinoides* CUPV237, y se cultivaron de forma rutinaria en el medio MRS (pH de 5,5), con un 2 % de inóculo, a 28 °C.

La cepa CUPV2371NR infra-productora de EPS fue obtenida por la doctora Idoia Ibarburu, a partir de la cepa salvaje CUPV2371 productora de heteropolisacárido. Para ello, la cepa salvaje se cultivó sucesivamente en el medio MRS suplementado con novobiocina 40 µg mL⁻¹ (Sigma) y durante 48 h, realizando tantos cultivos como fueron necesarios hasta no detectar el fenotipo *ropy*. Se sembró en MRS-agar, se seleccionó una colonia y se comprobó la ausencia de fenotipo *ropy*. Finalmente, este aislado se renombró como CUPV2371NR. Las colonias son rugosas, con bordes irregulares, a diferencia de las de la cepa salvaje CUPV2371, que son lisas y con bordes regulares (Figura 4.1). Se cuantificó la producción de EPS en los sobrenadantes de sus cultivos en el medio MSD (método del fenol-sulfúrico), obteniéndose valores inferiores a 10 mg mL⁻¹. Así mismo, el análisis del EPS aislado a partir de la biomasa mediante HPSEC mostró tres fracciones de diferente peso molecular: superior a 10³, 10 y 1 kDa, al igual que se observó en el caso de CUPV2371 (Tabla 1.3)

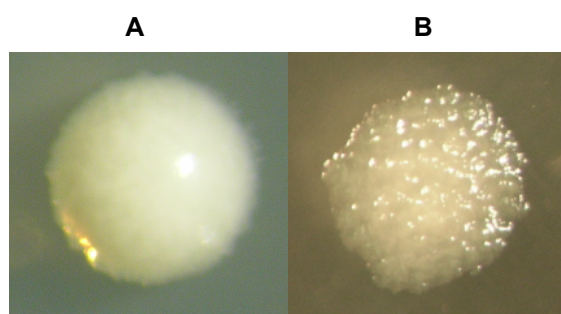


Figura 4.1. Colonias de las estirpes *L. collinoides* CUPV2371 (A) y *L. collinoides* CUPV2371NR (B). El tamaño de las colonias es de 0,6 mm.

2.2 Fermentación de matrices alimentarias

Se utilizaron tres tipos de bebidas: bebida de soja (pH de 6,54), y bebida de avena (pH 7,33) (Montsoy, Viladrau, Girona), y leche desnatada (10 %, p/v; pH 6,54, Sigma). Previamente, las bacterias se adaptaron a las diferentes bebidas mediante cultivos en medio MRS enriquecido con el alimento. Primero, se cultivaron en un

medio compuesto por MRS y matriz alimentaria (1:1), a continuación en otro medio con una mayor proporción del alimento (1:3), y tras 24 h de fermentación, este cultivo sirvió para inocular al 2 % las diferentes matrices alimentarias (suplementadas con un 2 % de glucosa). Los cultivos se incubaron durante 72 h a 28 °C, y posteriormente se mantuvieron a 4 °C durante 2 d (avena y soja) o 7 d en el caso de la leche. Tras el periodo de refrigeración se midió de pH. El recuento de células viables se realizó a las 0 y 72 h de incubación, y después del periodo a 4 °C, mediante la siembra en superficie en el medio MRS-agar.

2.3 Características probióticas

2.3.1 Supervivencia celular bajo un modelo *in vitro* de estrés gastrointestinal

Para el análisis de la supervivencia de las bacterias sometidas a estrés gástrico (G) y a estrés gastrointestinal (GI), se utilizaron suspensiones de células obtenidas a partir un cultivo crecido en el medio MRS con aproximadamente 10^9 UFC mL⁻¹. Las células contenidas en 25 mL de cultivo, se recogieron por centrifugación (8000 x g, 10 min) y se suspendieron en el mismo volumen de solución electrolítica estéril (apartado 2.5 del capítulo 3), leche, bebida de avena o bebida de soja. La solución electrolítica se preparó en el momento del ensayo y las matrices alimentarias se esterilizaron mediante un autoclave (120 °C, 4 min).

La simulación de las condiciones del tracto gastrointestinal humano se realizó utilizando el modelo *in vitro* del estrés gástrico y gastrointestinal descrito en el capítulo 3 (Figura 3.2). La evaluación de la supervivencia bacteriana se llevó a cabo mediante el recuento de células viables. Para ello se tomaron muestras en cada uno de los tratamientos, se realizaron diluciones sucesivas y se sembraron en MRS-agar (CO₂ 5 %, v/v, y 28 °C).

2.3.2 Autoagregación e hidrofobicidad celular

Los ensayos de autoagregación e hidrofobicidad celular se realizaron a partir de una suspensión de células obtenidas a partir de un cultivo realizado en el medio MRS, que había alcanzado la fase estacionaria de crecimiento (DO₆₀₀ aproximada de 5). Las células se recogieron por centrifugación (8.000 x g, 10 min) y se suspendieron

en PBS (pH 7,2) (Anexo I) con el mismo volumen del cultivo inicial. Las determinaciones se llevaron a cabo a por triplicado y a partir de tres cultivos independientes.

En el caso de los ensayos de auto-agregación bacteriana, se dispensaron 10 mL de la suspensión celular en tubos de vidrio estériles con un diámetro interior de 13 mm, y fueron agitados vigorosamente. Inmediatamente después, se tomaron 0,1 mL, se diluyeron en 2,4 mL de PBS, y se midió la densidad óptica a 600 nm (A_0). Los tubos se mantuvieron a temperatura ambiente en un lugar apartado de movimientos y vibraciones, y trascurridas 2 y 4 h se midió la DO_{600} (A_t). Para calcular el % de autoagregación de la cepa se aplicó la fórmula: $A \% = [1 - (A_t/A_0)] \times 100$ (Kos et al., 2003).

Para los ensayos de hidrofobicidad celular, las suspensiones celulares se diluyeron 5 veces con PBS y se midió la DO_{600} (H_0). Posteriormente, se tomaron 4 mL de la dilución, se le añadió 0,64 mL de xileno (Panreac) y se agitó vigorosamente durante 120 s. Los tubos se mantuvieron en reposo durante 30 min y se midió la DO_{600} de la fracción acuosa (H). El porcentaje de hidrofobicidad se obtuvo mediante la fórmula $H \% = [(H_0 - H)/H_0] \times 100$ (Pérez et., al. 1998).

2.3.3 Actividad antioxidante

La capacidad anti-radicales libres de las células bacterianas se determinó con suspensiones celulares preparadas a partir de cultivos en el medio MRS (28 °C durante 29 h). Se tomaron 4 mL, se centrifugaron a 8.000 x g durante 5 min y las células se lavaron un par de veces con solución Ringer®. Finalmente, se suspendieron en agua destilada para obtener suspensiones celulares de 10^9 , 10^8 , 10^7 y 10^6 UFC mL⁻¹ (Wang et al., 2009). Las determinaciones se llevaron a cabo al menos por triplicado y a partir de tres cultivos independientes.

Para hallar la capacidad anti-radicales hidroxilo (HO^{*}) de las células se tomó 1 mL de una solución de 1,10-fenantrolina 0,75 mM, a la cual se le añadieron 2 mL de PBS (pH 7,4) y 1 mL de FeSO₄ 0,75 mM. A continuación, se añadió 1 mL de la solución bacteriana, 1 mL de H₂O₂ 0,12 % (v/v) o 1 mL de PBS, y se incubó a 37 °C durante 90 min. Finalmente, se midió la absorbancia a 536 nm (A_{536}). Para expresar la actividad anti-radicales hidroxilo, se sustituyeron los valores de absorbancia obtenidos

en presencia de la muestra (A_S), del control (H_2O_2) en ausencia de la muestra (A_C), y sin muestra ni H_2O_2 (A_B), en la siguiente fórmula (Wang et al., 2009):

$$\% \text{ Actividad anti-radicales hidroxilo} = (A_S - A_C) / (A_B - A_C) \times 100$$

Para determinar la capacidad anti-radicales superóxido (O_2^-) de las células bacterianas, se mezclaron 400 μ L de la suspensión celular o agua destilada (blanco), con 1200 μ L de una solución tampón de Tris HCl 1 M (pH 8, incluyendo EDTA 0,1 mM), y se incubó 1 h a temperatura ambiente (Wang et al., 2009). A continuación, se tomaron 200 μ L de la mezcla anterior y se añadieron 10 μ L de pirogalol 0,45 mM (Sigma), se homogeneizó e inmediatamente, se tomaron las medidas de absorbancia (325 nm) a tiempo cero y cada minuto durante 4 min, en un lector de microplacas (Synology HT, BIOTEK). Se realizaron 6 réplicas por cada concentración de células, y el ensayo se llevó a cabo en placas de 96 pocillos (Corning). La actividad anti-radicales superóxido se obtuvo a partir de la velocidad de auto-oxidación del pirogalol (%), sustituyendo el incremento de la absorbancia medido en las mezclas de reacción con la suspensión celular (ΔA) o con el agua destilada (ΔA_0), en la siguiente fórmula: $\% \text{ Actividad anti-radicales } O_2^- = [1 - (\Delta A / \Delta A_0)] \times 100$.

La capacidad anti-radicales 1,1-difenil-2-picrilhidracilol (DPPH $^{\bullet}$) se determinó de acuerdo a la metodología descrita por Hafsa et al. (2016). Para ello se tomaron 2 mL de una solución de DPPH $^{\bullet}$ 0,2 mM preparada en metanol, y se mezclaron con 1 mL de una suspensión de células en etanol (10^9 , 10^8 , 10^7 o 10^6 UFC mL $^{-1}$), o con 1 mL de etanol. Tras 30 min en completa oscuridad y a temperatura ambiente, las mezclas fueron centrifugadas a 8000 x g durante 2 min, e inmediatamente se midió la absorbancia a 517 nm. Para hallar el % de actividad se sustituyeron los valores de absorbancia obtenidos en las mezclas de solución de DPPH $^{\bullet}$, con la suspensión de células en metanol (A_S), o con etanol (A_B) en la siguiente fórmula:

$$\% \text{ Actividad anti-radicales DPPH}^{\bullet} = [1 - (A_S / A_B)] \times 100$$

Para cada muestra se realizaron 5 réplicas del ensayo.

2.4 Transferencia del plásmido pRCR12 a las bacterias y expresión de la proteína mCherry

Estos ensayos fueron realizados bajo la supervisión de la doctora Paloma López en el Centro de Investigaciones Biológicas (Madrid).

El plásmido pRCR12 (Figura 4.2) es portador del gen que codifica la proteína monomérica fluorescente mCherry (Russo et al., 2015). Y fue construido a partir del plásmido pRCR (Mohedano et al., 2015), el cual contiene el promotor fuerte P_x de operón de la maltosa (*malXCD*) de *Streptococcus pneumoniae* corriente arriba del gen *mrfp* que codifica la proteína mCherry. Por esta razón, P_x -*mrfp* se transcribe de forma constitutiva. Además, el plásmido contiene el gen *cat*, que codifica la proteína cloranfenicol acetiltransferasa, responsable de la resistencia al cloranfenicol (Russo et al., 2015). pRCR12 está optimizado para ser expresado en bacterias del ácido láctico (García-Cayueta et al., 2012), y contiene el replicón del plásmido pSH71 de *Lactococcus lactis*, que es de amplio espectro de huésped y funcional en cepas pertenecientes al género *Lactobacillus* (Nacher, 2015).

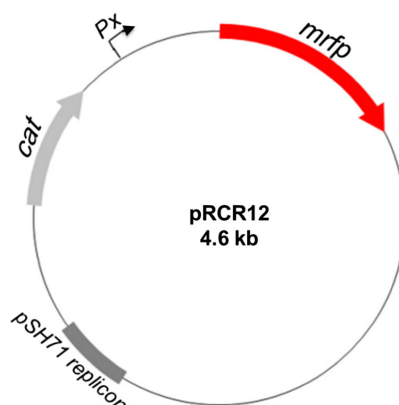


Figura 4.2. Mapa físico del plásmido pRCR12 (Russo et al., 2015).

2.4.1 Transformación de las células bacterianas con pRCR12

La transformación con el plásmido pRCR12 se llevó a cabo en las cepas *L. sicerae* CUPV261^T, *L. collinoides* CUPV237 y en la cepa *non-ropy* *L. collinoides* CUPV2371NR, aplicando el protocolo descrito por Berthier et al. (1996).

El plásmido pRCR12 se aisló a partir de cultivos de *Escherichia coli* DH5 α [pRCR12], mediante el kit comercial de purificación de plásmidos JetStar 2.0

(Genomed), siguiendo las instrucciones indicadas por el fabricante. La concentración de plásmido se ajustó a 100 ng mL^{-1} , y se conservó a -80 °C hasta el momento de su utilización.

Para la obtención de células competentes, se tomó un cultivo bacteriano crecido en el medio MRS hasta alcanzar 10^8 UFC mL^{-1} (fase exponencial de crecimiento). El cultivo se centrifugó ($5.500 \times g$, 4 °C , 10 min), se retiró el sobrenadante, y las células se lavaron con PBS con una agitación vigorosa durante 2 o 3 min con el fin de retirar el máximo de polisacárido adherido a las bacterias. La suspensión celular se centrifugó ($5.500 \times g$, 4 °C , 10 min), se lavó con PBS, y se añadió 10 mL de una solución fría de MgCl_2 10 mM. Las células se resuspendieron mediante movimientos suaves, se centrifugaron ($3.300 \times g$, 4 °C , 5 min), y se sometieron a un nuevo lavado con 10 mL de MgCl_2 10 mM. Seguidamente se realizaron dos lavados con 10 mL de solución de electroporación (sacarosa 0,5 M y glicerol 10 %, v/v) mantenida en hielo. Por último, las células competentes fueron suspendidas en 500 μL de solución de electroporación fría, y se mantuvieron en hielo.

Para el proceso de electroporación, tanto las soluciones como el material se mantuvieron en hielo. Se comenzó mezclando cuidadosamente 50 μL de células competentes y 5 μL de DNA plásmídico (100 ng mL^{-1}), y la mezcla se transfirió a una cubeta de electroporación estéril de 0,2 cm (Gene Pulser® Cuvette, BioRad). Las condiciones utilizadas en la electroporación fueron: una resistencia de 600Ω , una capacitancia de $25 \mu\text{F}$ y un voltaje de 1,8 kV, aplicados en un equipo de electroporación “Gene Pulser” acoplado al “Pulse controller” (Bio-Rad). Las constantes de tiempo encontradas fueron 8,9 ms para *L. sicerae* CUPV261^T, 11,2 ms para *L. collinoides* CUPV237 y 12,7 ms para CUPV2371NR. Se añadió 0,5 mL de MRS estéril (glucosa 3 %, p/v, y MgCl_2 80 mM) a la suspensión celular y se mantuvieron durante 2 h a 30 °C . Transcurrido el periodo de incubación, las células se sembraron en MRS-agar suplementado con cloranfenicol, $7,5 \mu\text{g mL}^{-1}$ en el caso de *L. sicerae* CUPV261 [pRCR12], o con $5 \mu\text{g mL}^{-1}$ para las cepas de *L. collinoides* CUPV237 [pRCR12] y CUPV2371NR [pRCR12], y se incubaron a 30 °C en microanaerobiosis (BD GasPak™ Ez Anaerobe Gas Generating Systems). Todas las colonias obtenidas presentaron una coloración magenta oscuro que está provocada por la expresión de la proteína mCherry (Figura 4.8 centro).

2.4.2 Detección de la expresión de la proteína fluorescente mCherry

Para la detección de la expresión de la proteína mCherry, los transformantes de *L. sicerae* y *L. collinoides* se cultivaron en medio MRS-cloranfenicol (apartado 2.5.1). El crecimiento fue monitorizado mediante la medida de la DO₆₀₀, y la fluorescencia fue cuantificada en un espectrofluorímetro (Spectometer RF-540, Shimadzu), con unas longitudes de onda de excitación y emisión, de λ_{ex} 587 nm y λ_{em} 610 nm (Mohedano et al., 2015).

Para la visualización de los transformantes, se tomaron microfotografías *in vivo* en un equipo de microscopía laser confocal (Microscopio confocal Láser (CLSM) LEICA TCS SP5 AOBS) en los Servicios Científicos del Centro de Investigaciones Biológicas de Madrid. Para el procesado de imágenes se utilizó el software ImageJ v1.47 (National Institutes of Health) (Rasband, 1997).

2.5 Ensayos de colonización y visualización de *Lactobacillus sp.* [pRCR12] en el modelo de larvas gnotobióticas de *Danio rerio*.

Estos ensayos se realizaron bajo la supervisión del doctor Miguel Ángel Pardo en el Centro Tecnológico AZTI-Tecnalia, Derio (Bizkaia).

2.5.1 Obtención de larvas gnotobióticas de pez cebra

Los adultos progenitores de *Danio rerio* (Hamilton, 1822), se criaron y se mantuvieron en las instalaciones de AZTI tal y como se describe en el capítulo 3 (apartado 2.6.1).

Para la obtención de larvas de pez cebra libres de gérmenes (axénicas o *germ-free*), los huevos fertilizados y aclarados con solución para embriones (EW, apartado 2.6.1 del capítulo 3), se sometieron a una serie de lavados para eliminar la microbiota que les acompañaba. Inicialmente, los huevos se depositaron en un tubo de centrifuga estéril de 15 mL, y se realizaron 10 lavados con la solución de antibióticos (Ab: solución EW suplementada con kanamicina 15 mg L⁻¹, ampicilina 300 mg L⁻¹ y anfotericina B 1,25 mg L⁻¹), invirtiendo el tubo mediante movimientos suaves. Después se lavaron con solución EW suplementada con polivinilpirrolidona 0,02 % (v/v) durante

2 min. Inmediatamente después, los huevos se sumergieron en EW suplementada con lejía 0,005 % (v/v) durante 1 h. Se retiró el sobrenadante, se lavaron 10 veces con solución EW para eliminar los restos de lejía, y se mantuvieron durante 15 h en solución Ab. Tras este tiempo se realizaron nuevamente 10 lavados con solución EW. Los huevos se distribuyeron en placas Petri estériles, a razón de 10 embriones mL⁻¹ y se aplicaron dos pulsos de luz de 1,8 kV. Tras una incubación a 27 °C durante 2,5 días, los huevos se lavaron 3 veces con PBS diluido 1:100, y permanecieron a 27 °C durante 24 h (Oyarbide et al., 2015).

2.5.2 Ensayos de colonización intestinal

Las estirpes *L. sicerae* CUPV261^T p[RRCR12], *L. collinoides* CUPV237 p[RRCR12] y *L. collinoides* CUPV2371NR p[RRCR12] se cultivaron en el medio MRS suplementado con cloranfenicol a 28 °C, hasta alcanzar una concentración en torno a 10⁸ UFC mL⁻¹. Las células se recogieron por centrifugación y se lavaron con PBS para eliminar los restos del medio de cultivo.

Grupos de 15 larvas axénicas de 4 días post-fecundación (dpf), fueron expuestas a concentraciones de 5×10⁷ bacterias mL⁻¹, con o sin EPS 150 mg L⁻¹, durante 18 h, a 27 °C y con una agitación orbital de 90 rpm. Posteriormente, se lavaron tres veces con una solución de PBS suplementada con Tween 20 0,1 % (v/v), se mantuvieron a 27 °C y 90 rpm durante 6, 24 y 48 h antes de ser visualizadas (periodos post-exposición). Cada experimento se realizó por triplicado y una vez finalizados, los embriones fueron sacrificados mediante shock frío.

Para medir el grado de colonización bacteriana en el epitelio intestinal, se llevó a cabo el recuento en placa de las células viables a partir de una larva. Una vez finalizados los periodos post-exposición, cada larva se depositó en un microtubo estéril de 1,5 mL, se añadió 0,5 mL de PBS y se trituró utilizando el homogeneizador Pellet Pestle Cordless Motor (Kimble Chase, Vineland, NJ). Para el recuento de células viables, se sembró el contenido del microtubo en MRS-agar suplementado con cloranfenicol, y se incubó a 28 °C en una atmósfera con un 5 % (v/v) de CO₂.

Para la visualización de las bacterias fluorescentes en el interior de las larvas se utilizó un estereomicroscopio Leica MZFL III con un rango de aumento de 8X a 100X. El microscopio estaba equipado con luz visible y luz UV (100 W Hg), y las

condiciones para la detección de la fluorescencia fueron: un rango de longitudes de onda de excitación de 450-490 nm y de emisión de 540-580 nm. Las imágenes se tomaron con una cámara Leica DFC 360FX y se procesaron con el programa informático ImageJ v1.47 (Russo et al., 2015)

2.6 Análisis estadístico

Los datos se expresan como la media \pm desviación estándar. Los análisis estadísticos se realizaron utilizando el programa informático SPSS (Versión 24.0). Para detectar las diferencias significativas, se realizó un análisis de la varianza (ANOVA) de un factor, seguido de un *Post-hoc* con el test DSM para varianzas iguales o un test T3 de Dunnett para varianzas distintas.

3. RESULTADOS

3.1 Fermentación de matrices alimentarias

Las matrices utilizadas (bebida de soja, bebida de avena y leche) se suplementaron con un 2 % (v/v) de glucosa, y se inocularon con las bacterias *L. sicerae* CUPV261^T y *L. collinoides* CUPV237. La Figura 4.3 muestra los crecimientos observados tras los periodos de fermentación y de refrigeración a 4 °C (48 h para los cultivos en avena y soja, y 7 días en leche).

La estirpe CUPV261^T creció en las tres bebidas (Figura 4.3 A), detectándose incrementos significativos de las poblaciones bacterianas al final del periodo de fermentación ($p < 0,001$), que fueron acompañados de un descenso de los valores de pH, a 4,94 en leche, 3,8 en soja y 4,11 en avena. Así mismo, después del periodo de almacenamiento a 4 °C la población bacteriana disminuyó significativamente en los cultivos en leche ($p < 0,01$).

Con respecto a las fermentaciones realizadas con la cepa CUPV237, se detectaron comportamientos diferentes en cada bebida (Figura 4.3 B). En la matriz leche no se observó crecimiento de la bacteria. Sin embargo, en los cultivos de soja y avena se observó un crecimiento significativo después de la incubación a 28 °C ($p < 0,001$), y se registraron unos valores de pH de 3,92 y 4,7, respectivamente. En la matriz soja se detectó crecimiento durante el periodo de refrigeración, en cambio, en avena la población disminuyó significativamente ($p < 0,01$).

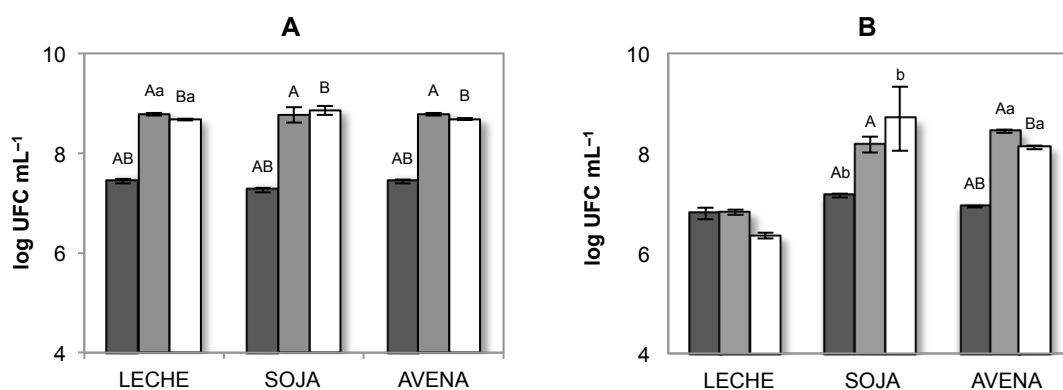


Figura 4.3. Fermentaciones en leche, avena y soja. Las gráficas representan el crecimiento de *L. sicerae* CUPV261^T (A) y de *L. collinoides* CUPV237 (B) observado en las diferentes matrices alimentarias. Las barras muestran la media del log UFC mL⁻¹ ± la desviación estándar cuantificadas a tiempo cero (■), tras la fermentación (▒) y después del periodo a 4 °C (□). Las diferencias significativas se indican con igual carácter para $p < 0,001$ (mayúscula), $p < 0,01$ (minúscula).

3.2 Tolerancia al estrés gástrico y gastrointestinal

Se determinó la supervivencia de *L. sicerae* CUPV261^T y *L. collinoides* CUPV237 al estrés gástrico y gastrointestinal utilizando un modelo *in vitro* (Fernández de Palencia et al., 2009). Las células cultivadas en el medio MRS, se suspendieron en solución gástrica, leche, bebida de avena o de soja, y se sometieron a acidificaciones y a la acción de enzimas gastrointestinales durante el tratamiento (Figura 3.2).

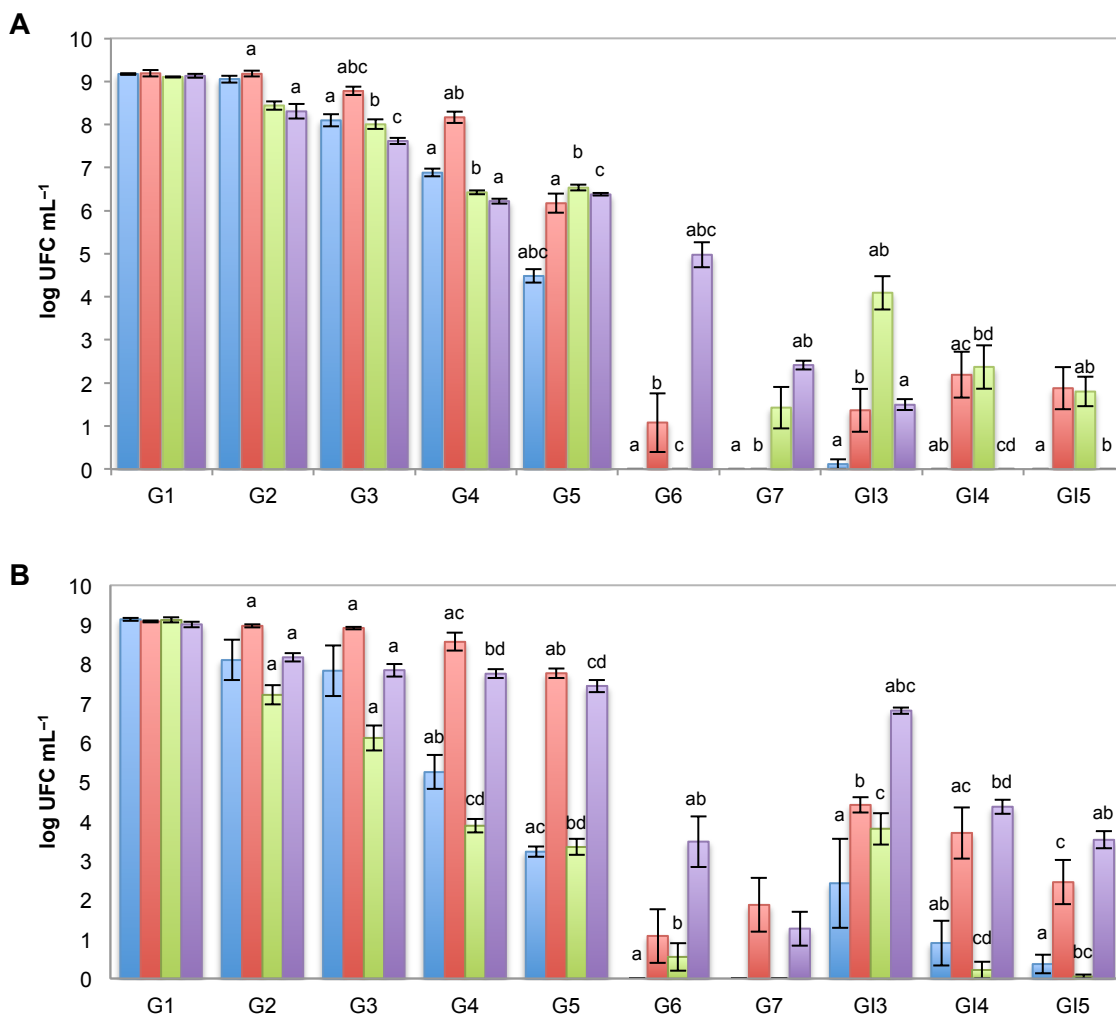


Figura 4.4. Tolerancia de *L. sicerae* CUPV261^T (A) y *L. collinoides* CUPV237 (B) frente a condiciones simuladas de estrés gastrointestinal. Las bacterias se suspendieron en solución gástrica (■), leche (■), avena (■) y soja (■). Las barras representan la media del número de células viables tras cada tratamiento ± el error estándar de la desviación, y en cada tratamiento, las diferencias significativas se representan con la misma letra ($p < 0,05$).

En los ensayos realizados con las cepas de *L. collinoides* y de *L. sicerae* se observaron que en ambas cepas el estrés gástrico y gastrointestinal afectó de forma drástica a las células suspendidas en solución gástrica y en las tres matrices alimentarias (Figura 4.3).

En la estirpe CUPV261^T, la supervivencia observada en el tratamiento G6 (pH 2,1) fue significativamente mayor en la bebida de soja (Figura 4.4 A), aunque las poblaciones fueron inferiores a 5 unidades logarítmicas. Por otro lado, una vez concluidos los tratamientos del estrés gastrointestinal (GI5, pH 3), solo se detectaron células viables en avena y leche (log 1,8).

De la misma manera, en el tratamiento de estrés gástrico (G6, pH 2,1) en la cepa CUPV237 se redujo sensiblemente la viabilidad celular (Figura 4.4 B), aunque los niveles fueron significativamente mayores en soja (log 3,4), y a pH 1,8, sólo se detectaron células viables en soja y leche (concentraciones inferiores a log 1,8). Así mismo, una vez concluido el tratamiento de estrés gastrointestinal (GI5), los mayores recuentos se observaron también en soja y leche (del orden de log 3,5 y log 2,4, respectivamente).

3.3 Evaluación de la actividad antioxidante

Para la determinación de la actividad antioxidante de las células de *L. sicerae* CUPV261^T y *L. collinoides* CUPV237, se analizó su comportamiento frente a radicales de hidroxilo (OH^{*}), superóxido y 1,1-difenil-2-picril-hidrazilo (DPPH^{*}).

Con respecto a la evaluación del actividad anti-OH^{*} (Figura 4.5 A), tanto CUPV261^T como CUPV237 mostraron un efecto dosis-dependiente, y se registró una mayor actividad con la concentración de 10⁹ UFC mL⁻¹ (36 y 53 %, respectivamente). Sin embargo, los resultados obtenidos para la actividad anti-O²⁻ mostraron en ambas cepas un valor similar para las 4 concentraciones celulares, que fue próximo a 25 % (Figura 4.5 B). Para la actividad anti-DPPH^{*} se observó un comportamiento diferente dependiendo de la cepa (Figura 4.5 C). Para la estirpe CUPV261 los valores fueron similares en las suspensiones de 10⁹ -10⁷ UFC mL⁻¹, en torno al 48 %, y la actividad descende hasta el 18 % en 10⁶ UFC mL⁻¹. En el caso de CUPV237, la actividad de 10⁹ y 10⁸ UFC mL⁻¹ fue de en torno al 26 %, y con 10⁷ y 10⁶ UFC mL⁻¹ del 18 %.

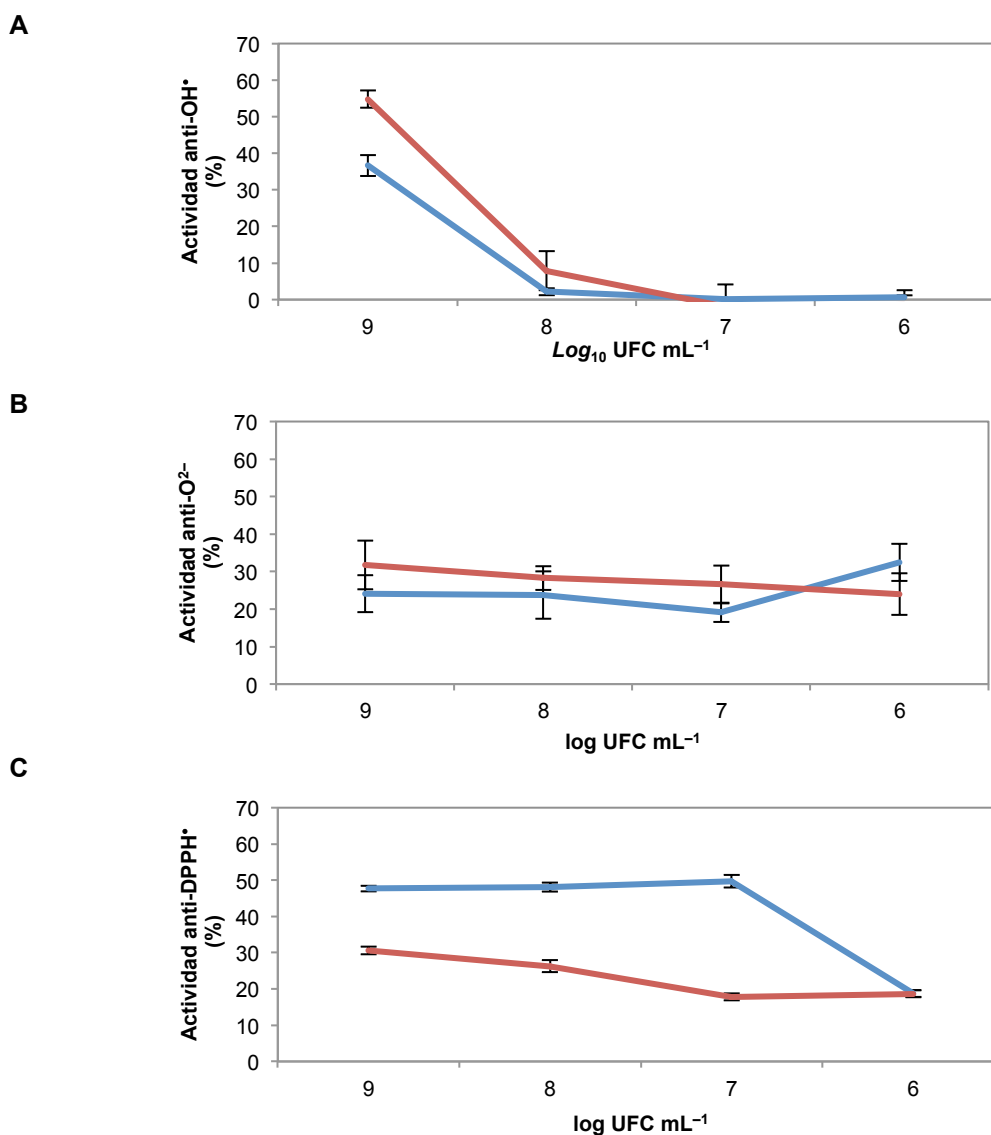


Figura 4.5. Actividad antioxidante de *L. sicerae* CUPV261^T (■) y *L. collinoides* CUPV237 (■) observada en modelos *in vitro*. **A**, actividad antiradicales hidroxilo (OH[•]); **B**, actividad antiradicales superóxido (O²⁻); y **C**, anti-radicales 1,1-difenil-2-picril-hidracilo (DPPH[•]). Las líneas representan la media aritmética ± la desviación estándar.

3.4 Capacidad de autoagregación e hidrofobicidad celular

La Figura 4.6 muestra la relación entre la capacidad de autoagregación y la hidrofobicidad celular de las suspensiones celulares de *L. sicerae* CUPV261^T y *L. collinoides* CUPV237.

El xileno, solvente orgánico de naturaleza hidrófoba, fue utilizado para hallar el índice de hidrofobicidad de la superficie celular. El valor de hidrofobicidad de CUPV237 fue del 39 %, aproximadamente el doble que el obtenido en CUPV261^T (16,49 %). Sin embargo, el porcentaje de autoagregación fue muy similar en ambas

estirpes, tras 2 horas de incubación se observaron valores en torno al 20 %, y a un 49 % al final del ensayo (4 h).

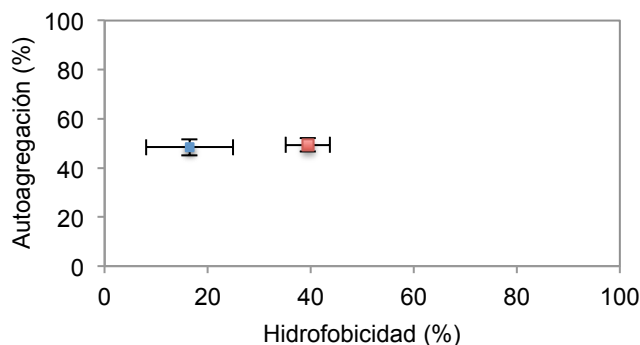


Figura 4.6. Hidrofobicidad y capacidad de autoagregación celular. En la gráfica se representa el porcentaje de autoagregación celular observado a las 4 h de reposo, respecto al porcentaje de hidrofobicidad encontrado en *L. sicerae* CUPV261^T (■) y en *L. collinoides* CUPV237 (■). En las gráficas se representa la media \pm la desviación estándar.

3.5 Ensayos de colonización gastrointestinal en el modelo *in vivo* de larvas gnotobióticas de pez cebra

Las cepas *L. sicerae* CUPV261^T, *L. collinoides* CUPV237 y la mutante *non-ropy* CUPV2371NR, fueron transformadas con el plásmido pRCR12. Este plásmido es portador del gen que codifica la proteína autofluorescente mCherry.

Como se aprecia en la Figura 4.7, los transformantes mostraron una coloración magenta durante los 11 días posteriores a la siembra en el medio MRS-agar suplementado con cloranfenicol. El rendimiento de transformantes fue bajo, únicamente se obtuvo un transformante para CUPV237 y CUPV2371NR, los cuales se nombraron como CUPV237 [pRCR12] y CUPV2371NR [pRCR12], respectivamente. En el caso de *L. sicerae* se obtuvieron 10 colonias rosadas y se seleccionó una de ellas que se denominó CUPV261^T [pRCR12].

Para el análisis de la expresión de la proteína mCherry en las estirpes CUPV261^T [pRCR12], CUPV237 [pRCR12] y CUPV2371NR [pRCR12] se utilizaron cultivos en el medio MRS suplementado con cloranfenicol. En estas tres estirpes se observó que el crecimiento estaba acompañado de un incremento de los niveles de fluorescencia (Figura 4.7). Esto indicó que la presencia del plásmido p[RCR12] confirió fluorescencia a los transformantes de *L. sicerae* y *L. collinoides*. Por otro lado, se observaron mediante microscopía óptica cultivos en fase exponencial de células

concentradas y suspendidas en PBS. Las imágenes mostraron la expresión de la proteína mCherry en células individuales de las 3 estirpes.

Se estudió la capacidad de las cepas de *L. sicerae* y *L. collinoides*, acompañadas o no de $150 \mu\text{g mL}^{-1}$ del EPS que producen, de colonizar el epitelio intestinal de larvas axénicas de pez cebra. Para ello, se utilizaron los transformantes *L. sicerae* CUPV261^T [pRCR12], *L. collinoides* CUPV237 [pRCR12] y la estirpe *non-ropy* *L. collinoides* CUPV2371NR [pRCR12], debido a su capacidad de producir la proteína fluorescente mCherry que facilitaría su localización dentro de las larvas transparentes. Una vez que las larvas se expusieron a los transformantes, se mantuvieron en PBS durante de 6, 24 y 48 horas (periodos post-exposición) antes de ser visualizadas mediante un estereomicroscopio (Figura 4.8). Las imágenes mostraron fluorescencia solo en un número muy reducido de larvas. Además, no se detectaron bacterias viables en aquellas en las que previamente se había visualizado fluorescencia, ni tampoco en el resto de las larvas tratadas.

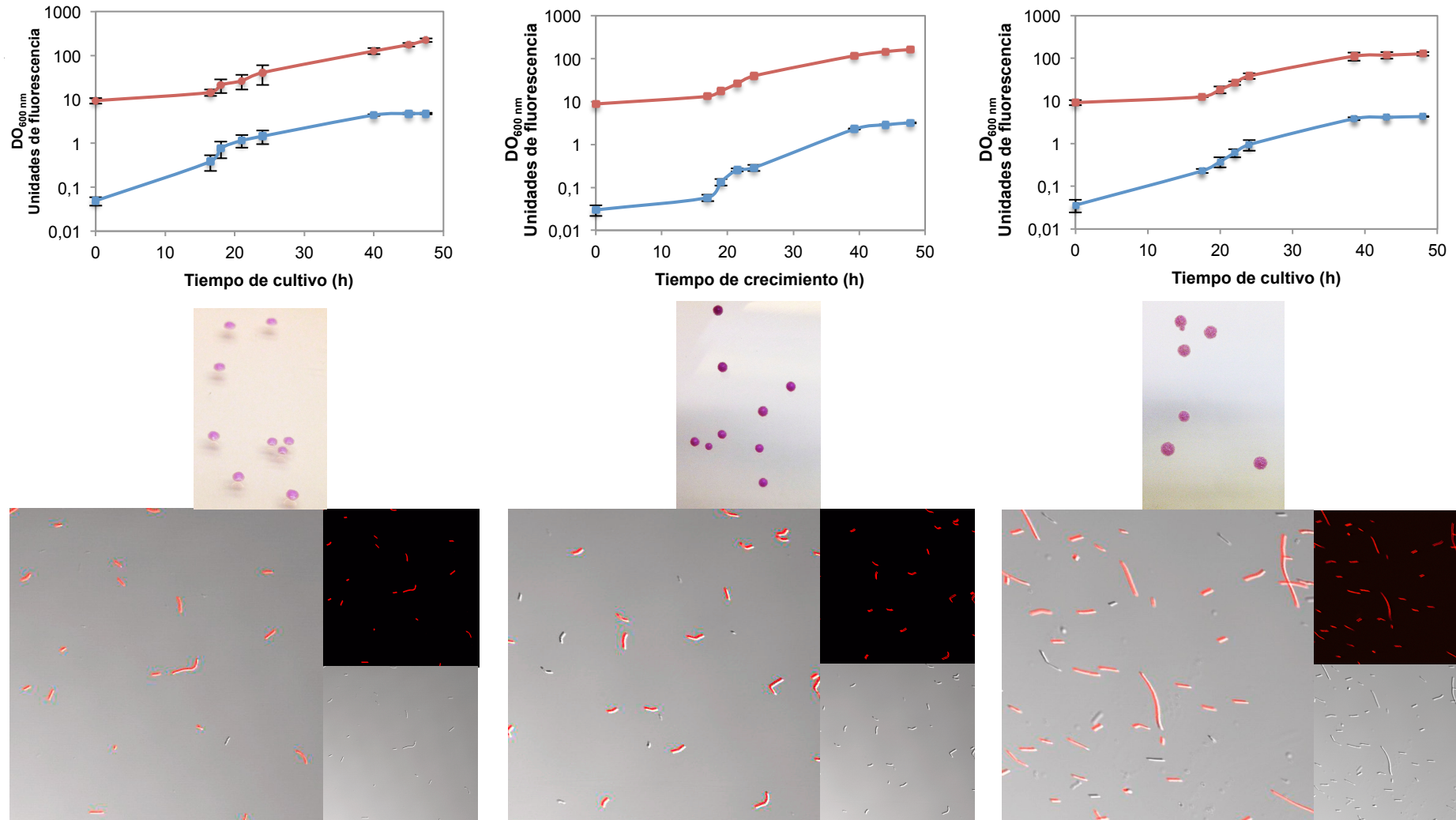


Figura 4.7. Detección de la expresión de la proteína fluorescente mCherry en *L. sicerae* CUPV261^T [pRCR12] (A), *L. collinoides* CUPV237 [pRCR12] (B) y *L. collinoides* CUPV2372 [pRCR12] (C). Arriba, se representan los valores de DO₆₀₀ (■) y de fluorescencia (■) ± error estándar de la media. Centro, colonias cultivadas en el medio MRS-agar suplementado con cloranfenicol. Abajo, se muestran las imágenes de las células suspendidas en PBS y procedentes de cultivos en fase exponencial, obtenidas por microscopía de contraste de fases (parte inferior derecha), por microscopía de fluorescencia (parte superior derecha), y del solapamiento de ambas (izquierda).

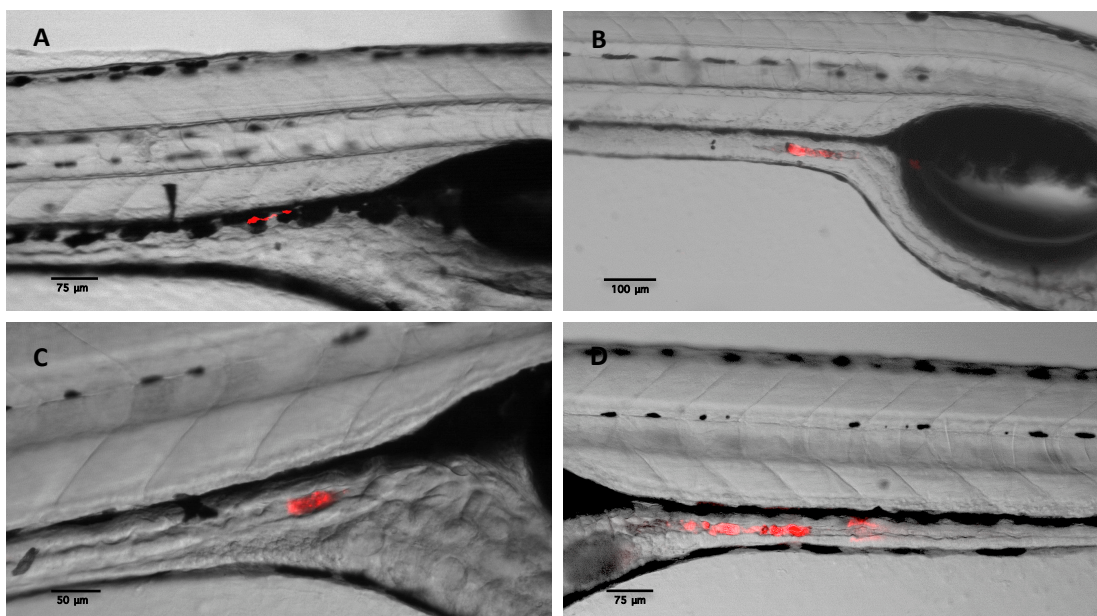


Figura 4.8. Detección de los transformantes de *L. sicerae* y *L. collinoides* en el intestino de larvas gnotobióticas de pez cebra. Los ensayos se llevaron a cabo con suspensiones celulares suplementadas o no con EPS (150 mg L^{-1}). En **A**, *L. sicerae* CUPV261^T [pRCR12] a las 24 horas post-exposición (hpe); **B**, *L. collinoides* CUPV2371NR [pRCR12] a las 48 hpe; **C**, *L. collinoides* CUPV237 [pRCR12] en presencia EPS a las 6 hpe; y **D**, *L. collinoides* CUPV2371NR a las 6 hpe.

4. DISCUSIÓN

La utilización de alimentos como vehículo para suministrar probióticos ha sido de interés para los científicos durante décadas, debido a sus beneficios en la salud de los consumidores (Trivedi et al., 2014). La dosis diaria recomendada para que un probiótico ejerza un efecto fisiológico o terapéutico debe de estar entre 10^8 - 10^{10} UFC (Fric, 2007). Tradicionalmente las bacterias lácticas son responsables de la elaboración de gran variedad de productos lácteos fermentados, aunque lo habitual para las especies del presente trabajo es encontrarlas en bebidas alcohólicas sin estabilizar (Carr & Davies, 1972; Fuji et al, 2005). *Lactobacillus collinoides* es una especie catalogada como QPS (*Qualified Presumption of Safety*) según la EFSA, además de otras especies de bacterias lácticas presentes en la sidra como son *L. diolivorans* o *P. parvulus* (EFSA, 2019). Las cepas *L. sicerae* CUPV261^T y *L. collinoides* CUPV237 fueron capaces de fermentar las matrices bebida de soja y avena, ambas suplementadas con glucosa. Cabe destacar, que después de incubar los productos a 4 °C, las poblaciones bacterianas se mantuvieron por encima de 10^8 UFC mL⁻¹, y estas concentraciones son similares a las descritas en leches fermentadas por diferentes cepas probióticas de *Lactobacillus* (Li et al., 2014; Blaiotta et al., 2017). Además, se ha descrito que la matriz bebida de soja es apropiada para suministrar probióticos viables de *L. reuteri* (Roy et al., 2016). Con respecto al crecimiento en leche, *L. collinoides* no fue capaz de fermentar esta matriz; y sin embargo, *L. sicerae* alcanzó poblaciones de 10^8 UFC mL⁻¹, y estos niveles se mantuvieron una vez concluido el periodo de refrigeración a 4 °C (7 días).

Uno de los requisitos para que una cepa sea considerada como probiótica es que debe de alcanzar su localización final en el hospedador (p. ej. el tracto gastrointestinal), y en un número suficientemente alto que permita ejercer su efecto beneficioso (Hill et al., 2014; Calatayud, Marcos & Margolles, 2016). Por este motivo, se decidió aplicar el modelo *in vitro* de estrés gástrico y gastrointestinal sobre suspensiones celulares de *L. sicerae* y *L. collinoides*. Los resultados mostraron un descenso importante de la viabilidad celular de CUPV261^T y CUPV237, y aunque las matrices alimentarias ejercieron un efecto protector, se alcanzaron poblaciones inferiores a 10^4 UFC mL⁻¹ debido a las agresivas condiciones ácido-enzimáticas de los tratamientos. El efecto protector de la matriz alimentaria sobre las células bacterianas sometidas a ensayos de estrés gástrico y gastrointestinal ha sido también observado en las cepas productoras de β-glucano *P. parvulus* CUPV22 y 2.6, cuando se incorporaron a yogur o zumo de naranja con leche (Elizaquível et al., 2011). Así mismo,

las estirpes *L. acidophilus* La5, *L. plantarum* CECT 8328 y *L. fermentum* CECT 8448 mejoraron su tolerancia al estrés cuando se incluyeron en pasta (Arena et al., 2014).

En el intestino delgado y en el intestino grueso se dan condiciones oxidantes que fundamentalmente son ocasionadas por la presencia de especies reactivas de oxígeno (radicales ROS), y parecen ser producidas por la actividad mitocondrial. Estas especies oxidantes pueden ser las responsables de la aparición de enfermedades tales como el cáncer (Sanders et al., 2004). Los ensayos *in vitro* realizados para medir la actividad antioxidante de células intactas de *L. sicerae* y *L. collinoides*, mostraron una actividad anti-radicales libres frente a los aniones superóxido (36 y 53 %, respectivamente), radicales hidroxilo (en torno al 25 %) y DPPH[•] (48 y 26 %, respectivamente). Resultados similares se han descrito en trabajos donde se les atribuye a las BAL una potencial capacidad antioxidante (Lin & Chang, 2000; Wang et al., 2009; Das & Goyal, 2015; Tang et al., 2017), y podría deberse a los diferentes componentes de la envuelta celular, como son las proteínas o polisacáridos y los ácidos teicoicos, muy abundantes en la superficie bacteriana (Yi et al., 2009; Tang et al., 2017).

Una propiedad importante de muchas cepas bacterianas utilizadas como probióticos es la de adherirse a las células epiteliales y a superficies mucosas (Kos et al., 2003). Se ha observado que la capacidad de agregación bacteriana y la hidrofobicidad de las superficies celulares, son solo unos de los factores a tener en cuenta dentro del mecanismo complejo que permite a los microorganismos interactuar con el hospedador y ejercer su efecto beneficioso (García-Cayueta et al., 2014). Las estirpes *L. collinoides* CUPV2371 y *L. sicerae* CUPV261^T presentaron valores de hidrofobicidad (16 y 39 %, respectivamente) y de autoagregación (en torno al 40 %) similares a los descritos por otros autores para ciertas estirpes de *Lactobacillus* (Lacerda et al., 2013; Tuo et al., 2013; García-Cayueta et al., 2014; Abdulla et al., 2014). La presencia de heteropolisacárido en la superficie celular de estas estirpes aisladas de sidra, podría influir en sus propiedades de adhesión. Con respecto a esto, se ha observado en cepas probióticas de *Lactobacillus* y *Bifidobacterium* que los niveles de adhesión dependen del tipo de HePS que producen (Ruas-Madiedo et al., 2006).

Para continuar el estudio sobre las características probióticas de las cepas de *L. sicerae* y *L. collinoides*, se utilizó el modelo animal alternativo de larvas gnotobióticas de pez cebra. Se analizó la habilidad de los transformantes de CUPV261^T, CUPV237 y

su cepa isógena *non-ropy* CUPV2371NR para colonizar el epitelio intestinal de larvas axénicas de *Danio rerio*. Para poder localizar a las bacterias dentro de las larvas, las estirpes se modificaron genéticamente introduciéndoles el vector plasmídico [pRCR12] que contiene el gen *mrfp* y que codifica la proteína fluorescente mCherry. Se ha comprobado que la presencia de este plásmido en *Lactobacillus* y en otras estirpes de bacterias lácticas, permite la detección de los transformantes y su expresión génica a tiempo real, debido a la valoración de la proteína fluorescente mCherry (García-Cayuela et al., 2012; Mohedano et al., 2015; Garai-Novillo et al., 2019). Inicialmente, se observó que todas las colonias de los transformantes *L. sicerae* CUPV261^T [pRCR12], y *L. collinoides* CUPV237 [pRCR12] y CUPV2371NR [pRCR12] adoptaron una coloración magenta que indicó que expresaban el gen *mrfp* (Figura 4.7). Así mismo, las curvas de crecimiento mostraron que el aumento de la fluorescencia estaba relacionado con el incremento de la DO₆₀₀. Además, mediante microscopía óptica de contraste de fases y de fluorescencia, se observó la fluorescencia individual de cada célula, aunque se detectaron variaciones en la intensidad entre los bacilos de un mismo cultivo. Las proteínas fluorescentes necesitan un tiempo de maduración postraducciona para la formación del cromóforo (Garai-Novillo et al., 2019). En concreto, se ha descrito en *Lactococcus lactis* que la proteína mCherry posee una velocidad de maduración lenta, con un valor máximo específico de fluorescencia de 6 h (Garai-Novillo et al., 2019). Las imágenes de los transformantes mostraron diferencias en la intensidad de la fluorescencia emitida por los lactobacilos (Figura 4.7), que podrían ser explicadas por el diferente estado de maduración de la proteína mCherry entre las células de un mismo cultivo. Finalmente, los resultados obtenidos nos permiten concluir que el gen de la mCherry es funcional en las estirpes *L. sicerae* CUPV261^T [pRCR12], y *L. collinoides* CUPV237 [pRCR12] y CUPV2371NR [pRCR12], y su presencia permite la detección de las células mediante fluorescencia.

Los ensayos de colonización bacteriana del epitelio intestinal se realizaron mediante el modelo de larvas gnotobióticas de pez cebra. Larvas axénicas fueron expuestas a suspensiones bacterianas de cada una de las estirpes transformadas de *L. sicerae* y *L. collinoides*, y suplementadas o no con 150 mg L⁻¹ del EPS que producen. A diferencia de los resultados obtenidos con estirpes de bacterias lácticas de las especies *L. plantarum*, *L. fermentum* y *Pediococcus parvulus* (Russo et al., 2015; Pérez-Ramos et al., 2018), únicamente se pudieron localizar bacterias fluorescentes en el interior del tracto intestinal de un número muy reducido de larvas, y no se detectaron células viables de las bacterias de este estudio a partir de las larvas tratadas. A pesar de ello, la perdurabilidad de la fluorescencia en larvas de 48 hpe y

que ésta esté concentrada en zonas de emisión definida dentro de las larvas, podría indicar que las células están intactas (sin roturas de membranas por muerte celular) (Figura 4.8). Éstas podrían encontrarse en un estado de viables no cultivables por las situaciones de estrés generadas por las condiciones del ensayo, pero no se han podido realizar ensayos adicionales que confirmen esta idea. El estado de viables no cultivables es una estrategia de supervivencia de las células expuestas a circunstancias ambientales adversas, como ha sido descrito *L. lindneri* y *L. paracollinoides* (Pinto et al., 2015; Suzuki et al., 2006).

5. CONCLUSIONES

En este trabajo se ha estudiado el potencial probiótico de las estirpes productoras de heteropolisacárido *L. sicerae* CUPV261^T y *L. collinoides* CUPV237 mediante ensayos realizados en modelos *in vivo* e *in vitro*.

Ambas cepas fermentan las matrices alimentarias de bebida de soja y avena, además de la matriz leche para la cepa de *L. sicerae*; y se mantuvieron en poblaciones superiores a 10⁸ UFC mL⁻¹ una vez concluido el periodo de refrigeración. Con respecto a los ensayos de tolerancia del estrés gastrointestinal llevados a cabo en un modelo *in vitro*, aunque las matrices alimentarias ejercieron un efecto protector, las severas condiciones ácido-enzimáticas provocaron un descenso importante de la viabilidad celular. Por otro lado, las células de estas estirpes presentaron una potencial capacidad antioxidante frente a los radicales hidroxilo, superóxido y DPPH, así como una hidrofobicidad de la superficie celular y un porcentaje de autoagregación similares a las descritas en otras estirpes de bacterias lácticas.

Para evaluar la capacidad de colonización intestinal en larvas de pez cebra de *L. sicerae* CUPV261^T y *L. collinoides* CUPV237, así como el mutante *non-ropy* *L. collinoides* CUPV2371NR, las estirpes fueron transformadas con el plásmido p[RCR12], el cual contiene el gen *mrfp* que codifica la proteína fluorescente mCherry. Los resultados obtenidos nos permitieron concluir que el gen de la mCherry es funcional en los transformantes CUPV261^Tp[RCR12], CUPV237 p[RCR12] y CUPV2371NR p[RCR12], y su presencia permite la detección de las células mediante fluorescencia. Finalmente, no se observaron evidencias de que estas estirpes sean capaces de colonizar el tracto gastrointestinal de larvas axénicas de pez cebra.

6. BIBLIOGRAFÍA

- Abdulla, A. A., Abed, T. A., & Saeed, A. M. (2014). Adhesion, autoaggregation and hydrophobicity of six *Lactobacillus* strains. *Microbiology Research Journal International*, 4(4) 381-391.
- Arena, M. P., Caggianiello, G., Fiocco, D., Russo, P., Torelli, M., Spano, G., & Capozzi, V. (2014). Barley β -glucans-containing food enhances probiotic performances of beneficial bacteria. *International Journal of Molecular Sciences*, 15(2), 3025-3039.
- Berthier, F., Zagorec, M., Champomier-Vergès, M., Ehrlich, S. D., & Morel-Deville, F. (1996). Efficient transformation of *Lactobacillus sakei* by electroporation. *Microbiology*, 142(5), 1273-1279.
- Bhushan, B., Tomar, S. K., & Chauhan, A. (2017). Techno-functional differentiation of two vitamin B12 producing *Lactobacillus plantarum* strains: an elucidation for diverse future use. *Applied Microbiology and Biotechnology*, 101(2), 697-709.
- Blaiotta, G., Murru, N., Di Cerbo, A., Succi, M., Coppola, R., & Aponte, M. (2017). Commercially standardized process for probiotic “Italico” cheese production. *LWT-Food Science and Technology*, 79, 601-608.
- Calatayud, G. Á., Marcos, A., & Margolles, A. (Eds.). (2016). *Probióticos, prebióticos y salud: evidencia científica*. Ergon.
- Capozzi, V., Russo, P., Dueñas, M. T., López, P., & Spano, G. (2012). Lactic acid bacteria producing B-group vitamins: a great potential for functional cereals products. *Applied microbiology and biotechnology*, 96(6), 1383-1394.
- Carr, J. G., & Davies, P. A. (1972). The ecology and classification of strains of *Lactobacillus collinoides* nov. spec.: a bacterium commonly found in fermenting apple juice. *Journal of Applied Bacteriology*, 35(3), 463-471.
- Chikkamath, V., Kummari, S., Naik, V., & Nagappa, A. N. (2018). The role of probiotics, prebiotics and synbiotic on human health and disease-A review. *Manipal Journal of Pharmaceutical Sciences*, 4(2), 19-24.
- Das, D., & Goyal, A. (2015). Antioxidant activity and γ -aminobutyric acid (GABA) producing ability of probiotic *Lactobacillus plantarum* DM5 isolated from Marcha of Sikkim. *LWT-Food Science and Technology*, 61(1), 263-268.
- EFSA BIOHAZ Panel (EFSA Panel on Biological Hazards), 2019. Scientific Opinion on the update of the list of QPS-recommended biological agents intentionally added to food or feed as notified to EFSA. *EFSA Journal EFSA Journal* 2019; 17(7):5555.

- Elizaquível, P., Sánchez, G., Salvador, A., Fiszman, S., Dueñas, M. T., López, P., Fernández de Palencia, P., & Aznar, R. (2011). Evaluation of yogurt and various beverages as carriers of lactic acid bacteria producing 2-branched (1, 3)- β -D-glucan. *Journal of Dairy Science*, *94*(7), 3271-3278.
- FAO, Probiotics in food. *Food Nutr. Pap.* 2001, *85*, 71.
- Fernández de Palencia, P., Werning, M. L., Sierra-Filardi, E., Dueñas, M. T., Irastorza, A., Corbí, A. L., & López, P. (2009). Probiotic properties of the 2-substituted (1, 3)- β -D-glucan-producing bacterium *Pediococcus parvulus* 2.6. *Applied and Environmental Microbiology*, *75*(14), 4887-4891.
- Figuroa-González, I., Quijano, G., Ramírez, G., & Cruz-Guerrero, A. (2011). Probiotics and prebiotics-perspectives and challenges. *Journal of the Science of Food and Agriculture*, *91*(8), 1341-1348.
- Fric, P. (2007). Probiotics and prebiotics—renaissance of a therapeutic principle. *Open Medicine*, *2*(3), 237-270.
- Fujii, T., Nakashima, K., & Hayashi, N. (2005). Random amplified polymorphic DNA-PCR based cloning of markers to identify the beer-spoilage strains of *Lactobacillus brevis*, *Pediococcus damnosus*, *Lactobacillus collinoides* and *Lactobacillus coryniformis*. *Journal of Applied Microbiology*, *98*(5), 1209-1220.
- García-Cayuela, T., de Cadiñanos, L. P. G., Mohedano, M. L., de Palencia, P. F., Boden, D., Wells, J., Peláez, C., López, P., & Requena, T. (2012). Fluorescent protein vectors for promoter analysis in lactic acid bacteria and *Escherichia coli*. *Applied Microbiology and Biotechnology*, *96*(1), 171-181.
- García-Cayuela, T., Korany, A. M., Bustos, I., de Cadiñanos, L. P. G., Requena, T., Peláez, C., & Martínez-Cuesta, M. C. (2014). Adhesion abilities of dairy *Lactobacillus plantarum* strains showing an aggregation phenotype. *Food Research International*, *57*, 44-50.
- Hafsa, J., ali Smach, M., Khedher, M. R. B., Charfeddine, B., Limem, K., Majdoub, H., & Rouatbi, S. (2016). Physical, antioxidant and antimicrobial properties of chitosan films containing Eucalyptus globulus essential oil. *LWT-Food Science and Technology*, *68*, 356-364.
- Harish, K., & Varghese, T. (2006). Probiotics in humans—evidence based review. *Calicut Med J*, *4*(4), e3.
- Hill, C., Guarner, F., Reid, G., Gibson, G. R., Merenstein, D. J., Pot, B., Morelli, L.,

- Canani, R. B., Flint, H. J., Salminen, S., Calder, P.C., & Sanders, M.E. (2014) .Expert consensus document. The International Scientific Association for Probiotics and Prebiotics consensus statement on the scope and appropriate use of the term probiotic. *Nat Rev Gastroenterol Hepatol*, 11(8):506-514.
- Kos, B., Šušković, J., Vuković, S., Šimpraga, M., Frece, J., & Matošić, S. (2003). Adhesion and aggregation ability of probiotic strain *Lactobacillus acidophilus* M92. *Journal of Applied Microbiology*, 94(6), 981-987
- Li, C., Li, W., Chen, X., Feng, M., Rui, X., Jiang, M., & Dong, M. (2014). Microbiological, physicochemical and rheological properties of fermented soymilk produced with exopolysaccharide (EPS) producing lactic acid bacteria strains. *LWT-Food Science and Technology*, 57(2), 477-485.
- Lin, M. Y., & Chang, F. J. (2000). Antioxidative effect of intestinal bacteria *Bifidobacterium longum* ATCC 15708 and *Lactobacillus acidophilus* ATCC 4356. *Digestive Diseases and Sciences*, 45(8), 1617-1622.
- Mohedano, M. L., García-Cayuela, T., Pérez-Ramos, A., Gaiser, R. A., Requena, T., & López, P. (2015). Construction and validation of a mCherry protein vector for promoter analysis in *Lactobacillus acidophilus*. *Journal of Industrial Microbiology & Biotechnology*, 42(2), 247-253.
- Nácher, M. (2015). *Dextranos de bacterias lácticas aisladas de productos cárnicos: caracterización y aplicaciones* (Tesis doctoral, Universidad de Valencia).
- Oyarbide, U., Iturria, I., Rainieri, S., & Pardo, M. A. (2015). Use of gnotobiotic zebrafish to study *Vibrio anguillarum* pathogenicity. *Zebrafish*, 12(1), 71-80.
- Panda, S. H., Das, S., Bal, P., Panda, S. K., Goli, J. K., & Mohanty, N. (2018). Characterization of novel folate producing *Lactobacillus rhamnosus* and its appliance in fortification of ragi (*Eleusine coracana*) gruel. *Food Bioscience*, 21, 100-106.
- Pandey, K.R., Naik, S.R. & Vakil, B.V., (2015). Probiotics, prebiotics and synbiotics- a review. *J Food Sci Technol*, 52(12), 7577-7587.
- Pérez, P. F., Minnaard, Y., Disalvo, E. A., & De Antoni, G. L. (1998). Surface properties of bifidobacterial strains of human origin. *Applied and Environmental Microbiology*, 64(1), 21-26.
- Pérez-Ramos, A., Mohedano, M. L., Pardo, M. Á., & López, P. (2018). β -glucan-producing *Pediococcus parvulus* 2.6: test of probiotic and

- immunomodulatory properties in Zebrafish models. *Frontiers in Microbiology*, 9, 1684.
- Pinto, D., Santos, M. A., & Chambel, L. (2015). Thirty years of viable but nonculturable state research: unsolved molecular mechanisms. *Critical Reviews in Microbiology*, 41(1), 61-76.
- Rasband, W. S. (1997). ImageJ software. *National Institutes of Health: Bethesda, MD, USA, 2012*.
- Roy, D., Savard, P., Guertin, N., Martoni, C. J., Jones, M. L., & Champagne, C. P. (2016). Viability of *Lactobacillus reuteri* NCIMB 30242 during storage in fruit juice and soy beverage. *The Journal of Microbiology, Biotechnology and Food Sciences*, 5(4), 320.
- Ruas-Madiedo, P., Gueimonde, M., Margolles, A., de los Reyes-Gavilán, C. G., & Salminen, S. (2006). Exopolysaccharides produced by probiotic strains modify the adhesion of probiotics and enteropathogens to human intestinal mucus. *Journal of Food Protection*, 69(8), 2011-2015.
- Russo, P., Iturria, I., Mohedano, M. L., Caggianiello, G., Rainieri, S., Fiocco, D., Pardo, P. A.; López, P., & Spano, G. (2015). Zebrafish gut colonization by mCherry-labelled lactic acid bacteria. *Applied Microbiology and Biotechnology*, 99(8), 3479-3490.
- Sánchez, B., Delgado, S., Blanco-Míguez, A., Lourenço, A., Gueimonde, M., & Margolles, A. (2017). Probiotics, gut microbiota, and their influence on host health and disease. *Molecular Nutrition & Food Research*, 61(1), 1600240.
- Sanders, L. M., Henderson, C. E., Hong, M. Y., Barhoumi, R., Burghardt, R. C., Carroll, R. J., Turner, N. D., Chapkin, R. S., & Lupton, J. R. (2004). Pro-oxidant environment of the colon compared to the small intestine may contribute to greater cancer susceptibility. *Cancer Letters*, 208(2), 155-161.
- Suzuki, K., Iijima, K., Asano, S., Kuriyama, H., & Kitagawa, Y. (2006). Induction of viable but nonculturable state in beer spoilage lactic acid bacteria. *Journal of the Institute of Brewing*, 112(4), 295-301.
- Tang, W., Xing, Z., Li, C., Wang, J., & Wang, Y. (2017). Molecular mechanisms and *in vitro* antioxidant effects of *Lactobacillus plantarum* MA2. *Food Chemistry*, 221, 1642-1649.

- Trivedi, J. B., Prajapati, J. B., Nair, B. M., Oste, R., & Aparnathi, K. D. (2014). Fermentation kinetics and sensory attributes of milk fermented by probiotic bacteria. *International Journal of Fermented Foods*, 3(1), 75.
- Tuo, Y., Yu, H., Ai, L., Wu, Z., Guo, B., & Chen, W. (2013). Aggregation and adhesion properties of 22 *Lactobacillus* strains. *Journal of Dairy Science*, 96(7), 4252-4257.
- Wang, A. N., Yi, X. W., Yu, H. F., Dong, B., & Qiao, S. Y. (2009). Free radical scavenging activity of *Lactobacillus fermentum in vitro* and its antioxidative effect on growing–finishing pigs. *Journal of Applied Microbiology*, 107(4), 1140-1148.
- Yi, Z. J., Fu, Y. R., Li, M., Gao, K. S., & Zhang, X. G. (2009). Effect of LTA isolated from bifidobacteria on D-galactose-induced aging. *Experimental Gerontology*, 44(12), 760-765.

5. Evaluación de la producción de riboflavina en bacterias lácticas
aisladas de sidra y de su contenido en sidra natural del País Vasco

1. INTRODUCCIÓN

La riboflavina (7,8-dimetil-10-(1-D-ribitol) isoaloxazina) (Figura 5.1), es una vitamina hidrosoluble del grupo B (vitamina B₂) necesaria para el desarrollo de los seres vivos. Algunas plantas, hongos y bacterias tienen la capacidad de sintetizarla, y otros organismos dependen del aporte nutricional.

El requerimiento diario de riboflavina en humanos se estima en 1,3 mg en hombres y 1,1 mg en mujeres (Stahmann et al., 2000). Los humanos adquieren esta vitamina mediante la ingestión de hongos, levaduras, vegetales de hoja verde, carne, pescados grasos y en menor medida de los cereales debido al procesado del grano (Burgess et al., 2009). Un exceso de ingesta de riboflavina es inofensivo (Stahmann et al., 2000), ya que es eliminada por la orina. Una deficiencia de riboflavina afecta al metabolismo de la glucosa, ácidos grasos y aminoácidos provocando la arriboflavinosis, enfermedad que se caracteriza por una estomatitis angular, glositis, quelosis, dermatitis seborreica alrededor de la nariz y la boca, y cambios oculares que incluyen reducción del lagrimeo, fotofobia, vascularización corneal y formación de cataratas. La deficiencia subclínica de riboflavina ha sido encontrada en diabéticos, niños y familias con bajo nivel socioeconómico. Además, en niños con enfermedades cardíacas crónicas y bebés con una terapia prolongada contra la hiperbilirrubinemia (Kliegman et al., 2014). En la actualidad, y con el fin de incrementar el valor nutricional de alimentos y piensos, la riboflavina es sintetizada de forma industrial mediante procesos fermentativos, en los que se utilizan principalmente cepas del hongo *Ashbya gossypii* (niveles de producción de 15 g L⁻¹) y de la bacteria *Bacillus subtilis* (Revueta et al., 2017).

La riboflavina es modificada en el interior celular para producir flavinas activas biológicamente, la coenzima riboflavina-5'-fosfato, también denominada flavina mononucleótido (FMN), y el dinucleótido de flavina y adenina o flavina adenina dinucleótido (FAD). La síntesis de ambas coenzimas está catalizada por una enzima bifuncional flavoquinasa/FAD-sintasa (RibC), que convierte la riboflavina en FMN por fosforilación y en FAD por una posterior adenosilación (Vitreschat et al., 2002) (Figura 5.1). Tanto el FMN como el FAD actúan como portadores de electrones en las reacciones de óxido-reducción, funcionando como coenzimas para cientos de enzimas FMN- o FAD-dependientes, llamadas flavoproteínas.

Algunas cepas de BAL son capaces de producir, liberar o incrementar componentes específicos en los alimentos que aportan beneficios a la salud,

incluyendo la prevención o tratamiento de una enfermedad (LeBlanc et al., 2011). Entre estos ingredientes cabe destacar las vitaminas del grupo B, tales como la riboflavina, folatos o cobalamina (B₁₂) (Thakur et al., 2016). Así, ciertas BAL son adecuadas para aumentar significativamente la concentración de riboflavina en productos fermentados (LeBlanc et al., 2011). Estas bacterias, aun produciendo pequeñas cantidades de riboflavina, son una mejor opción para ser utilizadas como cultivos iniciadores en la elaboración de productos fermentados en vez de los *starters* tradicionales, los cuales consumen riboflavina (Thakur, Tomar & De, 2015). Su utilización puede permitir obtener nuevos alimentos con un interés nutricional incrementado, y/o con propiedades beneficiosas para la salud (LeBlanc et al., 2011).

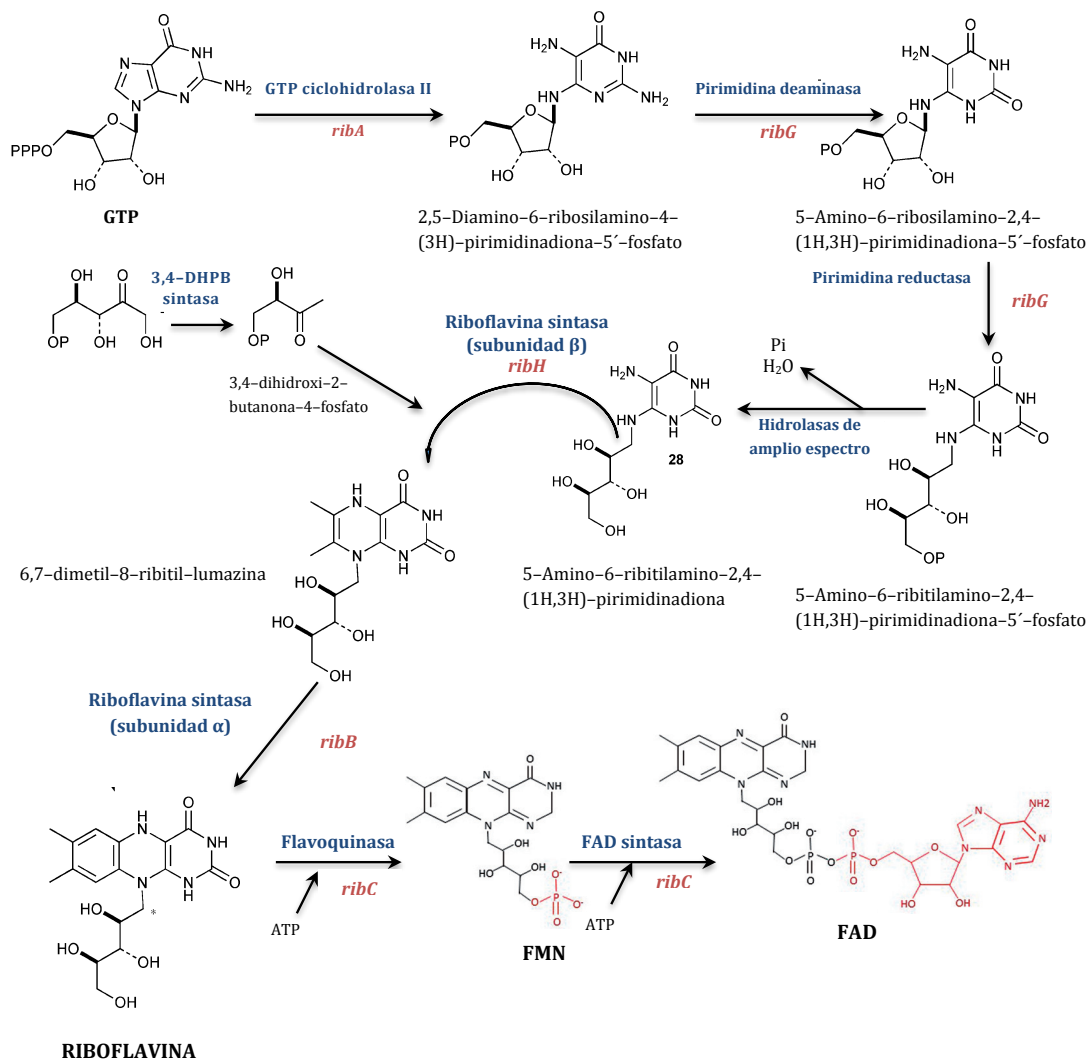


Figura 5.1. Ruta de producción de Vitamina B₂ y de sus vitámeros FMN y FAD en bacterias. La representación se ha realizado a partir de los trabajos de Webb et al. (2007), Capozzi et al. (2012), Thakur, Tomar & De (2015) y García-Angulo (2017). En rojo y azul se indican el gen y la proteína que codifica, respectivamente.

La biosíntesis de riboflavina ha sido descrita tanto en bacterias Gram-negativas como en Gram-positivas, y es llevada a cabo a partir de los precursores guanosina 5'-trifosfato (GTP) y ribulosa 5'-fosfato (Figura 5.1). El operón *rib* (Figura 5.2) está compuesto por cuatro genes (*ribG*, *ribB*, *ribA* y *ribH*), más el elemento RFN regulador localizado aguas arriba del primer gen (*ribG*) y un terminador en el extremo 3' de *ribH*. En primer lugar, la enzima GTP ciclohrolasa II (RibA) cataliza la formación de 2,5-diamino-6-ribosilamino-4-(3H)-pirimidinadiona-5'-fosfato. En *Bacillus subtilis*, RibA es una proteína bifuncional que cataliza también la formación de 3,4-dihidroxi-2-butanona-4-fosfato a partir de ribulosa 5'-fosfato, que es utilizado posteriormente por la enzima riboflavina sintasa subunidad β (RibH). En segundo lugar, ocurre una desaminación del anillo de pirimidina, seguida de la tercera transformación en la cual se reduce el grupo ribosil. Estas transformaciones, están catalizadas por RibG en su función pirimidina desaminasa y pirimidina reductasa, dando lugar a 5-amino-6-ribitilamino-2,4-(1H,3H)-pirimidinadiona-5'-fosfato. Este compuesto pierde el grupo fosfato y por medio de la enzima riboflavina sintasa subunidad β (RibH), se produce la condensación de este intermediario con 3,4-dihidroxi-2-butanona-4-fosfato, para formar 6,7-dimetil-8-ribitil-lumazina. Finalmente, la enzima riboflavina sintasa subunidad α (RibB) cataliza la síntesis de riboflavina. En el citoplasma, la riboflavina es rápidamente y casi exclusivamente convertida a FMN y FAD por RibC.

En la regulación de la síntesis y transporte de riboflavina interviene el elemento RFN (un aptámero del FMN *riboswitch*). Esta región reguladora está localizada en el extremo 5' del operón *rib* y del gen transportador de riboflavina *yapA/ribU*. Es una secuencia no traducida del mRNA, cuya estructura secundaria se cree dependiente de los niveles de los productos biológicamente activos de la ruta de la riboflavina (FMN y FAD). El *riboswitch* tiene dos plegamientos alternativos: el ON (antiterminador) o el OFF (terminador) (Figura 5.2). Cuando los niveles de riboflavina o de sus cofactores son suficientemente altos, el FMN interactúa directamente con el aptámero de mRNA naciente. Se estabiliza entonces una estructura pentafoliada que permite la formación de un terminador transcripcional entre ella y el inicio del primer gen. Y de esta manera, se induce la disociación prematura de la RNA polimerasa que reduce la expresión del operón (Mack & Grill, 2006; Pedrolli et al., 2015). Por el contrario, cuando la bacteria se encuentra en un entorno con bajos niveles de riboflavina o de sus cofactores, se forma una estructura secundaria hexafoliada compleja que impide la formación del terminador y favorece la expresión de los genes localizados aguas abajo. Se han propuesto dos mecanismos de regulación post-transcripcional: (i) atenuación transcripcional (Figura 5.2 A); y (ii) atenuación traduccional (Figura 5.2 B). En el primer

caso, se formaría corriente abajo de la estructura pentafoliada una estructura tallo-lazo que actuaría como terminador transcripcional, generando un transcrito abortivo. En el segundo caso, aguas abajo de la estructura pentafoliada, se formaría una estructura tallo-lazo que secuestraría el sitio de unión a los ribosomas (RBS) del gen *ribG* impidiendo su traducción y, en consecuencia, la catálisis de una de las primeras etapas de la ruta biosintética (Vitreschak et al., 2002).

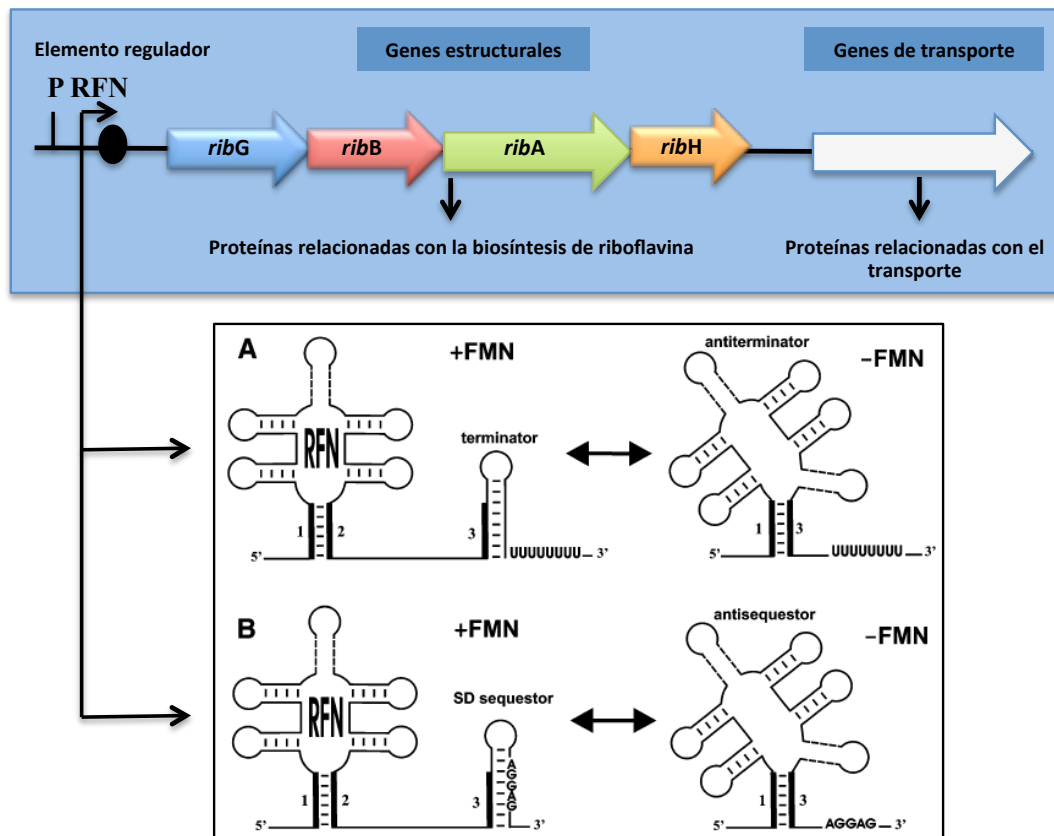


Figura 5.2. Los determinantes genéticos de la producción y transporte transmembrana de riboflavina. **Panel superior**, organización del operón *rib* y genes implicados en la biosíntesis y transporte de riboflavina (Thakur, Tomar & De, 2015). **Panel inferior**, predicción de los posibles mecanismos de regulación mediados por un elemento RFN del mRNA; (A) mediante atenuación transcripcional y (B) mediante atenuación traduccional (Vitreschak et al., 2002).

Se ha abordado la superproducción de riboflavina en bacterias mediante la sobreexpresión de genes implicados en la biosíntesis de la vitamina. Así, la sobreexpresión del gen *ribA* en *B. subtilis* incrementó la producción de riboflavina hasta un 25 %, sugiriendo que esta enzima limita la velocidad de la biosíntesis de riboflavina. Sin embargo, en *Lactococcus lactis*, la sobreexpresión única de *ribA* no produjo un incremento en la producción de esta vitamina (Burgess et al., 2009). Diversos autores han seleccionado BAL mutantes superproductoras de riboflavina por resistencia al tratamiento con roseoflavina, que es un compuesto tóxico y un análogo estructural de la vitamina B₂. Dichos mutantes contenían mutaciones en la región RFN

que conduce a la sobreexpresión de los genes *rib* (Burgess et al., 2006; Russo et al., 2014).

Con estos antecedentes, el trabajo experimental recogido en este capítulo estuvo enfocado a la verificación de la producción de riboflavina por BAL aisladas de sidra natural del País Vasco. El término riboflavina o B₂, se utilizará para describir todas las formas de flavina biológicamente activas de la vitamina B₂. Se optimizó un medio químicamente definido que permitió cultivar y mejorar el crecimiento de las cepas a estudio, así como cuantificar la riboflavina. Además, se estudió el operón *rib* de la cepa mutante superproductora de riboflavina *L. collinoides* CUPV237 y el mecanismo de regulación de la producción de vitamina B₂. Finalmente, se ha cuantificado la concentración de riboflavina en sidra natural del País Vasco.

2. MATERIAL Y MÉTODOS

2.1 Selección de cepas y medios de cultivo

Las bacterias utilizadas en estos ensayos proceden del análisis de las cepas productoras de exopolisacárido descritas en el capítulo 1, en concreto, 17 de ellas pertenecientes a la especie *L. collinoides*, una a *L. sicerae*, y 3 a *L. suebicus* (Tabla 5.5). Se incorporaron también en el estudio las estirpes productoras de (1,3)(1,2)- β -D-glucano *P. parvulus* 2.6 y *P. ethanolidurans* CUPV141 (Dueñas et al., 1997; Llamas-Arriba et al., 2018), y la cepa control productora de riboflavina *L. plantarum* subsp. *plantarum* CECT 748^T (Remagni, 2012). Las bacterias se cultivaron rutinariamente en MRS, y se almacenaron a $-80\text{ }^{\circ}\text{C}$ con un suplemento de glicerol al 20 % (v/v).

La cepa superproductora de riboflavina y productora de EPS *L. collinoides* CUPV237 se obtuvo por mutación espontánea de la cepa salvaje *L. collinoides* CUPV2371. Durante el crecimiento de la cepa salvaje en el medio semidefinido MSD se observó un cambio de color en el medio de cultivo, adoptando un fuerte carácter fluorescente amarillo-verdoso, y posteriormente se seleccionó en medio MRS-sólido una colonia amarilla (Figura 5.3). El genoma de CUPV237 está secuenciado y depositado en la base de datos del NCBI (Benson et al., 2006), con el número de acceso: JYDC00000000 (Puertas et al., 2016).

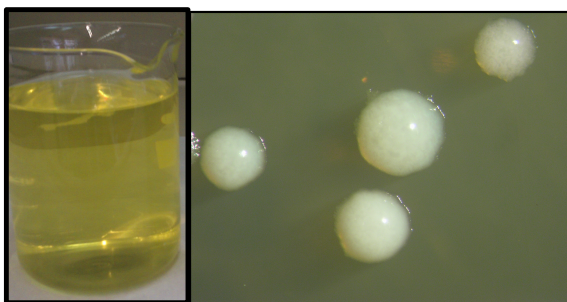


Figura 5.3. Cultivos de la cepa superproductora de riboflavina CUPV237. Izquierda, sobrenadante libre de células de un cultivo en MSD; derecha, colonias de un cultivo en MRS-sólido.

Para comprobar la capacidad de las cepas de crecer en ausencia de riboflavina se realizaron hasta 8 cultivos consecutivos en el medio semidefinido DifcoTM *Riboflavin Assay Medium*, apropiado para la detección de microorganismos productores de vitamina B₂ por no contenerla en su composición. Este medio fue ajustado a pH 6 con HCl 6 M y suplementado con el indicador de pH púrpura de bromocresol 0,014 % (p/v).

Para la determinación cuantitativa de la producción de riboflavina, se utilizaron los medios químicamente definidos, medio M5 (Tabla 5.1), medio CDM (Tabla 5.2) y medio PID (Tabla 5.3).

Tabla 5.1. Composición del medio químicamente definido M5 (Poolman et al., 1988).

Solución basal (pH 5,5)	g L⁻¹	Aminoácidos	g L⁻¹
K ₂ HPO ₄	3,0	Alanina	0,240
KH ₂ PO ₄	3,0	Arginina	0,120
Citrato diamónico	4,0	Asparagina	0,352
Acetato sódico	1,0	Aspartato	0,416
Clorhidrato de cisteína	2,4×10 ⁻⁴	Glutamato	0,496
Bases nitrogenadas		Glutamina	0,384
Adenina	0,010	Glicina	0,176
Guanina	0,010	Histidina	0,152
Uracilo	0,010	Isoleucina	0,208
Xantina	0,010	Leucina	0,456
Vitaminas		Lisina	0,440
Ácido <i>p</i> -aminobenzoico	0,005	Metionina	0,124
D-Biotina	2,5×10 ⁻³	Fenilalanina	0,276
Ácido Fólico	0,001	Prolina	0,676
Clorhidrato de piridoxamina	2,5×10 ⁻³	Tirosina	0,261
Clorhidrato de piridoxina	0,001	Micronutrientes	
Riboflavina	0,001	MgCl ₂	0,200
Clorhidrato de tiamina	0,001	CaCl ₂	0,038
Cianocobalamina	0,001	ZnSO ₄	5×10 ⁻⁴
Ácido lipoico	0,001	Glucosa	20,0

La esterilización se llevó a cabo mediante filtración, a excepción de la solución basal y la solución de glucosa que se realizó en un autoclave.

Tabla 5.2. Composición del medio químicamente definido (CDM) (Terrade et al., 2009).

Solución basal (pH 5,5)	g L⁻¹	Aminoácidos	g L⁻¹
K ₂ HPO ₄	1,0	Alanina	0,200
MnSO ₄ ·7H ₂ O	0,100	Arginina	0,750
MgSO ₄ ·7H ₂ O	0,100	Asparagina	0,150
CaCl ₂	0,440	Aspartato	0,350
CuSO ₄ ·5H ₂ O	1,5×10 ⁻⁵	Glutamato	0,500
FeSO ₄ ·7H ₂ O	2×10 ⁻⁴	Glutamina	0,200
ZnSO ₄ ·7H ₂ O	1,35×10 ⁻⁴	Glicina	0,500
Bases nitrogenadas		Clorhidrato de cisteína	0,200
Adenina	0,010	Histidina	0,500
Guanina	0,010	Isoleucina	0,200
Uracilo	0,010	Leucina	0,200
Citosina	0,010	Lisina	0,250
Timina	0,010	Metionina	0,150
Xantina	0,005	Fenilalanina	0,200
Vitaminas		Prolina	0,500
Ácido <i>p</i> -aminobenzoico	1×10 ⁻⁴	Serina	0,400
D-Biotina	0,002	Treonina	0,350
Ácido Fólico	0,002	Triptófano	0,200
Clorhidrato de piridoxina	0,002	Valina	0,200
Riboflavina	0,002	Tirosina	0,261
Clorhidrato de tiamina	0,001	Glucosa	20,0
Clorhidrato de colina	0,002		
Ácido nicotínico	0,002		
Ácido pantoténico	0,002		
Cianocobalamina	1×10 ⁻⁴		

La esterilización se llevó a cabo mediante filtración, a excepción de la solución basal y la solución de glucosa que se realizó en un autoclave.

El medio PID se diseñó a partir del descrito por Teusink et al. (2005) y fue modificado con el objetivo de mejorar el crecimiento de las cepas (Tabla 5.3).

Tabla 5.3. Composición y elaboración detallada del medio PID.

Sales o medio base (pH 5,5)	g L⁻¹	Aminoácidos	g L⁻¹
K ₂ HPO ₄	1,0	Alanina	0,240
KH ₂ PO ₄	5,0	Arginina	0,125
Acetato de sodio	1,0	Ácido aspártico	0,420
Citrato de amonio	0,6	Clorhidrato de cisteína	0,130
^a MgSO ₄ ·7H ₂ O	0,1	Ácido glutámico	0,500
^a MnSO ₄ ·H ₂ O	0,05	Glicina	0,175
Vitaminas		Histidina	0,150
Ácido lipoico	0,001 (disuelto en etanol absoluto)	Isoleucina	0,210
D-Biotina	0,0025 (disuelto en NaOH 2 M)	Leucina	0,475
Ácido fólico	0,001	Lisina	0,440
Ácido pantoténico	0,001	Metionina	0,125
Ácido nicotínico	0,001	Fenilalanina	0,275
Ácido <i>p</i> -aminobenzoico	0,010	Prolina	0,675
Clorhidrato de piridoxamina	0,005	Serina	0,340
Clorhidrato de piridoxina	0,002	Treonina	0,225
Riboflavina	0,001	Valina	0,325
Clorhidrato de tiamina	0,001	^a Asparagina	0,350
^a Cianocobalamina	0,001	^a Glutamina	0,390
Ácido ascórbico (Vit. C)	0,500	^a Triptófano	0,050
Bases nitrogenadas (disuelto en NaOH 0,1 M)		^a Tirosina	(disuelto en NaOH 0,05 M)
Adenina	0,010	Glucosa	20,0
Guanina	0,010		
Uracilo	0,010		
Xantina	0,010		

La esterilización se llevó a cabo mediante filtración, a excepción de la solución basal y la solución de glucosa que se realizó en un autoclave.

(a) variaciones en la concentración de estos compuestos, respecto al medio descrito por Teusink et al. (2005).

Condiciones de cultivo

Las bacterias se cultivaron por duplicado en los 3 medios definidos (completos y sin riboflavina). Los inóculos se obtuvieron a partir de cultivos en MRS en fase exponencial. Las células se recogieron por centrifugación ($8.161 \times g$, 2 min) y se lavaron con solución Ringer®. La incubación se realizó en completa oscuridad a 28 °C durante 68 h y en atmósfera enriquecida con un 5 % de CO₂. El crecimiento se monitorizó mediante la medida de la absorbancia a 600 nm (DO₆₀₀). La producción de vitamina B₂ se cuantificó en los sobrenadantes libres de células de los cultivos realizados en los medios CDM (Tabla 5.2) y PID (Tabla 5.3).

2.2 Producción de riboflavina por *L. collinoides* CUPV237

Los cultivos se realizaron en el medio MSD, partiendo de una DO_{600} inicial de 0,2. Se incubaron en completa oscuridad a 28 °C, en atmósfera de CO_2 al 5 % y durante 68 h. Las células se retiraron por centrifugación ($15.680 \times g$, 20 °C), evitando la exposición a la luz.

Para la identificación de la riboflavina en el sobrenadante, se empleó un espectrofluorímetro (Spectrometer RF-540 Shimadzu), con el cual se realizaron barridos del espectro de luz ultravioleta-visible. Se obtuvo un valor máximo con unas longitudes de onda de excitación y emisión, de λ_{ex} 450 nm y λ_{em} 525 nm, coincidiendo estos parámetros con los de la riboflavina (Homa et al., 2010). Este análisis se llevó a cabo junto con el profesor Iñaki Berregui, del departamento de Química Aplicada de la Facultad de Química de Donostia-San Sebastián (Universidad del País Vasco).

2.3 Cuantificación de riboflavina

Para la cuantificación de la riboflavina, las muestras se filtraron por un filtro de acetato de celulosa con un diámetro de poro de 0,2 μm . La concentración de riboflavina se determinó en un equipo de HPLC Shimadzu-Prominence (USA), equipado con un detector de fluorescencia Shimadzu-RF 10AXL (USA), con las condiciones de λ_{ex} 450 nm y λ_{em} 525 nm. La columna utilizada fue la EC 250/4.6 Nucleosil 120-5 C18 (Macherey-Nagel) junto con la precolumna Teknokroma TRC-160K1, ambas termostalizadas a 40 °C. El volumen de inyección fue de 20 μL . El método se llevó a cabo en condiciones isocráticas con un flujo de 0,8 $mL \text{ min}^{-1}$ y una fase móvil compuesta por acetato sódico 0,05 M:metanol, 60:40 (v/v), con un pH de 6,0 ajustado con ácido acético glacial.

Para la construcción de las curvas de calibrado se empleó un estándar analítico de riboflavina (Supelco, Sigma-Aldrich, St. Louis, MO). El compuesto fue disuelto en NaOH 0,05 M e inmediatamente se ajustó el pH a 5,0 con ácido acético glacial. Las soluciones estándar se prepararon en el momento de su utilización, evitando su exposición a la luz. El parámetro ganancia del detector de fluorescencia se fijó en el valor 4. Se elaboraron 3 curvas de calibrado modificando el parámetro sensibilidad. Los rangos de concentración lineal fueron entre 1 a 50 $\mu g \text{ L}^{-1}$ para la sensibilidad alta (Figura 5.4); de 0,020 a 2 $mg \text{ L}^{-1}$ para la media, y de 0,5 a 10 $mg \text{ L}^{-1}$ para la baja. Se obtuvo un límite de detección (LOD) de 1,19 $\mu g \text{ L}^{-1}$ y un límite de

cuantificación del método (LOQ) de $3,99 \mu\text{g L}^{-1}$, para la curva medida en sensibilidad alta. Los valores de LOD y LOQ se calcularon en base a la desviación estándar de la regresión (Sr) y al valor de la pendiente de la curva (m): $\text{LOD}=3\text{Sr}/m$; $\text{LOQ}=10\text{Sr}/m$ (Hossain et al., 2019).

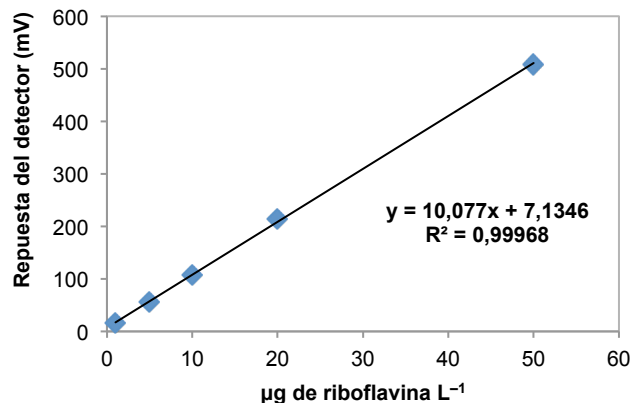


Figura 5.4. Curva de calibrado para la cuantificación de riboflavina con sensibilidad alta.

2.4 Fermentaciones de mostos de manzana

Obtención y tratamiento de los mostos

Se utilizaron 6 mostos monovarietales que fueron cedidos por el profesor Iñaki Berregi (campaña 2013), y para su elaboración, se emplearon las variedades de manzana autóctona Berde garratza, Gezamina, Merabi, Mozoloa, Urtebi txiki y Urdin. Además, se empleó un séptimo mosto (mosto mezcla), que fue obtenido mediante la mezcla de diferentes variedades de manzana de sidra procedentes de Normandía (Francia), y fue proporcionado por la sidrería Etxeberria (Hernani, Gipuzkoa). Para evitar la fermentación espontánea, las muestras se enfriaron de inmediato a $4\text{ }^{\circ}\text{C}$, y una vez en el laboratorio, se mantuvieron a $-20\text{ }^{\circ}\text{C}$ hasta su utilización.

El pH de los mostos se ajustó a 5,0 con NaOH y se centrifugaron a $4\text{ }^{\circ}\text{C}$ ($15.680 \times g$, 30 min) para eliminar las partículas en suspensión. Los sobrenadantes fueron esterilizados mediante autoclave a $120\text{ }^{\circ}\text{C}$ durante 6 min, para después añadirles un aporte extra de nitrógeno. El medio de cultivo (mosto modificado) constó de tres partes de mosto estéril y una parte de una solución de 12 g L^{-1} de ácidos casamino (BD™ Difco™, USA), esterilizada a $120\text{ }^{\circ}\text{C}$ durante 15 min. Durante todo este proceso se minimizó el tiempo de preparación para evitar la oxidación de los zumos.

Cepas y condiciones de cultivo

Se utilizaron la cepa superproductora de riboflavina *L. collinoides* CUPV237 y la estirpe *L. sicerae* CUPV261^T, además de la cepa control *L. plantarum* subsp. *plantarum* CECT 748^T. Los precultivos se realizaron en medio MRS, y las bacterias se sedimentaron y lavaron con solución Ringer® antes de ser inoculadas en los mostos. Los cultivos se mantuvieron a 28 °C, durante 7 días en jarras con generadores de anaerobiosis GasPakTM EZ Anaerobe Pouch System (BDTM) para evitar la oxidación de los caldos.

El crecimiento se monitorizó mediante la medida de la absorbancia a 600 nm (DO₆₀₀). Para la cuantificación de la riboflavina, los cultivos se centrifugaron durante 20 min a 15.680 × *g* (4 °C) y se filtraron (0,2 µm). El análisis se llevó a cabo mediante HPLC, tal y como se describe en el apartado 2.3, y se utilizó la curva de calibrado que se muestra en la Figura 5.4.

2.5 Determinación de riboflavina en sidras

Se determinó el contenido de riboflavina en 44 muestras de sidra natural que habían sido elaboradas en Gipuzkoa. Los doctores Iñaki Berregi y Andoni Zuriarrain de la Universidad del País Vasco EHU/UPV proporcionaron muestras de sidras embotelladas pertenecientes a su estudio de la evolución del perfil polifenólico en sidras monovarietales del País Vasco (Zuriarrain, 2017). Estas bebidas habían sido elaboradas con las variedades de manzana Urtebi txiki, Urtebi haundi, Moko, Txalaka, Goiko y Gezamina (campaña 2012). Además, se analizaron 7 sidras con la marca Eusko Label y elaboradas con manzana del País Vasco; unas fueron proporcionadas por el doctor Juan Zuriarrain y otras se adquirieron en un comercio de Oiartzun (Gipuzkoa).

Así mismo, en una sidrería localizada en el municipio de Hernani (Gipuzkoa) se tomaron muestras de sidra en barrica (19 depósitos, campaña 2013) y elaboradas con una mezcla de variedades de manzana (procedentes o no del País Vasco). Las muestras se conservaron en hielo y alejadas de la luz hasta su análisis. Esta sidrería también proporcionó sidras embotelladas de diferentes años: 4 de 2011, 7 de 2012, y 1 botella de 2013, que se incorporaron al estudio.

La cuantificación de riboflavina en las bebidas se realizó mediante HPLC tal y como se describe en el apartado 2.3.

2.6 Detección de genes implicados en la síntesis de riboflavina

La detección de genes implicados en la síntesis de vitamina B₂ se realizó mediante el método descrito por Capozzi et al. (2011), y la extracción de los DNA mediante el protocolo descrito en el capítulo 1 (apartado 2.6.1). Se llevaron a cabo PCR con los DNA de dos cultivos independientes de 19 cepas de la colección CUPV, pertenecientes a las especies *L. collinoides* (12), *L. suebicus* (2), *L. sicerae* (2), *L. diolivorans* G77, *P. parvulus* 2.6 y *O. oeni* I₄, más *L. plantarum* subsp. *plantarum* CECT 748^T como control positivo. La mezcla de PCR se realizó en un volumen de reacción de 20 µL, y estaba compuesta por: 1x de tampón de PCR, 100 µM de cada dNTP, 0,25 µM de cada cebador *ribF* y *ribR* (Tabla 5.4), 1 U de DNA polimerasa Phusion® de alta fidelidad (Thermo Scientific™) y 80 ng de DNA. El programa utilizado contenía un periodo de desnaturalización de 5 min a 94 °C; y 35 ciclos con 30 s a 94 °C, 31 s a 52 °C y 2 min a 72 °C. El producto de la PCR se visualizó mediante electroforesis en un gel de agarosa al 0,8 % (p/v) en tampón TAE, teñido con bromuro de etidio 0,2 µg mL⁻¹, y fue sometido a un voltaje de 80 V, durante 90 min.

Para la amplificación del operón *rib* se utilizaron los oligonucleótidos mostrados en la Tabla 5.4, que fueron diseñados a partir de la secuencia de DNA del operón *rib* y su región aguas arriba de la cepa CUPV237 (Puertas et al., 2016). El diseño de los cebadores se llevó a cabo con el software Primer3 web, versión 4.0 (<http://primer3.ut.ee>). La reacción de amplificación (40 µL) contenía: 1x de tampón de PCR, 1 U de DNA polimerasa Phusion® de alta fidelidad (Thermo Scientific™), 100 µM de cada dNTP, 1 pM de cada cebador y 160 µg de DNA purificado. Los programas de PCR utilizados para cada pareja de cebadores fueron los siguientes:

Con los cebadores **3Rib-F y 3Rib-R**, las condiciones fueron: 1 ciclo de 5 min a 94 °C; y 35 ciclos de 45 s a 94 °C, 35 s a 53 °C y 1 min a 72 °C.

Las amplificaciones con las parejas de cebadores **Rib-FA y Rib-RA, RibA-F y RibA-R, RibH-F y RibH-R, RibB-F y RibB-R, y RibD-F y RibD-R** se llevaron a cabo con: 1 ciclo de 5 min a 94 °C; y 35 ciclos de 1 min a 94 °C, 45 s a 50 °C y 1 min a 72 °C.

Tabla 5.4. Relación de cebadores destinados a la amplificación parcial del operón *rib*.

Cebador	Secuencia (5'→3')	Amplicón (pb)	Gen Diana	Referencia
ribF	CTTCRGGGCAGG GTG	2300	RFN- <i>ribA</i>	Capozzi et al., 2011
ribR	GGRAADABRTGNCCNGG			
RibA-F	GTGCATGATTCACGACGTTT	1100	Secuencia RFN- <i>ribG</i>	Este estudio
RibA-R	ATCCGGTAGCGAGAAGTTGA			
3Rib-F	GCAGGTCGGCATCAGTAGTC	991	Secuencia RFN- <i>ribG</i>	
3Rib-R	AGGTGACTAAGCGCGTTGAT			
RibD-F	TCTCGCTACCGGATATCACC	1062	<i>ribG</i>	
RibD-R	TGTCGCCAACCTGACTATGA			
RibB-F	CCAACTCACGATCGACACAA	1033	<i>ribB</i>	
RibB-R	TCGCAGATGTAAGCAACTGG			
RibA-F	ATACGGAAGCCGCTGTTGAT	850	<i>ribA</i>	
RibA-R	AAATTGAGCGACAACGATCC			
RibH-F	GAAGGGCTTGATACCGTTGA	819	<i>ribH</i> -terminador	
RibH-R	GTTGACATTCCGGGAAGTTATT			

Los productos de PCR se cargaron en un gel de agarosa al 0,8 % (p/v) en tampón TAE, con bromuro de etidio $0,2 \mu\text{g mL}^{-1}$, al que se le aplicó una corriente de 100 V durante 60 min. Los geles fueron documentados mediante el equipo GelDoc (BioRad). El tamaño de los fragmentos de DNA se estimó bajo luz ultravioleta, por comparación con el marcador de pesos moleculares de 1 Kb de Invitrogen. Las bandas fueron recuperadas y purificadas con el kit PCR Clean-Up Gel Extraction (Macherey-Nagel) y enviadas al servicio de secuenciación SECUGEN S.L. (Madrid).

Para el alineamiento de las secuencias de DNA, se utilizó el programa Clustalw 2.0 (<https://www.ebi.ac.uk/Tools/msa/clustalw2/>). El tratamiento de las mismas se realizó combinando los resultados obtenidos en BLASTn, BLASTp y en la base de datos de dominios conservados (CDD) disponible en el sitio web NCBI. Para realizar una predicción de las estructuras secundarias en el mRNA, se utilizó el programa mfold The RNA Institute Collage of Arts and Sciences, Universidad de Albany, NY, USA (<http://unafold.rna.aL.any.edu/?q=mfold/rna-folding-form>) (Zuker, 2003) y el servidor web PASIFIC (<http://www.weizmann.ac.il/molgen/Sorek/PASIFIC/>) que fue diseñado para la predicción de *riboswitches* (Millman et al., 2017).

3. RESULTADOS

3.1. Producción de riboflavina por *L. collinoides* CUPV237

Este estudio se inició con la cepa productora de heteropolisacárido *L. collinoides* CUPV2371 debido a la aparición de forma espontánea de un fenotipo que coloreaba el medio semidefinido MSD de un color amarillo-verdoso. Se seleccionó una colonia amarilla a partir de un cultivo en MRS-agar, y esta cepa mutante superproductora de riboflavina se nombró como CUPV237. El genoma de esta bacteria fue secuenciado (Puertas et al., 2016).

Con el fin de determinar la producción de riboflavina, esta estirpe fue cultivada en el medio semidefinido MSD, y como se muestra en la Figura 5.5, tras 39 h de incubación, la concentración de riboflavina y de EPS en el sobrenadante libre de células fue de $1,79 \pm 0,04 \text{ mg L}^{-1}$ y de $47,37 \pm 0,46 \text{ mg L}^{-1}$, respectivamente. El aumento de los niveles de riboflavina y de EPS entre las 39 y las 48 h podrían ser debidos a la lisis celular.

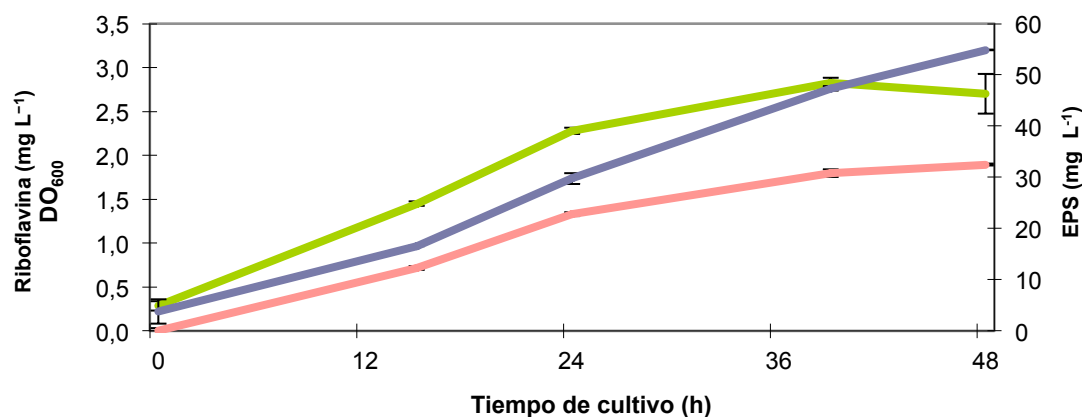


Figura 5.5. Cinética de crecimiento, de cuantificación de riboflavina y de EPS en el medio de cultivo de la cepa CUPV237. En verde se representa el crecimiento expresado como valores de densidad óptica medida a 600 nm; en violeta, el EPS producido (mg mL^{-1}) y en rojo los niveles de riboflavina (mg L^{-1}) presentes en el medio de cultivo.

3.2 Determinación de la producción de riboflavina en cepas de la colección CUPV

Se seleccionaron para el estudio 24 cepas de la colección CUPV y representativas de diferentes especies: *L. collinoides*, *L. sicerae*, *L. suebicus*, *P. parvulus* y *P. ethanolidurans* (Tabla 5.5). Inicialmente, y con el fin de evaluar el crecimiento en un medio sin riboflavina, se cultivaron en el medio semidefinido Difco™ *Riboflavin Assay Medium* suplementado con el indicador de pH púrpura de

bromocresol. Las cepas fueron crecidas durante 8 cultivos consecutivos en el mismo medio sin riboflavina (inóculo 1 %), y su crecimiento se observó de manera cualitativa mediante la detección de un cambio de color del cultivo. La mayoría de las cepas fueron capaces de crecer y modificar el pH del medio en los 8 cultivos consecutivos, a excepción de *L. sicerae* CUPV262, *L. collinoides* CUPV2324 y *P. parvulus* 2.6, en las que no se observó crecimiento a partir del segundo cultivo.

Así mismo, todas las cepas se cultivaron en los medios químicamente definidos M5, CDM y PID para determinar los niveles de riboflavina liberada al medio y comparar su crecimiento (Tabla 5.5). La mayor parte de las estirpes fueron capaces de crecer en los tres medios de cultivo, a excepción de *L. collinoides* CUPV2313 y CUPV2324; y de forma general, se alcanzaron valores de DO₆₀₀ superiores en el medio PID. En este medio, el valor de la DO₆₀₀ fue superior a 1 en todos los casos a excepción de las cepas citadas, y de *L. sicerae* CUPV261^T, *L. collinoides* CUPV2320, CUPV2322 y *P. ethanolidurans* CUPV141.

La concentración de riboflavina liberada al medio de cultivo (CDM y PID) fue estudiada mediante el análisis por HPLC de los sobrenadantes libres de células. En general, los niveles de riboflavina fueron ligeramente superiores en el medio CDM que en el medio PID. Sin embargo, este comportamiento fue distinto en las cepas *L. plantarum* subsp. *plantarum* CECT 748^T y *L. collinoides* CUPV237, que mostraron en el medio PID un incremento en la concentración de riboflavina de 4,7 y 2,7 veces, respectivamente, y que está relacionado con un aumento notable de su crecimiento en este medio. La cepa silvestre CUPV2371 y la control *L. plantarum* subsp. *plantarum* CECT 748^T secretaron niveles de riboflavina similares, $387,3 \pm 16,7$ y $330,1 \pm 13,9 \mu\text{g L}^{-1}$, respectivamente. Cabe destacar que en la estirpe mutante CUPV237 la acumulación de riboflavina en el medio fue del orden de 8 veces superior a la de la cepa silvestre.

Tabla 5.5. Crecimiento de las cepas de la colección CUPV en los medios definidos M5, CDM y PID, completos y sin vitamina B₂, y concentración de riboflavina en el sobrenadante.

Cepa	Medio de cultivo							
	^a M5		^b CDM			^b PID		
	Completo DO ₆₀₀	Sin riboflavina DO ₆₀₀	Completo DO ₆₀₀	Sin riboflavina DO ₆₀₀	Sin riboflavina µg L ⁻¹	Completo DO ₆₀₀	Sin riboflavina DO ₆₀₀	Sin riboflavina µg L ⁻¹
<i>L. plantarum</i> subsp. <i>plantarum</i> CECT 748 ^T	0,85±0,03	0,45±0,01	1,73±0,19	1,74±0,64	70,4±9,14	3,86±0,09	3,98±0,17	330,1±13,95
<i>L. sicerae</i> CUPV261 ^T	0,19±0,00	0,27±0,03	0,24±0,01	0,87±0,15	11,07±6,93	0,75±0,12	0,82±0,04	ND
<i>L. collinoides</i> CUPV2313	0,16±0,03	0,13±0,01	0,16±0,01	0,27±0,01	6,35±2,42	0,27±0,21	0,33±0,05	6,77±0,80
2315	0,12±0,02	0,11±0,01	0,45±0,02	0,22±0,07	7,55±0,08	0,31±0,08	0,32±0,04	6,77±0,00
2371	-	-	-	-	-	1,86±0,16	2,26±0,17	387,33±16,74
237	0,61±0,00	0,61±0,03	0,51±0,02	0,46±0,00	1097,25±0,64	1,63±0,80	2,67±0,06	3004,45±192,95
238	0,14±0,01	0,07±0,01	0,52±0,01	0,21±0,02	4,40±0,63	1,43±0,21	1,06±0,29	6,77±0,00
239	0,33±0,02	0,16±0,04	0,35±0,00	0,17±0,12	^(c) 2,78±0,04	1,08±0,26	1,25±0,12	4,09±0,28
2311	0,54±0,01	0,46±0,02	0,76±0,01	0,41±0,02	6,02±0,16	1,41±0,25	1,02±0,06	ND
2312	0,59±0,02	0,48±0,00	0,81±0,01	0,24±0,01	9,80±0,23	1,32±0,19	1,34±0,05	4,76±0,12
2317	0,39±0,00	0,31±0,00	0,24±0,00	0,18±0,00	4,00±0,09	1,41±0,17	1,05±0,07	ND
2320	0,40±0,00	0,37±0,01	1,10±0,05	0,21±0,00	11,15±0,08	0,64±0,41	0,61±0,10	7,61±0,40
2322	0,87±0,01	0,73±0,05	0,54±0,02	0,21±0,03	8,44±0,02	0,72±0,07	0,65±0,04	6,48±0,40
2323	0,34±0,00	0,26±0,02	1,24±0,11	0,96±0,01	21,74±0,86	0,68±0,07	1,25±0,07	ND
2324	0,08±0,01	0,07±0,01	0,44±0,01	0,44±0,04	10,55±0,03	0,19±0,24	0,3±0,08	^(c) 2,93±0,08
231	1,04±0,03	0,99±0,00	0,55±0,12	0,49±0,00	4,96±0,01	1,24±0,46	1,06±0,04	^(c) 3,24±0,68
232	-	-	0,49±0,03	0,52±0,03	^(c) 3,80±0,08	1,39±0,16	1,39±0,11	ND
234	1,37±0,01	1,32±0,02	0,81±0,03	0,67±0,05	9,07±0,03	1,18±0,07	1,23±0,06	ND
235	1,43±0,02	0,92±0,04	0,85±0,00	0,65±0,02	21,63±0,92	1,27±0,20	1,34±0,07	^(c) 3,04±0,16
2328	-	-	0,66±0,02	0,48±0,03	9,53±0,06	1,47±0,23	1,52±0,14	ND
<i>L. suebicus</i> CUPV225	0,43±0,19	0,53±0,02	0,2±0,00	0,22±0,00	^(c) 3,03±0,14	1,29±0,20	1,08±0,23	^(c) 1,92±0,4
226	0,90±0,06	0,87±0,08	0,91±0,02	0,53±0,03	^(c) 3,59±0,03	0,94±0,38	1,46±0,07	5,41±1,12
221	-	-	0,34±0,01	0,36±0,01	4,07±0,10	1,19±0,24	1,17±0,10	^(c) 3,47±0,20
<i>P. parvulus</i> 2.6	0,18±0,01	0,22±0,02	0,27±0,00	0,27±0,01	^(c) 2,44±0,03	1,83±0,62	1,30±0,02	^(c) 2,68 ±0,0
<i>P. ethanolidurans</i> CUPV141	0,80±0,09	0,73±0,03	0,45±0,01	0,38±0,00	^(c) 2,58±0,12	0,52±0,23	0,62±0,05	ND

(a) 120 h de fermentación.

(b) 65 h de fermentación.

(c) Concentraciones comprendidas entre el LOD (1,19 µg L⁻¹) y el LOQ (3,99 µg L⁻¹).

ND, no detectado.

3.3 Crecimiento y producción de riboflavina por *L. collinoides* CUPV237 y *L. siceræ* CUPV261^T en mostos de manzana.

La cepa superproductora de riboflavina *L. collinoides* CUPV237 y *L. siceræ* CUPV261^T fueron seleccionadas para evaluar la síntesis de la vitamina en mostos de manzana. Como control se incluyó la estirpe *L. plantarum* subsp. *plantarum* CECT 748^T. La Figura 5.6 A muestra el crecimiento en 7 mostos, 6 elaborados a partir de una única variedad de manzana y un mosto mezcla, todos ellos suplementados con ácidos casamino. Las cepas fueron capaces de crecer en estos medios, ya que se observó un incremento en los valores de la DO₆₀₀ tras 7 días de cultivo. El crecimiento varió en función de la variedad de manzana, y fue siempre superior para la cepa CUPV237.

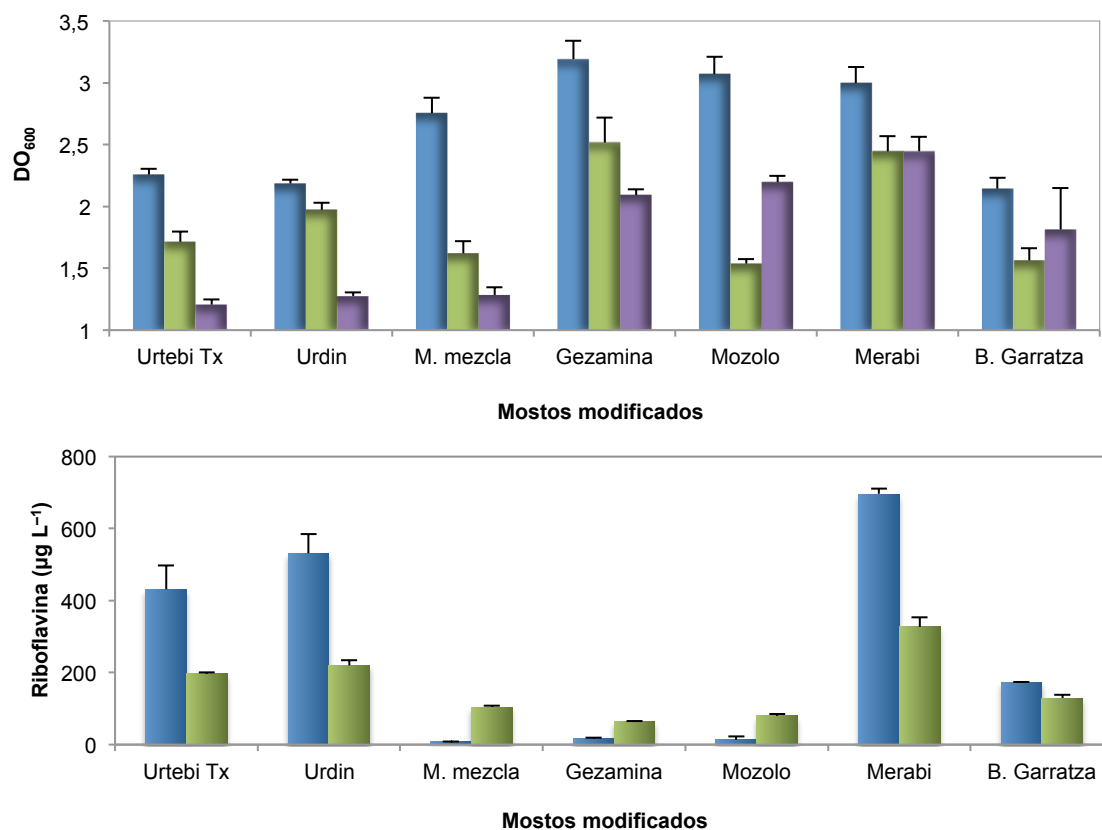


Figura 5.6. Fermentaciones en mostos modificados obtenidos a partir de diferentes variedades de manzana. En A, muestra el crecimiento de *L. collinoides* CUPV237 (■), *L. siceræ* CUPV261^T (■) y *L. plantarum* subsp. *plantarum* CECT 748^T (■), tras 7 días de cultivo. En la gráfica B, se representa el incremento en la concentración de riboflavina en los sobrenadantes de los cultivos. La concentración de riboflavina cuantificada en el sobrenadante de *L. siceræ* CUPV261^T fue inferior al límite de detección del método.

La Figura 5.6 B muestra la concentración de riboflavina en los sobrenadantes de los cultivos llevados a cabo por *L. collinoides* y *L. plantarum* subsp. *plantarum*, dado que en las fermentaciones con la estirpe *L. sicerae* no se detectó riboflavina en el medio. La concentración inicial de los mostos de manzana varió entre 4,59 $\mu\text{g L}^{-1}$ (mosto Merabi) y 20,72 $\mu\text{g L}^{-1}$ (mosto mezcla). En ambas cepas, las concentraciones más elevadas se observaron en los mostos de las variedades Merabi, Urdin y Urtebi txiki, y destacó CUPV237 con una concentración del orden de 700 $\mu\text{g L}^{-1}$ en Merabi.

3.4 Análisis del contenido de riboflavina en sidra natural

Con el fin de conocer el contenido de riboflavina en la sidra natural del País Vasco, se tomaron 44 muestras de distinta procedencia y elaboradas en Gipuzkoa.

Se analizaron 13 sidras en botella que habían sido elaboradas con manzana autóctona: 6 monovarietales y 7 sidras comerciales (Euskolabel). Se detectó riboflavina en 8 bebidas (Figura 5.7), y destacaron las sidras monovarietales Gezamina y Txalaka por poseer las concentraciones más altas (en torno a 50 $\mu\text{g L}^{-1}$).

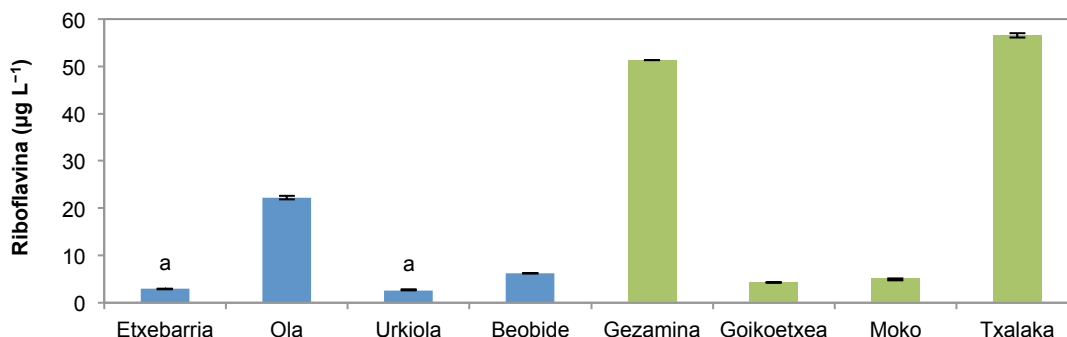


Figura 5.7. Concentración de riboflavina en sidras embotelladas elaboradas con variedades de manzana del País Vasco. Valores obtenidos en sidras comerciales elaboradas a partir de mezcla de mostos (■), y sidras monovarietales (■). a, detectada pero no cuantificable (valor comprendido entre los límites LOD y LOQ).

Durante la campaña 2013, se analizó toda la producción de sidra de una sidrería localizada en Hernani (Gipuzkoa) (19 depósitos). Las muestras fueron tomadas directamente de las barricas y exhibían un color amarillo-pajizo claro, sin aspecto de haber sufrido oxidaciones. Como se puede observar en la Figura 5.8, se detectó riboflavina en 15 muestras, alcanzando los 44,5 $\mu\text{g L}^{-1}$ en la barrica nº 27. Además, se analizaron 12 sidras embotelladas de diferentes campañas de producción (2011, 2012, 2013). En este caso, sólo en una de las botellas de la cosecha de 2011 se

cuantificaron $5,3 \pm 0,2 \mu\text{g L}^{-1}$ de riboflavina, mientras que en el resto no se detectó esta vitamina.

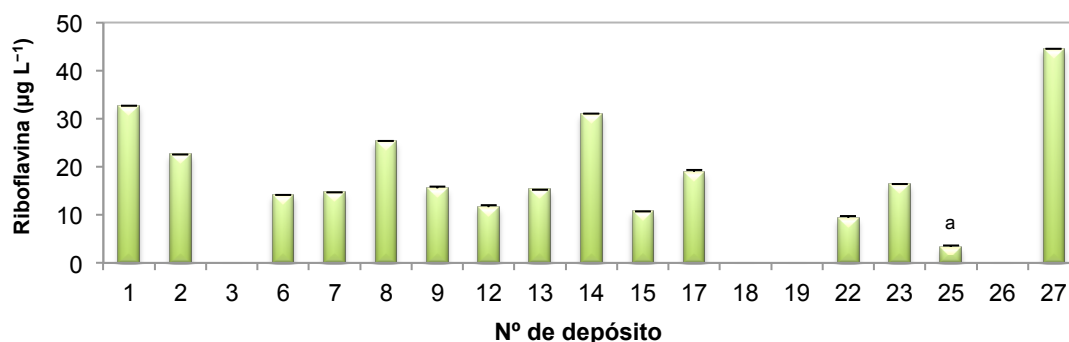


Figura 5.8. Análisis del contenido de riboflavina en la sidra elaborada por una sidrería de Hernani (Gipuzkoa). La gráfica muestra la concentración de vitamina de la sidra en barrica. Se analizaron 19 muestras numeradas según la sidrería. a, detectada pero no cuantificable (valor comprendido entre los límites LOD y LOQ).

3.5 Detección de genes implicados en la síntesis de riboflavina

Inicialmente, se llevaron a cabo PCR dirigidas a la amplificación parcial del operón de la riboflavina con los cebadores descritos por Capozzi et al. (2011), en un total de 19 cepas de las especies *L. collinoides*, *L. sicerae*, *L. suebicus*, *L. diolivorans*, *P. parvulus* y *O. oeni*. Únicamente se detectó la banda esperada, utilizando como sustrato los DNA aislados de las cepas: *L. plantarum* subsp. *plantarum* CECT 784^T (control) y *L. suebicus* CUPV225 y CUPV226.

El operón *rib* de *L. collinoides* CUPV237, se obtuvo a partir de su genoma (NZ_JYDC00000000; Puertas et al., 2016) depositado en la plataforma RAST (Brettin et al., 2015), y fue analizado utilizando el servidor BLASTn (Figura 5.9). Se observó un máximo de identidad del 75 % (valor-e de 0,0) con la secuencia comprendida desde la base 2.873.888 a la 2.877.233 del genoma de *Lactobacillus paracollinoides* TMW11994 (CP014915.1). El análisis de la secuencia de aminoácidos obtenida a partir de la secuencia de nucleótidos mostró que contenía los dominios: RibD (PRK10786, proteína bifuncional diaminodihidroxifosforibosilaminopirimidina deaminasa/5-amino-6-(5-fosforibosilamino) uracilo reductasa, valor-e de $2,38 \times 10^{-54}$), PRK09289 (riboflavina sintasa subunidad alfa, valor-e de $2,2 \times 10^{-52}$), RibH (PRK00061, 6,7-dimetil-8-ribitil lumazina sintasa, valor-e de $5,17 \times 10^{-47}$) y PRK09311 (proteína bifuncional 3,4-dihidroxi-2-butanona 4-fosfato sintasa/GTP ciclohidrolasa II, valor-e de $9,83 \times 10^{-108}$).

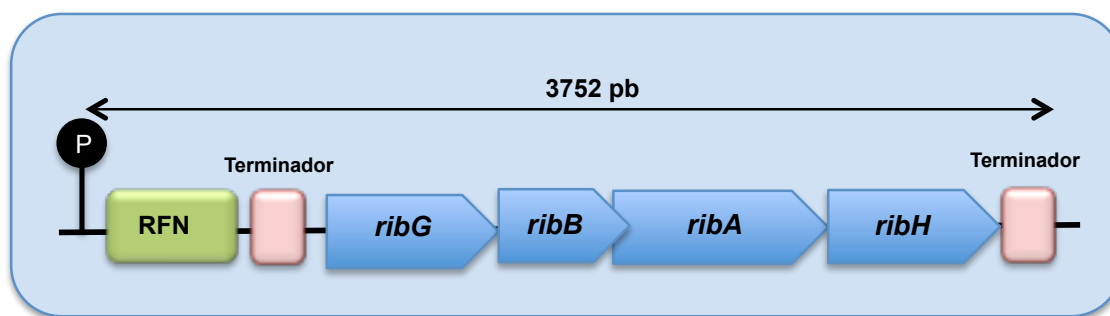


Figura 5.9. Operón *rib* perteneciente a la cepa *L. collinoides* CUPV237. Ha sido elaborado a partir de la secuencia (NZ_JYDC00000000) del genoma bacteriano descrito en Puertas et al. (2016).

Se seleccionaron las cepas *L. collinoides* CUPV2371, CUPV2313, CUPV2320, CUPV2323, CUPV231 y *L. sicerae* CUPV261^T (procedentes de diferentes botellas de sidra), para detectar y comparar su operón *rib* entre ellas y con la cepa superproductora CUPV237. Para ello, se diseñaron cebadores dirigidos a los genes de este operón utilizando como plantilla la secuencia del operón *rib* de la cepa secuenciada (Puertas et al., 2016). En todas las cepas de *L. collinoides* se obtuvo la banda esperada, y la secuenciación de los amplicones permitió obtener la secuencia de nucleótidos de los genes *ribG*, *ribB*, *ribA* y de la secuencia RFN. Sin embargo, aunque en la amplificación del gen *ribH* se detectó la banda correspondiente, no se pudo obtener la secuencia de nucleótidos de este gen y del terminador del operón localizado en su extremo 3', a excepción de la cepa CUPV2371, en cuyo caso se consiguió la secuencia del operón completo. En la cepa de *L. sicerae* CUPV261^T, se observaron las bandas correspondientes a los genes *ribG*, *ribA* y *ribH*, pero mediante secuenciación sólo se obtuvo la secuencia parcial de los genes *ribG* y *ribB*.

Las secuencias de los productos de amplificación de las cepas de *L. collinoides*, se compararon con el operón *rib* de la cepa superproductora CUPV237. Los alineamientos mostraron que éstas son idénticas entre sí, a excepción de la secuencia de la cepa CUPV237 (Anexo II.IV). La secuencia de esta cepa presentó un cambio en la base en la posición -151 respecto a la adenina inicial de la secuencia codificante del gen *ribG*, en el extremo 3' de la posible secuencia reguladora RFN (Figura 5.9). La mutación puntual en la cepa CUPV237 superproductora de riboflavina, es una transición consistente en el cambio de una guanina presente en la cepa silvestre, por una adenina (G153A).

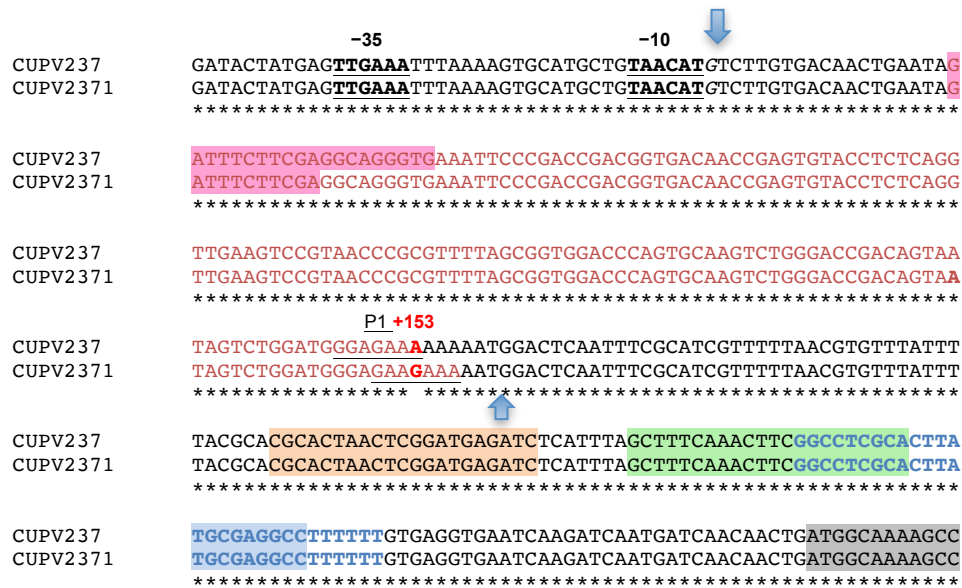


Figura 5.10. Región reguladora del operón *rib* de *L. collinoides*. En la figura se muestran las secuencias de las cepas CUPV2371 y CUPV237, y en ellas se representan: con letras granates, la secuencia del RFN o aptámero; con letras azules, el terminador; el sombreado gris, el extremo 5' del gen *ribG*; están subrayadas las regiones -35 y -10 del promotor; las bases subrayadas en la región P1 están implicadas en la formación del tallo del aptámero (predicción con mfold de la secuencia comprendida entre las flechas azules, Figura 5.10), y en rojo se indica la posición de la mutación. En base a las predicciones del *riboswitch* obtenidas con el servidor web PASIFIC de la secuencia comprendida entre el primer nucleótido del transcrito (cursiva) y el terminador, las bases sombreadas representan: en rosa, el anti-anti-terminador; en naranja, el anti-terminador; en verde, la secuencia del terminador que se conserva en los plegamientos ON/OFF; y en azul, la secuencia que participa en la formación del terminador en OFF.

La predicción del plegamiento del elemento RFN de la región reguladora del operón *rib* (aptámero), muestra 5 estructuras tallo-lazo (P2/L2-P6/L6) y un anillo central, que posee unas dimensiones ligeramente mayores en el plegamiento de la cepa CUPV2371 (Figura 5.11). Este modelo obtenido mediante mfold muestra que parte de la secuencia del mRNA que compone el tallo de esta estructura (P1) en su extremo 3', es diferente en la cepa salvaje y en la superproductora; y ambas contienen la posición 153 que corresponde con la mutación en CUPV237. Por otro lado, la predicción con el programa PASIFIC muestra la formación de las cinco horquillas en el plegamiento OFF de la cepa salvaje y localiza las secuencias implicadas en los plegamientos OFF y ON del elemento regulador o *riboswitch* (Figuras 4.10 y 4.12). Sin embargo, la predicción del plegamiento OFF del *riboswitch* de la cepa superproductora CUPV237, no muestra las 5 estructuras tallo-lazo del aptámero (Figura 5.13), aunque, el plegamiento en ON es idéntico al que se forma en la cepa silvestre.

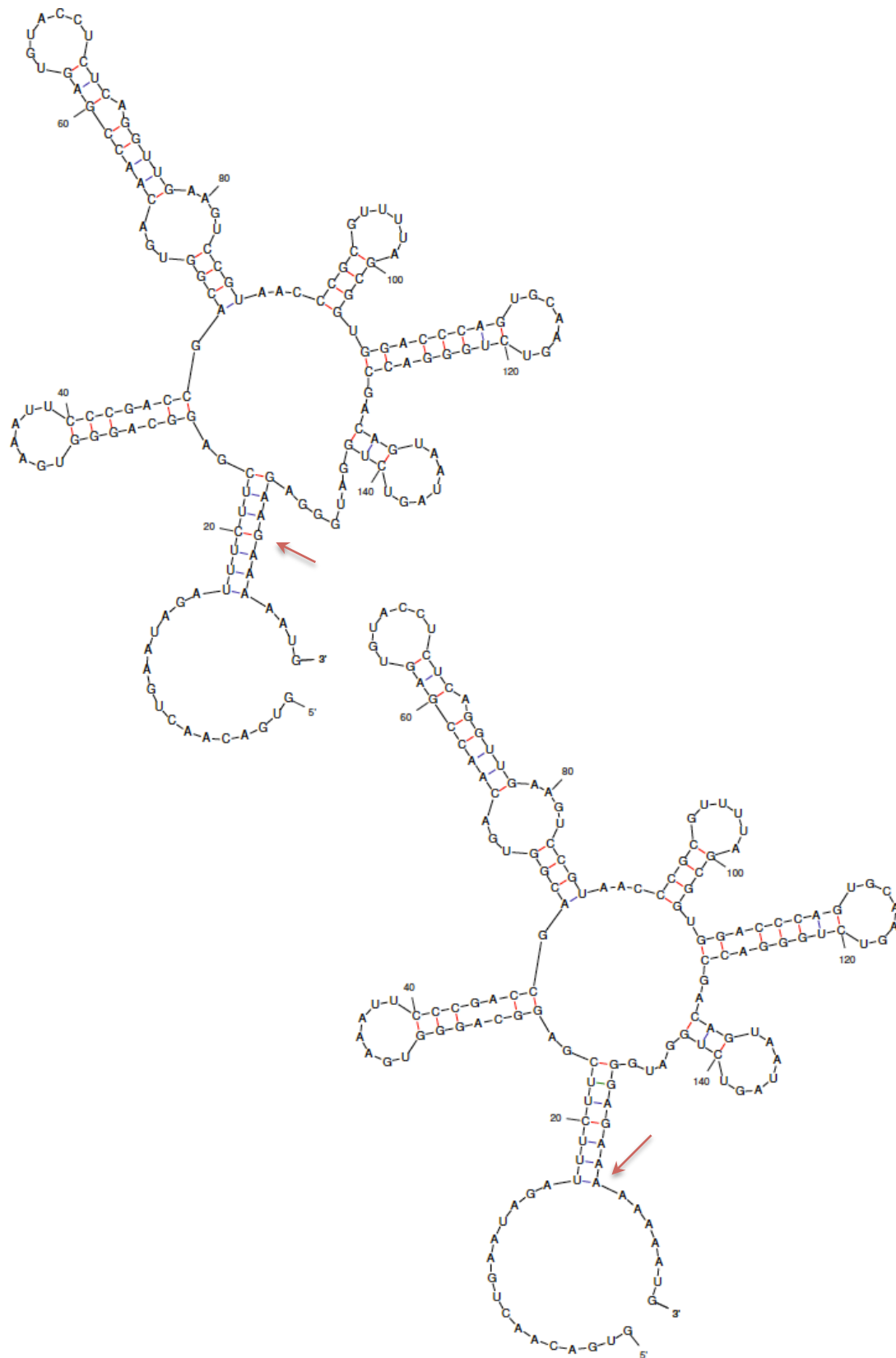


Figura 5.11. Predicción del plegamiento de la secuencia de mRNA del aptámero localizada en la región reguladora del operón *rib* en *L. collinoides* mediante el servidor web mfold. (A) CUPV2371 y (B) CUPV237. La flecha indica la posición de la base mutada. La estructura de lazo (L) y de tallo (P) se nombran de acuerdo a Serganov et al. (2009).

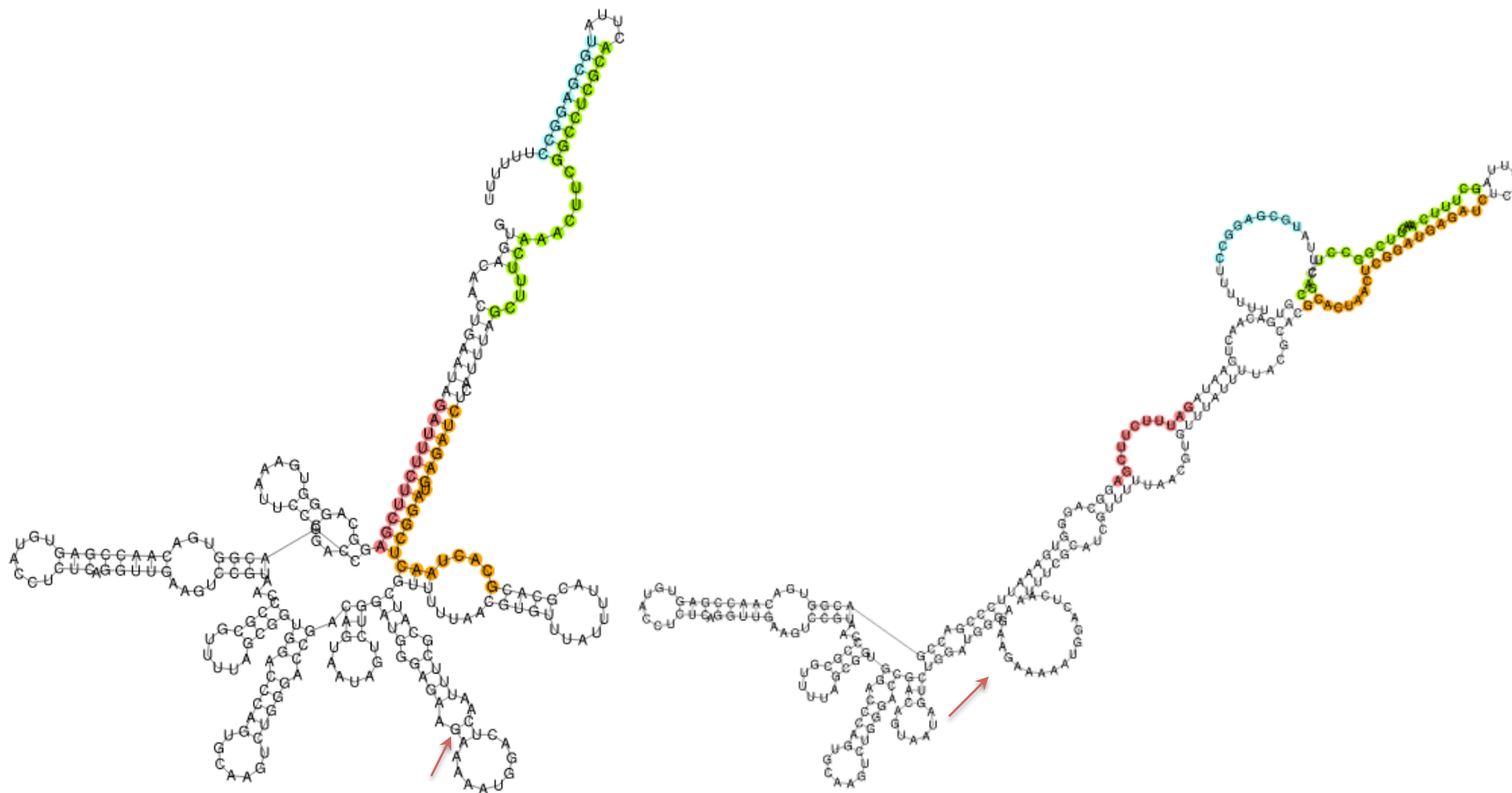


Figura 5.12. Plegamiento de la secuencia de mRNA de la porción reguladora del operon *rib* de *L. collinoides* CUPV2371. Se ha tenido en cuenta la secuencia comprendida desde la posición +1, hasta la secuencia de poliU del terminador (Figura 5.9). La predicción se realizó mediante el programa PASIFIC. A, no permite la transcripción del operón (OFF), y B, permite la transcripción (ON). La flecha indica la posición de la base mutada en CUPV237.

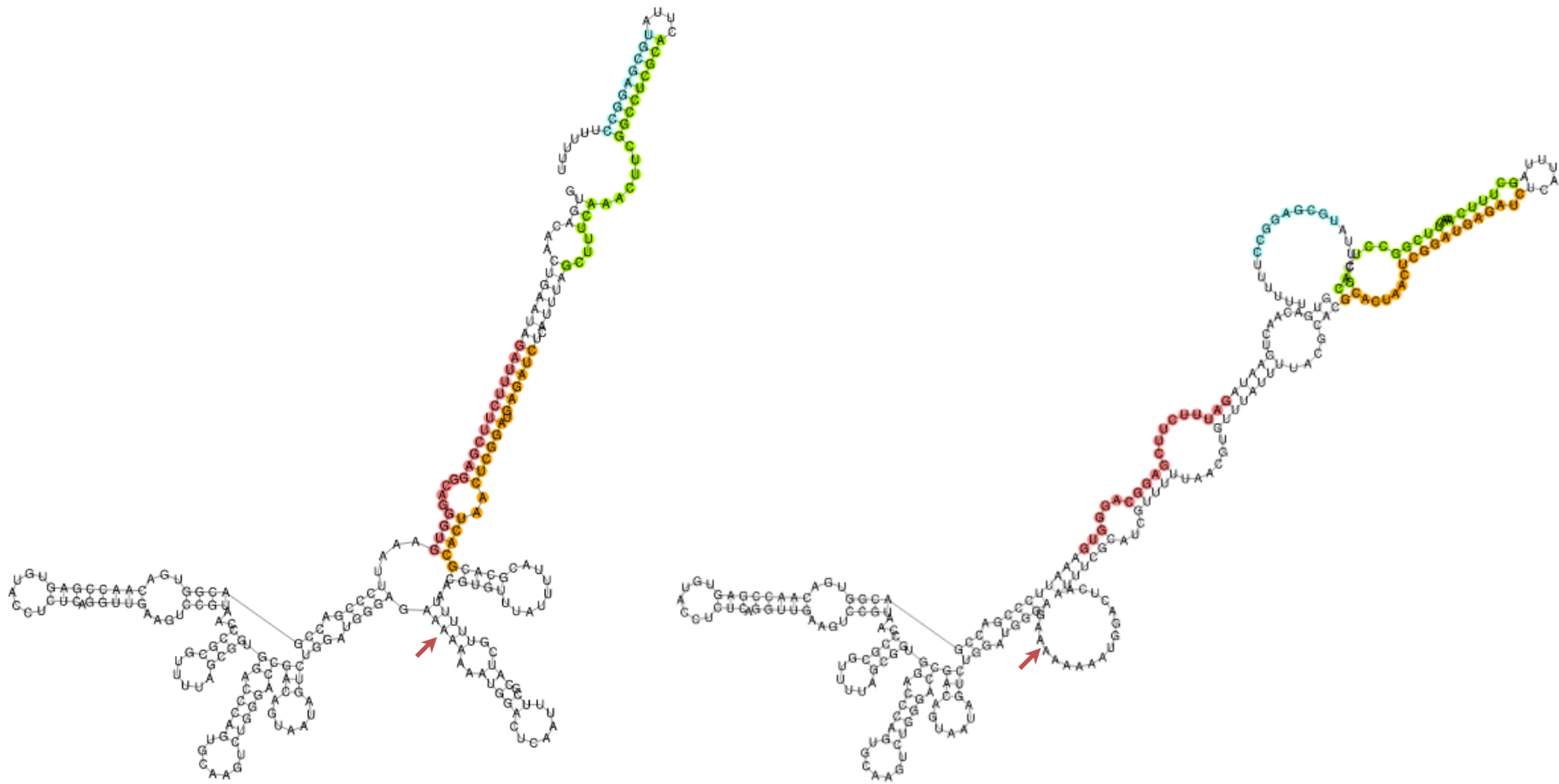


Figura 5.13. Plegamiento de la secuencia de mRNA de la porción reguladora del operon *rib* de *L. collinoides* CUPV237. Se ha tenido en cuenta la secuencia comprendida desde la posición +1, hasta la secuencia de poliU del terminador (Figura 5.9). La predicción se realizó mediante el programa PASIFIC. A, no permite la transcripción del operón (OFF), y B, permite la transcripción (ON). La flecha indica la posición de la base mutada.

4. DISCUSIÓN

Las BAL son bacterias utilizadas como cultivos iniciadores o adjuntos, algunas son probióticos naturales, y también pueden ser consideradas fábricas celulares ideales para producir un amplio rango de metabolitos denominados nutraceuticos, entre los que se encuentran las vitaminas del grupo B (Thakur, Tomar & De, 2015). Así, recientemente se ha propuesto el uso de ciertas BAL con capacidad de sintetizar estas vitaminas, y particularmente la riboflavina, para elaborar alimentos fermentados bio-enriquecidos en dichos compuestos (del Valle et al., 2014; Capozzi et al., 2011; Patel, Shah & Prajapati, 2013). En este campo de investigación, se han descrito cepas de *Lactobacillus sp.* cuyas producciones pueden alcanzar hasta 2,8 mg L⁻¹ de riboflavina (Jayashree et al., 2010; Russo et al., 2014; Yépez et al., 2019). Además, varios grupos de investigación han obtenido cepas probióticas mutantes con fenotipo superproductor, utilizando roseoflavina (compuesto análogo de la vitamina B₂), para ser aplicado en la fortificación de alimentos (Burgess et al., 2006; Capozzi et al., 2011; Yépez et al., 2019).

En este trabajo se ha analizado la capacidad de producción de riboflavina por 24 cepas de la colección de la UPV/EHU pertenecientes a las especies *L. collinoides*, *L. sicerae*, *L. suebicus*, *P. parvulus* y *P. ethanolidurans*, en dos medios químicamente definidos. La dificultad que presentan las cepas estudiadas para crecer en un medio definido, se resolvió con la optimización del medio químicamente definido PID, elaborado a partir del medio descrito por Teusink et al. (2005). En este medio, los cultivos de lactobacilos y pediococos, alcanzaron DO₆₀₀ superiores a las detectadas en los medios M5 (Poolman et al., 1988), CDM (Terrade et al., 2009) y en aquellas cultivadas en el medio MSD (Tabla 1.3). El análisis mediante HPLC de los sobrenadantes de los cultivos libres de células permitió la detección y la cuantificación de la riboflavina liberada al medio de cultivo. Las concentraciones más altas de vitamina B₂ se registraron en las fermentaciones llevadas a cabo por las cepas *L. collinoides* CUPV237 y CUPV2371, y por la cepa control *L. plantarum* subsp. *plantarum* CECT 748^T. En esta última estirpe de *L. plantarum* subsp. *plantarum*, Remagni (2012) describieron una producción de riboflavina-próxima a 0,30 mg L⁻¹ muy próxima a la obtenida en este trabajo (0,33 mg L⁻¹) al ser cultivada en el medio PID. En el presente trabajo, se ha detectado y caracterizado el mutante espontáneo *L. collinoides* CUPV237 superproductor de riboflavina. Esta cepa, es capaz de sintetizar y secretar hasta 3 mg L⁻¹ de riboflavina en el medio definido PID, que son 7,75 veces superiores a la observada en cepa silvestre CUPV2371. Cabe destacar que esta

producción es superior a la descrita hasta el momento para mutantes de BAL no seleccionados (del Valle et al., 2014).

Con el fin de comprobar la capacidad de las cepas estudiadas para sintetizar riboflavina en una matriz alimentaria, se realizaron fermentaciones en mostos monovarietales de manzana. La estirpe superproductora *L. collinoides* CUPV237 al igual que la cepa control *L. plantarum* subsp. *plantarum* CECT 748^T, incrementaron la concentración de riboflavina en los 7 zumos modificados. Además, se observó que una misma cepa produce diferentes niveles de vitamina dependiendo del tipo de manzana que se ha empleado para elaborar el mosto, e independientemente del crecimiento alcanzado en cada uno de ellos. Por consiguiente, las diferencias en la composición de los medios de cultivo influyeron manera muy notable en la producción de riboflavina. Sin embargo, la estirpe *L. siceræ* CUPV261^T presentó un comportamiento diferente dado que no se detectó vitamina en los sobrenadantes de estas matrices, aunque sí se observó crecimiento en todos los mostos. El contenido de riboflavina en los zumos modificados fue de entre 4 y 20 $\mu\text{g L}^{-1}$, y al igual que ocurre con ciertas cepas utilizadas en la elaboración de productos fermentados tradicionales, *L. siceræ* consumió la riboflavina del medio (Thakur, Tomar & De, 2015).

Así mismo, en el presente trabajo se ha determinado la concentración de riboflavina en la sidra natural elaborada en Gipuzkoa. Se detectó la vitamina en 24 de las 44 sidras analizadas, con un valor máximo de 56 $\mu\text{g L}^{-1}$ en una sidra monovarietal elaborada con la manzana autóctona Txalaka. En general, las sidras monovarietales presentaron concentraciones ligeramente superiores a las de las bebidas elaboradas con mezclas de variedades de manzana. Además, las concentraciones de riboflavina de las sidras en barrica fueron ligeramente superiores a las de la sidra en botella (Figuras 4.7 y 4.8). Las sidras analizadas en este trabajo muestran contenidos de vitamina B₂ inferiores a los reportados por otros autores en esta bebida, entre 30 y 500 $\mu\text{g L}^{-1}$ (Buglass, 2015; Pérez-Bibbins et al., 2015; Hucker et al., 2011), que podrían explicarse por los diferentes tipos de manzana empleados y por las diferencias en el proceso de elaboración. Por otro lado, la sidra Gezamina presentó la segunda concentración más elevada de vitamina B₂. Sin embargo, la fermentación de su mosto realizada con la cepa CUPV237 o CECT 748^T, mostró unas de las producciones de riboflavina más bajas del ensayo. Esto puede indicar, que el contenido de riboflavina en sidra depende tanto de la variedad de manzana utilizada, como de la microbiota presente en la bebida.

Con respecto a la detección de los genes implicados en la síntesis de riboflavina, en la amplificación parcial del operón *rib* realizada con los cebadores degenerados descritos por Capozzi et al. (2011), sólo se obtuvieron resultados positivos utilizando los DNA de las cepas de *L. suebicus*. Para los aislados de las especie *L. collinoides* y la estirpe *L. sicerae* CUPV261^T, el operón *rib* fue detectado con los cebadores diseñados a partir de la secuencia de *L. collinoides* CUPV237. Además, se consiguió amplificar la región comprendida entre el RFN y el gen *ribA* de las 5 cepas de *L. collinoides*. Estas secuencias mostraron un operón altamente conservado a nivel de nucleótido para la especie *L. collinoides* (Figura II.II del Anexo II).

La organización del operón *rib* en las cepas estudiadas de *L. collinoides* aparece representada en la Figura 5.9. La comparación de la secuencia de la cepa superproductora *L. collinoides* CUPV237 con la secuencia de la cepa silvestre CUPV2371, mostró la existencia de una región RFN posible, y la presencia de una mutación puntual consistente en el cambio de una base (G153A) en la cepa CUPV237 (Figuras 4.10 y 4.11). Además, en ambas cepas se detectó un terminador transcripcional ρ -independiente localizado entre la región RFN y el gen *ribG* (Figuras 4.12 y 4.13). Estos hechos indicarían que la expresión del operón *rib* en *L. collinoides* podría estar sometida a una regulación similar a la propuesta para otros lactobacilos (Figura 5.2, panel inferior A). La predicción de la localización del terminador transcripcional y la ausencia del sitio de unión a los ribosomas, revela que el mecanismo de regulación en la cepa silvestre correspondería a un mecanismo de atenuación transcripcional con una síntesis abortiva del mRNA. También, la localización de la mutación en CUPV237 en la región RFN, indicaba que podría ser responsable del fenotipo superproductor de riboflavina de la cepa, ya que este tipo de mutaciones han sido previamente descritas en BAL superproductoras de vitamina B₂ (Burgess et al., 2006, Russo et al., 2014).

Consecuentemente, pensamos que la mutación podría afectar a la formación de la estructura pentafoliada propuesta como sitio de unión del inhibidor transcripcional FMN en otras bacterias. Esta alteración podría impedir la unión del ligando al aptámero, lo que a su vez, repercutiría en el plegamiento a 3' del RFN, promoviendo la formación de la estructura ON (antiterminador). Por ese motivo, se realizó una predicción de la estructura secundaria de la región RFN en el transcrito de las cepas CUPV237 y CUPV2371 (Figura 5.11). Inesperadamente, en ambos casos se observó una estructura secundaria compleja constituida por cinco estructuras tallo-lazo

con una energía libre (ΔG) similar ($-45 \text{ kcal mol}^{-1}$), y donde la mutación se localizó próxima al extremo 3'. En este plegamiento se detectó un ligero desplazamiento de la secuencia de mRNA que forma el tallo del aptámero (en el extremo 3') (Figura 5.10 y 4.11). Esta variación produce que la secuencia del RFN de la cepa silvestre sea más parecida a la secuencia consenso descrita por Serganov et al. (2009), y por tanto este plegamiento poseería mayor estabilidad que el de la cepa mutante. Este hecho indica que la mutación podría afectar al plegamiento de regiones más extensas del mRNA.

Así, procedimos a predecir el plegamiento de las estructuras ON (permite la síntesis de riboflavina) y OFF (no hay síntesis de riboflavina) del *riboswitch*. En el plegamiento OFF de la cepa silvestre (Figura 5.12 A) se observa la formación de 5 horquillas (L2-L6) en el aptámero, mientras que en la cepa superproductora solo aparecen 4 (L2-L5) (Figura 5.13 A). Según estos modelos, se podría deducir que inicialmente en la cepa superproductora se formaría el aptámero pentafoliado y a medida que crece la molécula de mRNA, este plegamiento sería inestable obligando a adoptar la configuración ON que da lugar a la síntesis de vitamina B₂. En cuanto al FMN, tendría que interactuar con el aptámero para interrumpir la síntesis de riboflavina, pero podría ocurrir que no sea posible debido a que las dimensiones del anillo central han variado al igual que la secuencia de P1 (Figura 5.11), y/o a una posible variación de la estructura terciaria del aptámero debido a la variación del plegamiento OFF observado en la cepa mutante (Figura 5.13).

Mediante ensayos de cristalización, Serganov et al. (2009) estudiaron la estructura terciaria que adopta el elemento RFN de *Fusobacterium nucleatum*. Describieron que las mutaciones reguladoras G105U y G108A (localizadas en el tallo de la estructura pentafoliada del elemento RFN), previenen la formación y/o afectan a la estabilidad de la hélice reguladora P1 (del tallo) en la estructura terciaria. Al traducir estas posiciones a la secuencia del elemento RFN de CUPV237, se observa que la G108A del elemento RFN de *Fusobacterium nucleatum*, coincide exactamente con la mutación ocurrida en la estirpe superproductora de *L. collinoides*. De esta manera se podría explicar que la mutación en *L. collinoides* provoca una desestabilización en la formación de la estructura terciaria del elemento RFN en presencia o no de FMN, que podría permitir la traducción del operón *rib*.

5. CONCLUSIONES

En este capítulo se ha optimizado un medio de cultivo definido, denominado PID, que ha permitido mejorar el crecimiento de cepas de las especies *Lactobacillus collinoides*, *L. sicerae*, *L. suebicus*, *L. plantarum* subsp. *plantarum*, *Pediococcus parvulus* y *P. ethanolidurans*. Además, en este medio se obtuvieron las concentraciones de riboflavina más elevadas producidas por las estirpes *L. collinoides* CUPV237 y CUPV2371, y la cepa control *L. plantarum* subsp. *plantarum* CECT 748^T.

El mutante espontáneo *L. collinoides* CUPV237 productor de heteropolisacárido es capaz de producir en un medio de cultivo químicamente definido hasta 3 mg L⁻¹ de vitamina B₂, que es una concentración 7,75 veces superior a la producida por la cepa silvestre en idénticas condiciones. Este fenotipo superproductor se puede justificar mediante la existencia de una mutación en el tallo de la estructura secundaria del elemento regulador RFN del operón *rib*. Por otro lado, se sugiere que el mecanismo de regulación para la producción de riboflavina en la cepa silvestre correspondería a un mecanismo de atenuación transcripcional con una síntesis abortiva del mRNA.

Finalmente, en este trabajo se ha analizado por primera vez la presencia de riboflavina en la sidra natural producida en el País Vasco, y su concentración en las sidras analizadas alcanza los 57 µg L⁻¹. La concentración de vitamina B₂ en sidra, podría estar determinada tanto por la variedad de manzana utilizada para su producción, como por la microbiota presente en la bebida.

6. BIBLIOGRAFÍA

- Benson, D. A., Karsch-Mizrachi, I., Lipman, D. J., Ostell, J., & Wheeler, D. L. (2006). GenBank. *Nucleic Acids Research*, 34(suppl_1), D16-D20.
- Brettin, T., Davis, J. J., Disz, T., Edwards, R. A., Gerdes, S., Olsen, G. J., Olson, R., Overbeek, R., Parrello, B., Pusch, G. D., Shukla, M., Thomason, A., Stevens, R., Vonstein, V., Wattam, A.R., & Xia, F. (2015). RASTtk: a modular and extensible implementation of the RAST algorithm for building custom annotation pipelines and annotating batches of genomes. *Scientific Reports*, 5, srep08365.
- Buglass, A. J. (2015). Chemical composition of beverages and drinks. En: Handbook of Food Chemistry (pp. 225-300). Springer Berlin Heidelberg.
- Burgess, C. M., Smid, E. J., Rutten, G., & Van Sinderen, D. (2006). A general method for selection of riboflavin-overproducing food grade microorganisms. *Microbial Cell Factories*, 5(1), 24.
- Burgess, C. M., Smid, E. J., & van Sinderen, D. (2009). Bacterial vitamin B₂, B₁₁ and B₁₂ overproduction: an overview. *International Journal of Food Microbiology*, 133(1), 1-7.
- Capozzi, V., Menga, V., Digesu, A. M., De Vita, P., Van Sinderen, D., Cattivelli, L., Fares, C., & Spano, G. (2011). Biotechnological production of vitamin B₂-enriched bread and pasta. *Journal of Agricultural and Food Chemistry*, 59(14), 8013-8020.
- Capozzi, V., Russo, P., Dueñas, M. T., López, P., & Spano, G. (2012). Lactic acid bacteria producing B-group vitamins: a great potential for functional cereals products. *Applied Microbiology and Biotechnology*, 96(6), 1383-1394.
- Dueñas-Chasco, M. T., Rodríguez-Carvajal, M. A., Tejero Mateo, P., Franco-Rodríguez, G., Espartero, J. L., Irastorza-Iribas, A., & Gil-Serrano, A. M. (1997). Structural analysis of the exopolysaccharide produced by *Pediococcus damnosus* 2.6. *Carbohydrate Research*, 303(4), 453-458.
- García-Angulo, V. A. (2017). Overlapping riboflavin supply pathways in bacteria. *Critical Reviews in Microbiology*, 43(2), 196-209.
- Homa, J., Klimek, M., Kruk, J., Cocquerelle, C., Vandenbulcke, F., & Plytycz, B. (2010). Metal-specific effects on metallothionein gene induction and riboflavin content in coelomocytes of *Allolobophora chlorotica*. *Ecotoxicology and Environmental Safety*, 73(8), 1937-1943.

- Hossain, M. F., Rashid, M., Sidhu, R., Mullins, R., & Mayhew, S. L. (2019). A Simplified, Specific HPLC Method of Assaying Thiamine and Riboflavin in Mushrooms. *International Journal of Food Science*, 2019- 8716986, 8 p.
- Hucker, B., Wakeling, L., & Vriesekoop, F. (2011). The quantitative analysis of thiamin and riboflavin and their respective vitamers in fermented alcoholic beverages. *Journal of Agricultural and Food Chemistry*, 59(23), 12278-12285.
- Jayashree, S., Jayaraman, K., & Kalaichelvan, G. (2010). Isolation, screening and characterization of riboflavin producing lactic acid bacteria from Katpadi, Vellore district. *Recent Research in Science and Technology*, 2(1).
- Kliegman, R., Stanton, B. M., Geme, J. S., & Schor, N. F. (2014). *Nelson. Tratado de pediatría*. Elsevier Brasil.
- Llamas-Arriba, M. G., Pérez-Ramos, A., Puertas, A. I., López, P., Prieto, A., & Dueñas, M. T. (2018). Characterization of *Pediococcus ethanolidurans* CUPV141: a β -D-glucan and heteropolysaccharide-producing bacterium. *Frontiers in Microbiology*, 9, 2041.
- LeBlanc, J. G., Laiño, J. E., del Valle, M. J., Vannini, V., Van Sinderen, D., Taranto, M. P., Font de Valdez, G., Savoy de Giori, G., & Sesma, F. (2011). B-Group vitamin production by lactic acid bacteria—current knowledge and potential applications. *Journal of Applied Microbiology*, 111(6), 1297-1309.
- Mack, M., & Grill, S. (2006). Riboflavin analogs and inhibitors of riboflavin biosynthesis. *Applied Microbiology and Biotechnology*, 71(3), 265-275.
- Millman, A., Dar, D., Shamir, M., & Sorek, R. (2016). Computational prediction of regulatory, premature transcription termination in bacteria. *Nucleic Acids Research*, 45(2), 886-893.
- Patel, A., Shah, N., & Prajapati, J. B. (2013). Biosynthesis of vitamins and enzymes in fermented foods by lactic acid bacteria and related genera - A promising approach. *Croatian Journal of Food Science and Technology*, 5(2), 85-91.
- Pedrolli, D. B., Kühm, C., Sévin, D. C., Vockenhuber, M. P., Sauer, U., Suess, B., & Mack, M. (2015). A dual control mechanism synchronizes riboflavin and sulphur metabolism in *Bacillus subtilis*. *Proceedings of the National Academy of Sciences*, 112(45), 14054-14059.
- Pérez-Bibbins, B., Torrado-Agrasar, A., Salgado, J. M., de Souza Oliveira, R. P., & Dominguez, J. M. (2015). Potential of lees from wine, beer and cider

- manufacturing as a source of economic nutrients: An overview. *Waste Management*, 40, 72-81.
- Poolman, B., & Konings, W. N. (1988). Relation of growth of *Streptococcus lactis* and *Streptococcus cremoris* to amino acid transport. *Journal of Bacteriology*, 170(2), 700-707.
- Puertas, A. I., Capozzi, V., Llamas, M. G., López, P., Lamontanara, A., Orrù, L., Russo, P.; Spano, G., & Dueñas, M. T. (2016). Draft genome sequence of *Lactobacillus collinoides* CUPV 237, an exopolysaccharide and riboflavin producer isolated from cider. *Genome Announcements*, 4(3), e00506-16.
- Remagni, M. C. (2012). Biotechnological and spectroscopical evaluation of selected *Lactobacillus plantarum* strains with probiotic and nutraceutical potentialities. Tesis doctoral, *Università degli studi di Milano* (Italia).
- Reuelta, J. L., Ledesma-Amaro, R., Lozano-Mártinez, P., Díaz-Fernández, D., Buey, R. M., & Jiménez, A. (2017). Bioproduction of riboflavin: a bright yellow history. *Journal of Industrial Microbiology & Biotechnology*, 44(4-5), 659-665.
- Russo, P., Capozzi, V., Arena, M. P., Spadaccino, G., Dueñas, M. T., López, P., Fiocco D., & Spano, G. (2014). Riboflavin-overproducing strains of *Lactobacillus fermentum* for riboflavin-enriched bread, *Applied Microbiology and Biotechnology*, 98(8), 3691-3700.
- Serganov, A., Huang, L., & Patel, D. J. (2009). Coenzyme recognition and gene regulation by a flavin mononucleotide riboswitch. *Nature*, 458(7235), 233.
- Stahmann, K. P., Reuelta, J. L., & Seulberger, H. (2000). Three biotechnical processes using *Ashbya gossypii*, *Candida famata*, or *Bacillus subtilis* compete with chemical riboflavin production. *Applied Microbiology and Biotechnology*, 53(5), 509-516.
- Terrade, N., Noël, R., Couillaud, R., & de Orduña, R. M. (2009). A new chemically defined medium for wine lactic acid bacteria. *Food Research International*, 42(3), 363-367.
- Teusink, B., van Enkevort, F. H., Francke, C., Wiersma, A., Wegkamp, A., Smid, E. J., & Siezen, R. J. (2005). In silico reconstruction of the metabolic pathways of *Lactobacillus plantarum*: comparing predictions of nutrient requirements with those from growth experiments. *Applied and Environmental Microbiology*, 71(11), 7253-7262.

- Thakur, K., Tomar, S. K., & De S. Lactic acid bacteria as a cell factory for riboflavin production (2015). *Microbial Biotechnology*, 9(4), 441-451.
- Thakur, K., Lule, V. K., Rajni, C. S., Kumar, N., Mandal, S., Anand, S., Kumari, V., & Tomar, S. K. (2016). Riboflavin producing probiotic lactobacilli as a biotechnological strategy to obtain riboflavin-enriched fermented foods. *Journal of Pure and Applied Microbiology*. 10(1), 161-166.
- del Valle, M. J., Laiño, J. E., de Giori, G. S., & LeBlanc, J. G. (2014). Riboflavin producing lactic acid bacteria as a biotechnological strategy to obtain bio-enriched soymilk. *Food Research International*, 62, 1015-1019.
- Vitreschak, A. G., Rodionov, D. A., Mironov, A. A., & Gelfand, M. S. (2002). Regulation of riboflavin biosynthesis and transport genes in bacteria by transcriptional and translational attenuation. *Nucleic Acids Research*, 30(14), 3141-3151.
- Webb, M. E., Marquet, A., Mendel, R. R., Rébeillé, F., & Smith, A. G. (2007). Elucidating biosynthetic pathways for vitamins and cofactors. *Natural Product Reports*, 24(5), 988-1008.
- Yépez, A., Russo, P., Spano, G., Khomenko, I., Biasioli, F., Capozzi, V., & Aznar, R. (2019). In situ riboflavin fortification of different kefir-like cereal-based beverages using selected Andean LAB strains. *Food Microbiology*, 77, 61-68.
- Zuker, M. (2003). Mfold web server for nucleic acid folding and hybridization prediction. *Nucleic Acids Research*, 31(13), 3406-3415.
- Zuriarrain Ocio, A. (2017). Sagar barietatearen eta polifenolen eragina Euskal Herriko sagardoaren ezaugarrietan. Tesis doctoral, *Universidad del País Vasco EHU/UPV*.

Conclusiones Generales

En este trabajo, se ha profundizado en el estudio de las bacterias lácticas productoras de exopolisacárido del género *Lactobacillus* aisladas de sidra ahilada, y pertenecientes a la Colección de la Universidad del País Vasco (CUPV). De los resultados obtenidos se han extraído las siguientes conclusiones generales:

1. El estudio genotípico y bioquímico llevado a cabo en un total de 41 aislados, recogidos de sidras ahiladas entre los años 1992 y 2009, permitió la identificación de las siguientes especies alterantes: *L. collinoides*, *L. diolivorans*, *L. suebicus* y *L. sicerae*. La incidencia de estas especies alterantes varió en función del año de aislamiento.
2. Los análisis fenotípicos y genotípicos llevados a cabo en las cepas homofermentativas CUPV261^T y CUPV262, permitieron la descripción de una nueva especie del género *Lactobacillus*, y se propuso el nombre *Lactobacillus sicerae* sp. nov., cuya cepa tipo es CUPV261^T (=CECT 8227^T=KCTC 21012^T).
3. El análisis de los exopolisacáridos sintetizados por 14 cepas aisladas en la campaña de 2009, y pertenecientes a las especies *L. collinoides* y *L. sicerae*, reveló que producen entre 7 y 68 mg L⁻¹, y que están compuestos por tres fracciones de diferente peso molecular (1, 10 y en torno a 10³ kDa). La detección mediante PCR de genes *eps* sugiere que todas las cepas sintetizan heteropolisacáridos.
4. El análisis *in silico* del genoma completo de *L. collinoides* CUPV237 mostró predictivamente 4 *clusters eps*; mientras que en *L. sicerae* CUPV261^T se identificaron genes *eps* en 8 de los *contigs* obtenidos de la secuenciación parcial del su genoma. En ambas cepas, estos genes codificarían proteínas de la ruta biosintética Wzy-dependiente para la producción de heteropolisacáridos.
5. La caracterización estructural de los EPS ha confirmado que ambas cepas producen heteropolisacáridos, compuestos mayoritariamente por glucosa y galactosa, además de ramnosa en *L. sicerae* CUPV261^T, o glucosamina en *L. collinoides* CUPV237. Estos EPS presentan estabilidad térmica hasta los 244 °C.
6. Se ha analizado el efecto del estrés gastrointestinal sobre las estirpes CUPV261^T y CUPV237 y sus heteropolisacáridos, mediante el uso de un modelo *in vitro* de estrés gástrico y gastrointestinal. Las poblaciones bacterianas de *L. sicerae* y *L. collinoides* suspendidas en solución gástrica o en

las matrices alimentarias de soja, avena y leche, se vieron profundamente afectadas por los tratamientos ácido-enzimáticos aplicados en este modelo. Los exopolisacáridos producidos por estas dos estirpes mostraron resistencia a la degradación frente al estrés gástrico y gastrointestinal.

7. Los HePS producidos por *L. sicerae* CUPV261^T, *L. collinoides* CUPV237, así como por las bacterias probióticas *B. longum* INIA P132 y *B. infantis* INIA P731 poseen la capacidad de atenuar la mortalidad de las larvas de pez cebra, en el modelo *in vivo* de enfermedad inflamatoria intestinal inducido por el agente químico DSS.
8. La transformación de CUPV261^T, CUPV237 y de la estirpe *non ropy* CUPV2372 con el plásmido pRCR12 reveló que el gen de la mCherry es funcional en los transformantes CUPV261^T p[RCR12], CUPV237 p[RCR12] y CUPV2371NR p[RCR12], y su presencia permite la detección de las células mediante fluorescencia.
9. El mutante espontáneo *L. collinoides* CUPV237 productor de heteropolisacárido, y aislado durante la consecución de este trabajo, es capaz de producir en un medio de cultivo químicamente definido hasta 3 mg L⁻¹ de vitamina B₂, que es una concentración 7,75 veces superior a la producida por la cepa silvestre en idénticas condiciones. Este fenotipo superproductor se puede justificar mediante la existencia de una mutación en el tallo de la estructura secundaria del elemento regulador RFN del operón *rib*.
10. Se ha optimizado un medio de cultivo definido que mejora el crecimiento de cepas de bacterias lácticas aisladas de sidra de las especies *L. collinoides*, *L. sicerae*, *L. suebicus*, *Pediococcus parvulus* y *P. ethanolidurans*; y permite la cuantificación de la riboflavina mediante el método de HPLC que ha sido puesto a punto en este trabajo.

ANEXO I

Medio MRS de Man, Rogosa & Sharpe (1960)

Glucosa, 20 g L⁻¹; peptona bacteriológica, 10 g L⁻¹; extracto de carne, 10 g L⁻¹, extracto de levadura, 5 g L⁻¹; Tween® 80, 1 g L⁻¹; acetato de sodio, 5 g L⁻¹; MgSO₄·7H₂O, 0,1 g L⁻¹; MnSO₄·H₂O, 0,05 g L⁻¹ y K₂HPO₄, 2 g L⁻¹; pH final de 5,5.

Con agar bacteriológico, 2 g L⁻¹.

La esterilización se llevó a cabo a 120 °C durante 20 min en un autoclave.

Medio MRS-rojo de clorofenol

Glucosa, fructosa, sacarosa, lactosa, galactosa, maltosa, rafinosa, manitol, sorbitol, trehalosa, xilosa o ramnosa, 20 g L⁻¹; peptona bacteriológica, 10 g L⁻¹; extracto de levadura, 5 g L⁻¹; Tween® 80, 1 g L⁻¹; acetato de sodio, 5 g L⁻¹; MgSO₄·7H₂O, 0,1 g L⁻¹; MnSO₄·H₂O, 0,05 g L⁻¹ y K₂HPO₄, 2 g L⁻¹; rojo de clorofenol, 0,4 g L⁻¹; pH final de 4,8. La esterilización se llevó a cabo a 120 °C durante 20 min en un autoclave.

Medio API® 50CHL

Peptona bacteriológica, 10 g L⁻¹; extracto de levadura, 5 g L⁻¹; Tween® 80, 1 mL L⁻¹; K₂HPO₄, 2 g L⁻¹; acetato de sodio 3H₂O, 5 g L⁻¹; citrato diamónico 2 g L⁻¹; MgSO₄·7H₂O, 0,2 g L⁻¹; MnSO₄·H₂O, 0,05 g L⁻¹; púrpura de bromocresol, 0,17 g L⁻¹; pH de 6,2. La esterilización se llevó a cabo a 120 °C durante 20 min en un autoclave.

Medio MSD

Glucosa, 20 g L⁻¹; ácidos casamino (BD™ Difco™, USA), 5 g L⁻¹; *bacto yeast nitrogen base* (Difco), 6,7 g L⁻¹; Tween 80, 1 g L⁻¹; citrato diamónico, 2 g L⁻¹; MnSO₄·4H₂O, 0,05 g L⁻¹; K₂HPO₄, 2 g L⁻¹; acetato de sodio, 5 g L⁻¹; adenina, 0,005 g L⁻¹; guanina, 0,005 g L⁻¹; xantina, 0,005 g L⁻¹; uracilo, 0,005 g L⁻¹; ácido L-málico, 4 g L⁻¹; pH 5,5.

La esterilización se llevó a cabo a 120°C durante 20 min en un autoclave, por un lado la glucosa, y por otro, el resto de compuestos, a excepción del *bacto yeast nitrogen base* y las bases nitrogenadas que se esterilizaron mediante filtración (0,45 µm).

Tampón TAE (50 x)

Tris base	242 g L ⁻¹
Ácido acético glacial	57 mL L ⁻¹
Na ₂ EDTA 2H ₂ O 0,25 mM (pH 8)	200 mL L ⁻¹

Esterilizar por filtración (0,45 µm) y guardar a 4 °C

Tampón de carga

Glicerol	50 % (v/v)
Azul de bromofenol	0,25 % (p/v)
Xileno-cianol	0,25 % (p/v)

Solución de lisis

Tris HCl (pH 8)	30 mM
EDTA	2 mM
Triton X-100	1,2 % (v/v)

Esterilizar por filtración y guardar a 4 °C.

Solución de lisozima

Disolver la lisozima en la solución de lisis a una concentración de 30 mg mL⁻¹. Preparar en el momento de su utilización.

ANEXO II

II.I

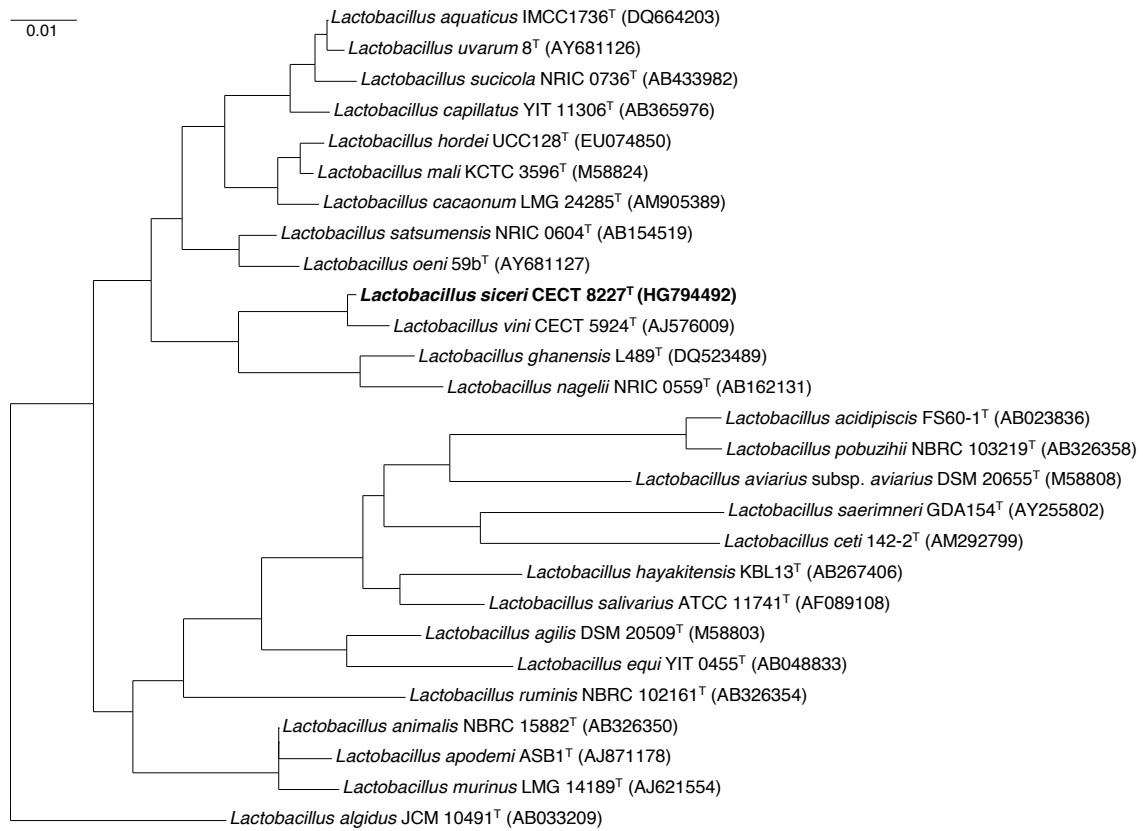


Figura II.I. Árbol filogenético de máxima verosimilitud. Basado en las secuencias casi completas del gen rRNA 16S de la estirpe *L. siceræ* CUPV261^T (=CECT 8227^T) y las especies estrechamente relacionadas. Entre paréntesis se indican los números de acceso de las secuencias. Barra de escala, número de sustituciones por posición.

II.II

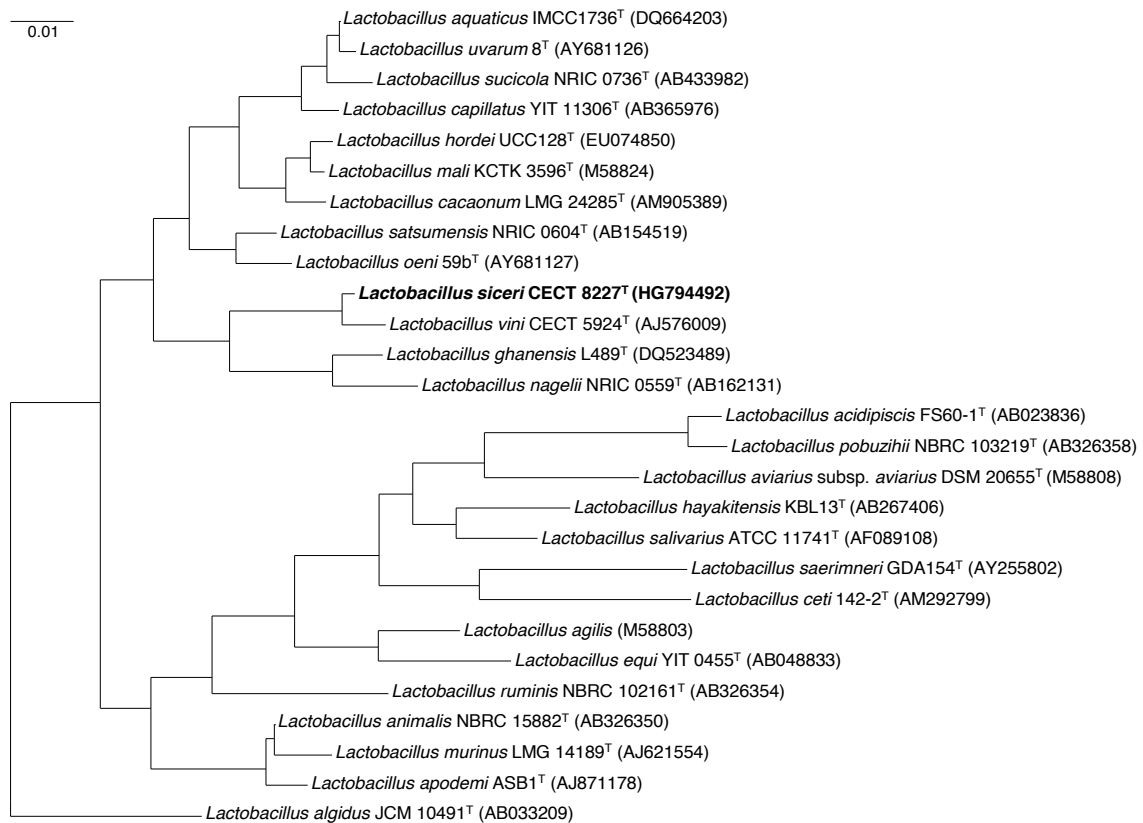


Figura II.II. Árbol filogenético de máxima parsimonia basado en las secuencias casi completas del gen rRNA 16S de la estirpe *L. siceræ* CUPV261^T (=CECT 8227^T) y las especies estrechamente relacionadas. Entre paréntesis se indican los números de acceso de las secuencias. Barra de escala, 1 sustitución por 100 posiciones de nucleótido.

II.III.

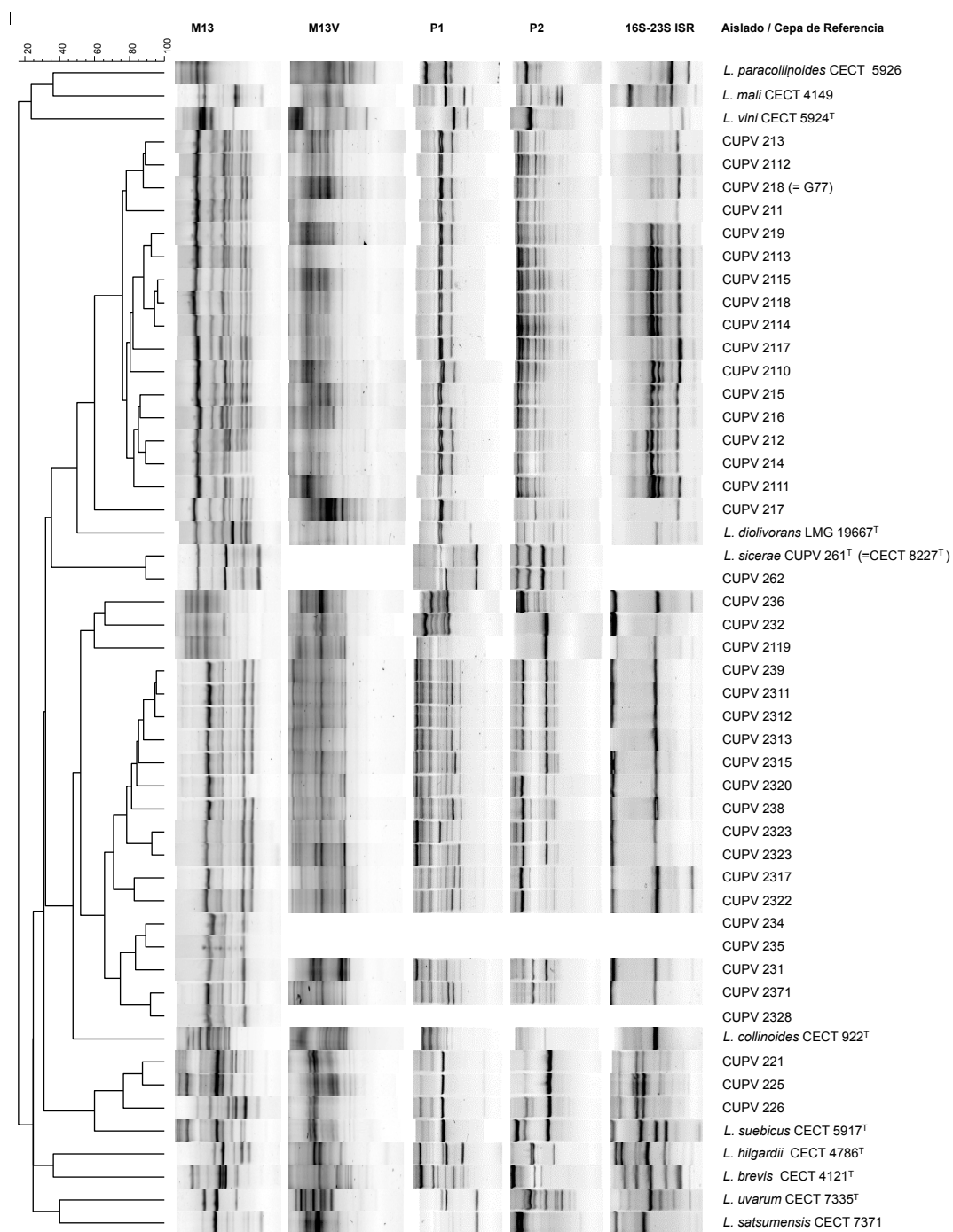


Figura II.III. Dendrograma derivado del agrupamiento UPGMA basado en la matriz de similitud obtenida a partir de los perfiles RAPD (M13, M13V, P1 y P2), de la amplificación 16S-23S ISR, y junto con los resultados mostrados en la fermentación de carbohidratos API® 50CH (bioMérieux). La escala indica el porcentaje de similitud.

II.IV.

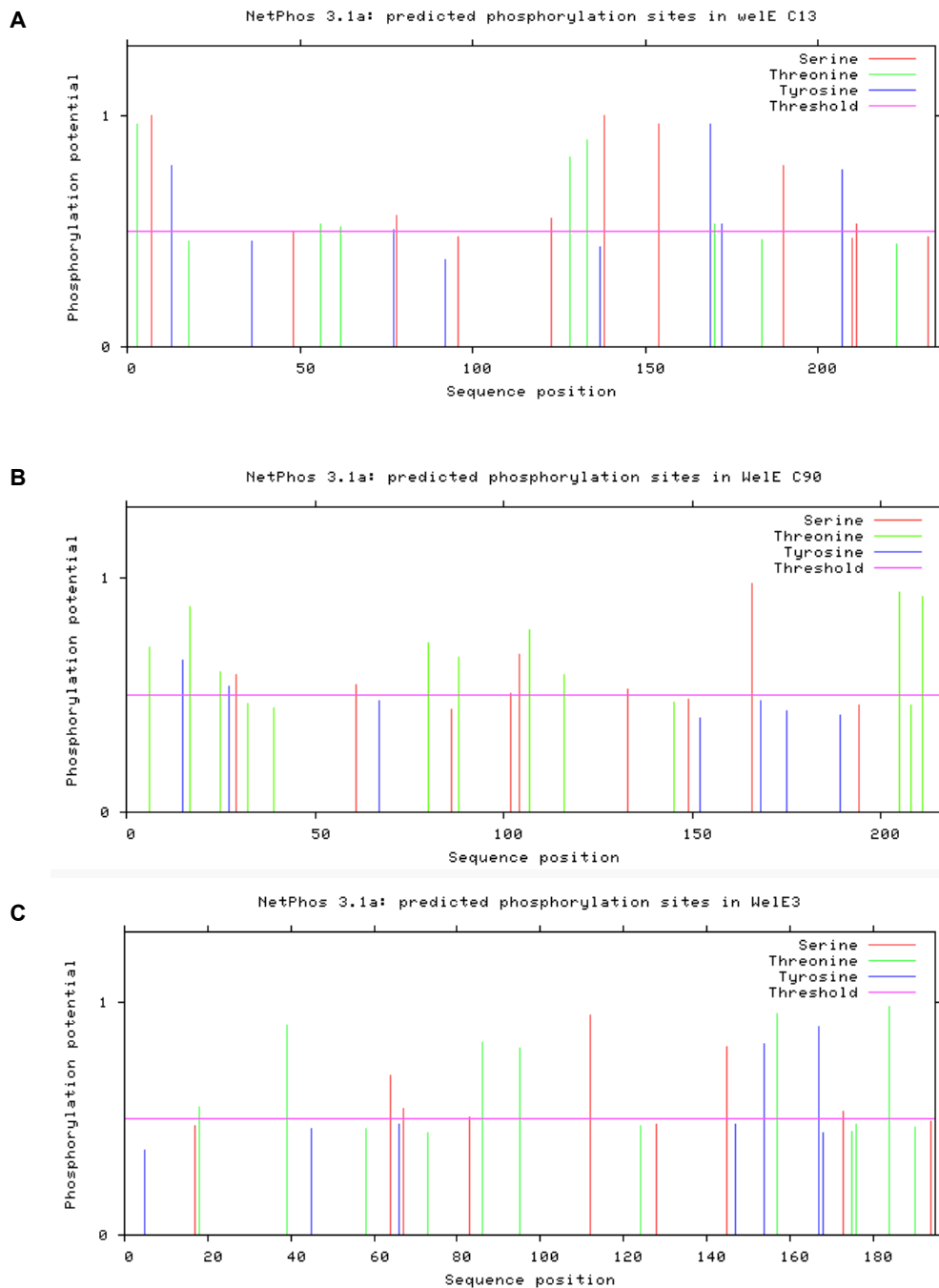


Figura II.IV. Residuos con probabilidad de ser fosforilados en las glicosiltransferasa iniciadora de CUPV237. Predicciones se realizaron sobre los residuos de tirosina (azul), treonina (verde) y serina (rojo), de las proteínas Wel1E (A), Wel2E (B) y Wel3E (C), mediante el programa NetPhos.

II.V.

Figura II.IV. Alineamiento múltiple (CLUSTALX 2.0) de 6 secuencias de nucleótidos que corresponden con las secuenciaciones parciales del operón *rib* de 5 cepas de *Lactobacillus collinoides* y *Lactobacillus sicerae* CUPV261^T. Se indican los nucleótidos idénticos en todas las secuencias (*). Las secuencias de nucleótidos provienen de amplificaciones elaboradas a partir de DNA genómico de las cepas CUPV2323, CUPV231, CUPV2313, CUPV2371 y CUPV2320, amplificadas con los cebadores descritos en la Tabla 5.1 y diseñados en este estudio. Posteriormente, han sido comparadas con la secuencia del operón *rib* de CUPV237 (JYDC00000000). En azul, se localiza la región RFN, con la base que ha sufrido variación en rojo; en púrpura, la secuencia referente al gen *ribB*; en verde, *ribA*; y en azul, el inicio del gen *ribH*.

Alineamientos de la región promotora

CUPV2323	-----	
CUPV231	-----	
CUPV2313	-----	
CUPV2371	-----GTTTGATTNNNCTTAAATTCGCAAAAAATCGCTGCAGGTCGGC	44
CUPV2320	-----CGCTGCAGGTCGGC	14
CUPV237	GTGCATGATTCACGACGTTTGATTCGGCTTAAATTCGCAAAAAATCGCTGCAGGTCGGC	60
CUPV2323	-----TCTGCACNTCAGCAATCCT	19
CUPV231	-----TAAGTTTCAAAA-CATCTGCACNTCAGCAATCCT	33
CUPV2313	-----	
CUPV2371	ATCAGTAGTCTTGTTAAGAATACCAATAAGTTTCAAAAACATCTGCACATCAGCAATCCT	104
CUPV2320	ATCAGTAGTCTTGTTAAGAATACCAATAAGTTTCAAAAACATCTGCACATCAGCAATCCT	74
CUPV237	ATCAGTAGTCTTGTTAAGAATACCAATAAGTTTCAAAAACATCTGCACATCAGCAATCCT	120
CUPV2323	TAGTAATGTGGCAAAGGGTTAACCAGCGCTTACTGATTCGGTTCGCCATAATCGTGCAC	79
CUPV231	TAGTAATGTGGCAAAGGGTTAACCAGCGCTTACTGATTCGGTTCGCCATAATCGTGCAC	93
CUPV2313	-----	
CUPV2371	TAGTAATGTGGCAAAGGGTTAACCAGCGCTTACTGATTCGGTTCGCCATAATCGTGCAC	164
CUPV2320	TAGTAATGTGGCAAAGGGTTAACCAGCGCTTACTGATTCGGTTCGCCATAATCGTGCAC	134
CUPV237	TAGTAATGTGGCAAAGGGTTAACCAGCGCTTACTGATTCGGTTCGCCATAATCGTGCAC	180
CUPV2323	TCATTCTTGCTGGCTGGACTTTGACGCGATATTCAGGCTCACATGCT	126
CUPV231	TCATTCTTGCTGGCTGGACTTTGACGCGATATTCAGGCTCACATGCT	153
CUPV2313	-----	
CUPV2371	TCATTCTTGCTGGCTGGACTTTGACGCGATATTCAGGCTCACATGCT	211
CUPV2320	TCATTCTTGCTGGCTGGACTTTGACGCGATATTCAGGCTCACATGCT	181
CUPV237	TCATTCTTGCTGGCTGGACTTTGACGCGATATTCAGGCTCACATGCT	227
CUPV2323	TAATCCAGCTCATGAACCATTACCAGCAGTCTTGACCACAGGTGTGCGCGATACACGATC	186
CUPV231	TAATCCAGCTCATGAACCATTACCAGCAGTCTTGACNNCAGGTGTGCGCGATACACGATC	213
CUPV2313	-----	
CUPV2371	TAATCCAGCTCATGAACCATTACCAGCAGTCTTGACCACAGGTGTGCGCGATACACGATC	271
CUPV2320	TAATCCAGCTCATGAACCATTACCAGCAGTCTTGACCACAGGTGTGCGCGATACACGATC	241
CUPV237	TAATCCAGCTCATGAACCATTACCAGCAGTCTTGACCACAGGTGTGCGCGATACACGATC	287
CUPV2323	ATTCACAATCTGGATTAGCTAGTTACAATATCATACAAAATAACGGAACGTTGCTTTTAGC	246
CUPV231	ATTCACAATCTGGATTAGCTAGTTACAATATCATACAAAATAACGGAACGTTGCTTTTAGC	273
CUPV2313	-----	
CUPV2371	ATTCACAATCTGGATTAGCTAGTTACAATATCATACAAAATAACGGAACGTTGCTTTTAGC	331
CUPV2320	ATTCACAATCTGGATTAGCTAGTTACAATATCATACAAAATAACGGAACGTTGCTTTTAGC	301
CUPV237	ATTCACAATCTGGATTAGCTAGTTACAATATCATACAAAATAACGGAACGTTGCTTTTAGC	347
CUPV2323	CAGTCTAAACCATTGATCGTCGTAAAAAAAATAAAAAAATCGCAAATCAACATGAAAG	306
CUPV231	CAGTCTAAACCATTGATCGTCGTAAAAAAAATAAAAAAATCGCAAATCAACATGAAAG	333
CUPV2313	-----	
CUPV2371	CAGTCTAAACCATTGATCGTCGTAAAAAAAATAAAAAAATCGCAAATCAACATGAAAG	391
CUPV2320	CAGTCTAAACCATTGATCGTCGTAAAAAAAATAAAAAAATCGCAAATCAACATGAAAG	361
CUPV237	CAGTCTAAACCATTGATCGTCGTAAAAAAAATAAAAAAATCGCAAATCAACATGAAAG	407
CUPV2323	CATTCTACCGCAAGGGTTACCCCATTTTTGAAAGCCATTTTCATTTAATAATAATTTAAC	366
CUPV231	CATTCTACCGCAAGGGTTACCCCATTTTTGAAAGCCATTTTCATTTAATAATAATTTAAC	393

CUPV2313	-----GCCATTTTCATTTAATAATAATTTAAC	26
CUPV2371	CATTTCTACCGCAAGGGTTACCCCATTTTTGAAAGCCATTTTCATTTAATAATAATTTAAC	451
CUPV2320	CATTTCTACCGCAAGGGTTACCCCATTTTTGAAAGCCATTTTCATTTAATAATAATTTAAC	421
CUPV237	CATTTCTACCGCAAGGGTTACCCCATTTTTGAAAGCCATTTTCATTTAATAATAATTTAAC	467

CUPV2323	CGCCATAACCCCGTCACGACAGCCTGCAAGCAGCTTCAACGACCACCATTGAATGATCG	426
CUPV231	CGCCATAACCCCGTCACGACAGCCTGCAAGCAGCTTCAACGACCACCATTGAATGATCG	453
CUPV2313	CGCCATAACCCCGTCACGACAGCCTGCAAGCAGCTTCAACGACCACCATTGAATGATCG	86
CUPV2371	CGCCATAACCCCGTCACGACAGCCTGCAAGCAGCTTCAACGACCACCATTGAATGATCG	511
CUPV2320	CGCCATAACCCCGTCACGACAGCCTGCAAGCAGCTTCAACGACCACCATTGAATGATCG	481
CUPV237	CGCCATAACCCCGTCACGACAGCCTGCAAGCAGCTTCAACGACCACCATTGAATGATCG	527

CUPV2323	GGTTATCAGATACTATGAGTTGAAATTTAAAAGTGCATGCTGTAACATGTCTTGTGACAA	486
CUPV231	GGTTATCAGATACTATGAGTTGAAATTTAAAAGTGCATGCTGTAACATGTCTTGTGACAA	513
CUPV2313	GGTTATCAGATACTATGAGTTGAAATTTAAAAGTGCATGCTGTAACATGTCTTGTGACAA	146
CUPV2371	GGTTATCAGATACTATGAGTTGAAATTTAAAAGTGCATGCTGTAACATGTCTTGTGACAA	571
CUPV2320	GGTTATCAGATACTATGAGTTGAAATTTAAAAGTGCATGCTGTAACATGTCTTGTGACAA	541
CUPV237	GGTTATCAGATACTATGAGTTGAAATTTAAAAGTGCATGCTGTAACATGTCTTGTGACAA	587

CUPV2323	CTGAATAGATTTCTTCGAGGCAGGGTGAAATTCGCCAGCCAGGTTGACAACCCGAGTGTAC	546
CUPV231	CTGAATAGATTTCTTCGAGGCAGGGTGAAATTCGCCAGCCAGGTTGACAACCCGAGTGTAC	573
CUPV2313	CTGAATAGATTTCTTCGAGGCAGGGTGAAATTCGCCAGCCAGGTTGACAACCCGAGTGTAC	206
CUPV2371	CTGAATAGATTTCTTCGAGGCAGGGTGAAATTCGCCAGCCAGGTTGACAACCCGAGTGTAC	631
CUPV2320	CTGAATAGATTTCTTCGAGGCAGGGTGAAATTCGCCAGCCAGGTTGACAACCCGAGTGTAC	601
CUPV237	CTGAATAGATTTCTTCGAGGCAGGGTGAAATTCGCCAGCCAGGTTGACAACCCGAGTGTAC	647

CUPV2323	CTCTCAGGTTGAAGTCCGTAACCCGCGTTTTAGCGGTGGACCCAGTGCAGTCTGGGACC	606
CUPV231	CTCTCAGGTTGAAGTCCGTAACCCGCGTTTTAGCGGTGGACCCAGTGCAGTCTGGGACC	633
CUPV2313	CTCTCAGGTTGAAGTCCGTAACCCGCGTTTTAGCGGTGGACCCAGTGCAGTCTGGGACC	266
CUPV2371	CTCTCAGGTTGAAGTCCGTAACCCGCGTTTTAGCGGTGGACCCAGTGCAGTCTGGGACC	691
CUPV2320	CTCTCAGGTTGAAGTCCGTAACCCGCGTTTTAGCGGTGGACCCAGTGCAGTCTGGGACC	661
CUPV237	CTCTCAGGTTGAAGTCCGTAACCCGCGTTTTAGCGGTGGACCCAGTGCAGTCTGGGACC	707

CUPV2323	GACAGTAATAGTCTGGATGGGAGAAAGAAAAATGGACTCAATTTTCGCATCGTTTTTAAACGT	666
CUPV231	GACAGTAATAGTCTGGATGGGAGAAAGAAAAATGGACTCAATTTTCGCATCGTTTTTAAACGT	693
CUPV2313	GACAGTAATAGTCTGGATGGGAGAAAGAAAAATGGACTCAATTTTCGCATCGTTTTTAAACGT	326
CUPV2371	GACAGTAATAGTCTGGATGGGAGAAAGAAAAATGGACTCAATTTTCGCATCGTTTTTAAACGT	751
CUPV2320	GACAGTAATAGTCTGGATGGGAGAAAGAAAAATGGACTCAATTTTCGCATCGTTTTTAAACGT	721
CUPV237	GACAGTAATAGTCTGGATGGGAGAAAGAAAAATGGACTCAATTTTCGCATCGTTTTTAAACGT	767

CUPV2323	GTTTATTTTACGCACGCACTAACTCGGATGAGATCTCATTAGCTTTCAAACCTTCGGCCT	726
CUPV231	GTTTATTTTACGCACGCACTAACTCGGATGAGATCTCATTAGCTTTCAAACCTTCGGCCT	753
CUPV2313	GTTTATTTTACGCACGCACTAACTCGGATGAGATCTCATTAGCTTTCAAACCTTCGGCCT	386
CUPV2371	GTTTATTTTACGCACGCACTAACTCGGATGAGATCTCATTAGCTTTCAAACCTTCGGCCT	811
CUPV2320	GTTTATTTTACGCACGCACTAACTCGGATGAGATCTCATTAGCTTTCAAACCTTCGGCCT	781
CUPV237	GTTTATTTTACGCACGCACTAACTCGGATGAGATCTCATTAGCTTTCAAACCTTCGGCCT	827

CUPV2323	CGCACTTATGCGAGGCCTTTTTTGTGAGGTGAATCAAGATCAATGATCAACAACCTGATGG	786
CUPV231	CGCACTTATGCGAGGCCTTTTTTGTGAGGTGAATCAAGATCAATGATCAACAACCTGATGG	813
CUPV2313	CGCACTTATGCGAGGCCTTTTTTGTGAGGTGAATCAAGATCAATGATCAACAACCTGATGG	446
CUPV2371	CGCACTTATGCGAGGCCTTTTTTGTGAGGTGAATCAAGATCAATGATCAACAACCTGATGG	871
CUPV2320	CGCACTTATGCGAGGCCTTTTTTGTGAGGTGAATCAAGATCAATGATCAACAACCTGATGG	841
CUPV237	CGCACTTATGCGAGGCCTTTTTTGTGAGGTGAATCAAGATCAATGATCAACAACCTGATGG	887

CUPV2323	CAAAAGCCATCGCGGCTGCCGGAACCGGAATCACCCACACGTGGACGAACCCCGTTGTTG	846
CUPV231	CAAAAGCCATCGCGGCTGCCGGAACCGGAATCACCCACACGTGGACGAACCCCGTTGTTG	873
CUPV2313	CAAAAGCCATCGCGGCTGCCGGAACCGGAATCACCCACACGTGGACGAACCCCGTTGTTG	503
CUPV2371	CAAAAGCCATCGCGGCTGCCGGAACCGGAATCACCCACACGTGGACGAACCCCGTTGTTG	931
CUPV2320	CAAAAGCCATCGCGGCTGCCGGAACCGGAATCACCCACACGTGGACGAACCCCGTTGTTG	896
CUPV237	CAAAAGCCATCGCGGCTGCCGGAACCGGAATCACCCACACGTGGACGAACCCCGTTGTTG	947

CUPV2323	GCGCCGTCATCGTTAAAAATAATCAACTTCTCGCTACCGGATATCACCACCGATTGGCN	906
CUPV231	GCGCCGTCATCGTTAAAAATAATCAACTTCTCGCTACCGGATATCACCACCGAT---GCG	930
CUPV2313	GCGC-----	507
CUPV2371	GCGCCGTCATCGTTAAAAATAATCA-----	956
CUPV2320	GTG-----	899
CUPV237	GCGCCGTCATCGTTAAAAATAATCAACTTCTCGCTACCGGATATCACCACCGATTGGCG	1007
	* *	

Alineamientos de la región ribG

CUPV2323	-----CGCGGA	6
CUPV261T	-----	
CUPV237	TAAAAATAATCAACTTCTCGCTACCGGATATCACCACCGATTTGGCGAAATGCACGCGGA	1020
CUPV2371	-----ACGCGGA	7
CUPV231	-----GCCGCGGA	8
CUPV2320	-----CCGCGGA	7
CUPV2313	-----ATGCCGCGGA	10
CUPV2323	GATCAACGCGCTTAGTCACCTTCAAATATCGAGGATGCCCGTGATGCCACAATGTATGT	66
CUPV261T	-----	
CUPV237	GATCAACGCGCTTAGTCACCTTCAAATATCGAGGATGCCCGTGATGCCACAATGTATGT	1080
CUPV2371	GATCAACGCGCTTAGTCNCCTTCAAATATCGAGGATGCCCGTGATGCCACAATGTATGT	67
CUPV231	GATCAACGCGCTTAGTCNCCTTCAAATATCGAGGANGCCCGTGATGCCACAATGTATGT	68
CUPV2320	GATCA-CGCGCTTAGTCACCTTCAAATATCGAGGATGCCCGTGATGCCACAATGTATGT	66
CUPV2313	GATCA-CGCGCTTAGTCNCCTTCAAATATCGAGGANGCCCGTGATGCCACAATGTATGT	69
CUPV2323	CACCCTCGAACCTGCAGCCACTACGGCAAGACGCCACCGTGCGCCAAACGGCTTGTGA	126
CUPV261T	-----	
CUPV237	CACCCTCGAACCTGCAGCCACTACGGCAAGACGCCACCGTGCGCCAAACGGCTTGTGA	1140
CUPV2371	CACCCTCGAACCTGCAGCCACTACGGCAAGACGCCACCGTGCGCCAAACGGCTTGTGA	127
CUPV231	CACCCTCGAACCTGCAGCCACTACGGCAAGACGCCACCGTGCGCCAAACGGCTTGTGA	128
CUPV2320	CACCCTCGAACCTGCAGCCACTACGGCAAGACGCCACCGTGCGCCAAACGGCTTGTGA	126
CUPV2313	CACCCTCGAACCTGCAGCCACTACGGCAAGACGCCACCGTGCGCCAAACGGCTTGTGA	129
CUPV2323	AGTCGGTATCAAGCGCGTCGTCATTGGGCAGCAGGACCCTAATCCTCAGGTAAGCGGTCA	186
CUPV261T	-----	
CUPV237	AGTCGGTATCAAGCGCGTCGTCATTGGGCAGCAGGACCCTAATCCTCAGGTAAGCGGTCA	1200
CUPV2371	AGTCGGTATCAAGCGCGTCGTCATTGGGCAGCAGGACCCTAATCCTCAGGTAAGCGGTCA	187
CUPV231	AGTCGGTATCAAGCGCGTCGTCATTGGGCAGCAGGACCCTAATCCTCAGGTAAGCGGTCA	188
CUPV2320	AGTCGGTATCAAGCGCGTCGTCATTGGGCAGCAGGACCCTAATCCTCAGGTAAGCGGTCA	186
CUPV2313	AGTCGGTATCAAGCGCGTCGTCATTGGGCAGCAGGACCCTAATCCTCAGGTAAGCGGTCA	189
CUPV2323	CGGTATCGCGATTCTAAAAGCCGCCAATATTGACGTGACCGTTTTAAACATCACGGACGA	246
CUPV261T	-----	
CUPV237	CGGTATCGCGATTCTAAAAGCCGCCAATATTGACGTGACCGTTTTAAACATCACGGACGA	1260
CUPV2371	CGGTATCGCGATTCTAAAAGCCGCCAATATTGACGTGACCGTTTTAAACATCACGGACGA	247
CUPV231	CGGTATCGCGATTCTAAAAGCCGCCAATATTGACGTGACCGTTTTAAACATCACGGACGA	248
CUPV2320	CGGTATCGCGATTCTAAAAGCCGCCAATATTGACGTGACCGTTTTAAACATCACGGACGA	246
CUPV2313	CGGTATCGCGATTCTAAAAGCCGCCAATATTGACGTGACCGTTTTAAACATCACGGACGA	249
CUPV2323	CCTCAACGTGGCCTACAACTTTTTTTACCGGCACAAACGGCCGCTCGTCACCCTCAAGTA	306
CUPV261T	-----	
CUPV237	CCTCAACGTGGCCTACAACTTTTTTTACCGGCACAAACGGCCGCTCGTCACCCTCAAGTA	1320
CUPV2371	CCTCAACGTGGCCTACAACTTTTTTTACCGGCACAAACGGCCGCTCGTCACCCTCAAGTA	307
CUPV231	CCTCAACGTGGCCTACAACTTTTTTTACCGGCACAAACGGCCGCTCGTCACCCTCAAGTA	308
CUPV2320	CCTCAACGTGGCCTACAACTTTTTTTACCGGCACAAACGGCCGCTCGTCACCCTCAAGTA	306
CUPV2313	CCTCAACGTGGCCTACAACTTTTTTTACCGGCACAAACGGCCGCTCGTCACCCTCAAGTA	309
CUPV2323	TGCCATGAGTATTGACGGCAAGCTCAACGATGGGTCAGGTAAGCGAACCCCTGCTGACCGG	366
CUPV261T	-----	
CUPV237	TGCCATGAGTATTGACGGCAAGCTCAACGATGGGTCAGGTAAGCGAACCCCTGCTGACCGG	1380
CUPV2371	TGCCATGAGTATTGACGGCAAGCTCAACGATGGGTCAGGTAAGCGAACCCCTGCTGACCGG	367
CUPV231	TGCCATGAGTATTGACGGCAAGCTCAACGATGGGTCAGGTAAGCGAACCCCTGCTGACCGG	368
CUPV2320	TGCCATGAGTATTGACGGCAAGCTCAACGATGGGTCAGGTAAGCGAACCCCTGCTGACCGG	366
CUPV2313	TGCCATGAGTATTGACGGCAAGCTCAACGATGGGTCAGGTAAGCGAACCCCTGCTGACCGG	369
CUPV2323	TAAACCCGCTTACCATGACAGTCAGAACCCTGCGCCTGCATCAGCAAGCAATCCTTATTGG	426
CUPV261T	-----	
CUPV237	TAAACCCGCTTACCATGACAGTCAGAACCCTGCGCCTGCATCAGCAAGCAATCCTTATTGG	1440
CUPV2371	TAAACCCGCTTACCATGACAGTCAGAACCCTGCGCCTGCATCAGCAAGCAATCCTTATTGG	427
CUPV231	TAAACCCGCTTACCATGACAGTCAGAACCCTGCGCCTGCATCAGCAAGCAATCCTTATTGG	428
CUPV2320	TAAACCCGCTTACCATGACAGTCAGAACCCTGCGCCTGCATCAGCAAGCAATCCTTATTGG	426
CUPV2313	TAAACCCGCTTACCATGACAGTCAGAACCCTGCGCCTGCATCAGCAAGCAATCCTTATTGG	429


```

CUPV2323      CCCAACTCACGATCGACACAAACCTGACTAATCNAATTCNTAGTCNGGGNTTGGNNNACA 1026
CUPV261T      CCCAACTCACGAT----- 422
CUPV237       CCCAACTCACGATCGACACAAACCTGACTAATCAAATTCATAGTCAGGTTGGCGACAGTA 2040
CUPV2371      CCCAACTCACGATCGAC----- 984
CUPV231       CCCAACTCACGANNNANACAAACCTGACTAATCAAATTCAT----- 1009
CUPV2320      CCCAACTCACGATCGACACA----- 985
CUPV2313      CCCAACTCACGATCGACACAAACCTGACTAATCAAATT----- 1007
*****

```

Alineamientos de la región ribB

```

CUPV2323      -----
CUPV231       -----
CUPV237       CCCAACTCACGATCGACACAAACCTGACTAATCAAATTCATAGTCAGGTTGGCGACAGTA 2040
CUPV2313      -----GTNNGGTTGGCGACNGTA 18
CUPV2371      -----AAATTCATAGTCAGGTTGGCGACAGTA 27
CUPV2320      -----TCTAGTCAGGTTGGCGACNGTA 22

```

```

CUPV2323_partial_1 -----ATCTGTTTAAACAGTTACTAACTTAACATCCNANNNTNCACAGCCG 46
CUPV2323_partial_2 -----
CUPV231       -----ACTAACTTAACATCCGATTCTTTCACAGCCG 31
CUPV237       TCGCTGTTGATGGTATCTGTTTAAACAGTTACTAACTTAACATCCGATTCTTTCACAGCCG 2100
CUPV2313      TCGCTGTTGATGGTATCTGTTTAAACAGTTACTAACTTAACATCCGATTCTTTCACAGCCG 78
CUPV2371      TCGCTGTTGATGGTATCTGTTTAAACAGTTACTAACTTAACATCCGATTCTTTCACAGCCG 87
CUPV2320      NCGCTGTTGATGGTATCTGTTTAAACAGTTACTAACTTAACATCCGATTCTTTCACAGCCG 82
***** * ** *****

```

```

CUPV2323_partial_1 ATGTTATGCCAGAAACAGTACACCGGACAAATCTGATGTNACTTGGAGAAGGCAGTCATG 106
CUPV2323_partial_2 -----
CUPV231       ATGTTATGCCAGAAACAGTACACCGGACAAATCTGATGTCACTTGGAGAAGGCAGTCATG 91
CUPV237       ATGTTATGCCAGAAACAGTACACCGGACAAATCTGATGTCACTTGGAGAAGGCAGTCATG 2160
CUPV2313      ATGTTATGCCAGAAACAGTACACCGGACAAATCTGATGTCACTTGGAGAAGGCAGTCATG 138
CUPV2371      ATGTTATGCCAGAAACAGTACACCGGACAAATCTGATGTCACTTGGAGAAGGCAGTCATG 147
CUPV2320      ATGTTATGCCAGAAACAGTACACCGGACAAATCTGATGTCACTTGGAGAAGGCAGTCATG 142
*****

```

```

CUPV2323_partial_1 TGAATCTGGAGNCTG----- 121
CUPV2323_partial_2 -----
CUPV231       TGAATCTGGAGCCTGCTTTAGCTGTAACAGATCGATTAGACGGTCACTTTGTCTGGGCC 151
CUPV237       TGAATCTGGAGCCTGCTTTAGCTGTAACAGATCGATTAGACGGTCACTTTGTCTGGGCC 2220
CUPV2313      TGAATCTGGAGCCTGCTTTAGCTGTAACAGATCGATTAGACGGTCACTTTGTCTGGGCC 198
CUPV2371      TGAATCTGGAGCCTGCTTTAGCTGTAACAGATCGATTAGACGGTCACTTTGTCTGGGCC 207
CUPV2320      TGAATCTGGAGCCTGCTTTAGCTGTAACAGATCGATTAGACGGTCACTTTGTCTGGGCC 202
*****

```

```

CUPV2323_partial_2 -----
CUPV231       ACATAGACGCAACGGCAACCCCTCATCCGTCAGGTGCAAGATCAAACAGCAGTCACACTGA 211
CUPV237       ACATAGACGCAACGGCAACCCCTCATCCGTCAGGTGCAAGATCAAACAGCAGTCACACTGA 2280
CUPV2313      ACATAGACGCAACGGCAACCCCTCATCCGTCAGGTGCAAGATCAAACAGCAGTCACACTGA 258
CUPV2371      ACATAGACGCAACGGCAACCCCTCATCCGTCAGGTGCAAGATCAAACAGCAGTCACACTGA 267
CUPV2320      ACATAGACGCAACGGCAACCCCTCATCCGTCAGGTGCAAGATCAAACAGCAGTCACACTGA 262
*****

```

```

CUPV2323_partial_2 -----
CUPV231       CTTTCTCGTTTCCAACCCACTATCAACCCCTACGTCATTGAAAAGGGGTCCGTGGCAATCA 271
CUPV237       CTTTCTCGTTTCCAACCCACTATCAACCCCTACGTCATTGAAAAGGGGTCCGTGGCAATCA 2340
CUPV2313      CTTTCTCGTTTCCAACCCACTATCAACCCCTACGTCATTGAAAAGGGGTCCGTGGCAATCA 318
CUPV2371      CTTTCTCGTTTCCAACCCACTATCAACCCCTACGTCATTGAAAAGGGGTCCGTGGCAATCA 327
CUPV2320      CTTTCTCGTTTCCAACCCACTATCAACCCCTACGTCATTGAAAAGGGGTCCGTGGCAATCA 322
*****

```

```

CUPV2323_partial_2 -----
CUPV231       ACGGTGTTAGTCTCACCATTACCGCGTTTCTTCGGGTCAGTTCAGCGTTAGTCTCATCC 331
CUPV237       ACGGTGTTAGTCTCACCATTACCGCGTTTCTTCGGGTCAGTTCAGCGTTAGTCTCATCC 2400
CUPV2313      ACGGTGTTAGTCTCACCATTACCGCGTTTCTTCGGGTCAGTTCAGCGTTAGTCTCATCC 378
CUPV2371      ACGGTGTTAGTCTCACCATTACCGCGTTTCTTCGGGTCAGTTCAGCGTTAGTCTCATCC 387
CUPV2320      ACGGTGTTAGTCTCACCATTACNNCNNTTCTTCGGGTCANNTCAGCGTTAGNCTCATCC 382
***** * *****

```

CUPV2323_partial_2	-----	
CUPV231	CCCACACCATGGCAGCCACCATGCTTGGCGATCTGCAAACGGTGACCCAATTAATCTTG	391
CUPV237	CCCACACCATGGCAGCCACCATGCTTGGCGATCTGCAAACGGTGACCCAATTAATCTTG	2460
CUPV2313	CCCACACCATGGCAGCCACCATGCTTGGCGATCTGCAAACGGTGACCCAATTAATCTTG	438
CUPV2371	CCCACACCATGGCAGCCACCATGCTTGGCGATCTGCAAACGGTGACCCAATTAATCTTG	447
CUPV2320	CCCACACCATGNCA-----	396

CUPV2323_partial_2	-----	
CUPV231_ribB	AAACCGACATTCTTGGTAAGTATCTTATCAACCAACAGGAGGTAAGCGCACATGACTAGT	451
CUPV237	AAACCGACATTCTTGGTAAGTATCTTATCAACCAACAGGAGGTAAGCGCACATGACTAGT	2520
CUPV2313_ribB	AAACCGACATTCTTGGTAAGTATCTTATCAACCAACAGGAGGTAAGCGCACATGACTAGT	498
CUPV2371_ribB	AAACCGACATTCTTGGTAAGTATCTTATCAACCAACAGGAGGTAAGCGCACATGACTAGT	507
CUPV2320_ribB	-----	

CUPV2323_partial_2	-----	
CUPV231	TCAGAATCAATTATTAACGCTGTAGAAAACGCCCTTGAAACATTGAAAAACGGCCAAC	511
CUPV237	TCAGAATCAATTATTAACGCTGTAGAAAACGCCCTTGAAACATTGAAAAACGGCCAAC	2580
CUPV2313	TCAGAATCAATTATTAACGCTGTAGAAAACGCCCTTGAAACATTGAAAAACGGCCAAC	558
CUPV2371	TCAGAATCAATTATTAACGCTGTAGAAAACGCCCTTGAAACATTGAAAAACGGCCAAC	567
CUPV2320	-----	

CUPV2323_partial_2	-----	
CUPV231	ATCATTGTCACCGATGATGATCACCGGGAGGCCGAAGGTGACATGGTTGGTTTAGCGCAG	571
CUPV237	ATCATTGTCACCGATGATGATCACCGGGAGGCCGAAGGTGACATGGTTGGTTTAGCGCAG	2640
CUPV2313	ATCATTGTCACCGATGATGATCACCGGGAGGCCGAAGGTGACATGGTTGGTTTAGCGCAG	618
CUPV2371	ATCATTGTCACCGATGATGATCACCGGGAGGCCGAAGGTGACATGGTTGGTTTAGCGCAG	627
CUPV2320	-----	

CUPV2323_partial_2	-----	
CUPV231	TATGCAACTGGAGAAACCGTCCGGACAATGGTAACTAACGCCCGTGGCTTACTGTGCGTG	631
CUPV237	TATGCAACTGGAGAAACCGTCCGGACAATGGTAACTAACGCCCGTGGCTTACTGTGCGTG	2700
CUPV2313	TATGCAACTGGAGAAACCGTCCGGACAATGGTAACTAACGCCCGTGGCTTACTGTGCGTG	678
CUPV2371	TATGCAACTGGAGAAACCGTCCGGACAATGGTAACTAACGCCCGTGGCTTACTGTGCGTG	687
CUPV2320	-----	

CUPV2323_partial_2	-----	
CUPV2320_partial_2	-----ACAAACAANTGCTTNGCGTNTAGGAANGANGCANANGTGACTAANGNNGN	52
CUPV231	CCCATGGCACAACAATTTGCTTCGGCTTAGGAATGACGCCGATGGTGACTAATGCGACC	691
CUPV237	CCCATGGCACAACAATTTGCTTCGGCTTAGGAATGACGCCGATGGTGACTAATGCGACC	2760
CUPV2313	CCCATGGCACAACAATTTGCTTCGGCTTAGGAATGACGCCGATGGTGACTAATGCGACC	738
CUPV2371	CCCATGGCACAACAATTTGCTTCGGCTTAGGAATGACGCCGATGGTGACTAATGCGACC	747
CUPV2320_partial_1	-----	
CUPV2323_partial_2	-----	
CUPV2320_partial_2	GANGNGTNNGGCACNNCTTCACCATCAGTACCGATGCAAAAACAACCTTCCACTGGAATC	112
CUPV231	GATGCGTACGGCACCGCTTCACCATCAGTACCGATGCAAAAACAACCTTCCACTGGAATC	751
CUPV237	GATGCGTACGGCACCGCTTCACCATCAGTACCGATGCAAAAACAACCTTCCACTGGAATC	2820
CUPV2313	GATGCGTACGGCACCGCTTCACCATCAGTACCGATGCAAAAACAACCTTCCACTGGAATC	798
CUPV2371	GATGCGTACGGCACCGCTTCACCATCAGTACCGATGCAAAAACAACCTTCCACTGGAATC	807
CUPV2320_partial_1	-----	
CUPV2323_partial_2	-----	
CUPV2320_partial_2	-----CCGAC	5
CUPV231	TCAGCGTTTGACCGGGCCGACACCATCCGCCAGCTCGCCGACCCGGAATCAAACCCGAC	171
CUPV237	TCAGCGTTTGACCGGGCCGACACCATCCGCCAGCTCGCCGACCCGGAATCAAACCCGAC	811
CUPV2313	TCAGCGTTTGACCGGGCCGACACCATCCGCCAGCTCGCCGACCCGGAATCAAACCCGAC	2880
CUPV2371	TCAGCGTTTGACCGGGCCGACACCATCCGCCAGCTCGCCGACCCGGAATCAAACCCGAC	858
CUPV2320_partial_1	-----	
CUPV2323_partial_2	-----	
CUPV2320_partial_2	GCCTTCTACCATCCTGGTCAATTTTTCCATTAATGCCAAGAATCGCGGTGTGATGGCA	65
CUPV231	GCCTTCTACCATCCTGGTCAATTTTTCCATTAATGCCAAGAATCGCGGTGTGATGGCA	231
CUPV237	GCCTTCTACCATCCTGGTCAATTTTTCCATTAATGCCAAGAATCGCGGTGTGATGGCA	871
CUPV2313	GCCTTCTACCATCCTGGTCAATTTTTCCATTAATGCCAAGAATCGCGGTGTGATGGCA	2940
CUPV2371	GCCTTCTACCATCCTGGTCAATTTTTCCATTAATGCCAAGAATCGCGGTGTGATGGCA	918
CUPV2320_partial_1	-----	
	GCCTTCTACCATCCTGGTCAATTTTTCCATTAATGCCAAGAATCGCGGTGTGATGGCA	927

CUPV2323_partial_2 CGAGGCGGGCATAACGAAGCCG----- 88
 CUPV2320_partial_2R CGAGGCGGGCATAACGAAGCCGTGT-GAT--GCGAA----- 266
 CUPV231 CGAGGCGGGCATAACGAAGCCGCTGTTGANTTGGCGAAACTCGCNAANGCTGCNC----- 926
 CUPV237 CGAGGCGGGCATAACGAAGCCGCTGTTGATTTGGCGAAACTCGCGAACGCTGCCCCAGTT 3000
 CUPV2313 CGAGGCGGGCATAACGAAGCCGCTGTTGATTTGGC----- 953
 CUPV2371 CGAGGCGGGCATAACGAAGCCGCTGTTGATTTGGCGAAA----- 966
 CUPV2320_partial_1 -----

Alineamientos de la región ribA

CUPV231 -----NNCTGTTGATTTGGCGAAACTCGCGAACGCTGCCCCAGTT 40
 CUPV2320 -----CCCCAGTT 8
 CUPV2313 -----CGCTGTTGATTTGGCGAAACTCGCGAACGCTGCCCCAGTT 40
 CUPV2371 -----TGTGATTTGGCGAAACTCGCGAACGCTGCCCCAGTT 37
 CUPV237 CGAGGCGGGCATAACGAAGCCGCTGTTGATTTGGCGAAACTCGCGAACGCTGCCCCAGTT 3000
 CUPV2323 -----GTT 3

CUPV231 GCTTACATCTGCGAAATTTGGCCAAGGACGGGCATATGGCGGGCGGCATGAACTCAA 100
 CUPV2320 GCTTACATNTGNGAAATTTGGCCAAGGACGGGCATATGGCGNGGCGGCATGAACTCAA 68
 CUPV2313 GCTTACATCTGCGAAATTTGGCCAAGGACGGGCATATGGCGGGCGGCATGAACTCAA 100
 CUPV2371 GCTTACATCTGCGAAATTTGGCCAAGGACGGGCATATGGCGGGCGGCATGAACTCAA 97
 CUPV237 GCTTACATCTGCGAAATTTGGCCAAGGACGGGCATATGGCGGGCGGCATGAACTCAA 3060
 CUPV2323 GCTTACNTCTGCGAAATTTGGCCAAGGACGGGCATATGGCGGGCGGCATGAACTCAA 63
 ***** * * * *****

CUPV231 CCATTTGCTGAAGGCATCCAAATGCCGTTGATTTCAATTCAGGACA 146
 CUPV2320 CCATTTGCTGAAGGCATCCAAATGCCGTTGATTTCAATTCAGGACA 114
 CUPV2313 CCATTTGCTGAAGGCATCCAAATGCCGTTGATTTCAATTCAGGACA 160
 CUPV2371 CCATTTGCTGAAGGCATCCAAATGCCGTTGATTTCAATTCAGGACA 143
 CUPV237 CCATTTGCTGAAGGCATCCAAATGCCGTTGATTTCAATTCAGGACA 3106
 CUPV2323 CCATTTGCTGAAGGCATCCAAATGCCGTTGATTTCAATTCAGGACA 109

CUPV231 TCAAAACAATACCGGTACATGAAAGATCGCGAAATGCTGATTTAATCACCAGTGTAAAC 206
 CUPV2320 TCAAAACAATACCGGTACATGAAAGATCGCGAAATGCTGATTTAATCACCAGTGTAAAC 174
 CUPV2313 TCAAAACAATACCGGTACATGAAAGATCGCGAAATGCTGATTTAATCACCAGTGTAAAC 220
 CUPV2371 TCAAAACAATACCGGTACATGAAAGATCGCGAAATGCTGATTTAATCACCAGTGTAAAC 203
 CUPV237 TCAAAACAATACCGGTACATGAAAGATCGCGAAATGCTGATTTAATCACCAGTGTAAAC 3166
 CUPV2323 TCAAAACAATACCGGTACATGAAAGATCGCGAAATGCTGATTTAATCACCAGTGTAAAC 169

CUPV231 TGCCACCAAATATGGTGATTTCCAGCTTGAGGCTTATGACACACGTGATGGCCATGAAC 266
 CUPV2320 TGCCACCAAATATGGTGATTTCCAGCTTGAGGCTTATGACACACGTGATGGCCATGAAC 234
 CUPV2313 TGCCACCAAATATGGTGATTTCCAGCTTGAGGCTTATGACACACGTGATGGCCATGAAC 280
 CUPV2371 TGCCACCAAATATGGTGATTTCCAGCTTGAGGCTTATGACACACGTGATGGCCATGAAC 263
 CUPV237 TGCCACCAAATATGGTGATTTCCAGCTTGAGGCTTATGACACACGTGATGGCCATGAAC 3226
 CUPV2323 TGCCACCAAATATGGTGATTTCCAGCTTGAGGCTTATGACACACGTGATGGCCATGAAC 229

CUPV231 CTACCCTGTTAATTTCAAAGGGTCTATTCAACCAAACGAACCACTGTTGTTACGAATGC 326
 CUPV2320 CTACCCTGTTAATTTCAAAGGGTCTATTCAACCAAACGAACCACTGTTGTTACGAATGC 294
 CUPV2313 CTACCCTGTTAATTTCAAAGGGTCTATTCAACCAAACGAACCACTGTTGTTACGAATGC 340
 CUPV2371 CTACCCTGTTAATTTCAAAGGGTCTATTCAACCAAACGAACCACTGTTGTTACGAATGC 323
 CUPV237 CTACCCTGTTAATTTCAAAGGGTCTATTCAACCAAACGAACCACTGTTGTTACGAATGC 3286
 CUPV2323 CTACCCTGTTAATTTCAAAGGGTCTATTCAACCAAACGAACCACTGTTGTTACGAATGC 289

CUPV231 ATTCTGAATGCTCACCGGTGATATTTGGGTTCAATTCGTTGCGATTGCGGCGAACAAT 386
 CUPV2320 ATTCTGAATGCTCACCGGTGATATTTGGGTTCAATTCGTTGCGATTGCGGCGAACAAT 354
 CUPV2313 ATTCTGAATGCTCACCGGTGATATTTGGGTTCAATTCGTTGCGATTGCGGCGAACAAT 400
 CUPV2371 ATTCTGAATGCTCACCGGTGATATTTGGGTTCAATTCGTTGCGATTGCGGCGAACAAT 383
 CUPV237 ATTCTGAATGCTCACCGGTGATATTTGGGTTCAATTCGTTGCGATTGCGGCGAACAAT 3346
 CUPV2323 ATTCTGAATGCTCACCGGTGATATTTGGGTTCAATTCGTTGCGATTGCGGCGAACAAT 349

CUPV231	TAGCAACTGCGCTGCGCACCATTGAAGCGGCCGGTCACGGCGCCGTGATCTATCTGCGAC	446
CUPV2320	TAGCAACTGCGCTGCGCACCATTGAAGCGGCCGGTCACGGCGCCGTGATCTATCTGCGAC	414
CUPV2313	TAGCAACTGCGCTGCGCACCATTGAAGCGGCCGGTCACGGCGCCGTGATCTATCTGCGAC	460
CUPV2371	TAGCAACTGCGCTGCGCACCATTGAAGCGGCCGGTCACGGCGCCGTGATCTATCTGCGAC	443
CUPV237	TAGCAACTGCGCTGCGCACCATTGAAGCGGCCGGTCACGGCGCCGTGATCTATCTGCGAC	3406
CUPV2323	TAGCAACTGCGCTGCGCACCATTGAAGCGGCCGGTCACGGCGCCGTGATCTATCTGCGAC	409

CUPV231	AGGAAGGCCGTGGCATTGGCCTGGCCAACAAGTTACGAGCCTACAACTGCAGGAAGAAG	506
CUPV2320	AGGAAGGCCGTGGCATTGGCCTGGCCAACAAGTTACGAGCCTACAACTGCAGGAAGAAG	474
CUPV2313	AGGAAGGCCGTGGCATTGGCCTGGCCAACAAGTTACGAGCCTACAACTGCAGGAAGAAG	520
CUPV2371	AGGAAGGCCGTGGCATTGGCCTGGCCAACAAGTTACGAGCCTACAACTGCAGGAAGAAG	503
CUPV237	AGGAAGGCCGTGGCATTGGCCTGGCCAACAAGTTACGAGCCTACAACTGCAGGAAGAAG	3466
CUPV2323	AGGAAGGCCGTGGCATTGGCCTGGCCAACAAGTTACGAGCCTACAACTGCAGGAAGAAG	469

CUPV231	GGCTTGATACCGTTGAGGCTAATGTGCATTAGGCTTTGAACCGGACGAACGCG	560
CUPV2320	GGCTTGATACCGTTGAGGCTAATGTGCATTAGGCTTTGAACCGGACGAACGCG	528
CUPV2313	GGCTTGATACCGTTGAGGCTAATGTGCATTAGGCTTTGAACCGGACGAACGCG	574
CUPV2371	GGCTTGATACCGTTGAGGCTAATGTGCATTAGGCTTTGAACCGGACGAACGCG	557
CUPV237	GGCTTGATACCGTTGAGGCTAATGTGCATTAGGCTTTGAACCGGACGAACGCG	3520
CUPV2323	GGCTTGATACCGTTGAGGCTAATGTGCATTAGGCTTTGAACCGGACGAACGCG	529

CUPV231	ATTATGGGTTGGTTGCAGCCATTTGCATAAGAAAAGGTCAGCGAAGTTACGCTGATGA	620
CUPV2320	ATTATGGGTTGGTTGCAGCCATTTGCATAAGAAAAGGTCAGCGAAGTTACGCTGATGA	588
CUPV2313	ATTATGGGTTGGTTGCAGCCATTTGCATAAGAAAAGGTCAGCGAAGTTACGCTGATGA	634
CUPV2371	ATTATGGGTTGGTTGCAGCCATTTGCATAAGAAAAGGTCAGCGAAGTTACGCTGATGA	617
CUPV237	ATTATGGGTTGGTTGCAGCCATTTGCATAAGAAAAGGTCAGCGAAGTTACGCTGATGA	3580
CUPV2323	ATTATGGGTTGGTTGCAGCCATTTGCATAAGAAAAGGTCAGCGAAGTTACGCTGATGA	589

CUPV231	CGAATAACCCAGATAAAGGTTTCATCAGCTAGAGGCTCTGGGCATCACCCCTAGATGCGCGTG	680
CUPV2320	CGAATAACCCAGATAAAGGTTTCATCAGCTAGAGGCTCTGGGCATCACCCCTAGATGCGCGTG	648
CUPV2313	CGAATAACCCAGATAAAGGTTTCATCAGCTAGAGGCTCTGGGCATCACCCCTAGATGCGCGTG	694
CUPV2371	CGAATAACCCAGATAAAGGTTTCATCAGCTAGAGGCTCTGGGCATCACCCCTAGATGCGCGTG	677
CUPV237	CGAATAACCCAGATAAAGGTTTCATCAGCTAGAGGCTCTGGGCATCACCCCTAGATGCGCGTG	3640
CUPV2323	CGAATAACCCAGATAAAGGTTTCATCAGCTAGAGGCTCTGGGCATCACCCCTAGATGCGCGTG	649

CUPV231	TGCCAATCGAAACAAAAGCTCGGCCGAAAATCGGCACATCTTTGAAACCAAAAAGCACA	740
CUPV2320	TGCCAATCGAAACAAAAGCTCGGCCGAAAATCGGCACATCTTTGAAACCAAAAAGCACA	708
CUPV2313	TGCCAATCGAAACAAAAGCTCGGCCGAAAATCGGCACATCTTTGAAACCAAAAAGCACA	754
CUPV2371	TGCCAATCGAAACAAAAGCTCGGCCGAAAATCGGCACATCTTTGAAACCAAAAAGCACA	737
CUPV237	TGCCAATCGAAACAAAAGCTCGGCCGAAAATCGGCACATCTTTGAAACCAAAAAGCACA	3700
CUPV2323	TGCCAATCGAAACAAAAGCTCGGCCGAAAATCGGCACATCTTTGAAACCAAAAAGCACA	709

CUPV231	AAATGCATCATCTACTCAAGGAGGTTCAATAACGATGAATACTTACACAGGAACGATCAA	800
CUPV2320	AAATGCATCATCTACTCAAGGAGGTTCAATAACGATGAATACT--CACAGGAACGATCAA	767
CUPV2313	AAATGCATCATCTACTCAAGGAGGTTCAATAACNATGAATACTTACACAGGAACGATCAA	814
CUPV2371	AAATGCATCATCTACTCAAGGAGGTTCAATAACGATGAATACTTACACA-----	786
CUPV237	AAATGCATCATCTACTCAAGGAGGTTCAATAACGATGAATACTTACACAGGAACGATCAA	3760
CUPV2323	AAATGCATCATCTACTCAAGGAGGTTCAATAACGANGAATACTTACACAG--AACGATCAA	768
	***** * ***** ****	
CUPV231	TGGCGAACATCAACGAATCGGGATCGNNNNNNNNNNAATTNNNNN-----	846
CUPV2320	TGGCGA-----	773
CUPV2313	TGGCGAACATCAACNAATCNGGNTCGTTG-----	844
CUPV2371	-----	
CUPV237	TGGCGAACATCAACGAATCGGG-ATCGTTGTCGCTCAATTTAATGATCTCGTCACCAAAC	3819
CUPV232	-----	
CUPV231	-----	
CUPV2320	-----	
CUPV2313	-----	
CUPV2371	-----	
CUPV237	GCCTATTGGAAGGCGCCCTATCAGCTCTTAAACAGTTCGGCGTGCCCAATAATGCCATTA	3879
CUPV2323	-----	

Alineamientos de la región ribH

CUPV237	ATTGGCCTGGCCAACAAGTTACGAGCCTACAACTGCAGGAAGAAGGGCTTGATACCGTT	3480
CUPV2371	-----GTT	3

CUPV237	GAGGCTAATGTGCATTTAGGCTTTGAACCGGACGAACGCGATTATGGGTTGGTTGCAGCC	3540
CUPV2371	GAGGCTAATGTGCATTTAGGCTTTGAACCGGACGAACGCGATTATGGGTTGGTTGCAGCC	63

CUPV237	ATTTTGCATAAGAAAAAGGTCAGCGAAGTTACGCTGATGACGAATAACCCAGATAAGGTT	3600
CUPV2371	ATTTTGCATAAGAAAAAGGTCAGCGAAGTTACGCTGATGACGAATAACCCAGATAAGGTT	123

CUPV237	CATCAGCTAGAGGCTCTGGGCATCACCCTAGATGCGCGTGTGCCAATCGAAACAAAAGCT	3660
CUPV2371	CATCAGCTAGAGGCTCTGGGCATCACCCTAGATGCGCGTGTGCCAATCGAAACAAAAGCT	183

CUPV237	CGGCCGAAAATCGGCACATCTTGAACCAAAAAGCACAAAATGCATCATCTACTCAAG	3720
CUPV2371	CGGCCGAAAATCGGCACATCTTGAACCAAAAAGCACAAAATGCATCATCTACTCAAG	243

CUPV237	GAGGTTCAATAACGATGAATACTTACACAGGAACGATCAATGGCGAACATCAACGAATCG	3780
CUPV2371	GAGGTTCAATAACGATGAATACTTACACAGGAACGATCAATGGCGAACATCAACGAATCG	303

CUPV237	GGATCGTTGTCGCTCAATTTAATGATCTCGTCACCAAACGCCTATTGGAAGGCGCCCTAT	3840
CUPV2371	GGATCGTTGTCGCTCAATTTAATGATCTCGTCACCAAACGCCTATTGGAAGGCGCCCTAT	363

CUPV237	CAGCTCTTAAACAGTTTCGGCGTGCCCAATAATGCCATTACGGTGACCTGGGTGCCAGGAG	3900
CUPV2371	CAGCTCTTAAACAGTTTCGGCGTGCCCAATAATGCCATTACGGTGACCTGGGTGCCAGGAG	423

CUPV237	CCTTAGAATTGCCACGGGCTGCCAATAATGGCTGGTTCGGCAAGGTTGACGGAATCA	3960
CUPV2371	CCTTAGAATTGCCACGGGCTGCCAATAATGGCTGGTTCGGCAAGGTTGACGGAATCA	483

CUPV237	TGCCTTAGGTGCAGTGGTCCGTGGGGAAACCTCACACTATGATTATGTTTGTGCTAACA	4020
CUPV2371	TGCCTTAGGTGCAGTGGTCCGTGGGGAAACCTCACACTATGATTATGTTTGTGCTAACA	543

CUPV237	CCGCCTCAGGCTGGCGGAAGTTTCCTTAAACGGCCAGTTCCTGTCATGTTGGTGTCC	4080
CUPV2371	CCGCCTCAGGCTGGCGGAAGTTTCCTTAAACGGCCAGTTCCTGTCATGTTGGTGTCC	603

CUPV237	TAACGACTGATAACATGAATCAAGCCATGAACCGAGCCGGCGGAAAAGCCGGAATAAAG	4140
CUPV2371	TAACGACTGATAACATGAATCAAGCCATGAACCGAGCCGGCGGAAAAGCCGGAATAAAG	663

CUPV237	GCAGCAAATGTGCCAGCGGCTTCTTGAATGATTCACCTGGCTGATT-GGATCACCGCC	4199
CUPV2371	GCAGCAAATGTGCCAGCGGCTTCTTGAATGATTCACCTGGCTGATTGGATCACCGCC	723

CUPV237	TAGGGCACCATACTGTGATGTTGAGAGTCGACATTAATGTCGGCTCTTTTTTATGTATT	4259
CUPV2371	TAGGGCACCATACTGTGATGTT-GAGAGTCGACATTAATGTCGGCTCTTTTTTATGTATT	782

CUPV237	AATAACTTC	4319
CUPV2371	AATAACTTC-----	791

CUPV237	TTGCT 4324	
CUPV2371	-----	

ANEXO III

Lactobacillus sicerae sp. nov., a lactic acid bacterium isolated from Spanish natural cider

Ana Isabel Puertas,¹ David R. Arahal,^{2,3} Idoia Ibarburu,¹
Patricia Elizaquível,^{3,4} Rosa Aznar^{2,3,4} and M. Teresa Dueñas¹

Correspondence
David R. Arahal
arahal@uv.es

¹Department of Applied Chemistry, University of Basque Country (UPV/EHU), Paseo Manuel de Lardizabal 3, 20018 Donostia, Spain

²Spanish Type Culture Collection (CECT), University of Valencia, Catedrático Agustín Escardino 9, 46980 Paterna, Spain

³Department of Microbiology and Ecology, University of Valencia, Dr. Moliner 50, 46100 Burjassot, Spain

⁴Institute of Agrochemistry and Food Technology (IATA), Spanish Council for Scientific Research (CSIC), Catedrático Agustín Escardino 7, 46980 Paterna, Spain

Strains CUPV261^T and CUPV262 were isolated from rosy natural ciders of the Basque Country, Spain, in 2007. Cells are Gram-stain positive, non-spore-forming, motile rods, facultative anaerobes and catalase-negative. The strains are obligately homofermentative (final product DL-lactate) and produce exopolysaccharides from sucrose. Phylogenetic analysis based on 16S rRNA gene sequences revealed that the highest similarity to both isolates corresponded to the type strain of *Lactobacillus vini* (99.1%), followed by *Lactobacillus satsumensis* (96.4%), and *Lactobacillus oeni* (96.2%), and for all other established species, 16S rRNA gene sequence similarities were below 96%. The species delineation of strains CUPV261^T and CUPV262 was evaluated through RAPD fingerprinting. In addition, a random partial genome pyrosequencing approach was performed on strain CUPV261^T in order to compare it with the genome sequence of *Lactobacillus vini* DSM 20605^T and calculate indexes of average nucleotide identity (ANI) between them. Results permit the conclusion that strains CUPV261^T and CUPV262 represent a novel species of the genus *Lactobacillus*, for which the name *Lactobacillus sicerae* sp. nov. is proposed. The type strain is CUPV261^T (=CECT 8227^T=KCTC 21012^T).

Lactic acid bacteria (LAB) of the genera *Lactobacillus*, *Oenococcus*, *Leuconostoc* and *Pediococcus* are involved in the cider making process (Beech & Carr, 1977; Dueñas *et al.*, 1994; Laplace *et al.*, 2001). The fermentation of apple juice is a microbiologically complex process involving the activities of acetic acid bacteria, lactic acid bacteria and yeasts. In Spain, especially in the Basque Country and Asturias, natural cider is usually produced in small cider factories by using traditional techniques, which implies, among other practices, that yeasts and LAB starters are not

added (Salih *et al.*, 1990; Dueñas *et al.*, 1994). Malolactic fermentation (MLF) occurs spontaneously by indigenous LAB present in the musts (Dueñas *et al.*, 1994). This transformation has a great importance from an organoleptic point view, and most of the LAB isolated from cider has this capacity (Beech & Carr, 1977; Dueñas *et al.*, 1994). Several species of the genus *Lactobacillus* have been isolated from juice and apple cider of different countries. The obligate homofermentative *Lactobacillus mali* (Carr & Davies, 1970), *Lactobacillus delbrueckii* subsp. *lactis* (Marshall & Walkley, 1951; Weiss *et al.*, 1983) and *Lactobacillus acidophilus* (Laplace *et al.*, 2001) are considerably rare. In contrast, the species most frequently found are the heterofermentative lactobacilli: *Lactobacillus collinoides* (Carr & Davies, 1972; Dueñas *et al.*, 1995; Claisse & Lonvaud-Funel, 2000; Sauvageot *et al.*, 2000; Garai *et al.*, 2007), *Lactobacillus paracollinoides* (Whiting & Carr, 1957), *Lactobacillus fermentum* (Carr & Davies, 1972; Dellaglio *et al.*, 2004), *Lactobacillus buchneri*, *Lactobacillus viridescens*, and *Lactobacillus hilgardii* (Carr & Davies, 1972), *Lactobacillus diolivorans*, *Lactobacillus plantarum* and *Lactobacillus suebicus* (Kleynmans *et al.*, 1989;

Abbreviations: ANI, average nucleotide identity; DDH, DNA–DNA hybridization; EPS, exopolysaccharides; LAB, lactic acid bacteria; MLF, malolactic fermentation; RAPD, randomly amplified polymorphic DNA; UPMGA, unweighted pair group method with arithmetic averages.

The GenBank/EMBL/DDJB accession number for the 16S rRNA gene sequence of strain CUPV261^T (=CECT 8227^T) is HG794492. Shotgun genome raw sequence data generated for this strain in this study is publicly available at the Sequence Read Archive (SRA) repository under study accession PRJEB5073 and run accession ERR385820.

Two supplementary figures and a supplementary table are available with the online version of this paper.

Marieta *et al.*, 2009). In natural cider from Basque Country, microbiological stabilization is not performed after MLF or before bottling. As a result, LAB becomes predominant in the microbiota, being able to promote detrimental effects, such as the alteration known as oiliness or ropiness (Dueñas *et al.*, 1995). This alteration is the consequence of exopolysaccharides (EPS) produced by some *Lactobacillus* sp. (Dueñas *et al.*, 1995), *Pediococcus parvulus* (Dueñas-Chasco *et al.*, 1997), *Lactobacillus diolivorans* (Dueñas-Chasco *et al.*, 1998), and *Oenococcus oeni* strains (Ibarburu *et al.*, 2007), increasing the consistency of the beverage, which causes important economic losses in the Basque Country cider industry. However, EPS-producing LAB are becoming industrially important micro-organisms for elaboration of functional food products, since they provide thickening properties and contribute to improve the texture and mouth-feel of the resulting fermented products. In this context, we have previously found that an EPS-producing strain of *Lactobacillus suebicus* isolated from cider is a potential candidate for the production of functional foods (Garai-Ibabe *et al.*, 2010). Moreover, certain EPS produced by LAB have beneficial effects on human health (Ruas-Madiedo *et al.*, 2008).

Strains CUPV261^T and CUPV262 were isolated from ropy natural ciders according to the methods described by Dueñas *et al.* (1994). We chose those colonies that showed 'ropy' phenotype in de Man, Rogosa and Sharpe (MRS) agar (Pronadisa). The colonies formed long filaments after being touched with the loop. The strains exhibited a ropy appearance in liquid culture and the cell deposit formed a long string upon agitation. Strains CUPV261^T and CUPV262 were preserved frozen at -80 °C in 20% (v/v) glycerol. Phenotypic characterization of strains was done following standardized methods. Morphological, cultural and biochemical testing according to standard techniques were performed at 28 °C unless otherwise stated. Catalase activity was assessed by bubble production after adding a drop of 10% (v/v) H₂O₂ solution. Gas production from glucose and gluconate was determined in MRS broth provided with 2% (w/v) of the carbohydrate and Durham tubes (Mañes-Lázaro *et al.*, 2008). Production of dextran from sucrose was assessed on MRS agar in which glucose was replaced with 5% (w/v) sucrose. The effects of temperature and various initial pH levels were tested in MRS broth for 5 days. Resistance to NaCl and ethanol was examined after 5 days incubation at 28 °C in MRS broth containing 5% (w/v) NaCl or 10% (v/v) ethanol. Biochemical characteristics were determined with the API 50CH, rapid ID32 STREP and API ZYM galleries (bioMérieux) according to the manufacturer's instructions. An increase in the viscosity of the medium was observed when cells were grown in a MRS-based broth (without glucose and meat extract at pH 6.2 and containing 0.04% (w/v) chlorophenol red) supplemented with 2% (w/v) of glucose, trehalose, fructose or sucrose, but not with galactose, maltose or lactose. Results are reported in the species description and summarized in Table 1.

Genomic DNA of strains CUPV261^T and CUPV262 was extracted and purified with the DNeasy Blood & Tissue kit (Qiagen) supplemented with mutanolysin 2 U µl⁻¹ (Sigma-Aldrich). DNA templates were amplified by PCR using three primers: flanking primers 616V and 630R (Ehrmann *et al.*, 2003) and internal primer 699R (Arahal *et al.*, 2008) to obtain two large fragments (1466 pb and 1009 pb) of the 16S rRNA gene. The PCR products were purified using a NucleoSpin Gel and PCR Clean-up kit (Macherey-Nagel) according to the manufacturer's instructions. Subsequent sequencing reactions were done on an Abi Prism 3730 automated sequencer using the Big Dye Terminator v3.1 cycle sequencing kit, premixed format. Sequencing primers were the same ones used in the amplification reaction but diluted ten-fold (5 pmol). The new sequences were identical (100% similarity) to each other so for the rest of the text we refer only to the sequence of strain CUPV261^T. The isolates were identified using the EzTaxon-e server (<http://eztaxon-e.ezbiocloud.net/>; Kim *et al.*, 2012) and the highest level of pairwise similarity was obtained with the type strain of *Lactobacillus vini* CECT 5924^T (99.1%), followed by *Lactobacillus satsumensis* NRIC 0604^T (96.4%) and *Lactobacillus oeni* 59b^T (96.2%).

The new sequence was compared with public sequences in the EMBL gene databases using the BLAST program (National Center for Biotechnology Information; <http://www.ncbi.nlm.nih.gov/>). Related sequences were further analysed using the ARB program package (Ludwig *et al.*, 2004; <http://www.arb-home.de>) using alternative treeing methods (maximum-parsimony, maximum-likelihood and distance matrix) and data subsets. Automated sequence alignments were corrected manually using the ARB_EDIT sequence editor and alignments retrieved from SILVA and LTP latest updates were also used as references (Pruesse *et al.*, 2007; Yarza *et al.*, 2010). The analysis of the 16S rRNA gene sequence showed that strain CUPV261^T forms a very stable pair with *Lactobacillus vini* CECT 5924^T and both of them with the pair formed by the type strains of *Lactobacillus ghanensis* and *Lactobacillus nagelii*. Bootstrap support to these nodes was maximal and the same topology was retrieved in different reconstructions (Fig. 1 and Figs S1 and S2, available in the online Supplementary Material). Other related species placed in the vicinity with high confidence are *Lactobacillus satsumensis*, *Lactobacillus oeni*, *Lactobacillus cacaonum*, *Lactobacillus mali*, *Lactobacillus hordei*, *Lactobacillus capillatus*, *Lactobacillus sucicola*, *Lactobacillus aquaticus* and *Lactobacillus uvarum*.

In addition, genotypic differentiation was approached by randomly amplified polymorphic DNA (RAPD) comparing the profiles with those of some reference strains: *Lactobacillus mali* CECT 4149, *Lactobacillus nagelii* CECT 5983^T, *Lactobacillus satsumensis* CECT 7371, *Lactobacillus uvarum* CECT 7335^T, *Lactobacillus vini* CECT 5924^T, *Lactobacillus vini* CECT 7072 and *Lactobacillus vini* CECT 7073. Analysis was performed using three universal primers: M13 (5'-GAGGGTGGCGGTTCT-3') (Pinto *et al.*, 2005), P1 (5'-ACGCGCCCT-3') and P2 (5'-ATGTAACGCC-3')

Table 1. Differential traits of strain CUPV261^T and strains of closely related species

Strains: 1, CUPV261^T; 2, *Lactobacillus vini* CECT 5924^T; 3, *Lactobacillus ghanensis* L489^T; 4, *Lactobacillus nagelii* CECT 5983^T; 5, *Lactobacillus satsumensis* CECT 7371; 6, *Lactobacillus oeni* CECT 7334^T; 7, *Lactobacillus uvarum* CECT 7335^T; 8, *Lactobacillus mali* CECT 4149. All data are from this study unless otherwise indicated. All strains were motile, catalase-negative and produced acid from D-mannose. Strain CUPV262 gave the same results as CUPV261^T except for fermentation of lactose (negative for CUPV262). +, Positive; -, negative; w, weakly positive; ND, no data available.

Characteristic	1	2	3*	4	5	6†	7	8
EPS formation from sucrose	+	-	-	+	+	+	+	+
Lactic acid isomer	DL	DL‡ ^a	DL	DL ^b	L ^c	L	L ^d	L ^e
Growth with/at:								
5 % NaCl	-	+	ND	+	+	+	+	-
15 °C	+	-	W	+	+	+	ND	+
45 °C	+	+	+	+	+	+	ND	-
Acid production from:								
L-Arabinose	-	+	-	-	-	-	-	-
D-Ribose	-	+	-	+	-	-	-	-
D-Galactose	+	-	+	+	+	-	-	-
L-Sorbose	-	-	+	+	-	+	-	-
L-Rhamnose	-	-	+	+	-	-	-	-
D-Mannitol	-	-	+	+	+	+	+	+
D-Sorbitol	-	-	-	+	+	+	-	+
Methyl α -D-mannopyranoside	+	-	ND	-	-	-	-	-
Methyl α -D-glucofuranoside	-	-	-	+	+	+	+	-
N-Acetylglucosamine	-	+	+	+	W	+	W	+
Amygdalin	-	+	+	+	+	-	+	+
Aesculin ferric citrate	-	+	+	+	+	-	+	+
Cellobiose	-	+	+	+	+	-	+	+
Maltose	W	+	-	+	-	-	-	+
Lactose	+	-	-	-	-	-	-	+
Melibiose	-	-	-	+	-	-	-	-
Melezitose	-	-	-	-	-	-	-	+
β -Gentiobiose	-	+	-	+	+	-	+	+
Turanose	-	-	-	-	+	-	+	-
D-Tagatose	+	-	-	+	+	-	-	-
D-Arabitol	-	+	ND	-	-	-	-	-
DNA G + C content (mol%)	37.5	39.4 ^a	37.8	37.7*	40.0 ^c	37.2	36.1 ^d	32.5 ^e

*Data from Nielsen *et al.* (2007).

†Data from Mañes-Lázaro *et al.* (2009).

‡Data from: a, Rodas *et al.* (2006); b, Edwards *et al.* (2000); c, Endo & Okada (2005); d, Mañes-Lázaro *et al.* (2008); e, Kaneuchi *et al.* (1988).

(Simpson *et al.*, 2002). The banding patterns of each strain obtained after the three amplifications were combined, and analysed with BioNumerics 2.5 software (Applied Maths) using the Dice coefficient and the unweighted pair group method with arithmetic averages (UPGMA) (Fig. 2). Strains CUPV261^T and CUPV262 clustered together at 83.17 % similarity, suggesting they pertain to the same species but are not clones; and joined with the reference strains at 20.51 % similarity, supporting they belong to a separate species. The calculated global cophenetic correlation value for the global analysis was 92 indicating a good level of reliability.

Although the results of RAPD fingerprinting were clear, we wanted to reinforce the genetic evidence that strain CUPV261^T and the type strain of *Lactobacillus vini* belong

to different species in spite of sharing 99.12 % 16S rRNA sequence similarity. It has been recently proposed that DNA-DNA hybridization (DDH) determinations, the gold standard of prokaryotic species definition, may be substituted by a comparison between sequenced genomes of the case strains, by using the average nucleotide identity (ANI) index applied to a minimum of 20 % of the randomly sequenced complete genome (Richter & Rosselló-Móra, 2009). Therefore, a random partial genome pyrosequencing approach was performed on strain CUPV261^T as previously reported (Lucena *et al.*, 2012a) using a GS-Junior (Roche) sequencing instrument at the Central Service of Support to Experimental Research (SCSIE) of the University of Valencia. Subsequent assembly produced 1.73 Mb (978 contigs); this represents 66 % of the estimated genome size. Calculation of ANI according to MUMmer (ANIm) and

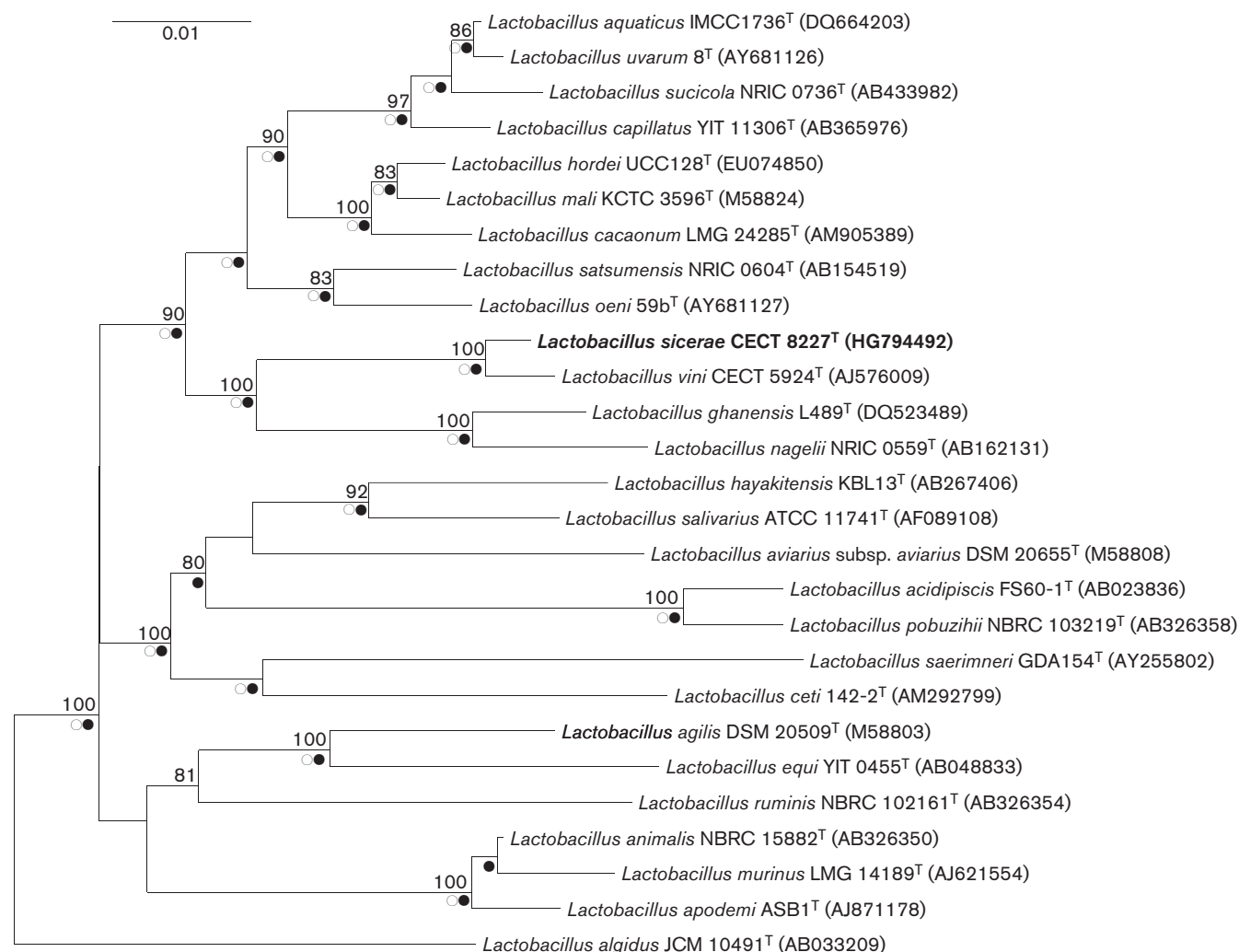


Fig. 1. Neighbour-joining phylogenetic tree based on almost complete 16S rRNA gene sequences of strain CUPV261^T (=CECT 8227^T) and closely related species. GenBank accession numbers are given in parentheses. Bootstrap values >70% confidence are shown at branching points (percentage of 1000 resamplings). Open circles and filled circles indicate nodes coincident in the maximum-likelihood and maximum-parsimony trees, respectively. Bar, 0.01 substitutions per position.

BLAST (ANIb) between *Lactobacillus vini* DSM 20605^T (AHYZ01000001–AHYZ01000220) and assembled data of strain CUPV261^T was performed on JSpecies as described in Richter & Rosselló-Móra (2009) and references therein. The low values obtained (ANIb 87.50–87.65% and ANIm 88.69–88.71%) were well-below the proposed boundary (96%) for genomic species definition. The same conclusion can be obtained from the predicted DDH value (37.7%, well-below the 70% threshold) using BLAST+ and the recommended formula (identities/high-score segment pair's length) of the genome-to-genome distance calculator (GGDC2.0) (Meier-Kolthoff *et al.*, 2013). The genomic assembled sequence of strain CUPV261^T also allowed the determination of its DNA G+C content, which was 37.5 mol%.

Colonies grown on MRS agar plates at 28 °C, 5% CO₂ after 6–7 days, were rubbery and bright, slightly convex, sometimes displayed a faint halo around, and measured just over 1 mm in diameter. Cells were rods occurring singly, in couples or in short chains. Bacterial suspensions were vitrified and imaged by cryo-transmission electron microscopy (cryo-TEM) and rods with a mean size of $0.52 \pm 0.10 \times 2.71 \pm 0.72 \mu\text{m}$ and an apical flagellum were observed (Fig. 3). One drop of the 48 h culture in MRS broth was vitrified by rapid freezing in liquid ethane using a Vitrobot Mark IV (FEI). This vitrified sample grid was transferred through 655 Turbo Pumping Station (Gatan) to a 626 DH Single Tilt Liquid Nitrogen Cryo-holder (Gatan), where it was maintained at approximately $-180 \text{ }^\circ\text{C}$. Copper grid (300 mesh Quantifoils) was hydrophilized by

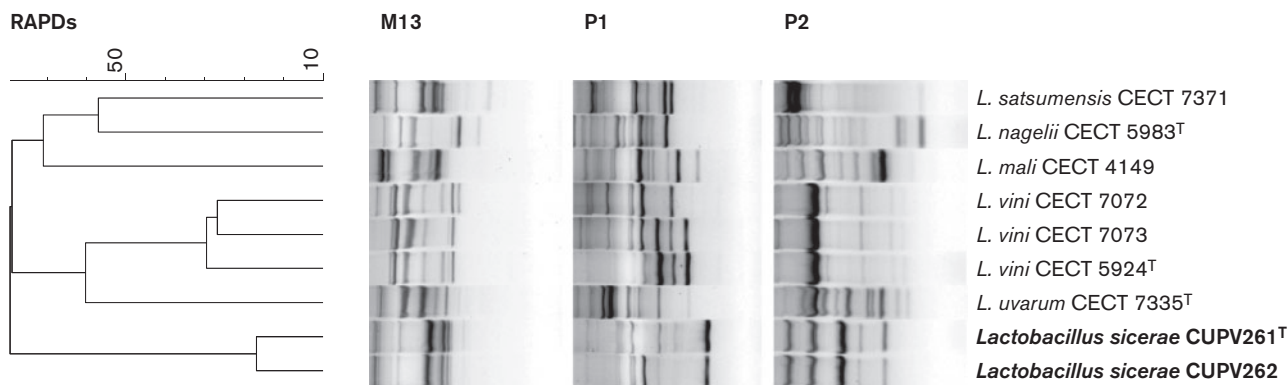


Fig. 2. Dendrogram derived from UPGMA cluster analysis based on the combined similarity matrix obtained from the M13, P1 and P2 RAPD fingerprinting. The tracks show the processed band patterns corresponding to RAPD M13, P1, and P2 after conversion, normalization, and subtraction of the background.

glow-discharge treatment. The sample was examined in a transmission electron microscope (TECNAI G2 20 TWIN; FEI) operating at an accelerating voltage of 200 KeV in a bright-field and low-dose image mode.

Strains CUPV261^T and CUPV262 were Gram-stain positive, facultatively anaerobic, non-spore-forming and catalase-negative lactobacilli. The strains grew in MRS broth at pH 3.7, 4.5 or 8.0 (28 °C). Growth occurred at 15–45 °C, but not at 5 °C (pH 5.5). Cells could grow with 10 % (v/v) ethanol, but not with 5 % (w/v) NaCl. The strains are obligately homofermentative: they form DL-lactate from glucose but not gas from glucose, and they do not ferment gluconate. The isomers of lactic acid were determined by the

L-lactic kit (ENOLOGY; BioSystems) and by HPLC (Velasco *et al.*, 2009), with the molar ratios of D-:L-lactic acid being 1:0.85. When malate and glucose were available, the bacteria were able to transform L-malic acid into L-lactic acid, and citrate utilization was also observed. In addition, cellular fatty acid composition was obtained at CECT following previously described procedures (Lucena *et al.*, 2012b). The fatty acid profiles of strains CUPV261^T and *Lactobacillus vini* CECT 5924^T contained the same fatty acids but with different relative abundance allowing their differentiation (Table 2). Differences were pronounced for C_{16:0}, C_{19:1ω7c/ω6c}, C_{18:1ω9c} and C_{14:0}. In addition, *Lactobacillus vini* CECT 5924^T contained a larger fraction of saturated fatty acids than strain CUPV261^T.

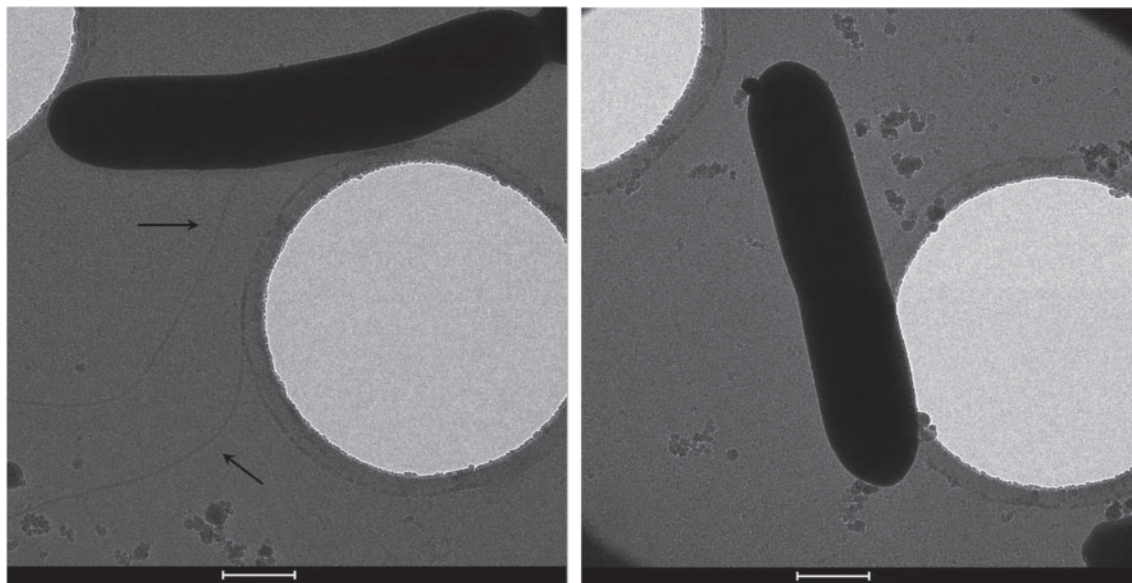


Fig. 3. Photographs taken by Cryo-TEM of strain CUPV261^T cultured in MRS broth. Arrows indicate a long apical flagellum. Bars, 500 nm.

Table 2. Comparison of cellular fatty acid contents (%) of strain CECT 8227^T and *Lactobacillus vini* CECT 5924^T (cells grown on MA, 48 h, 28 °C)

Data from this study (mean values of at least three replicates, carried out according to the Microbial Identification System, Microbial ID).

Cellular fatty acid	CECT 8227 ^T	<i>Lactobacillus vini</i> CECT 5924 ^T
Saturated		
C _{12:0}	1.1	1.0
C _{14:0}	5.3	10.0
C _{16:0}	12.4	26.4
C _{18:0}	2.8	2.0
Unsaturated		
C _{18:1ω9c}	40.0	30.7
Sum In Feature		
3 (C _{16:1ω7c} /C _{16:1ω6c})	3.9	5.1
7 (C _{19:1ω7c} /C _{19:1ω6c})	29.9	17.2
8 (C _{18:1ω7c} /C _{18:1ω6c})	4.6	7.6

Unlike the closest phylogenetic neighbour, strains CUPV261^T and CUPV262 were unable to utilize pentoses when tested in API 50 CHL galleries and in MRS-chlorophenol red fermentation broth supplemented with 2% (w/v) pentoses, following incubation. Table 1 contains further descriptive traits that permit a readily distinction of the novel isolates from related species including, among others, the ability to form EPS from sucrose, the isomer of lactic acid produced in fermentation, and the profile of fermentative substrates. In addition, strains CUPV261^T and CUPV262 showed less reactivity compared to *Lactobacillus vini* CECT 5924^T in miniaturized systems rapid ID32 STREP and API ZYM (Table S1).

Based on the data provided, strains CUPV261^T and CUPV262 represent a novel species of the genus *Lactobacillus*, for which the name *Lactobacillus sicerae* sp. nov. is proposed.

Description of *Lactobacillus sicerae* sp. nov.

Lactobacillus sicerae (si'ce.rae. L. fem. gen. n. *sicerae* of cider).

Cells are Gram-stain positive, non-spore-forming rods measuring $0.52 \pm 0.10 \times 2.71 \pm 0.72$ µm. Cells are found singly, in pairs and in short chains, and are motile with polar flagella (Fig. 3). Facultatively anaerobic and catalase-negative. Colonies on MRS agar after 6 days incubation at 28 °C are rubbery and bright, slightly convex, white, sometimes surrounded by a faint halo, and measure just over 1 mm in diameter. Growth occurs from 15 to 45 °C, at pH 3.7, pH 8.0, and with 10% ethanol. Growth does not occur at 5 °C, and 5% NaCl inhibits growth. Produces EPS from sucrose. Obligately homofermentative. DL-Lactic acid is the sole product from glucose fermentation (ratio 1:0.85). Both malic and citric acids are utilized in the presence of glucose. Aesculin and arginine are not hydrolysed. Acid is produced from D-galactose, D-glucose, D-fructose,

D-mannose, methyl α-D-mannopyranoside, arbutin, salicin, maltose (weak), lactose (strain CUPV261^T), sucrose, trehalose and D-tagatose, but not from glycerol, erythritol, D-arabinose, L-arabinose, D-ribose, D-xylose, L-xylose, D-adonitol, methyl β-D-xylopyranoside, L-sorbose, L-rhamnose, dulcitol, inositol, D-mannitol, D-sorbitol, methyl α-D-glucopyranoside, N-acetylglucosamine, amygdalin, aesculin, cellobiose, melibiose, inulin, melezitose, raffinose, starch, glycogen, xylitol, β-gentiobiose, turanose, D-lyxose, D-fucose, L-fucose, D-arabitol, L-arabitol, potassium gluconate, 2-ketogluconate or 5-ketogluconate. Results in rapid ID 32 STREP and API ZYM tests are given in Table S1.

The type strain, CUPV261^T (=CECT 8227^T=KCTC 21012^T), was isolated from a ropy natural cider of the Basque Country, Spain, in 2007. The DNA G+C content of the type strain is 37.5 mol% and the predominant cellular fatty acids are C_{18:1ω9c}, C_{19:1ω7c}/C_{19:1ω6c} and C_{16:0}. An additional strain of the species is CUPV262.

Acknowledgements

This study was supported by grants from the Spanish Ministry of Science and Innovation (grant nos AGL2009-12998-C03, AGL2012-40084-C03 and CSD2007-00063), the Basque Government (no. IT335-10) and the Generalitat Valenciana (PROMETEO/2012/040). A. I. P. acknowledges the 'Gobierno Vasco, Dpto. Agricultura, Pesca y Alimentación' for the fellowship. We also thank Microscopy: Polymer Characterization Service (SGIker) from the University of the Basque Country.

References

- Arahal, D. R., Sánchez, E., Macián, M. C. & Garay, E. (2008). Value of *recN* sequences for species identification and as a phylogenetic marker within the family "Leuconostocaceae". *Int Microbiol* **11**, 33–39.
- Beech, F. W. & Carr, J. G. (1977). Cider and Perry. In *Alcoholic Beverages*, vol. 1, pp.139–313. Edited by A. H. Rose. London: Academic Press.
- Carr, J. G. & Davies, P. A. (1970). Homofermentative Lactobacilli of ciders including *Lactobacillus mali* nov. spec. *J Appl Bacteriol* **33**, 768–774.
- Carr, J. G. & Davies, P. A. (1972). The ecology and classification of strains of *Lactobacillus collinoides* nov. spec.: a bacterium commonly found in fermenting apple juice. *J Appl Bacteriol* **35**, 463–471.
- Claisse, O. & Lonvaud-Funel, A. (2000). Assimilation of glycerol by a strain of *Lactobacillus collinoides* isolated from cider. *Food Microbiol* **17**, 513–519.
- Dellaglio, F., Torriani, S. & Felis, G. E. (2004). Reclassification of *Lactobacillus cellobiosus* Rogosa *et al.* 1953 as a later synonym of *Lactobacillus fermentum* Beijerinck 1901. *Int J Syst Evol Microbiol* **54**, 809–812.
- Dueñas, M., Irastorza, A., Fernandez, K., Bilbao, A. & Huerta, A. (1994). Microbial populations and malolactic fermentation of apple cider using traditional and modified methods. *J Food Sci* **59**, 1060–1064.
- Dueñas, M., Irastorza, A., Fernandez, K. & Bilbao, A. (1995). Heterofermentative lactobacilli causing ropiness in Basque Country ciders. *J Food Prot* **58**, 76–80.
- Dueñas-Chasco, M. T., Rodríguez-Carvajal, M. A., Tejero Mateo, P., Franco-Rodríguez, G., Espartero, J. L., Irastorza-Iribas, A. &

- Gil-Serrano, A. M. (1997). Structural analysis of the exopolysaccharide produced by *Pediococcus damnosus* 2.6. *Carbohydr Res* **303**, 453–458.
- Dueñas-Chasco, M. T., Rodríguez-Carvajal, M. A., Tejero-Mateo, P., Espartero, J. L., Irastorza-Iribas, A. & Gil-Serrano, A. M. (1998). Structural analysis of the exopolysaccharides produced by *Lactobacillus* spp. G-77. *Carbohydr Res* **307**, 125–133.
- Edwards, C. G., Collins, M. D., Lawson, P. A. & Rodríguez, A. V. (2000). *Lactobacillus nagelii* sp. nov., an organism isolated from a partially fermented wine. *Int J Syst Evol Microbiol* **50**, 699–702.
- Ehrmann, M. A., Müller, M. R. A. & Vogel, R. F. (2003). Molecular analysis of sourdough reveals *Lactobacillus mindensis* sp. nov. *Int J Syst Evol Microbiol* **53**, 7–13.
- Endo, A. & Okada, S. (2005). *Lactobacillus satsumensis* sp. nov., isolated from mashes of shochu, a traditional Japanese distilled spirit made from fermented rice and other starchy materials. *Int J Syst Evol Microbiol* **55**, 83–85.
- Garai, G., Dueñas, M. T., Irastorza, A. & Moreno-Arribas, M. V. (2007). Biogenic amine production by lactic acid bacteria isolated from cider. *Lett Appl Microbiol* **45**, 473–478.
- Garai-Ibabe, G., Dueñas, M. T., Irastorza, A., Sierra-Filardi, E., Werning, M. L., López, P., Corbí, A. L. & Fernández de Palencia, P. (2010). Naturally occurring 2-substituted (1,3)-beta-D-glucan producing *Lactobacillus suebicus* and *Pediococcus parvulus* strains with potential utility in the production of functional foods. *Bioresour Technol* **101**, 9254–9263.
- Ibarburu, I., Soria-Díaz, M. E., Rodríguez-Carvajal, M. A., Velasco, S. E., Tejero-Mateo, P., Gil-Serrano, A. M., Irastorza, A. & Dueñas, M. T. (2007). Growth and exopolysaccharide (EPS) production by *Oenococcus oeni* 14 and structural characterization of their EPSs. *J Appl Microbiol* **103**, 477–486.
- Kaneuchi, C., Seki, M. & Komagata, K. (1988). Taxonomic study of *Lactobacillus mali* Carr and Davis 1970 and related strains: validation of *Lactobacillus mali* Carr and Davis 1970 over *Lactobacillus yamanashiensis* Nomomura 1983. *Int J Syst Bacteriol* **38**, 269–272.
- Kim, O. S., Cho, Y. J., Lee, K., Yoon, S. H., Kim, M., Na, H., Park, S. C., Jeon, Y. S., Lee, J. H. & other authors (2012). Introducing EzTaxon-e: a prokaryotic 16S rRNA gene sequence database with phylotypes that represent uncultured species. *Int J Syst Evol Microbiol* **62**, 716–721.
- Kleynmans, U., Heinzl, H. & Hammes, W. P. (1989). *Lactobacillus suebicus* sp. nov., an obligately heterofermentative *Lactobacillus* species isolated from fruit mashes. *Syst Appl Microbiol* **11**, 267–271.
- Laplace, J. M., Jacquet, A., Travers, I., Simon, J. P. & Auffray, Y. (2001). Incidence of land and physicochemical composition of apples on the qualitative and quantitative development of microbial flora during cider fermentations. *J Inst Brew* **107**, 227–233.
- Lucena, T., Ruvira, M. A., Arahall, D. R., Macián, M. C. & Pujalte, M. J. (2012a). *Vibrio aestivus* sp. nov. and *Vibrio quintilis* sp. nov., related to Marisflavi and Gazogenes clades, respectively. *Syst Appl Microbiol* **35**, 427–431.
- Lucena, T., Pujalte, M. J., Ruvira, M. A., Garay, E., Macián, M. C. & Arahall, D. R. (2012b). *Tropiciobacter multivorans* sp. nov., an aerobic alphaproteobacterium isolated from surface seawater. *Int J Syst Evol Microbiol* **62**, 844–848.
- Ludwig, W., Strunk, O., Westram, R., Richter, L., Meier, H., Yadhukumar, Buchner, A., Lai, T., Steppi, S. & other authors (2004). ARB: a software environment for sequence data. *Nucleic Acids Res* **32**, 1363–1371.
- Mañes-Lázaro, R., Ferrer, S., Rosselló-Mora, R. & Pardo, I. (2008). *Lactobacillus uvarum* sp. nov.—a new lactic acid bacterium isolated from Spanish Bobal grape must. *Syst Appl Microbiol* **31**, 425–433.
- Mañes-Lázaro, R., Ferrer, S., Rosselló-Mora, R. & Pardo, I. (2009). *Lactobacillus oeni* sp. nov., from wine. *Int J Syst Evol Microbiol* **59**, 2010–2014.
- Marieta, C., Ibarburu, I., Dueñas, M. & Irastorza, A. (2009). Supramolecular structure and conformation of a (1→3)(1→2)-β-D-glucan from *Lactobacillus suebicus* CUPV221 as observed by tapping mode atomic force microscopy. *J Agric Food Chem* **57**, 6183–6188.
- Marshall, C. R. & Walkley, V. T. (1951). Some aspects of microbiology applied to commercial apple juice production. I. Distribution of microorganisms on the fruit. *J Food Sci* **16**, 448–456.
- Meier-Kolthoff, J. P., Auch, A. F., Klenk, H.-P. & Göker, M. (2013). Genome sequence-based species delimitation with confidence intervals and improved distance functions. *BMC Bioinformatics* **14**, 60.
- Nielsen, D. S., Schillinger, U., Franz, C. M., Bresciani, J., Amoa-Awua, W., Holzapfel, W. H. & Jakobsen, M. (2007). *Lactobacillus ghanensis* sp. nov., a motile lactic acid bacterium isolated from Ghanaian cocoa fermentations. *Int J Syst Evol Microbiol* **57**, 1468–1472.
- Pinto, B., Chenoll, E. & Aznar, R. (2005). Identification and typing of food-borne *Staphylococcus aureus* by PCR-based techniques. *Syst Appl Microbiol* **28**, 340–352.
- Pruesse, E., Quast, C., Knittel, K., Fuchs, B. M., Ludwig, W., Peplies, J. & Glöckner, F. O. (2007). SILVA: a comprehensive online resource for quality checked and aligned ribosomal RNA sequence data compatible with ARB. *Nucleic Acids Res* **35**, 7188–7196.
- Richter, M. & Rosselló-Móra, R. (2009). Shifting the genomic gold standard for the prokaryotic species definition. *Proc Natl Acad Sci U S A* **106**, 19126–19131.
- Rodas, A. M., Chenoll, E., Macián, M. C., Ferrer, S., Pardo, I. & Aznar, R. (2006). *Lactobacillus vini* sp. nov., a wine lactic acid bacterium homofermentative for pentoses. *Int J Syst Evol Microbiol* **56**, 513–517.
- Ruas-Madiedo, P., Abraham, A. G., Mozzi, F. & de los Reyes-Gavilán, C. G. (2008). Functionality of exopolysaccharides produced by lactic acid bacteria. In *Molecular Aspects of Lactic Acid Bacteria for Traditional and New Applications*, pp. 137–166. Edited by B. Mayo, P. López & G. Pérez-Martínez. Kerala, India: Research Signpost.
- Salih, A. G., Le Quéré, J. M., Drilleau, J. F. & Moreno, J. (1990). Lactic acid bacteria and malolactic fermentation in the manufacture of Spanish cider. *J Inst Brew* **96**, 369–372.
- Sauvageot, N., Gouffi, K., Laplace, J. M. & Auffray, Y. (2000). Glycerol metabolism in *Lactobacillus collinoides*: production of 3-hydroxypropionaldehyde, a precursor of acrolein. *Int J Food Microbiol* **55**, 167–170.
- Simpson, P. J., Stanton, C., Fitzgerald, G. F. & Ross, R. P. (2002). Genomic diversity within the genus *Pediococcus* as revealed by randomly amplified polymorphic DNA PCR and pulsed-field gel electrophoresis. *Appl Environ Microbiol* **68**, 765–771.
- Velasco, S. E., Areizaga, J., Irastorza, A., Dueñas, M. T., Santamaría, A. & Muñoz, M. E. (2009). Chemical and rheological properties of the beta-glucan produced by *Pediococcus parvulus* 2.6. *J Agric Food Chem* **57**, 1827–1834.
- Weiss, N., Schillinger, U. & Kandler, O. (1983). *Lactobacillus lactis*, *Lactobacillus leichmannii* and *Lactobacillus bulgaricus*, subjective synonyms of *Lactobacillus delbrueckii*, and description of *Lactobacillus delbrueckii* subsp. *lactis* comb. nov. and *Lactobacillus delbrueckii* subsp. *bulgaricus* comb. nov. *Syst Appl Microbiol* **4**, 552–557.
- Whiting, G. C. & Carr, J. G. (1957). Chlorogenic acid metabolism in cider fermentation. *Nature* **180**, 1479.
- Yarza, P., Ludwig, W., Euzéby, J., Amann, R., Schleifer, K. H., Glöckner, F. O. & Rosselló-Móra, R. (2010). Update of the All-Species Living Tree Project based on 16S and 23S rRNA sequence analyses. *Syst Appl Microbiol* **33**, 291–299.

Draft Genome Sequence of *Lactobacillus collinoides* CUPV237, an Exopolysaccharide and Riboflavin Producer Isolated from Cider

Ana Isabel Puertas,^a Vittorio Capozzi,^b María Goretti Llamas,^a Paloma López,^c Antonella Lamontanara,^d Luigi Orrù,^d Pasquale Russo,^b Giuseppe Spano,^b María Teresa Dueñas^a

Department of Applied Chemistry, University of Basque Country (UPV/EHU), San Sebastián, Spain^a; Department of Agriculture, Food and Environment Sciences, University of Foggia, Foggia, Italy^b; Department of Molecular Microbiology and Infection Biology, Centro de Investigaciones Biológicas (C.S.I.C.), Madrid, Spain^c; Council for Agricultural Research and Economics (CREA)-Genomics Research Centre, Fiorenzuola d'Arda (PC), Italy^d

***Lactobacillus collinoides* CUPV237 is a strain isolated from a Basque cider. *Lactobacillus collinoides* is one of the most frequent species found in cider from Spain, France, or England. A notable feature of the *L. collinoides* CUPV237 strain is its ability to produce exopolysaccharides.**

Received 29 April 2016 Accepted 2 May 2016 Published 9 June 2016

Citation Puertas AI, Capozzi V, Llamas MG, López P, Lamontanara A, Orrù L, Russo P, Spano G, Dueñas MT. 2016. Draft genome sequence of *Lactobacillus collinoides* CUPV237, an exopolysaccharide and riboflavin producer isolated from cider. *Genome Announc* 4(3):e00506-16. doi:10.1128/genomeA.00506-16.

Copyright © 2016 Puertas et al. This is an open-access article distributed under the terms of the [Creative Commons Attribution 4.0 International license](https://creativecommons.org/licenses/by/4.0/).

Address correspondence to María Teresa Dueñas, mariateresa.duenas@ehu.es.

Lactobacillus collinoides CUPV237 is a strain isolated from a Basque cider at the Department of Applied Chemistry, Faculty of Chemistry (University of the Basque Country UPV/EHU, San Sebastián, Spain). In the Basque Country (Northern Spain), natural cider is produced in small factories using traditional techniques, normally using juices obtained from many varieties of fresh cider apples (bitter, bittersweet, and sweet) to obtain a balanced content of sugars, acids, and polyphenols, without the addition of extra sugar or CO₂. Alcoholic and malolactic fermentations occur spontaneously due to the indigenous yeasts and lactic acid bacteria present in the musts (1–3). The microbial decarboxylation of L-malic acid into L-lactic acid is of great importance from an organoleptic point of view, and most of the lactic acid bacteria isolated from cider have this capacity (1, 4–7). *Lactobacillus collinoides* is one of the most frequent species found in cider from Spain, France, or England (5, 8–10). A notable feature of the *L. collinoides* CUPV237 strain is its ability to produce exopolysaccharides.

Using the TruSeq DNA sample prep kit FC-121-1001 according to the manufacturer's instructions, 2 μg of genomic DNA of *L. collinoides* was subjected to library preparation. Whole-genome sequencing was performed using the Illumina GAIIx platform at the CREA Genomics Research Centre (Fiorenzuola d'Arda). A total of 8,107,203 paired-end reads ranging from 90 to 115 bp in length were *de novo* assembled using CLC Genomics Workbench v7.0. The assembly resulted in 127 contigs with an N₅₀ length of 70,285 bp. The shortest contig was 203 bp and the longest was 243,224 bp. The draft genome consists of 3,707,616 bp. The genome sequence was annotated using the NCBI Prokaryotic Genome Annotation Pipeline (http://www.ncbi.nlm.nih.gov/genome/annotation_prok).

Nucleotide sequence accession numbers. This whole-genome shotgun project has been deposited at DDBJ/ENA/GenBank under the accession number [JYDC00000000](https://www.ncbi.nlm.nih.gov/nuclink/JYDC00000000). The version described in this paper is version JYDC01000000.

ACKNOWLEDGMENTS

This study was supported by grants from the Spanish Ministry of Science and Innovation (AGL2012-40084-C03 and AGL2015-65010-C3-1-R) and the Basque Government (IT866-13). V.C. was supported by a grant from the Apulian Region in the framework of the "FutureInResearch" program (practice code 9OJ4W81).

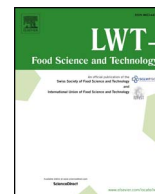
FUNDING INFORMATION

This work, including the efforts of Ana Isabel Puertas, was funded by Spanish Ministry of Science and Innovation (AGL2012-40084-C03 and AGL2015-65010-C3-1-R). This work, including the efforts of Ana Isabel Puertas, was funded by Basque Government (IT866-13). This work, including the efforts of Vittorio Capozzi, was funded by the Apulian Region in the framework of "FutureInResearch" program (practice code 9OJ4W81).

REFERENCES

1. Dueñas M, Irastorza A, Fernández K, Bilbao A, Huerta A. 1994. Microbial populations and malolactic fermentation of apple cider using traditional and modified methods. *J Food Sci* 59:1060–1064. <http://dx.doi.org/10.1111/j.1365-2621.1994.tb08190.x>.
2. Del Campo G, Santos JI, Berregi I, Velasco S, Ibarburu I, Dueñas MT, Irastorza A. 2003. Ciders produced by two types of presses and fermented in stainless steel and wooden vats. *J Inst Brewing* 109:342–348. <http://dx.doi.org/10.1002/j.2050-0416.2003.tb00608.x>.
3. Del Campo G, Berregi I, Santos JI, Dueñas M, Irastorza A. 2008. Development of alcoholic and malolactic fermentations in highly acidic and phenolic apple musts. *Bioresour Technol* 99:2857–2863. <http://dx.doi.org/10.1016/j.biortech.2007.06.007>.
4. Velasco SE, Yebra MJ, Monedero V, Ibarburu I, Dueñas MT, Irastorza A. 2007. Influence of the carbohydrate source on β-glucan production and enzyme activities involved in sugar metabolism in *Pediococcus parvulus* 2.6. *Int J Food Microbiol* 115:325–334. <http://dx.doi.org/10.1016/j.jifoodmicro.2006.12.023>.
5. Sánchez A, Rodríguez R, Coton M, Coton E, Herrero M, García LA, Díaz M. 2010. Population dynamics of lactic acid bacteria during spontaneous malolactic fermentation in industrial cider. *Food Res Int* 43:2101–2107. <http://dx.doi.org/10.1016/j.foodres.2010.07.010>.
6. Puertas AI, Arahal DR, Ibarburu I, Elizaquível P, Aznar R, Dueñas MT. 2014. *Lactobacillus sicerae* sp. nov., a lactic acid bacterium isolated from

- Spanish natural cider. *Int J Syst Evol Micr* **64**:2949–2955. <http://dx.doi.org/10.1099/ijss.0.059980-0>.
7. Ibarburu I, Puertas AI, Berregi I, Rodríguez-Carvajal MA, Prieto A, Dueñas MT. 2015. Production and partial characterization of exopolysaccharides produced by two *Lactobacillus suebicus* strains isolated from cider. *Int J Food Microbiol* **214**:54–62. <http://dx.doi.org/10.1016/j.ijfoodmicro.2015.07.012>.
 8. Werning ML, Ibarburu I, Dueñas MT, Irastorza A, Navas J, López P. 2006. *Pediococcus parvulus* gtf gene encoding the GTF glycosyltransferase and its application for specific PCR detection of β -D-glucan-producing bacteria in foods and beverages. *J Food Prot* **69**:161–169.
 9. Claisse O, Lonvaud-Funel A. 2000. Assimilation of glycerol by a strain of *Lactobacillus collinoides* isolated from cider. *Food Microbiol* **17**:513–519. <http://dx.doi.org/10.1006/fmic.2000.0342>.
 10. Carr JG, Davies PA. 1972. The ecology and classification of strains of *Lactobacillus collinoides* nov. spec.: a bacterium commonly found in fermenting apple juice. *J Appl Bacteriol* **35**:463–471. <http://dx.doi.org/10.1111/j.1365-2672.1972.tb03723.x>.



Disclosing diversity of exopolysaccharide-producing lactobacilli from Spanish natural ciders



Ana Isabel Puertas^a, Idoia Ibarburu^a, Patricia Elizaquivel^b, Andoni Zuriarrain^a, Iñaki Berregi^a, Paloma López^e, Alicia Prieto^e, Rosa Aznar^{b,c,d}, María Teresa Dueñas^{a,*}

^a Facultad de Ciencias Químicas, Universidad del País Vasco (UPV/EHU), Paseo Manuel de Lardizabal, 3, 2018, Donostia-San Sebastián, Spain

^b Colección Española de Cultivos Tipo (CECT), Burjassot, Spain

^c Departamento de Microbiología y Ecología, Universitat de València, Burjassot, Valencia, Spain

^d Instituto de Agroquímica y Tecnología de Alimentos (IATA), Consejo Superior de Investigaciones Científicas (CSIC), Burjassot, Valencia, Spain

^e Centro de Investigaciones Biológicas, Consejo Superior de Investigaciones Científicas, Ramiro de Maeztu 9, 28040, Madrid, Spain

ARTICLE INFO

Keywords:

Cider
Lactobacillus
Exopolysaccharides (EPS)
Ropy isolates

ABSTRACT

Lactic acid bacteria (LAB) are naturally occurring bacterial populations in traditional cider from the Basque Country (Spain), which is spontaneously fermented without starters. Some LAB are able to produce exopolysaccharides (EPS) thus causing viscosity, a cider spoilage called “ropiness” or “oiliness”. A total of 41 isolates recovered between 1992 and 2009 from ropy ciders of different cider factories were included in the present study. Identification by 16S rRNA gene sequencing, biochemical traits (API), RAPD-PCR using four universal primers (M13, M13V, P1 and P2) and 16S-23S ISRs amplification profiles revealed that the spoiler species were *L. collinoides*, *L. diolivorans*, *L. sicerae* and *L. suebicus*. EPS production in *L. collinoides* and *L. sicerae* strains approached by PCR amplification of *eps* genes encoding for homopolysaccharide and heteropolysaccharide revealed that these strains synthesize heteropolysaccharides and in addition, *L. collinoides* CUPV231 synthesizes a 2-branched (1,3)- β -D-glucan. The molecular weight of their EPS determined by HP-SEC revealed the presence of three polymers with average molecular weights (M_w) of around 10^6 g/mol, 10^4 g/mol and 10^3 g/mol. The middle-weight fraction was the most abundant except in *L. sicerae* CUPV261 which mainly produced the high M_w polymer.

1. Introduction

Natural cider from the Basque Country (Spain) is usually produced in small cider factories by using traditional techniques, and it is spontaneously fermented by indigenous LAB present in the musts (Del Campo et al., 2008; Dueñas, Irastorza, Fernández, Bilbao, & Huerta, 1994; Sánchez et al., 2010). Microbiological stabilization is not performed after malolactic fermentation (MLF) or before bottling and as result, LAB becomes predominant in the cider microbiota. Certain LAB isolated from cider and wine are able to produce exopolysaccharides (EPS), and their release to the culture medium strongly modifies the beverage rheological characteristics that might render products unpleasant to the palate. This alteration, called “ropiness” or “oiliness”, has also been described in red and white wines from the Bordeaux region in France. It was reported that *Pediococcus parvulus*, *Oenococcus oeni*, *Lactobacillus suebicus*, and *Lactobacillus diolivorans* strains isolated from ropy cider and wine (Dols-Lafargue et al., 2008; Dueñas-Chasco et al., 1997; Garai-Ibabe et al., 2010a; Ibarburu et al., 2007) synthesize a

characteristic homopolysaccharide (HoPS) 2-substituted- β -D-glucan. This β -glucan accumulates around the cells and forms a protective barrier, which confers to the ropy *P. parvulus* strains resistance to wine stress conditions (low pH, high ethanol or SO_2 concentrations) (Dols-Lafargue et al., 2008) and lysozyme treatment (Coulon, Houles, Dimopoulou, Maupeu, & Dols-Lafargue, 2012). The β -glucan also increases the adhesion of the β -glucan producing strains to abiotic and biotic surfaces (Dols-Lafargue et al., 2008; Fernández de Palencia et al., 2009; Garai-Ibabe et al., 2010b) and could provide a selective advantage for adhesion to fruit surfaces and beverage making equipment. LAB cider isolates can also synthesize other types of EPS [heteropolysaccharides (HePS) or other HoPS such as dextrans, which are α -glucans] (Dueñas et al. 1998; Ibarburu et al., 2015). Despite of spoilage, LAB EPS can also contribute to sensory characteristics such as mouth-feel and foaming of cider, in addition to the polysaccharides from raw material and yeasts (Mangas, Moreno, Rodríguez, Picinelli, & Suárez, 1999).

The aim of this work was to disclose the EPS-producing *Lactobacillus*

* Corresponding author.

E-mail address: mariateresa.duenas@ehu.eus (M.T. Dueñas).

Table 1
Strains used in the study.

Species	Source	Origin	Cider producer	Year of isolation
<i>Lactobacillus brevis</i> CECT 4121 ^T	CECT	Human faeces		
<i>L. collinoides</i> CECT 922 ^T	CECT	Fermenting apple juice		
CUPV238, CUPV239, CUPV2311, CUPV2312, CUPV2371	This study	Ropy cider	D	2009
CUPV236	CUPV	Cider	K	2003
CUPV231, CUPV232, CUPV234, CUPV235, CUPV2119, CUPV2328	CUPV	Spoiled cider	G	2000
CUPV2313, CUPV2315	This study	Ropy cider	H	2009
CUPV2317, CUPV2320, CUPV2322, CUPV2323, CUPV2324	This study	Ropy cider	I	2009
<i>L. diolivorans</i> LMG 19667 ^T	LMG	Maize silage		
CUPV213	CUPV	Ropy cider	A	1992
CUPV211, CUPV219, CUPV2112	CUPV	Cider	B	1992
CUPV212, CUPV214, CUPV215, CUPV216, CUPV217, CUPV 218 = G77, CUPV2110, CUPV 2111, CUPV2113	CUPV	Ropy cider	C	1992
CUPV2117, CUPV2118	CUPV	Spoiled cider	E	2003
CUPV2114, CUPV2115	CUPV	Cider	K	2003
<i>L. hilgardii</i> CECT 4786 ^T	CECT	Wine		
<i>L. mali</i> CECT 4149	CECT	Wine must		
<i>L. paracollinoides</i> CECT 5926, DSM 15502 ^T	CECT DSMZ	Beer Brewery environment		
<i>L. satsumensis</i> CECT 7371 ^T	CECT	Grape must		
<i>L. sicerae</i> CECT 8227 ^T = CUPV261 ^T , CUPV262	CUPV	Ropy cider	F	2009
<i>L. suebicus</i> CECT 5917 ^T	CECT	Apple mash		
CUPV225	CUPV	Ropy cider	E	2003
CUPV221	CUPV	Ropy cider	F	2003
CUPV226	CUPV	Ropy cider	J	2003
<i>L. uvarum</i> CECT 7335 ^T	CECT	Grape must		
<i>L. vini</i> CECT 5924	CECT	Fermenting grape must		

CUPV, Colección de la Universidad del País Vasco (Spain); CECT, Colección Española de Cultivo Tipo (Spanish Type Culture Collection, University of Valencia, Burjassot Spain); DSMZ, Leibniz Institute DSMZ-German Collection of Microorganisms and Cell Cultures (Braunschweig, Germany); LMG, BCCM/LMG Belgian Coordinated Collection of Microorganism (Brussels, Belgium).

isolated from cider which, despite causing spoilage in this beverage, might contribute to enhance organoleptic characteristics of cider or be useful for other food applications. On one hand, identification and genotypic differentiation was approached to trace the occurrence of spoiler strains. On the other hand, characterization of EPS produced by newly detected naturally occurring LAB species in ropy cider was carried out aiming at deeply analyzing the structural polysaccharides and genes associated with EPS synthesis.

2. Material and methods

2.1. Bacterial strains and culture conditions

The bacterial strains used in this work included 41 isolates from Spanish natural ciders and they belong to the genus *Lactobacillus*. Some of them were previously characterized: *L. diolivorans* G-77 (CUPV 218) (Dueñas et al. 1998); *L. suebicus* (CUPV 221, CUPV225, and CUPV226) (Garai-Ibabe et al., 2010a; Notararigo et al., 2013; Ibarburu et al., 2015); and *L. sicerae* (CUPV 261^T and CUPV 262) (Puertas et al., 2014). In addition, 12 reference strains representing 11 species (apart from *L. sicerae*) were also included for comparative purposes. Table 1 reports the species names and their sources. The isolates were recovered between 1992 and 2009 from ropy ciders of different factories that showed occurrence of spoilage. *Lactobacilli* included in this study were selected on the basis of the ropy phenotype exhibited by using the method described in Puertas et al. (2014); their colonies formed long filaments when touched with the loop, and also exhibited a ropy appearance in MRS broth. Strains were routinely cultured in de Man, Rogosa and Sharpe broth (MRS, De Man, Rogosa, & Sharpe, 1960) at pH 5.5 for 48 h at 28 °C in an atmosphere containing 5% CO₂, and stored in growth liquid medium containing 20% (v/v) glycerol at –80 °C.

For EPS isolation and quantification, strains were grown in a semi-defined-medium (SMD) at an initial pH of 5.5, according to Ibarburu et al. (2015). Batch fermentations without pH control were carried out in fully filled 250 mL screw-cap flasks for 65 h at 28 °C in an atmosphere containing 5% CO₂. Growth was monitored spectrophotometrically at 600 nm (OD600). Analysis of the fermentation products was carried out by HPLC as described by Ibarburu et al. (2015).

2.2. Identification and genotypic characterization

LAB strains were characterized by biochemical tests and PCR-based techniques. Carbohydrate utilization was determined with the API 50CH system (API bio-Mérieux, Marcy l'Etoile, France). API galleries were incubated for up to 7 days at 28 °C. Gas production from glucose and gluconate was determined in a modified MRS broth without citrate or meat extract and provided with 2% (w/v) of the carbohydrate and Durham tubes (Mañes-Lázaro et al., 2009).

Identification of isolates was approached by 16S rRNA gene partial sequencing as previously described in Ehrmann, Müller, and Vogel (2003). Genomic DNA was extracted and purified with the DNeasy[®] Blood & Tissue kit (Qiagen, Hilden, Germany) supplementing the enzymatic lysis buffer with lysozyme (30 mg/mL) and mutanolysin 2 U/μL (Sigma-Aldrich). The PCR products were purified using the QIAquick PCR purification kit (Qiagen, Hilden, Germany), according to the manufacturer's instructions. Sequences were obtained at the Sequencing and Genotyping Service (SGiker) of the University of the Basque Country (UPV/EHU) and they were analyzed using the EzTaxon-e server (<http://eztaxon-e.ezbiocloud.net/>; Kim et al., 2012).

Genomic diversity of the strains was analyzed by the randomly amplified polymorphic DNA (RAPD) method using four universal primers: M13 (5'-GAA ACA GCT ATG ACC ATG-3') (Pinto, Chenoll, & Aznar, 2005), P1 (5'-ACG CGC CCT-3') and P2 (5'-ATG TAA CGCC-3') (Simpson, Stanton, Fitzgerald, & Ross, 2002), and M13V (5'-GTT TTC CCA GTC AGC AC-3') (Ehrmann et al., 2003). In addition, amplification of 16S-23S ISRs with primers LA2-16S1F (5'-CACCCAAAGTCCGGTT CGG-3') and LA2-ITSMR (5'-GTTCTCGGCTTAATTACTG-3') was performed (Suzuki, Koyanagi, & Yamashita, 2004) to differentiate between *L. collinoides* and *L. paracollinoides*. PCR amplifications were conducted in duplicate with a final volume of 50 μL. Amplification products (20 μL) were electrophoresed on 1.9% (w/v) agarose gels at 80 V for 90 min. Gels were stained with ethidium bromide and photographed under U.V. light. Gel images were recorded using a Gel-Doc system (Bio-Rad) and stored as TIFF files.

The banding patterns of each strain obtained after the five

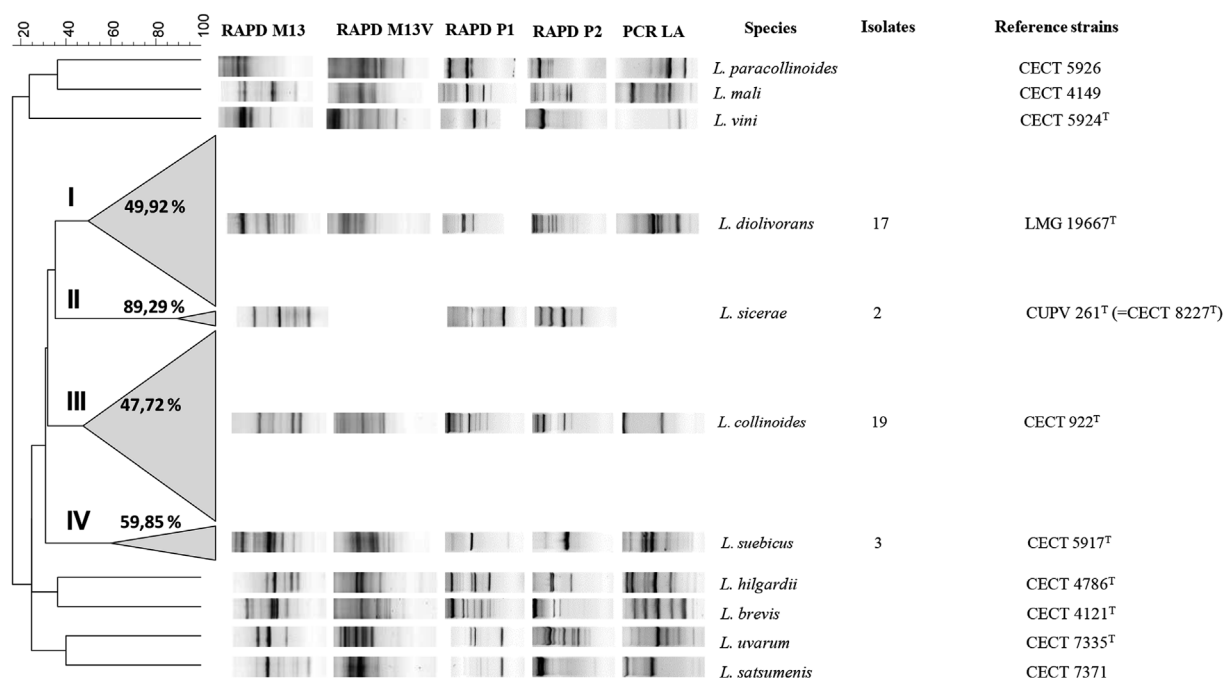


Fig. 1. Dendrogram derived from UPGMA cluster analysis based on the combined similarity matrix obtained from 16S-23S ISRs amplification profiles and RAPD-PCR using four universal primers (M13, M13V, P1 and P2) and API results corresponding to EPS-producing *Lactobacillus* isolates and reference strains. Strips show the combined representative profile for each cluster or strain after conversion, normalization, and subtraction of the background. The scale measures the percentage of similarity. Clusters are numbered.

amplifications were analysed with BioNumerics 2.5 software (Applied Maths) using the Pearson coefficient and the unweighted pair group method with arithmetic averages (UPGMA). Clustering of multiple data sets, combining banding patterns (RAPD M13, P1, P2, M13V and 16S-23S ISR) and API results on carbohydrate fermentations, was calculated taking averaged similarity values from the individual experiments with the aid of the “Composite data set” tool in BioNumerics.

2.3. PCR detection of the *eps* genes

Amplification reactions of the *eps* genes were performed using different primers targeting HoPS (*gtf*, *deg*, *lev*) and HePS (*epsD/E*, *epsA*, *epsB*, *epsEFG*, *epsF*) coding genes as previously described (Ibarburu et al., 2015). The PCR conditions were carried out according to the literature. The amplified products were purified by using the QIAquick Gel extraction kit (Qiagen, Hilden, Germany) in accordance with the manufacturer's recommendations. Both DNA strands of amplicons were sequenced and the predicted amino acid sequences were searched against the National Center of Biotechnology Information (NCBI) database by means of the BLASTP program available at the NCBI (<http://www.ncbi.nlm.nih.gov/>). Amino acid alignments were done using the ClustalW program (<http://www.ebi.ac.uk/Tools/msa/clustalw2/>).

2.4. Exopolysaccharide isolation and quantification

For quantification of EPS released to the culture media, *Lactobacillus* strains were grown in the SMD medium under the conditions described above. Bacterial cells were removed by centrifugation (12,000 × g, 20 °C, 30 min), and the EPS present in the supernatant was precipitated and recovered as previously described in Ibarburu et al. (2015). The concentration of EPS was estimated as neutral carbohydrate content determined by the phenol-sulphuric method (Dubois, Gilles, Hamilton, Rebers, & Smith, 1956), using glucose as standard. All determinations were made in triplicate. In addition, to obtain the EPS attached to the bacterial surface, strains were grown on agar-MRS for 7 days in an atmosphere containing 5% CO₂. The crude-EPS was collected from the biomass and purified as previously described by López et al., 2012. The

EPSs were frozen at −80 °C and lyophilized.

2.5. EPS molecular weight

The weight-average molecular weight (M_w) of the crude-EPS was determined by high-performance size exclusion chromatography (HPSEC) on an Agilent 1100 system (Hewlett-Packard, Germany) equipped with a PL-aquagel-OH guard column (8 μm, Agilent Technologies) and PL-aquagel-OH 40, 50, and 60 (Agilent Technologies) columns in series as described in Ibarburu et al. (2015).

3. Results and discussion

3.1. Identification and characterization of EPS-producing *Lactobacillus* strains

The ropy isolates included in this study are part of the CUPV collection, and were recovered from Spanish natural cider producers that suffered cider spoilage episodes (Table 1). Spoiled beverages from 2009 were additionally tested for the presence 2-substituted-(1,3)-β-D-glucan producing bacteria in cider (Ibarburu et al., 2010). Four ropy ciders gave a negative result, which indicated no β-glucan production, while 14 isolates showed ropy phenotype and are included in the present study.

The 41 cider strains, 6 previously identified and 35 new isolates, were obligate heterofermentative, producing CO₂, DL-lactate, acetate and ethanol from glucose. They were preliminarily identified by 16S rRNA coding gene sequencing (500 pb), and the isolates showed sequence similarity above 98% with *L. diolivorans* (17) and *L. collinoides*/*L. paracollinoides* (19). Since many LAB species have high 16S rRNA gene sequence similarity, i.e. *L. collinoides*/*L. paracollinoides*, their proper identification required additional tests. Therefore, 16S-23S ISRs amplification profiles and RAPD-PCR using four universal primers (M13, M13V, P1 and P2) were further approached to aid identification as well as to analyze the intraspecific genetic diversity of *Lactobacillus* isolates. The clustering analysis including reference strains and cider isolates was calculated individually for each RAPD and ISR-PCR profile

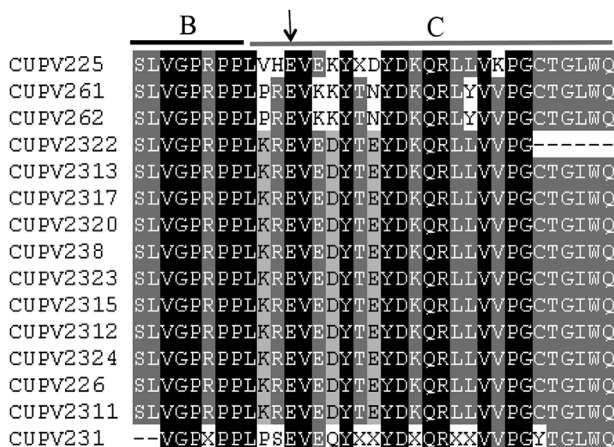


Fig. 2. Alignment of deduced amino acid sequences of PCR products obtained with PG primers. The letter X indicates an undetermined amino acid. Dark shading indicates identical amino acids, and light shading indicates conserved amino acids (only two different amino acids between strains); black arrow indicates a putative catalytic residue; dark and light line indicate two of the blocks in which the p-GT is divided (van Kranenburg et al., 1999).

and also by combining electrophoretic profiles and API results. The highest intraspecies differentiation was obtained with the combined RAPD, ISR-PCR and API profiles. Fig. 1 shows the dendrogram derived from UPGMA clustering including ropy cider isolates and reference strains. At 50% similarity four clusters were formed grouping cider isolates. Cluster I includes 17 isolates and the type strain of *L. diolivorans* LMG 19667^T; they were confirmed as members of the species by 99% 16S rRNA gene sequence similarity. Cluster II includes 2 isolates of *L. sicerae*, a new species described in another study (Puertas et al., 2014). Cluster III groups 19 isolates together with the type strain of the species *L. collinoides* CECT 922^T. This result corroborates their ascription to this species in addition to the ISR-PCR profiles, which allowed differentiation from *L. paracollinoides*. Cluster IV includes 3 isolates, the HePS-producing strains CUPV225 and CUPV226 (Ibarburu et al., 2015) and the O2-substituted (1,3)- β -D-glucan producing strain CUPV 221 (Garai-Ibabe et al., 2010b) previously identified as *L. suebicus*, and the reference strain *L. suebicus* CECT 5917^T. The RAPD analysis assessed the correct identification of isolates, which revealed that spoiler species were *L. diolivorans* in 1992, *L. collinoides* in 2000, these two species and *L. suebicus* in 2003, and *L. collinoides* and *L. sicerae* in 2009. The isolates analyzed were recovered from spoiled cider under demand of cider factories and only factory F was sampled in 2003 and 2009, the latter rendering the new species *L. sicerae* isolates. Therefore, there is no possibility to trace back the LAB species occurrence in each factory (Fig. S1). Nevertheless, *L. collinoides* and *L. diolivorans* were the main isolates recovered in three and two years, respectively, and they are the species most frequently associated with alterations and organoleptic defects in cider. Both species were related with bitterness production (via glycerol dehydratase pathway), which is characterized for an unpleasant bitter taste that is associated with the presence of acrolein combined to polyphenols (Garai-Ibabe et al., 2008). *L. collinoides* species was also implicated in phenolic off-flavour defects of ciders (Buron et al., 2012) that are due to volatile phenols (4-ethylcatechol, 4-ethylphenol and 4-ethylguaiaicol). In addition, *L. collinoides* strains isolated from Spanish and French ciders showed the ability to produce biogenic amines (Coton et al., 2010; Garai-Ibabe, Dueñas, Irastorza, & Moreno-Arribas, 2007). Intraspecific diversity analyzed by RAPD revealed differences between *L. suebicus* isolates, recovered from different cider factories, and separated *L. collinoides* isolates in three groups that clustered apart from the type strain; one included 2 isolates from 2000 and one from 2003, another 11 from 2009, and a third one, grouped 4 from 2000 and one from 2009.

3.2. PCR screening for HoPS and HePS genes

The presence of EPS coding genes in the ropy *L. collinoides* (12) and *L. sicerae* (2) isolates recovered in 2009 was assessed by PCR. No dextrans or levan producers could be detected using the primers targeting glucansucrase (*deg*) or levansucrase (*lev*) genes. PCR was also used to detect the presence of the *gtf* gene encoding the GTF glycosyltransferase, which catalyzes the synthesis of the 2-branched (1,3)- β -D-glucan (Werning et al., 2006). The expected amplicon was only detected in *L. collinoides* CUP V231, recovered in 2000. This strain agglutinated in the presence of anti-serotype 37 antibodies targeting the β -glucan (Garai-Ibabe et al., 2010a; Werning et al., 2014), suggesting that it was a 2-substituted-(1,3)- β -D-glucan producer. NMR and methylation analyses confirmed the β -glucan production (data not shown) along with other polysaccharides.

In addition, the presence of genes implicated in an essential step of bacterial HePS biosynthesis was sought using several sets of *eps* primers (*epsD/E*, *epsA*, *epsB*, *epsEFG*, *epsF*) previously described (Ibarburu et al., 2015). DNA from *L. collinoides* (12) and *L. sicerae* (2) isolates recovered in 2009 yielded only a 189-bp PCR product with the *epsD/E* primers, which amplifies the genes encoding the priming-glycosyltransferase (p-GTF) (Provencher, LaPointe, Sirois, Calsteren, & Roy, 2003). This enzyme catalyzes the transfer of the first phospho-sugar residue from an activated nucleotide sugar to the undecaprenyl phosphate-lipid carrier on the cytoplasmic face of the membrane in the first step of repeating unit synthesis of HePS (Lebeer et al., 2009). The predicted amino acid sequences of PCR products from *L. sicerae* strains showed identities above 77% (see Table S1 in the supplemental material) with respect to the partial sequence of EpsE protein of the HePS producer *Lactobacillus helveticus* CRL1176 (accession no. ABB59702.1, Mozzi et al., 2006). Nevertheless, *L. collinoides* strains showed identities ranging from 66% to 83% with EpsE protein of the HePS producer *L. fermentum* TDS030603 (accession no. BAI67356.1, Dan et al., 2009).

Similar to that described in HePS-producers belonging to the genera *Lactobacillus* and *Bifidobacterium* (Provencher et al., 2003; Ruas-Madiedo et al., 2007), the predicted amino acid sequences of the PCR products showed parts of two conserved blocks (Fig. 2), which are localized at the C-terminus of the p-GTF. Block B is involved in the interaction with the lipid carrier (Wang, Liu, & Reeves, 1996), and all sequences of block C of the HePS-producers isolated from cider contain a glutamate residue, which has been proposed as one of the catalytic residues in the p-GT of *Lactococcus lactis* (van Kranenburg, Vos, Van Swam, Kleerebezem, & DeVos, 1999).

Accordingly, all these data suggested that *L. collinoides* and *L. sicerae* strains recovered in 2009 synthesize HePS. In addition, *L. collinoides* CUPV 231 recovered in 2000 synthesizes the 2-branched (1,3)- β -D-glucan.

3.3. EPS production and molecular weight determinations

In previous studies, we described the EPS production by *L. diolivorans* G-77 (CUPV 218) and *L. suebicus* strains isolated from cider. *L. diolivorans* G-77 and *L. suebicus* CUPV221 synthesize the characteristic O-2-substituted (1,3)- β -D-glucan. Besides β -glucan, *L. diolivorans* G-77 synthesizes a (1,6)(1,2)- α -D-glucan (Dueñas et al. 1998). More recently, the HePS produced by two *L. suebicus* strains (CUPV 225 and CUPV226) were characterized (Ibarburu et al., 2015; Notararigo et al., 2013).

In the present study, we screened the EPS production and molecular weight of EPS produced by the ropy *L. collinoides* (12) and *L. sicerae* (2) isolates recovered in 2009. The EPS-producing *L. collinoides* and *L. sicerae* strains showed the characteristic ropy phenotype in MRS broth. However, some polysaccharide components of this complex medium, such as glucomannans in yeast extract, interfere with the EPS isolation procedure. Indeed, the analysis by HP-SEC of an extract from fresh MRS broth obtained by ethanol precipitation showed a very broad peak with a Mw of $1.29 \cdot 10^4$ g/mol and a polydispersity index of 4.89 (Mw/Mn,

Table 2

Growth characteristics and EPS production of *L. collinoides* and *L. sicerae* strains grown in SMD medium, and the molecular weight of their EPS fractions isolated from the cell biomass harvested from the surface of MRS-agar plates.

Strain	OD ₆₀₀	EPS (mg L ⁻¹)	pH	Mw (g/mol)			Ratio of fractions
				High	Medium	Low	
				(x10 ⁶)	(x 10 ⁴)	(x10 ³)	
<i>L. sicerae</i>							
CUPV261 ^T	1.36 ± 0.06	64.11 ± 4,66	4.48	2.26	1.69	4.49	4.9: 3.0: 2.0
CUPV262	1.72 ± 0.06	68.69 ± 3,65	4.21	–	2.77	4.10	0.0: 5.7: 4.3
<i>L. collinoides</i>							
CUPV2371	1.13 ± 0.07	37.98 ± 2.75	4.88	1.07	1.95	4.35	1.6: 6.5: 1.8
CUPV238	0.37 ± 0.01	7.91 ± 3.97	5.44	1.22	1.93	4.85	3.6: 6.6: 1.6
CUPV239	0.33 ± 0.01	7.14 ± 1.95	5.52	2.08	2.10	4.78	5.0: 4.6: 0.9
CUPV2311	0.28 ± 0.01	8.28 ± 3.83	5.66	1.76	2.07	4.21	5.0: 4.0: 1.0
CUPV2312	0.51 ± 0.01	7.91 ± 2.28	5.59	2.07	2.05	5.14	3.6: 4.8: 1.6
CUPV2313	0.26 ± 0.07	11.65 ± 3.57	5.55	1.41	2.26	5.04	2.5: 6.5: 9.4
CUPV2314	0.45 ± 0.03	10.84 ± 3.08	5.60	1.58	2.01	4.75	2.0: 6.9: 1.0
CUPV2317	0.76 ± 0.01	10.77 ± 2.00	5.54	1.65	2.02	4.87	2.5: 6.3: 1.2
CUPV2320	0.45 ± 0.01	10.91 ± 3.12	5.39	1.29	2.05	4.97	4.0: 5.0: 1.0
CUPV2322	0.44 ± 0.05	9.36 ± 5.44	5.43	1.21	2.02	4.76	3.2: 5.8: 1.1
CUPV2323	0.49 ± 0.05	8.72 ± 2.28	5.56	1.36	2.02	4.82	3.8: 5.2: 1.0
CUPV2324	0.32 ± 0.05	8.62 ± 2.25	5.51	1.89	2.00	4.48	2.7: 6.5: 0.8

Values are given as mean values ± standard deviations; Mw, weight-average molecular weight.

where Mw is the weight-average molar mass and Mn is the number-average molar mass). Due to this interference, the EPS producing ability of the *L. collinoides* (12) and *L. sicerae* (2) strains was tested in a SMD semi-defined-medium (Table 2) previously used to quantify EPS production (Ibarburu et al., 2015). Three strains (*L. sicerae* CUPV 261^T, CUPV 262 and *L. collinoides* CUPV 2371) were able to grow (Table 2) and to increase the viscosity of the medium as it was observed when touched with the loop. These strains yielded between 68.7 and 38.0 mg/L of EPS determined by the phenol-sulphuric method. The other strains exhibited a cell deposit that formed a long strip upon agitation. Therefore, due to the interference of the components of the MRS medium in the EPS-extraction, and the poor growth obtained in the semi-defined medium for the majority of the *L. collinoides* strains (Table 2), the EPSs were collected from cellular biomass harvested from agar-MRS plates (surface EPS).

Analysis of the surface EPS samples by HP-SEC revealed the presence of three peaks of different molecular weights (Table 2). The molecular weight distribution of the crude EPS was a high Mw-EPS with average M_w of around 10⁶ g/mol, a second polymer with an intermediate Mw (around 10⁴ g/mol), and a low Mw-polymer of around 10³ g/mol. In most of EPS the second fraction was the most abundant, although *L. sicerae* CUPV261 produced mainly the high Mw polymer.

The presence of several polymers in EPS has also been reported in other *Lactobacilli* (Baruah, Das, & Goyal, 2016; Ibarburu et al., 2015). It is also the case of the cider isolates *L. diolivorans* G77 and *O. oeni* I4 which, besides β-glucan, synthesize a (1,6) (1,2)-α-D-glucan (Dueñas et al. 1998), and two HePS (Ibarburu et al., 2007), respectively. In wine, HePS and β-glucan production has been also described for *O. oeni* strains as well as the HoPS synthesis from sucrose (dextrans or levans, which are β-fructans) (Dimopoulou et al., 2014; 2016). These authors showed the protective effect of either cell-linked HePS or dextrans during freeze drying of the malolactic *O. oeni* strains, and suggested that these EPS may help them to better survive during production and conservation.

4. Conclusions

In the present study, a deeper analysis on ropy cider *Lactobacillus* revealed diversity in species and EPS type of naturally occurring populations associated with cider spoilage in the Basque Country (Spain). EPS production was screened in *L. collinoides* and *L. sicerae* strains and

molecular weight of their surface polysaccharides were determined. The results of PCR screening to detect *eps* genes suggest that these strains synthesize HePS. This study contributes to improve our current knowledge about the EPS-producing *Lactobacillus* involved in the cider-making process and opens a new research line for biological control during cider manufacture. Further studies are in progress on the structural analysis of novel HePS synthesized by selected *L. collinoides* and *L. sicerae* strains and genes associated with HePS synthesis.

Acknowledgments

This study was supported by grants AGL2012-40084-C03 (co-funded by FEDER), AGL2015-65010-C3-1-R, IT866-13 from the Basque Government and PROMETEO/2012/040 from the Generalitat Valenciana. Technical and human support provided by the SGiker (UPV/EHU, MICINN, GV/EJ, FEDER and FSE) is also gratefully acknowledged. We thank Dr. Stephen W. Elson for critical reading of the manuscript.

Appendix A. Supplementary data

Supplementary data related to this article can be found at <http://dx.doi.org/10.1016/j.lwt.2017.12.048>.

References

- Baruah, R., Das, D., & Goyal, A. (2016). Heteropolysaccharides from lactic acid bacteria: Current trends and applications. *Journal of Probiotics & Health*, 4(141).
- Buron, N., Coton, M., Legendre, P., Ledauphin, J., Kientz-Bouchart, V., Guichard, H., et al. (2012). Implications of *Lactobacillus collinoides* and *Brettanomyces/Dekkera anomala* in phenolic off-flavour defects of ciders. *International Journal of Food Microbiology*, 153, 159–165.
- Coton, M., Romano, A., Spano, G., Ziegler, K., Vetrana, C., Desmarais, C., et al. (2010). Occurrence of biogenic amine-forming lactic acid bacteria in wine and cider. *Food Microbiology*, 27, 1078–1085.
- Coulon, J., Houlès, A., Dimopoulou, M., Maupeu, J., & Dols-Lafargue, M. (2012). Lysozyme resistance of the ropy strain *Pediococcus parvulus* IOEB 8801 is correlated with beta-glucan accumulation around the cell. *International Journal of Food Microbiology*, 159, 25–29.
- Dan, T., Fukuda, K., Sugai-Bannai, M., Takakuwa, N., Motoshima, H., & Urashima, T. (2009). Characterization and expression analysis of the exopolysaccharide gene cluster in *Lactobacillus fermentum* TDS030603. *Bioscience Biotechnology & Biochemistry*, 73, 2656–2664.
- De Man, J. C., Rogosa, D., & Sharpe, M. E. (1960). A medium for the cultivation of lactobacilli. *Journal of Applied Bacteriology*, 23, 130–135.
- Del Campo, G., Berregi, I., Santos, J. I., Dueñas, M., & Irastorza, A. (2008). Development

- of alcoholic and malolactic fermentations in highly acidic and phenolic apple musts. *Bioresource Technology*, 99, 2857–2863.
- Dimopoulou, M., Bardeau, T., Ramonet, P. Y., Miot-Certier, C., Claisse, O., Doco, T., et al. (2016). Exopolysaccharides produced by *Oenococcus oeni*: From genomic and phenotypic analysis to technological valorization. *Food Microbiology*, 53, 10–17.
- Dimopoulou, M., Vuillemin, M., Campbell-Sills, H., Lucas, P. M., Ballestra, P., Miot-Sertier, C., et al. (2014). Exopolysaccharide (EPS) synthesis by *Oenococcus oeni*: From genes to phenotypes. *PLoS One*, 9(6), e98898.
- Dols-Lafargue, M., Lee, H. Y., Le Marrec, C., Heyraud, A., Chambat, G., & Lonvaud-Funel, A. (2008). Characterization of *gtf*, a glucosyltransferase gene in the genome of *Pediococcus parvulus* and *Oenococcus oeni*, two bacterial species commonly found in wine. *Applied and Environmental Microbiology*, 74, 4079–4090.
- Dubois, M., Gilles, K. A., Hamilton, J. K., Rebers, P. A., & Smith, F. (1956). Colorimetric method for determination of sugars and related substances. *Analytical Chemistry*, 28, 350–356.
- Dueñas-Chasco, M. T., Rodríguez-Carvajal, M. A., Tejero Mateo, P., Franco-Rodríguez, G., Espartero, J. L., Irastorza-Iribas, A., et al. (1997). Structural analysis of the exopolysaccharide produced by *Pediococcus damnosus* 2.6. *Carbohydrate Research*, 303, 453–458.
- Dueñas-Chasco, M. T., Rodríguez-Carvajal, M. A., Tejero-Mateo, P., Espartero, J. L., Irastorza-Iribas, A., & Gil-Serrano, A. M. (1998). Structural analysis of the exopolysaccharides produced by *Lactobacillus* spp. G-77. *Carbohydrate Research*, 307, 125–133.
- Dueñas, M., Irastorza, A., Fernández, K., Bilbao, A., & Huerta, A. (1994). Microbial populations and malolactic fermentation of apple cider using traditional and modified methods. *Journal of Food Science*, 59, 1060–1064.
- Ehrmann, M. A., Müller, M. R., & Vogel, R. F. (2003). Molecular analysis of sourdough reveals *Lactobacillus mindensis* sp. nov. *International Journal of Systematic and Evolutionary Microbiology*, 53, 7–13.
- Fernández de Palencia, P. F., Werning, M. L., Sierra-Filardi, E., Dueñas, M. T., Irastorza, A., Corbí, A. L., et al. (2009). Probiotic properties of the 2-substituted (1,3)- β -D-glucan-producing bacterium *Pediococcus parvulus* 2.6. *Applied and Environmental Microbiology*, 75, 4887–4891.
- Garai-Ibabe, G., Areizaga, J., Aznar, R., Elizaguivel, P., Prieto, A., Irastorza, A., et al. (2010a). Screening and selection of 2-branched (1,3)- β -D-glucan producing lactic acid bacteria and exopolysaccharide characterization. *Journal of Agricultural and Food Chemistry*, 58, 6149–6156.
- Garai-Ibabe, G., Dueñas, M. T., Irastorza, A., & Moreno-Arribas, M. V. (2007). Biogenic amine production by lactic acid bacteria isolated from ciders. *Letters in Applied Microbiology*, 45, 473–478.
- Garai-Ibabe, G., Dueñas, M. T., Irastorza, A., Sierra-Filardi, E., Werning, M. L., López, P., et al. (2010b). Naturally occurring 2-substituted (1,3)- β -D-glucan producing *Lactobacillus suebicus* and *Pediococcus parvulus* strains with potential utility in the production of functional foods. *Bioresource Technology*, 101, 9254–9263.
- Garai-Ibabe, G., Ibarburu, I., Berregi, I., Claisse, O., Lonvaud-Funel, A., Irastorza, A., et al. (2008). Glycerol metabolism and bitterness producing lactic acid bacteria in cidermaking. *International Journal of Food Microbiology*, 121, 253–261.
- Ibarburu, I., Aznar, R., Elizaguivel, P., García-Quintás, N., López, P., Munduate, A., et al. (2010). A real-time PCR assay for detection and quantification of 2-branched (1,3)- β -D-glucan producing lactic acid bacteria in cider. *International Journal of Food Microbiology*, 143, 26–31.
- Ibarburu, I., Puertas, A. I., Berregi, I., Rodríguez-Carvajal, M. A., Prieto, A., & Dueñas, M. T. (2015). Production and partial characterization of exopolysaccharides produced by two *Lactobacillus suebicus* strains isolated from cider. *International Journal of Food Microbiology*, 214, 54–62.
- Ibarburu, I., Soria-Díaz, M. E., Rodríguez-Carvajal, M. A., Velasco, S. E., Tejero-Mateo, P., Gil-Serrano, A. M., et al. (2007). Growth and exopolysaccharide (EPS) production by *Oenococcus oeni* 14 and structural characterization of their EPSs. *Journal of Applied Microbiology*, 103, 477–486.
- Kim, O. S., Cho, Y. J., Lee, K., Yoon, S. H., Kim, M., Na, H., et al. (2012). Introducing EzTaxon-e: A prokaryotic 16S rRNA gene sequence database with phylotypes that represent uncultured species. *International Journal of Systematic and Evolutionary Microbiology*, 62, 716–721.
- van Kranenburg, R., Vos, H. R., Van Swam, I. I., Kleerebezem, M., & De Vos, W. M. (1999). Functional analysis of glycosyltransferase genes from *Lactococcus lactis* and other gram-positive cocci: Complementarity, expression, and diversity. *Journal of Bacteriology*, 181, 6347–6353.
- Lebeer, S., Verhoeven, T. L., Francius, G., Schoofs, G., Lambrichts, I., Dufrière, Y., et al. (2009). Identification of a gene cluster for the biosynthesis of a long, galactose-rich exopolysaccharide in *Lactobacillus rhamnosus* GG and functional analysis of the priming glycosyltransferase. *Applied and Environmental Microbiology*, 75, 3554–3563.
- López, P., Monteserín, D. C., Gueimonde, M., de los Reyes-Gavilán, C. G., Margolles, A., Suárez, A., et al. (2012). Exopolysaccharide-producing *Bifidobacterium* strains elicit different *in vitro* responses upon interaction with human cells. *Food Research International*, 46, 99–107.
- Mañes-Lázaro, R., Ferrer, S., Rosselló-Mora, R., & Pardo, I. (2009). *Lactobacillus oeni* sp. nov., from wine. *International Journal of Systematic and Evolutionary Microbiology*, 59, 2010–2014.
- Mangas, J. J., Moreno, J., Rodríguez, R., Picinelli, A., & Suárez, B. (1999). Analysis of polysaccharides in cider: Their effect on sensory foaming properties. *Journal of Agricultural and Food Chemistry*, 47, 152–156.
- Mozzi, F., Vaningelgem, F., Hébert, E. M., Van der Meulen, R., Moreno, M. R. F., de Valdez, G. F., et al. (2006). Diversity of heteropolysaccharide-producing lactic acid bacterium strains and their biopolymers. *Applied and Environmental Microbiology*, 72, 4431–4435.
- Notararigo, N., Náchter-Vázquez, M., Ibarburu, I., Werning, M. L., Fernández de Palencia, P., Dueñas, M. T., et al. (2013). Comparative analysis of production and purification of homo- and hetero-polysaccharides produced by lactic acid bacteria. *Carbohydrate Polymers*, 93, 57–64.
- Pinto, B., Chenoll, E., & Aznar, R. (2005). Identification and typing of foodborne *Staphylococcus aureus* by PCR-based techniques. *Systematic & Applied Microbiology*, 28, 340–352.
- Provencher, C., LaPointe, G., Sirois, S., Van Calsteren, M. R., & Roy, D. (2003). Consensus-degenerate hybrid oligonucleotide primers for amplification of priming glycosyltransferase genes of the exopolysaccharide locus in strains of the *Lactobacillus casei* group. *Applied and Environmental Microbiology*, 69, 3299–3307.
- Puertas, A. I., Arahál, D. R., Ibarburu, I., Elizaguivel, P., Aznar, R., & Dueñas, M. T. (2014). *Lactobacillus sicerae* sp. nov., a lactic acid bacterium isolated from Spanish natural cider. *International Journal of Systematic and Evolutionary Microbiology*, 64, 2949–2955.
- Ruas-Madiedo, P., Moreno, J. A., Salazar, N., Delgado, S., Mayo, B., Margolles, A., et al. (2007). Screening of exopolysaccharide-producing *Lactobacillus* and *Bifidobacterium* strains isolated from the human intestinal microbiota. *Applied and Environmental Microbiology*, 73, 4385–4388.
- Sánchez, A., Rodríguez, R., Coton, M., Coton, E., Herrero, M., García, L., et al. (2010). Population dynamics of lactic acid bacteria during spontaneous malolactic fermentation in industrial cider. *Food Research International*, 43, 2101–2107.
- Simpson, P. J., Stanton, C., Fitzgerald, G. F., & Ross, R. P. (2002). Genomic diversity within the genus *Pediococcus* as revealed by randomly amplified polymorphic DNA PCR and pulsed-field gel electrophoresis. *Applied and Environmental Microbiology*, 68, 765–771.
- Suzuki, K., Koyanagi, M., & Yamashita, H. (2004). Genetic characterization and specific detection of beer-spoilage *Lactobacillus* sp. LA2 and related strains. *Journal of Applied Microbiology*, 96, 677–683.
- Wang, L., Liu, D., & Reeves, P. R. (1996). C-terminal half of *Salmonella enterica* WbaP (RfbP) is the galactosyl-1-phosphate transferase domain catalyzing the first step of O-antigen synthesis. *Journal of Bacteriology*, 178, 2598–2604.
- Werning, M. L., Ibarburu, I., Dueñas, M. T., Irastorza, A., Navas, J., & López, P. (2006). *Pediococcus parvulus* *gtf* gene encoding the GTF glycosyltransferase and its application for specific PCR detection of β -D-glucan-producing bacteria in foods and beverages. *Journal of Food Protection*, 69, 161–169.
- Werning, M. L., Pérez-Ramos, A., Fernández de Palencia, P., Mohedano, M. L., Dueñas, M. T., Prieto, A., et al. (2014). A specific immunological method to detect and quantify bacterial 2-substituted (1,3)- β -D-glucan. *Carbohydrate Polymers*, 113, 39–45.

Article

Supramolecular Structure and Renaturation of a (1→3)-β-D-Glucan Compared with Curdlan and Scleroglucan

Ana Isabel Puertas ¹, M^a Teresa Dueñas ¹ and Cristina Marieta ^{1,2,*}

¹ Department of Applied Chemistry, University of the Basque Country, UPV/EHU, P^o Manuel Lardiazabal, 3, 20018 Donostia-San Sebastián, Spain; E-Mails: anaisabel.puertas@ehu.es (A.I.P.); mariateresa.duenas@ehu.es (M.T.D.)

² Department of Chemical Ingeniering and Environmental, EUPD, University of the Basque Country, UPV/EHU, Plaza Europa 1, 20018 Donostia-San Sebastián, Spain

* Author to whom correspondence should be addressed; E-Mail: cristina.marieta@ehu.es; Tel.: +34-943-017-190.

Received: 26 July 2014; in revised form: 25 August 2014 / Accepted: 5 September 2014 /

Published: 22 September 2014

Abstract: A (1→3)-β-D-Glucan produced by *Lactobacillus suebicus* CUPV221 strain was investigated by tapping mode atomic force microscopy (TM-AFM), to compare its supramolecular structure and conformation with two commercial polysaccharides: curdlan and scleroglucan. It was found that the β-D-Glucan was a (1→3)(1→2)-β-D-Glucan and at room temperature formed three-dimensional networks by entanglements between strands, as does scleroglucan. However, (1→3)(1→2)-β-D-Glucan strands seemed to be more stiff than those of scleroglucan. It was also observed that curdlan samples deposited from 5 mM NaOH aqueous solution showed supermolecular assemblies, recognized in the literature as micelles, which are controlled by hydrophobic hydration. The (1→3)(1→2)-β-D-Glucan in alkaline aqueous solutions produced different supramolecular structures depending on pH, and at 0.4 M NaOH (pH 13.16), denaturation took place. After neutralizing the alkaline solution with HCl, the formation of short linear, circular, and hairpin structures was observed.

Keywords: (1→3)-β-D-Glucans; curdlan; scleroglucan; atomic force microscope

1. Introduction

(1→3)-β-D-Glucans from several bacteria and fungi constitute a group of natural polysaccharides with a main chain of (1→3)-linked β-glucopyranosyl units. They can be linear or branched with either (1→6) or (1→2)-linked side chains of varying length and distribution. In plants, (1→3)-β-D-Glucans exhibit a linear structure with mixed β-(1→3) and β-(1→4) glycosidic bonds [1]. These β-glucans have applications in food, pharmaceutical and other industries as emulsifiers, stabilizers, binders, gelling agents, lubricants, and thickening agents [2]. However, a better understanding of the structure-function relationship of these biopolymers remains a challenge to further improve applications and to better satisfy the consumer demand for appealing, tasty and even healthier products [3]. Moreover, these polysaccharides have been extensively studied in the last decade because they have potential as biological response modifiers. Numerous publications describe their biological activities and therapeutic uses [4], such as antitumor, antibacterial, antiviral, and anticoagulatory effects [5]. The biological activity of these macromolecules is strongly dependent upon chemical as well as physical properties such as conformation or structure, which in turn depend on the environmental conditions [4].

With respect to the industrial uses of (1→3)-β-D-Glucans, the strictly linear polysaccharide curdlan is the most studied [6], due to its unique rheological and thermal gelling properties [7] and its ability to form an elastic gel with strong bioactivity [8]. Additionally, its use as an inert dietary fiber is approved in Japan and is registered in the United States as a food additive. Although curdlan has been widely studied [7–9], it is possible to contribute to the characterization of this biomacromolecule since unusual and conflicting results can still be found, especially related to its structural analysis [10]. Another (1→3)-β-D-Glucan of industrial importance is scleroglucan, which consists of a main linear chain of (1→3)-β-D-Glucopyranosyl units, with one β-D-Glucopyranosyl unit (1→6) linked to every third unit of the main chain [11]. The most important industrial application of this polymer is in oil recovery and drilling [2], and its use as an antitumor, antiviral, and antimicrobial compound is being investigated [12].

A new class of (1→3)-β-D-Glucans synthesized by some lactic acid bacteria (LAB) has been described. These polysaccharides have a primary structure consisting of a trisaccharide-repeating unit with two (1→3)-β linked glucose residues in the main chain, one of which is substituted in position 2 by a terminal glucose. Their gelling properties have also been reported. Since several LAB species have a “*Generally Regarded As Safe*” (GRAS) status by the American Food and Drug Association, these β-glucans could be an alternative to (1→3)-β-D-Glucans from non-GRAS microbiota. In addition, it has been shown that the (1→3)(1→2)-β-D-Glucan producing *Pediococcus parvulus* 2.6 exhibits probiotic properties [13] and assays on human ingestion of an oat-based product manufactured with this strain showed a decrease of serum cholesterol levels [14].

The objective of the work has been to study the supramolecular structure and renaturation of the 2-branched (1→3)-β-D-Glucan produced by *Lactobacillus suebicus* CUPV221, and to compare the results with those exhibited by curdlan and scleroglucan, which are already of commercial interest.

2. Experimental Section

The polymers used in the present study were as follows: curdlan C7821, which was supplied by Sigma-Aldrich, scleroglucan Actigum™ CS 11, kindly supplied by Cargill S.L.U. (Martorell, Spain), both polysaccharides were used without any treatment, and a (1→3)(1→2)-β-D-Glucan an exopolysaccharide from a *Lactobacillus suebicus* CUPV221, a bacterium isolated from a ropy Basque cider. Strain was routinely cultured at 28 °C in Man Rogosa Sharpe (MRS) broth (Pronadisa, Madrid, Spain), and stored in this medium with glycerol at 20% (v/v). For exopolysaccharide production a semidefined (SMD) broth was used without yeast extract, beef extract or peptone, as these ingredients interfere with the β-glucan purification; it contained (in grams per liter of distilled water): glucose 20, casamino acids (Difco) 10, sodium acetate 5, Bacto yeast nitrogen base (BYNB) (Difco) 6.7, K₂HPO₄ 1, KH₂PO₄ 1, Mg₂SO₄·7H₂O 0.2, MnSO₄·4H₂O 0.1, KCl 0.45, di-ammonium citrate 3.5, Tween 80 1, adenine, uracil, thymine and guanine 0.005. Both glucose and BYNB were sterilized by filtering through a 0.22-μm-pore size Millex-GS filter unit (Millipore, Bedford, TX, USA) and added to the other, autoclaved ingredients. The pH of the SMD medium was adjusted to 4.8 prior to sterilization. The clear supernatant obtained by centrifugation for 30 min at 16,000 g was collected. Crude EPS was precipitated from the supernatant by addition of three volumes of cold ethanol, followed by storage overnight at 4 °C. The polysaccharide was purified by precipitation with ethanol three times and the final precipitate was resuspended in distilled water, dialyzed (Mw cut-off 12,000–14,000 Da) against distilled water for 48 h with water replacement twice a day, and finally lyophilized.

The supramolecular structure and conformation of the polysaccharides were studied by tapping mode atomic force microscopy (TM-AFM) performed on a scanning probe microscope (SPM) (Nanoscope IVa, Multimode™ from Digital Instruments) operating in tapping mode (TM-AFM) at room temperature. Samples were placed on top of a “J” piezoelectric scanner, the maximum *xy* imaging range of which was ~100 μm, and scanned at a frequency of 0.2–1 Hz using the MPP-12100 silicon probes of Veeco. Several specimens were scanned in different regions and similar images were obtained, thus demonstrating the reproducibility of the results. All images are shown without any image processing except in some cases where horizontal leveling and contrast enhancement were used. The diameters of helical units and strands of the polysaccharide were measured with Digital Instruments Nanoscope IV Software version 5.12r5.

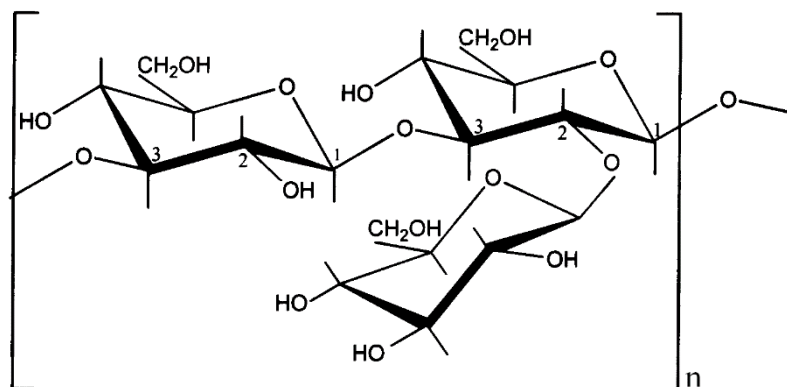
The drop deposition method was used to prepare the TM-AFM samples, thus dissolutions of the biopolymers were required. Scleroglucan and the β-D-Glucan from a *Lactobacillus suebicus* were dissolved in water at 10 mg/L, and curdlan, which is not soluble in pure water, was dissolved in 5 mM NaOH aqueous solution, at a concentration of 10 mg/L. 0.5 μL of the solutions were pipetted onto cleaved sheets of mica. The samples were air-dried in a desiccator at atmosphere pressure for 24 h.

We found that at 0.4 M NaOH (pH 13.16) the strand separation of triplexes took place (denaturation). Some authors have documented the ability of the triple helices to spontaneously re-form upon restoration of the thermodynamic conditions (renaturation) [4]. To study the renaturation of the (1→3)-β-D-Glucan, a 1-mg/L solution in 0.4 M NaOH was neutralized with HCl and the salt was removed by dialysis. Then, the previous described drop deposition method was used to prepare the samples for TM-AFM.

3. Results and Discussion

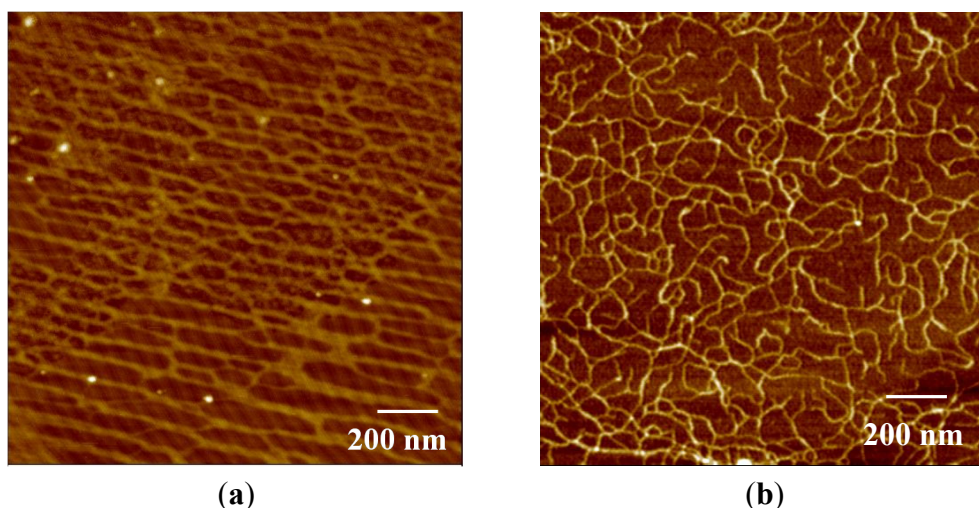
(1→3)-β-D-Glucan is produced by a lactic acid bacterium, *Lactobacillus suebicus* CUPV221 [15]. This biopolymer is a main linear chain of (1→3)-β-D-Glucopyranosyl units, with one (1→2)-β-D-Glucopyranosyl pendant unit attached to every two units of the main chain, as shown in Figure 1 [16].

Figure 1. Repeat unit of the polysaccharide produced by *Lactobacillus suebicus* CUPV221.



At room temperature, this (1→3)(1→2)-β-D-Glucan forms a gel network structure, that we probed by TM-AFM, Figure 2a.

Figure 2. TM-AFM height images of: (a) (1→3)(1→2)-β-D-Glucan; (b) scleroglucan. Images were obtained by depositing the glucans from 10 mg/L aqueous solutions onto mica and scanning in air. Height images of 1.5 μm × 1.5 μm.



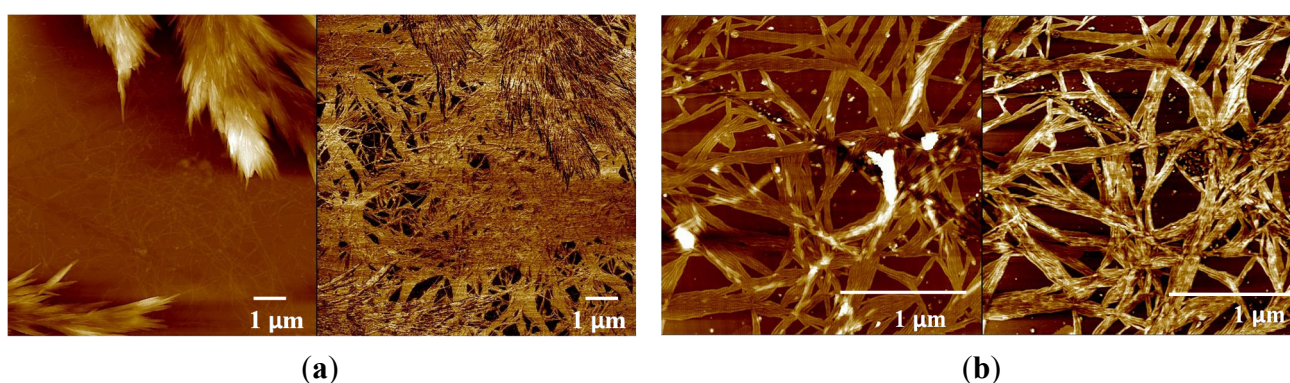
Additionally, we previously performed a study of an identical polysaccharide, a branched 2-substituted (1→3)-β-D-Glucan, produced by *P. parvulus* 2.6, and the existence of a physical network in water solution at room temperature was proved by rheological measurements [17]. Furthermore, two facts demonstrated that it was a low-set gel or weak gel: (i) viscosity decreased above a certain shear rate, and (ii) the viscous modulus (G'') was lower than the elastic modulus (G'), with a very slight dependence on frequency, behavior associated with weak gels [18]. Similar weak gel behavior has been

described for scleroglucan [19]. Figure 2b depicts a TM-AFM image of a sample from a 10 mg/L aqueous solution of scleroglucan. The image shows a three-dimensional network formed by entanglements between strands like that of the (1→3)(1→2)-β-D-Glucan and scleroglucan (Figure 2a).

Due to the rod like character of the (1→3)(1→2)-β-D-Glucan strands and their unwinding observed at 13.16 pH, a helical conformation was assigned [20]. The conformation of scleroglucan is also widely accepted as a rod-like triple helix [21,22]. However, in view of the TM-AFM images, Figure 2, and keeping in mind the repeating units of both biopolymers, it can be concluded that the strands of (1→3)(1→2)-β-D-Glucan are more stiff than those of scleroglucan.

In its solid-state, commercial curdlan is insoluble in water at room temperature. Therefore, to carry out the study by AFM it was necessary to prepare a solution with a suitable solvent. Due to the ionization of hydrogen bonds, curdlan dissolves easily in dilute alkaline solutions. When this solvent is used to carry out morphological and structural studies, curdlan shows different morphologies depending on pH, ranging from endless microfibrils to spindle-shaped fibrils of various lengths [23], or even thin lamellar hexagonal crystals [24], and the conformation varies from triple or single helix to random coil [25]. When a weak alkaline solution is used to prepare the AFM samples, the curdlan structure could almost be maintained [8]. Thus, 5 mM NaOH aqueous solution, pH 11.75, was chosen to develop the present study. Figure 3 shows the morphology of curdlan after the evaporation of the solvent at room temperature. A height image (left) reveals a fairly rough morphology with a high density of spike-like growth features. Observing the phase image (right), a homogenous color of the image is seen. This means that more curdlan exists between the spindle-shaped joined microfibrils forming the spike-like features. When a higher magnification of this area was made, 2.5 μm × 2.5 μm scan, an entanglement of fibrils composed of laterally associated strands were observed (Figure 3b).

Figure 3. TM-AFM height (left) and phase (right) images of curdlan. Images were obtained by depositing the glucan from a 10 mg/L 5 mM NaOH aqueous solution, pH 11.75, onto mica and scanned in air: (a) images of 10 μm × 10 μm; (b) images of 2.5 μm × 2.5 μm.



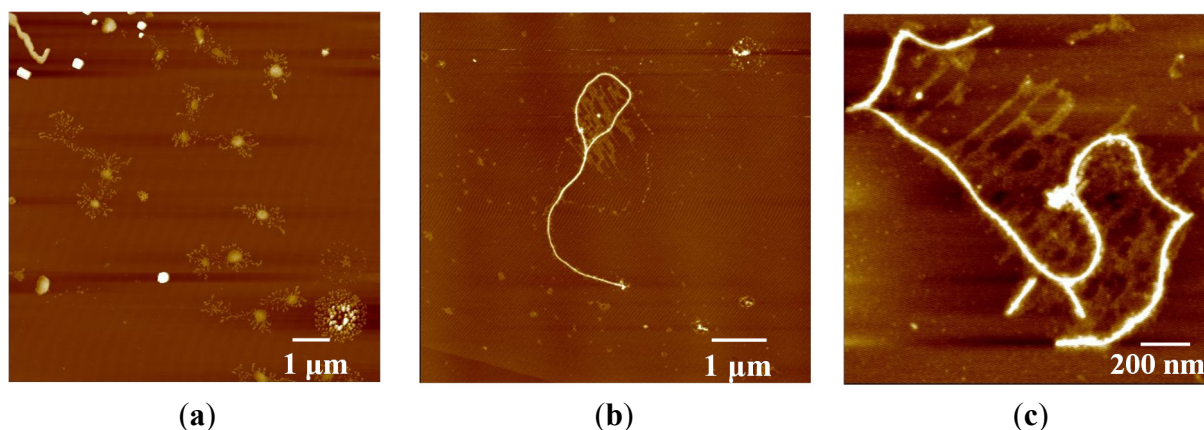
Trace analyses were also carried out to obtain quantitative information from AFM images. The diameter of the strands for curdlan was about 1.6 nm, slightly larger than that reported for the triple strand thickness by X-ray fiber diffraction, 1.56 nm [8,26]. Moreover, this discrepancy between values by AFM and those determined by other techniques has already been observed by other authors, and they propose that the dissimilarity might result from the fact that the molecules were distorted by desiccation or by interaction with the mica substrate, or that the molecules were partially embedded in a layer of

water adhering to the mica surface [27]. The diameter of the strands of the (1→3)(1→2)-β-D-Glucan was about 1.8 nm [20], similar to that found in the literature for scleroglucan [28].

The structure of the (1→3)(1→2)-β-D-Glucans in units of helical conformation is an important basis for their functional properties. Nevertheless, this helical conformation is not stable at high pH or by increasing the temperature above the helix melting temperature. Thus, breaking of intermolecular hydrogen bonds takes place and the multi-helical units dissociate into single stranded random coils (denaturation) [4]. However, the triple helix can be reformed by neutralizing. Different structures have been mentioned in literature for renatured species: linear, circular, hairpin, multichain (aggregated) structures, *etc.* [4,17]. The aim of the present work was to study the conformational transitions during the denaturation-renaturation for the (1→3)(1→2)-β-D-Glucan and to compare its behaviour with the scleroglucan behaviour from previous works found in the literature [4,29]. The denaturation of the (1→3)(1→2)-β-D-Glucan took place at 0.4 M NaOH aqueous solution (pH 13.16) and after the neutralization TM-AFM images were taken.

As can be seen in Figure 4, a mixture of linear, circular and hairpin structures in addition to larger clusters with less well-defined morphology were found. Similar behavior was observed for scleroglucan [4] and schizophyllan [30]. However, it should be mentioned that, for the (1→3)(1→2)-β-D-Glucan, a great dispersion structure sizes was observed (scales are shown below each image), small linear and circular structures (Figure 4a) coexisted with strands of 5 μm of length (Figure 4b) and small circular structures (Figure 4a) with rod-like linear strands (Figure 4c). This behavior could be attributed to the more stiff character of the (1→3)(1→2)-β-D-Glucan biomacromolecules. The strand separation of triplexes was originally considered to be irreversible [4], but later extensive analysis of many micrographs using scleroglucan samples in five different ranges of molecular weight suggested that the reconstituted molecules, both rods and rings, are substantially triple helical [31].

Figure 4. TM-AFM height images of renatured (1→3)(1→2)-β-D-Glucan. Images were obtained by depositing the glucan from the (1→3)(1→2)-β-D-Glucan neutralized solution. (a) Images of 10 μm × 10 μm; (b) image of 7.11 μm × 7.11 μm; (c) image of 1.5 μm × 1.5 μm.



4. Conclusions

We have shown that the (1→3)(1→2)-β-D-Glucan from *Lactobacillus suebicus* CUPV221 forms three-dimensional network structures by entanglements between strands, as occurs with scleroglucan.

Due to the macromolecular structure and also possibly to the direction of the helical arrangement, (1→3)(1→2)-β-D-Glucan strands are more stiff than those of scleroglucan. Curdlan samples deposited from 5 mM NaOH aqueous solution showed supermolecular assemblies, which are recognized in the literature as micelles.

(1→3)(1→2)-β-D-Glucan after exposure to a denaturation-renaturation cycle forms various molecular topologies: linear, circular and hairpin structures in addition to larger clusters with less well-defined morphology.

Acknowledgments

This study was supported by grants AGL2009-12998-C03 and AGL2012-40084 from the Spanish Ministry of Science and Innovation, and IT335-10 from the Basque Government. Ana Isabel Puertas acknowledges the “Gobierno Vasco, Dpto. Agricultura, Pesca y Alimentación” for the fellowship.

Author Contributions

The manuscript was finalized through contributions from all authors, and all authors also approved the final manuscript.

Conflicts of Interest

The authors declare no conflict of interest.

References

1. Laroche, C.; Michaud, P. New developments and prospective applications for β-(1,3) glucans. *Recent Pat. Biotechnol.* **2007**, *1*, 59–73.
2. Survase, S.A.; Saudagar, P.S.; Bajaj, I.B.; Singhal, R.S. Scleroglucan: Fermentative production, downstream processing and applications. *Food Technol. Biotechnol.* **2007**, *45*, 107–118.
3. Duboc, P.; Mollet, B. Applications of exopolysaccharides. *Int. Dairy J.* **2001**, *11*, 759–768.
4. Sletmoen, M.; Stokke, B.T. Higher order structure of (1,3)-β-D-glucans and its influence on their biological activities and complexation abilities. *Biopolymers* **2008**, *89*, 310–320.
5. Gawronski, M.; Park, J.T.; Magee, A.S.; Conrad, H. Microfibrillar structure of PGG-glucan in aqueous solution as Triple-helix aggregates by small angle x-ray scattering. *Biopolymers* **1999**, *50*, 569–578.
6. Harada, T.; Masada, M.; Fujimori, K.; Maeda, I. Production of a firm, resilient gel-forming polysaccharide by a mutant of *Alcaligenes faecalis* var. *myxogenes* 10C3. *Agric. Biol. Chem.* **1966**, *30*, 196–198.
7. McIntosh, M.; Stone, B.A.; Stanisich, V.A. Curdlan and other bacterial (1→3)-β-D-glucans. *Appl. Microbiol. Biotechnol.* **2005**, *68*, 163–173.
8. Jin, Y.; Zhang, H.; Yin, Y.; Nishinari, K. Conformation of curdlan as observed by tapping mode atomic force microscopy. *Colloid Polym. Sci.* **2006**, *284*, 1371–1377.

9. Sun, Y.; Liu, Y.; Li, Y.; Lv, M.; Li, P.; Xu, H.; Wang, L. Preparation and characterization of novel curdlan/chitosan blending membranes for antibacterial applications. *Carbohydr. Polym.* **2011**, *84*, 952–959.
10. Zhang, H.; Huang, L.; Nishinari, K.; Watase, M.; Konno, A. Thermal measurements of curdlan in aqueous suspension during gelation. *Food Hydrocolloids* **2000**, *14*, 121–124.
11. Vincendon, M. Scleroglucan derivatives: Aromatic carbamates. *J. Polym. Sci. Part A Polym. Chem.* **1999**, *37*, 3187–3192.
12. Kim, H.I.; Kim, J.H.; Yang, S.B.; Hong, S.G.; Lee, S.A.; Hwang, S.J.; Shin, K.S.; Suh, H.J.; Park, M.H. A polysaccharide extracted from rice bran fermented with *Lentinus edodes* enhances natural killer cell activity and exhibits anticancer effects. *J. Med. Food* **2007**, *10*, 25–31.
13. Fernández de Palencia, P.; Werning, M.L.; Sierra-Filardi, E.; Dueñas, M.T.; Irastorza, A.; Corbí, A.L.; López, P. Probiotic properties of the 2-substituted (1,3)- β -D-glucan-producing bacterium *Pediococcus parvulus* 2.6. *Appl. Environ. Microbiol.* **2009**, *75*, 4887–4891.
14. Mårtensson, O.; Björklund, M.; Lambo, A.M.; Dueñas-Chasco, M.T.; Irastorza, A.; Holst, O.; Norin, E.; Walling, G.; Öste, R.; Önning, G. Fermented røpy, oat-based products reduce cholesterol levels and stimulate the bifidobacteria flora in humans. *Nutr. Res.* **2005**, *25*, 429–442.
15. Garai-Ibabe, G.; Dueñas, M.T.; Irastorza, A.; Sierra-Filardi, E.; Werning, M.L.; López, P.; Corbí, A.L.; Fernández de Palencia, P. Naturally occurring 2-substituted (1,3)- β -D-glucan producing *Lactobacillus suebicus* and *Pediococcus parvulus* strains with potential utility in the production of functional foods. *Bioresour. Technol.* **2010**, *101*, 9254–9263.
16. Ibarburu, I. Exopolysaccharide-producing lactic acid bacteria: Structural analysis of polysaccharides and molecular detection of β -(1 \rightarrow 3)(1 \rightarrow 2)-D-glucan producer strains. Ph.D. Thesis, University of the Basque Country (UPV/EHU), Donostia-San Sebastián, Spain, 2009.
17. Velasco, S.; Irastorza, A.; Dueñas, M.; Santamaría, A.; Muñoz, M.E. Chemical and rheological properties of the β -glucan produced by *Pediococcus parvulus* 2.6. *J. Agric. Food Chem.* **2009**, *57*, 1827–1834.
18. Guenet, J.M. *Thermoreversible Gelation of Polymers and Biopolymers*; Academic Press Inc.: San Diego, CA, USA, 1992.
19. Grassi, M.; Lapasin, R.; Pricl, S. A study of the rheological behavior of scleroglucan weak gel systems. *Carbohydr. Polym.* **1995**, *29*, 169–181.
20. Marieta, C.; Ibarburu, I.; Dueñas, M.; Irastorza, A. Supramolecular structure and conformation of a røpy strain of *Lactobacillus suebicus* as observed by tapping mode atomic force microscopy. *J. Agric. Food Chem.* **2009**, *57*, 6183–6188.
21. Yanaki, T.; Norisuye, T. Triple helix and random coil scleroglucan in dilute solution. *Polym. J.* **1983**, *15*, 389–396.
22. Harada, T.; Misaki, A.; Saito, H. Curdlan: A bacterial-gel-forming β -1 \rightarrow 3 glucan. *Arch. Biochem. Biophys.* **1968**, *124*, 292–298.
23. Harada, T.; Harada, A. Gel Formation and Ultrastructure in Food Polysaccharides. In *Polysaccharide Association Structures in Food*; CRC Press: Boca Raton, FL, USA, 1998; pp. 37–40.
24. Pelosi, P.; Bulone, V.; Heux, L. Polymorphism of curdlan and (1 \rightarrow 3)- β -D-glucans synthesized *in vitro*: A13C CP-MAS and X-Ray diffraction analysis. *Carbohydr. Polym.* **2006**, *66*, 199–207.

25. Zhang, L.; Wang, C.; Cui, S.; Wang, Z.; Zhang, X. Single-molecules force spectroscopy on curdlan: Unwinding helical structures and random coils. *Nanoletters* **2003**, *3*, 1119–1124.
26. Nishinari, K. Rheological and DSC study of sol-gel transition in aqueous dispersions of industrially important polymers and colloids. *Colloid Polym. Sci.* **1997**, *275*, 1093–1107.
27. McIntire, T.M.; Brant, D.A. Imaging of individual biopolymers and supramolecular assemblies using noncontact atomic force microscopy. *Biopolymers* **1997**, *42*, 133–146.
28. McIntire, T.M.; Penner, R.M.; Brant, D.A. Observations of a circular, triple-helical polysaccharide using noncontact atomic force microscopy. *Macromolecules* **1995**, *28*, 6375–6377.
29. Vuppu, A.; Garcia, A.A.; Vernia, C. Tapping mode atomic force microscopy of scleroglucan networks. *Biopolymers* **1997**, *42*, 89–100.
30. Stokke, B.T.; Elgsaeter, A.; Brant, D.A.; Kuge, T.; Kitamura, S. Macromolecular cyclization of (1→6)-branched-(1→3)-β-D-glucans observed after denaturation-renaturation of the triple-helical structure. *Biopolymers* **1993**, *33*, 193–198.
31. Brant, D.A. Versatile polysaccharides: Ropes, rings, and rods. *AIM Mag.* **2005**, *60*, 40–49.

© 2014 by the authors; licensee MDPI, Basel, Switzerland. This article is an open access article distributed under the terms and conditions of the Creative Commons Attribution license (<http://creativecommons.org/licenses/by/3.0/>).



Production and partial characterization of exopolysaccharides produced by two *Lactobacillus suebicus* strains isolated from cider



Idoia Ibarburu^a, Ana Isabel Puertas^a, Iñaki Berregi^a, Miguel A. Rodríguez-Carvajal^c, Alicia Prieto^b, M^a. Teresa Dueñas^{a,*}

^a Departamento de Química Aplicada, Facultad de Ciencias Químicas, Universidad del País Vasco, Paseo Manuel de Lardizabal 3, 20018 San Sebastián, Spain

^b Departamento de Biología Medioambiental, Centro de Investigaciones Biológicas, Consejo Superior de Investigaciones Científicas, Ramiro de Maeztu 9, 28040 Madrid, Spain

^c Departamento de Química Orgánica, Facultad de Química, Universidad de Sevilla, Profesor García González, 1, 41012 Sevilla, Spain

ARTICLE INFO

Article history:

Received 30 January 2015

Received in revised form 19 June 2015

Accepted 9 July 2015

Available online 16 July 2015

Keywords:

Exopolysaccharides

Lactobacillus suebicus

Heteropolysaccharides

Lactic acid bacteria

ABSTRACT

Many lactic acid bacteria synthesize extracellular polysaccharides (exopolysaccharides, EPSs) with a large variation in structure and potential functional properties. Although EPS production can produce detrimental effects in alcoholic beverages, these polymers play an important role in the rheological behavior and texture of fermented products. In this work, EPS production by two *Lactobacillus suebicus* strains, which were isolated from ropy ciders, was examined in a semidefined medium. The existence of priming glycosyltransferase encoding genes was detected by PCR. In addition, the preliminary characterization of the polymers was undertaken. Molecular masses were determined by size exclusion chromatography revealing the presence of two peaks, corresponding to polymers of high- and low-molecular-weight in all fractions. The composition of the EPS fractions was analyzed by gas chromatography–mass spectrometry after acid hydrolysis, revealing that they contained glucose, galactose, *N*-acetylglucosamine and phosphate, although in different ratios, suggesting that a mixture of polysaccharides is being synthesized. We also examined the influence of the sugar source (glucose, ribose, xylose, or arabinose) and pH conditions on growth and EPS production.

© 2015 Elsevier B.V. All rights reserved.

1. Introduction

Certain strains of lactic acid bacteria (LAB) produce exopolysaccharide (EPS) with a large variation in composition, molecular mass, and structure. These molecules are secreted into the medium playing an important role in the rheology and texture of fermented foods, enhancing naturally the texture and viscosity, but in addition to being a biothickener, it has been reported that some EPSs can promote antitumoral, immunomodulatory and antimicrobial activity (Werning et al., 2012; Hidalgo-Cantabrana et al., 2012). Additionally, prebiotic effects of several EPS have also been demonstrated (Korakli et al., 2002). These properties generate interest in the food industry due to several LAB species have a “Generally Recognized As Safe” status by the American Food and Drug Association or a “Qualified Presumption of Safety” status by the European Food Safety Authority. However, extracellular polymers also produce deleterious effects to the organoleptic properties of fermented alcoholic beverages, as in cider (Dueñas et al., 1995) and in wine (Llaubères et al., 1990), being the origin of an alteration named oiliness or ropiness characterized by a viscous texture and oily feel. EPSs produced by *Pediococcus parvulus* 2.6 (Dueñas-Chasco et al., 1997), *Lactobacillus* sp. G77 (Dueñas-Chasco et al., 1998) or *Oenococcus oeni* I4 (Ibarburu et al., 2007) isolated

from ropy ciders have been characterized. Depending on the chemical composition, the bacterial EPSs are classified as homopolysaccharides (HoPSs), consisting of only one type of monosaccharide and heteropolysaccharides (HePSs) formed by two or more types of monosaccharides. Heteropolysaccharides are usually produced in small amounts by homofermentative and facultatively heterofermentative species (De Vuyst and Degeest, 1999), nevertheless, LAB synthesized a wide variety of HePSs composed of different sugar moieties (glucose, galactose, rhamnose, mannose, *N*-acetylglucosamine, *N*-acetylgalactosamine, glucuronic acid), molecular mass and structure, whose production are strongly influenced by culture conditions (De Vuyst et al., 2001; Mozzi et al., 2003). To obtain high EPS production, it is necessary to optimize growth conditions, which require an understanding of the different production parameters involved (Velasco et al., 2006). Previous works showed that physical (temperature, pH, oxygen tension) and chemical (carbohydrate source, nitrogen source) factors determined the EPS yield of lactic acid bacteria (Cerning et al., 1994; Degeest et al., 2002). Further, studies for different LAB species conducted on the molecular genetics of HePS biosynthesis suggested that the genetic diversity of the *eps* cluster determinate the structural diversity of HePSs (De Vuyst et al., 2011; Dimopoulou et al., 2014).

The genus *Lactobacillus* represents the largest group within the lactic acid bacteria and is also the predominant microbiota in natural fermented products. *Lactobacillus suebicus* is an uncommon obligately

* Corresponding author.

E-mail address: mariaateresa.duenas@ehu.es (M.^aT. Dueñas).

heterofermentative organism found in ropy cider (Werning et al., 2006) and in apple and pear mash (Kleynmans et al., 1989). This species is associated to particular flavors and ripening processes of apple mash (Nam et al., 2011).

In this work, two EPS-producing strains of *L. suebicus* isolated from ropy ciders were studied to examine the influence of carbohydrate source and pH of the culture medium on growth and EPS production. Taking into account that the technological and biological effects of polysaccharides depend on composition, sugar linkages, and molecular mass, the preliminary characterization of exopolysaccharides was undertaken.

2. Material and methods

2.1. Bacterial strains and growth conditions

The EPS-producing *L. suebicus* strains: CUPV225 (Notararigo et al., 2013) and CUPV226 were isolated from two ropy natural ciders of Basque Country (Spain). Strains were stored at -80°C in MRS broth containing 20% (v/v) glycerol. Before experimental use, bacteria were propagated in Man Rogosa Sharpe (MRS) broth (Pronadisa, Madrid, Spain) at 28°C in an atmosphere containing 5% CO_2 . For EPS production, strains were grown in a semi-defined (SMD) medium (Marieta et al., 2009) containing (in grams per liter): glucose 20, Casamino Acids (Becton Dickinson, Spain) 5, sodium acetate 5, Difco™ Yeast Nitrogen Base (DYNB, Becton Dickinson, Spain) 6.7, K_2HPO_4 2, $\text{MnSO}_4 \cdot 4\text{H}_2\text{O}$ 0.05, di-ammonium citrate 2, Tween 80 1, adenine, uracyl, xantine and guanine 0.005. Sugars and DYNB were sterilized by filtering them through a 0.45-pore size Minisart (Sartorius Stedium Biotech, Germany) and added to the medium (pH 5.5) after autoclaving.

2.2. Identification of EPS-producer strains

Strains CUPV225 (Notararigo et al., 2013) and CUPV226 were identified by biochemical tests and 16S rRNA gene sequence analysis. The homo- or heterofermentative characteristic was tested as described by Dueñas et al. (1995). Carbohydrate utilization was determined with the API 50CH system (API-BioMérieux, Marcy l'Etoile, France). Additional assays to study the carbohydrate fermentation profiles were carried out in MRS broth without glucose and meat extract, with 0.04% of chlorophenol red as pH indicator, and supplemented with 2% (wt/v) one of the sugars glucose, fructose, sucrose, lactose, galactose, or maltose. Incubation was performed for up to 7 days, at 28°C in an atmosphere containing 5% CO_2 . One-milliliter aliquots of MRS cultures were used for DNA extraction. Following centrifugation at $15,800 \times g$ for 5 min, pellets were washed in 1 mL of Ringer's solution (Oxoid) and centrifuged at

$15,800 \times g$ for 5 min. The resulting cell pellet was resuspended in $180 \mu\text{L}$ of an enzymatic lysis buffer containing 20 g/L lysozyme, and incubated for 30 min at 37°C . DNA was purified by DNeasy Blood and Tissue Kit (Qiagen GmbH, Hilden, Germany), according to the manufacturer's instructions. DNA samples were stored at -20°C until use. For identification of the ropy strains based on 16S rRNA gene sequencing, a fragment of the 16S rRNA gene was amplified as previously described (Werning et al., 2006). 16S rRNA sequences were identified with nucleotide identity at the species level higher than 98% by using the BLAST tool of the GenBank DNA database (<http://www.ncbi.nlm.nih.gov/>).

2.3. PCR detection of the eps genes

Amplification reactions of the *eps* gene were performed using different primers that target homopolysaccharide (*gtf*, *deg*, *lev*) and heteropolysaccharide (*epsD/E*, *epsA*, *epsB*, *epsEFG*, *epsF*) genes. The primers used are shown in Table 1. The PCR conditions were carried out according to the literature. The amplified products were purified by using the QIAquick Gel extraction kit (Qiagen, Hilden, Germany) in accordance with the manufacturer's recommendations. DNA strands of amplicons were sequenced at the sequencing service SGIker of University of Basque Country (UPV/EHU). Similarity searches were performed with the BLAST algorithm available at the National Center of Biotechnology Information (<http://www.ncbi.nlm.nih.gov/>).

2.4. Fermentation conditions

Batch fermentation assays were carried out in semi-defined medium (SMD) without pH control in fully filled 250 mL screw-cap flasks during 72 h at 28°C in an atmosphere containing 5% CO_2 . Overnight cultures grown at 28°C in MRS containing glucose (20 g/L) were inoculated until an absorbance (at 600 nm) value of 0.2. The effect of pH on growth and EPS production was analyzed at initial pH values of 4.8 and 5.5 at 28°C in an atmosphere containing 5% CO_2 , for 111 h in *L. suebicus* CUPV226 and for 72 h in CUPV225. Fermentations at controlled pH of two independent cultures of the *L. suebicus* CUPV226 strain were also performed in a 3 L fermenter (BIOFLO 110 Fermentor/Bioreactor, New Brunswick Scientific). Cultures were carried out in SMD broth at pH 5.5 that was adjusted with 5 N NaOH. The temperature was kept at 28°C and agitation was set to 50 rpm. Samples from cultures were taken at different times between 0 and 111 h. The plate dilution method was used to monitor cell viability on MRS agar plates, incubated at 28°C for 5–6 days in an incubator with 5% CO_2 and reported as CFU/mL. To evaluate their influence on growth and EPS production, glucose,

Table 1

Primer pairs used to screen for HoPS and HePS genes.

Primer	Sequence ^a (5'→3')	Gene target	Expected fragment size (bp)	Reference
<i>gtf</i> fw	CGGTAATGAAGCGTTTCCTG	Glycosyltransferase	417	Werning et al. (2006)
<i>gtf</i> rev	GCTAGTACGGTAGACTTG			
<i>deg</i> fw	GAYAAAYWSNAAYCCNRYNGTNC	Glucansucrase	660	Kralj et al. (2003)
<i>deg</i> rev	ADRTCNCRTARTANAVNYKNG			
<i>lev</i> fw	GAYGTI TGG GAYWSI TGGC	Levansucrase	800	Tieking et al. (2003)
<i>lev</i> rv	TCITYYTCRTCISWIRMCAT			
<i>eps</i> D/E fw	TCATTTTATTCGTAACCTCAATTGAYGARYTNCC	Priming glycosyltransferase (<i>L. casei</i> group and <i>S. thermophilus</i>)	189	Provencher et al. (2003)
<i>eps</i> D/E rv	AATATTATTACGACCTSWNAYYTGCCA			
<i>eps</i> A fw	TAGTGACAACGGTTGACTG	EPS regulation/ (<i>S. thermophilus</i>)	784	Low et al. (1998)
<i>eps</i> A rv	GATCATTATGGACTGTCAC			
<i>eps</i> B fw	CGTACGATTCGTACGACCAT	EPS chain length determination (<i>L. lactis</i>)	1150	Deveau and Moineau (2003)
<i>eps</i> B rv	TGACCACTGACACTTGAAGC			
<i>eps</i> EFG fw	GAYGARYTNCCNARYTNWKNAAAYGT	Priming glycosyltransferase (<i>L. delbrueckii</i> subsp. <i>bulgaricus</i> , <i>L. helveticus</i>)	1600	Mozzi et al. (2006)
<i>eps</i> EFG rv	TGCAGCYTCWCCACATG			
<i>eps</i> F fw	ACCAGATATTGTACATTGTC	Branching galactosyltransferase (<i>S. thermophilus</i>)	571	Low et al. (1998)
<i>eps</i> F rv	TGTCATAGGCTGTACAAC			

^a Y = C or T; R = A or G; W = A or T; K = G or T; S = C or G; M = A or C; V = A, C, or G; N = A, C, G, or T; I = inosine.

arabinose, ribose, maltose and xylose, were added as carbon sources to the medium (20 g/L) and cultured for 72 h at 28 °C in an atmosphere containing 5% CO₂. Samples from cultures were taken daily, monitoring bacterial growth spectrophotometrically at 600 nm (OD₆₀₀). All experiments were performed in duplicate independently. EPS production was quantified as described below.

2.5. Quantification of EPS, DNA, RNA and proteins

Lyophilized EPS preparations were suspended in water (0.1 mg/mL). EPS production was estimated from neutral carbohydrate content of these solutions, determined by the phenol–sulfuric acid method using glucose as the standard (Dubois et al., 1956). Proteins, DNA and RNA were measured in the same solutions with the Qubit® 2.0 fluorometer. This technique allows the core range detection of 1 ng/mL to 500 ng/mL of DNA, 25 ng/mL to 500 ng/mL of RNA, and 1.25 µg/mL to 25 µg/mL of proteins. Each reported value was the average of three independent determinations.

2.6. Analysis of the fermentation products

For chemical analysis of the products, batch fermentations were performed for 72 h at 28 °C, in an atmosphere containing 5% CO₂, in SMD broth with 20 g/L glucose, pH 5.5 (without pH control). Samples were centrifuged (12,000 ×g, 30 min) and the supernatants filtered through a 0.2 µm membrane filter (Minisart RC15, Sartorius). The concentration of sugars, organic acids and ethanol in the fermentation broth was quantified by HPLC (Agilent 1100, Hewlett-Packard, Germany) using an ion exchange column (Aminex HPX-87H, Bio-Rad, Hercules, CA), protected by a guard column (Supelguard Pb HPLC column, Supelco), coupled with an ultraviolet–visible (UV–vis) and refractive index (RI) detector. The column was eluted with diluted sulfuric acid (5 mM) at 65 °C, at a flow rate of 0.6 mL/min. The data are means of two independent experiments.

2.7. EPS isolation and quantification

To examine EPS production, *L. suebicus* CUPV225 and CUPV226 were grown under the conditions described above. Bacterial cells were removed from the fermented media by centrifugation (12,000 ×g, 4 °C, 30 min). The clear supernatant was collected, and the EPSs precipitated by adding three volumes of cold ethanol, followed by overnight storage at 4 °C. First, a floating fraction was recovered by spinning and resuspended in ultrapure water (fraction F). Then, the remaining cloudy ethanol mixture was maintained overnight at 4 °C and centrifuged at 12,000 ×g for 30 min at 4 °C to collect the polysaccharide as a precipitate. This fraction was washed 3 times with 70% (v/v) ethanol and centrifuged (fraction P). Fractions F and P were suspended in ultrapure water, dialyzed for 3 days (changed twice each day) through a 12–14 kDa cutoff dialysis membrane (Medicell International, Ltd., London, U.K.), and lyophilized. The samples were redissolved to analyze EPSs, protein, DNA and RNA content. In addition, samples from cultures with a controlled pH of 5.5, with glucose, ribose (72 h), or xylose (24 h) as the sole carbon source, were also analyzed. For EPS quantification in different fermentation steps, 1-mL aliquots were withdrawn from cultures and centrifuged (30 min, 12,000 ×g) to remove cells. 0.5 mL of the clear supernatant were collected, and the EPSs precipitated by adding three volumes of cold ethanol, followed by overnight storage at 4 °C. The precipitate was recovered by centrifugation (12,000 ×g, 20 min, 4 °C), dissolved in ultrapure water, and the precipitation process repeated three times to clean the preparations that were finally resuspended in purified water to estimate the concentration of EPS.

2.8. EPS characterization

2.8.1. Molecular mass determination

The weight-average molecular weight (M_w) of the polysaccharides was determined by high-performance size exclusion chromatography (HPLC-SEC, Agilent 1100 Series System, Hewlett-Packard, Germany) with refractive index (RI) detection. Data processing was performed using the Agilent ChemStation with integrated GPC data analysis software. The HPLC system was equipped with a guard column (PL-aquagel–OH Guard, 8 µm, Agilent Technologies) and a PL aquagel–OH Mixed-H column (8 µm, Agilent Technologies). The column was eluted with 0.1 M NaNO₃ and 0.02% NaN₃ (pH 7), at 35 °C and at a flow rate of 0.9 mL min⁻¹. The polymer solutions were prepared at 0.75-mg/mL and 100 µL were injected. The calibration curve was obtained by using dextran standards (10³, 5 × 10³, 1.2 × 10⁴, 5 × 10⁴, 8 × 10⁴, 1.5 × 10⁵, 2.7 × 10⁵, 4.1 × 10⁵, 6.7 × 10⁵, 1.4 × 10⁶ and 2 × 10⁶ Da) obtained from Sigma-Aldrich. Samples and standards were filtered through 0.2 µm filters (Chromafil Xtra, Macherey-Nagel) prior to the injection.

2.8.2. Determination of monosaccharide composition and phosphate content

Neutral sugar composition was determined after hydrolysis of the polysaccharides with 3 M trifluoroacetic acid (121 °C, 1 h). The hydrolyzed monosaccharides were converted into their corresponding trimethylsilyl-oximes, and analyzed and quantified by gas chromatography as previously described (Notararigo et al., 2013). Phosphate content (from solutions 500 µg/mL in water) was deduced from inorganic phosphate determination on a 5500 inductively coupled plasma instrument (Perkin Elmer).

2.8.3. Fourier-transform infrared (FTIR) spectroscopy

The presence of *N*-acetyl, carboxyl, phosphate or sulfate groups and the α- or β-anomeric configuration of the monosaccharides was investigated by FTIR spectroscopy. The spectra were recorded on KBr pellets of the samples in a FTIR 4200 type A instrument (Jasco Corporation, Tokyo, Japan), with a light source in the middle infrared range (400–4000 cm⁻¹), and a triglycine-sulfate (TGS) detector, with a resolution of 4 cm⁻¹.

2.8.4. Methylation analysis

The polysaccharides (1–5 mg) were methylated according to the method of Ciucanu and Kerek (1984). The permethylated polysaccharides were hydrolyzed with 3 M trifluoroacetic acid (TFA) at 121 °C for 1 h. The resulting partially methylated monosaccharides were converted into their corresponding alditol acetates by reduction with NaBD₄ and subsequent acetylation with 250 µL of pyridine:acetic anhydride (1:1) for 1 h at 100 °C, as described by Laine et al. (1972). The partially methylated alditol acetates obtained were analyzed by gas chromatography–mass spectrometry (GC–MS) on a 6890A/5975C instrument from Agilent, with He as the carrier gas. The injector was programmed at 250 °C. Samples (1 µL) were injected with a split ratio of 1:50 and their components separated in a HP5MS (Agilent) fused silica column (30 m × 0.25 mm I.D. × 0.2 µm film thickness), with a temperature program starting at 160 °C (1 min) and then rising 2 °C min⁻¹ up to 200 °C. An *m/z* range between 40 and 450 amu was scanned. Identification was done on the basis of the retention time and mass spectra of the compounds. Quantification was performed according to peak area.

2.8.5. NMR analysis

The floating and precipitated EPS fractions were deuterium exchanged several times by freeze drying from D₂O and then examined as solutions (3 mg/mL) in 99.98% D₂O. Spectra were recorded at 300 K on a Bruker AMX500 spectrometer operating at 500 · 13 MHz (¹H-nuclear magnetic resonance). Chemical shifts are given in parts

per million using the HDO (semi heavy water) signal (4.75 ppm) (^1H) as reference.

3. Results and discussion

3.1. Characterization of the EPS-producing strains

In the present work, two LAB strains isolated from ropy ciders were investigated for their ability to produce exopolysaccharide. They exhibited a ropy phenotype when cultured in MRS broth and on MRS agar, suggesting that they were exopolysaccharide producers. The colonies formed long filaments after being touched with a loop. On the basis of partial 16S rRNA gene sequence analysis, both strains were assigned to *L. suebicus* species with 99% nucleotide identity to the type strain DSM 5007, and named *L. suebicus* CUPV225 (Notararigo et al., 2013) and CUPV226. Sugar fermentation patterns of both EPS-producer strains were tested to detect the potential raw materials to be fermented. These strains were able to ferment, and grow on D-glucose, L-arabinose, D-ribose, D-xylose and D-arabitol, and after 6 days of incubation, maltose was also fermented. Moreover *L. suebicus* CUPV225 fermented methyl- β -D-xyloside. Both strains fermented few sugars regarding the type obligately heterofermentative strain *L. suebicus* DSM 5007 described by Kleynmans et al. (1989), that also fermented D-galactose, cellobiose, melibiose and sucrose. Besides, the authors observed no slime production from sucrose.

Extracellular polysaccharides are synthesized by strains of several *Lactobacillus* species that are isolated mainly from fermented foods, as dairy or meat products (De Vuyst and Degeest, 1999), or cereal products (Van der Meulen et al., 2007). Heterofermentative lactobacilli and pediococci were involved in the ropiness of cider and wine due to the production of glucan homopolysaccharides (Llaubères et al., 1990; Dueñas et al., 1995; Dueñas-Chasco et al., 1998). *P. parvulus* was the predominant EPS-producer in the spoiled beverages (Garai-Ibabe et al., 2010a; Dols-Lafargue et al., 2008). In our laboratory, several strains of *L. suebicus* were isolated from spoiled ciders, but three of them were capable to produce EPSs: CUPV226, CUPV225 and CUPV221, a strain identified as β -(1,3)-D-glucan producer (Marieta et al., 2009; Garai-Ibabe et al., 2010b; Notararigo et al., 2013). To our knowledge, these are the unique exopolysaccharide-producer strains of *L. suebicus* reported up to now.

3.2. PCR screening for HoPS and HePS genes

The presence of *eps* genes in the ropy strains *L. suebicus* CUPV226 and CUPV225 was assessed by PCR. The results revealed that any of the strains possessed genes coding for HoPS-synthesizing enzymes such as glucan- or fructansucrases (Table 1). One of the tested genes was *gtf* that codifies for a glucosyltransferase involved in the synthesis of the 2-branched (1,3)- β -D-glucan HoPSs by *P. parvulus* 2.6, whose presence served for the specific detection of (1,3)- β -D-glucan producers among several LAB species isolated from ropy ciders, such as *O. oeni*, *Lactobacillus diolivorans*, *L. suebicus* and *Lactobacillus collinoides* (Werning et al., 2006). Although HoPS-producing bacteria have mainly been described in ropy ciders and wines, *O. oeni* I4 (Ibarburu et al., 2007) and *O. oeni* IOEB 0205 (Dimopoulou et al., 2014) showed the unusual ability to synthesize both homo- and heteropolysaccharides. Therefore, the absence of the expected amplicon for HoPSs in both ropy strains suggested heteropolysaccharide production. The presence of genes implicated in an essential step of bacterial HePS biosynthesis was sought using several sets of *eps* primers previously described in the literature (Table 1). Regarding the HePS *eps* primers, DNA of both strains yielded only a 189-bp PCR product with the *epsD/E* primers, which amplify the genes coding for the priming-glycosyltransferase (p-GTF) (Provencher et al., 2003). This enzyme catalyze the transfer of the first phospho-sugar residue from an activated nucleotide sugar to the undecaprenyl phosphate-lipid carrier on the cytoplasmic face

of the membrane, at the first step of repeating unit synthesis of HePSs (Werning et al., 2012). No PCR products were obtained with any of the other primers used. The sequenced PCR products of CUPV225 and CUPV226 strains (see Table S1 in the Supplemental material) showed 79% and 81% identity, respectively, with the *epsE* gene of the HePS producer *Lactobacillus helveticus* CRL1176 (accession no. DQ222973). All these data suggested that both strains synthesize heteropolysaccharides (Notararigo et al., 2013).

3.3. Effect of initial pH on growth and EPS production

Lactobacilli have a more favorable growth in culture media with a slightly acidic pH of 6.4–5.4. Usually, bacterial growth decreases below these pH values and stops at pH values around 3.6–4.0, depending on the strains. However, *L. suebicus* strains isolated from fruit mashes were able to grow even at pH 2.8 (Kleynmans et al., 1989). Based on these premises, and since initial pH was reported as one of the factors affecting the properties and amount of EPS produced by LAB (De Vuyst and Degeest, 1999), the influence of different pH values (4.8, 5.5, 6) on growth and EPS production was analyzed. Incubations were performed at 28 °C in a semi-defined medium, without adding yeast extract, beef extract, or peptone, as these ingredients interfere with EPS analysis. Samples were collected at various incubation times to estimate bacterial growth and the amount of EPS produced.

The growth curves for both strains were similar at pH 5.5 and 6.0 (data not shown), whereas biomass production was lower at pH 4.8 (Table 2). The highest optical density value was detected at 48 h in CUPV225 and 72 h in CUPV226. Velasco et al. (2006) reported the maximum EPS production by the β -glucan producer *P. parvulus* 2.6 at pH 5.2 and according to Torino et al. (2001), pH 5 was the optimal value for general metabolism and EPS production in *L. helveticus* ATCC 15807. As shown in Fig. 2, EPSs were released to the culture medium along the incubation period, and amounts close to 100 mg L⁻¹ were recovered at the end of exponential growth phase. Similar EPS concentrations have been reported for most of the HePS-producing *Lactobacillus* strains (De Vuyst and Degeest, 1999; Werning et al., 2012) as well as the β -glucan producing LAB strains isolated from cider and wine (Ibarburu et al., 2007; Garai-Ibabe et al., 2010a; Dols-Lafargue et al., 2008). In addition, growth and EPS production by *L. suebicus* CUPV226 strain was compared under controlled pH (5.5) and a large incubation period (Table 2). CUPV226 cells growing under controlled pH synthesized and released EPSs into the growth medium mainly during the exponential growth phase and continued in the stationary phase, in agreement with that found for EPS-producing *Pediococcus*, *Lactobacillus* and *Oenococcus* strains isolated from cider (Velasco et al., 2006; Ibarburu et al., 2007; Garai-Ibabe et al., 2010b). No significant differences in EPS accumulation were observed up to 88-h of incubation, as compared with cultures grown without pH control. In the latter, the increase in the amount of neutral carbohydrates observed at longer incubation times occurred in parallel with a decrease in cell count and optical density, and was probably due to cell lysis. However, when pH was controlled, the cell viability decrease was slower and more gradual, and only a slight increase in the EPS concentration was detected after 111 h of incubation. In addition, Table 2 shows the EPS yield expressed in mg/L EPS per cell number/L. The EPS yield profile between 15 and 48 h of fermentation without pH control, at pH values of 4.8 and 5.5, showed that EPS/cell ratio is similar and higher than that with the controlled pH. After 63 h of fermentation, the EPS yield became higher with pH 5.5 due to the decreased cell number.

To check the EPS purity after ethanol precipitation, dialysis, and lyophilisation, the concentration of neutral carbohydrates, protein, DNA, and RNA was analyzed in aqueous solutions of the EPS preparations from cultures at pH 5.5. The results show that the proportion of the EPSs was variable depending on the fraction, being higher in the precipitated fractions (75.56 and 82.32%) of both strains (Table 4). As discussed below, the EPSs produced by *L. suebicus* CUPV225 and

Table 2
Microbial count and EPS production by *L. suebicus* CUPV226 in SMD medium with 4.8, 5.5 and controlled pH.

Incubation time (h)	pH 4.8			pH 5.5			Controlled pH 5.5		
	Cell count (CFU/mL)	EPS (mg/L)	EPS yield (mgEPS/cell)	Cell count (CFU/mL)	EPS (mg/L)	EPS yield (mgEPS/cell)	Cell count (CFU/mL)	EPS (mg/L)	EPS yield (mg EPS/cell)
0	2.62E+08	4.99 ± 0.44	–	2.76E+08	5.8 ± 1.06	–	1.62E+08	4.62 ± 0.89	–
15	2.31E+08	21.64 ± 0.10	9.39E–08	3.31E+08	33.46 ± 3.63	1.01E–07	3.16E+08	27.46 ± 2.72	8.69E–08
24	2.55E+08	28.88 ± 0.92	1.13E–07	4.56E+08	44.37 ± 2.53	9.73E–08	1.08E+09	41.23 ± 4.68	3.82E–08
39	5.53E+08	47.95 ± 1.38	8.68E–08	6.63E+08	68.34 ± 1.68	1.03E–07	2.85E+09	68.51 ± 2.43	2.40E–08
48	8.55E+08	58.75 ± 0.53	6.87E–08	1.17E+09	96.64 ± 1.17	8.26E–08	2.77E+09	79.63 ± 2.54	2.87E–08
63	1.04E+09	62.85 ± 2.67	6.06E–08	2.35E+09	92.29 ± 1.12	3.93E–08	2.34E+09	93.07 ± 1.84	3.98E–08
72	1.23E+09	91.78 ± 1.64	7.46E–08	1.16E+09	94.03 ± 0.19	8.11E–08	2.23E+09	92.20 ± 3.10	4.13E–08
88	8.68E+08	125.16 ± 1.01	1.44E–07	3.45E+08	124.77 ± 0.29	3.62E–07	1.49E+09	108.98 ± 1.70	7.31E–08
111	9.63E+08	130.71 ± 1.52	1.36E–07	2.07E+07	261.91 ± 2.63	1.27E–05	1.54E+09	102.01 ± 3.34	6.62E–08

CUPV226 are heteropolysaccharides composed of neutral sugars, glucosamine and phosphate. Since the EPS amount was estimated by the phenol–sulphuric acid method, which detects neutral sugars but does not give positive reaction with aminosugars, carbohydrate content was underestimated. Protein contamination from 10 to 22% was detected in the EPS preparations (data not shown). Proteins and residual DNA and RNA in the EPS preparations were presumably due to cell lysis.

3.4. Fermentative metabolism

The batch fermentation profiles of *L. suebicus* CUPV226 and CUPV225 were analyzed by HPLC. Incubations were performed without pH control, at the optimal initial pH value of 5.5 (Table 3). Both strains metabolized L-malic acid to L-lactic acid by malolactic fermentation (FML), similar to that described for other LAB isolates from cider (Dueñas et al., 1995). Apple juice, like grape juice, contains this C4-dicarboxylic acid, and the FML is the physiological significance in cidermaking and winemaking processes (du Toit et al., 2011). The malic acid consumption rate was higher for CUPV225 than CUPV226. Amounts close to 85% were consumed by CUPV225 at 72 h of incubation, while malic acid was partially consumed by CUPV226 strain (23%). Glucose was metabolized by *L. suebicus* strains via the phosphoketolase pathway to mixtures of lactic acid and ethanol and besides, EPS production occurred during the active growth phase. At the end of the incubation period (72 h), the hexose was practically consumed by *L. suebicus* CUPV226 and completely by CUPV225, and traces of acetic acid (0.2 g/L) were only detected in cultures of *L. suebicus* CUPV226 strain. Similar to that found in other heterofermentative LAB, the NAD(P)H released during conversion of the hexose to a pentose was reoxidized in the ethanol pathway yielding ethanol instead of acetate (Zaunmüller et al., 2006). Similar concentrations of lactic acid were found at the end of incubation.

3.5. Influence of the sugar source on growth and EPS production

Several studies have previously reported that medium composition influence EPS production by *Lactobacillus* strains (Cerning et al., 1994; Petry et al., 2000). In this work, the effect of several carbohydrate

sources on growth and EPS production was analyzed. Both strains were grown in the semidefined SMD medium with glucose, arabinose, ribose or xylose as these monosaccharides are both fermented and contained in apple musts and ciders (Blanco et al., 2001; Arnous and Meyer, 2008). Fermentations proceeded without pH control for 3 days at 28 °C (Fig. 1). Although maltose was fermented in the complex medium MRS, during the first 3 days of incubation the growth in the semidefined medium was negligible (data not shown). As shown in Fig. 1, both *L. suebicus* strains showed similar growth profiles on all monosaccharides assayed. The growth with xylose and arabinose provided the highest and the lowest maximal biomass values, respectively. Similar to that found in *Lactobacillus brevis* strains (Falck et al., 2013), xylose stimulated growth to a higher degree than glucose, the maximum optical densities being detected after 24 h and 48 h incubation respectively. EPS production was also influenced by the carbohydrate source. In the presence of xylose, culture supernatants contained about 100 mg/L after 24 h. The results represented in Fig. 1b show that the cultures with arabinose produced the lowest EPS synthesis after 48–72 h, which agrees with the growth curve tendency with this sugar. However after 24 h proportionally more EPSs were obtained when arabinose was used instead of ribose, and the same amount of EPSs was obtained in glucose.

Instead, ribose seemed to be a favorable sugar source for growth, and both biomass and EPS concentration increased along the incubation period (EPS amounts close to 150 mg/L after 72 h). Ribose was previously used as an additional carbohydrate source to increase EPS production by *Streptococcus thermophilus* LY03 (Degeest et al., 2002), as this pentose is the main component of the sugar nucleotides, the precursor molecules in EPS biosynthesis; however, no significant increase of the EPS yield was observed.

On account of cell lysis, analysis of the EPS preparation showed a slight contamination by DNA and RNA, and between 10–12% protein was also detected in the EPS fractions from cultures with xylose and ribose, except in the floating fraction from fermentation with ribose that did not contain protein (data not shown). Furthermore, as in fermentations with glucose, the analysis of the chemical composition of the EPS fractions underscored the carbohydrate content in these

Table 3
Batch fermentation profile of *L. suebicus* CUPV226 and CUPV225, grown in SMD medium with glucose (20 g L⁻¹) at 28 °C, and without pH control (initial pH value of 5.5).

Incubation time (h)	OD ₆₀₀	pH	EPS (mg/L)	Residual glucose (g/L)	Malic acid (g/L)	Lactic acid (g/L)	Ethanol (g/L)
<i>L. suebicus</i> CUPV226	0	0.198 ± 0.008	5.52	6.4 ± 1.7	20.75 ± 0	4.35 ± 0	0
	24	1.190 ± 0.013	4.89	44.4 ± 2.5	15.28 ± 0.03	3.90 ± 0.03	2.41 ± 0.00
	48	2.784 ± 0.097	4.32	94.9 ± 3.2	3.59 ± 0.04	3.33 ± 0.00	8.03 ± 0.13
	72	2.924 ± 0.164	4.25	105.5 ± 13.6	0.57 ± 0.00	3.28 ± 0.02	9.92 ± 0.00
<i>L. suebicus</i> CUPV225	0	0.268 ± 0.000	5.27	6.9 ± 1.6	20.75 ± 0	4.35 ± 0	0
	24	2.871 ± 0.013	4.30	65.8 ± 4.1	9.11 ± 0.04	2.27 ± 0.04	5.35 ± 0.03
	48	3.563 ± 0.049	4.22	109.2 ± 4.0	0.12 ± 0.00	2.26 ± 0.00	9.15 ± 0.01
	72	2.031 ± 0.038	4.28	189.0 ± 5.0	0	0.67 ± 0.00	9.48 ± 0.24

The results are presented as means ± standard deviations of two independent experiments. OD₆₀₀, optical density at 600 nm.

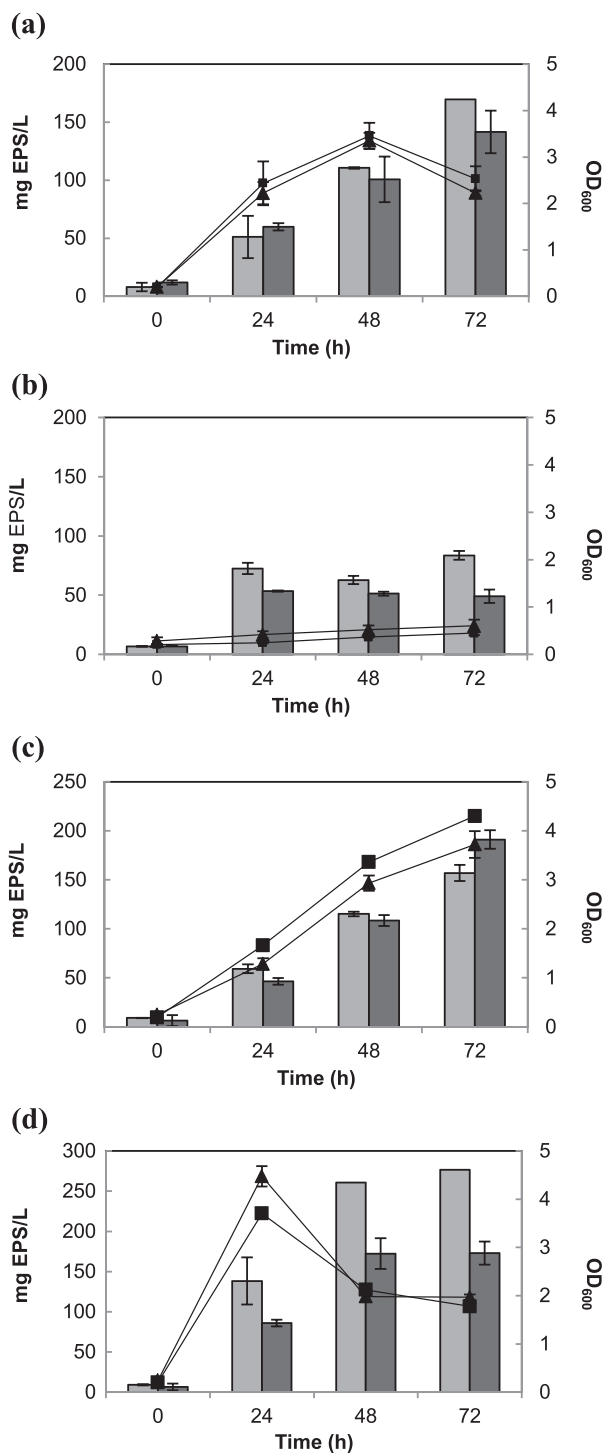


Fig. 1. Influence of carbohydrate source on growth (\blacktriangle CUPV226; \blacksquare CUPV225) and EPS production (CUPV226, light gray; CUPV225, dark gray) grown, (a) glucose, (b) arabinose, (c) ribose, and (d) xylose.

samples, which was estimated to be between 48 and 82% depending on the fraction (Table 4).

3.6. Isolation and partial characterization of EPSs

Monosaccharide composition of EPSs from lactic acid bacteria depends on the strain and can be influenced by media and culture conditions. Cultures of *L. suebicus* CUPV226 and CUPV225 in SMD broth supplemented with glucose and without pH control were grown

for 72 h to collect the EPSs. Moreover, EPSs were recovered from cultures of *L. suebicus* CUPV226 in the same medium supplemented with ribose or xylose, to test the effect of using pentoses as carbon sources on EPS composition. When ethanol was added to the culture media, two polysaccharide fractions were distinguished. One of them was collected while floating in 25% ethanol (F) and the other fraction was recovered as a precipitate after centrifugation (P). The composition of fractions F and P was analyzed by GLC–MS and the relative proportions of their components are gathered in Table 4, showing to have the same components (glucose, galactose, *N*-acetylglucosamine, and phosphate) but in different proportions. In glucose-fed cultures fraction F showed higher glucose/galactose ratios and *N*-acetylglucosamine content than fraction P. Nevertheless, when pentoses were used as the carbon source, the glucose/galactose ratio and the *N*-acetylglucosamine content were similar in F and P fractions.

In HePSs from lactic acid bacteria glucose and galactose are both common sugars and, to a lesser extent, *N*-acetyl-glucosamine (Werning et al., 2012). This amino-sugar was reported in the EPSs produced by LAB belonging to different species, such as *Lactobacillus rhamnosus* (Shao et al. 2014; Landersjö et al., 2002), *Lactococcus lactis* subsp. *cremoris* (Marshall et al., 1995) and *S. thermophilus* (Almirón-Roig et al., 2000). In addition the HePSs from both *L. suebicus* strains contain phosphate. This inorganic molecule has been described in HePSs from *Lactobacillus plantarum* (Tallon et al., 2003), *L. lactis* subsp. *cremoris* (van Casteren et al., 1998) and *Lactobacillus delbrueckii* ssp. *bulgaricus* (Makino et al., 2006). On the other hand, it has been shown the relevant role of PO_4^- in immune stimulation of polysaccharides synthesized by *L. delbrueckii* ssp. *bulgaricus* (Makino et al., 2006).

Fig. 2 shows the infrared spectra of these fractions, synthesized with D-glucose as carbon source, recorded in the transmission mode between 3700 and 700 cm^{-1} and analyzed after Fourier transform. The bands in the spectrum of the F fraction coincide to that previously reported by Notararigo et al. (2013) for the same material. In fraction P, the spectrum was also comparable, with a broad stretching characteristic peak around 3400 cm^{-1} from hydroxyl groups and a C–H stretching band around 2920 cm^{-1} . In the range between 1090–1030 cm^{-1} , a band characteristic of phosphoric esters was observed in all the spectra. The presence of two bands at approximately 1550 cm^{-1} (amide I) from C=O stretching vibration and 1650 cm^{-1} (amide II) from N–H bending and C–N stretching, confirmed that the glucosamine residues detected by GC were *N*-acetylated. Likewise, all spectra showed the bands typical of polysaccharides in the region 1200–950 cm^{-1} (fingerprint region) with an intense peak at 1038 cm^{-1} (Shang et al., 2013). An absorption peak at 850 cm^{-1} was observed only in the IR spectrum of *L. suebicus* CUPV225 floating fraction, suggesting α configuration of sugars (Shang et al., 2013). This absorption peak or others regarding the anomeric configuration of sugars were not observed in the other samples analyzed, probably due to the presence of more than one anomeric type in the EPS preparation.

The $^1\text{H-NMR}$ analysis of P and F fractions from both strains revealed a very complex set of signals that obstructed its resolution (Fig. 3). $^1\text{H-NMR}$ spectra were very similar, with several signals between 5.4 and 5.0 ppm, compatible with the presence of α -anomers, and several signals between 5.0 and 4.4 ppm indicating the presence of β -anomers. When comparing the anomeric regions, two sets of signals can be found: a set of five relatively narrow signals at approximately 5.2 ppm (two) and 4.6 ppm (three), and a second set of broad signals close to 4.8 ppm. The relative intensity of both sets are different in these fractions, which agrees with a mixture of polysaccharides. Moreover, the intensity of signal around 2 ppm, characteristic of *N*-acetyl groups from glucosamine increases with signals from broad set. These data are compatible with the presence of a polysaccharide of relatively low molecular weight (narrow signals) and a second polysaccharide of high molecular weight (broad signals), which would contain *N*-acetylglucosamine residues.

Table 4
Composition and molecular masses of EPS fractions produced by *L. suebicus* strains grown on different carbohydrate sources.

<i>L. suebicus</i> strain	Fraction	Carbon source	EPS (%) ^a	Relative ratio of sugar composition			Phosphoric acid (%)	Mw, g/mol (polydispersity) ^b		EPS H:EPS L ^c
				Gal	Glc	N-acetylglucosamine		EPS H	EPS L	
CUPV225	F	Glucose	53.5	1	2.8	1.9	2.4	1.67 × 10 ⁶ (2.86)	2.53 × 10 ⁴ (1.33)	1:1
	P	Glucose	75.5	1.1	1.8	1	4.5	7.80 × 10 ⁶ (2.92)	2.17 × 10 ⁴ (1.73)	1:1
CUPV226	F	Glucose	66.3	1	5.1	5.4	1.7	1.51 × 10 ⁶ (2.86)	2.51 × 10 ⁴ (1.34)	2:1
	P	Glucose	82.3	1	2.8	1.1	8.8	4.20 × 10 ⁶ (2.28)	1.90 × 10 ⁴ (1.77)	1:3
	F	Ribose	48.2	1.2	1.6	1	n.d.	4.49 × 10 ⁶ (2.63)	2.55 × 10 ⁴ (1.29)	1:1
	P	Ribose	67.9	3.5	4.4	1	n.d.	1.98 × 10 ⁶ (3.44)	2.04 × 10 ⁴ (1.28)	1:8
	F	Xylose	66.7	1	1.5	1.1	n.d.	4.39 × 10 ⁶ (2.66)	2.63 × 10 ⁴ (1.51)	1:1
	P	Xylose	51.6	9.3	9.6	1	n.d.	1.52 × 10 ⁶ (3.0)	2.17 × 10 ⁴ (1.31)	1:18

F, floating fraction; P, precipitated fraction. H, high molecular weight polymer; L, low molecular weight polymer. n.d., not determined.

^a Data obtained by phenol-sulphuric acid method.

^b Mw/Mn is a measure of polydispersity.

^c Data are ratio of peak area from EPS H and EPS L.

To test this point, and for weight-average molecular weight determination, size exclusion chromatography (SEC) was carried out, revealing the presence of two peaks, corresponding to polymers of high- (EPS H) and low-molecular-weight (EPS L) in all fractions (Table 4). The high-Mw polymers of both strains ranged between 1.5 and 7.8 × 10⁶ g/mol, except that in P fraction of CUPV226 grown in glucose (10⁵ g/mol). The low-Mw polymer ranged between 1.90 and 2.63 × 10⁴ g/mol, presenting polydispersity values lower than those obtained from high-Mw polymers. EPS H and EPS L polymers were not completely separated through ethanol precipitation, unlike two types of EPSs produced simultaneously by *S. thermophilus* LY03 isolated from the fermentation broth separately (De Vuyst and Degeest, 1999).

Monosaccharide analysis of the H fractions revealed the presence of glucose and N-acetylglucosamine as their main components, while the L fractions contained similar amounts of glucose and galactose, and phosphate. The production of EPSs with these components

has not previously reported for lactobacilli, and then their structural characterization merits further investigation.

It is interesting to note that in cultures grown with pentoses as the carbon source, the low-Mw EPS (EPS L) was mostly recovered in P fraction (ratios H:L of 1:18 with xylose and 1:8 with ribose), which agrees with the monosaccharide composition detected for fractions F and P. These results indicate that EPS L is preferably synthesized when only C5-carbon sources were available, and then that the synthesis of EPSs is dependent on the carbon source, as reported by Sánchez et al. (2006) for a *Lactobacillus pentosus* strain.

HePS production by different *Lactobacillus* species is being studied in the last years for food and human health applications (Ryan et al., 2015), and it should be noted that both structure and molecular mass depend on the EPS producing strain. In this work, the EPS synthesis by two *L. suebicus* strains isolated from ropy ciders of different cidemaker cellars and the apple juice sugars that could be potentially used for EPS synthesis was studied. In addition to glucose, both strains were able to

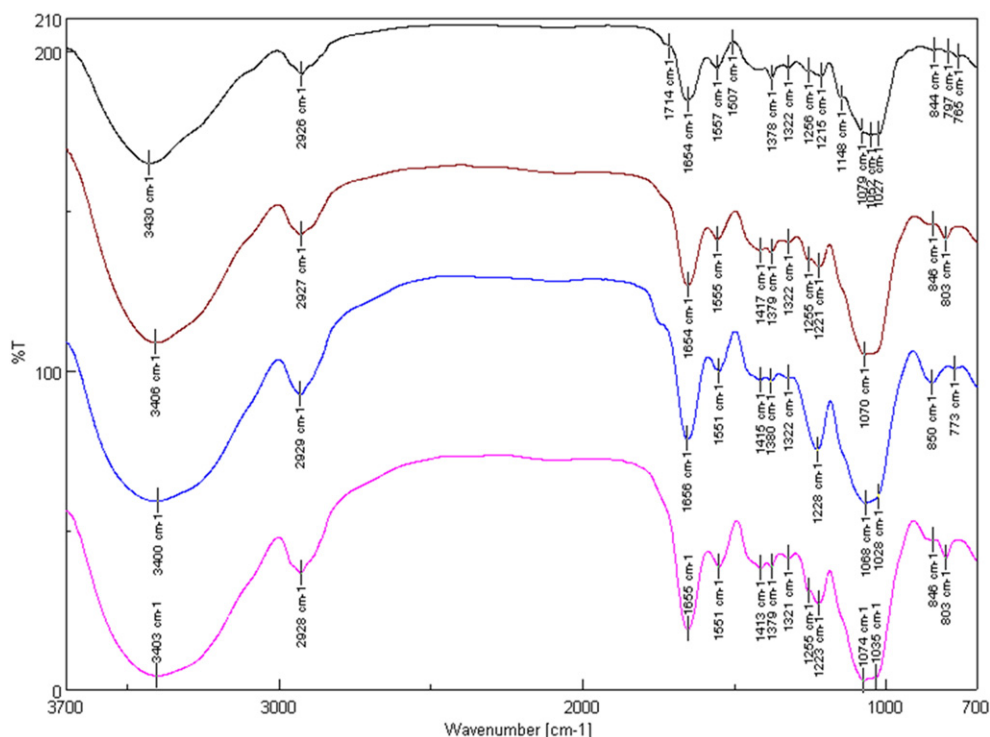


Fig. 2. Fourier-transform infrared spectra of EPS fractions synthesized by *L. suebicus* CUPV226 and CUPV225. Fractions: 226F (black), 226P (red), 225F (blue), and 225P (pink).

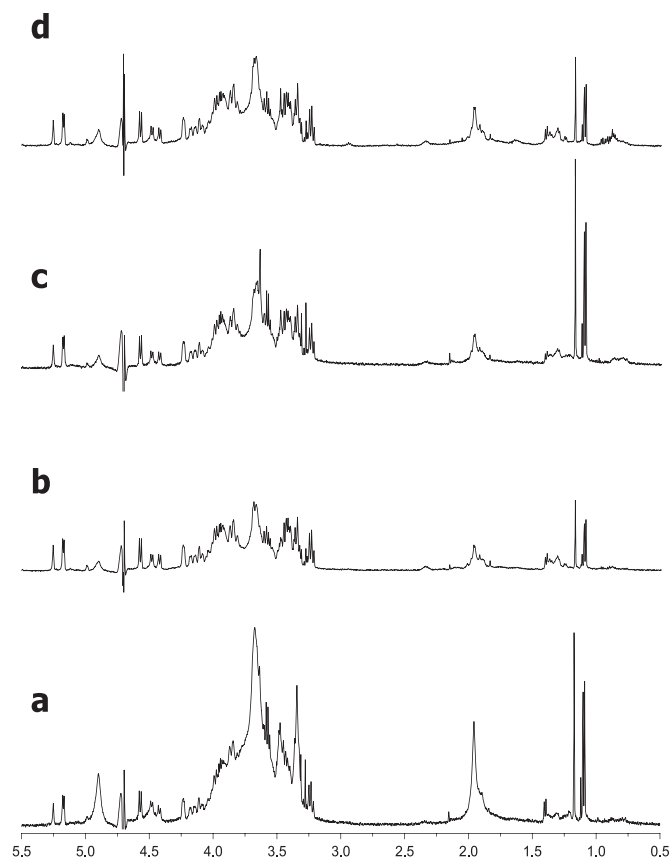


Fig. 3. $^1\text{H-NMR}$ (500 MHz) spectra of the fractions containing polysaccharides: a) CUPV226F, b) CUPV226P, c) CUPV225F, and d) CUPV225P.

produce EPSs from ribose and xylose. The crude-EPS analyses showed that were constituted by two polymers of high- and low-molecular weight. Both strains synthesized a mixture of complex HePSs, one of them acidic, containing glucose, galactose, and phosphate, and other composed of glucose and N-acetylglucosamine. However, the relative proportion of both polysaccharides is different depending on the monosaccharide source. Taking into account the relevant role of PO_4^- in immune stimulation of exopolysaccharides, their structural characterization and immunological properties are currently under investigation.

Abbreviations

LAB	lactic acid bacteria
MRS	Man Rogosa Sharpe medium
EPS	exopolysaccharide
HPLC	high-performance liquid chromatography
SMD	semidefined medium
HePS	heteropolysaccharide
HoPS	homopolysaccharide

Supplementary data to this article can be found online at <http://dx.doi.org/10.1016/j.ijfoodmicro.2015.07.012>.

Acknowledgments

This study was supported by grants AGL2009-12998-C03, AGL2012-40084-C03 (co-funded by FEDER) and IT866-13 from the Basque Government. Technical and human support provided by the SGiker (UPV/EHU, MICINN, GV/EJ, FEDER y FSE) is also gratefully acknowledged.

References

- Almirón-Roig, E., Mulholland, F., Gasson, M.J., Griffin, A.M., 2000. The complete *cps* gene cluster from *Streptococcus thermophilus* NCFB 2393 involved in the biosynthesis of a new exopolysaccharide. *Microbiology* 146, 2793–2802.
- Arnous, A., Meyer, A.S., 2008. Comparison of methods for compositional characterization of grape (*Vitis vinifera* L.) and apple (*Malus domestica*) skins. *Food Bioprod. Process.* 86, 79–86.
- Blanco, D., Muro, D., Mangas, J., 2001. Determination of monosaccharides in cider by reversed-phase liquid chromatography. *Anal. Chim. Acta* 436, 173–180.
- Cerning, J., Renard, C.M.G.C., Thibault, J.F., Bouillanne, C., Landon, M., Desmazeaud, M., Topisirovic, L., 1994. Carbon source requirements for exopolysaccharide production by *Lactobacillus casei* CG11 and partial structure analysis of the polymer. *Appl. Environ. Microbiol.* 7460, 3914–3919.
- Ciucanu, I., Kerek, F., 1984. A simple and rapid method for the permethylation of carbohydrates. *Carbohydr. Res.* 131, 209–217.
- De Vuyst, L., Degeest, B., 1999. Heteropolysaccharides from lactic acid bacteria. *FEMS Microbiol. Rev.* 23, 153–177.
- De Vuyst, L., de Vin, F., Vaningelgem, F., Degeest, B., 2001. Recent developments in the biosynthesis and applications of heteropolysaccharides from lactic acid bacteria. *Int. Dairy J.* 11, 687–707.
- De Vuyst, L., Weckx, S., Ravyts, F., Herman, L., Leroy, F., 2011. New insights into the exopolysaccharide production of *Streptococcus thermophilus*. *Int. Dairy J.* 21, 586–591.
- Degeest, B., Mozzi, F., De Vuyst, L., 2002. Effect of medium composition and temperature and pH changes on exopolysaccharide yields and stability during *Streptococcus thermophilus* LY03 fermentations. *Int. J. Food Microbiol.* 79, 161–174.
- Deveau, H., Moineau, S., 2003. Use of RFLP to characterize *Lactococcus lactis* strains producing exopolysaccharides. *J. Dairy Sci.* 86, 1472–1475.
- Dimopoulou, M., Vuillemin, M., Campbell-Sills, H., Lucas, P.M., Ballestra, P., Miot-Sertier, C., Favier, M., Coulon, J., Moine, V., Doco, T., Roques, M., Williams, P., Petrel, M., Gontier, E., Moulis, C., Remaud-Simeon, M., Dols-Lafargue, M., 2014. Exopolysaccharide (EPS) synthesis by *Oenococcus oeni*: from genes to phenotypes. *PLoS ONE* 9 (6), e98898.
- Dols-Lafargue, M., Lee, H.Y., Le Marrec, D., Heyraud, A., Chambat, G., Lonvaud-Funel, A., 2008. Characterization of *gtf*, a glucosyltransferase gene in the genomes of *Pediococcus parvulus* and *Oenococcus oeni*, two bacterial species commonly found in wine. *Appl. Environ. Microbiol.* 74, 4079–4090.
- du Toit, M., Engelbrecht, L., Lerm, E., Krieger-Weber, S., 2011. *Lactobacillus*: the next generation of malolactic fermentation starter cultures—an overview. *Food Bioprocess Technol.* 4, 876–906.
- Dubois, M., Gilles, K.A., Hamilton, J.K., Rebers, P.A., Smith, F., 1956. Colorimetric method for determination of sugars and related substances. *Anal. Chem.* 28, 350–356.
- Dueñas, M., Irastorza, A., Fernández, K., Bilbao, A., 1995. Heterofermentative *Lactobacilli* causing ropiness in Basque country ciders. *J. Food Prot.* 58, 76–80.
- Dueñas-Chasco, M.T., Rodríguez-Carvajal, M.A., Tejero-Mateo, P., Franco-Rodríguez, G., Espartero, J.L., Irastorza-Iribas, A., Gil-Serrano, A.M., 1997. Structural analysis of the exopolysaccharide produced by *Pediococcus damnosus* 2.6. *Carbohydr. Res.* 303, 453–458.
- Dueñas-Chasco, M.T., Rodríguez-Carvajal, M.A., Tejero-Mateo, P., Espartero, J.L., Irastorza-Iribas, A., Gil-Serrano, A.M., 1998. Structural analysis of the exopolysaccharides produced by *Lactobacillus* spp. G-77. *Carbohydr. Res.* 307, 125–133.
- Falck, P., Precha-Atsawan, S., Grey, C., Immerzeel, P., Staišlbrand, H., Adlercreutz, P., Nordberg Karlsson, E., 2013. Xylooligosaccharides from hardwood and cereal xylans produced by a thermostable xylanase as carbon sources for *Lactobacillus brevis* and *Bifidobacterium adolescentis*. *J. Agric. Food Chem.* 61, 7333–7340.
- Garai-Ibabe, G., Areizaga, J., Aznar, R., Elizaguivel, P., Prieto, A., Irastorza, A., Dueñas, M.T., 2010a. Screening and selection of 2-branched (1,3)- β -D-glucan producing lactic acid bacteria and exopolysaccharide characterization. *J. Agric. Food Chem.* 58, 6149–6156.
- Garai-Ibabe, G., Dueñas, M.T., Irastorza, A., Sierra-Filardi, E., Werning, M.L., López, P., Corbí, A.L., Fernández de Palencia, P., 2010b. Naturally occurring 2-substituted (1,3)- β -D-glucan producing *Lactobacillus suebicus* and *Pediococcus parvulus* strains with potential utility in the production of functional foods. *Bioresour. Technol.* 101, 9254–9263.
- Hidalgo-Cantabrana, C., Patricia López, P., Gueimonde, M., de los Reyes-Gavilán, C.G., Suárez, A., Margolles, A., Ruas-Madiedo, P., 2012. Immune modulation capability of exopolysaccharides synthesised by lactic acid bacteria and bifidobacteria. *Probiot. Antimicrob. Proteins* 4, 227–237.
- Ibarburu, I., Soria-Díaz, M.E., Rodríguez-Carvajal, M.A., Velasco, S.E., Tejero-Mateo, P., Gil-Serrano, A.M., Irastorza, A., Dueñas, M.T., 2007. Growth and exopolysaccharide (EPS) production by *Oenococcus oeni* 14 and structural characterization of their EPSs. *J. Appl. Microbiol.* 103, 477–486.
- Kleynmans, U., Heinzl, H., Hammes, W.P., 1989. *Lactobacillus suebicus* sp. nov., an obligately heterofermentative *Lactobacillus* species. *Syst. Appl. Microbiol.* 11, 267–271.
- Korakli, M., Ganzle, M.G., Vogel, R.F., 2002. Metabolism by bifidobacteria and lactic acid bacteria of polysaccharides from wheat and rye, and exopolysaccharides produced by *Lactobacillus sanfranciscensis*. *J. Appl. Microbiol.* 92, 958–965.
- Kralj, S., van Geel-Schutten, G.H., van der Maarel, M., Dijkhuizen, L., 2003. Efficient screening methods for glucosyltransferase genes in *Lactobacillus* strains. *Biocatal. Biotransf.* 21, 181–187.
- Laine, R.A., Esselman, W.J., Sweeley, C.C., 1972. Gas-liquid chromatography of carbohydrates. *Methods Enzymol.* 28, 159–167.
- Landersjö, C., Yang, Z., Huttunen, E., Widmalm, G., 2002. Structural studies of the exopolysaccharide produced by *Lactobacillus rhamnosus* strain GG (ATCC 53103). *Biomacromolecules* 3, 880–884.
- Llaubères, R.M., Richard, B., Lonvaud, A., Doubourdieu, D., Fournet, B., 1990. Structure of an extracellular β -D-glucan from *Pediococcus* sp., a wine lactic bacteria. *Carbohydr. Res.* 203, 103–107.

- Low, D., Ahlgren, J.A., Horne, D., McMahon, D.J., Oberg, C.J., Broadbent, J.R., 1998. Role of *Streptococcus thermophilus* MR-1C capsular exopolysaccharide in cheese moisture retention. *Appl. Environ. Microbiol.* 64, 2147–2151.
- Makino, S., Ikegami, S., Kano, H., Sashihara, T., Sugano, H., Horiuchi, H., Saito, T., Oda, M., 2006. Immunomodulatory effects of polysaccharides produced by *Lactobacillus delbrueckii* ssp. *bulgaricus* OLL1073R-1. 2006. *J. Dairy Sci.* 89, 2873–2878.
- Marieta, C., Ibarburu, I., Dueñas, M., Irastorza, A., 2009. Supramolecular structure and conformation of a (1,3)(1,2)- β -D-glucan from *Lactobacillus suebicus* CUPV221 as observed by tapping mode atomic force microscopy. *J. Agric. Food Chem.* 57, 6183–6188.
- Marshall, V.M., Cowie, E.N., Moreton, R.S., 1995. Analysis and production of two exopolysaccharides from *Lactococcus lactis* subsp. *cremoris* LC330. *J. Dairy Res.* 62, 621–628.
- Mozzi, F., Savoy de Giori, G., Font de Valdez, G., 2003. UDP-galactose 4-epimerase: a key enzyme in exopolysaccharide formation by *Lactobacillus casei* CRL 87 in controlled pH batch cultures. *J. Appl. Microbiol.* 94, 175–183.
- Mozzi, F., Vaningelgem, F., Hébert, E.M., Van der Meulen, R., Foulquié Moreno, M.R., Font de Valdez, G., De Vuyst, L., 2006. Diversity of heteropolysaccharide-producing lactic acid bacterium strains and their biopolymers. *Appl. Environ. Microbiol.* 72, 4431–4435.
- Nam, S.H., Choi, S.H., Kang, A., Kim, D.W., Kim, R.N., Kim, D.S., Kim, A., Park, H.S., 2011. Genome sequence of *Lactobacillus suebicus* KCTC 3549. *J. Bacteriol.* 193, 5532–5533.
- Notararigo, N., Náchter-Vázquez, M., Ibarburu, I., Werning, M.L., Fernández de Palencia, P., Dueñas, M.T., Aznar, R., López, P., Prieto, A., 2013. Comparative analysis of production and purification of homo- and hetero-polysaccharides produced by lactic acid bacteria. *Carbohydr. Polym.* 93, 57–64.
- Petry, S., Furlan, S., Crepeau, M.J., Cerning, J., Desmazeaud, M., 2000. Factors affecting exocellular polysaccharide production by *Lactobacillus delbrueckii* subsp. *bulgaricus* grown in a chemically defined medium. *Appl. Environ. Microbiol.* 66, 3427–3431.
- Provencher, C., La Pointe, G., Sirois, S., Van Calsteren, M.R., Roy, D., 2003. Consensus-degenerate hybrid oligonucleotide primers for amplification of priming glycosyltransferase genes of the exopolysaccharide locus in strains of the *Lactobacillus casei* group. *Appl. Environ. Microbiol.* 69, 3299–3307.
- Ryan, P.M., Ross, R.P., Fitzgerald, G.F., Caplice, N.M., Stanton, C., 2015. Sugar-coated: exopolysaccharide producing lactic acid bacteria for food and human health applications. *Food Funct.* 6, 679–693.
- Sánchez, J.I., Martínez, B., Guillén, R., Jiménez-Díaz, R., Rodríguez, A., 2006. Culture conditions determine the balance between two different exopolysaccharides produced by *Lactobacillus pentosus* LPS2. *Appl. Environ. Microbiol.* 72, 7495–7502.
- Shang, N., Xua, R., Li, P., 2013. Structure characterization of an exopolysaccharide produced by *Bifidobacterium animalis* RH. *Carbohydr. Polym.* 91, 128–134.
- Shao, L., Zhang, H., Chen, W., Ai, L., Guo, B., 2014. Partial characterization and immunostimulatory activity of exopolysaccharides from *Lactobacillus rhamnosus*. *Carbohydr. Polym.* 107, 51–56.
- Tallon, R., Bressollier, P., Urdaci, M.C., 2003. Isolation and characterization of two exopolysaccharides produced by *Lactobacillus plantarum* EP56. *Res. Microbiol.* 154, 705–712.
- Tieking, M., Korakli, M., Ehrmann, M.A., Gänzle, M.G., Vogel, R.F., 2003. In situ production of exopolysaccharides during sourdough fermentation by cereal and intestinal isolates of lactic acid bacteria. *Appl. Environ. Microbiol.* 69, 945–952.
- Torino, M.I., Taranto, M.P., Sesma, F., de Valdez, G.F., 2001. Heterofermentative pattern and exopolysaccharide production by *Lactobacillus helveticus* ATCC 15807 in response to environmental pH. *J. Appl. Microbiol.* 91, 846–852.
- van Casteren, W.H.M., Dijkema, C., Schols, H.A., Beldman, G., Voragen, A.G.J., 1998. Characterisation and modification of the exopolysaccharide produced by *Lactococcus lactis* subsp. *cremoris* B40. *Carbohydr. Polym.* 37, 123–130.
- Van der Meulen, R., Grosu-Tudor, S., Mozzi, F., Vaningelgem, F., Zamfir, M., Font de Valdez, G., De Vuyst, L., 2007. Screening of lactic acid bacteria isolates from dairy and cereal products for exopolysaccharide production and genes involved. *Int. J. Food Microbiol.* 118, 250–258.
- Velasco, S., Arskod, E., Paese, M., Grage, H., Irastorza, A., Radstrom, P., van Niel, E.W.J., 2006. Environmental factors influencing growth and exopolysaccharide formation by *Pediococcus parvulus* 2.6. *Int. J. Food Microbiol.* 111, 252–258.
- Werning, M.L., Ibarburu, I., Dueñas, M.T., Irastorza, A., Navas, J., López, P., 2006. *Pediococcus parvulus* *gff* gene encoding the GTF glycosyltransferase and its application for specific PCR detection of β -D-glucan-producing bacteria in foods and beverages. *J. Food Prot.* 69, 161–169.
- Werning, M.L., Notararigo, S., Náchter, M., Fernández de Palencia, P., Aznar, R., López, P., 2012. Biosynthesis, purification and biotechnological use of exopolysaccharides produced by lactic acid bacteria. In: El-Samragy, Y. (Ed.), *Food Additives*. InTech, Croatia, pp. 83–114.
- Zaunmüller, T., Eichert, M., Richter, H., Uden, G., 2006. Variations in the energy metabolism of biotechnologically relevant heterofermentative lactic acid bacteria during growth on sugars and organic acids. *Appl. Microbiol. Biotechnol.* 72, 421–429.



Quantitative determination of lactic and acetic acids in cider by ^1H NMR spectrometry



Andoni Zuriarrain, Juan Zuriarrain, Ana Isabel Puertas, María Teresa Dueñas, Iñaki Berregi*

University of the Basque Country EHU/UPV, Faculty of Chemistry, Manuel Lardizabal 3, 20018 Donostia-San Sebastián, Gipuzkoa, Spain

ARTICLE INFO

Article history:

Received 4 November 2014

Received in revised form

19 December 2014

Accepted 20 December 2014

Available online 29 December 2014

Keywords:

Lactic acid

Acetic acid

Cider

Nuclear magnetic resonance

ABSTRACT

A quantitative determination method of lactic and acetic acids in cider is proposed by means of the proton nuclear magnetic resonance (^1H NMR) technique. Lactic acid gives a doublet signal at 1.42 ppm in the spectrum and acetic acid a singlet signal at 2.09 ppm, whose area is used to determine the concentration of these compounds. 3-(Trimethylsilyl)-2,2,3,3- d^4 -propionic acid sodium salt is added to the cider with a double purpose: as a reference for 0.00 ppm and as an internal standard for ^1H NMR measurement. Enzymatic analysis methods are used to validate the method. Good correlations are found between the lactic and acetic acids concentrations obtained by ^1H NMR and those obtained by enzymatic methods in different commercial ciders. For lactic acid, the 95% confidence interval for the slope is 1.05 ± 0.08 (includes 1) and for the intercept 0.27 ± 0.42 (includes 0). For acetic acid, these intervals are 1.01 ± 0.06 for the slope and 0.03 ± 0.08 for the intercept. The described method is fast and direct.

© 2015 Elsevier Ltd. All rights reserved.

1. Introduction

L-Malic acid is the major organic acid in apples (Belitz, Grosch, & Shieberle, 2009). In the Basque Country, cider is made from apple juice as a result of two spontaneous fermentations, carried out by indigenous microflora. The first one, called alcoholic fermentation, is the conversion of sugar into ethanol by yeasts. The second, called malolactic fermentation, involves the transformation of L-malic acid into L-lactic acid by lactic acid bacteria (Dueñas, Irastorza, Fernández, Bilbao, & del Campo, 1997). The malolactic fermentation is essential in Basque cider because it decreases the strong acid perception given by malic acid into the smoother flavor given by lactic acid. Therefore, it is crucial to have analytical methods to monitor this fermentation.

On the other hand, as no control over lactic acid bacteria is carried out after malolactic fermentation, a large number of lactic acid bacteria is found (Dueñas, Irastorza, Fernández, Bilbao, & Huerta, 1994) and these bacteria are a potential source of different cider alterations. One of the most widespread cider alterations is the production of excess of acetic acid (Irastorza, Munduate, González, Aierbe, & del Campo, 1993) by using residual sugars and other compounds such as glycerol or lactic acid. Acetic acid is always present in cider, but an excess leads to spoilage

of the product. Spanish regulation allows a maximum content of 2.2 g L^{-1} , which means that the acetic acid concentration needs to be strongly controlled.

Different techniques are used for the determination of acids in fruit juices and their fermentative derivatives. Among them, HPLC is more extensively used, permitting the quantification of the main acids in 20–30 min (Shui & Leong, 2002; Zhang et al., 2008). Enzymatic methods to determine lactic, acetic and other organic acids are also used (R-Biopharm AG), their main advantages being high selectivity and sensitivity. However, they require specific kits for each individual organic acid, which are rather costly and time-consuming.

The ^1H NMR spectroscopy offers a high number of signals of different molecules in a single spectrum. This means that many chemicals might be simultaneously determined. It also offers advantages in terms of speed and simplicity of sample preparations (Košir & Kidrič, 2002). We have already proposed determination methods by means of ^1H NMR spectroscopy for some compounds found in apples and other fruits, specifically for chlorogenic acid (Berregi, Santos, del Campo, Miranda, & Aizpurua, 2003), (–)-epicatechin (Berregi, Santos, del Campo, & Miranda, 2003), malic and citric acids (del Campo, Berregi, Caracena, & Santos, 2006), and formic acid (Berregi, del Campo, Caracena, & Miranda, 2007); also for some important coffee compounds (del Campo, Berregi, Caracena, & Zuriarrain, 2010) and recently for ethanol in ciders (Zuriarrain, Zuriarrain, Villar, & Berregi, 2015).

* Corresponding author. Tel.: +34 943 018210; fax: +34 943 015270.

E-mail address: i.berregi@ehu.es (I. Berregi).

In this work, a new ^1H NMR method is evaluated for the simultaneous determination of lactic and acetic acids in fermenting apple musts and ciders. The method proposed here will make it possible to monitor the malolactic fermentation by ^1H NMR, and also to prevent the spoilage of cider due to the production of excess of acetic acid.

Nord, Vaag, and Duus (2004) determined lactic and acetic acids by ^1H NMR, but in beers, not in ciders. In addition, they obtained lower correlations with standard methods, specially for acetic acid. The reason for this might be that they used CD_3COOD to fix the pH, and the signal of the residual CHD_2COOD contained in it as an internal standard. We think that the choice of the internal standard is not adequate, since its signal overlaps partially with that of acetic acid. They also did not consider the possible presence of the isomers l-lactic and D-lactic acid.

Monakhova et al. (2014) published recently an excellent work, in where almost 30 compounds were determined in apple juices, including lactic and acetic acids, by means of ^1H NMR spectroscopy. However, apple juice is a matrix very different from cider, as it has different acid, sugar, alcohol and polyphenolic profile.

Godelmann et al. (2013) used the ^1H NMR signals of lactic and acetic acids (among others) in wine analysis, but not for determining them but to differentiate important parameters of the wines, as grape variety, geographical origin and year of vintage. Lachenmeier et al. (2005) used also the ^1H NMR signals of lactic acid, among many others, but this time the purpose was the quality control and authenticity assessment of beers.

2. Material and methods

All chemicals used are of an analytical reagent grade. Solutions are prepared with twice-distilled water (from this point on, “water”).

2.1. Preparing the TSP– D_2O solution

Exactly 0.2500 g of 3-(trimethylsilyl)-2,2,3,3-tetradeuteriopropionic acid sodium salt (TSP) are dissolved in 17.5 mL of D_2O and made up to 25 mL with water. The final concentrations are 10.00 g L^{-1} of TSP and 70% (v/v) D_2O .

2.2. Recording of ^1H NMR spectra: general procedure

600 μL of the calibration standard or the must sample are placed in a 5 mm outer diameter NMR tube and 100 μL of the TSP– D_2O solution are added. The final concentrations are TSP $1.426 \pm 0.014 \text{ g L}^{-1}$ and D_2O 10% (v/v). D_2O serves as the field frequency lock and all the spectra are referenced to the signal from TSP at $\delta = 0.00 \text{ ppm}$, which is also used as an internal standard.

The 500 MHz ^1H NMR spectra are recorded at a temperature of 30°C using a Bruker Avance 500 spectrometer. 64 scans of 32K data points are acquired with a spectral width of 8012 Hz (16 ppm), acquisition time of 4.0 s, recycle delay of 2.0 s, flip angle of 90° and constant gain of 28.5, requiring about 8 min per sample. Water suppression is achieved using the presaturation pulse sequence used by Nord et al. (2004). As a comment, we have used a 500 MHz NMR spectrometer, only because it is the one that we have in our University. A simpler and cheaper one, as for example a 50 MHz spectrometer, could have been used for the purpose of this article.

Preliminary data processing is carried out using Bruker software, version 2.5. The Free Induction Decay signals are Fourier transformed (1.0 Hz line broadening) and the spectra are phased and the baseline corrected. The resulting spectra are aligned by right or left shifting as necessary, using the TSP signal as a

reference. Data analysis is achieved with MestReNova 6.1.1-6384 software package.

2.3. Determination of the longitudinal relaxation time, T_1

A solution is prepared by directly adding to an NMR tube $\sim 1.6 \text{ mg}$ of %98 lactic acid, $\sim 1 \mu\text{L}$ of glacial acetic acid, 650 μL of D_2O and 50 μL of DCl (to ensure strong acidity). To measure the T_1 of lactic and acetic acids, the longitudinal relaxation delays of the selected protons are determined by the inversion recovery pulse sequence method, using T_1 cal Bruker program which fits the data to the exponential equation $I = I_0 + P \exp(-\tau/T_1)$ where I is the intensity of each proton resonance at inversion delay τ and I_0 at the equilibrium state and P is a constant. Inversion delays used are 0.10, 0.50, 1.00, 2.00, 3.00, 7.00, 10.00, 20.00, 30.00 and 45.00 s.

2.4. Calibration graph

A 32 g L^{-1} stock solution of lactic acid is prepared by dissolving the appropriate quantity of %98 lactic acid in 50 mL water. By diluting the stock solution, 10 standards are prepared with lactic acid concentrations in the $0.5\text{--}5 \text{ g L}^{-1}$ range. In the same way, a 20 g L^{-1} stock solution of acetic acid is prepared by diluting the appropriate volume of glacial acetic acid to 50 mL with water, and standardizing it with NaOH in order to know the exact concentration. By diluting the stock solution, 10 standards are prepared with acetic acid concentrations in the range of $0.3\text{--}3 \text{ g L}^{-1}$. The pH of all the standards is adjusted at 1.0 by adding concentrate H_2SO_4 . A 600 μL volume of each standard is placed in an NMR tube, 100 μL of the TSP– D_2O solution are added and ^1H NMR spectra are recorded following the general procedure.

The calibration graph is obtained by plotting the ratio between the peak areas of lactic or acetic acid and the internal standard TSP against lactic or acetic acid concentration.

2.5. Preparing the cider samples

10 Commercial ciders, previously degassed with a vacuum flask, have been used in this study. 15 mL of each sample are placed in a precipitate flask to adjust the pH at 1.0 with concentrate H_2SO_4 , and later diluted to 25 mL with pH-1.0-water. A fraction of the solution ($<2 \text{ mL}$) is immediately used for ^1H NMR spectra recording and the determination of lactic and acetic acid is performed by means of this technique. The remaining solution is frozen until the determination of both acids by enzymatic methods is fulfilled.

2.6. Analysis of samples by enzymatic methods

After thawing the sample, commercial enzymatic methods (BioSystems) are used to determine lactic and acetic acids. In contrast to the NMR method, these methods determine l- and D- lactic acids.

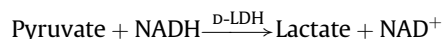
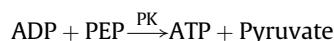
l-Lactic acid (as l-lactate) is quantitatively oxidized to pyruvate by nicotinamide-adenine dinucleotide (NAD^+) in the presence of $\text{l-lactate dehydrogenase}$ (l-LDH):



The amount of NADH formed, measured by its absorbance at 340 nm, is stoichiometric to the amount of l-lactate . D-Lactate is determined by the same reaction, but in the presence of $\text{D-lactate dehydrogenase}$.

Acetic acid (as acetate) reacts quantitatively with ATP, in the presence of acetate kinase (AK), to yield acetylphosphate and ADP; the latter reacts with phosphoenolpyruvate (PEP), in the presence

of pyruvate kinase (PK), to produce ATP and pyruvate, which subsequently reacts with NADH in the presence of D-lactate dehydrogenase (D-LDH):



The amount of NADH consumed, measured by its absorbance at 340 nm, is stoichiometric to the amount of acetic acid.

3. Results and discussion

3.1. ^1H NMR spectra of ciders

Fig. 1 displays the ^1H NMR spectrum of a commercial Basque cider, with the working signals of lactic acid, acetic acid and TSP indicated. Qualitatively similar spectra are obtained with other ciders.

Lactic acid ($\text{CH}_3\text{—CHOH—COOH}$) gives a doublet signal at 1.42 ppm and acetic acid ($\text{CH}_3\text{—COOH}$) a singlet signal at 2.09 ppm, both corresponding to the methyl group, $\text{CH}_3\text{—}$. The carboxylic protons of both acids, as well as those of the —CHOH group of lactic acid, are not visible because they appear near the signal of water, at ~ 4.9 ppm, which is eliminated by the presaturation pulse sequence used.

The two great signals observed in the spectrum are given by ethanol ($\text{CH}_3\text{—CH}_2\text{OH}$): a triplet signal at 1.19 ppm, corresponding to the protons from the methyl group, $\text{CH}_3\text{—}$, and a multiplet signal at 3.66 ppm, produced by the protons of methylene group, $\text{—CH}_2\text{—}$. They are not eliminated by the presaturation pulse sequence used.

We chose TSP as an internal standard in a previous work (del Campo et al., 2006) because it is soluble in water, stable in the sample media, available in high purity and has a very simple ^1H NMR spectrum consisting of a single nine proton singlet, which never overlaps with any other signal of the cider. This singlet is used simultaneously to fix the chemical shift at 0.0 ppm in the ^1H NMR spectra.

The chemical shift of lactic acid and acetic acid signals is hardly influenced by pH, at values smaller than 5, while that of TSP signal is not influenced at all. In any case, we have adjusted the pH at 1.0 with concentrate H_2SO_4 , in order to reproduce the working pH used

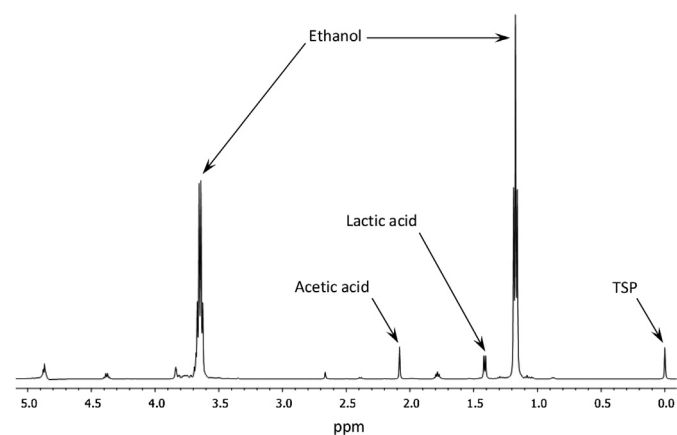


Fig. 1. ^1H NMR spectrum of a commercial cider. Working signals of acetic acid, lactic acid and TSP are indicated.

in the determination of malic acid (del Campo et al., 2006). This potentially gives the chance to determine the three compounds in the same analysis and to follow the malolactic fermentation by both the increase of lactic acid and the decrease of malic acid.

The longitudinal relaxation time of the working protons, obtained from the inversion recovery pulse sequence method, is 1.829 ± 0.044 s for lactic acid, and 5.640 ± 0.090 s for acetic acid. The value for the nine protons of TSP, obtained in a previous work (del Campo et al., 2010), is 3.769 ± 0.016 s. According to this, the critical factor for the ^1H NMR acquisition conditions is the relaxation time of the working protons of acetic acid. To obtain maximum relaxation of the molecule after each data acquisition and so that the registry times of the spectra are not excessively long, the conditions selected are acquisition time 4.0 s, recycle delay time 2.0 s and number of scans 64. The sum of acquisition time and recycle delay time is 6.0 s, longer than the relaxation time of the working protons of acetic acid, so, the protons involved will relax completely and no loss of sensitivity will occur. Under these conditions the ^1H NMR spectra are recorded in 8 min, which we consider to be an adequate value if we want the determination method to be competitive with other techniques.

3.2. Calibration equation and limit of detection

The calibration graphs are obtained by plotting the ratio between peak areas of lactic or acetic acids (A) and the internal standard TSP (A_{TSP}) against lactic or acetic concentration (C , g L^{-1}). The general equation is $A/A_{\text{TSP}} = a \times C (\text{g L}^{-1}) + b$. By processing the experimental data with Excel 2007, the calibration equations listed in Table 1 are obtained. The high correlation coefficients obtained (>0.999) indicate a good linearity response within the concentration range studied. This is confirmed by the t test (Miller & Miller, 2005), which gives high t values (79.2 for lactic acid and 180.5 for acetic acid) with a significance lower than 0.01. The limits of detection, also listed in the table, are calculated from “ $3S_y/x + \text{intercept}$ ”.

3.3. Precision

The precision of the method is verified by an intra- and inter-day repeatability test. Following the general procedure, we have obtained the ^1H NMR spectra of many samples prepared with a 2.57 g L^{-1} standard of lactic acid and a 1.68 g L^{-1} standard of acetic acid, that is, the middle concentrations of the calibration ranges used for each compound. Then, using the calibration equation, we calculated the concentration of both compounds in each sample. For five measurements taken in the same day – intra-day repeatability – a coefficient of variation of 2.34% is obtained with lactic acid, and 4.47% with acetic acid. For twenty measurements performed throughout seventeen days – inter-day repeatability –, five in the first day, five in the third, five in the seventh and five in the seventeenth, a value of 2.76% is achieved with lactic acid, and 5.02% with acetic acid.

3.4. Application to commercial ciders and fermenting musts

To validate the ^1H NMR procedure described, we applied it to determine lactic and acetic acids in ten commercial ciders. For comparison purposes, we have determined the acids of the same commercial ciders via standard enzymatic methods, which are normally used for this purpose in the Basque Country. The results obtained by the two techniques are listed in Table 2.

By plotting the results obtained by ^1H NMR against those obtained by enzymatic methods in the same samples and fitting the data by least squares method (Miller & Miller, 2005), a Pearson

Table 1Calibration data for the general equation $A/A_{TSP} = a \times C (\text{g L}^{-1}) + b$.

Analyte	$a \pm S_a$	$b \pm S_b$	R	N	$S_{y/x}$	LOD (g L^{-1})
Lactic acid	0.4364 ± 0.0055	0.0216 ± 0.0175	0.9994	10	2.5674×10^{-2}	0.18
Acetic acid	0.6184 ± 0.0034	-0.0097 ± 0.0071	0.9999	10	1.0428×10^{-2}	0.05

S_a : standard error for slope; S_b : standard error for intercept; $S_{y/x}$: standard error for regression; R: regression coefficient; LOD: limit of detection; N = number of experimental points.

Table 2Concentrations^a of lactic and acetic acids (g L^{-1}) in real samples, obtained by ^1H NMR and enzymatic standard methods.

Sample	Lactic acid L		Lactic acid D		Lactic acid total		Acetic acid	
	Enzymatic	Enzymatic	Enzymatic	Enzymatic	^1H NMR	^1H NMR	Enzymatic	^1H NMR
1	3.02 ± 0.04	3.19 ± 0.14	6.21 ± 0.14	6.86 ± 0.13	2.52 ± 0.05	2.56 ± 0.03		
2	2.87 ± 0.05	2.84 ± 0.12	5.71 ± 0.13	6.18 ± 0.04	1.45 ± 0.07	1.55 ± 0.04		
3	4.86 ± 0.17	0.29 ± 0.01	5.15 ± 0.17	5.88 ± 0.06	1.68 ± 0.10	1.78 ± 0.06		
4	0.91 ± 0.03	0.96 ± 0.03	1.87 ± 0.05	1.98 ± 0.01	1.98 ± 0.01	2.06 ± 0.02		
5	8.42 ± 0.29	0.31 ± 0.02	8.73 ± 0.29	9.45 ± 0.20	0.30 ± 0.06	0.33 ± 0.03		
6	6.65 ± 0.26	0.32 ± 0.01	6.97 ± 0.26	7.29 ± 0.14	0.92 ± 0.03	0.97 ± 0.02		
7	1.12 ± 0.02	0.83 ± 0.01	1.95 ± 0.02	2.39 ± 0.02	1.30 ± 0.05	1.24 ± 0.02		
8	2.12 ± 0.04	2.30 ± 0.01	4.42 ± 0.04	5.09 ± 0.03	1.71 ± 0.04	1.75 ± 0.02		
9	2.18 ± 0.04	1.97 ± 0.01	4.15 ± 0.04	4.85 ± 0.06	0.48 ± 0.09	0.55 ± 0.01		
10	4.38 ± 0.12	0.33 ± 0.03	4.71 ± 0.13	4.93 ± 0.09	0.84 ± 0.02	0.87 ± 0.02		

^a Average of three measurements \pm SD.

correlation coefficient of 0.9958 is achieved for lactic acid and 0.9977 for acetic acid. Besides, 95% confidence interval for the slope is 1.05 ± 0.08 for lactic acid and 1.01 ± 0.06 for acetic acid, including the 1.0, and that for the intercept is 0.27 ± 0.42 for lactic acid and 0.03 ± 0.08 for acetic acid, including the zero. We conclude that ^1H NMR method is valid for the determination of lactic and acetic acids in cider samples.

To check the usefulness of the method to analyze fermenting ciders, we have obtained an apple juice made of Basque apples and subjected it to fermentation conditions. We have then taken several samples at different stages of the fermentative process and equally determined the lactic and acetic acid content by the ^1H NMR method proposed here. We have also determined the malic acid content from its multiplet signal at 2.88 ppm, as we proposed in a previous article for different fruit juices (del Campo et al., 2006). In that article the interference of citric acid was discussed but it does

not apply here because its content in apple musts is very small. On the other hand, the ^1H NMR spectra recording conditions used for malic acid are those described in the present article for lactic and acetic acids, in order to obtain all the results from the same spectrum. This does not suppose any kind of problem because the conditions described for malic acid in the previous article were very similar.

Fig. 2 shows the evolution of the three acids. It can be seen that the decrease in malic acid content is accompanied by a similar increase in lactic acid content, indicating that the malolactic fermentation is taking place. The concentrations are given in mmol L^{-1} units, to facilitate the comparison. On the other hand, acetic acid content increases during the fermentation at different rates, which is a typical behavior in fermenting apple musts. We can see in this figure that ^1H NMR technique is appropriate for monitoring the malolactic fermentation in ciders, and also to follow the increase of acetic acid content, which is a frequent source of problems in cidermaking.

The method proposed here will be useful to all cidermakers who have an NMR service nearby, which is the norm in almost all the cider producers of the Basque Country. In this case, the method proposed is more economical than the enzymatic method, because the enzymatic reagents are quite expensive. Obviously, this will not be the case if the cider producers have to buy the NMR spectrometer.

On the other hand, enzymatic method distinguishes L and D isomers of lactic acid and NMR technique does not. In most cases this will not be a problem, because usually the total amount of lactic acid is evaluated. This will be a disadvantage only if we have special interest in D -lactic acid, because sometimes its presence is indicative of a cider spoilage.

Acknowledgments

We are grateful to the Basque Government (grant number UE09+/54 and PA12/26), the University of the Basque Country UPV/EHU, the Gipuzkoa Natural Cider Association (grant number Zabalduz 2012) and the Fraisoro Agro-environmental Laboratory for their financial and technical support.

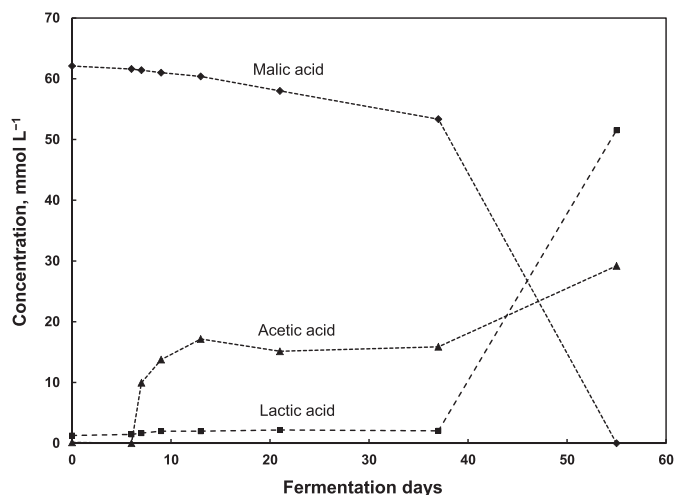


Fig. 2. Evolution of malic, lactic and acetic acids during fermentation of an apple must, followed by ^1H NMR technique.

References

- Belitz, H. D., Grosch, W., & Shieberle, P. (2009). *Food chemistry* (3rd ed.). Berlin-Heidelberg: Springer-Verlag (chapter 18).
- Berregi, I., del Campo, G., Caracena, R., & Miranda, J. I. (2007). Quantitative determination of formic acid in apple juices by ^1H NMR spectrometry. *Talanta*, *72*, 1049–1053.
- Berregi, I., Santos, J. I., del Campo, G., & Miranda, J. I. (2003). Quantitative determination of (–)-epicatechin in cider apple juices by ^1H NMR. *Talanta*, *61*, 139–145.
- Berregi, I., Santos, J. I., del Campo, G., Miranda, J. I., & Aizpurua, J. M. (2003). Quantitative determination of chlorogenic acid in cider apple juices by ^1H NMR spectrometry. *Analytica Chimica Acta*, *486*, 269–274.
- BioSystems, Reagents & Instruments. Barcelona, Spain. Reagents enology/enzymatic. <http://www.biosystems.es> Accessed 16.12.14.
- del Campo, G., Berregi, I., Caracena, R., & Santos, J. I. (2006). Quantitative analysis of malic and citric acid in fruit juices using proton nuclear magnetic resonance spectroscopy. *Analytica Chimica Acta*, *556*, 462–468.
- del Campo, G., Berregi, I., Caracena, R., & Zuriarrain, J. (2010). Quantitative determination of caffeine, formic acid, trigonelline and 5-(hydroxymethyl)furfural in soluble coffees by ^1H NMR spectrometry. *Talanta*, *81*, 367–371.
- Dueñas, M., Irastorza, A., Fernández, C., Bilbao, A., & del Campo, G. (1997). Influence of apple juice treatments on the cider making process. *Journal of the Institute of Brewing*, *103*, 251–255.
- Dueñas, M., Irastorza, A., Fernández, K., Bilbao, A., & Huerta, A. (1994). Microbial populations and malolactic fermentation of apple cider using traditional and modified methods. *Journal of Food Science*, *59*, 1060–1064.
- Godelmann, R., Fang, F., Humpfer, E., Schütz, B., Bansbach, M., Schäfer, H., et al. (2013). Targeted and nontargeted wine analysis by ^1H NMR spectroscopy combined with multivariate statistical analysis. Differentiation of important parameters: grape variety, geographical origin, year of vintage. *Journal of Agricultural and Food Chemistry*, *61*, 5610–5619.
- Irastorza, A., Munduate, A., González, A., Aierbe, T., & del Campo, G. (1993). Caractéristiques analytiques des cidres de la province de Guipúzcoa (Pays Basque). *Journal International des Sciences de la Vigne et du Vin*, *27*, 55–63.
- Košir, I. J., & Kidrič, J. (2002). Use of modern nuclear magnetic resonance spectroscopy in wine analysis: determination of minor compounds. *Analytica Chimica Acta*, *458*, 77–84.
- Lachenmeier, D. W., Frank, W., Humpfer, E., Schäfer, H., Keller, S., Mörtter, M., et al. (2005). Quality control of beer using high-resolution nuclear magnetic resonance spectroscopy and multivariate analysis. *European Food Research and Technology*, *220*, 215–221.
- Miller, J. N., & Miller, J. C. (2005). *Statistics and chemometrics for analytical chemistry* (5th ed.). London: Pearson Education (pp. 110–114, 126–131).
- Monakhova, Y. B., Schütz, B., Schäfer, H., Spraul, M., Kuballa, T., Hahn, H., et al. (2014). Validation studies for multicomponent quantitative NMR analysis: the example of apple fruit juice. *Accreditation and Quality Assurance*, *19*, 17–29.
- Nord, L. I., Vaag, P., & Duus, J.Ø. (2004). Quantification of organic and amino acids in beer by ^1H NMR spectroscopy. *Analytical Chemistry*, *76*, 4790–4798.
- R-Biopharm AG. Darmstadt, Germany. Food & feed analysis/constituents/enzymatic analysis/Roche yellow line. <http://www.r-biopharm.com> Accessed 16.12.14.
- Shui, G., & Leong, L. P. (2002). Separation and determination of organic acids and phenolic compounds in fruit juices and drinks by high-performance liquid chromatography. *Journal of Chromatography A*, *977*, 89–96.
- Zhang, H., Zhou, F., Ji, B., Nout, R. M. J., Fang, Q., & Yang, Z. (2008). Determination of organic acids evolution during apple cider fermentation using an improved HPLC analysis method. *European Food Research and Technology*, *227*, 1183–1190.
- Zuriarrain, A., Zuriarrain, J., Villar, M., & Berregi, I. (2015). Quantitative determination of ethanol in cider by ^1H NMR spectrometry. *Food Control*, *50*, 758–762.

Polyphenolic profile in cider and antioxidant power

Andoni Zuriarrain, Juan Zuriarrain, Ana Isabel Puertas, María Teresa Dueñas, Miren Ostra and Iñaki Berregi*

Abstract

BACKGROUND: The aim of this work was to find the effect of polyphenolic compounds in Basque ciders on the following parameters: antioxidant activity, browning, protein-precipitating capacity, turbidity and reduction potential. These five parameters are highly important, as they affect the taste, the visual aspect and the preservation of cider, and are mainly related to polyphenolic compounds.

RESULTS: Procyanidin B1 and procyanidin B2 showed a significant positive effect on antioxidant activity. *p*-Coumaric acid, (–)-epicatechin and hyperin had a significant positive effect on protein-precipitating capacity. Tyrosol had a significant negative effect on reduction potential.

CONCLUSION: Procyanidin B1 and procyanidin B2 are the most powerful antioxidants in Basque cider, while *p*-coumaric acid, (–)-epicatechin and hyperin are those with greatest capacity to precipitate proteins. Ciders with higher tyrosol concentration will have less reduction potential and higher antioxidant reservoir.

© 2014 Society of Chemical Industry

Keywords: cider; polyphenolic compounds; antioxidant activity; antioxidant reservoir

INTRODUCTION

Cider apple varieties contain relatively large amounts of polyphenolic compounds, which can be divided into four classes: hydroxycinnamic acid derivatives, flavan-3-ols, either monomeric (catechins) or oligomeric (procyanidins), flavonols and dihydrochalcones.¹

Polyphenolic compounds, particularly procyanidins, are responsible for haze and sediment formation because of their interaction with proteins.^{2,3} They are also involved in browning processes because of the effect of polyphenol oxidases.⁴ From the organoleptic point of view, polyphenols are related to bitterness and astringency, whose balance defines the overall mouth feel of the beverage.⁵

The aim of this work was to find correlations between the individual polyphenolic compounds in Basque ciders and the following parameters: antioxidant activity, browning, protein-precipitating capacity, turbidity and reduction potential. These five parameters are related mainly to polyphenols and are vital as they affect the taste, the visual aspect and the preservation of the cider.

Among the different methods available to measure the antioxidant activity,⁶ we have chosen the ferric-reducing antioxidant power (FRAP) assay because it is simple and fast. It is based on the reduction of the Fe³⁺ complex of 2,4,6-tripyridyl-*s*-triazine, Fe(TPTZ)³⁺, to the intensely blue-coloured Fe²⁺ complex Fe(TPTZ)²⁺ by antioxidants in acidic medium. Results are obtained as absorbance increases at 593 nm and are usually expressed as micromolar equivalents of an antioxidant standard such as Trolox or ascorbic acid. The reaction is non-specific, so the change in absorbance is directly related to the total

reducing power of the antioxidants present in the reaction mixture.

Enzymatic browning is one of the most limiting factors when fruits are cut or crushed, such as happens to apples in cider production. The vegetal cells are broken, the enzymes are liberated from tissues and they come into contact with their main substrates, the polyphenolic compounds. The major enzyme involved in the browning reaction is polyphenol oxidase (mixture of EC 1.14.18.1 and EC 1.10.3.1). In the presence of oxygen, this enzyme catalyses the oxidation of phenol to *ortho*-quinones, which rapidly polymerize to form brown pigments.⁷ Browning is measured as the absorbance at 420 nm, the absorption maximum of these pigments.⁸

Many polyphenolic compounds have the ability to precipitate proteins. In fact, the interaction between polyphenolics and proteins is the most frequent cause of haze in beverages.³ The method we have chosen to quantify the protein-precipitating capacity measures the amount of polyphenolic compounds precipitated by a standard protein, bovine serum albumin. The precipitate is dissolved at high pH in the presence of a detergent, and the coloured iron–phenolate complex is determined by spectrophotometry. The method is robust and works well with virtually all

* Correspondence to: Iñaki Berregi, Department of Applied Chemistry, Faculty of Chemistry, University of the Basque Country UPV/EHU, Manuel Lardizabal 3, E-20018 Donostia-San Sebastián, Spain. E-mail: i.berregi@ehu.es

Department of Applied Chemistry, Faculty of Chemistry, University of the Basque Country UPV/EHU, Manuel Lardizabal 3, E-20018, Donostia-San Sebastián, Spain

Table 1. Calibration data for $N = 5$ and general equation: peak area = $a \times C$ (mg L⁻¹) + b

Polyphenol	Linear range (mg L ⁻¹)	a	b	r	LOD (mg L ⁻¹)
Hydroxycinnamic acids					
Caffeic acid	2.0–10.0	346.0	–34.7	0.9998	0.2
Chlorogenic acid	23.8–237.5	158.3	–316.8	0.9998	5.4
<i>p</i> -Coumaric acid	0.5–6.1	432.0	2.7	0.9999	0.1
Hydrocaffeic acid	9.9–99.2	56.5	–389.5	0.9864	5.8
(<i>trans</i>)-Ferulic acid	1.3–5.0	242.8	24.3	0.9815	1.3
Flavan-3-ols					
(+)-Catechin	4.7–18.7	39.0	–13.5	0.9998	0.4
(–)-Epicatechin	18.3–183.2	46.7	–63.7	0.9996	6.5
Dihydrochalcones					
Phloridzin	2.0–20.1	120.5	11.7	0.9993	1.0
Flavonols					
Avicularin	2.7–20.7	129.1	–69.2	0.9948	2.7
Hyperin	0.2–2.0	114.5	–2.5	0.9998	0.05
Isoquercitrin	2.0–20.0	121.8	–2.3	0.9985	1.4
Quercitrin	0.2–2.0	98.7	–3.9	1.0000	0.02
Benzoic acids					
Gallic acid	2.2–10.5	164.2	–59.2	0.9990	0.5
<i>p</i> -Hydroxybenzoic acid	0.5–6.0	92.9	–1.9	1.0000	0.04
Protocatechuic acid	1.0–8.3	92.8	–0.8	0.9986	0.5
Volatile polyphenols					
Catechol	1.6–7.8	67.2	–4.1	0.9868	1.6
Tyrosol	4.9–49.4	36.4	–8.0	0.9999	1.1

LOD, limit of detection.

Table 2. Calibration data for $N = 1$

Polyphenol	Standard (mg L ⁻¹)	Response factor	LOD (mg L ⁻¹)
Hydroxycinnamic acids			
4- <i>p</i> -Coumaroylquinic acid	104.2	71.7	2.3
Flavan-3-ols			
Procyanidin B1	45.2	4.7	4.0
Procyanidin B2	113.4	7.8	6.4
Procyanidin B5	52.6	13.6	5.8
Dihydrochalcones			
Phloretin 2'- <i>O</i> -xyloglucoside	98.6	22.7	3.3

LOD, limit of detection.

plant extracts.⁹ Besides, the turbidity caused by polyphenolics or by other factors in the must (newly pressed apple juice) or the cider can be measured with a conventional turbidimeter/nephelometer.

The reduction potential gives information on the ability of a redox couple to be oxidized or reduced. The methodologies developed for the measurement of the antioxidant activity, including FRAP, are kinetic methods that provide information about the most reactive compounds. On the other hand, the reduction potential is a thermodynamic quantity that accounts for all antioxidants present in the must or the cider, including the slowest but most efficient ones, as they represent the antioxidant reservoir of the beverage.¹⁰

In this work, we have obtained six different musts by using five different varieties of apples of the Basque Country (northern Spain). Five are monovarietal and the sixth is obtained by mixing

the varieties used in the other five musts in equal weight proportions. Monovarietal musts have been used mainly in order to obtain polyphenolic profiles as different as possible. By spontaneous fermentation of these musts, six different ciders have been obtained. The evolution of the ciders has been followed during 5 months, by measuring the concentration of polyphenolics and the five parameters mentioned throughout five samplings, and a multivariate linear regression study has been performed.

EXPERIMENTAL

All chemicals used were of analytical reagent grade. Solutions were prepared with doubly distilled water (hereinafter 'water').

Obtaining musts and fermentation

Six musts were obtained from six 250 kg lots of cider apples harvested in October 2010 in an experimental orchard of Hondarribia (Basque Country, Spain). Each lot was crushed separately and pressed in a vertical press, and the must obtained was introduced into a 250 L stainless steel tank where the fermentations took place. The temperature was kept at 15 °C. Alcoholic and malolactic fermentations took place spontaneously by indigenous microflora. The tanks were kept uncovered for 38 days until the tumultuous phase of fermentation had finished. Immediately afterwards, they were hermetically sealed and connected to a CO₂ cylinder, with an overpressure of 0.2 atm, in order to protect the ciders from oxidation. After 114 days of fermentation, the ciders were racked to remove the sediments deposited at the bottom of the tanks.

Five musts were monovarietal, obtained from the indigenous varieties Goikoetxea, Manttoni, Moko, Patzuloa and Txalaka, widely used to elaborate cider in the Basque Country. These varieties are

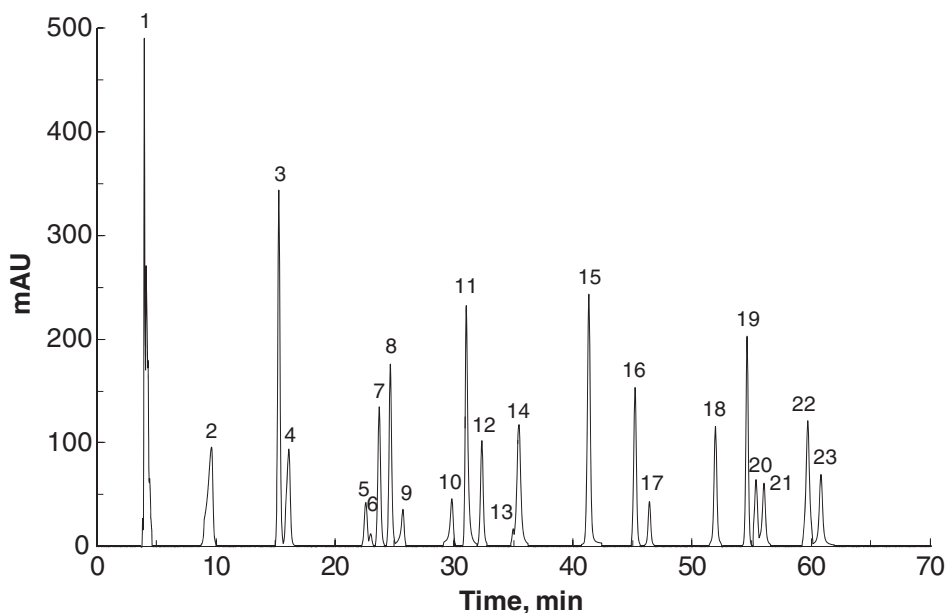


Figure 1. Chromatogram obtained at 280 nm with pure standards: 1, ascorbic acid; 2, gallic acid; 3, catechol; 4, protocatechuic acid; 5, tyrosol; 6, procyanidin B1; 7, *p*-hydroxybenzoic acid; 8, hydrocaffeic acid; 9, (+)-catechin; 10, procyanidin B2; 11, chlorogenic acid; 12, caffeic acid; 13, (–)-epicatechin; 14, 4-*p*-coumaroylquinic acid; 15, *p*-coumaric acid; 16, (*trans*)-ferulic acid; 17, procyanidin B5; 18, phloretin 2'-*O*-xyloglucoside; 19, phloridzin; 20, hyperin; 21, isoquercitrin; 22, avicularin; 23, quercitrin.

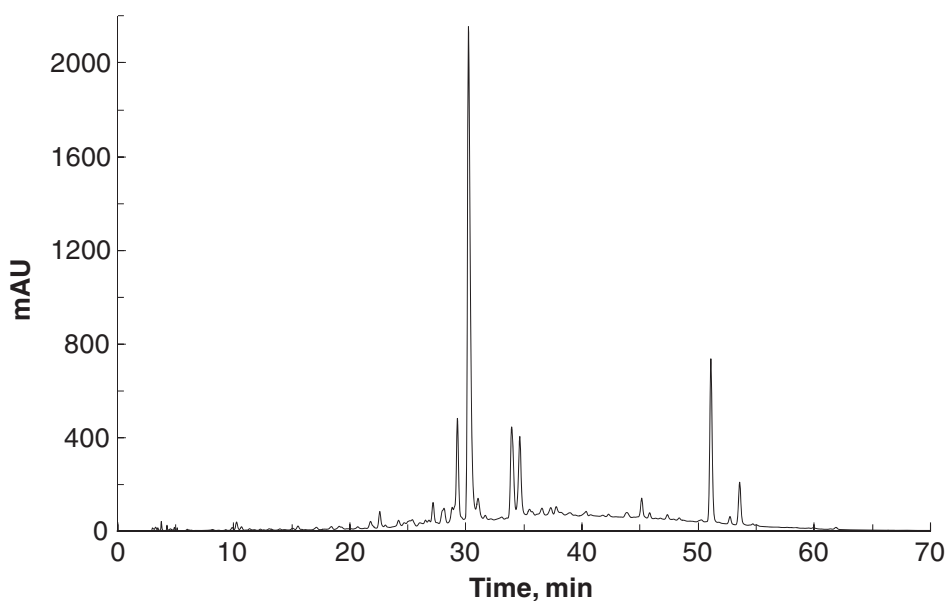


Figure 2. Chromatogram obtained at 280 nm with a cider sample of Moko variety.

quite different regarding polyphenolic content and acidity, which introduces variability in the study.

The sixth must, called Mixture, was obtained by crushing together 50 kg of each of the five varieties (total 250 kg). Cider in the Basque Country is always obtained from a mixture of varieties, so we considered it convenient to also include a must like this one.

Sampling

Must or cider samples of about 250 mL were taken from the six tanks during 5 months, from October 2010 to March 2011, at 0, 30, 60, 90 and 140 day intervals (there were minor differences in the number of days for the different tanks).

Each sample was homogenized by shaking and then degasified (except initial musts). Immediately afterwards, reduction potential and turbidity were measured. A 100 mL portion was centrifuged at $10\,000 \times g$ for 20 min and used to measure Folin–Ciocalteu index, FRAP, absorbance at 280 nm (total polyphenol index), absorbance at 320 nm (hydroxycinnamic acid derivatives), absorbance at 420 nm (browning) and protein-precipitating capacity. A fraction of the centrifuged sample was filtered through a 0.45 μm filter and distributed into two vials for later determination of polyphenolic compounds. The vials were stored in a freezer at -20°C until analysis. The sampling procedure described was always performed in 1 day to avoid oxidation of polyphenols and continuation of fermentation.

Table 3. Phenolic compound contents (mg L⁻¹) and parameters in Goikoetxea must^a

Compound	Fermentation days				
	0	30	63	98	140
Hydroxycinnamic acids					
Caffeic acid	0.73 ± 0.08	1.03 ± 0.12	ND	ND	0.24 ± 0.03
Chlorogenic acid	120.0 ± 0.6	124.5 ± 0.6	23.4 ± 0.1	9.21 ± 0.05	ND
<i>p</i> -Coumaric acid	1.47 ± 0.03	1.53 ± 0.03	0.31 ± 0.01	ND	ND
4- <i>p</i> -Coumaroylquinic acid	61.3 ± 0.2	92.2 ± 0.3	85.8 ± 0.2	80.8 ± 0.2	74.7 ± 0.2
Hydrocaffeic acid	7.37 ± 0.01	29.29 ± 0.06	79.1 ± 0.2	84.2 ± 0.2	84.2 ± 0.2
(<i>trans</i>)-Ferulic acid	ND	2.3 ± 0.2	2.6 ± 0.2	2.1 ± 0.1	2.2 ± 0.1
Flavan-3-ols					
(+)-Catechin	1.9 ± 0.4	6.5 ± 1.2	ND	ND	1.1 ± 0.2
(-)-Epicatechin	ND	13.12 ± 0.09	10.95 ± 0.07	ND	ND
Procyanidin B1	ND	20.9 ± 1.1	30.9 ± 1.6	36.4 ± 1.9	33.4 ± 1.7
Procyanidin B2	8.42 ± 0.01	4.99 ± 0.01	ND	ND	43.84 ± 0.06
Procyanidin B5	ND	ND	ND	ND	ND
Dihydrochalcones					
Phloretin 2'- <i>O</i> -xyloglucoside	52.2 ± 0.3	229.3 ± 1.3	36.9 ± 0.2	13.81 ± 0.08	15.09 ± 0.09
Phloridzin	ND	13.4 ± 3.5	29.8 ± 7.7	26.4 ± 6.8	23.4 ± 6.0
Flavonols					
Avicularin	ND	ND	ND	ND	ND
Hyperin	ND	0.15 ± 0.01	0.23 ± 0.01	0.19 ± 0.01	0.15 ± 0.01
Isoquercitrin	ND	ND	ND	ND	ND
Quercitrin	ND	0.58 ± 0.04	0.90 ± 0.07	0.78 ± 0.06	0.69 ± 0.05
Benzoic acids					
Gallic acid	ND	ND	ND	ND	ND
<i>p</i> -Hydroxybenzoic acid	0.13 ± 0.05	1.1 ± 0.4	1.5 ± 0.6	1.7 ± 0.6	1.7 ± 0.6
Protocatechuic acid	ND	0.9 ± 0.2	1.8 ± 0.4	1.8 ± 0.3	ND
Volatile polyphenols					
Catechol	ND	3.2 ± 0.1	12.8 ± 0.2	ND	12.4 ± 0.2
Tyrosol	1.20 ± 0.01	22.6 ± 0.1	22.6 ± 0.1	23.5 ± 0.1	23.0 ± 0.1
Overall polyphenols					
FCI (g tannic acid L ⁻¹)	1.37 ± 0.03	0.96 ± 0.01	0.97 ± 0.02	0.93 ± 0.02	0.80 ± 0.01
TPI (A _{280nm})	31.0 ± 0.1	24.8 ± 0.1	21.6 ± 0.1	19.4 ± 0.1	18.4 ± 0.1
Hydroxycinnamics (A _{320nm})	24.0 ± 0.1	17.7 ± 0.1	11.9 ± 0.1	9.4 ± 0.1	8.6 ± 0.1
Parameters					
FRAP (mmol Trolox L ⁻¹)	2.8 ± 0.1	2.9 ± 0.1	3.5 ± 0.2	4.2 ± 0.1	4.1 ± 0.1
PPC (g tannic acid L ⁻¹)	0.551 ± 0.008	0.431 ± 0.005	0.425 ± 0.010	0.394 ± 0.009	0.397 ± 0.002
Turbidity (NTU)	610 ± 2	304 ± 1	58 ± 1	19.8 ± 0.2	16.6 ± 0.1
Browning (A _{420nm})	3.38 ± 0.02	1.32 ± 0.01	1.02 ± 0.01	0.684 ± 0.001	0.221 ± 0.001
<i>E</i> (mV)	324 ± 2	235 ± 2	167 ± 1	166 ± 1	175 ± 1

FCI, Folin–Ciocalteu index; TPI, total polyphenol index; FRAP, ferric-reducing antioxidant power; PPC, protein-precipitating capacity; *E*, reduction potential against Ag/AgCl reference; ND, not detected.

^a Average of two measurements ± standard deviation.

Turbidity and reduction potential (*E*)

Turbidity was measured with a Hanna HI 83749-02 turbidimeter (Hanna Instruments SL, Eibar, Spain) and is given in nephelometric turbidity units (NTU). Reduction potential was measured with a Mettler Inlab[®] Redox Pro redox combination electrode (Mettler–Toledo, S.A.E., Barcelona, Spain) against an AgCl/Ag reference and is given in mV.

Folin–Ciocalteu index (FCI)

This index gives an idea of the total polyphenolic content of the must or the cider. All polyphenolic compounds are oxidized by means of the so-called Folin–Ciocalteu reagent. This reagent is available commercially and is formed from a mixture

of phosphotungstic acid (H₃PW₁₂O₄₀) and phosphomolybdic acid (H₃PMo₁₂O₄₀), which, after oxidation of the phenols, is reduced to a mixture of blue oxides of tungsten (W₈O₂₃) and molybdenum (Mo₈O₂₃). The blue coloration produced has a maximum absorption in the region of 750 nm and is proportional to the total quantity of polyphenolic compounds originally present. The result is expressed as an index, absorbance at 750 nm. It was determined as follows according to the OIV method.¹¹

Introduce into a 100 mL volumetric flask, strictly in the indicated order, 1 mL of the sample, 50 mL of distilled water, 5 mL of Folin–Ciocalteu reagent and 20 mL of sodium carbonate (200 g L⁻¹ solution), then make up to 100 mL with distilled water. Mix to dissolve. Leave for 30 min for the reaction to stabilize. Determine

Table 4. Phenolic compound contents (mg L⁻¹) and parameters in Manttoni must^a

Compound	Fermentation days				
	0	30	62	97	139
Hydroxycinnamic acids					
Caffeic acid	nd	0.25 ± 0.03	0.36 ± 0.04	nd	nd
Chlorogenic acid	17.04 ± 0.06	34.5 ± 0.1	12.26 ± 0.04	nd	nd
<i>p</i> -Coumaric acid	nd	0.6 ± 0.3	nd	nd	nd
4- <i>p</i> -Coumaroylquinic acid	nd	72.46 ± 0.05	65.73 ± 0.04	56.88 ± 0.04	57.42 ± 0.04
Hydrocaffeic acid	7.37 ± 0.04	19.4 ± 0.1	7.58 ± 0.04	35.0 ± 0.3	35.6 ± 0.3
(trans)-Ferulic acid	nd	nd	nd	nd	nd
Flavan-3-ols					
(+)-Catechin	1.3 ± 0.2	2.4 ± 0.2	nd	0.7 ± 0.1	2.3 ± 0.2
(-)-Epicatechin	nd	nd	nd	nd	nd
Procyanidin B1	nd	nd	18.4 ± 0.6	9.5 ± 0.3	6.6 ± 0.2
Procyanidin B2	19.0 ± 2.8	nd	16.9 ± 2.5	10.2 ± 1.5	nd
Procyanidin B5	nd	nd	nd	nd	nd
Dihydrochalcones					
Phloretin 2'-O-xyloglucoside	nd	20.78 ± 0.07	nd	nd	nd
Phloridzin	nd	2.5 ± 0.5	5.0 ± 0.9	1.4 ± 0.3	1.2 ± 0.2
Flavonols					
Avicularin	nd	nd	nd	nd	nd
Hyperin	nd	nd	nd	nd	nd
Isoquercitrin	nd	nd	nd	nd	nd
Quercitrin	nd	nd	0.3 ± 0.1	nd	nd
Benzoic acids					
Gallic acid	nd	0.6 ± 0.1	0.5 ± 0.1	nd	1.6 ± 0.2
<i>p</i> -Hydroxybenzoic acid	0.64 ± 0.03	0.56 ± 0.03	1.19 ± 0.06	1.03 ± 0.05	0.83 ± 0.04
Protocatechuic acid	nd	0.9 ± 0.2	0.6 ± 0.1	nd	nd
Volatile polyphenols					
Catechol	nd	4.35 ± 0.04	10.2 ± 0.1	9.68 ± 0.09	9.78 ± 0.09
Tyrosol	nd	22.0 ± 0.8	23.9 ± 0.9	21.1 ± 0.8	21.7 ± 0.8
Overall polyphenols					
FCI (tannic acid g L ⁻¹)	0.87 ± 0.02	0.72 ± 0.01	0.64 ± 0.02	0.54 ± 0.01	0.40 ± 0.01
TPI (A _{280nm})	19.8 ± 0.1	11.6 ± 0.1	11.4 ± 0.1	9.8 ± 0.1	9.0 ± 0.1
Hydroxycinnamics (A _{320nm})	13.7 ± 0.1	7.3 ± 0.1	6.5 ± 0.1	4.9 ± 0.1	4.2 ± 0.1
Parameters					
FRAP (trolox mmol L ⁻¹)	1.56 ± 0.07	1.65 ± 0.06	1.61 ± 0.03	1.73 ± 0.04	1.88 ± 0.06
PPC (tannic acid g L ⁻¹)	0.657 ± 0.053	0.296 ± 0.008	0.292 ± 0.003	0.277 ± 0.001	0.269 ± 0.009
Turbidity (NTU)	717 ± 1	60.1 ± 0.1	29.2 ± 0.1	21.95 ± 0.07	8.44 ± 0.05
Browning (A _{420 nm})	3.012 ± 0.012	0.410 ± 0.001	0.491 ± 0.002	0.211 ± 0.001	0.000 ± 0.001
E (mV)	341 ± 3	204 ± 2	183 ± 2	183 ± 2	180 ± 2

FCI, Folin–Ciocalteu index; TPI, total polyphenol index; FRAP, ferric-reducing antioxidant power; PPC, protein-precipitating capacity; E, reduction potential against Ag/AgCl reference; ND, not detected.

^a Average of two measurements ± standard deviation.

the absorbance at 750 nm through a path length of 10 mm with respect to a blank prepared with water in place of the sample. Making use of the Folin–Ciocalteu index (FCI), we calculated the total polyphenolic compounds in g tannic acid L⁻¹ by reference to a calibration curve prepared using tannic acid standards ((2–16) × 10⁻³ g L⁻¹).

Ferric-reducing antioxidant power

This parameter was measured according to the procedure of Benzie and Strain¹² but using Trolox as a standard instead of ascorbic acid. To perform the assay, the following solutions are prepared.

- Acetate buffer 300 mmol L⁻¹, pH 3.6: 3.1 g of sodium acetate trihydrate, 16 mL of glacial acetic acid and distilled water until 1 L.
- 2,4,6-Tripyridyl-s-triazine 10 mmol L⁻¹ in 40 mmol L⁻¹ HCl.
- FeCl₃·6H₂O 20 mmol L⁻¹.
- Working FRAP reagent: mixture of the above three reagents in the ratio 10:1:1 prepared at the time of use.

The assay is achieved as follows. The sample (100 μL) is mixed with 3 mL of working FRAP reagent thermostated at 37 °C and the absorption at 593 nm (A) is measured after 4 min. Trolox standards

Table 5. Phenolic compound contents (mg L⁻¹) and parameters in Mixture must^a

Compound	Fermentation days				
	0	30	58	92	139
Hydroxycinnamic acids					
Caffeic acid	1.0 ± 0.3	18.6 ± 5.9	6.1 ± 1.9	1.2 ± 0.4	0.9 ± 0.3
Chlorogenic acid	106.0 ± 2.0	208.4 ± 3.9	178.3 ± 3.4	107.2 ± 2.0	75.7 ± 1.4
<i>p</i> -Coumaric acid	1.0 ± 0.2	1.9 ± 0.3	1.6 ± 0.3	1.0 ± 0.2	0.8 ± 0.1
4- <i>p</i> -Coumaroylquinic acid	81.1 ± 1.3	205.6 ± 3.2	207.9 ± 3.2	199.9 ± 3.1	194.8 ± 3.0
Hydrocaffeic acid	11.48 ± 0.05	ND	14.25 ± 0.07	80.7 ± 0.4	92.7 ± 0.4
(<i>trans</i>)-Ferulic acid	ND	1.4 ± 0.3	1.3 ± 0.3	ND	ND
Flavan-3-ols					
(+)-Catechin	3.4 ± 0.3	13.1 ± 1.1	10.1 ± 0.8	11.4 ± 0.9	8.2 ± 0.7
(-)-Epicatechin	32.7 ± 3.3	62.7 ± 6.4	69.4 ± 7.0	57.1 ± 5.8	31.5 ± 3.2
Procyanidin B1	5.8 ± 0.3	148.9 ± 7.1	149.4 ± 7.1	112.4 ± 5.3	87.6 ± 4.2
Procyanidin B2	281 ± 18	293 ± 19	313 ± 20	278 ± 18	176 ± 11
Procyanidin B5	ND	8.3 ± 0.8	9.0 ± 0.8	9.5 ± 0.9	ND
Dihydrochalcones					
Phloretin 2'- <i>O</i> -xyloglucoside	20.8 ± 0.4	188.4 ± 3.9	201.1 ± 4.2	200.5 ± 4.1	162.2 ± 3.4
Phloridzin	ND	15.1 ± 1.6	18.2 ± 1.9	19.0 ± 2.0	12.1 ± 1.3
Flavonols					
Avicularin	ND	ND	ND	ND	ND
Hyperin	ND	0.31 ± 0.02	0.31 ± 0.02	0.27 ± 0.01	0.15 ± 0.01
Isoquercitrin	ND	ND	ND	ND	ND
Quercitrin	ND	1.07 ± 0.01	1.03 ± 0.01	0.84 ± 0.01	0.409 ± 0.004
Benzoic acids					
Gallic acid	ND	0.82 ± 0.03	1.07 ± 0.04	1.02 ± 0.04	1.00 ± 0.04
<i>p</i> -Hydroxybenzoic acid	0.08 ± 0.01	ND	ND	ND	1.4 ± 0.2
Protocatechuic acid	ND	3.7 ± 0.2	2.4 ± 0.2	1.20 ± 0.08	1.27 ± 0.08
Volatile polyphenols					
Catechol	ND	ND	ND	2.8 ± 0.2	7.8 ± 0.6
Tyrosol	ND	24.4 ± 0.7	26.0 ± 0.8	26.0 ± 0.8	26.7 ± 0.8
Overall polyphenols					
FCI (g tannic acid L ⁻¹)	2.06 ± 0.04	1.83 ± 0.04	1.70 ± 0.02	1.63 ± 0.03	1.35 ± 0.03
TPI (A _{280nm})	40.3 ± 0.1	36.2 ± 0.1	34.2 ± 0.1	32.2 ± 0.1	32.2 ± 0.1
Hydroxycinnamatics (A _{320nm})	29.5 ± 0.1	26.8 ± 0.1	22.8 ± 0.1	18.2 ± 0.1	17.0 ± 0.1
Parameters					
FRAP (mmol Trolox L ⁻¹)	5.0 ± 0.2	5.4 ± 0.3	6.0 ± 0.4	5.8 ± 0.3	5.6 ± 0.3
PPC (g tannic acid L ⁻¹)	0.776 ± 0.017	0.662 ± 0.014	0.658 ± 0.012	0.627 ± 0.007	0.662 ± 0.007
Turbidity (NTU)	732 ± 4	486.5 ± 0.7	41.15 ± 0.07	17.85 ± 0.07	5.7 ± 0.1
Browning (A _{420nm})	2.53 ± 0.03	1.14 ± 0.01	0.871 ± 0.004	0.615 ± 0.001	0.999 ± 0.001
<i>E</i> (mV)	328 ± 3	284 ± 2	228 ± 2	210 ± 2	200 ± 2

FCI, Folin–Ciocalteu index; TPI, total polyphenol index; FRAP, ferric-reducing antioxidant power; PPC, protein-precipitating capacity; *E*, reduction potential against Ag/AgCl reference; ND, not detected.

^a Average of two measurements ± standard deviation.

(0.2–1 mmol L⁻¹), as well as a blank, are processed in the same way to construct the calibration curve (*A* versus mmol Trolox L⁻¹). The results are given in mmol Trolox L⁻¹.

Absorbances at 280, 320 and 420 nm

These were measured in 10 mm cuvettes against water by means of an Agilent 8453 spectrophotometer (Agilent Technologies, Santa Clara, CA, USA). The absorbance at 280 nm is proportional to the total polyphenolic content and is called the total polyphenol index (TPI). The absorbance at 320 nm is proportional to the total hydroxycinnamic acid content.¹³ Dilutions, usually 1:50, were made with water when necessary and the absorbance was corrected by the dilution factor. In the case of absorbance at 420 nm

(browning), where dilutions are not allowed, cuvettes of smaller optical paths were used and the value obtained was corrected to a 10 mm optical path.¹¹

Protein-precipitating capacity (PPC)

To measure this parameter, the following reagents are prepared.⁹

- Buffer A: 0.20 mol L⁻¹ acetic acid, 0.17 mol L⁻¹ NaCl, pH adjusted to 4.9 with NaOH (11.4 mL of glacial acetic acid, 9.86 g of NaCl dissolved in about 800 mL of water, adjust to pH 4.9 with a solution of NaOH, make up to a final volume of 1 L with water).
- BSA: 1 mg mL⁻¹ bovine serum albumin (BSA) in buffer A.

Table 6. Phenolic compound contents (mg L⁻¹) and parameters in Moko must^a

Compound	Fermentation days				
	0	30	58	92	142
Hydroxycinnamic acids					
Caffeic acid	2.1 ± 0.2	3.4 ± 0.4	5.9 ± 0.6	7.1 ± 0.8	6.6 ± 0.2
Chlorogenic acid	396.1 ± 4.5	429.5 ± 4.9	398.5 ± 4.6	420.5 ± 4.8	400.9 ± 0.2
<i>p</i> -Coumaric acid	1.9 ± 0.4	2.3 ± 0.4	2.7 ± 0.5	2.7 ± 0.5	2.7 ± 0.4
4- <i>p</i> -Coumaroylquinic acid	96.3 ± 1.6	106.1 ± 1.8	134.3 ± 2.3	134.2 ± 2.3	133.7 ± 0.3
Hydrocaffeic acid	13.9 ± 0.1	12.8 ± 0.1	15.8 ± 0.1	12.9 ± 0.1	13.2 ± 0.1
(<i>trans</i>)-Ferulic acid	1.58 ± 0.08	ND	ND	ND	ND
Flavan-3-ols					
(+)-Catechin	18.9 ± 2.7	18.2 ± 2.6	25.9 ± 3.7	24.6 ± 3.5	10.6 ± 1.1
(-)-Epicatechin	114.5 ± 1.8	92.2 ± 1.5	145.0 ± 2.3	166.2 ± 2.6	152.9 ± 0.2
Procyanidin B1	87.8 ± 1.8	90.4 ± 1.9	93.5 ± 2.0	104.0 ± 2.2	83.3 ± 2.9
Procyanidin B2	674 ± 12	856 ± 15	855 ± 15	843 ± 15	771 ± 10
Procyanidin B5	23.5 ± 0.8	18.2 ± 0.6	23.9 ± 0.5	26.2 ± 0.8	23.2 ± 0.7
Dihydrochalcones					
Phloretin 2'- <i>O</i> -xyloglucoside	377 ± 15	460 ± 18	455 ± 18	452 ± 18	435 ± 6
Phloridzin	11.9 ± 0.7	11.2 ± 0.6	18.3 ± 1.1	28.5 ± 1.7	27.4 ± 0.2
Flavonols					
Avicularin	ND	ND	ND	ND	ND
Hyperin	0.60 ± 0.05	0.41 ± 0.03	0.54 ± 0.04	0.59 ± 0.05	0.58 ± 0.04
Isoquercitrin	0.33 ± 0.01	0.46 ± 0.02	0.56 ± 0.02	0.80 ± 0.03	0.30 ± 0.02
Quercitrin	1.25 ± 0.02	1.02 ± 0.02	1.47 ± 0.02	1.74 ± 0.03	1.64 ± 0.02
Benzoic acids					
Gallic acid	0.58 ± 0.02	ND	0.54 ± 0.02	0.56 ± 0.02	0.57 ± 0.01
<i>p</i> -Hydroxybenzoic acid	1.38 ± 0.07	ND	1.17 ± 0.06	1.71 ± 0.09	1.68 ± 0.04
Protocatechuic acid	ND	1.60 ± 0.01	2.73 ± 0.02	1.97 ± 0.02	2.01 ± 0.02
Volatile polyphenols					
Catechol	1.8 ± 0.2	1.7 ± 0.1	2.0 ± 0.2	1.7 ± 0.1	ND
Tyrosol	ND	12.2 ± 0.1	14.7 ± 0.3	14.6 ± 0.3	14.8 ± 0.2
Overall polyphenols					
FCI (g tannic acid L ⁻¹)	3.37 ± 0.04	3.04 ± 0.02	3.12 ± 0.03	2.86 ± 0.03	2.64 ± 0.02
TPI (A _{280 nm})	58.4 ± 0.1	59.1 ± 0.1	59.2 ± 0.1	59.2 ± 0.1	58.2 ± 0.1
Hydroxycinnamics (A _{320 nm})	36.0 ± 0.1	37.3 ± 0.1	37.1 ± 0.1	36.9 ± 0.1	36.2 ± 0.1
Parameters					
FRAP (mmol Trolox L ⁻¹)	9.8 ± 0.2	9.3 ± 0.2	10.0 ± 0.3	9.5 ± 0.3	9.3 ± 0.2
PPC (g tannic acid L ⁻¹)	1.055 ± 0.012	1.070 ± 0.009	1.121 ± 0.023	1.063 ± 0.004	1.079 ± 0.025
Turbidity (NTU)	432 ± 3	471 ± 3	138 ± 1	64.4 ± 0.2	15.1 ± 0.1
Browning (A _{420 nm})	1.56 ± 0.01	1.31 ± 0.01	0.953 ± 0.004	0.821 ± 0.001	0.959 ± 0.003
<i>E</i> (mV)	324 ± 2	275 ± 2	233 ± 2	214 ± 2	191 ± 1

FCI, Folin–Ciocalteu index; TPI, total polyphenol index; FRAP, ferric-reducing antioxidant power; PPC, protein-precipitating capacity; *E*, reduction potential against Ag/AgCl reference; ND, not detected.

^a Average of two measurements ± standard deviation.

- SDS/TEA: 50 mL L⁻¹ triethanolamine (TEA), 10 g L⁻¹ sodium dodecyl sulfate (SDS) (50 mL of TEA, 10 g of SDS, make up to 1 L with water).
- FeCl₃: 0.01 mol L⁻¹ FeCl₃ in 0.01 mol L⁻¹ HCl. To make 0.01 mol L⁻¹ HCl, dilute 0.83 mL of concentrated HCl to 1 L with water. Dissolve 1.62 g of FeCl₃ in 1 L of the acid solution and allow it to sit for several hours. Gravity filter through paper.

The assay is performed as follows. Dispense 2 mL of BSA into a 15 mL centrifuge tube and add 1 mL of sample solution. The solution cannot contain any acetone, since even traces of acetone inhibit the precipitation reaction. Mix immediately and allow to sit for 24 h at 4 °C. Centrifuge at 3000 × *g* for 15 min and pour off the

supernatant. Redissolve the pellet in 4 mL of SDS/TEA, add 1 mL of FeCl₃ and vortex immediately. After about 15 min, read the absorbance at 510 nm (*A*). Tannic acid standards (0.2–1.4 g L⁻¹ in water), as well as a blank (FeCl₃ in SDS/TEA), are processed in the same way to construct the calibration curve (*A* versus g tannic acid L⁻¹), except that they need to sit for only 15 min at room temperature after mixing with BSA. The results are given in g tannic acid L⁻¹.

Polyphenolic compounds

The determination of individual polyphenolic compounds was performed by high-performance liquid chromatography (HPLC) using the filtered samples. The method of Suárez *et al.*¹⁴ was employed. An Agilent 1100 Series liquid chromatograph (Agilent

Table 7. Phenolic compound contents (mg L⁻¹) and parameters in Patzuloa must^a

Compound	Fermentation days				
	0	30	58	92	134
Hydroxycinnamic acids					
Caffeic acid	0.24 ± 0.06	2.3 ± 0.3	2.1 ± 0.4	1.2 ± 0.1	1.2 ± 0.1
Chlorogenic acid	180.2 ± 1.9	292.6 ± 3.2	197.1 ± 2.1	118.4 ± 1.3	72.3 ± 0.8
<i>p</i> -Coumaric acid	2.35 ± 0.09	2.88 ± 0.11	2.11 ± 0.08	1.37 ± 0.05	0.95 ± 0.04
4- <i>p</i> -Coumaroylquinic acid	218.6 ± 0.5	585.7 ± 1.4	545.5 ± 1.3	504.3 ± 1.2	481.7 ± 1.2
Hydrocaffeic acid	7.37 ± 0.04	55.9 ± 0.3	92.4 ± 0.4	149.4 ± 0.7	168.5 ± 0.8
(<i>trans</i>)-Ferulic acid	ND	3.22 ± 0.08	3.19 ± 0.08	2.80 ± 0.07	2.41 ± 0.06
Flavan-3-ols					
(+)-Catechin	2.5 ± 0.1	13.6 ± 0.7	18.1 ± 1.0	14.8 ± 0.8	12.2 ± 0.6
(-)-Epicatechin	30.1 ± 7.5	33.6 ± 8.4	36.6 ± 9.1	31.9 ± 8.0	26.5 ± 6.6
Procyanidin B1	ND	130.5 ± 7.8	151.9 ± 9.1	142.4 ± 8.5	137.9 ± 8.2
Procyanidin B2	100.1 ± 0.5	114.4 ± 0.6	109.7 ± 0.5	112.1 ± 0.6	112.3 ± 0.6
Procyanidin B5	ND	ND	ND	ND	ND
Dihydrochalcones					
Phloretin 2'- <i>O</i> -xyloglucoside	5.01 ± 0.01	169.1 ± 0.5	160.2 ± 0.5	143.4 ± 0.4	120.6 ± 0.4
Phloridzin	ND	4.07 ± 0.06	4.26 ± 0.06	3.11 ± 0.04	3.11 ± 0.04
Flavonols					
Avicularin	ND	ND	ND	ND	ND
Hyperin	ND	ND	ND	ND	ND
Isoquercitrin	ND	ND	ND	ND	ND
Quercitrin	ND	1.25 ± 0.02	1.61 ± 0.03	0.87 ± 0.01	0.68 ± 0.01
Benzoic acids					
Gallic acid	ND	1.31 ± 0.01	1.38 ± 0.01	1.33 ± 0.01	1.39 ± 0.01
<i>p</i> -Hydroxybenzoic acid	0.64 ± 0.06	3.5 ± 0.3	ND	ND	2.8 ± 0.3
Protocatechuic acid	ND	1.9 ± 0.1	2.1 ± 0.1	1.81 ± 0.09	1.76 ± 0.09
Volatile polyphenols					
Catechol	ND	4.3 ± 0.3	6.0 ± 0.4	4.2 ± 0.2	5.4 ± 0.3
Tyrosol	ND	25.6 ± 0.1	25.2 ± 0.1	25.2 ± 0.1	25.4 ± 0.1
Overall polyphenols					
FCI (g tannic acid L ⁻¹)	2.33 ± 0.03	1.90 ± 0.01	1.90 ± 0.02	1.77 ± 0.01	1.64 ± 0.01
TPI (A _{280nm})	61.8 ± 0.1	44.1 ± 0.1	41.3 ± 0.1	37.8 ± 0.1	35.4 ± 0.1
Hydroxycinnamics (A _{320nm})	60.7 ± 0.1	41.6 ± 0.1	36.4 ± 0.1	30.1 ± 0.1	26.2 ± 0.1
Parameters					
FRAP (mmol Trolox L ⁻¹)	5.39 ± 0.04	5.28 ± 0.05	6.11 ± 0.07	6.17 ± 0.07	6.32 ± 0.06
PPC (g tannic acid L ⁻¹)	1.07 ± 0.01	0.65 ± 0.01	0.60 ± 0.02	0.56 ± 0.01	0.546 ± 0.007
Turbidity (NTU)	1023 ± 1	390 ± 6	155.5 ± 0.7	114.0 ± 0.5	38.8 ± 0.5
Browning (A _{420nm})	6.11 ± 0.03	1.29 ± 0.01	0.963 ± 0.007	0.987 ± 0.007	0.550 ± 0.005
<i>E</i> (mV)	280 ± 2	255 ± 2	175 ± 1	163 ± 1	157 ± 1

FCI, Folin–Ciocalteu index; TPI, total polyphenol index; FRAP, ferric-reducing antioxidant power; PPC, protein-precipitating capacity; *E*, reduction potential against Ag/AgCl reference; ND, not detected.

^a Average of two measurements ± standard deviation.

Technologies) was used with a Nucleosil® 120-3 C₁₈ column (250 mm × 4.6 mm, 3 μm; Macherey-Nagel, Düren, Germany). The flow rate was 0.8 mL min⁻¹, the column temperature 25 °C and the injected volume 50 μL. The elution solvents were aqueous 20 mL L⁻¹ acetic acid (solvent A) and pure methanol (solvent B). The samples were eluted according to the following gradient: a linear increase from 0 to 45% solvent B in 55 min, followed by a 20 min isocratic step and finally a return to the initial conditions (0% solvent B), allowing 5 min for stabilization. Column effluents were monitored at four wavelengths: 280 nm for benzoic acids, flavan-3-ols, dihydrochalcones, catechol and tyrosol, 313 nm for hydroxycinnamic acids and 355 nm for flavonols. Phenolic compounds were quantified by the external standard method from

peak areas. They were identified by means of their retention times and their 190–900 nm spectra, which were previously recorded by injecting the pure compounds.

The polyphenolic compounds determined are listed in Tables 1 and 2, where calibration data are also given. Polyphenols of Table 2 were calibrated to a single point owing to their high cost. Polyphenols of Table 1 were dissolved in 900 mL L⁻¹ ethanol containing 10 g L⁻¹ ascorbic acid to avoid oxidation. By dilution of these stock solutions with water, standards of appropriate concentrations were obtained, in which ethanol was adjusted to 60 mL L⁻¹ to avoid precipitation, and ascorbic acid to 10 g L⁻¹ to avoid oxidation. Polyphenols of Table 2 were dissolved in 60 mL L⁻¹ ethanol containing 10 g L⁻¹ ascorbic acid.

Table 8. Phenolic compound contents (mg L⁻¹) and parameters in Txalaka must^a

Compound	Fermentation days				
	0	30	64	98	139
Hydroxycinnamic acids					
Caffeic acid	0.91 ± 0.02	8.5 ± 0.2	8.9 ± 0.2	2.6 ± 0.6	1.1 ± 0.2
Chlorogenic acid	54.6 ± 4.2	17.5 ± 1.4	45.2 ± 3.5	40.6 ± 3.1	36.3 ± 2.8
<i>p</i> -Coumaric acid	0.40 ± 0.04	0.32 ± 0.03	0.17 ± 0.02	0.37 ± 0.04	0.20 ± 0.02
4- <i>p</i> -Coumaroylquinic acid	89.9 ± 6.4	119.9 ± 8.5	128.1 ± 9.1	124.3 ± 8.9	117.9 ± 8.4
Hydrocaffeic acid	10.32 ± 0.02	ND	10.89 ± 0.02	18.77 ± 0.04	21.50 ± 0.04
(<i>trans</i>)-Ferulic acid	ND	ND	ND	ND	ND
Flavan-3-ols					
(+)-Catechin	4.3 ± 0.3	12.3 ± 0.9	4.6 ± 0.4	8.6 ± 0.7	5.1 ± 0.4
(-)-Epicatechin	23.5 ± 1.8	52.3 ± 4.0	63.9 ± 4.9	60.9 ± 4.6	49.6 ± 3.8
Procyanidin B1	27.5 ± 1.1	47.6 ± 1.8	62.5 ± 2.3	57.4 ± 2.2	57.2 ± 2.1
Procyanidin B2	130 ± 1	263 ± 3	266 ± 4	262 ± 3	230 ± 3
Procyanidin B5	ND	6.4 ± 0.6	7.4 ± 0.7	7.8 ± 0.7	6.0 ± 0.6
Dihydrochalcones					
Phloretin 2'- <i>O</i> -xyloglucoside	17.5 ± 1.0	32.1 ± 1.9	35.9 ± 2.1	37.7 ± 2.2	32.6 ± 1.9
Phloridzin	1.4 ± 0.1	5.3 ± 0.4	7.9 ± 0.5	9.9 ± 0.7	6.2 ± 0.4
Flavonols					
Avicularin	ND	ND	ND	ND	ND
Hyperin	ND	0.24 ± 0.01	0.29 ± 0.01	0.32 ± 0.02	0.17 ± 0.01
Isoquercitrin	ND	ND	ND	ND	ND
Quercitrin	ND	0.46 ± 0.03	0.63 ± 0.04	0.83 ± 0.05	0.49 ± 0.03
Benzoic acids					
Gallic acid	0.55 ± 0.07	0.68 ± 0.08	0.78 ± 0.09	0.82 ± 0.09	0.82 ± 0.10
<i>p</i> -Hydroxybenzoic acid	ND	ND	ND	ND	2.4 ± 0.1
Protocatechuic acid	ND	2.8 ± 0.2	2.2 ± 0.2	1.5 ± 0.1	1.6 ± 0.1
Volatile polyphenols					
Catechol	ND	ND	ND	ND	ND
Tyrosol	ND	13.59 ± 0.04	15.62 ± 0.05	16.35 ± 0.05	16.34 ± 0.05
Overall polyphenols					
FCI (g tannic acid L ⁻¹)	1.62 ± 0.01	1.29 ± 0.02	1.24 ± 0.01	1.13 ± 0.01	0.98 ± 0.01
TPI (A _{280nm})	22.8 ± 0.1	22.3 ± 0.1	21.8 ± 0.1	21.2 ± 0.1	19.5 ± 0.1
Hydroxycinnamics (A _{320nm})	12.1 ± 0.1	11.3 ± 0.1	11.2 ± 0.1	10.0 ± 0.1	8.4 ± 0.1
Parameters					
FRAP (mmol Trolox L ⁻¹)	4.10 ± 0.09	3.47 ± 0.07	3.98 ± 0.08	3.95 ± 0.06	3.60 ± 0.06
PPC (g tannic acid L ⁻¹)	0.71 ± 0.02	0.56 ± 0.02	0.53 ± 0.01	0.520 ± 0.006	0.525 ± 0.008
Turbidity (NTU)	244 ± 4	544 ± 2	99.6 ± 0.4	36.8 ± 0.3	15.2 ± 0.1
Browning (A _{420nm})	0.870 ± 0.007	0.585 ± 0.005	0.490 ± 0.005	0.493 ± 0.002	0.000 ± 0.001
<i>E</i> (mV)	308 ± 2	231 ± 2	173 ± 2	177 ± 1	164 ± 1

FCI, Folin–Ciocalteu index; TPI, total polyphenol index; FRAP, ferric-reducing antioxidant power; PPC, protein-precipitating capacity; *E*, reduction potential against Ag/AgCl reference; ND, not detected.

^a Average of two measurements ± standard deviation.

RESULTS AND DISCUSSION

The following calibration equations were obtained from *n* experimental points for FCI, FRAP and PPC to calculate the concentration of the standard used (*C*) from the absorbance (*A*) at the given wavelength.

$$\text{FCI} : A_{750} = 88.8393C + 0.0448, C = \text{g tannic acid L}^{-1}, \\ n = 8, R = 0.9999$$

$$\text{FRAP} : A_{593} = 1.3564C + 0.1160, C = \text{mmol Trolox L}^{-1}, \\ n = 6, R = 0.9998$$

$$\text{PPC} : A_{510} = -0.4982C^2 + 1.8721C - 0.3034, C = \text{g tannic acid L}^{-1}, \\ n = 7, R = 0.9997$$

Table 9. Correlations between parameters and polyphenolics: Pearson coefficients^a

Polyphenolic compound	FRAP	PPC	Turbidity	Browning	<i>E</i>
Hydroxycinnamic acids					
Caffeic acid	0.347	0.313	0.086	-0.128	0.105
Chlorogenic acid	0.889	0.858	0.178	0.180	0.316
<i>p</i> -Coumaric acid	0.774	0.771	0.281	0.343	0.300
4- <i>p</i> -Coumaroylquinic acid	0.294	0.077	-0.058	-0.013	-0.241
Hydrocaffeic acid	0.065	-0.280	-0.417	-0.251	-0.546
(<i>trans</i>)-Ferulic acid	0.091	-0.201	-0.133	-0.120	-0.250
Flavan-3-ols					
(+)-Catechin	0.840	0.658	-0.052	-0.148	0.042
(-)-Epicatechin	0.866	0.806	-0.068	-0.074	0.081
Procyanidin B1	0.594	0.283	-0.258	-0.279	-0.210
Procyanidin B2	0.876	0.835	0.008	-0.054	0.184
Procyanidin B5	0.809	0.748	-0.084	-0.116	0.124
Dihydrochalcones					
Phloretin 2'- <i>O</i> -xyloglucoside	0.880	0.741	-0.070	-0.067	0.133
Phloridzin	0.448	0.227	-0.437	-0.298	-0.314
Flavonols					
Hyperin	0.739	0.629	-0.177	-0.194	0.011
Quercitrin	0.774	0.494	-0.300	-0.270	-0.230
Benzoic acids					
Gallic acid	0.151	-0.105	-0.409	-0.422	-0.385
<i>p</i> -Hydroxybenzoic acid	0.114	-0.017	-0.264	-0.172	-0.282
Protocatechuic acid	0.387	0.171	-0.242	-0.344	-0.327
Volatile polyphenols					
Catechol	-0.292	-0.511	-0.454	-0.353	-0.491
Tyrosol	-0.096	-0.498	-0.710	-0.640	-0.768
Overall polyphenols					
FCI	0.937	0.942	0.306	0.299	0.398
TPI	0.902	0.936	0.365	0.440	0.352
Hydroxycinnamics	0.719	0.810	0.514	0.617	0.378

FRAP, ferric-reducing antioxidant power; PPC, protein-precipitating capacity; *E*, reduction potential against Ag/AgCl reference; FCI, Folin–Ciocalteu index; TPI, total polyphenol index.

^a The significant correlations are indicated in **bold** type.

In the original description of the PPC assay, Hagerman and Butler⁹ reported a straight line. However, we obtained a much better fit with a second-order polynomial, hence we used it in all calculations. Besides, in the original method the absorbance at 510 nm is plotted against mg tannic acid, while we considered it more convenient to express tannic acid content in concentration units, so we used g L⁻¹ (mg mL⁻¹).

The polyphenolic compounds determined were the most habitual in Basque musts and ciders:^{15,16}

- Hydroxycinnamic acids: caffeic acid, chlorogenic acid, *p*-coumaric acid, 4-*p*-coumaroylquinic acid, hydrocaffeic acid and (*trans*)-ferulic acid.
- Flavan-3-ols: (+)-catechin, (-)-epicatechin, procyanidin B1, procyanidin B2 and procyanidin B5.
- Dihydrochalcones: phloretin 2'-*O*-xyloglucoside and phloridzin.
- Flavonols: avicularin, hyperin (or hyperoside), isoquercitrin and quercitrin.

Besides, we determined the benzoic acids gallic acid, *p*-hydroxybenzoic acid and protocatechuic acid as well as the volatile phenols catechol and tyrosol, which are determined by many authors.^{17,18}

Figure 1 shows the chromatogram obtained with pure standards. The overlapping of some peaks (e.g. peaks 13 and 14) was avoided by measuring at three different wavelengths, as explained above. Figure 2 shows a representative chromatogram obtained with one of our cider samples.

Tables 3–8 show the concentrations obtained throughout the five samplings for the individual polyphenolic compounds, as well as the values for the parameters FRAP, PPC, turbidity, browning and reduction potential. From these data, correlations between the five parameters and the polyphenols were calculated as Pearson coefficients at the 0.01 level. They are listed in Table 9.

As expected, FRAP and PPC parameters are significantly correlated with FCI and TPI. These two indices are related to total polyphenolic content, and polyphenolic compounds have antioxidant and precipitating properties. Besides, FRAP and PPC are also significantly correlated with hydroxycinnamics, and so are turbidity and browning.

Regarding individual polyphenolics, multivariate analysis was performed on data in order to explore the effect of the individual phenol contents in a multivariate way. Separate multivariate linear regression (MLR) models were built for parameters FRAP, PPC, turbidity, browning and reduction potential as dependent *Y* variable and individual phenol contents as predictor *X*

Table 10. MLR parameters for regression models^a using significant phenol contents to estimate cider parameters and % estimation (mean \pm standard deviation) obtained after applying MLR equations

Parameter	Multiple correlation	MLR equation		% estimation
		X variables ^b	B coefficients	
FRAP	0.944	x1: Caffeic acid x2: Procyanidin B1 x3: Procyanidin B2	b0: 2.3568 b1: -0.1435 b2: 0.0193 b3: 0.0076	106 \pm 27
PPC	0.964	x1: <i>p</i> -Coumaric acid x2: (-)-Epicatechin x3: Procyanidin B2 x4: Procyanidin B5 x5: Hyperin x6: Tyrosol	b0: 0.5262 b1: 0.1047 b2: 0.0018 b3: 0.0007 b4: -0.0247 b5: 0.0388 b6: -0.0105	101 \pm 12
Turbidity	0.787	x1: Phloridzin x2: Quercitrin x3: Gallic acid x4: Tyrosol	b0: 625.93 b1: -16.6404 b2: 167.5879 b3: -211.6035 b4: -12.6223	210 \pm 480
Browning	0.743	x1: <i>p</i>-Coumaric acid x2: Gallic acid x3: Protocatechuic acid x4: Tyrosol	b0: 2.0655 b1: 0.5001 b2: -0.4566 b3: -0.2539 b4: -0.0517	127 \pm 105
Potential	0.802	x1: <i>p</i> -Coumaric acid x2: Tyrosol	b0: 286.1248 b1: 13.5755 b2: -4.5877	102 \pm 16

^a The regression models are significant at 0.01 level.
^b Variables in **bold** type are significant at 0.01 level.

variables. Those phenols showing individual correlations higher than 0.300 (absolute value) with the parameter under evaluation were used to perform the MLR analysis. MLR models provided information about phenols with a significant effect on the studied parameter. Individual phenols showing a significant effect ($P = 0.05$) were selected to compute a final MLR model for each of the parameters. The regression models were significant at 0.01 level in all cases and the variables shown in Table 10 are the significant ones at 0.05 level. Finally, the value of the parameter was predicted ($\text{PARAMETER}_{\text{predicted}}$) for all samples using the MLR equation (Table 10) and compared with the observed value ($\text{PARAMETER}_{\text{observed}}$) according to the expression¹⁹

$$\% \text{ estimation} = \left(\frac{\text{PARAMETER}_{\text{predicted}}}{\text{PARAMETER}_{\text{observed}}} \right) \times 100$$

MLR models provided high values for multiple correlation coefficients and good estimation percentages for FRAP and PPC. Lower multiple correlation values were obtained for turbidity, browning and potential. However, the last of these was quite well predicted, with an average estimation value of 102%. Estimated values corresponding to turbidity and browning show that, even though significant regression models are obtained when individual phenol contents are used as predictor variables, these variables do not provide enough information to predict these two parameters properly.

Procyanidin B1 and procyanidin B2 show a significant positive effect on FRAP, so they are the polyphenolic compounds which most contribute to the antioxidant power in Basque ciders. On

the other hand, *p*-coumaric acid, (-)-epicatechin, procyanidin B2 and hyperin have a significant positive effect on PPC, being therefore the polyphenolic compounds which most contribute to the precipitating capacity. With respect to reduction potential *E*, only *p*-coumaric acid shows a positive effect on it.

It should be stressed that the main positive contribution to antioxidant power, precipitating capacity or reduction potential does not come necessarily from the most concentrated polyphenols. Although chlorogenic acid, 4-*p*-coumaroylquinic acid, procyanidin B2 and phloretin 2'-*O*-xyloglucoside are the most concentrated polyphenols in the studied ciders, only procyanidin B2 shows a significant effect on antioxidant power and precipitating capacity, and none of them does on reduction potential. On the other hand, less concentrated polyphenols such as *p*-coumaric acid and (-)-epicatechin offer remarkable contributions to some of these parameters. Even minor polyphenols such as hyperin contribute.

Although some significant effects were found on turbidity and browning, the regression models did not provide satisfactory predictions for these parameters. Some authors report a correlation between initial chlorogenic acid content and final browning,²⁰ but we have not seen this in our results.

With respect to negative contributions, caffeic acid has a significant negative effect on FRAP, and procyanidin B5 and tyrosol on PPC. However, the most remarkable negative contribution is that of tyrosol (a fermentation product) on reduction potential. This is interesting because it means that ciders with higher tyrosol

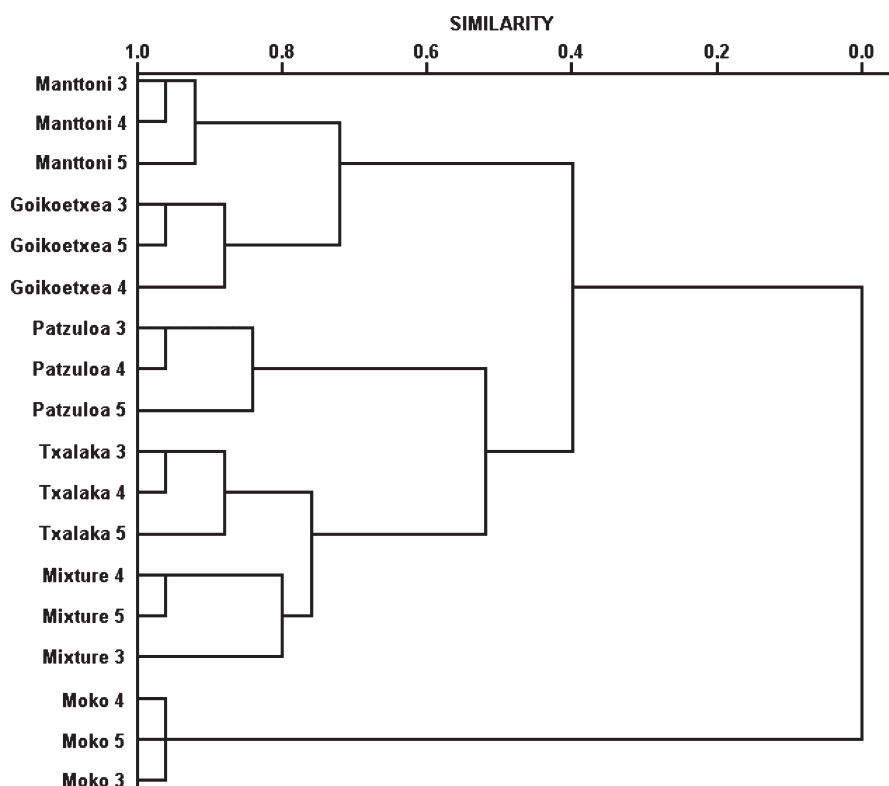


Figure 3. Cluster analysis: dendrogram for last three samplings.

concentration will have less reduction potential, which indicates higher antioxidant reservoir.

Tyrosol is a metabolite from tyrosine formed by yeasts during alcoholic fermentation and is present in wine, olive oil and other plant-derived products. Increasing interest has been focused on this compound because of its antioxidant, anticarcinogenic, cardioprotective and antimicrobial properties.²¹ It has been determined in many beverages such as Spanish Jerez red wines (20.38–44.46 mg L⁻¹),²¹ Suavia ‘Le Rive’ white wine (17.06 mg L⁻¹),²² Spanish white wines (10.15–24.77 mg L⁻¹)²³ and Spanish Merlot red wine (31.36 mg L⁻¹).²⁴ It has been suggested that white wines can provide cardioprotection similar to red wines, although containing lower quantities of polyphenols, if they are rich in tyrosol.^{25–27} This is consistent with the negative effect of tyrosol on reduction potential found in our work. As the tyrosol contents in our ciders (14.8–26.7 mg L⁻¹) and in white wines are similar, ciders are supposed to provide similar health benefits to white wines.

To conclude the study, we have used hierarchical cluster analysis in order to find patterns of clustering between the ciders obtained, based on the individual polyphenol profile. The data matrix included as objects the last three samplings (3, 4 and 5) of the six ciders studied (18 objects). These samplings correspond to ciders with completed alcoholic and malolactic fermentation, which means that they are finished or almost finished. The variables were the 22 individual polyphenols determined. Data were normalized by autoscaling. Square Euclidean distance was used as similarity criterion and furthest neighbour as clustering method. The results are presented in Fig. 3 as a dendrogram. Six groups are obtained, corresponding to the six ciders elaborated. Consequently, ciders can be classified attending only to their polyphenol composition. The smallest difference is obtained between Txalaka

and Mixture ciders. As Mixture cider was obtained by mixing the other five, it is not surprising that it is similar to some of them.

ACKNOWLEDGEMENTS

We are grateful to the Basque Government, the University of the Basque Country UPV/EHU, the Gipuzkoa Natural Cider Association and the Fraisoro Agro-environmental Laboratory for their financial and technical support.

REFERENCES

- Guyot S, Marnet N, Laraba D, Sanoner P and Drilleau JF, Reversed-phase HPLC following thiolysis for quantitative estimation and characterization of the four main classes of phenolic compounds in different tissue zones of a French cider apple variety. *J Agric Food Chem* **46**:1698–1705 (1998).
- Spanos GA and Wrolstad RE, Phenolics of apple, pear, and white grape juices and their changes with processing and storage – a review. *J Agric Food Chem* **40**:1478–1487 (1992).
- Siebert KJ, Haze formation in beverages. *LWT – Food Sci Technol* **39**:987–994 (2006).
- Le Bourvellec C, Le Quéré JM, Sanoner P, Drilleau JF and Guyot S, Inhibition of apple polyphenol oxidase activity by procyanidins and polyphenol oxidation products. *J Agric Food Chem* **52**:122–130 (2004).
- Lea AGH and Drilleau JF, Cidermaking, in *Fermented Beverage Production*. Kluwer Academic/Plenum Publishers, New York, NY, pp. 59–87 (2003).
- Antolovich M, Prenzler PD, Patsalides E, McDonald S and Robards K, Methods for testing antioxidant activity. *Analyst* **127**:183–198 (2002).
- Gacche RN, Shinde BT, Dhole NA, Pund MM and Jadhav AD, Evaluation of floral honey for inhibition of polyphenol oxidase-mediated browning, antioxidant and antimicrobial activities. *J Food Biochem* **33**:693–706 (2009).

- 8 Burdurlu HS and Karadeniz F, Effect of storage on nonenzymatic browning of apple juice concentrates. *Food Chem* **80**:91–97 (2003).
- 9 Hagerman AE and Butler LG, Protein precipitation method for the quantitative determination of tannins. *J Agric Food Chem* **26**:809–812 (1978).
- 10 Nicoli MC, Toniolo R and Anese M, Relationship between redox potential and chain-breaking activity of model systems and foods. *Food Chem* **88**:79–83 (2004).
- 11 OIV, *Compendium of International Methods of Analysis of Wines and Musts*, Vols 1 and 2. International Organisation of Vine and Wine, Paris (2013).
- 12 Benzie IFF and Strain JJ, The ferric reducing ability of plasma (FRAP) as a measure of 'antioxidant power': the FRAP assay. *Anal Biochem* **239**:70–76 (1996).
- 13 Gómez-Alonso S, García-Romero E and Hermosín-Gutiérrez I, HPLC analysis of diverse grape and wine phenolics using direct injection and multidetection by DAD and fluorescence. *J Food Compos Anal* **20**:618–626 (2007).
- 14 Suárez B, Palacios N, Fraga N and Rodríguez R, Liquid chromatographic method for quantifying polyphenols in ciders by direct injection. *J Chromatogr A* **1066**:105–110 (2005).
- 15 Alonso-Salces RM, Barranco A, Abad B, Berrueta LA, Gallo B and Vicente F, Polyphenolic profiles of Basque cider apple cultivars and their technological properties. *J Agric Food Chem* **52**:2938–2952 (2004).
- 16 Alonso-Salces RM, Herrero C, Barranco A, López-Márquez DM, Berrueta LA, Gallo B, *et al.*, Polyphenolic compositions of Basque natural ciders: a chemometric study. *Food Chem* **97**:438–446 (2006).
- 17 Arranz S, Saura-Calixto F, Shaha S and Kroon PA, High contents of nonextractable polyphenols in fruits suggest that polyphenol contents of plant foods have been underestimated. *J Agric Food Chem* **57**:7298–7303 (2009).
- 18 Rodríguez Madrera R, Picinelli Lobo A and Suárez Valles B, Phenolic profile of Asturian (Spain) natural cider. *J Agric Food Chem* **54**:120–124 (2006).
- 19 Picinelli Lobo A, Diñeiro García Y, Mangas Sánchez J, Rodríguez Madrera R and Suárez Valles B, Phenolic and antioxidant composition of cider. *J Food Compos Anal* **22**:644–648 (2009).
- 20 Robards K, Prenzler PD, Tucker G, Swatsitang P and Glover W, Phenolic compounds and their role in oxidative processes in fruits. *Food Chem* **66**:401–436 (1999).
- 21 Piñeiro Z, Cantos-Villar E, Palma M and Puertas B, Direct liquid chromatography method for the simultaneous quantification of hydroxytyrosol and tyrosol in red wines. *J Agric Food Chem* **59**:11683–11689 (2011).
- 22 Thirunavukkarasu M, Penumathsa SV, Samuel SM, Akita Y, Zhan L, Bertelli AAE, *et al.*, White wine induced cardioprotection against ischemia-reperfusion injury is mediated by life extending Akt/FOXO3a/NF κ B survival pathway. *J Agric Food Chem* **56**:6733–6739 (2008).
- 23 Gómez-Míguez MJ, González-Miret ML, Hernanz D, Fernández MA, Vicario IM and Heredia FJ, Effects of prefermentative skin contact conditions on colour and phenolic content of white wines. *J Food Eng* **78**:238–245 (2007).
- 24 Martín S, González-Burgos E, Carretero ME and Gómez-Serranillos MP, Neuroprotective properties of Spanish red wine and its isolated polyphenols on astrocytes. *Food Chem* **128**:40–48 (2011).
- 25 Bertelli AAE, Migliori M, Panichi V, Longoni B, Origlia N, Ferretti A, *et al.*, Oxidative stress and inflammatory reaction modulation by white wine. *Ann NY Acad Sci* **957**:295–301 (2002).
- 26 Bertelli AAE, Wine, research and cardiovascular disease: instructions for use. *Atherosclerosis* **195**:242–247 (2007).
- 27 Dudley JI, Lekli I, Mukherjee S, Das M, Bertelli AAA and Das DK, Does white wine qualify for French paradox? Comparison of the cardioprotective effects of red and white wines and their constituents: resveratrol, tyrosol, and hydroxytyrosol. *J Agric Food Chem* **56**:9362–9373 (2008).

Draft Genome Sequence of *Pediococcus parvulus* 2.6, a Probiotic β -Glucan Producer Strain

Adrián Pérez-Ramos,^a M. Luz Mohedano,^a Ana Puertas,^b Antonella Lamontanara,^c Luigi Orru,^c Giuseppe Spano,^d Vittorio Capozzi,^d M. Teresa Dueñas,^b Paloma López^a

Centro de Investigaciones Biológicas, C.S.I.C., Madrid, Spain^a; Department of Applied Chemistry, University of Basque Country (UPV/EHU), San Sebastián, Spain^b; Council for Agricultural Research and Economics (CREA)-Genomics Research Centre, Fiorenzuola d'Arda (PC), Italy^c; Department of Agriculture, Food and Environment Sciences, University of Foggia, Foggia, Italy^d

We report here the draft genome sequence of the probiotic *Pediococcus parvulus* 2.6, a lactic acid bacterial strain isolated from ropy cider. The bacterium produces a prebiotic and immunomodulatory exopolysaccharide, and this is the first strain of the *P. parvulus* species whose genome has been characterized.

Received 18 October 2016 Accepted 21 October 2016 Published 15 December 2016

Citation Pérez-Ramos A, Mohedano ML, Puertas A, Lamontanara A, Orru L, Spano G, Capozzi V, Dueñas MT, López P. 2016. Draft genome sequence of *Pediococcus parvulus* 2.6, a probiotic β -glucan producer strain. *Genome Announc* 4(6):e01381-16. doi:10.1128/genomeA.01381-16.

Copyright © 2016 Pérez-Ramos et al. This is an open-access article distributed under the terms of the [Creative Commons Attribution 4.0 International license](https://creativecommons.org/licenses/by/4.0/).

Address correspondence to Paloma López, plg@cib.csic.es.

We report here the draft genome sequence of *Pediococcus parvulus* 2.6 (formerly *Pediococcus damnosus*), a lactic acid bacterium isolated from ropy cider (1). This is the first strain of *P. parvulus* whose genome has been characterized. The 2.6 strain produces the immunomodulatory exopolysaccharide 2-substituted (1,3)- β -D-glucan (2), which is synthesized by a limited number of bacteria and confers probiotic properties to the producing strains. This polysaccharide differs from the β -glucans produced by plants and other microorganisms. The synthesis of 2-substituted (1,3)- β -D-glucan by *P. parvulus* 2.6 is controlled by a single heterotransmembrane glucosyltransferase (GTF), which polymerizes glucosyl residues from UDP glucose (3–5). Some of the conditions that influence the homopolysaccharide (HoPS) synthesis by *P. parvulus* 2.6, as well as the enzymatic activities involved in sugar metabolism in this strain, have been examined (6, 7). The physicochemical properties of the HoPS have also been determined, and nuclear magnetic resonance (NMR) analysis showed that the same HoPS was synthesized, irrespective of the sugar source used for growth (8). The molecular masses of these β -glucans are high ($>10^6$ Da), and their rheological properties showed that they have potential utility as biothickeners (8). An oat-based product fermented by *P. parvulus* 2.6 showed improved rheology (9), thereby decreasing the need for added stabilizers and texturizers.

The potential of *P. parvulus* 2.6 as a probiotic strain has also been examined; it resists gastrointestinal stress, adheres to Caco-2 cells, and its HoPS reduces the production of inflammatory cytokines by polarized macrophages (10). We have also shown that *P. parvulus* HoPS improves the growth and viability of probiotic microorganisms, as well as their adhesion to human enterocytes (11). The 2-substituted (1,3)- β -D-glucan increases *in vitro* the ratio of interleukin 10 (IL10) (anti-inflammatory) to tumor necrosis factor alpha (TNF α) (inflammatory) in human macrophages and decreases the levels of the proinflammatory IL8 in human intes-

tine organ cultures (reference 12 and Notararigo S., Antolin M., Guarner F., López P., unpublished data).

An oat-based product fermented by *P. parvulus* 2.6 had a bifidogenic effect and decreased serum cholesterol levels in humans (13). Possibly, the 2-substituted (1,3)- β -D-glucan has a synergistic effect with the hypocholesterolemic action of oat β -glucans. Finally, *P. parvulus* 2.6 displays antibacterial activity against several bacterial species (14), including natural contaminants in oats, a property that reduces the need for chemical preservatives and improves the functionality of the final product.

Two micrograms of genomic DNA was subjected to library preparation using the TruSeq DNA sample prep kit FC-121-1001, according to the manufacturer's instructions. Whole-genome sequencing used the Illumina GAIIx at the Genomics Research Centre (Fiorenzuola d'Arda, Italy). A total of 26,018,224 paired-end reads (2×110 -bp length) were assembled into 115 contigs. The genome was calculated to be 2,236,754 long. The size of the shortest contig was 206 bp, while the length of the longest contig was 171,226 bp. The genome sequence was annotated by the NCBI Prokaryotic Genomes Annotation Pipeline. A total of 2,241 genes were predicted to encode 2,069 proteins, three rRNAs, 60 tRNAs, and four noncoding RNAs (ncRNAs), and 105 are pseudogenes.

Accession number(s). The complete genome of *P. parvulus* 2.6 has been deposited at DDBJ/EMBL/GenBank under accession number [LXND000000000](https://www.ncbi.nlm.nih.gov/nuclink/LXND000000000).

ACKNOWLEDGMENT

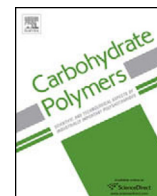
We thank Dr. Stephen Elson for the critical reading of the manuscript.

FUNDING INFORMATION

P.L., M.T.D., and G.S. are supported by the Spanish Ministry of Economy and Competitiveness grants AGL2012-40084-C03 and AGL2015-65010-C3-1-R. A.P.-R. is a Ph.D. student supported by the Spanish Ministry of Economy and Competitiveness grant BES-2013-065157. V.C. was supported by a grant from the Apulian Region in the framework of the "FutureInResearch" program (practice code 9OJ4W81).

REFERENCES

1. Fernández K, Dueñas M, Irastorza A, Bilbao A, del Campo G. 1995. Characterization and DNA plasmid analysis of ropy *Pediococcus* spp. strains isolated from Basque Country ciders. *J Food Protect* 59:35–40.
2. Dueñas-Chasco MT, Rodríguez-Carvajal MA, Mateo PT, Franco-Rodríguez G, Espartero J, Irastorza-Iribas A, Gil-Serrano AM. 1997. Structural analysis of the exopolysaccharide produced by *Pediococcus damnosus* 2.6. *Carbohydr Res* 303:453–458. [http://dx.doi.org/10.1016/S0008-6215\(97\)00192-4](http://dx.doi.org/10.1016/S0008-6215(97)00192-4).
3. Werning ML, Ibarburu I, Dueñas MT, Irastorza A, Navas J, López P. 2006. *Pediococcus parvulus* *gtf* gene encoding the GTF glycosyltransferase and its application for specific PCR detection of β -D-glucan-producing bacteria in foods and beverages. *J Food Prot* 69:161–169.
4. Werning ML, Corrales MA, Prieto A, de Palencia PF, Navas J, López P. 2008. Heterologous expression of a position 2-substituted (1 \rightarrow 3)- β -D-glucan in *Lactococcus lactis*. *Appl Environ Microbiol* 74:5259–5262. <http://dx.doi.org/10.1128/AEM.00463-08>.
5. Werning ML, Pérez-Ramos A, Fernández de Palencia P, Mohedano ML, Dueñas MT, Prieto A, López P. 2014. A specific immunological method to detect and quantify bacterial 2-substituted (1,3)- β -D-glucan. *Carbohydr Polym* 113:39–45. <http://dx.doi.org/10.1016/j.carbpol.2014.06.072>.
6. Velasco S, Arsköld E, Paese M, Grage H, Irastorza A, Rådström P, van Niel EW. 2006. Environmental factors influencing growth of and exopolysaccharide formation by *Pediococcus parvulus* 2.6. *Int J Food Microbiol* 111:252–258. <http://dx.doi.org/10.1016/j.ijfoodmicro.2006.06.008>.
7. Velasco SE, Yebra MJ, Monedero V, Ibarburu I, Dueñas MT, Irastorza A. 2007. Influence of the carbohydrate source on β -glucan production and enzyme activities involved in sugar metabolism in *Pediococcus parvulus* 2.6. *Int J Food Microbiol* 115:325–334. <http://dx.doi.org/10.1016/j.ijfoodmicro.2006.12.023>.
8. Velasco SE, Areizaga J, Irastorza A, Dueñas MT, Santamaria A, Muñoz ME. 2009. Chemical and rheological properties of the β -glucan produced by *Pediococcus parvulus* 2.6. *J Agric Food Chem* 57:1827–1834. <http://dx.doi.org/10.1021/jf803065w>.
9. Mårtensson O, Staaf J, Dueñas-Chasco MT, Irastorza A, Oste R, Holst O. 2002. A fermented ropy non-dairy oat product based on the exopolysaccharide-producing strain *Pediococcus damnosus* 2.6. *Adv Food Sci* 24: 4–11. <http://dx.doi.org/10.1016/j.nutres.2005.03.004>.
10. de Palencia PF, Werning ML, Sierra-Filardi E, Dueñas MT, Irastorza A, Corbí AL, López P. 2009. Probiotic properties of the 2-substituted (1,3)- β -D-glucan producing *Pediococcus parvulus* 2.6. *Appl Environ Microbiol* 75:4887–4891. <http://dx.doi.org/10.1128/AEM.00394-09>.
11. Russo P, López P, Capozzi V, de Palencia PF, Dueñas MT, Spano G, Fiocco D. 2012. Beta-glucans improve growth, viability and colonization of probiotic microorganisms. *Int J Mol Sci* 13:6026–6039. <http://dx.doi.org/10.1128/AEM.00394-09>.
12. Notararigo S, de las Casas-Engel M, Fernández de Palencia P, Corbí AL, López P. 2014. Immunomodulation of human macrophages and myeloid cells by 2-substituted (1,3)- β -D-glucan from *P. parvulus* 2.6. *Carbohydr Polym* 112:109–113. <http://dx.doi.org/10.1016/j.carbpol.2014.05.073>.
13. Mårtensson O, Björklund M, Lambo AM, Dueñas-Chasco M, Irastorza A, Holst O, Norin E, Welling G, Öste R, Önning G. 2005. Fermented ropy, oat-based products reduce cholesterol levels and stimulate the bifidobacteria flora in humans. *Nutr Res* 25:429–442. <http://dx.doi.org/10.1016/j.nutres.2005.03.004>.
14. Immerstrand T, Paul CJ, Rosenquist A, Deraz S, Mårtensson OB, Ljungh A, Blücher A, Öste R, Holst O, Karlsson EN. 2010. Characterization of the properties of *Pediococcus parvulus* for probiotic or protective culture use. *J Food Prot* 73:960–967.



Lactobacillus plantarum CIDCA 8327: An α -glucan producing-strain isolated from kefir grains



M.V. Gangoiti^{a,b}, A.I. Puertas^b, M.F. Hamet^c, P.J. Peruzzo^d, M.G. Llamas^b, M. Medrano^c, A. Prieto^e, M.T. Dueñas^b, A.G. Abraham^{a,c,*}

^a Área Bioquímica y Control de Alimentos, Dpto. Ciencias Biológicas, Facultad de Ciencias Exactas, Universidad Nacional de La Plata, 47 y 115, La Plata, Buenos Aires, Argentina

^b Dpto. de Química Aplicada, Facultad de Ciencias Químicas, Universidad del País Vasco (UPV/EHU), Paseo Manuel de Lardizabal 3, San Sebastián, País Vasco, Spain

^c Centro de Investigación y Desarrollo en Criotecología de Alimentos (CIDCA), Facultad de Ciencias Exactas, Universidad Nacional de La Plata – CONICET CCT La Plata – CIC, 47 y 116, La Plata, Buenos Aires, Argentina

^d Instituto de Investigaciones Físicoquímicas Teóricas y Aplicadas (INIFTA), Facultad de Ciencias Exactas, Universidad Nacional de La Plata – CONICET CCT La Plata, Diag. 113 y 64, La Plata, Buenos Aires, Argentina

^e Departamento de Biología Medioambiental, Centro de Investigaciones Biológicas, Consejo Superior de Investigaciones Científicas, Ramiro de Maeztu 9, Madrid, Spain

ARTICLE INFO

Article history:

Received 16 January 2017

Received in revised form 7 April 2017

Accepted 19 April 2017

Available online 23 April 2017

Keywords:

Lactobacillus plantarum

Kefir

Exopolysaccharides

Glucans

ABSTRACT

Lactobacillus plantarum CIDCA 8327 is an exopolysaccharide (EPS)-producer strain isolated from kefir with promising properties for the development of functional foods. The aim of the present study was to characterize the structure of the EPS synthesized by this strain grown in skim milk or semidefined medium (SDM). Additionally, genes involved in EPS synthesis were detected by PCR. *L. plantarum* produces an EPS with a molecular weight of 10^4 Da in both media. When grown in SDM produce an heteropolysaccharide composed mainly of glucose, glucosamine and rhamnose meanwhile the EPS produced in milk was composed exclusively of glucose indicating the influence of the sugar source. FTIR spectra of this EPS showed signals attributable to an α -glucan. Both by ^1H NMR and methylation analysis it was possible to determine that this polysaccharide is a branched α -(1 \rightarrow 4)-D-glucan composed of 80% linear α -(1 \rightarrow 4)-D-glucopyranosyl units and 19% (1 \rightarrow 4)-D-glucopyranosyl units substituted at O-3 by single α -D-glucopyranosyl residues.

© 2017 Elsevier Ltd. All rights reserved.

1. Introduction

Among the “Food-Grade” biopolymers obtained from natural sources, exopolysaccharides (EPS) synthesized by lactic acid bacteria (LAB) have focused the attention of researchers and manufacturers since these EPS contribute to the rheology of the fermented product and –on account of EPS potential health promoting properties– may also contribute to the development of functional foods (Das, Baruah, & Goyal, 2014; Patten & Laws, 2015).

EPS produced by LAB present a wide range of compositions, structures, molecular masses and conformations depending on the

strain. The EPS can stay attached to the cell surface (capsular) or can be released to the culture media (Patten & Laws, 2015). High molecular weight polysaccharides are widely used in the food industry as stabilizers, emulsifiers, and to improve texture and viscosity. The functionality of these polymers is originated from the structural differences in the sugar subunits, which is also the reason of the great diversity among bacterial EPS and novel EPS structures among LAB (Mozzi et al., 2006; Patten & Laws, 2015). Complex genetic mechanisms of EPS production, carbohydrate source, incubation temperature and time, or pH of the culture medium were reported to affect *in situ* EPS production levels as well as their conformational characteristics, sugar linkages, and molecular mass (Ibarburu et al., 2015).

Many EPS synthesized by LAB have demonstrated to elicit some biological effect (Patten & Laws, 2015). It has been reported that some EPS can have immunomodulatory (Hidalgo-Cantabrana et al., 2012; Medrano, Racedo, Rolny, Abraham, & Pérez, 2011; Notararigo et al., 2014) and antitumoral activity *in vivo* (Wang et al., 2014), as

* Corresponding author at: Centro de Investigación y Desarrollo en Criotecología de Alimentos (CIDCA), Facultad de Ciencias Exactas, Universidad Nacional de La Plata – CONICET CCT La Plata – CIC, 47 y 116, La Plata, Buenos Aires, Argentina.

E-mail addresses: analiabraham@yahoo.com.ar, aga@biol.unlp.edu.ar (A.G. Abraham).

well as an antagonistic effect against some intestinal pathogens *in vitro* (Medrano, Hamet, Abraham, & Pérez, 2009; Živković et al., 2016), among other health benefits. Additionally, the prebiotic effect of several EPS of LAB has been demonstrated *in vitro* (Korakli, Gänzle, & Vogel, 2002) and *in vivo* (Hamet, Medrano, Pérez, & Abraham, 2016).

Lactobacillus plantarum is a versatile microorganism that can be found in a wide range of habitats such as dairy, meat, and many plant fermentations, and it can reach high cell densities which are desirable for industrial applications. Different *L. plantarum* strains are able to produce heteropolysaccharides after grown in glucose or lactose (Dilna et al., 2015; Tallon, Bressollier, & Urdaci, 2003; Wang et al., 2010; Zhang et al., 2013; Zhang, Liu, Tao, & Wei, 2016) or homopolysaccharides: galactanes when lactose is the unique sugar source (Wang et al., 2014) or glucans when sucrose is the sugar source (Das & Goyal, 2013).

Among the health benefits of EPS produced by some strains of *L. plantarum* it can be mentioned antioxidant activity (Zhang et al., 2013), antagonistic activity against *Bacillus cereus* enterotoxin (Zhang et al., 2016), and antitumoral activity (Wang et al., 2014).

Kefir is a traditional beverage obtained by fermentation of milk with kefir grains that contain a wide diversity of lactic and acetic acid bacteria and yeasts immersed in a matrix composed of protein and the polysaccharide kefiran (Garrote, Abraham, & De Antoni, 2001). Kefiran production was associated to *Lactobacillus kefiranofaciens* though another lactobacilli isolated from kefir were described to produce EPS after growth in milk (Hamet, Piermaria, & Abraham, 2015; Wang, Zhao, Tian, Yang, & Yang, 2015).

L. plantarum CIDCA 8327 is a facultative heterofermentative *Lactobacillus* isolated from kefir grains (Garrote et al., 2001). This strain presents a hydrophilic surface and a moderate adhesion to intestinal cells (Caco-2 cell line), while it had a strong inhibitory activity against *Salmonella typhimurium*, *S. enterica*, *S. gallinarum*, *S. sonnei* and *Escherichia coli* (Golowczyc et al., 2008). Besides, it is able to grow in the presence of bile salts and survives after one hour of exposure to pH 2.5 (Golowczyc et al., 2008). Moreover, some studies demonstrate that this strain is able to produce organic acids such as lactic and acetic acid, and substances of low molecular weight with antifungal properties after growth in whey media (Londero et al., 2011). In addition this strain is able to grow in milk and produces *in situ* an EPS of low molecular mass (Hamet et al., 2015).

The above mentioned characteristics, that turn *L. plantarum* CIDCA 8327 into a promising starter to be potentially included in functional foods, prompted us to study the production and chemical composition of the EPS synthesized *in situ* by this strain.

2. Materials and methods

2.1. Strains and growth conditions

L. plantarum CIDCA 8327 isolated originally from kefir grains (Garrote et al., 2001) was stored at -80°C in sterile skim milk and reactivated in MRS broth at 30°C for 24 h (De Man, Rogosa, & Sharpe, 1960). After that, *L. plantarum* was grown in UHT skim milk (Composition g/L: Protein 32, Fat 15, lactose 47; ashes 6.). La Serenisima, General Rodriguez, Argentina or in a semidefined medium (SDM) (Marieta, Ibarburu, Duenñas, & Irastorza, 2009) for 21 h or 96 h, depending on the determination. The SDM had the following composition: glucose 20 g/L, Casamino Acids (Becton Dickinson, Spain) 5 g/L, Difco™ Yeast Nitrogen Base (DYNB, Becton Dickinson, Spain) 6.7 g/L, $\text{MnSO}_4 \cdot \text{H}_2\text{O}$ 0.05 g/L, K_2HPO_4 2 g/L, NaAcO 5 g/L, adenine 0.005 g/L, guanine 0.005 g/L, xanthine 0.005 g/L, uracil 0.005 g/L, and L-malic acid 4 g/L pH 5.0.

2.2. Transmission electron microscopy

Analysis of the bacteria and the EPS by transmission electron microscopy (TEM) (Tecnai G2 Twin) was performed using samples prepared as follows. Glow-discharged carbon-coated grids were placed facedown over a droplet of each culture concentrated five-fold in 0.1 M AcNH_4 , pH 7. After 1 min, each grid was removed, blotted briefly with filter paper, and without being dried, negatively stained with 2% uranyl acetate for 30 s and then blotted quickly and air dried.

2.3. DNA extraction and detection of genes

Genomic DNA was prepared from late-logarithmic phase *L. plantarum* CIDCA 8327 cells using the DNeasy Blood & Tissue Kit (Qiagen GmbH, Hilden, Germany) according to the manufacturer's instructions, except that we preincubated the cells with 2 U/ μL mutanolysin (Sigma-Aldrich), and adjusted to a final DNA concentration of 40 ng/ μL with water-free DNase and RNase.

For detection of polymerase genes in *L. plantarum* CIDCA 8327 associated with polysaccharide production, PCR primers were designed based on the predicted polymerase-cps genes sequences of *L. plantarum* WCFS1 available in the GenBank database (AL935263; Lp_1185, Lp_1204, Lp_1222, Lp_2101) (Table 1). Internal primers were also used to determine the sequence of both strands of genes. Primers were designed using the Primer V0.4.0 software (<http://prodo.wi.mit.edu/primer3/>). PCR reactions were carried out with Phusion High-Fidelity DNA Polymerase (Thermo Scientific, 163 Schwerte, Germany). Two annealing temperatures were used: 49°C for *cps1I*, *cps2H* and *cps4H*, and 53°C for *cps3F*. The PCR products were subjected to electrophoresis using a 1% (w/v) agarose gel. The amplicons were purified using NucleoSpin® Gel and PCR Clean-up kit (Macherey-Nagel, GmbH & Co., KG Düren, Germany), according to the manufacturer's instructions. Sequencing of the amplicons was carried out by Secugen S.L. (Madrid, Spain). The resulting sequences were analyzed by using the BLAST tool of the GenBank DNA database (<http://www.ncbi.nlm.nih.gov/>).

2.4. EPSs isolation and purification

The EPSs were isolated and purified from SDM or milk inoculated with *L. plantarum* CIDCA 8327. For the EPS produced in SDM, *L. plantarum* was cultured for 21 h or 96 h at 30°C . After that, cells were removed by centrifugation for 30 min at $12,000 \times g$. The clear supernatant was collected, and the EPS was precipitated by adding 3 volumes of cold ethanol, followed by storage overnight at -20°C . The precipitate was recovered by centrifugation at $12,000 \times g$ for 20 min at 4°C , dissolved in hot distilled water and dialyzed against deionized water, using a membrane (Medicell International Ltd., London, UK) having a cut-off of 3.5 kDa, for 2–3 days (water changed twice daily). Then, the retentate was lyophilized.

In the case of the EPS produced in milk, *L. plantarum* was incubated for 96 h at 30°C . A volume of 1000 mL of fermented milk was treated in boiling water for 30 min with discontinuous stirring. The mixture was centrifuged at $10,000 \times g$ for 20 min at 20°C (Avanti J25 Beckman Coulter Inc. centrifuge, Palo Alto, California). The polysaccharide in the supernatant was precipitated by addition of two volumes of cold ethanol and left at -20°C overnight. The mixture was centrifuged at $10,000 \times g$ for 20 min at 4°C . Pellets were dissolved in hot distilled water and dialyzed using a membrane (Spectra/Por, The Spectrum Companies, Gardena, CA, USA) having a cut-off of 1000 Da for 48 h at 4°C against four changes of twice-distilled water (Rimada & Abraham, 2003).

Table 1
Primers designed in this work to screen for CPS genes.

Gene name	Locus.tag	Primer sequences (5' → 3')	Expected fragment size (bp)
<i>cps1I</i>	Lp.1185	F: GGAATTTTACATGCCCGTTG R: ACATGAGCGTTGAAAGTGG I: TTATGCTCAGAACGATACTTCTGT	1431
<i>cps2H</i>	Lp.1204	F: AATACTGGTAAGCATAAGATGATTTG R: CAAATACTATTGCAATATAAACTCA I: TTGGAACTCAAATGGCCTC	1415
<i>cps3E</i> <i>cps3F</i>	Lp.1221 Lp.1222	F: GCGTGAGACGAACGTGATT R: CCGGTACGTTGATACAAAA I: TGTGTGCGGCGTATTTGTAT	1148
<i>cps4I</i> <i>cps4H</i>	Lp.2100 Lp.2101	F: GCCTGGTTTATGCGAGTGAT R: ACTCCCTCGCAAATAGGTT I: TTGACCTGGATGCTATGGAT	1531

F: forward, R: reverse and I: intermediate primer.

The samples were tested for the absence of other sugars by qualitative thin layer chromatography (TLC) and of proteins the Bradford method according to [Rimada and Abraham \(2003\)](#).

2.5. Exopolysaccharides quantification and molecular mass determination

EPS produced in milk or SDM was quantified by the anthrone method ([Hamet et al., 2015](#)). The molecular weight of the EPS obtained were determined by high-performance size exclusion chromatography (HPLC-SEC, Agilent 1100 Series System, Hewlett-Packard, Germany) associated to a refractive index (RI) detection system, as described by [Ibarburu et al. \(2015\)](#), using as molecular mass dextran standards of molecular weight range from 10^3 to 2×10^6 Da (Sigma-Aldrich).

2.6. Sugar composition

The sugar composition of the EPSs was determined by a method described by [Notararigo et al. \(2013\)](#) after hydrolysis of the polysaccharides with 3 M trifluoroacetic acid (TFA) at 121 °C for 1 h. The hydrolysed monosaccharides were converted into their corresponding alditol acetates, and analyzed and quantified by gas chromatography (GC 6890A, Agilent, Palo Alto, California, USA).

2.7. Fourier-transform infrared (FTIR) spectroscopy

Fourier-transformed Infrared Spectroscopy (FTIR) studies were performed using a Nicolet 380 instrument (Thermo Fisher Scientific) with a ZnSe single reflection ATR in the range 4000–650 cm^{-1} . The number of scans per experiment was 64, with a resolution of 4 cm^{-1} .

2.8. Methylation analysis

The EPS obtained after grown in milk was methylated according to the method described by [Ciucanu and Kerek \(1984\)](#). The permethylated polysaccharide was hydrolyzed with 3 M TFA at 121 °C for 1 h.

After hydrolysis, the partially methylated monosaccharides were reduced with deuterated NaBH_4 and converted into their corresponding alditol acetates with 500 μL of pyridine:acetic anhydride (1:1) for 1 h at 100 °C, as described by [Laine, Sweeley, Li, Kistic, and Rapport \(1972\)](#). Gas chromatography–mass spectrometry GC–MS analysis was carried out in a 6890A/5975C instrument from Agilent (Palo Alto, California, USA), with He as the carrier gas. The injector was programmed at 250 °C. Samples (1 μL) were injected with a split ratio of 1:50 and their components separated in a HP5MS (Agilent) fused silica column (30 m \times 0.25 mm I.D. \times 0.2 μm film thickness), with a temperature program starting

at 160 °C (1 min) and then rising 2 °C min^{-1} up to 200 °C. An m/z range between 40 and 450 amu was scanned. Identification was done on the basis of the retention time and mass spectra of the compounds. Quantification was performed according to peak area ([Ibarburu et al., 2015](#)).

2.9. NMR analysis

Purified EPS were deuterium exchanged several times by freeze drying from D_2O and then examined as solutions (3 mg/mL) in 99.98% D_2O . Spectra were recorded at 60 °C on a Bruker AMX500 spectrometer operating at 500.13 MHz (^1H -nuclear magnetic resonance). Chemical shifts were given in parts per million ([Ibarburu et al., 2015](#)).

3. Results

3.1. *L. plantarum* CIDCA 8327 contains polysaccharide polymerase genes associated with surface/exopolysaccharide production

L. plantarum strains that produce EPS contain several gene clusters involved in the synthesis of the biopolymer ([Remus et al., 2012](#)). To detect the presence of polysaccharide polymerase genes in the EPS-producing *L. plantarum* CIDCA 8327 strain, several *cps* primers were designed based on the *L. plantarum* WCFS1 complete genome sequence (GenBank accession number AL93526) ([Table 1](#)). In this strain 4 gene clusters (designated *cps1*, *cps2*, *cps3* and *cps4*) independently contribute to the overall surface-associated polysaccharide. DNA of *L. plantarum* CIDCA 8327 yielded an 1148 bp PCR product with the *cps3E-F* primers, covering the 3'-end of *cps3E* gene and the *cps3F* gene. No PCR products were obtained with any of the other primers used. Comparison with nucleotide sequences in the database revealed that the sequenced fragment showed 98% identity with the *cps3E-F* region encoding putative polysaccharide biosynthesis proteins in *L. plantarum* WCFS1, ST-III, and ZJ316 strains (Accession Numbers: AL935263.2, CP002222.1, CP004082, respectively). In addition, TEM analysis of *L. plantarum* CIDCA 8327 grown in a semidefined medium (SDM) revealed the presence of extracellular material loosely attached to the bacterial surface ([Fig. 1](#)).

3.2. The EPS produced by *L. plantarum* CIDCA 8327 depends on the growth medium

EPS production was first quantified in SDM. Two time points of fermentation were sampled, 21 h (EPS 1) and 96 h (EPS 2), obtaining 40 mg/L and 120 mg/L, respectively ([Table 2](#)). Both samples lacked protein based on the negative responses for Bradford test and absorption at 260 nm/280 nm spectra (data not shown). Differ-

Table 2

Molecular weight distribution and sugar ratios of EPS produced by *L. plantarum* CIDCA 8327 in different growth conditions. EPS1: EPS produced at 21 h in semidefined medium (SDM); EPS2: EPS produced at 96 h in SDM; and EPS3: EPS produced after 96 h in milk.

EPS	Medium	Hours of culture	pH	Total EPS (mg/L ⁻¹)	Molecular weight distribution (%)			Monosaccharide ratio			
					10 ⁵ Da	10 ⁴ Da	10 ³ Da	Glc	Gal	GlcN	Rha
1	SDM	21	3.9	40	–	61.2	38.8	10	0.6	6.6	2.7
2	SDM	96	3.6	120	5.9	87.4	6.6	10	0.5	7	1.4
3	milk	96	4.2	160		100	–	10	–	–	–

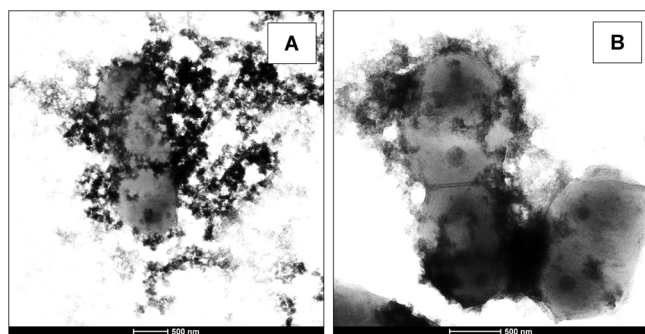


Fig. 1. Micrographs of *L. plantarum* CIDCA 8327 and its EPS obtained by Transmission Electron Microscopy. (A) Negative staining with uranyl acetate of whole cells of *L. plantarum* surrounded by exopolysaccharide (x 9600). (B) Detail of the cells and EPS (x 14,500).

ent patterns of molecular weight distribution were observed for the EPS recovered at the two times of fermentation (Table 2). While in EPS 1 there were 61.2% of the 10⁴ Da and 38.7% of the 10³ Da fraction, in EPS 2 most glucidic material (87.4%) appears as a 10⁴ Da fraction accompanied to two minor fractions of 10⁵ Da and 10³ Da, indicating that incubation for longer period enables oligosaccharides polymerization.

With these data in mind, sterile skim milk was inoculated with *L. plantarum* CIDCA 8327 and after 96 h of fermentation 160 mg/L of an EPS (EPS 3) with a molecular mass of 10⁴ Da was obtained (Table 1). Sugar composition of the three EPS obtained was analyzed by HPAEC-PAD and it is presented in Table 2. The EPS 1 and EPS 2 produced in SDM were composed mainly of glucose, rhamnose and glucosamine (Table 2). Galactose was also detected in both EPS at lower percentage. Moreover, trace amounts of galacturonic acid were detected. On the other hand the EPS 3, produced in milk, was composed exclusively of glucose (Table 2) indicating that the sugar source influences the composition of the EPS produced by this strain.

The FTIR spectra of the three EPS are presented in Fig. 2. They show the typical signals of polysaccharides documented in literature, such as a broad band around 3260 cm⁻¹ and a band at 2933 cm⁻¹, arising from O–H stretching and C–H stretching, respectively, and a broad band located at 1000–1200 cm⁻¹ assigned to overlapped C–O, C–C stretching and C–OH bending modes (Bremer & Geesey, 1991; Howe, Ishida, & Clark, 2002; Nataraj, Schomacker, Kraume, Mishra, & Drews, 2008). The spectra of EPS 1 and EPS 2 showed also two peaks around 1540 cm⁻¹ and 1639 cm⁻¹, corresponding to C–N and C=O stretching, that are related to the amide linkage of aminosugars in the polysaccharides structure and a band at 1747 cm⁻¹ typical of uronic acids (Kovács, Nyerges, & Izvekov, 2008). These findings confirm the results from monosaccharide analysis. Absorptions in the “anomeric region” (950–750 cm⁻¹) contain weak bands that inform on the anomeric configuration of the monosaccharides (Synytsya & Novak, 2014). For these samples, the spectra presented a characteristic band located at 835 cm⁻¹ from the α -anomer of the glucose pyranoid ring as well as a signal at 873 cm⁻¹ from galactose units (Kačuráková, Capek, Sasinkova, Wellner, & Ebringerova, 2000).

Table 3

Results from the methylation analysis of the α -glucan produced by *L. plantarum* CIDCA 8327 in milk.

Position of the O-methyl groups	Deduced linkages	%
1,5-diacetyl-2,3,4,6-tetramethyl-Glcp	Terminal (non-reducing end)	4.7
1,4,5-triacetyl-2,3,6-trimethyl-Glcp	1 \rightarrow 4	81.5
1,3,4,5-tetracetyl-2,6-dimethyl-Glcp	1 \rightarrow 3,4	13.8

On the other hand, all the vibrational peaks of the EPS 3 sample were similar to those obtained for α -glucans. The bands at 1155, 1022, 930, 850 and 760 cm⁻¹ evidenced the presence of a polysaccharide with α - linkages in the structure of this EPS (Kačuráková et al., 2000; Synytsya & Novak, 2014). The absence of a band at 1745 cm⁻¹ indicates that there are no carboxylic sugars in this EPS. In addition, there is no band around 1650 cm⁻¹, confirming that the sample does not contain amino sugars. These observations are in agreement with the sugar compositional analysis.

3.3. *L. plantarum* CIDCA 8327 produces an α -glucan during fermentation of milk

Since *L. plantarum* CIDCA 8327 was isolated from kefir and the research was focused on the use of this strain as milk starter, further studies were performed in order to elucidate the structure of the EPS produced by this strain during milk fermentation (EPS 3). Sugar linkages were determined and quantified upon analyzing by gas-liquid chromatography (GLC) the partially methylated alditol acetates (PMAAs) obtained from the sample (Table 3).

Methylation analysis showed the presence of 2,3,4,6-tetra-O-methyl glucitol corresponding to the non-reducing ends in the EPS chain, 2,3,6-tri-O-methyl glucitol indicating linear 1,4 glucosidic linkages, and 2,6-di-O-methyl glucitol resultant from branching points in glucose units attached through their positions 1,4, and 3.

The ¹H NMR spectrum of the EPS 3 (Fig. 3) showed resonances of hydrogen corresponding to the glucosyl residue. The ¹H NMR spectrum of a polysaccharide can generally be divided into two major regions: the anomeric region (δ = 4.3–5.5 ppm), and the ring proton region (δ = 3.2–4.3 ppm).

As shown in Fig. 3, signals in the region between 5.3 and 4.5 ppm related to H1-4 and H1-3 are well resolved and indicate α -D-glucans (Synytsya & Novak, 2014). The main signals in the anomeric region correspond to protons bound to C1 in the primary α 1 \rightarrow 4 glycosidic bond (δ = 5.36 ppm), and C1 in the branching α 1 \rightarrow 3 (δ = 5.32 ppm), and a small signal at δ = 4.95 ppm, attributable to α 1 \rightarrow 6 glycosidic bonds was also observed (Cheng & Neiss, 2012; Zang, Howseman, & Shulman, 1991; Zang, Rothman, & Shulman, 1990). The signals obtained in the spectrum in the ring proton region were poorly resolved due to the overlapping chemical shifts. However, it is possible to observe clearly the H4' peak corresponding to the protons bound to the free C4 non reducing ends (δ = 3.41 ppm) and other intense peaks from the H2 (δ = 3.63 ppm), H3 (δ = 3.95 ppm), H4 (δ = 3.62 ppm), H5 (δ = 3.81 ppm) and H6a and H6b (δ = 3.86 and 3.79 ppm, respectively) (Cheng & Neiss, 2012; Nilsson, Bergquist, Nilsson, & Gorton, 1996; Zang et al., 1990, 1991), but better assignments will require more specific identifications.

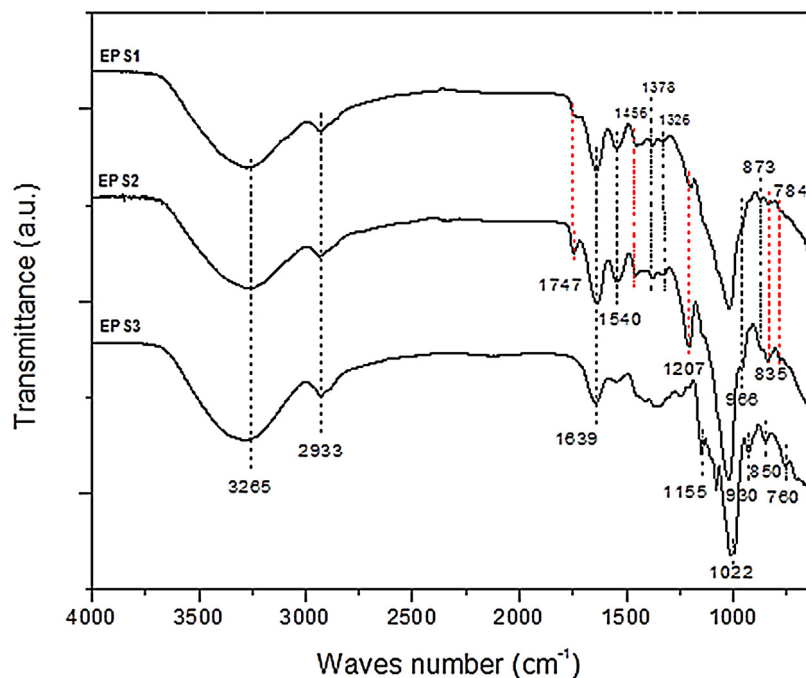


Fig. 2. FTIR spectra in the range of 700–4000 cm^{-1} of the EPS produced by *L. plantarum* CIDCA 8327 in different growth conditions EPS1: EPS produced at 21 h in semidefined medium (SDM); EPS2: EPS produced at 96 h in SDM; and EPS3: EPS produced after 96 h in milk.

The intensities of the resonances contain information about the branched structure of the molecule. In this case, the ratio of the integrated peaks of H1-4, H1-3, H1-6 and H4' is 47:12:0.38:1.

Gathering all data collected for EPS 3, this polysaccharide can be described as a branched α -(1 \rightarrow 4)-D-glucan with a molecular mass of around 9000 Da, composed of 80% linear α -(1 \rightarrow 4)-D-glucopyranosyl units and 19% (1 \rightarrow 4)-D-glucopyranosyl units substituted at O-3 by single α -D-glucopyranosyl residues or α -(1 \rightarrow 4) disaccharidic side chains (Fig. 4A and B).

4. Discussion

The functional aspects of fermented foods are mostly related to the concept of probiotic bacteria however the microbial production of functional molecules, such as bioactive EPS, is targeted (Leroy & De Vuyst, 2016). Kefir grains are an interesting source of EPS-producing bacteria (Hamet et al., 2015; Moura de Paiva et al., 2016). Herein we demonstrated that *L. plantarum* CIDCA 8327 isolated from kefir is able to produce EPS in milk or SDM, whose composition depends on the growth conditions. Otherwise, this is the first report of the production of α -glucan by a strain of *L. plantarum* isolated from kefir after growth in milk. Accordingly, by amplification and sequencing of a PCR fragment with a high degree of homology with the *cps3* cluster of *L. plantarum* WCSF1, we are proving the presence of genes involved in the CPS/EPS polysaccharide synthesis in the genome of *L. plantarum* CIDCA 8327.

It is noteworthy that *L. plantarum* CIDCA 8327 EPS remains in part loosely bound to the surface of the bacteria and may be involved in the interactions with their environment playing an important role in the communication between bacteria and the host organisms (Abraham, Medrano, Piermaria, & Mozzi, 2010; Chap. 10). Therefore, improved knowledge on these molecules is of great importance to understand the strain-specific and proposed beneficial modes of probiotic action (Remus et al., 2012).

The EPS produced by *L. plantarum* CIDCA 8327 in SDM was a heteropolysaccharide composed mainly of glucose, glucosamine and rhamnose. Harvesting the EPS at two incubation times allowed

observing that the molecular mass of the EPS recovered was higher upon a longer period, but without relevant changes in monosaccharide composition, suggesting that polymerization continues even in the stationary growth phase. Analysis of previous reports about characterization of EPS produced by different strains of *L. plantarum*, allows concluding that most of the strains produce heteropolysaccharides when grown in media containing glucose or lactose as the carbon source (Ismail & Nampoothiri, 2010; Remus et al., 2012; Tallon et al., 2003; Wang et al., 2010; Zhou et al., 2016). On the contrary, *L. plantarum* 70810 grown in a SD with lactose as unique carbon source produce a galactan (Wang et al., 2014).

Biosynthesis of CPS/EPS inside the cell occurs by activation of the precursor molecules by enzymes producing activated sugars/sugar acids by three possible mechanisms: the Wzx/Wzy-dependent pathway, the synthase-dependent pathway and the ATP binding cassette (ABC) transporter-dependent pathway. Alternatively, the extracellular synthesis by use of a single sucrose protein is used for the polymer strand elongation (Schmid, Sieber, & Rehm, 2015). Studies of the *L. plantarum* WCFS1 genome demonstrates that 4 gene clusters (designated *cps* genes), associated in two regions, independently contribute to the overall surface-associated polysaccharide. The first region has three *cps* gene clusters (1–3), and the second region comprises the *cps4* gene cluster and is conserved in other *L. plantarum* strains (ST-III, ATCC14917). In *L. plantarum* WCFS1, the polymerase genes implicated in the polymerization of the polysaccharide repeating units were found in the 4 *cps* clusters (Remus et al., 2012). DNA of *L. plantarum* CIDCA 8327 was amplified with the *cps3E-F* primers giving only one PCR product. At the 1112418 base position of the genome of WCFS1 strain, a guanine breaks the reading frame of the *cps3F* gene, but this not is the case in *L. plantarum* CIDCA 8327, like other strains sequenced (*L. plantarum* subsp. *plantarum* ST-III, Accession Number CP002222.1 or *L. plantarum* ZJ316, Accession Number CP004082.1).

In *L. plantarum* WCFS1, Remus et al. (2012) reported that it was unclear if a functional Wzy protein can be composed of Cps3F and CpsG. In *L. plantarum* CIDCA 8327, no putative conserved domains were detected, although the predicted amino acid sequence of the

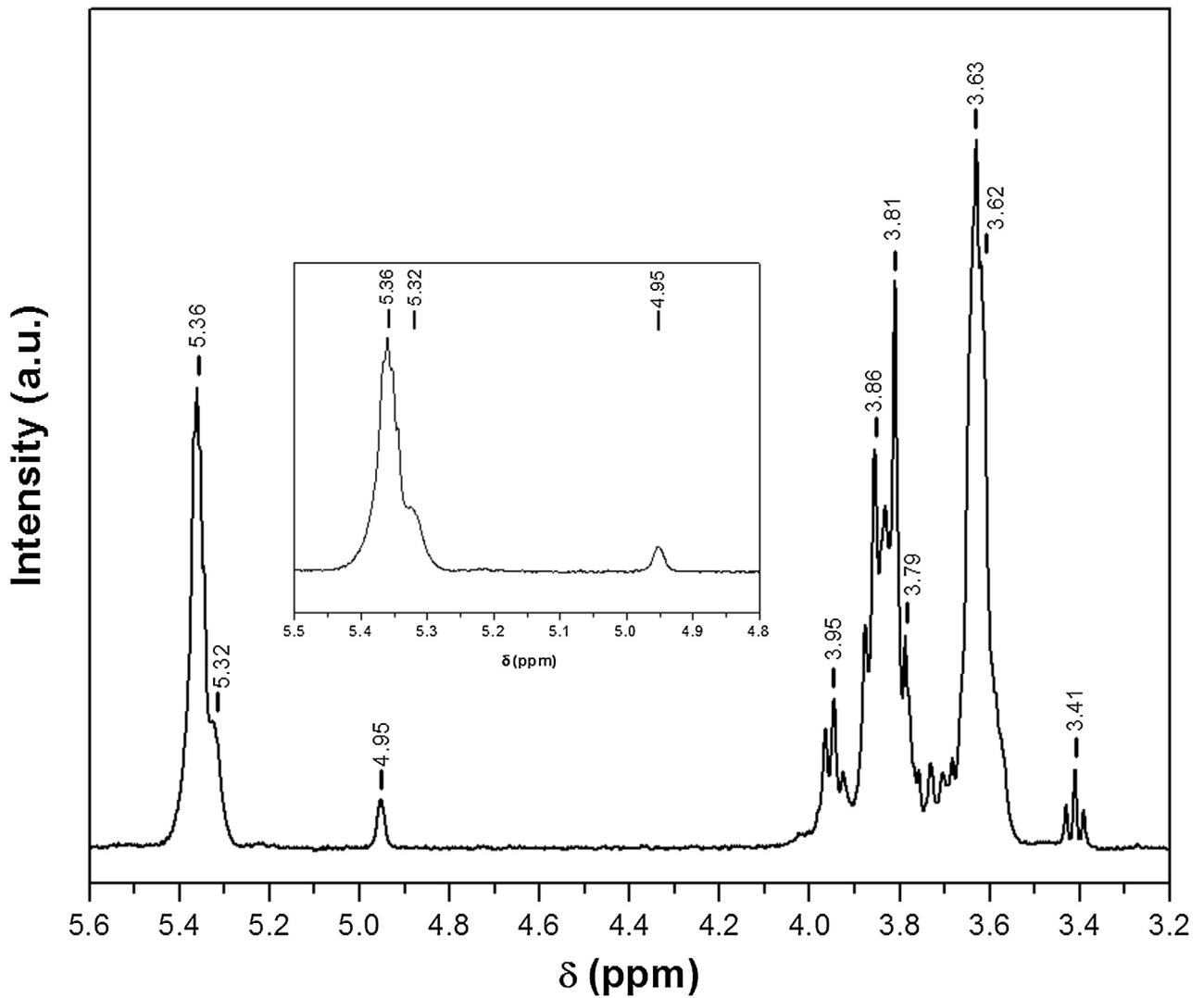


Fig. 3. ^1H NMR spectra of EPS produced by *L. plantarum* CIDCA 8327 in milk (EPS3).

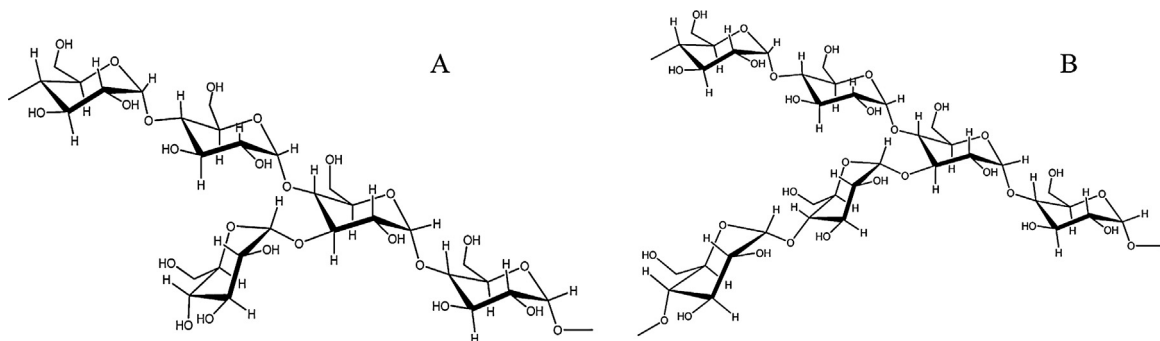


Fig. 4. Suggested structures for EPS produced by *L. plantarum* CIDCA 8327 in milk. Linear α -(1 \rightarrow 4)-D-glucopyranosyl units and (1 \rightarrow 4)-D-glucopyranosyl units substituted at O-3 by single α -D-glucopyranosyl residues (A) or α -(1 \rightarrow 4) disaccharidic side chains (B).

PCR fragment presented high identity with polysaccharide polymerase Wzy proteins like *L. rhamnosus* GG strain that produces a galactose-rich EPS (Lebeer et al., 2009).

When grown in milk, *L. plantarum* CIDCA 8327 produces a homopolysaccharide of around 10^4 Da composed only of glucose. The milk fermented with this strain presented a pseudoplastic behavior with a hysteresis loop that did not differ from the flow

curve of an acid gel obtained with D-gluconolactone (Hamet et al., 2015) in concordance to the expected behavior of an EPS with low molecular mass distribution. The FTIR spectrum of the EPS produced in milk showed typical polysaccharide signals, and all the vibrational peaks were similar to those obtained for α -glucans. Enzymes involved in α -glucans synthesis are glucansucrases that catalyze the polymerization of the homopolysaccharide out of

sucrose as donor of the corresponding monosaccharide, and transfer the molecule to the reducing end of the glucan (Leemhuis et al., 2013). *L. plantarum* CIDCA 8327 synthesize α -glucan from lactose, in consequence the existence of another pathway involved could not be ruled out. According to the main glycosidic linkages, α -glucans are classified into dextrans (α -1,6), mutans (α -1,3), reuterans (α -1,4) and alternans (α -1,3 and α -1,6) (Leemhuis et al., 2013). Both ^1H NMR and methylation analysis allowed to determine that this polysaccharide consists of a α -(1 \rightarrow 4)-D-glucan with 19% branching at positions O-3. Side chains could be made up of a single α -D-glucopyranosil unit or of a α -(1 \rightarrow 4)-glucopyranose disaccharide.

Dextran-producer lactic acid bacteria belong to the genera *Lactobacillus*, *Pediococcus*, *Leuconostoc* and *Weissella* (Torino, de Valdez, & Mozzi, 2015). Focusing on *Lactobacillus* isolated from sugary kefir, Moura de Paiva et al. (2016) demonstrated that *L. kefirifaciens* 1P3 and *L. satsumensis* 10P and 10P2 grown in the presence of sucrose produced an α -glucan linked by α -(1,6) glycosidic bonds (~90%).

Production of α -glucans by *L. plantarum* strains was reported by Das and Goyal (2013). When grown in medium with sucrose, *L. plantarum* DM5 produces an α -glucan that contains 86.5% α -(1 \rightarrow 6) linear linkages, with 13.5% α -(1 \rightarrow 3) branched linkages. *L. plantarum* CIDCA 8327 produces an α -glucan with α -(1 \rightarrow 4) glycosidic linkages similar to reuteran, but in this case the main chain is branched at positions O-3 and not in O-6, which distinguishes the EPS described here from other α -(1 \rightarrow 4)-glucans. To the best of our knowledge, this is the first report of a polysaccharide from LAB with this structure. Up to the moment, strains of *L. reuteri* were described as reuteran producers (Patel, Majumder, & Goyal, 2012; Tiekling & Gänzle, 2005). It is noteworthy that *L. plantarum* CIDCA 8327 produces α -glucan after growth in milk and this fact may contribute to the probiotic properties of this strain.

Among α -glucans, dextran and dextran-derived oligosaccharides have been reported to elicit some prebiotic effect *in vitro* (Das et al., 2014; Rao & Goyal, 2013). Sarbini, Kolida, Deville, Gibson, and Rastall (2014) correlated this effect on intestinal microbiota elicited by dextran with obesity management. Recently, two dextrans synthesized by *L. sakei* MN1 and *L. mesenteroides* RTF10 demonstrated to have antiviral and immunomodulatory activity against salmonid viruses (Nácher-Vázquez et al., 2015). Otherwise, it was described that α -(1 \rightarrow 4) glucans have a role in the induction of phagocytosis (Bittencourt et al., 2006; Nair, Melnick, Ramachandran, Escalon, & Ramachandran, 2006), nevertheless the ability to escape digestion of each EPS should be demonstrated.

It can be concluded that *L. plantarum* CIDCA 8327 isolated from kefir grain produces EPS with different sugar composition depending on the growth medium. In a SDM with glucose as the carbon source, several monosaccharides are released upon acid hydrolysis of the obtained polymer, suggesting the presence of heteropolysaccharides, while when grown in milk an extracellular α -glucan was synthesized. The EPS remains loosely bond to the bacterial cell. Taking into account that these strains associate to epithelial cells *in vitro* and exert a protective *in vitro* effect against *Salmonella* invasion (Golowczyk et al., 2008; Londero et al., 2012) the presence of this EPS could be a relevant factor in health promoting properties. This is the first report of an α -glucan producer strain isolated from kefir after growth in milk. Further studies to provide additional information on the structure of the glucan (periodate oxidation, Smith-degradation of oxidized products, more detailed NMR characterization) will be performed in future work. Our results encourage further investigations about the role of α -glucans produced by *L. plantarum* CIDCA 8327 that could contribute to comprehend the potential probiotic properties of this strain.

Acknowledgments

MVG is a member of the Researcher Career of CICPBA. PP, MM and AGA are members of Scientific Career of CONICET. AIP and MTD are supported by Universidad del País Vasco. AP is researcher from CSIC.

This study was supported by grants from the Agencia Nacional de Promoción Científica y Tecnológica (ANPCyT), CONICET and UNLP, the Spanish Ministry of Science and Innovation (AGL2012-40084-C03), the Basque Government (no. IT866-13). M.G.LI. acknowledges the 'Gobierno Vasco, Dpto. Agricultura, Pesca y Alimentación' for the fellowship. We also thank Microscopy: Polymer Characterization Service (SGIker) from the University of the Basque Country.

References

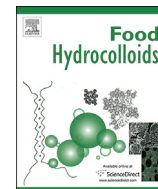
- Abraham, A. G., Medrano, M., Piermaria, J. A., & Mozzi, F. (2010). Novel applications of polysaccharides from lactic acid bacteria: A focus on kefir (Review article). In C. S. Hollingworth (Ed.), *Food hydrocolloids: Characteristics, properties and structures* (pp. 253–271). New York: Nova Publishers, Inc.
- Bittencourt, V. C. B., Figueiredo, R. T., da Silva, R. B., Mourão-Sá, D. S., Fernandez, P. L., Sasaki, G. L., et al. (2006). An α -glucan of *Pseudallescheria boydii* is involved in fungal phagocytosis and Toll-like receptor activation. *Journal of Biological Chemistry*, 281, 22614–22623.
- Bremer, P. J., & Geesey, G. G. (1991). An evaluation of biofilm development utilizing non-destructive attenuated total reflectance Fourier transform infrared spectroscopy. *Biofouling*, 3, 89–100.
- Cheng, H. N., & Neiss, T. G. (2012). Solution NMR spectroscopy of food polysaccharides. *Polymer Reviews*, 52, 81–114.
- Ciucanu, I., & Kerek, F. (1984). Rapid and simultaneous methylation of fatty and hydroxy fatty acids for gas-liquid chromatographic analysis. *Journal of Chromatography A*, 284, 179–185.
- Das, D., & Goyal, A. (2013). Characterization and biocompatibility of glucan: A safe food additive from probiotic *Lactobacillus plantarum* DM5. *Journal of the Science of Food and Agriculture*, 94, 683–690.
- Das, D., Baruah, R., & Goyal, A. (2014). A food additive with prebiotic properties of an α -D-glucan from *Lactobacillus plantarum* DM5. *International Journal of Biological Macromolecules*, 69, 20–26.
- De Man, J. C., Rogosa, D., & Sharpe, M. E. (1960). A medium for the cultivation of lactobacilli. *Journal of Applied Bacteriology*, 23, 130–135.
- Dilna, S. V., Surya, H., Aswathy, R. G., Varsha, K. K., Sakthikumar, D. N., Pandey, A., et al. (2015). Characterization of an exopolysaccharide with potential health-benefit properties from a probiotic *Lactobacillus plantarum* RJF 4. *LWT-Food Science and Technology*, 64, 1179–1186.
- Garrote, G. L., Abraham, A. G., & De Antoni, G. L. (2001). Chemical and microbiological characterisation of kefir grains. *Journal of Dairy Research*, 68, 639–652.
- Golowczyk, M. A., Gugliada, M. J., Hollmann, A. J., Delfederico, L., Garrote, G. L., Abraham, A. G., et al. (2008). Characterization of homofermentative lactobacilli isolated from kefir grains: Potential use as probiotic. *Journal of Dairy Research*, 75, 211–217.
- Hamet, M. F., Piermaria, J. A., & Abraham, A. G. (2015). Selection of EPS-producing *Lactobacillus* strains isolated from kefir grains and rheological characterization of the fermented milks. *LWT-Food Science and Technology*, 63, 129–135.
- Hamet, M. F., Medrano, M., Pérez, P. F., & Abraham, A. G. (2016). Oral administration of kefir exerts a bifidogenic effect on Balb/c mice intestinal microbiota. *Beneficial Microbes*, 7, 237–246.
- Hidalgo-Cantabrana, C., Patricia López, P., Gueimonde, M., de los Reyes-Gavilán, G., Suárez, A., Margolles, A., et al. (2012). Immune modulation capability of exopolysaccharides synthesised by lactic acid bacteria and bifidobacteria. *Probiotics and Antimicrobial Proteins*, 4, 227–237.
- Howe, K. J., Ishida, K. P., & Clark, M. M. (2002). Use of ATR/FT-IR spectrometry to study fouling of microfiltration membranes by natural waters. *Desalination*, 147, 251–255.
- Ibarburu, I., Puertas, A. I., Berregi, I., Rodríguez-Carvajal, M. A., Prieto, A., & Dueñas, M. T. (2015). Production and partial characterization of exopolysaccharides produced by two *Lactobacillus sakei* strains isolated from cider. *International Journal of Food Microbiology*, 214, 54–62.
- Ismail, B., & Nampoothiri, K. M. (2010). Production, purification and structural characterization of an exopolysaccharide produced by a probiotic *Lactobacillus plantarum* MTCC 9510. *Archives of Microbiology*, 192, 1049–1057.
- Káčuráková, M., Capek, P., Sasinkova, V., Wellner, N., & Ebringerova, A. (2000). FT-IR study of plant cell wall model compounds: Pectic polysaccharides and hemicelluloses. *Carbohydrate Polymers*, 43, 195–203.
- Korakli, M., Gänzle, M. G., & Vogel, R. F. (2002). Metabolism by bifidobacteria and lactic acid bacteria of polysaccharides from wheat and rye, and exopolysaccharides produced by *Lactobacillus sanfranciscensis*. *Journal of Applied Microbiology*, 92, 958–965.

- Kovács, A., Nyerges, B., & Izvekov, V. (2008). Vibrational analysis of N-acetyl- α -D-glucosamine and β -D-glucuronic acid. *Journal Physics of Chemistry*, 112, 5728–5735.
- Laine, R., Sweeley, C. C., Li, Y. T., Kisic, A., & Rapport, M. M. (1972). On the structure of cytolipin R, a ceramide tetrahexoside hapten from rat lymphosarcoma. *Journal of Lipid Research*, 13, 519–524.
- Lebeer, S., Verhoeven, T. L., Francius, G., Schoofs, G., Lambrechts, I., Dufrière, Y., et al. (2009). Identification of a gene cluster for the biosynthesis of a long, galactose-rich exopolysaccharide in *Lactobacillus rhamnosus* GG and functional analysis of the priming glycosyltransferase. *Applied and Environmental Microbiology*, 75, 3554–3563.
- Leemhuis, H., Pijning, T., Dobruchowska, J. M., van Leeuwen, S. S., Kralj, S., Dijkstra, B. W., et al. (2013). Glucansucrases: Three-dimensional structures, reactions, mechanism, α -glucan analysis and their implications in biotechnology and food applications. *Journal of Biotechnology*, 163, 250–272.
- Leroy, F., & De Vuyst, L. (2016). Advances in production and simplified methods for recovery and quantification of exopolysaccharides for applications in food and health. *Journal of Dairy Science*, 99, 3229–3238.
- Londero, A., Quinta, R., Abraham, A. G., Sereno, R., De Antoni, G., & Garrote, G. L. (2011). Inhibitory activity of cheese whey fermented with kefir grains. *Journal of Food Protection*, 1, 94–100.
- Marieta, C., Ibarburu, I., Duenas, M., & Irastorza, A. (2009). Supramolecular structure and conformation of a (1 \rightarrow 3)(1 \rightarrow 2)- β -D-glucan from *Lactobacillus subeubicus* CUPV221 as observed by tapping mode atomic force microscopy. *Journal of Agricultural and Food Chemistry*, 57, 6183–6188.
- Medrano, M., Hamet, M. F., Abraham, A. G., & Pérez, P. F. (2009). Kefiran protects Caco-2 cells from cytopathic effects induced by *Bacillus cereus* infection. *Antonie Van Leeuwenhoek*, 96, 505–513.
- Medrano, M., Racedo, S. M., Rolny, I. S., Abraham, A. G., & Pérez, P. F. (2011). Oral administration of kefiran modulates the immune cell balance of lymphoid tissues associated to intestinal mucosa. *Journal of Agricultural and Food Chemistry*, 59, 5299–5304.
- Moura de Paiva, I., da Silva Steinberg, R., Lula, I. S., de Souza-Fagundes, E. M., de Oliveira Mendes, T., Bell, M. J. V., et al. (2016). *Lactobacillus kefirifaciens* and *Lactobacillus satsumensis* isolated from Brazilian kefir grains produce alpha-glucans that are potentially suitable for food applications. *LWT-Food Science and Technology*, 72, 390–398.
- Mozzi, F., Vaningelgem, F., Hébert, E. M., Van der Meulen, R., Moreno, M. R. F., de Valdez, G. F., et al. (2006). Diversity of heteropolysaccharide-producing lactic acid bacterium strains and their biopolymers. *Applied and Environmental Microbiology*, 72, 4431–4435.
- Nácher-Vázquez, M., Ballesteros, N., Canales, A., Rodríguez Saint-Jean, S., Pérez-Prieto, S. I., Prieto, A., et al. (2015). Dextrans produced by lactic acid bacteria exhibit antiviral and immunomodulatory activity against salmonid viruses. *Carbohydrate Polymers*, 124, 292–301.
- Nair, P. R., Melnick, S. J., Ramachandran, R., Escalon, E., & Ramachandran, C. (2006). Mechanism of macrophage activation by (1,4)- α -D-glucan isolated from *Tinospora cordifolia*. *International Immunopharmacology*, 6, 1815–1824.
- Nataraj, S., Schomacker, R., Kraume, M., Mishra, M. I., & Drews, A. (2008). Analyses of polysaccharide fouling mechanisms during crossflow membrane filtration. *Journal of the Membrane Science*, 308, 152–161.
- Nilsson, G. S., Bergquist, K. E., Nilsson, U., & Gorton, L. (1996). Determination of the degree of branching in Normal and amylopectin type potato starch with ^1H NMR spectroscopy. Improved resolution and two-dimensional spectroscopy. *Starch*, 48, 352–357.
- Notararigo, N., Nácher-Vázquez, M., Ibarburu, I., Werning, M. L., Fernández de Palencia, P., Dueñas, M. T., et al. (2013). Comparative analysis of production and purification of homo- and hetero-polysaccharides produced by lactic acid bacteria. *Carbohydrate Polymers*, 93, 57–64.
- Patel, S., Majumder, A., & Goyal, A. (2012). Potentials of exopolysaccharides from lactic acid bacteria. *Indian Journal of Microbiology*, 52, 3–12.
- Patten, D. A., & Laws, A. P. (2015). *Lactobacillus*-produced exopolysaccharides and their potential health benefits: A review. *Beneficial Microbes*, 6, 1–15.
- Rao, J. M., & Goyal, A. (2013). A novel high dextran yielding *Weissella cibaria* JAG8 for cereal food application. *International Journal of Food Science & Nutrition*, 64, 346–354.
- Remus, D. M., van Kranenburg, R., van Swam, I. I., Taverne, N., Bongers, R. S., Wels, M., et al. (2012). Impact of 4 *Lactobacillus plantarum* capsular polysaccharide clusters on surface glyca composition and host cell signaling. *Microbial Cell Factories*, 11, 149.
- Rimada, P., & Abraham, A. G. (2003). Comparative study of different methodologies to determine the exopolysaccharide produced by kefir grains in milk and whey. *Le Lait*, 83, 79–88.
- Sarbini, S. R., Kolida, S., Deaville, E. R., Gibson, G. R., & Rastall, R. A. (2014). Potential of novel dextran oligosaccharides as prebiotics for obesity management through *in vitro* experimentation. *British Journal of Nutrition*, 112, 1303–1314.
- Schmid, J., Sieber, V., & Rehm, B. (2015). Bacterial exopolysaccharides: biosynthesis pathways and engineering strategies. *Frontiers in Microbiology*, 6, 496.
- Synytysya, A., & Novak, M. (2014). Structural analysis of glucans. *Annals Translation Medicine*, 2, 17.
- Tallon, R., Bressollier, P., & Urdaci, M. C. (2003). Isolation and characterization of two exopolysaccharides produced by *Lactobacillus plantarum* EP56. *Research in Microbiology*, 154, 705–712.
- Tiekling, M., & Gänzle, M. G. (2005). Exopolysaccharides from cereal-associated lactobacilli. *Trends in Food Science & Technology*, 16, 79–84.
- Torino, M. I., de Valdez, G. F., & Mozzi, F. (2015). Biopolymers from lactic acid bacteria. Novel applications in foods and beverages. *Frontiers in Microbiology*, 6.
- Wang, K., Li, W., Liu, P., Ahmed, Z., Xiao, P., & Bai, X. (2010). Physical characterization of exopolysaccharide produced by *Lactobacillus plantarum* KF5 isolated from Tibet Kefir. *Carbohydrate Polymers*, 82, 895–903.
- Wang, K., Li, W., Rui, X., Chen, X., Jiang, M., & Dong, M. (2014). Characterization of a novel exopolysaccharide with antitumor activity from *Lactobacillus plantarum* 70810. *International Journal of Biological Macromolecules*, 63, 133–139.
- Wang, J., Zhao, X., Tian, Z., Yang, Y., & Yang, Z. (2015). Characterization of an exopolysaccharide produced by *Lactobacillus plantarum* YW11 isolated from Tibet Kefir. *Carbohydrate Polymers*, 125, 16–25.
- Zang, L.-H., Rothman, D. L., & Shulman, R. G. (1990). ^1H NMR visibility of mammalian glycogen in solution. *Biophysics*, 87, 1678–1680.
- Zang, L.-H., Howseman, A. M., & Shulman, R. G. (1991). Assignment of the ^1H chemical shifts of glycogen. *Carbohydrate Research*, 220, 1–9.
- Zhang, L., Liu, C., Li, D., Zhao, Y., Zhang, X., Zeng, X., et al. (2013). Antioxidant activity of an exopolysaccharide isolated from *Lactobacillus plantarum* C88. *International Journal of Biological Macromolecules*, 54, 270–275.
- Zhang, L., Liu, C., Tao, X., & Wei, H. (2016). Characterization and sulfated modification of an exopolysaccharide from *Lactobacillus plantarum* ZDY2013 and its biological activities. *Carbohydrate Polymers*, 153, 25–33.
- Zhou, K., Zeng, Y., Yang, M., Chen, S., He, L., Ao, X., et al. (2016). Production: purification and structural study of an exopolysaccharide from *Lactobacillus plantarum* BC-25. *Carbohydrate Polymers*, 144, 205–214.
- Živković, M., Miljković, M. S., Ruas-Madiedo, P., Markelić, M. B., Veljović, K., Tolinački, M., et al. (2016). EPS-SJ exopolysaccharide produced by the strain *Lactobacillus paracasei* subsp. *paracasei* BGSJ2-8 is involved in adhesion to epithelial intestinal cells and decrease on *E. coli* association to Caco-2 cells. *Frontiers in Microbiology*, 7, 286.



Contents lists available at ScienceDirect

Food Hydrocolloids

journal homepage: www.elsevier.com/locate/foodhyd

Citric acid-incorporated fish gelatin/chitosan composite films

J. Uranga^a, A.I. Puertas^b, A. Etxabide^a, M.T. Dueñas^b, P. Guerrero^a, K. de la Caba^{a,*}^a BIOMAT Research Group, University of the Basque Country (UPV/EHU), Engineering College of Gipuzkoa, Plaza de Europa 1, 20018, Donostia-San Sebastián, Spain^b Department of Applied Chemistry, University of the Basque Country (UPV/EHU), Faculty of Chemistry, Paseo Manuel de Lardizabal 3, 20018, Donostia-San Sebastián, Spain

ARTICLE INFO

Article history:

Received 20 August 2017

Received in revised form

27 December 2017

Accepted 12 February 2018

Available online xxx

Keywords:

Fish gelatin

Citric acid

Chitosan

Composite film

Antibacterial

ABSTRACT

Transparent and colorless citric acid-incorporated fish gelatin/chitosan composite films were prepared in this work. The addition of citric acid into film forming formulations slowed down the swelling rate and swelling values of the films, which maintained their integrity and resulted in flexible hydrated films. Furthermore, citric acid acted as plasticizer, increasing the elongation at break of the films. Additionally, films showed good UV barrier properties and the incorporation of citric acid and chitosan reduced the *E. coli* growth, especially for the films prepared with 20 wt % citric acid, highlighting the potential use of these films as active food packaging. These results were related to the changes observed by Fourier transform infrared (FTIR) analysis, which revealed the different protein structure achieved as a function of citric acid and chitosan contents.

© 2018 Elsevier Ltd. All rights reserved.

1. Introduction

Functional properties, such as chemical and mechanical resistance, make plastic films useful for a huge range of applications in food and pharmaceutical industries, among others (Dormer, Finn, Ward, & Cullen, 2013; Wang, Wang, & Liu, 2015). However, plastic films are derived from non-renewable resources and lead to environmental problems associated to their treatment after disposal, especially when they are employed for short-term or single-use applications (Gigli et al., 2013). Therefore, research on alternative materials is needed to reduce the use of these non-biodegradable and non-renewable films (Kovalcik, Machovsky, Kozakova, & Koller, 2015; Narayanan, Loganathan, Valupa, Thomas, & Barghese, 2017; Sanyang, Sapuan, Jawaid, Ishak, & Sahari, 2016). In this context, fish gelatin can be extracted from fish bones and skins, promoting the valorization of food processing wastes. Fish gelatin is a protein that can provide materials with good mechanical and UV and oxygen barrier properties and, thus, represents an alternative raw material for a wide range of applications (Etxabide, Urdanpilleta, Guerrero, & de la Caba, 2015; Nur Hanani, Roos, & Kerry, 2014). In particular, fish gelatin can be

used to manufacture films for food packaging applications (Etxabide, Uranga, Guerrero, & de la Caba, 2017; Fu et al., 2017).

Since microbial contamination is considered one of the main causes of spoilage leading to food quality deterioration (Clarke et al., 2017), the development of active films is attracting much attention in the field of food science and technology. The active compound used in this work was citric acid, whose antimicrobial character has been reported in some recent works (Denghani, Hosseini, & Regenstein, 2018; Kim & Rhee, 2015; Olaimat et al., 2017). Citric acid is a bio-based polycarboxylic acid, commercially available at low cost, which has nontoxic nature since it is produced as a metabolic product of the body (Krebs or citric acid cycle) in all living cells that use oxygen as part of the cellular respiration (Rocha-García, Guerra-Contreras, Reyes-Hernández, & Palestino, 2017). In a previous work (Uranga, Leceta, Etxabide, Guerrero, & de la Caba, 2016), citric acid-modified fish gelatin films were prepared at basic conditions. This previous study reported that citric acid contents higher than 20 wt % did not provide further interactions between gelatin and citric acid and, thus, 10 and 20 wt % citric acid concentrations were selected in this work to provide mild acidity conditions and dissolve the chitosan used as antimicrobial biopolymer, whose antibacterial activity is attributed to the positively charged amino groups that interact with the negatively charged surface of bacteria (Bano, Arshad, Yasin, Ghauri, & Younus, 2017; Ganesan, 2017).

* Corresponding author. University of the Basque Country (UPV/EHU), Escuela de Ingeniería de Gipuzkoa, Plaza Europa 1, 20018, Donostia-San Sebastián, Spain.

E-mail address: koro.delacaba@ehu.eus (K. de la Caba).

Like fish gelatin, chitosan is also extracted from food processing waste, mainly shrimp shells (Muxika, Etxabide, Uranga, Guerrero, & de la Caba, 2017). The development of fish gelatin/chitosan films (BenBettaieb, Karbowiak, Bornaz, & Debeaufort, 2015; Gómez-Estaca, Gómez-Guillén, Fernández-Martín, & Montero, 2011), as well as the effects of the incorporation of active compounds, such as plant extracts (Benbettaieb et al., 2016; Bonilla & Sobral, 2016) and essential oils (Hosseini, Rezaei, Zandi, & Farahmandghavi, 2015; Kakaei & Shahbazi, 2016) into film forming formulations have been recently documented. However, to the best of our knowledge no manuscript has been focused on the effects of both citric acid and chitosan on the functional properties of fish gelatin-based films. Therefore, the combined effect of citric acid and chitosan on the antibacterial activity of the films and on their physico-chemical, thermal, optical, barrier and mechanical properties was analyzed in this work.

2. Materials and methods

2.1. Materials

Type A fish gelatin with a 240 bloom value (Healan Ingredients, UK) was used as the main component of film forming formulations. Anhydrous citric acid (Panreac, Spain) and high molecular weight chitosan with a deacetylation degree higher than 75% (Sigma–Aldrich, Spain) were used as active compounds. Glycerol with a purity of 99.01% (Panreac, Spain) was used as plasticizer. All chemicals were food grade and they were used as received without further purification.

2.2. Film preparation

Fish gelatin (FG) films were prepared by solution casting. Firstly, 10 wt % and 20 wt % (on gelatin basis) citric acid (CA) solutions (0.026 M and 0.052 M, respectively) were prepared. These CA concentrations were selected based on a previous work (Uranga et al., 2016). Then, chitosan (CHI) was dissolved in 100 mL of CA solution and it was maintained under continuous stirring for 30 min. After that, 5 g gelatin were added and the resultant solution was heated at 80 °C for 30 min and stirred at 200 rpm. Finally, 20 wt % glycerol (on gelatin basis), used as plasticizer, was added, pH was adjusted to 4.5 using 1 N NaOH, and the solution was stirred for other 30 min at 80 °C and 200 rpm. Film forming solutions were poured into Petri dishes and allowed to dry for 48 h at room temperature. The amount of CHI in films was 0, 3, 6 and 9 wt % (on gelatin basis) and films were designated as 10CAXCHI or 20CAXCHI for the films prepared with 10 and 20 wt % CA, respectively, as a function of the CHI content (X). Furthermore, control films without CA and CHI (0CA0CHI) were prepared. All films were conditioned in a controlled environment chamber (ACS SU700V) at 25 °C and 50% relative humidity before testing. The film thickness was measured to the nearest 0.001 mm with a hand-held QuantuMike digimatic micrometer (Mitutoyo Spain, Elgoibar, Spain) and the obtained values were $50 \pm 2 \mu\text{m}$.

2.3. Fourier transform infrared (FTIR) spectroscopy

FTIR spectra were recorded on a Nicolet 380 FTIR spectrometer with ATR Golden Gate. The measurements were recorded between 4000 and 800 cm^{-1} . A total of 32 scans were performed at a resolution of 4 cm^{-1} . All spectra were smoothed using the Savitzky-Golay function. Second-derivative spectra of the amide region were used at peak position guides for the curve fitting, according to the procedure described by Byler and Susi (1986), using OriginPro 9.0 software.

2.4. Moisture content (MC) and total soluble matter (TSM)

To determine the MC of films, samples were weighed (w_0) and then dried in an oven at 105 °C for 24 h. After that, samples were reweighed (w_1) and MC was calculated as:

$$\text{MC (\%)} = \frac{w_0 - w_1}{w_0} 100$$

TSM values were calculated using dried specimens. Immersion of samples into 200 mL of distilled water was performed for 24 h. After this time, the films were dried in an oven at 105 °C for 24 h and weighed (w_2). TSM values were calculated as follows:

$$\text{TSM (\%)} = \frac{w_1 - w_2}{w_1} 100$$

2.5. Swelling

In order to study the swelling of films, first, film disks with a diameter of 52 mm were weighed (w_h) and then, immersed into distilled water. Samples were weighed after immersion into water for specific times (w_t), until getting constant values. The swelling was calculated according to the following equation:

$$\text{Swelling (\%)} = \frac{w_t - w_h}{w_h} 100$$

2.6. Differential scanning calorimetry (DSC)

DSC was carried out in a Mettler Toledo DSC 822. Samples (3.0 ± 0.2 mg) were sealed in aluminum pans to avoid mass loss during the experiment. Filled pans were heated from 25 to 250 °C at a rate of 10 °C/min under inert atmosphere conditions (10 mL N_2 /min) to avoid thermo-oxidative reactions.

2.7. Thermo-gravimetric analysis (TGA)

Thermal stability of films was analyzed by TGA. Measurements were performed in a Mettler Toledo TGA SDTA 851 equipment. The samples were heated from 25 to 800 °C at a heating rate of 10 °C/min under inert atmosphere conditions (10 mL N_2 /min) to avoid thermo-oxidative reactions.

2.8. Color and gloss

Color was analyzed with a CR-400 Konica Minolta Chroma-Meter. L^* , a^* and b^* parameters were measured by placing the films on the surface of a standard white plate. The CIELAB color scale was used: $L^* = 0$ (black) to $L^* = 100$ (white), $-a^*$ (greenness) to $+a^*$ (redness), and $-b^*$ (blueness) to $+b^*$ (yellowness). Color difference (ΔE^*) was calculated referred to the control film (0CA0CHI):

$$\Delta E^* = \sqrt{(\Delta L^*)^2 + (\Delta a^*)^2 + (\Delta b^*)^2}$$

Film gloss was determined using a Multi Gloss 268 Plus gloss meter. Gloss values were measured at 60° incidence angle, according to ASTM D523-99 (ASTM, 1999).

2.9. Ultraviolet–visible (UV–vis) spectroscopy

UV-vis spectroscopy was performed in the range from 200 to

800 nm using a UV-Jasco spectrophotometer, model V-630. Transparency (T) values were measured at 600 nm (A_{600}) and normalized considering the film thickness (x):

$$T = \frac{A_{600}}{x}$$

2.10. Water contact angle (WCA)

WCA measurements were performed using a Dataphysic Contact Angle System, Oca 20 model. For each measurement, a 3 μ L droplet of distilled water was placed on the film surface. The image of the drop was taken using SCA20 software.

2.11. Water vapor permeability (WVP)

WVP values were measured in a W3/0120 tester. Film disks were sealed to cups containing distilled water. Then, cups were placed into the tester at 38 °C and 90% relative humidity, according to ASTM E96-00 (ASTM, 2000). WVP was determined gravimetrically as follows:

$$WVP \left(g \text{ cm}^{-1} \text{ s}^{-1} \text{ Pa}^{-1} \right) = \frac{w \cdot x}{A \cdot t \cdot \Delta P}$$

where w is the weight change (g), x is the film thickness (cm), A is the film area (cm²), t is time (s) and ΔP is the partial pressure difference of water vapor across the film (Pa).

2.12. Mechanical properties

Tensile strength (TS) and elongation at break (EB) were determined using MTS Insight 10 Electromechanical Testing System, equipped with a tensile load cell of 250 N. According to ASTM D1708-93 (ASTM, 1993), the cross-head speed was set at 1 mm/min and samples with 22.25 mm length and 4.75 mm width were used.

2.13. Antibacterial assessment

The antibacterial activity of fish gelatin films was tested against the growth of a Gram-negative bacteria, *E. coli* DH5 α , to analyze the influence of CA and CHI. *E. coli* DH5 α was grown overnight in Luria Bertani (LB) broth (Sambrook, Fritsch, & Maniatis, 1989) at 37 °C with shaking (160 rpm). Then, it was inoculated into fresh LB medium and grown up to the mid-exponential phase at 37 °C and it was used to inoculate 10 mL media containing 0.04 g of film and incubated for 24 h at 37 °C and 160 rpm. Samples from cultures were taken at 5 h since *E. coli* DH5 α had grown up actively after this time. The plate dilution method was used to monitor cell viability on LB agar plates incubated at 37 °C and results were reported as CFU/mL.

2.14. Statistical analysis

Analysis of variance (ANOVA) was used to determine the significance of differences among samples. The analysis was performed with a SPSS computer program (SPSS Statistic 23.0) and Tukey's test was used for multiple comparisons. All the assays were done at least in triplicate. Differences were statistically significant at the $P < 0.05$ level. This analysis was carried out separately for the systems with 10 wt % CA and 20 wt % CA in order to estimate the significant differences as a function of CHI content.

3. Results and discussion

3.1. Physicochemical properties

The effect of CHI and CA in fish gelatin films was assessed by FTIR analysis. As can be seen in Fig. 1, the most noticeable change occurred in the relative intensity between the band corresponding to amide I (C=O stretching at $\sim 1630 \text{ cm}^{-1}$) and the one associated to amide II (N-H bending coupled with C-N stretching at $\sim 1540 \text{ cm}^{-1}$) (Muyonga, Cole, & Duodu, 2004). In particular, the intensity of the amide I band was higher than that of the amide II for the control film (OCA0CHI); however, the difference in the relative intensity of these two bands became smaller for the films with 10 wt % CA (10CA0CHI and 10CA9CHI), similar for the films with 20 wt % CA without CHI (20CA0CHI), and the intensity of the amide II band became larger with respect to that of amide I for the films with 20 wt % CA and 9 wt % CHI (20CA9CHI).

According to Lagaron, Fernandez-Saiz, and Ocio (2007), the band at $\sim 1540 \text{ cm}^{-1}$ can be related to the biocide activity of chitosan associated to the protonated amino groups and, thus, a relative increase of this band might indicate an increase of the antibacterial capacity of the films, as corroborated below by the antimicrobial assessment. Additionally, the band at $\sim 1400 \text{ cm}^{-1}$ has been also associated to biocide activity related to carboxyl groups (Lagaron et al., 2007; Leceta, Guerrero, Ibarburu, Dueñas, & de la Caba, 2013). As can be seen in Fig. 1, the relative intensity of this band with respect to the band at 1450 cm^{-1} , corresponding to the CH₂ groups in proline, was lower for the films without CA and CHI (OCA0CHI), became similar for the films with 10 wt % CA (10CA0CHI and 10CA9CHI) and larger for the films with 20 wt % CA, especially for the films with 9 wt % CHI (10CA9CHI), in accordance with the antimicrobial results shown in Fig. 7. Furthermore, the bands in the 1100-1000 cm^{-1} region became a single band for the 20CA9CHI film.

These differences in the relative intensity of FTIR bands suggest different interactions among the polar groups of the formulation components (FG, CHI, CA and glycerol) depending on CHI, but mainly on CA content. The interactions between gelatin and chitosan are mainly produced by hydrogen bonding between carboxyl,

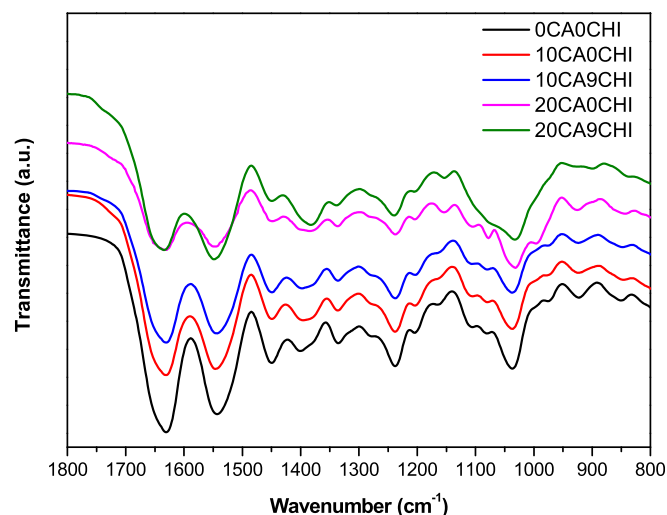


Fig. 1. FTIR spectra of the control film (OCA0CHI), the films with 10 or 20 wt % CA without CHI (10CA0CHI and 20CA0CHI) and the films with 9 wt % CHI (10CA9CHI and 20CA9CHI).

amino and hydroxyl groups of gelatin and amino and hydroxyl groups of chitosan (Gómez-Estaca et al., 2011). These interactions seem to be influenced by the CA content incorporated into the film forming solutions; therefore, in order to further analyze the effect of CA and CHI on the protein structure, the curve fitting of the amide I band was carried out.

The amide I profile of gelatin contains three major components: a band associated to the α -helix/random coil conformation at 1650 cm^{-1} , and two bands corresponding to the β -sheet conformation at $1615\text{--}1630\text{ cm}^{-1}$ and $1680\text{--}1700\text{ cm}^{-1}$ (Etxabide, Leceta, Cabezudo, Guerrero, & de la Caba, 2016; Guerrero, Kerry, & de la Caba, 2014). As can be seen in Table 1, no difference was observed in the protein structure with respect to the control film (OCA0CHI) when 10 wt % CA was incorporated (10CA0CHI); however a decrease in the content of the β -sheet conformation and an increase of the α -helix/random coil conformation was observed when 20 wt % CA was incorporated (20CA0CHI), indicating the great influence of CA content in the protein structure. Furthermore, the difference between the contents of β -sheet and α -helix/random coil conformations was bigger for the films prepared with 20 wt % CA, which showed higher content of α -helix/random coil than the films prepared with 10 wt % CA. This behavior could be due to a partial gelatin renaturation (Sow & Yang, 2015), which could be favored in the presence of higher CA contents due to the plasticizing effect of CA, as shown below when mechanical properties are analyzed.

The protein structure was also affected by the addition of CHI. Specifically, the content of β -sheet decreased and the content of α -helix/random coil increased with the incorporation of CHI. However, the changes observed when CHI content increased were different for the films prepared with 10 or 20 wt % CA. In particular, β -sheet content decreased and α -helix/random coil content increased when CHI content increased in the films prepared with 10 wt % CA, while the opposite trend, increase of β -sheet content and decrease of α -helix/random coil content, was observed for the films with 20 wt % CA. These results indicate the different extension of hydrogen bonding and, as a consequence, the different network formed as a function of the CA content in the film forming formulations.

The moisture content (MC) and total soluble matter (TSM) of the films were also analyzed and values are shown in Table 2. On the one hand, all films showed mean MC values from 11.21 to 13.41%, in agreement with the weight loss associated to the first step of TGA curves (Fig. 3). On the other hand, TSM values were around 40%, probably due to the dissolution of glycerol and CA, since the interactions among these components and the biopolymers used in this work (FG and CHI) occurred by hydrogen bonding, as indicated

Table 2

Moisture content (MC) and total soluble matter (TSM) of FG films prepared with different contents of citric acid (CA) and chitosan (CHI).

Film	MC (%)	TSM (%)
OCA0CHI	11.21 ± 0.33 ^d	37.33 ± 1.05 ^b
10CA0CHI	12.33 ± 0.05 ^a	44.96 ± 1.97 ^a
10CA3CHI	12.15 ± 0.06 ^b	38.67 ± 0.87 ^a
10CA6CHI	12.20 ± 0.06 ^{ab}	45.78 ± 1.76 ^a
10CA9CHI	11.93 ± 0.06 ^c	42.71 ± 4.68 ^a
OCA0CHI	11.21 ± 0.33 ^c	37.33 ± 1.05 ^c
20CA0CHI	13.46 ± 0.09 ^a	44.73 ± 1.86 ^a
20CA3CHI	13.32 ± 0.03 ^{ab}	42.99 ± 2.01 ^{ab}
20CA6CHI	13.41 ± 0.10 ^a	41.34 ± 0.82 ^{ab}
20CA9CHI	12.96 ± 0.24 ^b	40.27 ± 1.30 ^b

Two means followed by the same letter in the same section and column are not significantly ($P > 0.05$) different through the Turkey's multiple range test.

by FTIR analysis (Fig. 1). It is worth noting that all films maintained their integrity. Although no significant ($P > 0.05$) change was observed for the films with 10 wt % CA, in the case of the films with 20 wt % CA, the addition of CHI significantly ($P < 0.05$) decreased film solubility, as also shown by other authors for gelatin-chitosan films (Gómez-Estaca et al., 2011; Hosseini, Rezaei, Zandi, & Ghavi, 2013; Matiacevich, Cofré, Schebor, & Enrione, 2013).

Since the swelling behavior is indicative of crosslinking, the swelling values of the films were measured. First of all, the effect of CA was analyzed and the swelling curves are shown in Fig. 2. In general, gelatin films swell rapidly at short times but the swelling rate slows down at longer times (Gordon, Brooker, Chew, Wilson, & York, 2010). In the case of the control film (OCA0CHI), the swelling increased up to values next to 2000%, whereas the swelling values for the films prepared with CA were below 600% after 24 h. The increase of CA content from 10% to 20 wt % decreased swelling values. It is worth noting that the CA-incorporated films maintained their integrity up to the end of the swelling test and the hydrated films obtained were flexible.

Regarding the effect of CHI addition, swelling curves for the films prepared with CHI are shown in Fig. 3, in which two stages can be distinguished. The first stage until 420 min showed a fast swelling up to 460–620% for the films prepared with 10 wt % CA and up to 400–470% for the films prepared with 20 wt % CA. In all cases, the highest values were measured for the films without CHI, suggesting that the incorporation of CHI promoted the interactions with the polar groups of the formulation components, so less polar

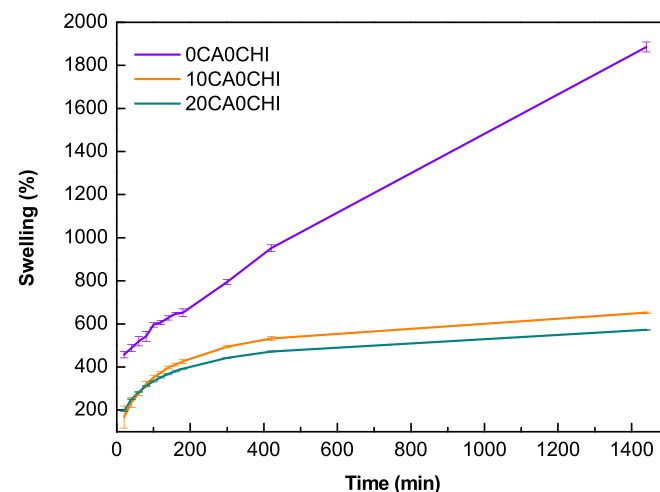


Fig. 2. Swelling behavior of the control film (OCA0CHI) and the FG films prepared with 10 wt % CA (10CA0CHI) or 20 wt % CA (20CA0CHI) without CHI.

Table 1

Protein conformations in FG films prepared with different contents of citric acid (CA) and chitosan (CHI).

Protein conformation	Film	Content (%)	Film	Content (%)
β sheet (1615–1630 cm^{-1})	OCA0CHI	42	OCA0CHI	42
	10CA0CHI	43	20CA0CHI	29
	10CA3CHI	41	20CA3CHI	22
	10CA6CHI	36	20CA6CHI	23
	10CA9CHI	35	20CA9CHI	25
α -helix/random coil	OCA0CHI	54	OCA0CHI	54
	10CA0CHI	53	20CA0CHI	68
	10CA3CHI	55	20CA3CHI	74
	10CA6CHI	60	20CA6CHI	72
	10CA9CHI	61	20CA9CHI	69
β sheet(1680–1700 cm^{-1})	OCA0CHI	4	OCA0CHI	4
	10CA0CHI	4	20CA0CHI	2
	10CA3CHI	4	20CA3CHI	4
	10CA6CHI	4	20CA6CHI	5
	10CA9CHI	4	20CA9CHI	5

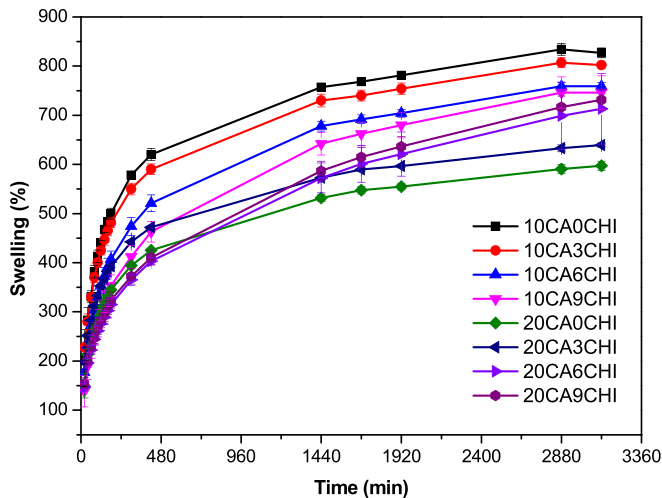


Fig. 3. Swelling behavior of the films prepared with different CA and CHI contents.

groups were accessible to interact with water molecules, leading to a lower swelling degree. This trend was maintained for the films prepared with 10 wt% CA until the end of the swelling test, when constant swelling values were reached. These final swelling values decreased from 825 to 750% when CHI content increased from 0 to 9 wt %. In contrast, this trend was reversed for the films prepared with 20 wt % CA. These results are in agreement with the different protein structures developed in the films with 10 or 20 wt % CA, as previously shown by FTIR analysis in Table 1.

3.2. Thermal properties

In order to relate the physicochemical changes observed as a function of CA and CHI content to thermal properties, DSC measurements were carried out and the curves obtained are shown in Fig. 4. As can be seen, the most noticeable change occurred when CA or CHI was incorporated, regardless of the CHI content added. In relation to the films with 10 wt % CA (Fig. 4a), all films, except the film with the highest CHI content (10CA9CHI), showed one single band related to water evaporation. As can be seen, the maximum of this band shifted from 83 to 95 °C when CA was incorporated into the formulation, and from 95 to 107 °C when CHI content increased from 0 to 9 wt %. These results are indicative of the interactions of CA and CHI with gelatin, which would hinder water evaporation.

Furthermore, the film with 9 wt % CHI showed a second peak around 220 °C, associated to CHI deacetylation (Almeida, Frollini, Castellán, & Coma, 2010). In contrast, all the films prepared with 20 wt % CA and CHI (Fig. 4b) showed two peaks. Moreover, the maximum temperature corresponding to this second peak decreased when CHI content increased, which can be related to the decrease of α -helix/random coil conformation from 3 to 9 wt % CHI content, as shown in Table 1.

Regarding TGA, derivative thermo-gravimetric (DTG) curves are shown in Fig. 5, with the weight loss curves in the inset. As can be seen, there are three main weight loss steps. The first one around 100 °C is related to water evaporation, as also shown by DSC in Fig. 4, and its value was around 10%, in accordance with the MC values shown in Table 2. The second weight loss step appeared around 250 °C and it is associated to the evaporation of glycerol (Castelló, Dweck, & Aranda, 2009) and the decomposition of CA (Choppali & Gorman, 2008). The maximum temperature corresponding to this second step appeared at lower temperatures for the films prepared with 20 wt % CA, which could be related to the different structure of the network formed as a function of CA content, as previously shown by FTIR results (Table 1); in contrast, the highest value was observed for the control film (0CA0CHI). Finally, the main weight loss step appeared at 310–320 °C and it corresponds to FG (Mohajer, Rezaei, & Hosseini, 2017) and CHI degradation (Corazzari et al., 2015). Films showed a residual mass around 30%, except the control film, which showed a residual mass around 20%.

3.3. Optical properties

In addition to the physicochemical and thermal behavior, the properties related to the appearance of the films were analyzed, in particular, color, gloss and transparency. As can be seen in Table 3, CIELab color parameters were similar for the films regardless of CA and CHI content. As a consequence, the total color difference was lower than 1 for all the films, indicating that there was no visual color difference produced by the incorporation of CA or CHI into the formulations.

Regarding gloss values (Table 4), the most significant difference occurred when CHI was incorporated into the formulations, which caused a significant ($P < 0.05$) decrease in gloss values. In spite of the gloss decrease, the films prepared with 10 wt % CA maintained a glossy surface with values around 100 GU, regardless of CHI content, indicative of a smooth surface. In contrast, the surface of the films prepared with 20 wt % CA changed from smooth to rough with

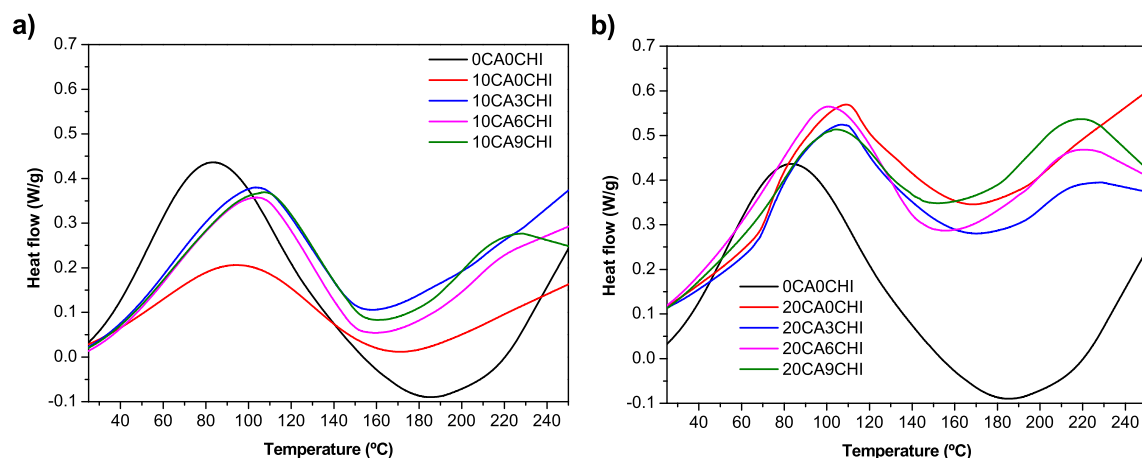


Fig. 4. DSC thermograms of the films prepared with a) 10 wt % CA and b) 20 wt % CA and different CHI contents in comparison to the control film (0CA0CHI).

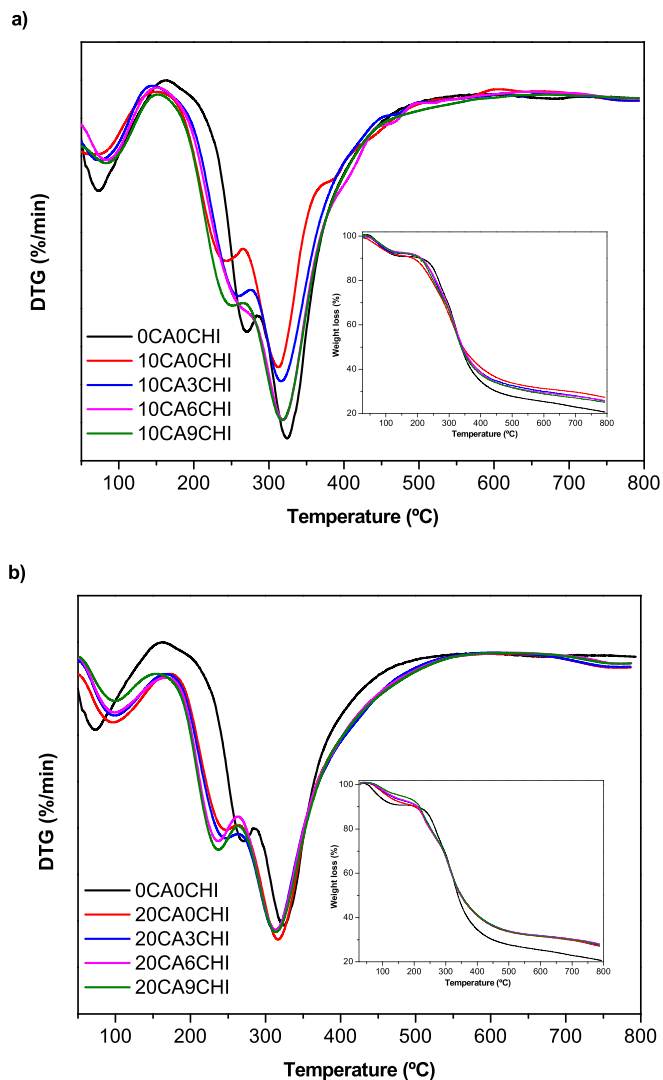


Fig. 5. Weight loss and DTG curves of the films prepared with a) 10 wt % CA and b) 20 wt % CA and different CHI contents in comparison to the control film (0CA0CHI).

Table 3
CIELab color parameters (L^* , a^* , b^*) and total color difference (ΔE^*) for FG films prepared with different contents of citric acid (CA) and chitosan (CHI).

Film	L^*	a^*	b^*	ΔE^*
0CA0CHI	96.81 ± 0.17 ^a	-0.05 ± 0.02 ^b	2.36 ± 0.03 ^b	–
10CA0CHI	96.48 ± 0.07 ^b	0.00 ± 0.02 ^a	2.26 ± 0.04 ^a	0.34 ± 0.07 ^a
10CA3CHI	96.17 ± 0.22 ^c	-0.05 ± 0.01 ^b	2.42 ± 0.11 ^b	0.64 ± 0.12 ^b
10CA6CHI	96.03 ± 0.14 ^c	-0.12 ± 0.02 ^c	2.52 ± 0.06 ^b	0.80 ± 0.09 ^c
10CA9CHI	96.04 ± 0.05 ^c	-0.20 ± 0.02 ^d	2.77 ± 0.08 ^c	0.88 ± 0.06 ^c
0CA0CHI	96.81 ± 0.17 ^a	-0.05 ± 0.02 ^b	2.36 ± 0.03 ^b	–
20CA0CHI	96.69 ± 0.04 ^a	-0.06 ± 0.01 ^a	2.27 ± 0.05 ^a	0.15 ± 0.05 ^b
20CA3CHI	96.51 ± 0.12 ^{ab}	-0.17 ± 0.01 ^b	2.47 ± 0.05 ^c	0.34 ± 0.11 ^a
20CA6CHI	96.50 ± 0.19 ^{ab}	-0.19 ± 0.01 ^c	2.58 ± 0.05 ^d	0.41 ± 0.09 ^a
20CA9CHI	96.12 ± 0.36 ^b	-0.28 ± 0.02 ^d	2.79 ± 0.02 ^e	0.84 ± 0.06 ^b

Two means followed by the same letter in the same section and column are not significantly ($P > 0.05$) different through the Turkey's multiple range test.

the incorporation of CHI, although CHI content did not significantly ($P > 0.05$) affect the gloss values. These variations between the films prepared with 10 or 20 wt % CA are in accordance with the different physicochemical properties shown in 3.1 section. Finally, concerning transparency, fish gelatin films did not absorb light at 600 nm, as can be seen by the low transparency values shown in Table 4, so

Table 4

Gloss and transparency values of FG films prepared with different contents of citric acid (CA) and chitosan (CHI).

Film	Gloss (GU)	Transparency
0CA0CHI	145.5 ± 5.7 ^a	0.66 ± 0.01 ^a
10CA0CHI	155.0 ± 0.7 ^a	1.18 ± 0.05 ^b
10CA3CHI	100.5 ± 2.3 ^b	1.38 ± 0.05 ^{bc}
10CA6CHI	98.1 ± 3.4 ^{bc}	0.85 ± 0.06 ^a
10CA9CHI	96.3 ± 0.5 ^c	1.63 ± 0.17 ^c
0CA0CHI	145.5 ± 5.7 ^a	0.66 ± 0.01 ^a
20CA0CHI	127.8 ± 3.2 ^b	0.71 ± 0.03 ^a
20CA3CHI	38.5 ± 0.5 ^c	1.63 ± 0.03 ^{bc}
20CA6CHI	26.7 ± 3.7 ^c	1.43 ± 0.16 ^b
20CA9CHI	25.9 ± 1.1 ^c	1.74 ± 0.08 ^c

Two means followed by the same letter in the same section and column are not significantly ($P > 0.05$) different through the Turkey's multiple range test.

it can be said that films were transparent regardless of CA and CHI content.

3.4. Light barrier and mechanical properties

Regarding light barrier properties, UV-vis spectra are shown in Fig. 6. As can be seen, films provided UV light barrier from 200 to 250 nm, thanks to tyrosine and phenylalanine amino acid residues in gelatin (Gómez-Guillén et al., 2009; Nagarajan, Benjakul, Prodpran, & Songtipya, 2015). Moreover, UV light absorbance in the 250–280 range increased with the incorporation of CA and with the increase of CHI content due to the carboxyl and hydroxyl auxochrome groups of CA and CHI (Jadhav & Phugare, 2012).

Film hydrophobicity was analyzed by the measurement of water contact angles (Karbowiak, Debeaufort, & Voilley, 2006; Kokoszka, Debeaufort, Lenart, & Voilley, 2010; Oymaci & Altinkaya, 2016). As shown in Table 5, WCA values increased by the incorporation of CA or CHI with respect to the control film, leading to hydrophobic surfaces. These values did not significantly ($P > 0.05$) change with CHI content for the films prepared with 10 wt % CA, while WCA values significantly ($P < 0.05$) increased for the films with 20 wt % CA when CHI increased from 0 to 9%, reaching a similar value for the films with 9 wt % CHI, regardless of CA content. This increase in the hydrophobic character of the films can be related to the interactions among polar groups shown by FTIR analysis, which hinder the orientation of polar groups towards the surface. Finally, regarding WVP, similar values were found for all films, indicating that the addition of CA and CHI did not unfavorably affect the film WVP. Water vapor permeability is a two-step process that includes water vapor sorption and water vapor diffusion (Roy, Gennadios, Weller, & Testin, 2000). The latter depends on protein structure, which changes as a function of the interactions of protein polar groups, causing the depart from the expected behavior (Su et al., 2010), as shown by WVP values in this work.

As displayed in Table 5, mechanical properties were also influenced by the addition of CA. Since the residual free CA can act as a plasticizer (Shi et al., 2008), TS significantly ($P < 0.05$) decreased, while EB significantly ($P < 0.05$) increased when CA was added. This effect was more pronounced when CHI was incorporated into the films with 10 wt % CA. However, the effect of CHI on the films prepared with 20 wt % CA was different, since both TS and EB values increased when CHI content was increased. This behavior is in agreement with the different physicochemical properties shown in 3.1 section. The mechanical performance, especially for the films prepared with 20 wt % CA, was better than that observed for gelatin/chitosan films with other organic acids, such as gallic acid (Rui et al., 2017) or ferulic acid (Benbettaieb, Karbowiak, Brachais, & Debeaufort, 2015).

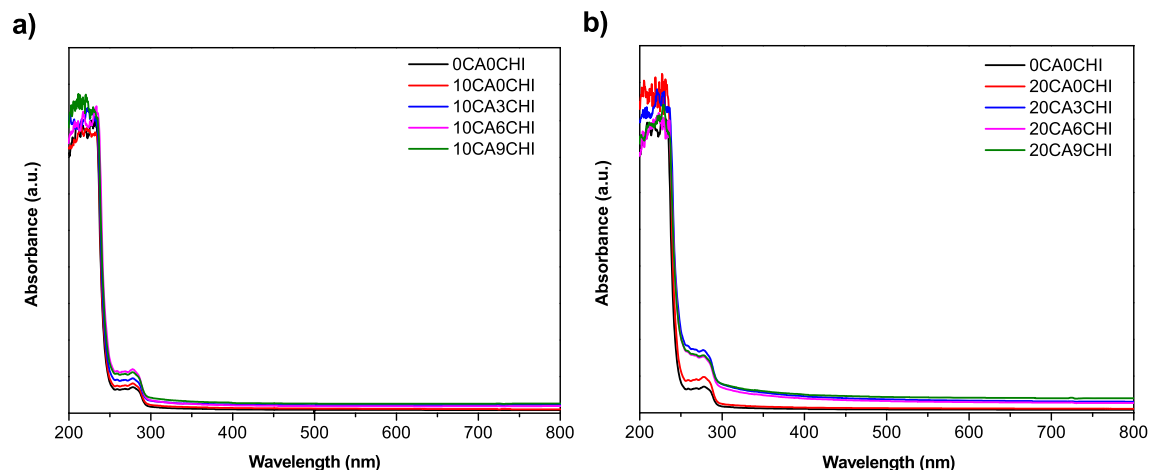


Fig. 6. UV-vis spectra of the films prepared with a) 10 wt % CA and b) 20 wt % CA and different CHI contents in comparison to the control film (0CA0CHI).

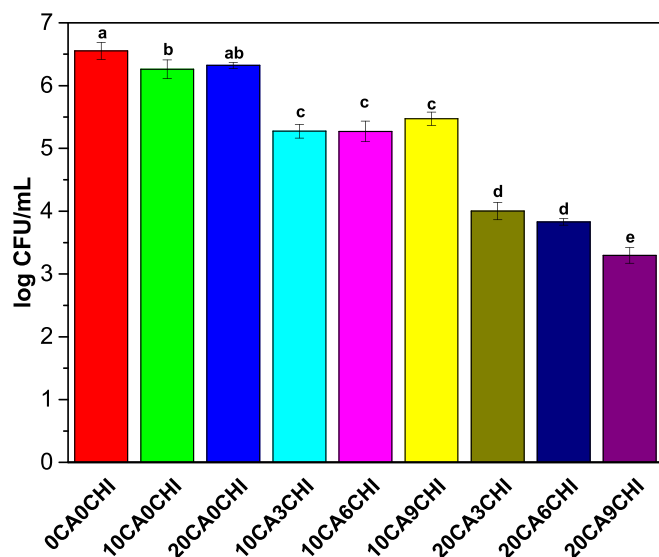


Fig. 7. Antibacterial activity of the films prepared with a) 10 wt % CA and b) 20 wt % CA and different CHI content.

Table 5

Barrier properties (water contact angle, WCA; water vapor permeability, WVP) and mechanical properties (tensile strength, TS; elongation at break, EB) of FG films prepared with different contents of citric acid (CA) and chitosan (CHI).

Film	WCA (°)	WVP · 10 ¹² (g · cm ⁻¹ · s ⁻¹ · Pa ⁻¹)	TS (MPa)	EB (%)
0CA0CHI	71 ± 4 ^a	1.9 ± 0.1 ^a	68 ± 5 ^a	8 ± 2 ^a
10CA0CHI	112 ± 10 ^b	1.8 ± 0.2 ^a	39 ± 2 ^b	23 ± 3 ^b
10CA3CHI	100 ± 14 ^b	2.5 ± 0.5 ^b	35 ± 1 ^b	18 ± 3 ^c
10CA6CHI	125 ± 13 ^b	2.6 ± 0.2 ^b	30 ± 3 ^c	15 ± 3 ^c
10CA9CHI	118 ± 3 ^b	2.6 ± 0.3 ^b	28 ± 2 ^c	5 ± 1 ^a
20CA0CHI	71 ± 4 ^a	1.9 ± 0.1 ^a	68 ± 5 ^a	8 ± 2 ^a
20CA3CHI	78 ± 5 ^b	2.1 ± 0.3 ^a	29 ± 4 ^b	17 ± 1 ^b
20CA6CHI	64 ± 4 ^a	2.3 ± 0.3 ^a	33 ± 2 ^c	22 ± 3 ^c
20CA9CHI	86 ± 2 ^b	2.5 ± 0.4 ^a	35 ± 3 ^c	18 ± 2 ^b
20CA9CHI	114 ± 1 ^c	2.7 ± 0.5 ^a	39 ± 3 ^d	22 ± 2 ^c

Two means followed by the same letter in the same section and column are not significantly ($P > 0.05$) different through the Turkey's multiple range test.

3.5. Antibacterial assessment

The antimicrobial activity of films was evaluated against *E. coli* and results are shown in Fig. 7. Although free CA has been found to

be active against some bacteria (Mahmoud, 2014), including *E. coli* (Firouzbadi, Noori, Edalatpanah, & Mirhosseini, 2014), films prepared with citric acid showed a slight ($P < 0.05$) reduction of growth, probably due to the fact that CA interacted with gelatin, as shown by FTIR results. The incorporation of CHI significantly ($P < 0.05$) decreased the bacterial growth for the films with 10 wt % CA, regardless of CHI content. In contrast, the increase of CHI content promoted a further decrease ($P < 0.05$) of bacterial growth for the films prepared with 20 wt % CA, in accordance with the FTIR analysis carried out (Fig. 1).

4. Conclusions

The incorporation of citric acid into gelatin film forming solutions decreased the swelling of the resulting films, which were flexible and easy to handle. This behavior could be explained by the new interactions of citric acid with gelatin and glycerol, as shown by FTIR analysis, which suggested the great influence of CA content on protein structure and antibacterial activity. In particular, a reduction in the growth of *E. coli* was shown especially for those films prepared with 20 wt % of citric acid and 9 wt % of chitosan, indicating the combined effect of citric acid and chitosan as natural antimicrobial compounds. The resulting films were transparent, colorless and showed good UV barrier properties and hydrophobic surfaces, essential properties for food packaging applications, highlighting the potential use of these films as active packaging.

Acknowledgments

The authors thank the University of the Basque Country UPV/EHU (PPG17/18 research group) and the Provincial Council of Gipuzkoa (Exp. 81/17) for their financial support. Jone Uranga thanks the Basque Government (fellowship PRE_2015_1_0205) and Alaitz Etxabide thanks UPV/EHU (fellowship DOCREC17/04). Also thanks are due to the Advanced Research Facilities (SGIker) from the UPV/EHU.

References

- Almeida, E. V. R., Frollini, E., Castellán, A., & Coma, V. (2010). Chitosan, sisal cellulose, and biocomposite chitosan/sisal cellulose films prepared from thiourea/NaOH aqueous solution. *Carbohydrate Polymers*, 80, 655–664.
- ASTM D1708-93. (1993). Standard test method for tensile properties of plastics by use of microtensile specimens. In *Annual book of ASTM standards*. Philadelphia, PA: American Society for Testing and Materials.
- ASTM D523-99. (1999). Standard test method for specular gloss. In *Annual book of*

- ASTM standards. Philadelphia, PA: American Society for Testing and Materials. ASTM E96-00. (2000). Standard test methods for water vapour transmission of material, E96-00. In *Annual book of ASTM standards*. Philadelphia, PA: American Society for Testing and Materials.
- Bano, I., Arshad, M., Yasin, T., Ghauri, M. A., & Younus, M. (2017). Chitosan: A potential biopolymer for wound management. *International Journal of Biological Macromolecules*, *102*, 380–383.
- Benbettaieb, N., Chambin, O., Assifaoui, A., Al-Assaf, S., Karbowski, T., & Debeaufort, F. (2016). Release of coumarin incorporated into chitosan-gelatin irradiated films. *Food Hydrocolloids*, *56*, 266–276.
- BenBettaieb, N., Karbowski, T., Bornaz, S., & Debeaufort, F. (2015). Spectroscopic analyses of the influence of electron beam irradiation doses on mechanical, transport properties and microstructure of chitosan-fish gelatin blend films. *Food Hydrocolloids*, *46*, 37–51.
- Benbettaieb, N., Karbowski, T., Brachais, C. H., & Debeaufort, F. (2015). Coupling tyrosol, quercetin or ferulic acid and electron beam irradiation to cross-link chitosan-gelatin films: A structure-function approach. *European Polymer Journal*, *67*, 113–127.
- Bonilla, J., & Sobral, P. J. A. (2016). Investigation of the physicochemical, antimicrobial and antioxidant properties of gelatin-chitosan edible film mixed with plant ethanolic extracts. *Food Bioscience*, *16*, 17–25.
- Byler, D. M., & Susi, H. (1986). Examination of the secondary structure of proteins by deconvolved FTIR spectra. *Biopolymers*, *25*, 469–487.
- Castelló, M. L., Dweck, J., & Aranda, D. A. G. (2009). Thermal stability and water content determination of glycerol by thermogravimetry. *Journal of Thermal Analysis and Calorimetry*, *97*, 627–630.
- Choppali, U., & Gorman, B. P. (2008). Structural and optical properties of nanocrystalline ZnO thin films synthesized by the citrate precursor route. *Journal of Luminescence*, *128*, 1641–1648.
- Clarke, D., Tyuftin, A. A., Cruz-Romero, M. C., Bolton, D., Fanning, S., Pankaj, S. K., et al. (2017). Surface attachment of active antimicrobial coatings onto conventional plastic-based laminates and performance assessment of these materials on the storage life of vacuum packaged beef sub-primals. *Food Microbiology*, *62*, 196–201.
- Corazzari, I., Nisticò, R., Turci, F., Faga, M. G., Franzoso, F., Tabasso, S., et al. (2015). Advanced physico-chemical characterization of chitosan by means of TGA coupled on-line with FTIR and GCMS: Thermal degradation and water adsorption capacity. *Polymer Degradation and Stability*, *112*, 1–9.
- Denghani, S., Hosseini, S. V., & Regensten, J. M. (2018). Edible films and coatings in seafood preservation: A review. *Food Chemistry*, *240*, 505–513.
- Dormer, A., Finn, D. P., Ward, P., & Cullen, J. (2013). Carbon footprint analysis in plastics manufacturing. *Journal of Cleaner Production*, *51*, 133–141.
- Etxabide, A., Leceta, I., Cabezudo, S., Guerrero, P., & de la Caba, K. (2016). Sustainable fish gelatin films: From food processing waste to compost. *ACS Sustainable Chemistry & Engineering*, *4*, 4626–4634.
- Etxabide, A., Uranga, J., Guerrero, P., & de la Caba, K. (2017). Development of active gelatin films by means of valorisation of food processing waste: A review. *Food Hydrocolloids*, *68*, 192–198.
- Etxabide, A., Urdanpilleta, M., Guerrero, P., & de la Caba, K. (2015). Effects of cross-linking in nanostructure and physicochemical properties of fish gelatins for bio-applications. *Reactive and Functional Polymers*, *94*, 55–62.
- Firouzabadi, F. B., Noori, M., Edalatpanah, Y., & Mirhosseini, M. (2014). ZnO nanoparticle suspensions containing citric acid as antimicrobial to control *Listeria monocytogenes*, *Escherichia coli*, *Staphylococcus aureus* and *Bacillus cereus* in mango juice. *Food Control*, *42*, 310–314.
- Fu, S., Wu, C., Wu, T., Yu, H., Yang, S., & Hu, Y. (2017). Preparation and characterisation of chlorogenic acid-gelatin type of biologically active film for coating preservation. *Food Chemistry*, *221*, 657–663.
- Ganesan, P. (2017). Natural and bio polymer curative films for wound dressing medical applications. *Wound medicine*, *18*, 33–40.
- Gigli, M., Negroni, A., Zanaroli, G., Lotti, N., Fava, F., & Munari, A. (2013). Environmentally friendly PBS-based copolyesters containing PEG-like subunit: Effect of block length on solid-state properties and enzymatic degradation. *Reactive and Functional Polymers*, *73*, 764–771.
- Gómez-Estaca, J., Gómez-Guillén, M. C., Fernández-Martín, F., & Montero, P. (2011). Effects of gelatin origin, bovine-hide and tuna skin, on the properties of compound gelatin-chitosan films. *Food Hydrocolloids*, *25*, 1461–1469.
- Gómez-Guillén, M. C., Pérez-Mateos, M., Gómez-Estaca, J., López-Caballero, E., Giménez, B., & Montero, P. (2009). Fish gelatin: A renewable material for developing active biodegradable films. *Trends in Food Science & Technology*, *20*, 3–16.
- Gordon, P. W., Brooker, A. D. M., Chew, Y. M. J., Wilson, D. I., & York, D. W. (2010). Studies into the swelling of gelatine films using a scanning fluid dynamic gauge. *Food and Bioprocess Processing*, *88*, 357–364.
- Guerrero, P., Kerry, J. P., & de la Caba, K. (2014). FTIR characterization of protein-polysaccharide interactions in extruded blends. *Carbohydrate Polymers*, *111*, 598–605.
- Hosseini, S. F., Rezaei, M., Zandi, M., & Farahmandghavi, F. (2015). Bio-based composite edible films containing *Origanum vulgare* L. essential oil. *Industrial Crops and Products*, *67*, 403–413.
- Hosseini, S. F., Rezaei, M., Zandi, M., & Ghavi, F. F. (2013). Preparation and functional properties of fish gelatin-chitosan blend edible films. *Food Chemistry*, *136*, 1490–1495.
- Jadhav, J. P., & Phugare, S. S. (2012). Textile dyes: General information and environmental aspects. In A. El Nemer (Ed.), *Non-conventional textile waste water treatment* (pp. 1–29). New York: Nova Science Publisher Inc.
- Kakaei, S., & Shahbazi, Y. (2016). Effect of chitosan-gelatin film incorporated with ethanolic red grape seed extract and Ziziphora clinopodioides essential oil on survival of *Listeria monocytogenes* and chemical, microbial and sensory properties of minced trout fillet. *Lebensmittel-Wissenschaft und -Technologie- Food Science and Technology*, *72*, 432–438.
- Karbowski, T., Debeaufort, F., & Voilley, A. (2006). Importance of surface tension characterization for food, pharmaceutical and packaging products: A review. *Critical Reviews in Food Science and Nutrition*, *46*, 391–407.
- Kim, S. A., & Rhee, M. S. (2015). Synergistic antimicrobial activity of caprylic acid in combination with citric acid against both *Escherichia coli* O157:H7 and indigenous microflora in carrot juice. *Food Microbiology*, *49*, 166–172.
- Kokoszka, S., Debeaufort, F., Lenart, A., & Voilley, A. (2010). Water vapour permeability, thermal and wetting properties of whey protein isolate based edible films. *International Dairy Journal*, *20*, 53–60.
- Kovalcik, A., Machovsky, M., Kozakova, Z., & Koller, M. (2015). Designing packaging materials with viscoelastic and gas barrier properties by optimized processing of poly(3-hydroxybutyrate-co-3-hydroxyvalerate) with lignin. *Reactive and Functional Polymers*, *94*, 25–34.
- Lagaron, J. M., Fernandez-Saiz, P., & Ocio, M. J. (2007). Using ATR-FTIR spectroscopy to design active antimicrobial food packaging structures based on high molecular weight chitosan polysaccharide. *Journal of Agricultural and Food Chemistry*, *55*, 2554–2562.
- Leceta, I., Guerrero, P., Ibarburu, I., Dueñas, M. T., & de la Caba, K. (2013). Characterization and antimicrobial analysis of chitosan-based films. *Journal of Food Engineering*, *116*, 889–899.
- Mahmoud, B. S. M. (2014). The efficacy of grape seed extract, citric acid and lactic acid on the inactivation of *Vibrio parahaemolyticus* in shucked oysters. *Food Control*, *41*, 13–16.
- Matiacevich, S., Cofré, D. C., Schebor, C., & Enrione, J. (2013). Physicochemical and antimicrobial properties of bovine and salmon gelatin-chitosan films. *CyTA - Journal of Food*, *11*, 366–378.
- Mohajer, S., Rezaei, M., & Hosseini, S. F. (2017). Physico-chemical and microstructural properties of fish gelatin/agar bio-based blend films. *Carbohydrate Polymers*, *157*, 784–793.
- Muxika, A., Etxabide, A., Uranga, J., Guerrero, P., & de la Caba, K. (2017). *International Journal of Biological Macromolecules*, *105*, 1358–1368. <https://doi.org/10.1016/j.ijbiomac.2017.07.087>.
- Muyonga, J. H., Cole, C. G. B., & Duodu, K. G. (2004). Fourier transform infrared (FTIR) spectroscopic study of acid soluble collagen and gelatin from skins and bones of young and adult Nile perch (*Lates niloticus*). *Food Chemistry*, *86*, 325–332.
- Nagarajan, M., Benjakul, S., Prodpran, T., & Songtipya, P. (2015). Properties and characteristics of nanocomposite films from tilapia skin gelatin incorporated with ethanolic extract from coconut husk. *Journal of Food Science & Technology*, *52*, 7669–7682.
- Narayanan, M., Loganathan, S., Valupa, R. B., Thomas, S., & Barghese, T. O. (2017). UV protective poly(lactic acid)/rosin films for sustainable packaging. *International Journal of Biological Macromolecules*, *99*, 37–45.
- Nur Hanani, Z. A., Roos, Y. H., & Kerry, J. P. (2014). Use and application of gelatin as potential biodegradable packaging materials for food products. *International Journal of Biological Macromolecules*, *71*, 94–102.
- Olaimat, A. N., Al-Nabulsi, A. A., Osaili, T. M., Al-Holy, M., Ayyash, M. M., Mehyar, G. F., et al. (2017). Survival and inhibition of *Staphylococcus aureus* in commercial and hydrated tahini using acetic and citric acids. *Food Control*, *77*, 179–186.
- Oymaci, P., & Altinkaya, S. A. (2016). Improvement of barrier and mechanical properties of whey protein isolate based food packaging films by incorporation of zein nanoparticles as a novel bionanocomposite. *Food Hydrocolloids*, *54*, 1–9.
- Rocha-García, D., Guerra-Contreras, A., Reyes-Hernández, J., & Palestino, G. (2017). Thermal and kinetic evaluation of biodegradable thermo-sensitive gelatin/poly(ethylene glycol) diamine crosslinked citric acid hydrogels for controlled release of tramadol. *European Polymer Journal*, *89*, 42–56.
- Roy, S., Gennadios, A., Weller, C. L., & Testin, R. F. (2000). Water vapor transport parameters of a cast wheat gluten film. *Industrial Crops and Products*, *11*, 43–50.
- Rui, L., Xie, M., Hu, B., Zhou, L., Yin, D., & Zeng, X. (2017). A comparative study on chitosan/gelatin composite films with conjugated or incorporated gallic acid. *Carbohydrate Polymers*, *173*, 473–481.
- Sambrook, J., Fritsch, E. F., & Maniatis, T. (1989). *Molecular cloning: A laboratory manual* (2nd ed.). New York: Cold Spring Harbor Laboratory Press.
- Sanyang, M. L., Sapuan, S. M., Jawaid, M., Ishak, M. R., & Sahari, J. (2016). Development and characterization of sugar palm starch and poly(lactic acid) bilayer films. *Carbohydrate Polymers*, *146*, 36–45.
- Shi, R., Bi, J., Zhang, Z., Zhu, A., Chen, D., Zhou, X., et al. (2008). The effect of citric acid on the structural properties and cytotoxicity of the polyvinyl alcohol/starch films when molding at high temperature. *Carbohydrate Polymers*, *74*, 763–770.
- Sow, L. C., & Yang, H. (2015). Effects of salt and sugar addition on the physico-chemical properties and nanostructure of fish gelatin. *Food Hydrocolloids*, *45*, 72–82.

- Su, J. F., Huang, Z., Zhao, Y. H., Yuan, X. Y., Wang, X. Y., & Li, M. (2010). Moisture sorption and water vapor permeability of soy protein isolate/poly(vinyl alcohol)/glycerol blend films. *Industrial Crops and Products*, 31, 266–276.
- Uranga, J., Leceta, I., Etxabide, A., Guerrero, P., & de la Caba, K. (2016). Cross-linking of fish gelatins to develop sustainable films with enhanced properties. *European Polymer Journal*, 78, 82–90.
- Wang, C., Wang, H., & Liu, Y. (2015). Separation of aluminum and plastic by metallurgy method for recycling waste pharmaceutical blisters. *Journal of Cleaner Production*, 102, 378–383.



Characterization of *Pediococcus ethanolidurans* CUPV141: A β -D-glucan- and Heteropolysaccharide-Producing Bacterium

María G. Llamas-Arriba^{1,2}, Adrián Pérez-Ramos², Ana I. Puertas¹, Paloma López², María T. Dueñas¹ and Alicia Prieto^{2*}

¹ Chemistry Faculty, Department of Applied Chemistry, University of the Basque Country (UPV/EHU), San Sebastián, Spain,

² Department of Microorganisms and Plant Technology, Biological Research Center, Spanish National Research Council (CIB-CSIC), Madrid, Spain

OPEN ACCESS

Edited by:

Vittorio Capozzi,
University of Foggia, Italy

Reviewed by:

María Dimopoulou,
Aristotle University of Thessaloniki,
Greece

Claudio Hidalgo Cantabrana,
North Carolina State University,
United States

*Correspondence:

Alicia Prieto
aliprieto@cib.csic.es

Specialty section:

This article was submitted to
Food Microbiology,
a section of the journal
Frontiers in Microbiology

Received: 16 June 2018

Accepted: 13 August 2018

Published: 04 September 2018

Citation:

Llamas-Arriba MG, Pérez-Ramos A, Puertas AI, López P, Dueñas MT and Prieto A (2018) Characterization of *Pediococcus ethanolidurans* CUPV141: A β -D-glucan- and Heteropolysaccharide-Producing Bacterium. *Front. Microbiol.* 9:2041. doi: 10.3389/fmicb.2018.02041

Pediococcus ethanolidurans CUPV141 is an exopolysaccharide (EPS)-producing lactic acid bacterium, first isolated from Basque Country cider (Spain). Physicochemical analysis of the EPS synthesized by the bacterium revealed that CUPV141 produces mostly a homopolysaccharide (HoPS), characterized as a 2-substituted (1,3)- β -D-glucan, together with a small quantity of a heteropolysaccharide (HePS) composed of glucose, galactose, glucosamine, and glycerol-3-phosphate, this being the first *Pediococcus* strain described to produce this kind of polymer. On the contrary, an isogenic strain CUPV141NR, generated by chemical mutagenesis of CUPV141, produced the HePS as the main extracellular polysaccharide and a barely detectable amount of 2-substituted (1,3)- β -D-glucan. This HoPS is synthesized by the transmembrane GTF glycosyltransferase (GTF), encoded by the *gtf* gene, which has been previously reported to be located in the pPP2 plasmid of the *Pediococcus parvulus* 2.6 strain. Southern blot hybridization revealed that in CUPV141 the *gtf* gene is located in a plasmid designated as pPE3, whose molecular mass (34.4 kbp) is different from that of pPP2 (24.5 kbp). Analysis of the influence of the EPS on the ability of the producing bacteria to adhere to the eukaryotic Caco-2 cells revealed higher affinity for the human enterocytes of CUPV141NR compared to that of CUPV141. This result indicates that, in contrast to the 2.6 strain, the presence of the HoPS does not potentiate the binding ability of *P. ethanolidurans*. Moreover, it supports that the phosphate-containing bacterial HePS improved the interaction between *P. ethanolidurans* and the eukaryotic cells.

Keywords: *Pediococcus ethanolidurans*, β -glucan, *gtf*, heteropolysaccharides, priming-glycosyltransferase, plasmid, adhesion

INTRODUCTION

Some lactic acid bacteria (LAB) produce exopolysaccharides (EPS), extracellular polymers that may remain tightly attached to the bacteria, constituting a capsule, or may be released to the environment (De Vuyst et al., 2001). These polymers often possess useful properties, such as improvement of the rheological properties of food and even beneficial effects for health as

prebiotics and immunomodulators (Bajpai et al., 2016; Caggianiello et al., 2016). The EPS can be homopolysaccharides (HoPS) or heteropolysaccharides (HePS), constituted, respectively, by one or various types of monosaccharides (Werning et al., 2012). Only one protein is responsible for the synthesis and the extracellular location of the HoPS, whereas the HePS synthesis and secretion requires the joint action of several proteins usually encoded by genes located in operons (Sanlibaba and Aybige Çakmak, 2016). A priming-glycosyltransferase (priming-GTF or p-GTF), which is phosphorylated by a tyrosine kinase (Minic et al., 2007), catalyzes the first step of the synthesis of HePS by the formation of a phosphoanhydride bond between the first hexose-1-phosphate of the repeating unit and an undecaprenyl phosphate lipid carrier anchored to the membrane. Then, the repeating-unit is synthesized, by sequential transfer of nucleotide sugar residues onto the growing chain by other glycosyltransferases (Whitfield, 2006). HePS are mainly composed of different ratios of glucose, galactose and rhamnose, and occasionally, they can be substituted by amino-sugars or polyols (glycerol) as well as by glucuronic acids and also phosphates (Badel et al., 2011). For LAB and bifidobacteria, genetic studies and characterization of the EPS produced by them have shown that these bacteria are able to synthesize more than one EPS. Characterization of these polymers has revealed that some strains produce HoPS and HePS (Ibarburu et al., 2007, 2015; Puertas et al., 2018) or several HePS (Remus et al., 2012; Salazar et al., 2012; Hidalgo-Cantabrana et al., 2013; Lee et al., 2016). In addition, HePS-producing *Streptococcus thermophilus* strains have been widely used for fermentations to generate dairy products as cheeses and yogurts because of the rheological properties their EPS confer to the final products (De Vuyst et al., 2003; Ravyts et al., 2011; Wu et al., 2011; Kanamarlapudi and Muddada, 2017). However, until now simultaneous production of HePS and HoPS by a pediococcal strain has not been reported. The most common EPS produced by strains belonging to this genus is a 2-substituted (1,3)- β -D-glucan (β -D-glucan) (Llaubères et al., 1990; Dueñas-Chasco et al., 1997) synthesized by the GTF glycosyltransferase (GTF) (Werning et al., 2008, 2014). This HoPS is produced by LAB isolated from alcoholic beverages: *Pediococcus damnosus* or *Oenococcus oeni* strains in wines (Lonvaud-Funel and Joyeux, 1988; Dols-Lafargue et al., 2008), *Lactobacillus* and *Pediococcus* strains in ciders (Dueñas et al., 1995; Fernández et al., 1995; Ibarburu et al., 2007; Garai-Ibabe et al., 2010a; Puertas et al., 2018) and *Lactobacillus* strains in beers (Fraunhofer et al., 2018). The GTF is encoded by the *gtf* gene, which is generally present in plasmids (Lonvaud-Funel et al., 1993; Werning et al., 2006), although a chromosomal location has been observed in *O. oeni* (Werning et al., 2006; Dols-Lafargue et al., 2008).

The interest in the identification and characterization of new LAB producing the β -D-glucan is due to the fact that this polymer immunomodulates human macrophages, and its presence increases the adhesion capability to enterocytes of the producing bacteria (Fernández de Palencia et al., 2009; Garai-Ibabe et al., 2010b). Moreover, this EPS has prebiotic activity (Russo et al., 2012; Pérez-Ramos et al., 2016b) and confers resistance to both technological and gastrointestinal

stresses to lactobacilli upon heterologous expression (Stack et al., 2010).

This work reports on the characterization of *Pediococcus ethanolidurans* CUPV141, a novel strain isolated from cider that produces the 2-substituted (1,3)- β -D-glucan and a phosphorylated HePS. As far as we know this is the first instance of detection of this species in cider and the first characterized example of a *Pediococcus* producing HoPS and HePS. Moreover, the presence of these two EPS seems to play a role for adhesion of the bacteria to biotic surfaces.

MATERIALS AND METHODS

Bacterial Strains and Growth Conditions

The EPS-producing *P. ethanolidurans* CUPV141 strain was isolated from Basque Country (Spain) ropy cider (containing 6% ethanol and at pH 3.4–3.8) as previously described (Dueñas et al., 1995) in Carr-agar medium (g/L; yeast extract, 4; casaminoacids, 5; DL malic acid, 5; glucose, 20; KH_2PO_4 , 0.5; KCl, 0.425; $\text{CaCl}_2 \cdot 2\text{H}_2\text{O}$, 0.125; MgSO_4 , 0.125; MnSO_4 , 0.0025) supplemented with pimarinin at 50 mg/mL to avoid the growth of yeasts and molds. The isogenic, non-ropy strain *P. ethanolidurans* CUPV141NR was generated in this work by chemical mutagenesis with the antibiotic novobiocin (Sigma-Aldrich) at a final concentration of 50 $\mu\text{g/mL}$. The *P. parvulus* 2.6 strain (Dueñas-Chasco et al., 1997) was used for comparative purposes. All strains were stored at -80°C in MRS medium (De Man et al., 1960) containing 20% glycerol. The experimental assays were performed in MRS medium pH 5.5 at 28°C and under an atmosphere containing 5% CO_2 . For EPS isolation, a semi-defined medium (SMD) was used (Dueñas-Chasco et al., 1997).

Genomic and Plasmidic DNA Preparations

For genomic DNA extraction, NucleoSpin® Tissue kit (Macherey-Nagel) was used according to the manufacturer's instructions and supplementing the lysis buffer with lysozyme (Sigma-Aldrich) at 30 mg/mL and mutanolysin (Sigma-Aldrich) at 2 U/ μL . Once isolated, samples were stored at -20°C until use.

Total plasmid DNA preparations of *P. ethanolidurans* CUPV141 and CUPV141NR strains were obtained and purified by isopycnic CsCl density gradient to eliminate non-supercoiled forms of the plasmids as previously described (Pérez-Ramos et al., 2017b). Plasmidic samples were maintained at -80°C until use.

Fluorescent quantification of the DNA in genomic and plasmidic DNA preparations was determined with a Qubit fluorometer using the Qubit HS dsDNA Assay Kit (Molecular Probes).

16S rDNA Amplification by PCR

The template for PCR amplification was genomic DNA from *P. ethanolidurans* CUPV141. The flanking primers 616V and 630R (Ehrmann et al., 2003) and the internal primer 699R (Arahal et al., 2008) were used to obtain two amplicons (1466

and 1009 pb) of the 16S rRNA gene. The PCR products were purified with a NucleoSpin® Gel and PCR Clean-up kit (Macherey-Nagel) according to the manufacturer's instructions. Subsequent sequencing reactions were performed at Secugen (Madrid, Spain). The DNA sequences obtained were used as templates for the identification of the strain in the public database EZBioCloud¹ (Kim et al., 2012).

Quantification of the 2-Substituted (1,3)- β -D-Glucan Produced by *P. ethanolidurans* Strains

A competition enzyme-linked immunosorbent assay (ELISA) was performed for the specific detection of the EPS synthesized by strains of *P. ethanolidurans*, based on *S. pneumoniae* serotype 37 antibody, as previously described (Werning et al., 2014). The EPS of *P. parvulus* 2.6 was isolated according to Notararigo et al. (2013) and immobilized in each well of a 96-Well Nunc-Immuno MicroWell MaxiSorp plate (Thermo Fisher Scientific). EPS quantification was performed using a standard curve of serial dilutions of the purified *P. parvulus* 2.6 EPS dissolved in PBS, generated by competition for the primary antibody.

To quantify the amount of EPS released to the growth medium or attached to the bacteria, *P. ethanolidurans* strains were grown in MRS medium (1 mL) to a final concentration of 1×10^8 colony forming units (cfu)/mL in 1.5 mL Eppendorf tubes. Then, the cultures were centrifuged ($9300 \times g$, 4°C, 10 min), the supernatants were transferred to another Eppendorf tube and the bacteria were resuspended in 1 mL of phosphate buffered saline (PBS) pH 7.2. Dilutions of the culture supernatants and of the bacterial suspension in PBS were used for quantification, measuring the OD at 415 nm in a microtiter plate reader model 680 (Bio-Rad). The determinations were performed in triplicate.

Characterization of the *gtf* and *p-gtf* Genes

Plasmid DNA from the *P. ethanolidurans* CUPV141 strain was used to determine the 1,704 bp nucleotide sequence of the *gtf* gene by the dideoxy method at Secugen as previously described for the *gtf* gene of *P. parvulus* strains (Garai-Ibabe et al., 2010b).

For detection of the priming-GTF coding gene (*p-gtf*), degenerate primers (Provencher et al., 2003) and genomic DNA from the two *P. ethanolidurans* strains were used for DNA amplification. The 20 μ L reaction mixtures for each sample contained: 1 U of Taq DNA polymerase (Sigma), 1X PCR Buffer (Sigma), 2.5 mM MgCl₂ (Sigma), 0.1 mM dNTP mixture (TaKaRa), 6.25 mM of each primer, and 200 ng of total template DNA. Conditions for the PCR were as follows. First, an incubation at 94°C for 9 min. Then, 5 cycles at 94°C for 30 s, 62°C for 31 s and 72°C for 32 s. Finally, 40 cycles at 94°C for 30 s, 52°C for 31 s, and 72°C for 32 s.

After fractionation in 2.5% agarose gels, the amplicons were purified using the 'NucleoSpin® Gel and PCR Clean-up' kit, according to the manufacturer's instructions, and the nucleotide sequence determined at Secugen.

¹<https://www.ezbiocloud.net>

Informatics Analysis of Genes and Inferred Protein Sequences

The amino acid sequence of the GTF was inferred from the nucleotide sequence of the *gtf* gene with EditSeq 15 software (DNASTAR® Lasergene 15). The sequences of the protein, the *gtf* gene as well as of the DNA fragment of *p-gtf* and its translated product were compared with those of other bacteria, deposited at the National Center for Biotechnology Information (NCBI) database², using the Basic Local Alignment Search Tool (BLAST³). Multiple sequence alignments (MSA) of the sequences obtained in the search were performed with MegAlign Pro 15 software (DNASTAR Lasergene 15) using the Clustal Omega algorithm. In addition, phylogenetic trees were obtained using Tamura-Nei (Tamura and Nei, 1993) or Kimura (Kimura, 1983) metrics for DNA and protein sequences, respectively. Finally, mutations in the amino acid sequence of the GTF of each bacterium were gathered in a secondary structure model of the *P. parvulus* 2.6 enzyme, previously inferred using the SOSUI program (Werning et al., 2006).

Detection of the *gtf* Gene by Southern Blot Hybridization

Genetic localization of the *gtf* gene was performed following the protocol previously described (Pérez-Ramos et al., 2017b). Briefly, samples of plasmid DNA preparations from *Pediococcus* strains and from *Escherichia coli* V517 (Macrina et al., 1978) were fractionated by electrophoresis in a 0.7% agarose gel and DNA molecules were revealed by staining with ethidium bromide at 0.5 μ g/mL. The gels' images were obtained with Gel Doc 200 (Bio-Rad). Plasmids from *E. coli* V517 were used to generate a standard curve in which their relative migration in the gel was represented *versus* their known size (Macrina et al., 1978), which was used to determine the molecular mass of the pediococcal plasmids. The plasmidic DNA bands were transferred to a nylon membrane prior to hybridization. The internal regions of the *gtf* gene used as probes were generated by PCR amplification, in a reaction catalyzed by Phusion High Fidelity Polymerase (New England BioLabs), using as substrate total plasmid DNA preparation of *P. parvulus* 2.6 and the previously described primers GTFSF and GTFSR (Werning et al., 2006). Then, the amplicon was labeled with digoxigenin-dUTP using the DIG high prime DNA labeling and detection starter kit II (Roche). Each DIG-labeled DNA probe (25 ng/mL) was used for hybridization at 40°C following the specifications of the kit's supplier. The hybridization bands were revealed with the chemiluminescent substrate CSPD, and the signals were detected with the LAS-3000 imaging system (Fujifilm).

Agglutination Immunological Analysis

Agglutination tests were performed with *S. pneumoniae* type 37-specific antisera according to the protocol previously described (Werning et al., 2006). Briefly, cultures in late-exponential phase (1×10^9 cfu/mL) from the two *Pediococcus* strains were

²<http://www.ncbi.nlm.nih.gov/>

³<https://blast.ncbi.nlm.nih.gov/>

centrifuged at $8609 \times g$ for 47 min at 4°C and after removal of the supernatants, the sedimented bacteria were concentrated 100-fold by resuspension in PBS pH 7.2 with vigorous vortexing. Then, $10 \mu\text{L}$ of each bacterial suspension was mixed with $1 \mu\text{L}$ of anti-type 37 antibody, and incubated for 2 h at 4°C . Afterwards, each sample ($4 \mu\text{L}$) was observed by phase contrast microscopy using a Leica DM 1000 microscope.

Isolation of EPS

Pediococcus ethanolidurans CUPV141 and CUPV141NR were grown in MRS broth for 24 h. Then, the volume of bacteria corresponding to a 2% inoculum was sedimented by centrifugation ($18500 \times g$, 10 min, 4°C), resuspended in fresh MRS pH 5.5 medium and incubated at 28°C in a 5% CO_2 atmosphere for 24 h. Finally, a 2% inoculum was sedimented again, in the same conditions, to inoculate the final fermentation in SMD pH 5.5 medium (Dueñas-Chasco et al., 1997). When the cultures reached the late-exponential phase of growth, bacteria were sedimented by centrifugation of the cultures ($18500 \times g$, 20 min, 4°C), and the EPS were precipitated from the supernatants by addition of 3 volumes of cold absolute ethanol and kept at -20°C for 16 h. Afterwards, the polymers were recovered by centrifugation ($18500 \times g$, 10 min, 4°C) and the crude EPS were washed three times with 80% (v/v) cold ethanol and dialyzed in 12–14 kDa MWCO membranes (Iberlabo) against distilled water, freeze-dried and kept at room temperature.

Lyophilized EPS were dissolved in ultrapure water (0.1 mg/mL) and concentration was estimated from the neutral carbohydrate content as determined by the phenol-sulphuric acid method (Dubois et al., 1956) using glucose as standard.

Partial Characterization of the Crude EPS

Pediococcus ethanolidurans CUPV141 and CUPV141NR were incubated in MRS broth for 21 h. Then, the volume corresponding to an OD_{600} of 1.0 was centrifuged ($9600 \times g$, 10 min, 4°C). Supernatants were discarded and the sediments were resuspended in 0.5 mL of PBS pH 7.2. Then, in order to visualize similarities or differences in the EPS production between the two *P. ethanolidurans* strains, transmission electron microscopy (TEM) was used following the protocol of Zarour et al. (2017) with modifications. Briefly, a drop of each solution was independently deposited on a carbon film copper grid, previously hydrophilized by a glow discharge process of ca. 30 s, and the preparations were washed with water for 15 s. Then, each grid was stained for 15 s with a uranyl acetate water solution (0.5% w/v) in order to improve the image contrast, and washed again with water. Finally, the samples were air-dried and examined in a TECNAI G2 20 TWIN (FEI) microscope, operating at an accelerating voltage of 200 kV in a bright-field image mode, at the Microscopy Service of the University of Basque Country (UPV/EHU). Monosaccharide composition of the polymers, as well as methylation analysis for the elucidation of the O-glycosidic linkages involved in the structure of the EPS were developed following the protocols described by Notarigo

et al. (2013). Finally, proton nuclear magnetic resonance (^1H NMR) analysis of the EPS produced by the ropy strain was performed as previously described (Dueñas-Chasco et al., 1997) at the UPV/EHU NMR Service (SGIker).

Adhesion Properties

Self-Aggregation Assay

Pediococcus ethanolidurans CUPV141 and CUPV141NR strains were grown in MRS medium pH 5.5 (1% inoculum) for 15 h. Then, the volume corresponding to $1 \times 10^8 \text{ cfu/mL}$ was centrifuged ($12000 \times g$, 10 min, 4°C) and after removal of the supernatant, 1 mL of fresh MRS pH 5.5 medium was added. Two tubes of each strain were incubated at 28°C . Samples were recovered at 5 and 24 h (one tube of each strain for each time) as follows: the tubes were gently centrifuged ($5000 \times g$, 3 min, 4°C), and after removal of the supernatants the bacteria were carefully resuspended in $50 \mu\text{L}$ PBS pH 7.2. Aliquots of $5 \mu\text{L}$ of this suspension were visualized by phase contrast microscopy using a Leica DM 1000 microscope.

Caco-2 Cell Culture Adhesion Assay

The Caco-2 enterocyte cell line was obtained from the cell bank at the CIB. They were seeded and maintained as previously described (Garai-Ibabe et al., 2010b). For adhesion assays, exponential-phase cultures of the *P. ethanolidurans* strains after sedimentation were resuspended in DMEM medium (Invitrogen), to give a concentration of $1.25 \times 10^6 \text{ cfu/mL}$, and added to Caco-2 cells (ratio 10:1, bacteria:Caco-2 cells) in a final volume of 0.1 mL per well. After incubation for 1 h at 37°C under a 5% CO_2 atmosphere, unattached bacteria were removed by three washes with 0.2 mL of PBS pH 7.2. Then, the Caco-2 cells were detached from the plastic surface by addition of 0.1 mL of 0.05% trypsin-EDTA per well and incubation for 5 min at 37°C . The detachment was stopped by adding 0.1 mL of PBS pH 7.2. To determine the number of cell-associated bacteria, appropriate dilutions were plated onto MRS-agar plates. The experiments were performed in triplicate. Adhesion data were analyzed by two-way analysis of variance (ANOVA) to determine the significant differences between the variables at $p \leq 0.05$. The analysis was performed using the SAS 9.4 software (SAS Institute Inc., Cary, NC, United States).

RESULTS AND DISCUSSION

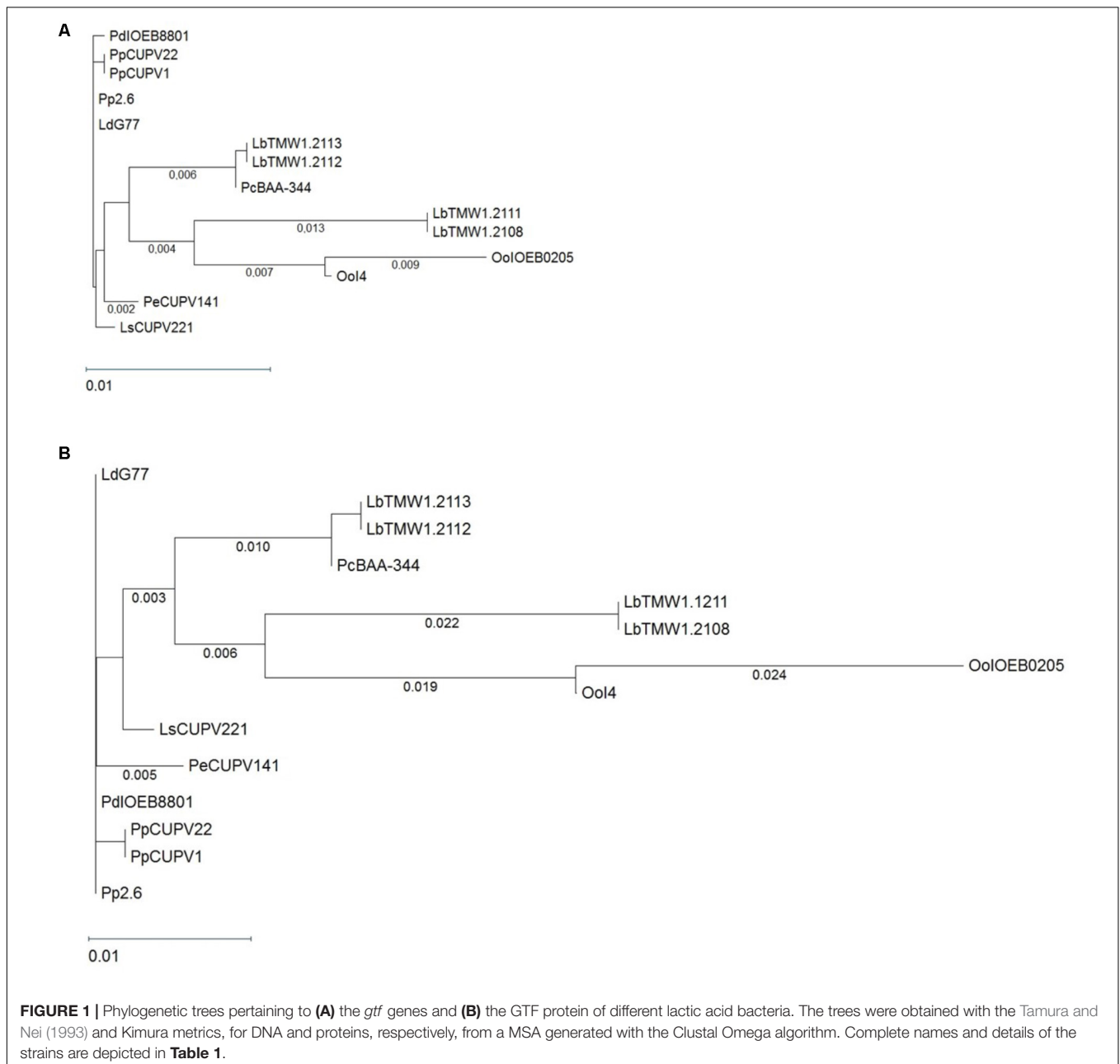
P. ethanolidurans CUPV141 Produces a HoPS

The mucosal (ropy) phenotype of some bacteria is related to the production of EPS (Torino et al., 2015), and among others, we have previously isolated the 2-substituted (1,3)- β -D-glucan-producing *P. parvulus* 2.6 strain from cider due to its ropy phenotype (Fernández et al., 1995). In the search for novel β -D-glucan-producing bacteria, the CUPV141 strain was isolated from a ropy cider and selected by its mucosal phenotype upon growth in a medium containing glucose. Determination of the nucleotide sequence of the 16S RNA coding gene (accession number in GenBank: MH298647) identified this strain as

P. ethanolidurans and, as far as we know, this is the first instance of isolation of this species from a ropy cider.

A specific ELISA method developed in our group (Werning et al., 2014) was used to test and quantify the production of the 2-substituted (1,3)- β -D-glucan by *P. ethanolidurans* CUPV141 cultures ($OD_{600\text{ nm}} = 1.0$), which amounted to 59.8 ± 4.8 mg/L. Afterwards, we proceeded to characterize the genetic determinant responsible for the β -D-glucan synthesis, which is synthesized by the GTF enzyme. Previously designed oligonucleotides (Werning et al., 2006) were used to amplify the *gtf* gene of CUPV141, and to determine its nucleotide sequence (accession number in GenBank: MH028492), which was compared to those of the *gtf* genes from GenBank at

the NCBI site. The BLASTn analysis revealed a 99% identity of the CUPV141 *gtf* with its homologs from *Lactobacillus suebicus* CUPV221, *Lactobacillus diolivorans* G77 (CUPV218) and *P. parvulus* CUPV22, CUPV1 and 2.6 strains isolated from Spanish cider and from *P. damnosus* IOEB8801 isolated from French wine, showing that these genes have evolved from a common ancestor. Thirteen *gtf* nucleotide sequences encoded by several LAB, belonging to the *Pediococcus*, *Lactobacillus*, and *Oenococcus* genera, were compared to that of CUPV141 strain to obtain the MSA depicted in **Supplementary Figure S1** and the phylogenetic unrooted tree shown in **Figure 1A**. According to the phylogenetic tree, the *gtf* gene is highly conserved among the species and genera studied, although the



MSA showed some nucleotide changes. Also, a high identity was observed between the *gtf* genes of *P. ethanolidurans* CUPV141 and *P. parvulus* 2.6, the reference bacterium for this gene. Only four changes, located at positions 86, 217, 1291, and 1524, differentiate these strains. The last was a silent mutation and the other three resulted in changes of the GTF of *P. parvulus* 2.6 (Trp29Leu, Leu73Phe, and H43Y). Thus, two divisions can be made according to the origin from which the species were isolated. The bacteria isolated from cider and *P. parvulus* IOEB8801 (from wine) are grouped together. All of them contain a plasmid harboring the *gtf* gene, except *L. suebicus* CUPV221 for which the location of the gene has not been established. The second division mainly grouped isolates from beer, besides two *O. oeni* strains isolated from champagne and cider, both described as having the *gtf* gene at a chromosomal localization. Taking into consideration this classification, there are also some mutations to emphasize. For instance, those having changes at positions 272, 1524, or 1548, where the majority of *gtf* genes of bacteria isolated from cider harbor two cytosines and one adenine, while the genes of beer isolates carry two thymines and one guanine, respectively. Moreover, the mutation in position 272 (a change Ala91Val) only occurred in the GTF of the isolates from cider. The other two were silent mutations. Although the physiological role of the 2-substituted (1,3)- β -D-glucan production is unknown, the high conservation of the *gtf* gene could be due to a bacterial adaptation to the alcoholic environment of the different beverages. The plasmidic location of the gene in the *Pediococcus* and *Lactobacillus* strains suggests a horizontal transfer of the gene, which might have conferred an evolutionary advantage.

The translated *P. ethanolidurans* CUPV141 *gtf* gene was used as a template for a BLASTp search. Most of the high identity hits coincided with those detected for the GTF enzymes, but the search also revealed identities, not detected at the nucleotide level, such as the GTF from *Propionibacterium freudenreichii* (33%) or the Tts glycosyltransferase of *S. pneumoniae* (36%). These results indicate a convergent functional evolution to yield glycosyltransferases encoded from unrelated genes. Similar results were reported for the GTF of *S. pneumoniae* Tts and *Propionibacterium freudenreichii* (Deutsch et al., 2008), and for those of *P. parvulus* 2.6, *P. damnosus* IOEB8801, and *O. oeni* 14 (Werning et al., 2006; Dols-Lafargue et al., 2008).

Moreover, the amino acid sequences of CUPV14 and 13 glycosyltransferases, encoded by related genes (Figure 1A) were aligned (Supplementary Figure S2). A phylogenetic tree was also generated (Figure 1B) disclosing a high degree of conservation, with small evolutionary distances among the GTF of different LAB species. Again, the species clustered according to the source from which they were isolated, with a clear grouping of the isolates from cider and beer, and high similarities in the active center of all the enzymes compared.

In addition, the differences in amino acids of the fourteen glycosyltransferases were assembled (Figure 2) in a previous topological prediction of the GTF of *P. parvulus* 2.6 and *L. diolivorans* G77 (CUPV218) (Werning et al., 2006). According to this model, the translated polypeptide seems to have four

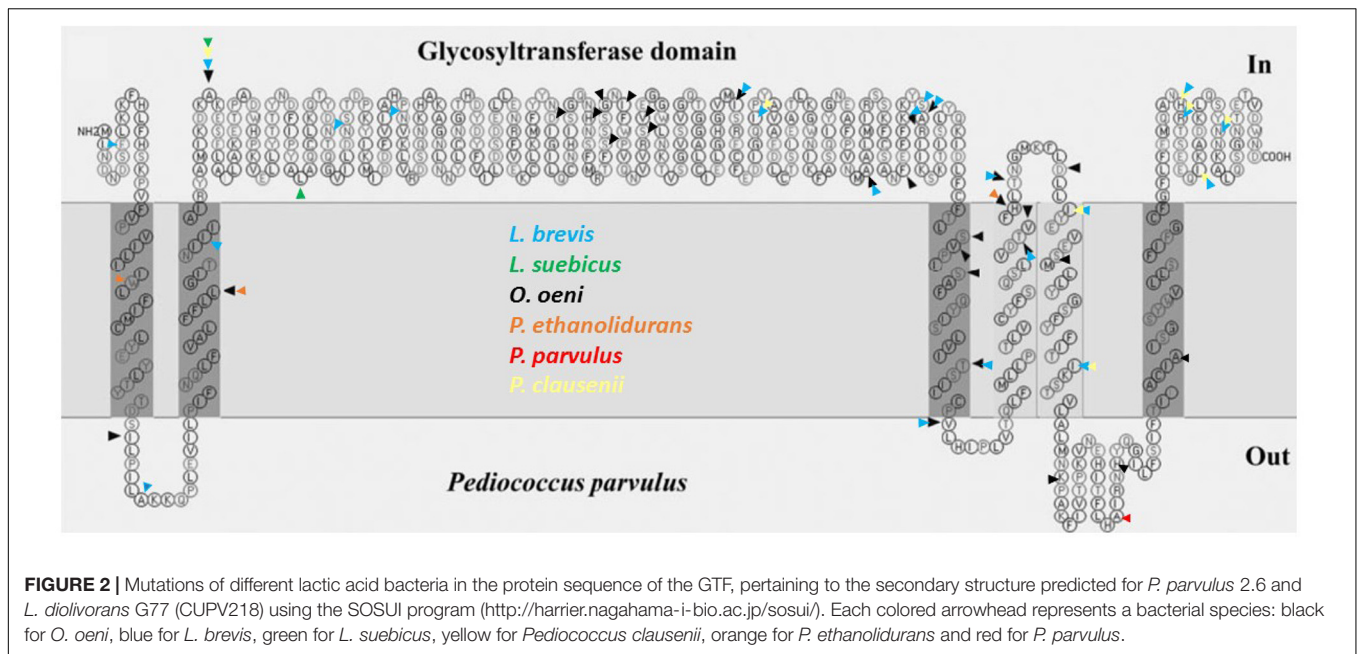
transmembrane regions at the C-terminal domain and two more at its N-terminus flanking the catalytic domain. This suggests that the enzyme synthesizes the EPS in the cytosol and that the active protein could be an oligomer of the polypeptide, which could form a membrane pore through which the polymer could be secreted to the environment. The alignment (Supplementary Figure S2) and superimposition (Figure 2) of the amino acid sequences revealed that the main differences are located at the transmembrane regions, which could be explained as an adaptation for optimal insertion into the membrane of each particular bacterium. Some variations were also observed in the sequence of the active center of the proteins, especially in *O. oeni* IOEB0205, but none of them affected the aspartic acid residues (Asp143, Asp198 and Asp200 or Asp295) that seem to constitute the essential catalytic tetrad (Werning et al., 2012). The GTF of *P. parvulus* CUPV1 and CUPV22 only differ with the enzyme of *P. parvulus* 2.6 in one amino acid (T489A), located at the loop between the fifth and sixth predicted transmembrane regions (Garai-Ibabe et al., 2010b). Finally, the four nucleotide mutations present in CUPV141 *gtf* gene resulted in three changes in the encoded polypeptide, L29W, F73L and Y431H, highlighted in orange in Figure 2 and located at the first, second, and fourth predicted transmembrane regions, respectively, and the fourth change in the nucleotide sequence in position 1524 resulted in a silent mutation.

Isolation and Partial Characterization of the EPS From *P. ethanolidurans* CUPV141

Culture media for routine growth often contain components that interfere with the quantification of the EPS released to the medium by bacteria, i.e., MRS medium (De Man et al., 1960). For this reason, SMD medium was used for the isolation of the EPS produced by CUPV141. As reported before (Velasco et al., 2006), the production of EPS can be affected by growth conditions, as well as by the growth media. Therefore the bacterial strain was cultivated for 48 h at two different pHs in SMD medium, giving a slightly higher production of EPS when the medium was adjusted to pH 5.5 (58.9 ± 2.2 mg/L) rather than pH 4.8 (53.5 ± 1.2 mg/L). Thus, for the subsequent isolation of EPS from the supernatants, both *Pediococcus* strains were grown in SMD medium at pH 5.5 for 48 h at 28°C in an atmosphere containing 5% CO₂.

The yield of EPS recovered from the supernatant of CUPV141 was 69 mg per liter of culture. Among the cider isolates, *P. parvulus* CUPV1 and *L. suebicus* CUPV221 produced similar amounts of EPS, while *P. parvulus* 2.6 or *P. parvulus* CUPV22 have been reported to produce 193 and 243 mg per liter, respectively (Garai-Ibabe et al., 2010a).

In order to elucidate the partial chemical structure of the EPS, several analyses were carried out. The polymer released to the medium by CUPV141 contained glucose as the major monosaccharide, and small amounts of galactose and galactosamine were also detected (less than 5%). In addition, a peak was identified as glycerol-3-phosphate using the NIST library included in the chromatographic software, which is an uncommon component of EPS from *Pediococcus* strains.



Methylation analysis gave evidence of three main units of partially methylated alditol acetates corresponding to terminal, 3-*O*-substituted and 2,3-di-*O*-substituted glucopyranose in relative proportions 1:1:1. In addition, the ¹H NMR spectrum of the EPS (**Figure 3**) showed the signals reported for the 2-substituted (1,3)-β-D-glucan of *P. parvulus* 2.6 (Dueñas-Chasco et al., 1997), which confirmed that *P. ethanolidurans* CUPV141 releases this β-D-glucan as the major extracellular polysaccharide. However, other minor components were identified in this EPS: (1,2)-galactopyranose, (1,6) and (1,3,6)-glucopyranose, and (1,4)-glucosamine, suggesting that *P. ethanolidurans* CUPV141 produced also a HePS. To the best of our knowledge, the production of both a HoPS and a HePS by *Pediococcus* strains has not been previously reported.

The *P. ethanolidurans* CUPV141NR Mutant Strain

Chemical mutagenesis of *P. parvulus* 2.6 resulted in the generation of the 2.6NR isogenic strain that did not produce β-D-glucan (Fernández et al., 1995). Therefore, with the aim of abolishing the production of the HoPS for further studies on the biological activity of the EPS, and for a better characterization of the HePS synthesized, *P. ethanolidurans* CUPV141 was subjected to chemical mutagenesis and the isogenic non-ropy CUPV141NR strain was generated. The Tts glycosyltransferase of *S. pneumoniae* serotype 37, which is homologous to the GTF of *P. parvulus* 2.6 and *P. ethanolidurans* CUPV141, synthesizes a capsular HoPS (Lull et al., 1999) very similar to the β-D-glucan produced by the pediococcal enzyme. Thus, anti-serotype 37 antibodies are able to agglutinate 2-substituted (1,3)-β-D-glucan-producing bacteria (Lull et al., 1999; Werning et al., 2006). Therefore, an evaluation of the HoPS production of the mutant and the parental strain by an agglutination immunoassay

with anti-serotype 37 antibodies was performed. The results revealed a clear difference between the aggregation capabilities of the two strains, showing, after a 24 h-incubation period, that *P. ethanolidurans* CUPV141 formed huge aggregates in the presence of the antibodies, while CUPV141NR strain produced small aggregates (**Figure 4**). These results suggested that the mutant strain still produced the β-D-glucan, although at very low levels. Specific quantification of the 2-substituted (1,3)-β-D-glucan with the ELISA immunoassay using anti-serotype 37 antibodies confirmed that, at an OD_{600 nm} = 1.0, the non-ropy CUPV141NR strain released 0.096 ± 0.002 mg/L of β-glucan to the supernatant, whereas the wild-type CUPV141 strain produced 42.40 ± 0.05 mg/L.

The recovery of EPS from the supernatant of CUPV141NR yielded 29 mg per liter of culture, a quantity much lower than that produced by the ropy strain. Acid hydrolysis of the EPS released glucose, galactose and glucosamine in a molar ratio 2.4:1:0.9, and the peak of glycerol-3-phosphate was observed again in the chromatogram. The main linkage types in the EPS, deduced from a methylation assay, revealed a polymer structurally different from the major β-glucan produced by the ropy strain, but with the same components detected in minor amounts in that preparation, namely: *O*-2 substituted galactopyranose, terminal glucopyranose, *O*-6, *O*-2,6, and *O*-3,6 substituted glucose, and *O*-4 substituted glucosamine. The proportion of terminal residues was far lower than that expected from the amount of branching points, which suggests that the glycerol 3-phosphate units detected in the hydrolysates may occupy terminal positions in the side chains of this branched polymer. Further analyses are needed to determine the structure of this polymer, but the current data confirm that *P. ethanolidurans* CUPV141 synthesizes and secretes at least two polysaccharides: the 2-substituted (1,3)-β-D-glucan and a HePS with glycerol-3-phosphate. This is the first instance of a *Pediococcus* strain producing both a HoPS and a

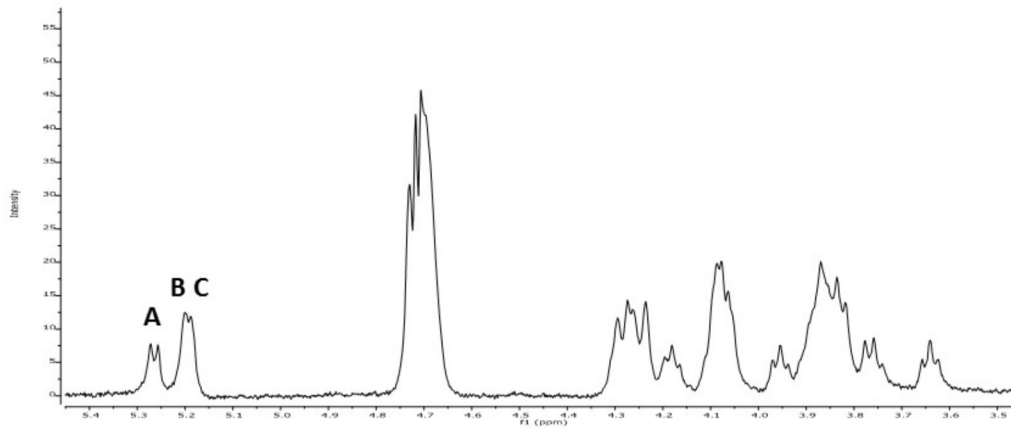


FIGURE 3 | ^1H RMN spectra of CUPV141 EPS recovered from the supernatant. A, B, and C signals correspond to the anomeric protons of terminal β -D-glucopyranose units, 3-linked- β -D-glucopyranose residues and 2,3-linked- β -D-glucopyranose units, respectively, as described in Dueñas-Chasco et al. (1997) for the 2-substituted (1,3)- β -D-glucan produced by *P. parvulus* 2.6.

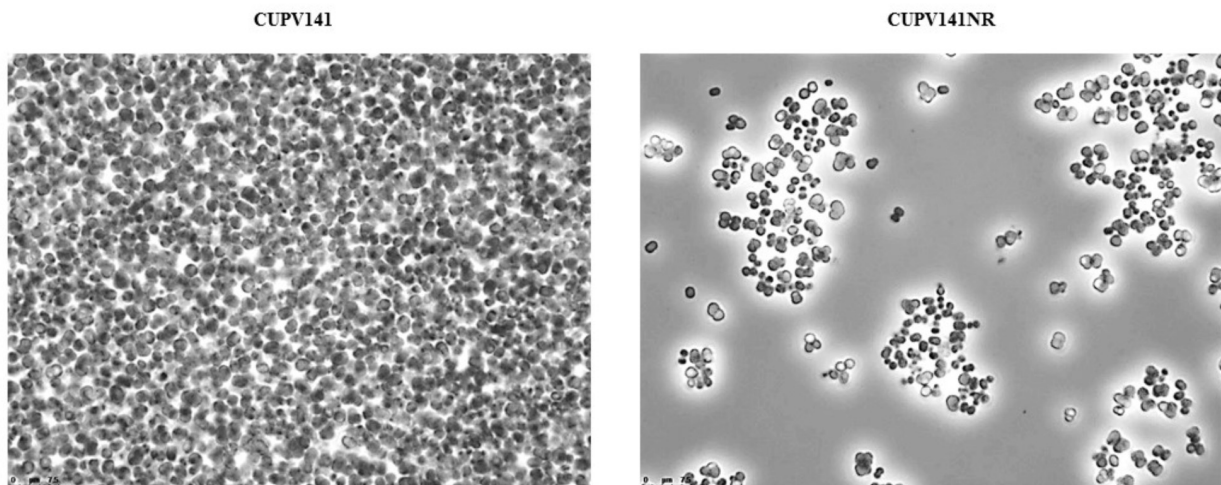


FIGURE 4 | Immunoagglutination in the presence of anti-serotype 37 antibody of (1,3)(1,2)- β -D-glucan producing *P. ethanolidurans* strains CUPV141 and CUPV141NR.

HePS, and the first report of a phosphorylated EPS in this genus, although other HePS with phosphorylated glycerol have been reported in *Lactobacillus delbrueckii* ssp. *bulgaricus* OLL 1073R-1 (Kitazawa et al., 1998), *Lactobacillus plantarum* EP56 (Tallon et al., 2003), and *Lactobacillus johnsonii* FI9785 (Dertli et al., 2013).

Detection of the Plasmidic Location of *P. ethanolidurans* *gtf* Gene

The *gtf* gene of *P. parvulus* 2.6 is located in the pPP2 plasmid, which is not present in the 2.6NR strain (Fernández et al., 1995; Werning et al., 2006; Pérez-Ramos et al., 2017b). Thus, by homology, the *gtf* gene in *P. ethanolidurans* CUPV141 could be located in a plasmid, and the reason for the non-ropy phenotype of the isogenic CUPV141NR strain could be the loss

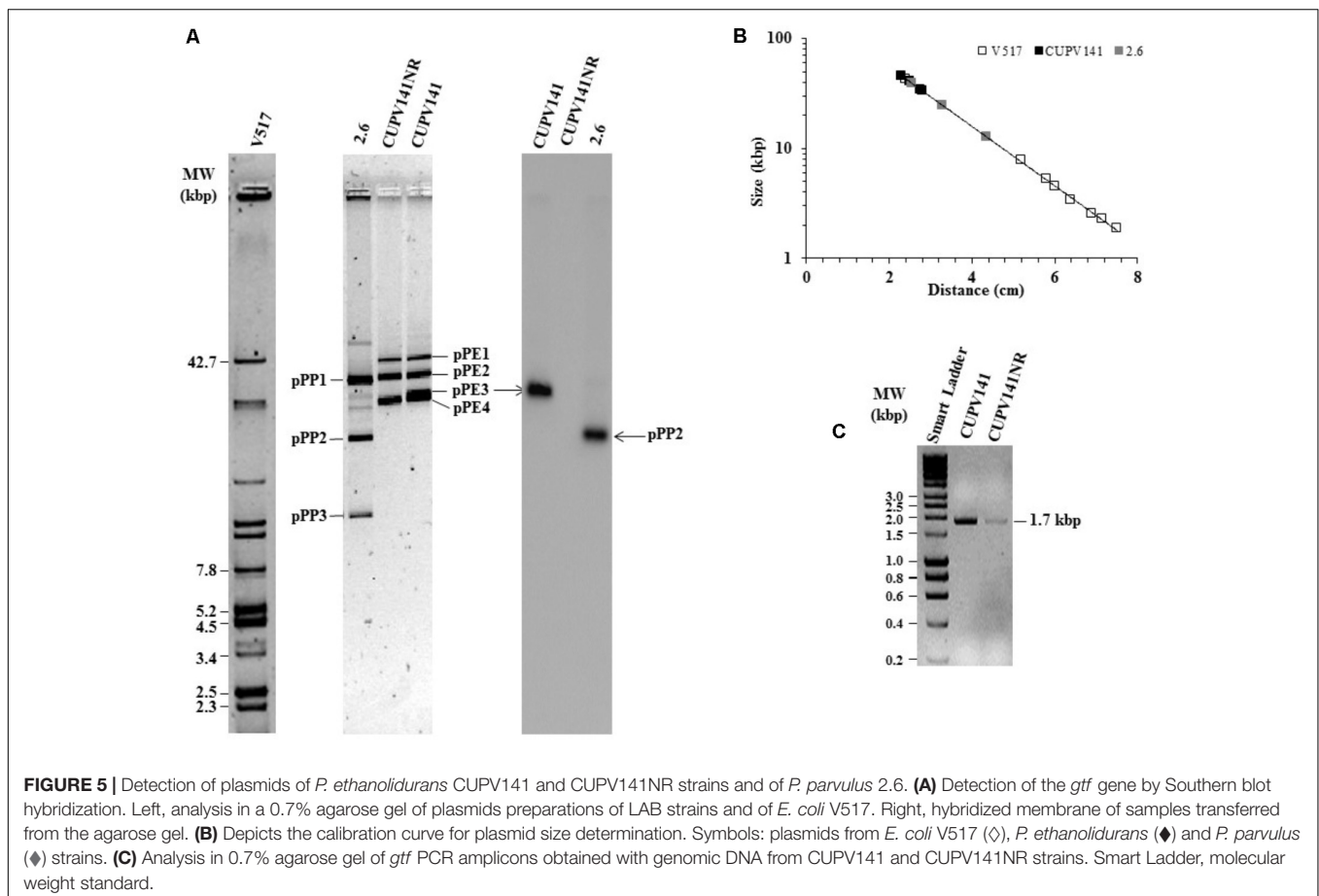
of this plasmid. To confirm this hypothesis, total plasmid DNA preparations from *P. ethanolidurans* CUPV141, CUPV141NR and *P. parvulus* 2.6 were purified by fractionation in a CsCl gradient to eliminate open circles and linear forms of the plasmids. Then, the purified plasmid DNA preparations were fractionated in an agarose gel (Figure 5A). As expected, three bands were detected in the preparation of *P. parvulus* 2.6 corresponding to the previously identified pPP1, pPP2, and pPP3 plasmids with molecular weights of 39.1, 24.5, and 12.7 kbp, respectively (Pérez-Ramos et al., 2017a and molecular weight inferred in Figure 5B). A different plasmidic pattern was detected in the *P. ethanolidurans* CUPV141 DNA preparation, including four bands, which should correspond to plasmids named pPE1, pPE2, pPE3, and pPE4 with an inferred molecular weight of 45.6, 40.2, 34.4, and 33.4 kbp, respectively (Figure 5B). Only three bands were observed in

the preparations of the *P. ethanolidurans* CUPV141NR strain, which lacked the pPE3 plasmid. Southern blot hybridization gave evidence of the presence of the *gtf* gene in *P. parvulus* 2.6 and in the *P. ethanolidurans* wild-type strain and not in the mutant (Figure 5A). Moreover, the hybridization bands revealed that pPE3 harbors the *gtf* gene in CUPV141, whose molecular weight differs from that of the pPP2 *gtf*-carrier plasmid in *P. parvulus* 2.6. The non-detection of *gtf* in the CUPV141NR strain correlated with its non-ropy phenotype, however, as stated above, the immunodetection and specific quantification of the (1,3)- β -D-glucan indicated that this bacterium produces low levels of the HoPS. This could be due to the presence of pPE3 in CUPV141NR with a low copy number undetectable by Southern blot hybridization. Thus, plasmidic DNA from both *Pediococcus* strains was used for the detection of the *gtf* gene by the more sensitive PCR amplification method. The reaction products were analyzed in agarose gel (Figure 5C), and the analysis revealed that the expected amplicon of 1.7 kbp had been generated with both plasmidic DNA preparations. However, the intensity of the band was very weak in the CUPV141NR DNA preparation even though a fivefold higher reaction volume, compared to that of CUPV141 DNA, was loaded in the gel (Figure 5C). Consequently, the overall results support a drastic decrease of the copy number of pPE3 as a consequence of the

novobiocin treatment of CUPV141 to generate the CUPV141NR strain.

Genetic Determinant of the Initiation of HePS Synthesis in *Pediococcus* Strains

HePS are synthesized by a more complex molecular mechanism than HoPS, which requires the action of several proteins. It is known that the first enzyme in the process is the p-GTF, which transfers the first phospho-sugar residue from an activated nucleotide sugar to the undecaprenyl phosphate-lipid carrier embedded in the membrane (Lebeer et al., 2009). The pGTF from *O. oeni* has been recently characterized (Dimopoulou et al., 2017), but no studies in *P. ethanolidurans* have been performed until now. Thus, the detection of the p-GTF coding gene was approached by PCR amplification of the highly conserved C-terminal sugar transferase domain of the enzyme, using degenerate primers previously described (Provencher et al., 2003). The nucleotide sequence of the obtained fragments was the same for the ropy and non-ropy strains. Furthermore, BLASTn analysis revealed 96, 85, and 74% identities with regions of genes encoding putative proteins annotated as a sugar transferase of *Lactobacillus sanfranciscensis* TMV1.1304, a glycosylphosphotransferase of *Vagococcus lutrae* MIS7, and a p-GTF of *Lactobacillus plantarum* 26.1, respectively. These nucleotide sequences were aligned using the Clustal Omega



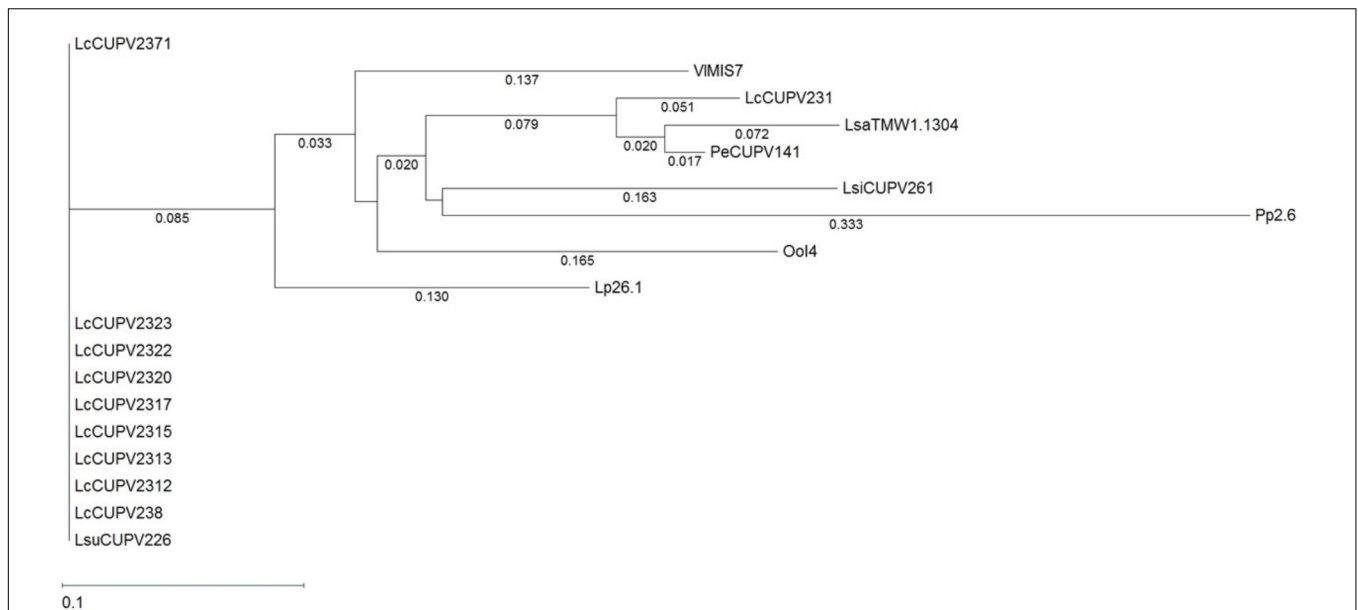


FIGURE 6 | Phylogenetic tree pertaining to the *p-gtf* gene nucleotide sequences of different lactic acid bacteria. The tree was obtained with the Tamura and Nei (1993) metric from a MSA generated with the Clustal Omega algorithm. Complete names and details of the strains are depicted in **Table 2**.

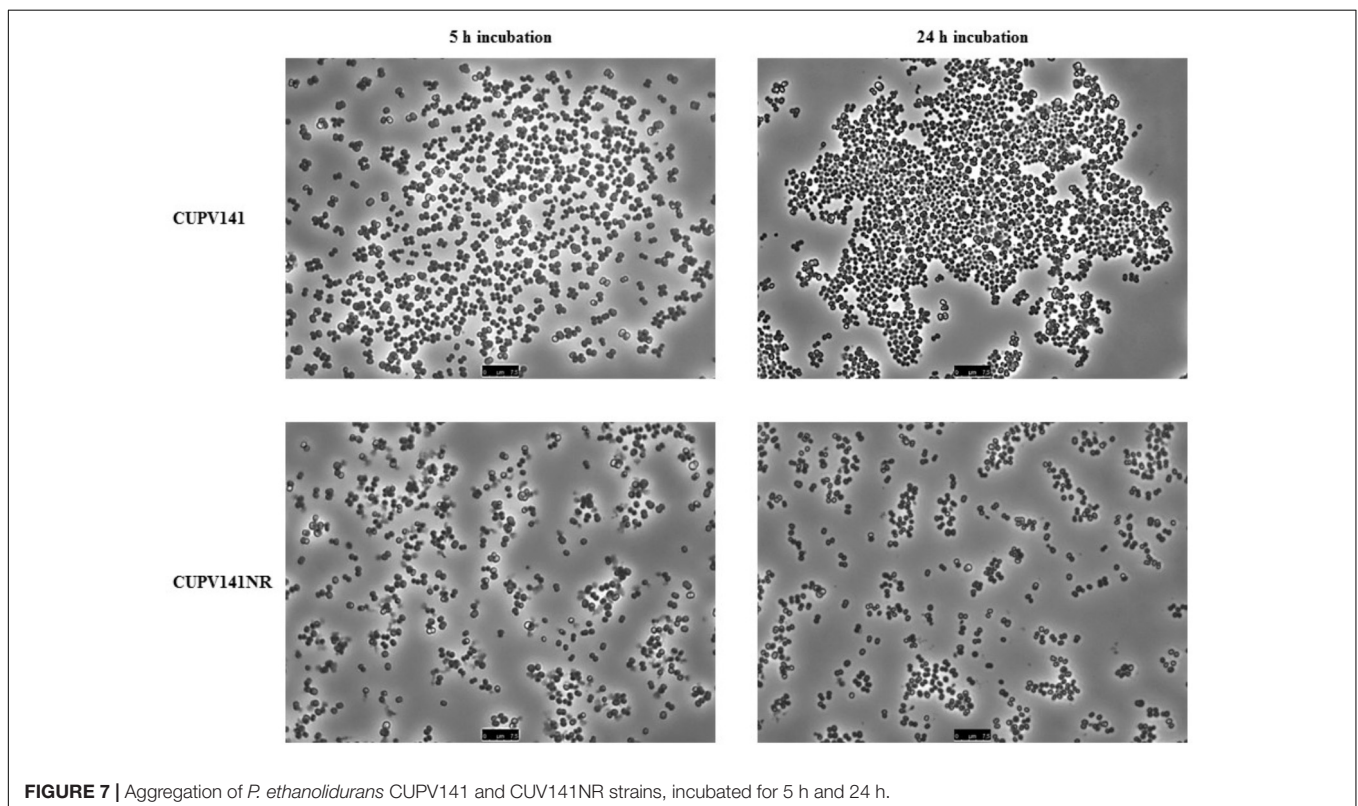
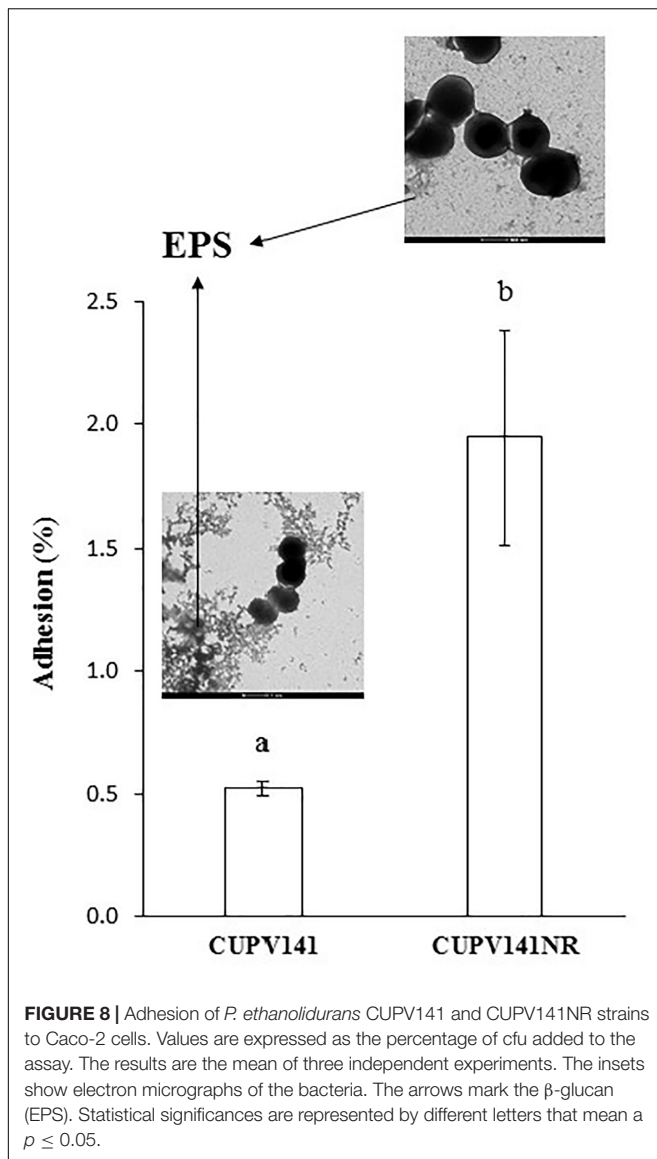


FIGURE 7 | Aggregation of *P. ethanolidurans* CUPV141 and CUPV141NR strains, incubated for 5 h and 24 h.

algorithm (**Supplementary Figure S3**) and a phylogenetic tree was also obtained (**Figure 6**). In addition, the MSA included a DNA sequence of a gene encoding a putative undecaprenyl-phosphate galactosephosphotransferase from the genome of *P. parvulus* 2.6 (Pérez-Ramos et al., 2016a), and the partial DNA

sequences of the *p-gtf* genes from different bacteria isolated from cider in a previous work (Puertas et al., 2018). The MSA showed a very poor conservation of the gene between different species. For instance, *P. parvulus* 2.6 showed three triplets more than the rest of the bacteria at position 125. However, the



homology was very high among different strains of *Lactobacillus collinoides*, as is also observed in the phylogenetic tree, except for the CUPV231 strain, which has an identity of 63.4% (104 out of 164 nucleotides) with the other *L. collinoides p-gtf* analyzed. The evolutionary distances between different species, which are depicted in the tree, would confirm this fact, being inexistent between *L. collinoides* strains. For the CUPV141 *p-gtf* DNA fragment, the amino acidic sequence of the encoded polypeptide was inferred with the EditSeq program and it was subjected to BLASTp analysis, where various hits were found. The amino acid sequences, like their corresponding coding ones, showed a high degree of identity among different strains of the same species, and less conservation between different species (**Supplementary Figure S4**). The C-terminal region of the LAB p-GTFs includes two blocks, B and C related, respectively, to either the interaction with the lipid carrier or conferring the specificity for sugar recognition (Wang et al., 1996). All of the amino acid sequences

aligned have a Glu at position 5 of block C except for that of *P. parvulus* 2.6, which carries a Phe (**Supplementary Figure S4**), previously proposed to be a catalytic residue (Van Kranenburg et al., 1999). In addition, two Tyr present in the C block had been proposed to be implicated in the phosphorylation of the enzyme in *S. thermophilus* (Minic et al., 2007). The one located at position 9 of the block is present in all of the sequences except for that of the 2.6 strain, which carries a phenylalanine (F), substitution that has no effect in the *S. thermophilus* p-GTF (Minic et al., 2007). In addition, an *in silico* analysis to find the genomic location of the *P. parvulus* 2.6 *p-gtf* gene revealed that it is included in a cluster of 11 genes involved in HePS synthesis and secretion (**Supplementary Figure S5**). Therefore, production of HePS by *Pediococcus* does not seem to be limited to the *P. ethanolidurans* species. However, we have never detected synthesis of HePS by the 2.6 strain and this could be due to lack of functionality of its p-GTF.

Analysis of the Adhesion Ability of the *P. ethanolidurans* CUPV141 and CUPV141NR Strains

To carry out this test, bacteria have to be sedimented and thus the supernatant containing part of the EPS is removed. Therefore, the concentration of the 2-substituted (1,3)- β -D-glucan bound to the bacteria after sedimentation and resuspension was determined by the specific ELISA immunoassay method prior to the analysis. As expected, the results revealed differences between the two strains, since CUPV141 and CUPV141NR carry 80.2 ± 6.0 ng/mL and $<0.30 \pm 0.06$ ng/mL HoPS, respectively. Consequently, a comparative analysis of the two strains analyzed should provide information on the contribution of the HoPS to adhesion.

First, the ability of the bacteria for self-aggregation was investigated (**Figure 7**). After 5 h of incubation, the culture of *P. ethanolidurans* CUPV141 showed some aggregates, whereas fewer complexes appeared in the culture of CUPV141NR. However, the differences at this incubation time were not very appreciable. By contrast, after 24 h of incubation the aggregates formed by the CUPV141 strain were bigger than those in the 5-h culture. An increase of aggregation of the CUPV141NR strain was not observed for the 5 h to 24 h incubation period. Thus, these results indicated that bacterial cell-to-cell interactions are mediated or potentiated by the 2-substituted (1,3)- β -D-glucan.

Secondly, the capacity of *P. ethanolidurans* CUPV141 and CUPV141NR to interact with human epithelial cells was also assessed using the enterocyte-like Caco-2 cell line (**Figure 8**). Visualization of the two strains by TEM (inset in **Figure 8**) showed differences in EPS production, which in CUPV141 formed a kind of net in the medium, while in CUPV141NR appeared as small aggregates. The ability of both strains to bind the enterocytes was significantly lower than that reported by Fernández De Palencia et al. (2008) for the commercial probiotic *Lactobacillus acidophilus* La-5 (7%). However, comparing the two strains described in this work, the non-ropy bacterium showed higher adhesion ($1.95 \pm 0.44\%$) to the eukaryotic cells than the ropy strain ($0.52 \pm 0.03\%$), which can be attributed to the presence of the phosphorylated HePS. Phosphate groups increase

TABLE 1 | Bacterial strains used for the *gtf* MSA and their codes.

Code	Strain	<i>gtf</i> gene location	Source of isolation	Reference
Pediococcus				
PeCUPV141	<i>P. ethanolidurans</i> CUPV141	Plasmid pPE3	Cider	This work
Pp2.6	<i>P. parvulus</i> 2.6	Plasmid pPP2	Cider	Werning et al., 2006
PpCUPV1	<i>P. parvulus</i> CUPV1	Plasmid	Cider	Garai-Ibabe et al., 2010a
PpCUPV22	<i>P. parvulus</i> CUPV22	Plasmid	Cider	
PdIOEB8801	<i>P. damnosus</i> IOEB8801	Plasmid pF8801	Red wine	Gindreau et al., 2001
PcBAA-344	<i>P. claussenii</i> ATCC BAA-344	Plasmid	Beer	Pittet et al., 2012
Oenococcus				
Ool4	<i>O. oeni</i> 14	Chromosome	Cider	Werning et al., 2006
OoIOEB0205	<i>O. oeni</i> IOEB205	Chromosome	Champagne	Dols-Lafargue et al., 2008
Lactobacillus				
LsCUPV221	<i>L. suebicus</i> CUPV221	Unknown	Cider	Garai-Ibabe et al., 2010b
LdG77	<i>L. diolivorans</i> G77 = CUPV218	Plasmid pLD1	Cider	Werning et al., 2006
LbTMV1.2108	<i>L. brevis</i> TMV1.2108	Plasmid pl12108-6	Beer	Fraunhofer et al., 2018
LbTMV1.2111	<i>L. brevis</i> TMV1.2111	Plasmid pl12111-5	Beer	Fraunhofer et al., 2018
LbTMV1.2112	<i>L. brevis</i> TMV1.2112	Plasmid pl12112-4	Beer	Fraunhofer et al., 2018
LbTMV1.2113	<i>L. brevis</i> TMV1.2113	Plasmid pl12113-4	Brewery surface	Fraunhofer et al., 2018

TABLE 2 | Bacterial strains used for the *p-gtf* MSA and their codes.

Code	Strain	Source of isolation	Reference
PeCUPV141	<i>P. ethanolidurans</i> CUPV141	Cider	This work
Pp2.6	<i>P. parvulus</i> 2.6	Cider	Pérez-Ramos et al., 2016a
Lp26.1	<i>L. plantarum</i> 26.1	Dairy and cereals	Van der Meulen et al., 2007
LsaTMV1.1304	<i>L. sanfranciscensis</i> TMV1.1304	Sourdough	Vogel et al., 2011
LsiCUPV261	<i>L. sicerae</i> CUPV261	Cider	Puertas et al., 2018
LsuCUPV226	<i>L. suebicus</i> CUPV226	Cider	Puertas et al., 2018
LcCUPV238	<i>L. collinoides</i> CUPV238	Cider	Puertas et al., 2018
LcCUPV2312	<i>L. collinoides</i> CUPV2312	Cider	Puertas et al., 2018
LcCUPV2313	<i>L. collinoides</i> CUPV2313	Cider	Puertas et al., 2018
LcCUPV2315	<i>L. collinoides</i> CUPV2315	Cider	Puertas et al., 2018
LcCUPV2317	<i>L. collinoides</i> CUPV2317	Cider	Puertas et al., 2018
LcCUPV2320	<i>L. collinoides</i> CUPV2320	Cider	Puertas et al., 2018
LcCUPV2322	<i>L. collinoides</i> CUPV2322	Cider	Puertas et al., 2018
LcCUPV2323	<i>L. collinoides</i> CUPV2323	Cider	Puertas et al., 2018
LcCUPV2371	<i>L. collinoides</i> CUPV2371	Cider	Puertas et al., 2018
LcCUPV231	<i>L. collinoides</i> CUPV231	Cider	Puertas et al., 2018
Ool4	<i>O. oeni</i> 14	Cider	Puertas et al., 2018
VIMIS7	<i>Vagococcus lutrae</i> MIS7	Fermented food	Unpublished, GenBank: AGM39429.1

the net charge of the EPS and can be very important to mediate the interactions between bacteria and their hosts, as reported for several *Lactobacillus* strains (Kitazawa et al., 1998; Tallon et al., 2003; Dertli et al., 2013). Similarly, chemical phosphorylation of a dextran produced by *Leuconostoc mesenteroides* enhanced its immunostimulatory capacity (Sato et al., 2004). For neutral EPS, some authors have reported that their presence in the surface of bacteria has a negative effect in their adhesive properties (López et al., 2012; Castro-Bravo et al., 2017; Náchter-Vázquez et al., 2017), while others described the production of these polymers as useful for probiotics to interact with eukaryotic cells (Fernández de Palencia et al., 2009; Garai-Ibabe et al., 2010b; Živković et al., 2016).

The positive effect of the HoPS on binding to intestinal cells was demonstrated for the β -glucan-producing *P. parvulus* 2.6 and CUPV22 strains, which showed adhesion capacities to Caco-2 cells of 6.1 and 10.5%, respectively, that were reduced when the EPS was removed by washing prior to the binding assay (Fernández de Palencia et al., 2009; Garai-Ibabe et al., 2010b). Thus, the different behavior of the CUPV141 ropy strain could be due to its lower production of 2-substituted (1,3)- β -D-glucan. The overall results obtained for *P. ethanolidurans* illustrate the different roles of the two polysaccharides produced by this species: there is an involvement of the 2-substituted (1,3)- β -D-glucan in cell-to-cell adhesion, while the HePS would lead these bacteria to interact with eukaryotic cells, for colonization of new

environments. However, further research would be necessary for the elucidation of the mechanism through which these kinds of adhesions take place.

CONCLUSION

Bacterial EPS (especially from LAB) are currently exploited in the food and beverage industries as the fermented products have improved texture and flavor. There is evidence that consumption of such products can have health benefits. This in turn has led to research to specifically identify EPS that could be potentially developed as medicines for human and animal use (Castro-Bravo et al., 2017; Dimopoulou et al., 2018; Pérez-Ramos et al., 2017a,b, 2018). Therefore, in the search for novel bacterial producers of the extracellular 2-substituted-(1,3)- β -D-glucan, we isolated a *P. ethanolidurans* (CUPV141) strain for the first time from a ropy cider of the Basque Country. In this work, we demonstrate that this isolate secretes not only that β -glucan, but also a HePS composed of glucose, galactose, glucosamine, and glycerol-3-phosphate, being the first *Pediococcus* strain described to produce this kind of polymer. However, our *in silico* analysis of priming-glycosyltransferase coding genes involved in HePS synthesis suggests that this is a general characteristic shared by different pediococci. Southern blot hybridization allowed localizing the GTF-coding gene responsible for the synthesis of the β -D-glucan in a 34.4 kbp-pPE3 plasmid of this strain. The role of the HoPS in bacterial self-aggregation, as well as the most relevant role of the HePS in bacteria-eukaryotic cells interactions were inferred from interactomic experiments using the ropy and the non-ropy strains. Nevertheless, the molecular mechanisms by which *P. ethanolidurans* performs biotic interactions, the detailed structure of the HePS produced by this strain, and its existence in other pediococci remain unknown and deserve further work.

DATA AVAILABILITY

All datasets generated for this study are included in the manuscript and the **Supplementary Files**.

AUTHOR CONTRIBUTIONS

ML-A was responsible for the manuscript's preparation and performed the majority of the assays described. AP-R was

REFERENCES

- Arahal, D. R., Sánchez, E., Macián, M. C., and Garay, E. (2008). Value of recN sequences for species identification and as a phylogenetic marker within the family "Leuconostocaceae." *Int. Microbiol.* 11, 33–39. doi: 10.2436/20.1501.01.42
- Badel, S., Bernardi, T., and Michaud, P. (2011). New perspectives for lactobacilli exopolysaccharides. *Biotechnol. Adv.* 29, 54–66. doi: 10.1016/j.biotechadv.2010.08.011
- Bajpai, V. K., Rather, I. A., Majumder, R., Shukla, S., Aeron, A., Kim, K., et al. (2016). Exopolysaccharide and lactic acid bacteria: perception, functionality and prospects. *Bangladesh J. Pharmacol.* 11, 1–23. doi: 10.3329/bjp.v11i1.23819

responsible for the extraction of the plasmids and the performance of the southern-blot hybridization assay. AP was responsible for the strain identification and determination of the DNA sequences of the priming-GTF coding gene from different LAB isolated from cider. AP was responsible for the planning of the experimental work and for the performance of the methylation and monosaccharide composition analysis in the characterization of the EPS. In addition, she participated in the manuscript corrections. PL and MD contributed to the discussions of the results, had a critical reading of the manuscript and corrected it.

FUNDING

This work was supported by a grant from the Department of Environment, Territorial Planification, Agriculture and Fishing and the project no. IT 866-13 from the Basque Government and by the Spanish Ministry of Science and Innovation (AGL 2015-65010-C3-1-R).

ACKNOWLEDGMENTS

We thank Dr. Guillermo Padilla Alonso for his valuable assistance in the bio-statistical analysis and Dr. Stephen Elson for the critical reading of the manuscript. Technical and human support by Mariano Barrado, Ph.D. (Microscopy Facility) and José I. Miranda, Ph.D. (NMR facility) of the general services of investigation (SGIker) at the University of Basque Country (UPV/EHU) and by Leonor Rodríguez (Ph.D.) and Mercedes Sánchez of the Gas Chromatography Facility of the CIB-CSIC are also gratefully acknowledged. We acknowledge support of the publication fee by the CSIC Open Access Publication Support Initiative through its Unit of Information Resources for Research (URICI).

SUPPLEMENTARY MATERIAL

The Supplementary Material for this article can be found online at: <https://www.frontiersin.org/articles/10.3389/fmicb.2018.02041/full#supplementary-material>

- Caggianiello, G., Kleerebezem, M., and Spano, G. (2016). Exopolysaccharides produced by lactic acid bacteria: from health-promoting benefits to stress tolerance mechanisms. *Appl. Microbiol. Biotechnol.* 100, 3877–3886. doi: 10.1007/s00253-016-7471-2
- Castro-Bravo, N., Hidalgo-Cantabrana, C., Rodríguez Carvajal, M. A., Ruas-Madiedo, P., and Margolles, A. (2017). Gene replacement and fluorescent labeling to study the functional role of exopolysaccharides in *Bifidobacterium animalis* subsp. *lactis*. *Front. Microbiol.* 8:1405. doi: 10.3389/fmicb.2017.01405
- De Man, J. C., Rogosa, M., and Sharpe, M. E. (1960). A medium for the cultivation of lactobacilli. *J. Appl. Bacteriol.* 23, 130–135. doi: 10.1111/j.1365-2672.1960.tb00188.x
- De Vuyst, L., De Vin, F., Vanangelgem, F., and Degeest, B. (2001). Recent developments in the biosynthesis and applications of heteropolysaccharides

- from lactic acid bacteria. *Int. Dairy J.* 11, 687–707. doi: 10.1016/S0958-6946(01)00114-5
- De Vuyst, L., Zamfir, M., Mozzi, F., Adriany, T., Marshall, V., Degeest, B., et al. (2003). Exopolysaccharide-producing *Streptococcus thermophilus* strains as functional starter cultures in the production of fermented milks. *Int. Dairy J.* 13, 707–717. doi: 10.1016/S0958-6946(03)00105-5
- Dertli, E., Colquhoun, I. J., Gunning, A. P., Bongaerts, R. J., Le Gall, G., Bonev, B. B., et al. (2013). Structure and biosynthesis of two exopolysaccharides produced by *Lactobacillus johnsonii* F19785. *J. Biol. Chem.* 288, 31938–31951. doi: 10.1074/jbc.M113.507418
- Deutsch, S. M., Falentin, H., Dols-Lafargue, M., LaPointe, G., and Roy, D. (2008). Capsular exopolysaccharide biosynthesis gene of *Propionibacterium freudenreichii* subsp. *shermanii*. *Int. J. Food Microbiol.* 125, 252–258. doi: 10.1016/j.ijfoodmicro.2008.04.006
- Dimopoulou, M., Claisse, O., Dutilh, L., Miot-Sertier, C., Ballestra, P., Lucas, P. M., et al. (2017). Molecular cloning, expression and characterization of *Oenococcus oeni* priming glycosyltransferases. *Mol. Biotechnol.* 59, 323–333. doi: 10.1007/s12033-017-0021-z
- Dimopoulou, M., Raffenne, J., Claisse, O., Miot-Sertier, C., Iturmendi, N., Moine, V., et al. (2018). *Oenococcus oeni* exopolysaccharide biosynthesis, a tool to improve malolactic starter performance. *Front. Microbiol.* 9:1276. doi: 10.3389/fmicb.2018.01276
- Dols-Lafargue, M., Lee, H. Y., Le Marrec, C., Heyraud, A., Chambat, G., and Lonvaud-Funel, A. (2008). Characterization of *gtf*, a glucosyltransferase gene in the genomes of *Pediococcus parvulus* and *Oenococcus oeni*, two bacterial species commonly found in wine. *Appl. Environ. Microbiol.* 74, 4079–4090. doi: 10.1128/AEM.00673-08
- Dubois, M., Gilles, K., Hamilton, J., Rebers, P., and Smith, F. (1956). Colorimetric method for determination of sugars and related substances. *Anal. Chem.* 28, 350–356. doi: 10.1021/ac60111a017
- Dueñas, M., Irastorza, A., Fernández, K., and Bilbao, A. (1995). Heterofermentative *Lactobacilli* causing ropiness in Basque Country ciders. *J. Food Prot.* 58, 76–80. doi: 10.4315/0362-028X-58.1.76
- Dueñas-Chasco, M. T., Rodríguez-Carvajal, M. A., Tejero Mateo, P., Franco-Rodríguez, G., Espartero, J. L., Irastorza-Iribas, A., et al. (1997). Structural analysis of the exopolysaccharide produced by *Pediococcus damnosus* 2.6. *Carbohydr. Res.* 303, 453–458. doi: 10.1016/S0008-6215(97)00192-4
- Ehrmann, M. A., Müller, M. R. A., and Vogel, R. F. (2003). Molecular analysis of sourdough reveals *Lactobacillus mindensis* sp. nov. *Int. J. Syst. Evol. Microbiol.* 53, 7–13. doi: 10.1099/ijs.0.02202-0
- Fernández, K., Dueñ, M., Irastorza, A., Bilbao, A., and Del Campo, G. (1995). Characterization and DNA plasmid analysis of ropy *Pediococcus* spp. strains isolated from Basque Country ciders. *J. Food Prot.* 59, 35–40. doi: 10.4315/0362-028X-59.1.35
- Fernández De Palencia, P., López, P., Corbí, A. L., Peláez, C., and Requena, T. (2008). Probiotic strains: survival under simulated gastrointestinal conditions, in vitro adhesion to Caco-2 cells and effect on cytokine secretion. *Eur. Food Res. Technol.* 227, 1475–1484. doi: 10.1007/s00217-008-0870-6
- Fernández de Palencia, P., Werning, M. L., Sierra-Filardi, E., Dueñas, M. T., Irastorza, A., Corbí, A. L., et al. (2009). Probiotic properties of the 2-substituted (1,3)- β -D-glucan-producing bacterium *Pediococcus parvulus* 2.6. *Appl. Environ. Microbiol.* 75, 4887–4891. doi: 10.1128/AEM.00394-09
- Fraunhofer, M. E., Geissler, A. J., Wefers, D., Bunzel, M., Jakob, F., and Vogel, R. F. (2018). Characterization of β -glucan formation by *Lactobacillus brevis* TMW 1.2112 isolated from slimy spoiled beer. *Int. J. Biol. Macromol.* 107, 874–881. doi: 10.1016/j.ijbiomac.2017.09.063
- Garai-Ibabe, G., Areizaga, J., Aznar, R., Elizaquivel, P., Prieto, A., Irastorza, A., et al. (2010a). Screening and selection of 2-branched (1,3)- β -D-glucan producing lactic acid bacteria and exopolysaccharide characterization. *J. Agric. Food Chem.* 58, 6149–6156. doi: 10.1021/jf904529q
- Garai-Ibabe, G., Dueñas, M. T., Irastorza, A., Sierra-Filardi, E., Werning, M. L., López, P., et al. (2010b). Naturally occurring 2-substituted (1,3)- β -D-glucan producing *Lactobacillus suebicus* and *Pediococcus parvulus* strains with potential utility in the production of functional foods. *Bioresour. Technol.* 101, 9254–9263. doi: 10.1016/j.biortech.2010.07.050
- Gindreau, E., Walling, E., and Lonvaud-Funel, A. (2001). Direct polymerase chain reaction detection of ropy *Pediococcus damnosus* strains in wine. *J. Appl. Microbiol.* 90, 535–542. doi: 10.1046/j.1365-2672.2001.01277.x
- Hidalgo-Cantabrana, C., Sánchez, B., Moine, D., Berger, B., de los Reyes-Gavilán, G., Gueimonde, M., et al. (2013). Insights into the ropy phenotype of the exopolysaccharide-producing strain *Bifidobacterium animalis* subsp. *lactis* A1dOxR. *Appl. Environ. Microbiol.* 79, 3870–3874. doi: 10.1128/AEM.00633-13
- Ibarburu, I., Puertas, A. I., Berregi, I., Rodríguez-Carvajal, M. A., Prieto, A., and Dueñas, M. T. (2015). Production and partial characterization of exopolysaccharides produced by two *Lactobacillus suebicus* strains isolated from cider. *Int. J. Food Microbiol.* 214, 54–62. doi: 10.1016/j.ijfoodmicro.2015.07.012
- Ibarburu, I., Soria-Díaz, M. E., Rodríguez-Carvajal, M. A., Velasco, S. E., Tejero-Mateo, P., Gil-Serrano, A. M., et al. (2007). Growth and exopolysaccharide (EPS) production by *Oenococcus oeni* 14 and structural characterization of their EPSs. *J. Appl. Microbiol.* 103, 477–486. doi: 10.1111/j.1365-2672.2006.03266.x
- Kanamarpaludi, S. L. R. K., and Muddada, S. (2017). Characterization of exopolysaccharide produced by *Streptococcus thermophilus* CC30. *Biomed. Res. Int.* 2017, 1–11. doi: 10.1155/2017/4201809
- Kim, O. S., Cho, Y. J., Lee, K., Yoon, S. H., Kim, M., Na, H., et al. (2012). Introducing EzTaxon-e: a prokaryotic 16S rRNA gene sequence database with phylogenies that represent uncultured species. *Int. J. Syst. Evol. Microbiol.* 62, 716–721. doi: 10.1099/ijs.0.038075-0
- Kimura, M. (1983). *The Neutral Theory of Molecular Evolution*. Cambridge: Cambridge University Press. doi: 10.1017/CBO9780511623486
- Kitazawa, H., Harata, T., Uemura, J., Saito, T., Kaneko, T., and Itoh, T. (1998). Phosphate group requirement for mitogenic activation of lymphocytes by an extracellular phosphopolysaccharide from *Lactobacillus delbrueckii* ssp. *bulgaricus*. *Int. J. Food Microbiol.* 40, 169–175. doi: 10.1016/S0168-1605(98)00030-0
- Leber, S., Verhoeven, T. L. A., Francius, G., Schoofs, G., Lambrichts, I., Dufrière, Y., et al. (2009). Identification of a gene cluster for the biosynthesis of a long, galactose-rich exopolysaccharide in *Lactobacillus rhamnosus* GG and functional analysis of the priming glycosyltransferase. *Appl. Environ. Microbiol.* 75, 3554–3563. doi: 10.1128/AEM.02919-08
- Lee, I. C., Caggianiello, G., van Swam, I. I., Taverne, N., Meijerink, M., Bron, P. A., et al. (2016). Strain-specific features of extracellular polysaccharides and their impact on *Lactobacillus plantarum*-host interactions. *Appl. Environ. Microbiol.* 82, 3959–3970. doi: 10.1128/AEM.00306-16
- Llaubères, R. M., Richard, B., Lonvaud, A., and Dubourdieu, D. (1990). Structure of an exocellular β -D-glucan from *Pediococcus* sp., a wine lactic bacteria. *Carbohydr. Res.* 203, 103–107. doi: 10.1016/0008-6215(90)80049-9
- Llull, D., Muñoz, R., López, R., and García, E. (1999). A single gene (*tts*) located outside the cap locus directs the formation of *Streptococcus pneumoniae* type 37 capsular polysaccharide: type 37 Pneumococci are natural, genetically binary strains. *J. Exp. Med.* 190, 241–251. doi: 10.1084/jem.190.2.241
- Lonvaud-Funel, A., Guilloux, Y., and Joyeux, A. (1993). Isolation of a DNA probe for identification of glucan-producing *Pediococcus damnosus* in wines. *J. Appl. Microbiol.* 74, 41–47. doi: 10.1111/j.1365-2672.1993.tb02994.x
- Lonvaud-Funel, A., and Joyeux, A. (1988). Une altération bactérienne des vins: la “maladie des vins filants.”. *Sci. Aliment.* 8, 33–49.
- López, P., Monteserín, D. C., Gueimonde, M., de los Reyes-Gavilán, C. G., Margolles, A., Suárez, A., et al. (2012). Exopolysaccharide-producing *Bifidobacterium* strains elicit different *in vitro* responses upon interaction with human cells. *Food Res. Int.* 46, 99–107. doi: 10.1016/j.foodres.2011.11.020
- Macrina, F. L., Kopecko, D. J., Jones, K. R., Ayers, D. J., and McCowen, S. M. (1978). A multiple plasmid-containing *Escherichia coli* strain: convenient source of size reference plasmid molecules. *Plasmid* 1, 417–420. doi: 10.1016/0147-619X(78)90056-2
- Minic, Z., Marie, C., Delorme, C., Faurie, J. M., Mercier, G., Ehrlich, D., et al. (2007). Control of EpsE, the phosphoglycosyltransferase initiating exopolysaccharide synthesis in *Streptococcus thermophilus*, by EpsD tyrosine kinase. *J. Bacteriol.* 189, 1351–1357. doi: 10.1128/JB.01122-06
- Nácher-Vázquez, M., Iturria, I., Zarour, K., Mohedano, M. L., Aznar, R., Pardo, M. Á., et al. (2017). Dextran production by *Lactobacillus sakei* MN1 coincides with reduced autoagglutination, biofilm formation and epithelial cell adhesion. *Carbohydr. Polym.* 168, 22–31. doi: 10.1016/j.carbpol.2017.03.024
- Notararigo, S., Nácher-Vázquez, M., Ibarburu, I., Werning, M. L., Fernández de Palencia, P., Dueñas, M. T., et al. (2013). Comparative analysis of production and purification of homo- and hetero-polysaccharides produced by lactic acid bacteria. *Carbohydr. Polym.* 94, 57–64. doi: 10.1016/j.carbpol.2012.05.016

- Pérez-Ramos, A., Mohedano, M. L., López, P., Spano, G., Fiocco, D., Russo, P., et al. (2017a). In situ β -Glucan fortification of cereal-based matrices by *Pediococcus parvulus* 2.6: technological aspects and prebiotic potential. *Int. J. Mol. Sci.* 18:1588. doi: 10.3390/ijms18071588
- Pérez-Ramos, A., Werning, M. L., Prieto, A., Russo, P., Spano, G., Mohedano, M. L., et al. (2017b). Characterization of the sorbitol utilization cluster of the probiotic *Pediococcus parvulus* 2.6: genetic, functional and complementation studies in heterologous hosts. *Front. Microbiol.* 8:2393. doi: 10.3389/fmicb.2017.02393
- Pérez-Ramos, A., Mohedano, M. L., Pardo, M. A., and López, P. (2018). β -Glucan-Producing *Pediococcus parvulus* 2.6: test of probiotic and immunomodulatory properties in Zebrafish models. *Front. Microbiol.* 9:1684. doi: 10.3389/fmicb.2018.01684
- Pérez-Ramos, A., Mohedano, M. L., Puertas, A., Lamontanara, A., Orru, L., Spano, G., et al. (2016a). Draft genome sequence of *Pediococcus parvulus* 2.6, a probiotic β -glucan producer strain. *Am. Soc. Microbiol. Genome Announc.* 4, 1–2. doi: 10.1128/genomeA.01141-15
- Pérez-Ramos, A., Nacher-Vázquez, M., Notararigo, S., López, P., and Mohedano, M. L. (2016b). "Current and future applications of bacterial extracellular polysaccharides," in *Probiotics, Prebiotics and Synbiotics: Bioactive Foods in Health Promotion*, eds R. R. Watson and V. R. Preedy (London: Academic Press), 329–344.
- Pittet, V., Abegunde, T., Marfleet, T., Haakensen, M., Morrow, K., Jayaprakash, T., et al. (2012). Complete genome sequence of the beer spoilage organism *Pediococcus clausenii* ATCC BAA-344^T. *J. Bacteriol.* 194, 1271–1272. doi: 10.1128/JB.06759-11
- Provencher, C., LaPointe, G., Sirois, S., Van Calsteren, M. R., and Roy, D. (2003). Consensus-degenerate hybrid oligonucleotide primers for amplification of priming glycosyltransferase genes of the exopolysaccharide locus in strains of the *Lactobacillus casei* group. *Appl. Environ. Microbiol.* 69, 3299–3307. doi: 10.1128/AEM.69.6.3299
- Puertas, A. I., Ibarburu, I., Elizaquível, P., Zuriarrain, A., Berregi, I., López, P., et al. (2018). Disclosing diversity of exopolysaccharide-producing lactobacilli from Spanish natural ciders. *Food Sci. Technol.* 90, 469–474. doi: 10.1016/j.lwt.2017.12.048
- Ravyts, F., de Vuyst, L., and Leroy, F. (2011). The effect of heteropolysaccharide-producing strains of *Streptococcus thermophilus* on the texture and organoleptic properties of low-fat yoghurt. *Int. J. Dairy Technol.* 64, 536–543. doi: 10.1111/j.1471-0307.2011.00714.x
- Remus, D. M., van Kranenburg, R., van Swam, I. I., Taverne, N., Bongers, R. S., Wels, M., et al. (2012). Impact of 4 *Lactobacillus plantarum* capsular polysaccharide clusters on surface glycan composition and host cell signaling. *Microb. Cell Fact.* 11:149. doi: 10.1186/1475-2859-11-149
- Russo, P., López, P., Capozzi, V., Fernández de Palencia, P., Dueñas, M. T., Spano, G., et al. (2012). Beta-glucans improve growth, viability and colonization of probiotic microorganisms. *Int. J. Mol. Sci.* 13, 6026–6039. doi: 10.3390/ijms13056026
- Salazar, N., Ruas-Madiedo, P., Prieto, A., Calle, L. P., and de los Reyes-Gavilán, C. G. (2012). Characterization of exopolysaccharides produced by *Bifidobacterium longum* NB667 and its cholate-resistant derivative strain IPLA B667dCo. *J. Agric. Food Chem.* 60, 1028–1035. doi: 10.1021/jf204034n
- Sanlibaba, P., and Aybige Çakmak, G. (2016). Exopolysaccharides production by lactic acid bacteria. *Appl. Microbiol. Open Access.* 2:115. doi: 10.4172/2471-9315.1000115
- Sato, T., Nishimura-Uemura, J., Shimosato, T., Kawai, Y., Kitazawa, H., and Saito, T. (2004). Dextran from *Leuconostoc mesenteroides* augments immunostimulatory effects by the introduction of phosphate groups. *J. Food Prot.* 67, 1719–1724. doi: 10.4315/0362-028X-67.8.1719
- Stack, H. M., Kearney, N., Stanton, C., Fitzgerald, G. F., and Ross, R. P. (2010). Association of beta-glucan endogenous production with increased stress tolerance of intestinal lactobacilli. *Appl. Environ. Microbiol.* 76, 500–507. doi: 10.1128/AEM.01524-09
- Tallon, R., Bressollier, P., and Urdaci, M. C. (2003). Isolation and characterization of two exopolysaccharides produced by *Lactobacillus plantarum* EP56. *Res. Microbiol.* 154, 705–712. doi: 10.1016/j.resmic.2003.09.006
- Tamura, K., and Nei, M. (1993). Estimation of the number of nucleotide substitutions in the control region of mitochondrial DNA in humans and chimpanzees. *Mol. Biol. Evol.* 10, 512–526. doi: 10.1093/molbev/msl149
- Torino, M. I., Font de Valdez, G., and Mozzi, F. (2015). Biopolymers from lactic acid bacteria. Novel applications in foods and beverages. *Front. Microbiol.* 6:834. doi: 10.3389/fmicb.2015.00834
- Van der Meulen, R., Grosu-Tudor, S., Mozzi, F., Vaningelgem, F., Zamfir, M., Font de Valdez, G., et al. (2007). Screening of lactic acid bacteria isolates from dairy and cereal products for exopolysaccharide production and genes involved. *Int. J. Food Microbiol.* 118, 250–258. doi: 10.1016/j.ijfoodmicro.2007.07.014
- Van Kranenburg, R., Vos, H. R., Van Swam, I. I., Kleerebezem, M., and De Vos, W. M. (1999). Functional analysis of glycosyltransferase genes from *Lactococcus lactis* and other gram-positive cocci: complementation, expression, and diversity. *J. Bacteriol.* 181, 6347–6353.
- Velasco, S., Årsköld, E., Paese, M., Grage, H., Irastorza, A., Rådström, P., et al. (2006). Environmental factors influencing growth of and exopolysaccharide formation by *Pediococcus parvulus* 2.6. *Int. J. Food Microbiol.* 111, 252–258. doi: 10.1016/j.ijfoodmicro.2006.06.008
- Vogel, R. F., Pavlovic, M., Ehrmann, M. A., Wiezer, A., Liesegang, H., Offschanka, S., et al. (2011). Genomic analysis reveals *Lactobacillus sanfranciscensis* as stable element in traditional sourdoughs. *Microb. Cell Fact.* 10, 1–11. doi: 10.1186/1475-2859-10-S1-S6
- Wang, L., Liu, D., and Reeves, P. R. (1996). C-terminal half of *Salmonella enterica* WbaP (RfbP) is the galactosyl-1-phosphate transferase domain catalyzing the first step of O-antigen synthesis. *J. Bacteriol.* 178, 2598–2604. doi: 10.1128/jb.178.9.2598-2604.1996
- Werning, M. L., Corrales, M. A., Prieto, A., Fernández de Palencia, P., Navas, J., and López, P. (2008). Heterologous expression of a position 2-substituted (1 \rightarrow 3)- β -D-glucan in *Lactococcus lactis*. *Appl. Environ. Microbiol.* 74, 5259–5262. doi: 10.1128/AEM.00463-08
- Werning, M. L., Ibarburu, I., Dueñas, M. T., Irastorza, A., Navas, J., and López, P. (2006). *Pediococcus parvulus* gtf gene encoding the GTF glycosyltransferase and its application for specific PCR detection of β -D-glucan-producing bacteria in foods and beverages. *J. Food Prot.* 69, 161–169. doi: 10.4315/0362-028X-69.1.161
- Werning, M. L., Notararigo, S., Nacher, M., Fernández de Palencia, P., Aznar, R., and López, P. (2012). "Biosynthesis, purification and biotechnological use of exopolysaccharides produced by lactic acid bacteria," in *Food Additives*, ed. Y. El-Samragy (Croatia: Intech), 83–114.
- Werning, M. L., Pérez-Ramos, A., Fernández De Palencia, P., Mohedano, M. L., Dueñas, M. T., Prieto, A., et al. (2014). A specific immunological method to detect and quantify bacterial 2-substituted (1,3)- β -D-glucan. *Carbohydr. Polym.* 113, 39–45. doi: 10.1016/j.carbpol.2014.06.072
- Whitfield, C. (2006). Biosynthesis and assembly of capsular polysaccharides. *Microb. Glycobiol.* 75, 39–68. doi: 10.1016/B978-0-12-374546-0.00020-1
- Wu, Q., Tun, H. M., Leung, F. C. C., Shah, N. P., Ravyts, F., de Vuyst, L., et al. (2011). Genomic insights into high exopolysaccharide-producing dairy starter bacterium *Streptococcus thermophilus* ASCC 1275. *Sci. Rep.* 4, 536–543. doi: 10.1111/j.1471-0307.2011.00714.x
- Zarour, K., Llamas, M. G., Prieto, A., Ruas-Madiedo, P., Dueñas, M. T., Fernández de Palencia, P., et al. (2017). Rheology and bioactivity of high molecular weight dextrans synthesised by lactic acid bacteria. *Carbohydr. Polym.* 174, 646–657. doi: 10.1016/j.carbpol.2017.06.113
- Živković, M., Miljković, M. S., Ruas-Madiedo, P., Markelić, M. B., Veljović, K., Tolinački, M., et al. (2016). EPS-SJ exopolysaccharide produced by the strain *Lactobacillus paracasei* subsp. *paracasei* BGSJ-2-8 is involved in adhesion to epithelial intestinal cells and decrease on *E. coli* association to Caco-2 cells. *Front. Microbiol.* 7:286. doi: 10.3389/fmicb.2016.00286

Conflict of Interest Statement: The authors declare that the research was conducted in the absence of any commercial or financial relationships that could be construed as a potential conflict of interest.

The handling editor declared a past co-authorship with several of the authors AP-R and PL.

Copyright © 2018 Llamas-Arriba, Pérez-Ramos, Puertas, López, Dueñas and Prieto. This is an open-access article distributed under the terms of the Creative Commons Attribution License (CC BY). The use, distribution or reproduction in other forums is permitted, provided the original author(s) and the copyright owner(s) are credited and that the original publication in this journal is cited, in accordance with accepted academic practice. No use, distribution or reproduction is permitted which does not comply with these terms.



Heteropolysaccharide-producing bifidobacteria for the development of functional dairy products

María Goretti Llamas-Arriba^{a,c}, Ángela Peirotén^b, Ana Isabel Puertas^a, Alicia Prieto^c, Paloma López^c, Miguel Á. Pardo^d, Eva Rodríguez^b, María Teresa Dueñas^{a,*}

^a Department of Applied Chemistry, University of Basque Country, Paseo Manuel de Lardizabal 3, 20018 San Sebastián, Spain

^b Department of Food Technology, National Institute for Agricultural Food Research and Technology (INIA), Ctra. de la Coruña km 7,5, 28040 Madrid, Spain

^c Biological Research Centre, Spanish National Research Council (CSIC), Ramiro de Maeztu 9, 28040 Madrid, Spain

^d Food Research Unit, Food and Marine Research Technologic Centre AZTI, Parque Tecnológico de Vizcaya, Astondo Bidea Edif. 609 Derio, Vizcaya, Spain

ARTICLE INFO

Keywords:

Bifidobacteria
Exopolysaccharide
Immunomodulation
Zebrafish
Technological properties
Adhesion

ABSTRACT

Bifidobacterium longum INIA P132 and *Bifidobacterium infantis* INIA P731, isolated from infant-faeces, were investigated in this work. Regarding the probiotic and technological potential of the bifidobacteria, both were resistant to gastrointestinal tract simulated conditions. *B. longum* showed high survival upon freezing and thawing as well as lyophilisation and was able to grow in milk. *B. infantis* had higher adhesion capacity to human Caco-2 cells than the commercial probiotic *Bifidobacterium animalis* BB12 strain. Moreover, both bacteria secrete heteropolysaccharides (HePS) composed of rhamnose, galactose and glucose. In a dextran sodium sulphate-induced enterocolitis model in zebra fish larvae, treatment with each HePS preparation resulted in a decrease of the larval mortality. In addition, the HePS from *B. longum* immunomodulated *in vitro* human macrophages treated with the inflammatory *Escherichia coli* O111:B4 lipopolysaccharide. Thus, both studied bifidobacteria and their HePS have potential beneficial effects on health and thus, to their application in functional foods.

1. Introduction

Bifidobacteria are a predominant bacterial group present in the human gastrointestinal tract. They have a long history of safe use in food and as probiotics, because they can protect the host by acting as a barrier against exogenous food-borne pathogens, promote nutrient supply and contribute to maintain normal mucosa immunity (Alp & Aslim, 2010; Ruas-Madiedo et al., 2007, 2009). Some of their beneficial effects on the host's health (anti-tumour, cholesterol-lowering, immunomodulating activity, etc) have been attributed to the exopolysaccharides (EPS) that they produce (Hidalgo-Cantabrana et al., 2014a; Inturri et al., 2017). Bifidobacteria synthesise heteropolysaccharides (HePS) and a molecular approach to determine the mechanism of their synthesis is under investigation (Ferrario et al., 2016; Hidalgo-

Cantabrana et al., 2014b; Inturri et al., 2017; Ruas-Madiedo et al., 2007), but it still remains unclear and seems to differ from one strain to another. *Bifidobacterium* genes involved in this synthesis are organised in clusters, called *eps* clusters, but there is not a consensus in their structural organization, their number and the role of their products. The HePS protect bifidobacteria from the acidity and bile salts during their passage through the gastrointestinal tract and can improve their adherence to the intestinal mucosa (Alp & Aslim, 2010; Fanning et al., 2012). Thus, bifidobacteria are currently used to directly produce their EPS in fermented products to exert their probiotic role after ingestion. However, *Bifidobacterium* strains have very stringent growth requirements. Some of them are very sensitive to oxygen, their growth in milk is poor and not all can survive processes used in the food industry (Roy, 2005). Thus, these characteristics of the *Bifidobacterium* strains must be

Abbreviations: DMEM, Dulbecco's Modified Eagle medium; DSS, dextran sodium sulphate; EDTA, ethylenediaminetetraacetic acid; EPS, exopolysaccharides; EW, embryo water; HePS, heteropolysaccharides; HoPS, homopolysaccharides; HPLC-SEC, high-performance size exclusion liquid chromatography; IR, infrared; LAB, lactic acid bacteria; mTSB, modified tryptic soy broth; LPS, lipopolysaccharide; MEM-Alpha, minimum essential medium-alpha; p-GTF, priming-glycosyltransferase; PMA, phorbol-12-myristate-13-acetate; PMA-THP-1, THP-1 monocytes differentiated to macrophages with PMA; RCM, reinforced clostridial medium; RPMI, Roswell Park memorial institute medium; RT, room temperature; TEM, transmission electron microscopy; TFA, trifluoroacetic acid

* Corresponding author.

E-mail addresses: gorettillamas@gmail.com (M.G. Llamas-Arriba), angela.peiroten@inia.es (Á. Peirotén), ana.isabel.puertas@gmail.com (A.I. Puertas), aliprieto@cib.csic.es (A. Prieto), plg@cib.csic.es (P. López), mpardo@azti.es (M.Á. Pardo), minguez@inia.es (E. Rodríguez), maria.teresa.duenas@ehu.es (M.T. Dueñas).

<https://doi.org/10.1016/j.lwt.2018.12.044>

Received 3 May 2018; Received in revised form 17 November 2018; Accepted 15 December 2018

Available online 17 December 2018

0023-6438/ © 2018 Published by Elsevier Ltd.

taken into account when searching for a new probiotic. The aims of the present work were to characterise the structure and functionality of the EPS produced by two bifidobacteria, and to evaluate the bacterial technological and probiotic properties.

2. Materials and methods

2.1. Bacterial strains and culture conditions

B. longum INIA P132 and *B. infantis* INIA P731, isolated from healthy breast-fed infant faeces (Rodríguez et al., 2012), were selected to be studied on the basis of their rosy phenotype. The commercial probiotic strain *B. animalis* BB12 (Chr. Hansen A/S, Hørsholm, Denmark) was used for comparison. All bifidobacteria were routinely cultured on Reinforced Clostridial Medium (RCM) broth (Becton, Dickinson and Company), incubated at 37 °C for 48 h in an anaerobic atmosphere (anaerobiosis generators, BD GasPak™), and conserved at –80 °C upon addition of 10% glycerol.

2.2. Amplification by PCR of priming-glycosyltransferase genes (p-GTF)

p-GTF enzymes are involved in the synthesis of EPS and can be encoded by different genes in different strains of *Bifidobacterium* (Hidalgo-Cantabrana, Ordoñez, Ruas-Madiedo, & Margolles, 2015). To detect the p-GTF coding genes of the two *Bifidobacterium* strains, their genomic DNA was isolated using the 'Wizard' Genomic DNA Purification kit (Promega) following the manufacturer's instructions. Two sets of degenerated primers previously designed by Hidalgo-Cantabrana et al. (2015) were used: *cpsD_F4-cpsD_R6* and *rfbP_F5-rfbP_R5*. PCRs were performed with Taq polymerase (Invitrogen) and conditions were: 3 min at 94 °C, 30 cycles of 45 s at 94 °C, 30 s at 60 °C or 56 °C for *rfbP_F5-rfbP_R5* or *cpsD_F4-cpsD_R6* and 50 s at 72 °C, with a 10 min final step at 72 °C. The DNA sequence of the resulting amplicons was determined at Secugen (Madrid, Spain). Homologies of the DNA sequence of the amplicons and the inferred amino acid sequences with the genes and proteins deposited in the data banks were searched with BLAST (www.ncbi.nlm.nih.gov/) and Clustal Omega (www.ebi.ac.uk/Tools/msa/clustalo/).

2.3. EPS isolation and purification

The bifidobacteria were seeded on RCM agar plates, collecting the polymers from the biomass on the plates' surfaces with ultrapure water (1.5 mL/plate) according to López et al. (2012) with modifications. Briefly, cell suspensions were mixed with one volume of 2 M NaOH and incubated overnight at room temperature (RT) with shaking at 180 rpm. Then, trichloroacetic acid was added at a final concentration of 20% (v/v) and kept 1–2 h at 4 °C under stirring. Supernatants were collected after centrifugation at 18566 × g at 4 °C (20 min) and pH was adjusted to 6.5 by addition of NaOH. Then, the EPS were precipitated with 3 vol of cold absolute ethanol, incubating overnight at –20 °C. The precipitates were sedimented by centrifugation at 18566 × g at 4 °C for 10 min and washed 3 times with 80% (v/v) cold ethanol. Finally, EPS-preparations were dialyzed in 12–14 kDa MWCO membranes (Iberlabo) against deionized water, and freeze-dried.

For further reduction of DNA, RNA and proteins, the freeze-dried EPS were dissolved (1 mg/mL) in a solution with 50 mM Tris-HCl, 100 mM MgSO₄·7H₂O, pH 7.5, and kept at 70 °C overnight. To eliminate non-dissolved material, the preparations were centrifuged at 8609 × g for 15 min at RT. Then, DNase I and RNase A (both from Sigma-Aldrich) were added to the supernatants at a final concentration of 2.5 µg/mL and 10 µg/mL, respectively, and enzymatic digestions were performed at 37 °C for 6 h with shaking. Afterwards, the EPS-preparations were deproteinized by: (i) treatment with proteinase K (Sigma) at 30 µg/mL for 18 h at 37 °C with moderate stirring and (ii) two phenolization processes. The latter were performed by addition of 1 mL

phenol:chloroform:isoamyl alcohol (25:24:1) to each EPS solution, vortex for 7 min, centrifugation at 8609 × g at RT for 5 min and recovery of the aqueous phases containing the EPS. Afterwards, the EPS preparations were treated with one volume of chloroform:isoamyl alcohol (24:1), vortexed for 7 min and fractionated as indicated above. Finally, samples were dialyzed and freeze-dried. Lyophilized EPS were dissolved in ultrapure water (0.1 mg/mL) and concentration was estimated from the neutral carbohydrate content, determined by the phenol-sulphuric acid method (Dubois, Gilles, Hamilton, Rebers, & Smith, 1956) using glucose as standard. Contaminant DNA, RNA and protein contents were determined in EPS suspensions at 1 mg/mL using specific fluorescent staining kits and the Qubit 2.0 fluorometric detection methods (ThermoFisher Scientific).

2.4. Detection of EPS by electron microscopy

To detect EPS by transmission electron microscopy (TEM), the bifidobacteria were grown in RCM broth. Aliquots (100 µL) of the cultures were centrifuged (5 min, 15700 × g at 4 °C) and the sediments were resuspended in 100 µL of deionized water. For visualisation, bacterial suspensions (50 µL) were processed as previously described (Zarour et al., 2017), with some modifications. Briefly, after the grids were discharged, they were placed facedown over a droplet of each suspension for 15 s and in the negative staining step, the uranyl acetate concentration used was reduced to 1% (w/v). Samples were examined in the Electron Microscopy Facility at the Biological Research Centre (CIB, Madrid, Spain).

2.5. EPS characterization

Neutral sugar composition and linkage types were determined as previously described (Notararigo et al., 2013). The presence of N-acetyl, carboxyl, phosphate or sulphate groups and the α- or β-anomeric configuration of the monosaccharides, as well as the average molecular weight (M_w) of the EPS, were assessed by infrared (IR) spectroscopy and high-performance size exclusion liquid chromatography (HPLC-SEC), respectively, as previously described (Ibarburu et al., 2015).

2.6. In vivo protective effect of EPS in a dextran sodium sulphate (DSS)-induced enterocolitis model of zebrafish larvae

Zebrafish embryos were obtained from wild-type adult zebrafish (*Danio rerio*, Hamilton 1822), bred and maintained in the AZTI Zebrafish Facility (REGA number ES489010006105; Derio, Spain) as previously described (Russo et al., 2015) following standard conditions (Sullivan & Kim, 2008). All experimental procedures were approved by the Regional Animal-Welfare Body. Embryos were recovered and cleaned with embryo water (EW; CaCl₂ at 294 mg/mL, MgSO₄·7H₂O at 123.3 mg/mL, NaHCO₃ at 63 mg/mL and KCl at 5.5 mg/mL) and maintained in EW supplemented with methylene blue 0.01% (w/v) at 27 °C. Pools of 20–30 embryos of 1-day post fertilization (dpf) were distributed in Petri dishes containing EW supplemented with the corresponding EPS (150 µg/mL), and incubated at 27 °C. Co-treatment with the EPS and 0.8% (w/v) of DSS (dextran sodium sulphate, Mw 6500–10,000 Da, Across Organics) extended from 4 dpf to 7 dpf. Treatments were replaced daily, and the dead larvae were counted at 5, 6 and 7 dpf. Plates in which only DSS was added were used as positive controls of mortality.

To evaluate if the attenuating effect was dose-dependent, the same protocol was performed assaying three different concentrations (50, 100 and 150 µg/mL) of the EPS produced by *B. infantis* INIA P731 strain. Tests were done in triplicate in two independent experiments.

2.7. THP-1 cell line culture and immunomodulation assay

The human monocytic cell line THP-1, obtained from the CIB cell

bank, was used for the immunomodulation assay. First, human monocytic THP-1 cells were differentiated to macrophages by treatment with phorbol-12-myristate-13-acetate (PMA), which results in their inability to proliferate (Kohro et al., 2004). Then, PMA-THP-1 cells were treated with the lipopolysaccharide (LPS) of *E. coli* O111:B4 to induce an inflammatory response and the EPS were tested as previously described (Zarour et al., 2017). Each EPS was tested in triplicate in two independent experiments.

2.8. Survival to simulated gastrointestinal conditions

Bifidobacterial survival to gastric and intestinal (GI) conditions was tested based on Haller et al. (2001) and consisted in consecutive exposure of bacterial suspensions to phosphate-buffered saline to pH 3 (adjusted with HCl) and to bile salts (Oxoid) at 1.5 g/L. Each step was performed over 1 h at 37 °C and anaerobic atmosphere. Experiments were performed in duplicate and viable cell population variation was determined by plate counting on RCM agar.

2.9. Biofilm formation

Bifidobacteria grown on RCM agar were resuspended in mTSB (tryptic soy broth, (Biolife), supplemented with 20 g/L of bacto proteose-peptone (Oxoid)). This suspension was used to inoculate (10%) either mTSB or mTSB supplemented with 0.2% oxgall (Oxoid), and each inoculated broth was loaded into the wells of polystyrene microtiter plates (Nunc 167008) and incubated at 37 °C for 24 h under anaerobic conditions. Biofilm formation was assessed by the crystal violet method (Lebeer, Verhoeven, Perea Vélez, Vanderleyden, & De Keersmaecker, 2007). Control wells with non-inoculated broth were used as blanks and negative controls. Each strain and treatment were tested in at least three independent experiments, each with eight biological replicates.

2.10. Caco-2 cell culture and adhesion assays

The Caco-2 human enterocyte cell line, obtained from the cell bank at CIB, was seeded in 96-well tissue culture plates (Falcon Microtest™, Becton Dickinson) at a final concentration of 1.25×10^5 cells/mL and grown as monolayers of differentiated and polarised cells for 15 days. Cell concentrations were determined as previously described (Garai-Ibabe et al., 2010).

For adhesion experiments, late exponential-phase cultures of the bifidobacteria were diluted in a final volume of 1 mL of DMEM (Invitrogen), to give 1.25×10^5 colony forming units (cfu)/mL, and added to Caco-2 cells (ratio 1:1) in a final volume of 0.1 mL per well. After incubation for 1 h at 37 °C and 5% CO₂, un-adhered bacteria were removed and the cell-associated bacteria quantified after plating onto RCM plates, as previously described (Nácher-Vázquez et al., 2017). All adhesion assays were conducted in triplicate, with two biological replicates in each.

2.11. Technological properties

Survival of frozen bifidobacterial cultures was measured after 21 days of storage at –80 °C. The strains were grown in RCM for 48 h at 37 °C in anaerobic conditions and glycerol was added as cryopreservant to a final concentration of 5% (w/v). Viable cell population was determined by plate counting on RCM agar before and after the process.

For freeze-drying survival assays, bacteria were grown, collected and resuspended in reconstituted skimmed milk (10% w/v; Central Lechera Asturiana) as protective medium, aliquoted into cryotubes and frozen at –80 °C for 24 h. Subsequently, aliquots were lyophilized and stored at 5 °C for 21 days. Freeze-dried bifidobacteria were reconstituted using peptone water and viability was determined by plate counting in RCM agar.

Growth and survival in milk was tested by inoculating the

bifidobacteria in reconstituted skimmed milk (10% w/v), incubating in anaerobic conditions at 37 °C for 24 h. Changes in bifidobacteria levels were assessed by plate counting on RCM agar.

Survival in milk under refrigerated conditions was performed by collecting the bacteria grown on RCM agar, resuspending them in skimmed milk and storing the suspensions at 5 °C. Viable cell population was determined by plate counting on RCM agar and checked at 14 and 28 days.

2.12. Statistical analysis

The bacterial adhesion to Caco-2 cells was evaluated by two-way analysis of variance (ANOVA). For tests of EPS immunomodulation of THP-1 cells the SAS 9.4 software (SAS Institute Inc.) applying the T-Student test to assess the significance of the addition of the lipopolysaccharide (LPS) from *E. coli* O111:B4 and then, Dunnett's test to evaluate the significance of the differences between samples and controls. The SPSS-PC 24.0 Software (SPSS Inc) was used for zebrafish larvae experiments, subjecting data to a one-way ANOVA followed by a *post hoc* Dunnett's T3 test. Results of survival to gastrointestinal conditions and biofilm formation tests were subjected to ANOVA analysis using a general linear model (GLM) and means' comparison was carried out by Tukey's test, performed using SPSS Statistics 22.0 software (IBM Corp.)

3. Results and discussion

3.1. Detection of EPS by electron microscopy

B. longum INIA P132 and *B. infantis* INIA P731 were selected for use in a former work because of their mucous and ropy phenotype. This characteristic has been related to the production of EPS (Ruas-Madiedo & de los Reyes-Gavilán, 2005; Torino, Font de Valdez, & Mozzi, 2015). Accordingly, analysis of bifidobacterial cultures by TEM revealed cells with EPS attached to them as well as un-attached EPS (Fig. 1B). Representative examples of *B. infantis* INIA P731 suspensions are depicted in Fig. 1A and B. Bifidobacteria are pleomorphic, thus, their shape varies depending on the strain and the growth medium adopting conventional rod or bifurcated 'Y'/'V' morphologies (Biavati, Vescovo,

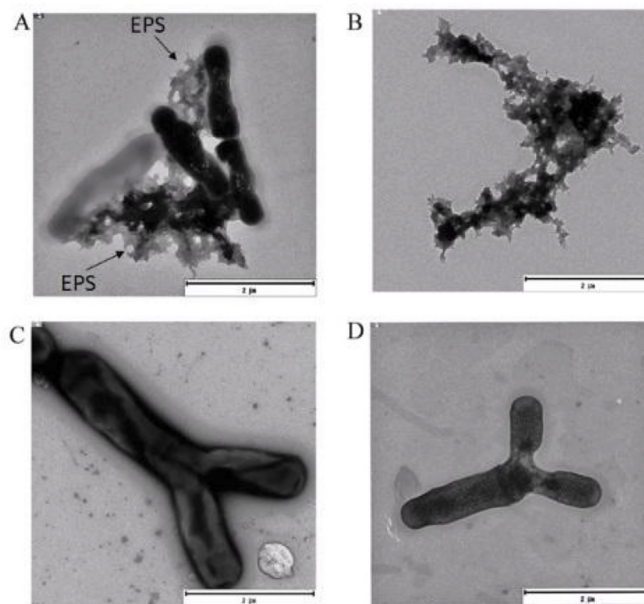


Fig. 1. Visualization of bifidobacteria and their EPS by TEM. *B. infantis* INIA P731 (A) and its EPS (B). Detection of 'Y' morphology of *B. infantis* INIA P731 (C) and *B. longum* INIA P132 (D).

Torriani, & Bottazzi, 2000; Hidalgo-Cantabrana et al., 2014b). As observed in Fig. 1C and D, the two bifidobacteria analysed have the “Y” morphology.

3.2. Detection of genes encoding the priming-glycosyltransferase

It has been reported that a p-GTF enzyme catalyses the first step of the synthesis of the *Bifidobacterium* HePS, by transferring a sugar-1-phosphate to a lipophilic carrier molecule embedded in the bacterial membrane (Ferrario et al., 2016). Moreover, two genes included in *eps* clusters, *cpsD* and *rfbP*, which encode putative p-GTF, have been detected in bifidobacteria and are annotated in the data banks as ‘galactosyl-transferase’ and ‘undecaprenyl-phosphate sugar phosphotransferase’, respectively. The two proteins only have homology at their C-terminal region, which includes the catalytic domain, and are highly conserved in bifidobacteria, which harbour one or both coding genes depending on the strain. Thus, the differences between the amino acid sequences of the p-GTF could be due to a domain responsible for the sugar specificity of each enzyme, located at their N-terminal regions (Hidalgo-Cantabrana et al., 2014b).

The PCR amplification of the 3'-region of the p-GTF coding genes with two different pairs of oligonucleotides produced only a high yield of one of the expected amplicons for each strain: the 373 bp DNA fragment of *rfbP* for *B. infantis* INIA P731 and the 301 bp DNA fragment of *cpsD* for *B. longum* INIA P132 (Fig. 2A). The determination of the DNA sequence of the specific amplicons and the homology search with the BLAST program confirmed that *B. infantis* INIA P731 harbours a gene with 99%–90% identity to the *rfbP* of several *Bifidobacterium breve* and *B. longum* strains as well as that *B. longum* INIA P132 carries a gene with 100%–96% identity to the *cpsD* of other *B. longum* strains. Also, the sequenced region of the genes from *B. infantis* INIA P731 and *B. longum* INIA P132 showed between them an identity of 70.1% indicating that the DNA region encoding the catalytic domain of the p-GTF protein has evolved from a common ancestral gene. Finally, the alignment of the predicted amino acid sequence of the two gene products (Fig. 2B)

revealed a fragment of the C-terminal region of the proteins highly-conserved in p-GTF (73.9% identity) (Hidalgo-Cantabrana et al., 2015; Ruas-Madiedo et al., 2007), with a glutamate (E) described as a probable catalytic residue in the p-GTF of *Lactococcus lactis*, and a tyrosine (Y) specific for galactosyltransferases (Ruas-Madiedo et al., 2007; Van Kranenburg, Vos, Van Swam, Kleerebezem, & De Vos, 1999). These data, together with the observation of mucoid colonies with ropy phenotype on RCM-agar plates and the visualization of EPS by TEM, encouraged us to isolate the EPS produced by the two strains.

3.3. Isolation and partial characterization of the EPS

The EPS were separated from biomass harvested from RCM-agar plates, recovering 0.5–0.8 mg and 0.2–0.3 mg of the polymers per plate for *B. longum* INIA P132 and *B. infantis* INIA P731, respectively. These recoveries are much lower than those ranges obtained previously for other bifidobacteria: 0.78–4.34 mg EPS/plate for different *Bifidobacterium* species (Salazar, Gueimonde, Hernández-Barranco, Ruas-Madiedo, & de los Reyes-Gavilán, 2008) and 3.6–3.8 mg/plate reported for *Bifidobacterium longum* NB667 (Salazar, Ruas-Madiedo, Prieto, Calle, & de los Reyes-Gavilán, 2012). The isolation of the EPS from cultures of bifidobacteria is complex and can lead to a different recovery, and then to different yields, depending on the method used. Therefore, it would be very difficult for these two EPS to be produced as prebiotics by the food industry, due to the low amount recovered. However, their synthesis *in situ* by the producing bifidobacteria in different fermented food would be more suitable to exert their beneficial effects.

The crude EPS precipitates contained residual amounts of DNA (0.01–0.03%), RNA (0.026–0.04%) and protein (1.5–2.5%) and, after enzymatic elimination of nucleic acids and deproteinization these values were further reduced to < 0.01%, < 0.02% and < 1%. Higher protein levels (1.9–8.9%) were reported for EPS preparations from other intestinal *Bifidobacterium* strains (Ruas-Madiedo et al., 2010; Salazar et al., 2008).

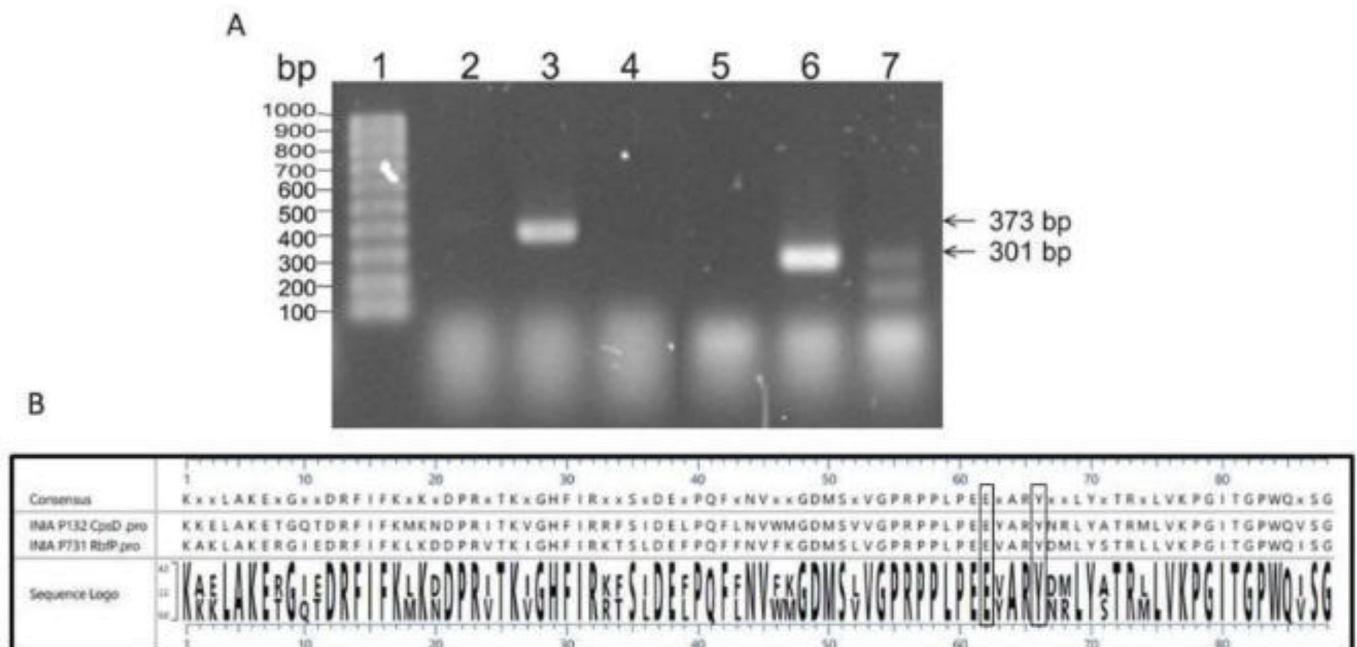


Fig. 2. Genetic analysis of EPS production by *Bifidobacterium* strains. (A) Detection by PCR of *cpsD* and *rfbP* in 1% agarose gel. Lanes: 1, BIORAD Ez Load 100 bp Molecular Ruler; 2, Negative control (*rfbP* F5-R5); 3, INIA P731 DNA with *rfbP* F5-R5 primers; 4, INIA P132 DNA with *rfbP* F5-R5 primers; 5, Negative control (*cpsD* F4-R6 primers); 6, INIA P132 DNA with *cpsD* F4-R6 primers; 7, INIA P731 DNA with *cpsD* F4-R6 primers. (B) Clustal omega alignment and consensus sequences of the inferred amino acid sequences of CpsD from INIA P132 and RfbP from INIA P731 are depicted. Conserved glutamate (E) and tyrosine (Y) residues among p-GTF at the putative catalytic centre are boxed.

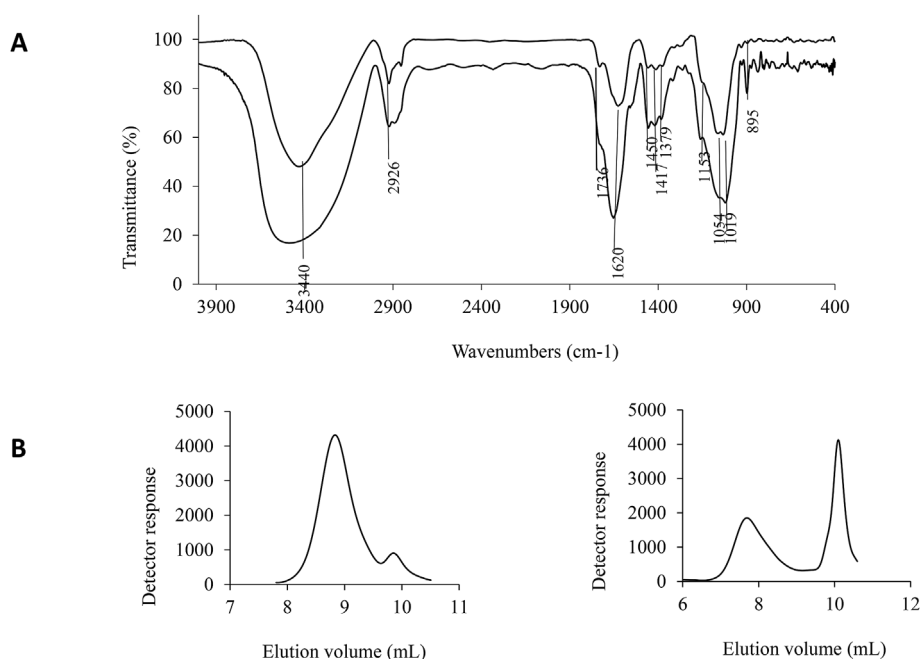


Fig. 3. Physicochemical analysis of bifidobacterial EPS preparations. (A) IR spectra. Up, EPS from *B. longum* INIA P132. Down, EPS from *B. infantis* INIA P731. (B) HPLC-SEC elugrams. Left, EPS fractions from *B. infantis* INIA P731. Right, EPS fractions from *B. longum* INIA P132.

Both EPS preparations were partially characterised to analyse their similarities and/or differences. IR spectra (Fig. 3A) showed the typical profile of polysaccharides. Absorption bands in the region of 3400, 1400 and 1060 cm^{-1} , correspond to the hydroxyl stretching vibration (Salazar et al., 2012). Those around 2925–2930 cm^{-1} are due to C-H stretching (Ahmad, Anjum, Zahoor, Nawaz, & Ahmed, 2010; Han et al., 2014; Xu, Shen, Ding, Gao, & Li, 2011), and signals in the 1860–1660 cm^{-1} region result from carbonyl stretching (Salazar et al., 2012; Xu et al., 2011). Absorption between 1200 and 1000 cm^{-1} is due to the stretching vibration of glycosidic linkage (C-O-C) and C-O or C-O-H groups (Ahmad et al., 2010; Han et al., 2014). The fingerprint region ($< 1500 \text{ cm}^{-1}$), characteristic of each molecule (Xu et al., 2011), presented a band around 1020 cm^{-1} . In the anomeric region, 950–700 cm^{-1} (Xu et al., 2011), a band at 895 cm^{-1} was observed in the spectrum of the crude *B. infantis* INIA P731 EPS, indicating its predominance of β anomers (Ahmad et al., 2010), while no bands were observed in this region for the EPS produced by the other strain studied, highlighting a first difference between them.

Regarding monosaccharide composition, both strains contained glucose, galactose and rhamnose, although in different proportions: 16:10:1 for *B. longum* INIA P132 and 28:10:8 for *B. infantis* INIA P731. These results correlate with the fact that bifidobacteria synthesise various HePS composed of these three monosaccharides (Hidalgo-Cantabrana et al., 2015; Kohno et al., 2009; Mozzi et al., 2006; Salazar et al., 2009). As several repeating units have been reported for bifidobacterial HePS, the types of O-glycosidic linkages in the two HePS preparations were investigated by methylation analysis. The results, depicted in Table 1, revealed the same seven predominant types of residues in both of them. The majority of glucose molecules were present as linear-chain units 1,4-linked, and at terminal positions of the side-chains, and also low percentages of 1,6 and (1,4,6)-linked glucopyranose were also detected. The relative proportion of the glucopyranose residues in both samples was similar. On the contrary, as already expected from monosaccharide analysis, the amount of rhamnose and galactose units differed considerably in the two HePS analysed. Rhamnose was exclusively attached to its adjacent residue in the polysaccharide chain by 1,3 linkages, representing almost 20% in the HePS from *B. infantis* INIA P731. Galactose was found in branching points, as a pyranose substituted at O-3 and O-6, and as linear-chain

Table 1

Linkage types and their proportions (%) in the crude EPS of each strain, deduced from a methylation analysis.

Linkage types	Proportion (%)	
	<i>B. infantis</i> INIA P731	<i>B. longum</i> INIA P132
Rhap-(1–3)	10.3	1.6
Glc-(1-	14.9	22.1
Galp-(1–4)	0.8	15.2
Glc-(1–4)	59.3	39.9
Galp-(1–3)	1.6	0.0
Glc-(1–6)	1.1	2.3
Glc-(1–4,6)	1.2	3.4
Galp-(1–3,6)	10.0	15.7

units 1,4-linked or 1,5-linked, representing about 30% of the HePS from *B. longum* INIA P132. Unfortunately, this uncertainty could not be resolved with this methodology since both residues are transformed into the same partially methylated alditol acetate: 1,4,5-tri-O-acetyl-2,3,6-tri-O-methyl galactose. The presence of either 1,4-Galp and 1,5-Galp in HePS from bifidobacteria has been reported (Hidalgo-Cantabrana et al., 2014b). In addition, the backbone of the extracellular HePS from *B. longum* JLB05 contains α -(1,4)-Galp, and no galactofuranose (Kohno et al., 2009). Moreover, pyruvic acid was reported in these HePS, and this or another organic acid could be present in the polymers analysed in the current work, since a slight carbonyl band (1736 cm^{-1}), more evident in the sample from *B. longum* INIA P132, was observed in the IR spectra (Fig. 3A). Analysis of the HePS preparations from the two bifidobacteria by analytical HPLC-SEC (Fig. 3B) indicated that they contained two fractions of different M_w , as reported before by other authors (Ruas-Madiedo et al., 2010; Salazar et al., 2008; Xu et al., 2011). *B. infantis* INIA P731 contained a major peak of M_w about 1.9×10^5 Da and a smaller one of 1.2×10^4 Da. In *B. longum* INIA P132 the two polysaccharides were in similar amounts, with the peak of high M_w being ca. 1.0×10^6 Da and the other of 1.3×10^5 Da. These M_w are in the range of those of other HePS produced by bifidobacteria (Kohno et al., 2009; Xu et al., 2011).

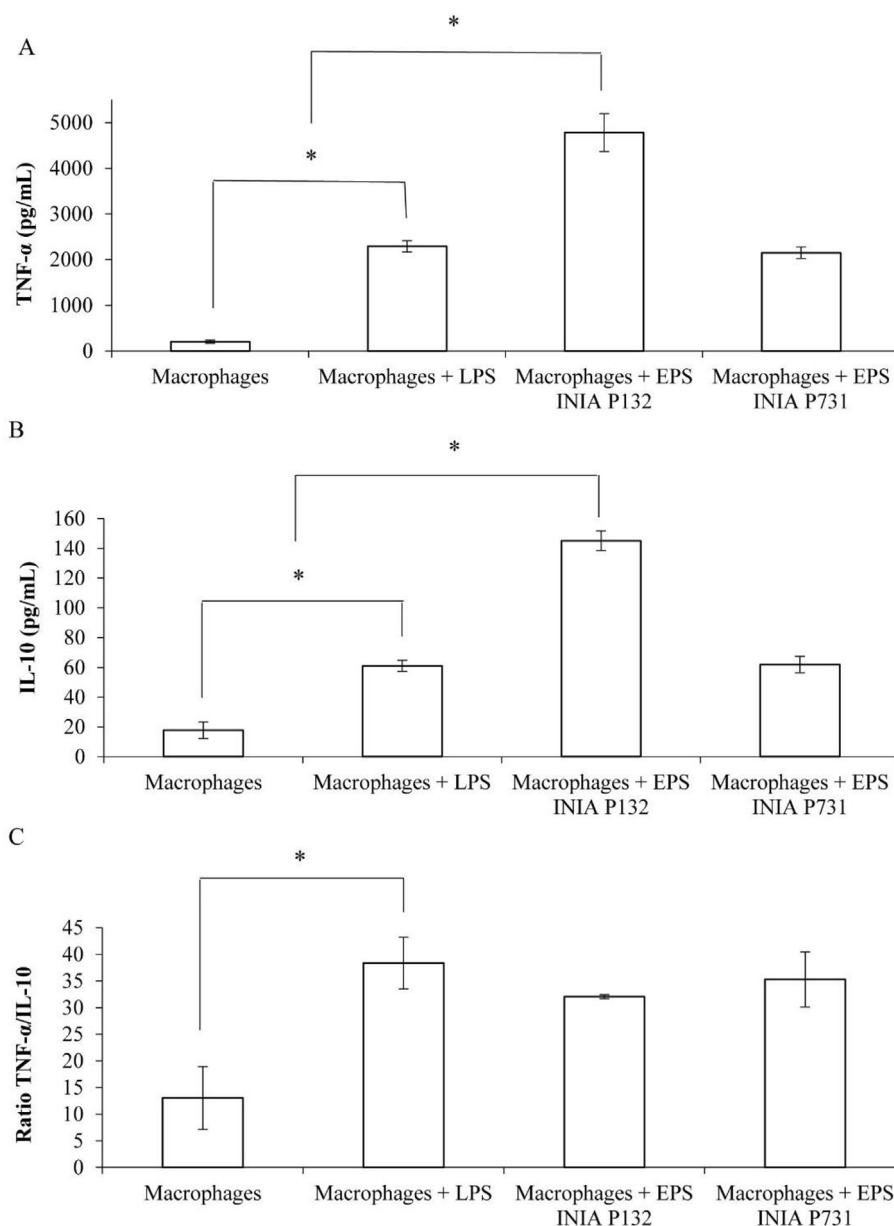


Fig. 4. Evaluation of the cytokines production in the supernatants of THP-1-PMA macrophages after the co-treatment with LPS and the HePS produced by bifidobacteria. Levels of TNF- α (A), IL-10 (B) and ratio TNF- α /IL-10 (C) are depicted. Data were analysed by the T-student's t-test. Then, Dunnett's test was employed to assess the significant differences between the samples and the controls. When significance was $p \leq 0.05$, it was indicated with *.

3.4. Immunomodulatory activity of HePS from bifidobacteria

The EPS seem to play a role in counteracting the inflammatory effect produced by probiotic strains, thus, preventing them from being attacked by the immune system (Schiavi et al., 2016; Yasuda, Serata, & Sako, 2008). Moreover, the EPS' physicochemical differences (negative charges, high or low molecular weight, etc) seem to affect their immunostimulation capacity.

Thus, we evaluated the immunomodulatory activity of the HePS of the two bifidobacteria *in vitro*. To this end, human PMA-THP-1 macrophages were treated with the HePS preparations and with *E. coli* LPS to induce an inflammatory response. The levels of the TNF- α inflammatory and IL-10 anti-inflammatory cytokines secreted by treated PMA-THP1 were compared to those secreted by macrophages either untreated or exposed only to LPS, which were used as controls (Fig. 4). All treatments induced the production of both cytokines (Fig. 4A and B). The levels of the individual cytokines were similar for treatments

with LPS alone and in co-treatment with HePS from *B. infantis* INIA P731, but in the presence of the HePS from *B. longum* INIA P132 a significantly higher production of TNF- α and IL-10 ($p < 0.05$) was observed. The TNF- α /IL-10 ratios calculated for the challenged macrophages were consistent with an inflammatory response (Fig. 4C) but, even though the differences among the ratios in the three treatments were not statistically significant, an anti-inflammatory trend of the HePS tested can be observed in this model (Fig. 4C). According to Hidalgo-Cantabrana et al. (2014b), high molecular mass EPS show a lower capacity to influence the release of anti- and pro-inflammatory cytokines by macrophages. However, these results could also be explained by an over-stimulation of the eukaryotic cells provoked by the LPS, which can mask the effect of the EPS.

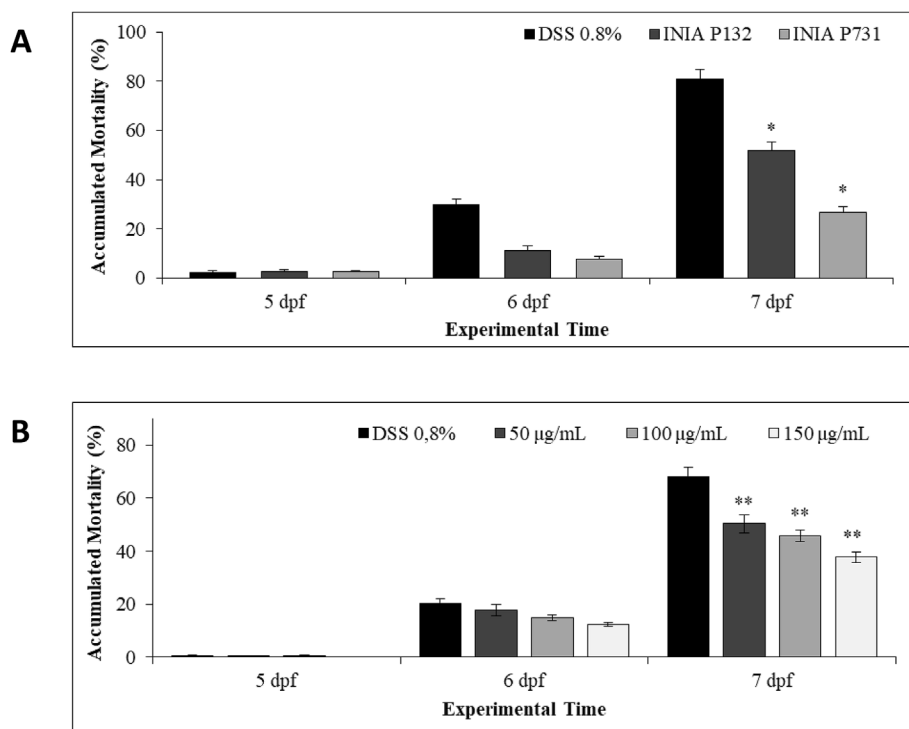


Fig. 5. Protective effect *in vivo* of bifidobacterial HePS in a DSS-induced enterocolitis zebrafish model. (A) Analysis of the mortality of zebrafish larvae treated with DSS 0.8% and HePS of *B. longum* and *B. infantis* strains. (B) Evaluation of dose-dependent effect of HePS produced by *B. infantis* INIA P731 on survival of zebrafish larvae treated with DSS 0.8%. The results are expressed as mean \pm standard deviation (SD) and data were subjected to a one-way ANOVA followed by a post hoc Dunnett's T3 test with significances of $p < 0.05$ (*) and $p < 0.01$ (**).

3.5. Protective effect of bifidobacterial HePS in an *in vivo* zebrafish model of enterocolitis

To assess the anti-inflammatory effect of the HePS preparations isolated from the two bifidobacteria, we used an *in vivo* enterocolitis model of zebrafish, induced by the chemical agent DSS. The data in Fig. 5A show that both HePS reduce the negative effects caused by the DSS. Around 80% of the larvae died upon 7 days of exposure to 0.8% DSS, while a reduced mortality was observed in a co-treatment with the *B. longum* INIA P132 HePS preparation ($51.7 \pm 3.6\%$, $p < 0.05$) and, more notably, with that of *B. infantis* INIA P731 ($26.7 \pm 2.2\%$, $p < 0.05$). Considering that polymers of *B. infantis* strain exerted the highest protection against DSS damage, we used this mixture to test if the effect was dose-dependent. Three different HePS concentrations (50, 100 and 150 $\mu\text{g/mL}$) were evaluated and, as expected, the highest reduction in larvae mortality ($31.68 \pm 1.32\%$, $p < 0.01$) was achieved when 150 $\mu\text{g/mL}$ of the EPS were administered, confirming a dose-dependent effect (Fig. 5B). The mechanism by which these polymers reduce mortality is still unknown. However, according to the experiments performed in a DSS-induced colitis mouse model with the strain *B. animalis* subsp. *lactis* Balat_1410^{S89L} (Hidalgo-Cantabrana et al., 2016), they could present an anti-inflammatory activity mediated by the induction of Treg cells in mesenteric lymphoid nodes, rather than acting as a physical barrier avoiding DSS action. However, further immunological assays should be performed to confirm this hypothesis.

3.6. Survival of bifidobacteria to simulated gastrointestinal conditions

The probiotic potential of the two EPS-producing bifidobacteria was first assessed by measuring their survival under *in vitro* GI conditions (Table 2A). The two *Bifidobacterium* strains showed good stability to the GI conditions, with reductions around 0.3 log cfu/mL, although their survival was lower than that of *B. animalis* BB12. This tolerance to acidic pH and bile salts exhibited by the two strains suggests their potential to survive passage through the GI tract and to reach the intestine at sufficient levels to exert their effects.

3.7. Biofilm formation by bifidobacteria

The HePS involved in biofilm formation can affect colonisation and survival of bifidobacteria in the gut (Hidalgo-Cantabrana et al., 2014b). In the present work, *B. infantis* INIA P731, in the absence of oxgall, showed the better result for biofilm formation of the two EPS-producing bifidobacteria (Table 2B). Neither of the two strains increased the biofilm formation in the presence of oxgall, as has been described before for certain strains of bifidobacteria and lactobacilli (Ambalam, Kiran Kondepudi, Nilsson, Wadström, & Ljungh, 2014; Lebeer et al., 2007) and both new bifidobacterial strains showed lower biofilm formation than *B. animalis* BB12 (Table 2B).

3.8. Analysis of the adhesion ability of the bifidobacteria

Adherence to human epithelial cells is one of the *in vitro* tests listed in the guideline for the evaluation of probiotics in food (FAO/WHO, 2002). Thus, the adhesion capacity of *B. longum* INIA P132 and *B. infantis* INIA P731 was assessed using the enterocyte-like Caco-2 cell line. Some authors have reported that the presence of EPS in the surface of bacteria has a negative effect on their adhesive properties (Castro-Bravo, Hidalgo-Cantabrana, Rodríguez Carvajal, Ruas-Madiedo, & Margolles, 2017; López et al., 2012; Nacher-Vázquez et al., 2017), while others described the production of these polymers as useful for probiotics to interact with eukaryotic cells (Fernández de Palencia et al., 2009; Garai-Ibabe et al., 2010; Živković et al., 2016). In this work, in accordance with the results obtained for the biofilm formation, *B. longum* INIA P132 showed low binding capacity to the enterocytes, whereas adhesion of *B. infantis* INIA P731 to the epithelial intestinal cells was significantly high ($p < 0.05$), exceeding *B. animalis* BB12 levels (Table 2C).

3.9. Technological properties of *Bifidobacterium* strains

The development of a functional food containing live probiotic cultures requires that the probiotic strain is able to survive both the manufacturing process and during the shelf life of the product. A preliminary technological characterization of the two bifidobacterial

Table 2
Probiotic characterization of bifidobacterial strains.

Strain	¹ Survival to gastrointestinal conditions	² Biofilm formation		
		mTSB	mTSB + 0.2% oxgall	³ Adherence to Caco2 cells
<i>B. longum</i> INIA P132	−0.32 ± 0.27 ^a	0.02 ± 0.01 ^{ab}	0.01 ± 0.01 ^a	1.45 ± 0.29 ^a
<i>B. infantis</i> INIA P731	−0.31 ± 0.05 ^a	0.21 ± 0.13 ^c	0.08 ± 0.06 ^b	35.91 ± 5.24 ^b
<i>B. animalis</i> BB12	0.18 ± 0.05 ^b	0.62 ± 0.14 ^d	0.71 ± 0.20 ^c	20.34 ± 5.48 ^c

¹Survival to gastrointestinal conditions expressed as change in log cfu/mL (mean ± SD). Values with different superscript differ significantly (Tukey test, $p < 0.05$). Two independent experiments were carried out with two replications in each (N = 4).

²Biofilm formation expressed as increment of OD570 nm (mean ± SD). Values with different superscript differ significantly (Tukey test, $p < 0.05$). Three independent experiments were carried out with 8 replications in each (N = 24).

³Adhesion to Caco-2 cells, expressed as the percentage of cfu (mean ± standard error (SE)). Values in each column with different superscript differ significantly (Two-way ANOVA, $p \leq 0.05$). Three independent experiments were carried out with two replicates in each (N = 6).

Table 3
Technological characteristics of the two *Bifidobacterium* strains.

Strain	−80 °C survival (21 d)	Freeze-drying survival (21 d)	Growth in milk (24 h)	4 °C storage (14 d)	4 °C storage (28 d)
<i>B. longum</i> INIA P132	−0.53 ± 0.15	−0.65 ± 0.03	1.52 ± 0.54	−0.92 ± 0.14	−1.70 ± 0.11
<i>B. infantis</i> INIA P731	−1.06 ± 0.15	−1.81 ± 0.26	−0.99 ± 0.21	−0.61 ± 0.10	−1.21 ± 0.05

Data are expressed as change in log cfu/mL-1 (mean ± SD) after each procedure. Two independent experiments were carried out with two replicates in each (N = 4).

strains was performed by assessing their survival as frozen or freeze-dried cultures, and their growth and survival in milk under refrigeration conditions. *B. longum* INIA P132 showed better stability as frozen and freeze-dried culture than *B. infantis* INIA P731 (Table 3). Moreover, *B. longum* was able to grow in milk, while the levels of *B. infantis* INIA P731 decreased in these conditions. This strain showed better stability in milk under refrigerated conditions. According to these results, more research is needed to improve the yield and survival of the strains under the manufacturing conditions and to test their behaviour in different food matrices.

4. Conclusions

The mucoid aspect and the ropiness of *B. longum* INIA P132 and *B. infantis* INIA P731 colonies suggested them as EPS producers, which was confirmed after obtaining EPS preparations from solid cultures. The polymers were partially characterised as mixtures of HePS with different ratios of rhamnose, galactose and glucose. The same linkage types were detected in both EPS preparations, although their proportions varied. Additionally, the biological activity of these HePS mixtures was studied. Both EPS showed a protective effect to DSS-treated zebrafish larvae. Although not conclusive, an anti-inflammatory tendency was also observed in experiments performed with PMA-THP-1 macrophages. Along with the EPS activities, both strains showed good survival under gastrointestinal conditions, and *B. infantis* INIA P731 displayed higher biofilm formation and adhesion capacity to enterocytes, which is a very remarkable property of probiotic strains. On the other hand, *B. longum* INIA P132 showed better technological suitability. Taken together, these findings suggest that the two strains evaluated, might be used as adjuncts in the food industry and give an added value to fermented products when synthesizing their HePS *in situ*.

Conflicts of interest

None.

Funding

This work was supported by a grant from de Department of Environment, Territorial Planification, Agriculture and Fishing and the project no. IT 866-13 from the Basque Government, by the Spanish

Ministry of Science and Innovation (AGL 2015-65010-C3-1-R) and by the Spanish Ministry of Economy and Competitiveness (RM12-00004-00-00 and RTA2013-00029-00-00).

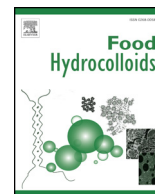
Acknowledgments

We thank Dr. Guillermo Padilla Alonso for his valuable assistance in the bio-statistical analysis. We thank Dr. Stephen Elson for the critical reading of the manuscript.

References

- Ahmad, A., Anjum, F. M., Zahoor, T., Nawaz, H., & Ahmed, Z. (2010). Extraction and characterization of β -D-glucan from oat for industrial utilization. *International Journal of Biological Macromolecules*, 46(3), 304–309. <https://doi.org/10.1016/j.ijbiomac.2010.01.002>.
- Alp, G., & Aslim, B. (2010). Relationship between the resistance to bile salts and low pH with exopolysaccharide (EPS) production of *Bifidobacterium* spp. isolated from infants feces and breast milk. *Anaerobe*, 16(2), 101–105. <https://doi.org/10.1016/j.anaerobe.2009.06.006>.
- Ambalam, P., Kiran Kondepudi, K., Nilsson, I., Wadström, T., & Ljungh, Å. (2014). Bile enhances cell surface hydrophobicity and biofilm formation of bifidobacteria. *Applied Biochemistry and Biotechnology*, 172(4), 1970–1981. <https://doi.org/10.1007/s12010-013-0596-1>.
- Biavati, B., Vescovo, M., Torriani, S., & Bottazzi, V. (2000). Bifidobacteria: history, ecology, physiology and applications. *Annals of Microbiology*, 50, 117–131.
- Castro-Bravo, N., Hidalgo-Cantabrana, C., Rodríguez Carvajal, M. A., Ruas-Madiedo, P., & Margolles, A. (2017). Gene replacement and fluorescent labeling to study the functional role of exopolysaccharides in *Bifidobacterium animalis* subsp. *lactis*. *Frontiers in Microbiology*, 8(July), 1–14. <https://doi.org/10.3389/fmicb.2017.01405>.
- Dubois, M., Gilles, K., Hamilton, J., Rebers, P., & Smith, F. (1956). Colorimetric method for determination of sugars and related substances. *Analytical Chemistry*, 28(3), 350–356. <https://doi.org/10.1021/ac60111a017>.
- Fanning, S., Hall, L. J., Cronin, M., Zomer, A., MacSharry, J., Goulding, D., et al. (2012). Bifidobacterial surface-exopolysaccharide facilitates commensal-host interaction through immune modulation and pathogen protection. *Proceedings of the National Academy of Sciences*, 109(6), 2108–2113. <https://doi.org/10.1073/pnas.1115621109>.
- FAO/WHO (2002). *Guidelines for the evaluation of probiotics in food* Report of a joint FAO/WHO working group on drafting guidelines for the evaluation of probiotics in food Geneva, Switzerland: World Health Organization. Retrieved from http://who.int/foodsafety/fs_management/en/probiotic_guidelines.pdf.
- Fernández de Palencia, P., Werning, M. L., Sierra-Filardi, E., Dueñas, M. T., Irastorza, A., Corbi, A. L., et al. (2009). Probiotic properties of the 2-substituted (1,3)- β -D-glucan-producing bacterium *Pediococcus parvulus* 2.6. *Applied and Environmental Microbiology*, 75(14), 4887–4891. <https://doi.org/10.1128/AEM.00394-09>.
- Ferrario, C., Milani, C., Mancabelli, L., Lugli, G. A., Duranti, S., Mangifesta, M., et al. (2016). Modulation of the *eps*-ome transcription of bifidobacteria through simulation of human intestinal environment. *FEMS Microbiology Ecology*, 92(4), 1–12. <https://doi.org/10.1093/femsec/fiw056>.

- Garai-Ibabe, G., Dueñas, M. T., Irastorza, A., Sierra-Filardi, E., Werning, M. L., López, P., et al. (2010). Naturally occurring 2-substituted (1,3)- β -D-glucan producing *Lactobacillus suebicus* and *Pediococcus parvulus* strains with potential utility in the production of functional foods. *Bioresour. Technology*, 101(23), 9254–9263. <https://doi.org/10.1016/j.biortech.2010.07.050>.
- Haller, D., Colbus, H., Gänze, M. G., Scherenbacher, P., Bode, C., & Hammes, W. P. (2001). Metabolic and functional properties of lactic acid bacteria in the gastro-intestinal ecosystem: A comparative in vitro study between bacteria of intestinal and fermented food origin. *Systematic & Applied Microbiology*, 24(2), 218–226. <https://doi.org/10.1078/0723-2020-00023>.
- Han, J., Hang, F., Guo, B., Liu, Z., You, C., & Wu, Z. (2014). Dextran synthesized by *Leuconostoc mesenteroides* BD1710 in tomato juice supplemented with sucrose. *Carbohydrate Polymers*, 112, 556–562. <https://doi.org/10.1016/j.carbpol.2014.06.035>.
- Hidalgo-Cantabrana, C., Algieri, F., Rodríguez-Nogales, A., Vezza, T., Martínez-Cambor, P., Margolles, A., et al. (2016). Effect of a rosy exopolysaccharide-producing *Bifidobacterium animalis* subsp. *lactis* strain orally administered on DSS-induced colitis mice model. *Frontiers in Microbiology*, 7, 1–11. <https://doi.org/10.3389/fmicb.2016.00868>.
- Hidalgo-Cantabrana, C., Nikolic, M., López, P., Suárez, A., Miljkovic, M., Kojic, M., et al. (2014a). Exopolysaccharide-producing *Bifidobacterium animalis* subsp. *lactis* strains and their polymers elicit different responses on immune cells from blood and gut associated lymphoid tissue. *Anaerobe*, 26, 24–30. <https://doi.org/10.1016/j.anaerobe.2014.01.003>.
- Hidalgo-Cantabrana, C., Ordoñez, I., Ruas-Madiedo, P., & Margolles, A. (2015). Degenerate PCR primers for detecting putative glycosyltransferase genes in *Bifidobacterium* strains. *Beneficial Microbes*, 6(4), 553–562. <https://doi.org/10.3920/BM2014.0046>.
- Hidalgo-Cantabrana, C., Sánchez, B., Milani, C., Ventura, M., Margolles, A., & Ruas-Madiedo, P. (2014b). Genomic overview and biological functions of exopolysaccharide biosynthesis in *Bifidobacterium* spp. *Applied and Environmental Microbiology*, 80(1), 9–18. <https://doi.org/10.1128/AEM.02977-13>.
- Ibarburu, I., Puertas, A. I., Berregi, I., Rodríguez-Carvajal, M. A., Prieto, A., & Dueñas, M. T. (2015). Production and partial characterization of exopolysaccharides produced by two *Lactobacillus suebicus* strains isolated from cider. *International Journal of Food Microbiology*, 214, 54–62. <https://doi.org/10.1016/j.ijfoodmicro.2015.07.012>.
- Inturri, R., Molinaro, A., Di Lorenzo, F., Blandino, G., Tomasello, B., Hidalgo-Cantabrana, C., et al. (2017). Chemical and biological properties of the novel exopolysaccharide produced by a probiotic strain of *Bifidobacterium longum*. *Carbohydrate Polymers*, 174, 1172–1180. <https://doi.org/10.1016/j.carbpol.2017.07.039>.
- Kohno, M., Suzuki, S., Kanaya, T., Yoshino, T., Matsuura, Y., Asada, M., et al. (2009). Structural characterization of the extracellular polysaccharide produced by *Bifidobacterium longum* JBL05. *Carbohydrate Polymers*, 77(2), 351–357. <https://doi.org/10.1016/j.carbpol.2009.01.013>.
- Kohro, T., Tanaka, T., Murakami, T., Wada, Y., Aburatani, H., Hamakubo, T., et al. (2004). A comparison of differences in the gene expression profiles of phorbol 12-myristate 13-acetate differentiated THP-1 cells and human monocyte-derived macrophage. *Journal of Atherosclerosis and Thrombosis*, 11(2), 88–97. <https://doi.org/10.5551/jat.11.88>.
- Lebeer, S., Verhoeven, T. L. A., Perea Vélez, M., Vanderleyden, J., & De Keersmaecker, S. C. J. (2007). Impact of environmental and genetic factors on biofilm formation by the probiotic strain *Lactobacillus rhamnosus* GG. *Applied and Environmental Microbiology*, 73(21), 6768–6775. <https://doi.org/10.1128/AEM.01393-07>.
- López, P., Monteserin, D. C., Gueimonde, M., de los Reyes-Gavilán, C. G., Margolles, A., Suárez, A., et al. (2012). Exopolysaccharide-producing *Bifidobacterium* strains elicit different in vitro responses upon interaction with human cells. *Food Research International*, 46(1), 99–107. <https://doi.org/10.1016/j.foodres.2011.11.020>.
- Mozzi, F., Vaningelgem, F., Hébert, E. M., Van der Meulen, R., Foulquié Moreno, M. R., Font De Valdez, G., et al. (2006). Diversity of heteropolysaccharide-producing lactic acid bacterium strains and their biopolymers. *Applied and Environmental Microbiology*, 72(6), 4431–4435. <https://doi.org/10.1128/AEM.02780-05>.
- Nácher-Vázquez, M., Iturria, I., Zarour, K., Mohedano, M. L., Aznar, R., Pardo, M.Á., et al. (2017). Dextran production by *Lactobacillus sakei* MN1 coincides with reduced autoagglutination, biofilm formation and epithelial cell adhesion. *Carbohydrate Polymers*, 168, 22–31. <https://doi.org/10.1016/j.carbpol.2017.03.024>.
- Notararigo, S., Nácher-Vázquez, M., Ibarburu, I., Werning, M. L., Fernández de Palencia, P., Dueñas, M. T., et al. (2013). Comparative analysis of production and purification of homo- and hetero-polysaccharides produced by lactic acid bacteria. *Carbohydrate Polymers*, 94(1), 57–64. <https://doi.org/10.1016/j.carbpol.2012.05.016>.
- Rodríguez, E., Arqués, J. L., Rodríguez, R., Peiróten, Á., Landete, J. M., & Medina, M. (2012). Antimicrobial properties of probiotic strains isolated from breast-fed infants. *Journal of Functional Foods*, 4(2), 542–551. <https://doi.org/10.1016/j.jff.2012.02.015>.
- Roy, D. (2005). Technological aspects related to the use of bifidobacteria in dairy products. *Le Lait*, 85, 39–56. <https://doi.org/10.1051/lait:2004026>.
- Ruas-Madiedo, P., & de los Reyes-Gavilán, C. G. (2005). Invited Review: methods for the screening, isolation, and characterization of exopolysaccharides produced by lactic acid bacteria. *Journal of Dairy Science*, 88, 843–856. [https://doi.org/10.3168/jds.S0022-0302\(05\)72750-8](https://doi.org/10.3168/jds.S0022-0302(05)72750-8).
- Ruas-Madiedo, P., Gueimonde, M., Arigoni, F., de los Reyes-Gavilán, C. G., & Margolles, A. (2009). Bile affects the synthesis of exopolysaccharides by *Bifidobacterium animalis*. *Applied and Environmental Microbiology*, 75(4), 1204–1207. <https://doi.org/10.1128/AEM.00908-08>.
- Ruas-Madiedo, P., Medrano, M., Salazar, N., de los Reyes-Gavilán, C. G., Pérez, P. F., & Abraham, A. G. (2010). Exopolysaccharides produced by *Lactobacillus* and *Bifidobacterium* strains abrogate in vitro the cytotoxic effect of bacterial toxins on eukaryotic cells. *Journal of Applied Microbiology*, 109(6), 2079–2086. <https://doi.org/10.1111/j.1365-2672.2010.04839.x>.
- Ruas-Madiedo, P., Moreno, J. A., Salazar, N., Delgado, S., Mayo, B., Margolles, A., et al. (2007). Screening of exopolysaccharide-producing *Lactobacillus* and *Bifidobacterium* strains isolated from the human intestinal microbiota. *Applied and Environmental Microbiology*, 73(13), 4385–4388. <https://doi.org/10.1128/AEM.02470-06>.
- Russo, P., Iturria, I., Mohedano, M. L., Caggiariello, G., Rainieri, S., Fiocco, D., et al. (2015). Zebrafish gut colonization by mCherry-labelled lactic acid bacteria. *Applied Microbiology and Biotechnology*, 99, 3479–3490. <https://doi.org/10.1007/s00253-014-6351-x>.
- Salazar, N., Gueimonde, M., Hernández-Barranco, A. M., Ruas-Madiedo, P., & de los Reyes-Gavilán, C. G. (2008). Exopolysaccharides produced by intestinal *Bifidobacterium* strains act as fermentable substrates for human intestinal bacteria. *Applied and Environmental Microbiology*, 74(15), 4737–4745. <https://doi.org/10.1128/AEM.00325-08>.
- Salazar, N., Ruas-Madiedo, P., Kolida, S., Collins, M., Rastall, R., Gibson, G., et al. (2009). Exopolysaccharides produced by *Bifidobacterium longum* IPLA E44 and *Bifidobacterium animalis* subsp. *lactis* IPLA R1 modify the composition and metabolic activity of human faecal microbiota in pH-controlled batch cultures. *International Journal of Food Microbiology*, 135(3), 260–267. <https://doi.org/10.1016/j.ijfoodmicro.2009.08.017>.
- Salazar, N., Ruas-Madiedo, P., Prieto, A., Calle, L. P., & de los Reyes-Gavilán, C. G. (2012). Characterization of exopolysaccharides produced by *Bifidobacterium longum* NB667 and its cholate-resistant derivative strain IPLA B667dCo. *Journal of Agricultural and Food Chemistry*, 60(4), 1028–1035. <https://doi.org/10.1021/jf204034n>.
- Schiavi, E., Gleinser, M., Molloy, E., Groeger, D., Frei, R., Ferstl, R., et al. (2016). *The Surface-associated Exopolysaccharide of Bifidobacterium longum 35624 Plays an Essential Role in Dampening Host Proinflammatory Responses and Repressing Local T_H17 Responses*, vol. 82, 7185–7196. (24) <https://doi.org/10.1128/AEM.02238-16> Editor .
- Sullivan, C., & Kim, C. H. (2008). Zebrafish as a model for infectious disease and immune function. *Fish & Shellfish Immunology*, 25(4), 341–350. <https://doi.org/10.1016/j.fsi.2008.05.005>.
- Torino, M. I., Font de Valdez, G., & Mozzi, F. (2015). Biopolymers from lactic acid bacteria. Novel applications in foods and beverages. *Frontiers in Microbiology*, 6, 1–16. <https://doi.org/10.3389/fmicb.2015.00834>.
- Van Kranenburg, R., Vos, H. R., Van Swam, I. I., Kleerebezem, M., & De Vos, W. M. (1999). Functional analysis of glycosyltransferase genes from *Lactococcus lactis* and other gram-positive cocci: complementation, expression, and diversity. *Journal of Bacteriology*, 181(20), 6347–6353.
- Xu, R., Shen, Q., Ding, X., Gao, W., & Li, P. (2011). Chemical characterization and antioxidant activity of an exopolysaccharide fraction isolated from *Bifidobacterium animalis* RH. *European Food Research and Technology*, 232(2), 231–240. <https://doi.org/10.1007/s00217-010-1382-8>.
- Yasuda, E., Serata, M., & Sako, T. (2008). Suppressive effect on activation of macrophages by *Lactobacillus casei* strain Shirota genes determining the synthesis of cell wall-associated polysaccharides. *Applied and Environmental Microbiology*, 74(15), 4746–4755. <https://doi.org/10.1128/AEM.00412-08>.
- Zarour, K., Llamas, M. G., Prieto, A., Ruas-Madiedo, P., Dueñas, M. T., Fernández de Palencia, P., et al. (2017). Rheology and bioactivity of high molecular weight dextrans synthesised by lactic acid bacteria. *Carbohydrate Polymers*, 174, 646–657. <https://doi.org/10.1016/j.carbpol.2017.06.113>.
- Živković, M., Miljković, M. S., Ruas-Madiedo, P., Markelić, M. B., Veljović, K., Tolinački, M., et al. (2016). EPS-SJ exopolysaccharide produced by the strain *Lactobacillus paracasei* subsp. *paracasei* BGSJ2-8 is involved in adhesion to epithelial intestinal cells and decrease on *E. coli* association to Caco-2 cells. *Frontiers in Microbiology*, 7(286), 1–14. <https://doi.org/10.3389/fmicb.2016.00286>.



Characterization of dextrans produced by *Lactobacillus mali* CUPV271 and *Leuconostoc carnosum* CUPV411

María Goretti Llamas-Arriba^a, Ana I. Puertas^a, Alicia Prieto^b, Paloma López^b, Mónica Cobos^a, José I. Miranda^a, Cristina Marieta^a, Patricia Ruas-Madiedo^c, M^a Teresa Dueñas^{a,*}

^a University of Basque Country (UPV/EHU), San Sebastián, Spain

^b Biological Research Centre (CIB), Spanish National Research Council (CSIC), Madrid, Spain

^c Asturias Dairy Centre (IPLA), Spanish National Research Council (CSIC), Villaviciosa, Spain

ARTICLE INFO

Keywords:

Dextran
Lactobacillus
Leuconostoc
Characterization
Adhesion

ABSTRACT

The exopolysaccharide (EPS)-producing *Lactobacillus mali* CUPV271 and *Leuconostoc carnosum* CUPV411 were isolated from Spanish rosy apple must and slimy ham, respectively. The polymers were purified from bacterial cultures' supernatants and subjected to physicochemical and rheological characterization with the aim to evaluate their potential for future industrial utilization. Methylation analysis, Fourier-Transform Infrared Spectroscopy (FT-IR) and Nuclear Magnetic Resonance (NMR) revealed that both polymers were dextrans, partially branched at O-3 and O-4 positions of the main α -(1 \rightarrow 6)-D-glucopyranose backbone. The molar masses of the EPS of *L. mali* and *Lc. carnosum* were of 1.23×10^8 g/mol and 3.58×10^8 g/mol, respectively. The bacterial strains were tested for binding to the human Caco-2 cell line in the presence and absence of their respective dextran, revealing that the EPS production by *L. mali* decreased the binding capacity of the bacterium while the adhesiveness of *Lc. carnosum* did not change. As the structure and molecular mass of both dextrans were comparable, other characteristics of the dextrans were studied to explain this behavior. Atomic force micrographs showed some differences at the supramolecular level, suggesting that the different spatial distribution of the dextrans might be on the basis of the results of the adhesion studies. Both polysaccharides resulted to be amorphous materials with T_g around 226 °C and showed slightly different thermal degradation patterns. Rheologically, they showed to have a pseudoplastic behavior, but very different critical concentrations: 3.8% for the EPS of *L. mali* and 0.4% for that of *Lc. carnosum*.

1. Introduction

Lactic acid bacteria (LAB) can produce a variety of EPS, either homopolysaccharides (HoPS), with a single type of sugar monomer, or heteropolysaccharides (HePS), made up by two or more different monosaccharides (Torino, Font de Valdez, & Mozzi, 2015). LAB are considered good glucan-producers, and among these HoPS, specifically, they synthesize α -glucans, which are composed of α -glucose. Dextrans are classified within this group and are composed of a main chain of α -(1 \rightarrow 6)-linked glucopyranose units, which can be branched by α -(1 \rightarrow 2), α -(1 \rightarrow 3) or α -(1 \rightarrow 4) linkages, in a proportion lower than 50%. Dextrans' production by LAB is not always desirable, for example, when they form the slime film that spoils meat products, although in general dextrans help to obtain better products. For instance, they can improve the texture, rheology and palatability of some beverages, and they serve as cryoprotectants or moisture-increasers (Lakshmi Bhavani & Nisha,

2010). In addition, they can be produced *in situ* in fermented dairy food, developing their prebiotic role, or during sourdough fermentation to improve texture and storage life of bread (Hu & Gänzle, 2018; Kothari, Das, Patel, & Goyal, 2014). Moreover, dextrans are applied in other fields than food industry. They have been reported as having antiviral activity in salmonids, to serve as plasma substitutes or as coating for columns with separation purposes (Chang, Crawford, & West, 1980; Lakshmi Bhavani & Nisha, 2010; Nacher-Vázquez et al., 2015; Pérez-Ramos, Nacher-Vázquez, Notararigo, López, & Mohedano, 2015). In 1878, Van Tiehem described the first microorganism responsible for dextran production and named it *Leuconostoc mesenteroides* (Meng et al., 2016). Since then, a lot of different bacteria have been isolated as dextran-producers, from other *Leuconostoc* to *Lactobacillus*, *Weissella*, *Streptococcus* or *Oenococcus* species (Dimopoulou et al., 2014; Dueñas-Chasco et al., 1998; Hu & Gänzle, 2018; Nacher-Vázquez et al., 2015; Vuillemin et al., 2018; Zarour et al., 2017). Dextrans are synthesized

* Corresponding author.

E-mail address: mariateresa.duenas@ehu.es (M.T. Dueñas).

<https://doi.org/10.1016/j.foodhyd.2018.10.053>

Received 27 July 2018; Received in revised form 9 October 2018; Accepted 27 October 2018

Available online 03 November 2018

0268-005X/ © 2018 Elsevier Ltd. All rights reserved.

from sucrose by dextransucrases, a type of glucansucrases mostly belonging to the glycoside hydrolase family 70 (Meng et al., 2016). Depending on the linkage specificity of the dextransucrase, dextrans are different in branches and proportion. Thus, depending on each bacterium and its specific dextransucrase, dextrans can be different one from another. Still nowadays, the most used dextran in industry is that produced by *Lc. mesenteroides* NRRL B-512F, with a 95% of α -(1 → 6) glucosidic linkages (Naessens, Cerdobbel, Soetaert, & Vandamme, 2005). However, the multiple applications of dextrans, as well as the increasing demand on free-additive products, make necessary the search for new dextran-producers. Thus, the aim of this work was the isolation of dextran-producing bacteria from different food origins and the characterization of the dextrans they produce.

2. Materials and methods

2.1. Bacterial strains and growth conditions

Two LAB strains were isolated, respectively, from the ropy slime of the surface of a vacuum-packed sliced cooked ham and from an apple must from a Spanish cider producer (Basque Country) as follows. Serial dilutions in Ringer's solution of the slime and the apple must were cultivated in MRS (De Man, Rogosa, & Sharpe, 1960) agar plates (pH 6.0), containing 2 μ L/mL pimaricin and 5% sucrose, at 28 °C under a microaerophilic atmosphere (CampyGen™, ThermoScientific) for 24 h. These bacteria were identified as *Leuconostoc carnosum* CUPV411 and *Lactobacillus mali* CUPV271 by sequencing a fragment of their 16 rRNA coding genes at Secugen (Madrid, Spain). The data were deposited in GenBank with accession numbers MH628089 and MH628046, respectively. LAB were grown at 30 °C without shaking in MRS medium containing either 2% glucose (MRSG) or 2% sucrose (MRSS). The media were buffered at pH 6.8 or 5.5 for growth of either *Lc. carnosum* or *L. mali*. The strains were stored in MRSG containing 20% (v/v) glycerol at –80 °C. For EPS production, a semi-defined (SMD) medium containing 2% sucrose (SMDS) and no glucose (Dueñas-Chasco et al., 1997) was used with the aim of avoiding the contamination with polysaccharides present in the MRS medium.

2.2. Production, purification and quantification of EPS from LAB

First, *L. mali* and *Lc. carnosum* were grown in MRSS for 24 h and the bacterial cultures were used as inoculum for further growth in SMDS medium at pH 5.5 and 6.8 respectively, for 48 h at 28 °C in a 5% CO₂-atmosphere. Then, the bacteria were sedimented by centrifugation (18500 × g, 4 °C, 10 min) and the EPS were recovered from the supernatants by precipitation with 1 volume of cold ethanol for 15 h at –20 °C. Afterwards, EPS were sedimented by centrifugation (18500 × g, 4 °C, 15 min), dialysed in 12–14 kDa MWCO membranes (Iberlabo) against distilled water for 3 days, freeze-dried and kept at room temperature. Finally, lyophilised EPS were dissolved in ultrapure water (0.1 mg/mL) and their concentration was determined from their neutral carbohydrate content, quantified by the phenol-sulphuric acid method (Dubois, Gilles, Hamilton, Rebers, & Smith, 1956) using glucose as standard.

2.3. Monosaccharide composition, methylation and FT-IR analyses

With the aim of elucidating the type of EPS isolated from the two strains neutral sugar composition and linkage types were determined as previously described (Notararigo et al., 2013). Neutral sugars were identified and quantified by gas chromatography, after hydrolysis of polysaccharides' samples with 3 M trifluoroacetic acid (TFA) for 90 min and derivatization to alditol acetates. To determine linkage types, the polysaccharides were methylated according to Ciucanu and Kerek (Ciucanu & Kerek, 1984), hydrolyzed with TFA 3 M for 1 h at 120 °C, converted into partially methylated alditol acetates using sodium

borodeuteride as the reducing agent and analyzed by gas-chromatography/mass spectrometry. The linkages in the polysaccharides were deduced from the mass spectra and retention time of the peaks, and their relative amount from the area under each peak. For Fourier-Transformed Infrared Spectroscopy (FTIR) analysis, KBr pellets of the samples were first prepared, recording the spectra in a FTIR 4200 instrument (Jasco Corporation) in the range 4000–700 cm⁻¹. The number of scans per experiment was 50, with a resolution of 4 cm⁻¹.

2.4. NMR spectroscopy analysis

Samples were weighted (ca. 1 mg) and dissolved 1:1 (w/v) in D₂O and their spectra were recorded at 333 K on a Bruker Avance NEO spectrometer operating at 500.13 MHz (¹H) and 125.75 MHz (¹³C), BBOF probe with z-gradients. Chemical shifts are given in ppm, using the acetone signal (2.16 ppm) (¹H) and (30.7 and 215.7 ppm) (¹³C) as reference. To record the 1D spectra, solvent suppression (WATERGATE) was used. The homonuclear COSY spectra were recorded using a pre-saturation to remove the residual signal of solvent (3K x 512 increments) with 8 scans. The heteronuclear single quantum coherence spectroscopy (HSQC) with solvent suppression was performed (2K x 256 increments) with 128 scans. The heteronuclear multiple bond correlation (HMBC) experiment was performed (4K x 256 increments) with 128 scans. To improve the sensitivity, a BBI with z-gradient probe was used to record the HSQC and HMBC spectra.

2.5. Detection of dextrans' production at cellular level

For phenotypic determination at cellular level, LAB cultures were grown in MRSG liquid medium to A₆₀₀ = 1.0. Then, 100 μ L of appropriate dilutions were streaked on MRSS- and MRSG-agar plates and incubated for 11 days. The detection of EPS in the LAB colonies was performed by transmission electron microscopy (TEM). Three or four colonies of each strain from MRSS- and MRSG-agar plates were carefully suspended in 50 μ L of sterile distilled water to form a turbid suspension, which was subjected to negative staining with uranyl acetate, prior TEM analysis as previously described (Zarour et al., 2017).

2.6. Caco-2 cell culture and adhesion assays

The Caco-2 human enterocyte cell line, obtained from the cell bank at Centro de Investigaciones Biológicas (CIB, Madrid, Spain), was seeded in 96-well tissue culture plates (Falcon Microtest™) at a final concentration of 1.25 × 10⁵ cells/mL, and grew as monolayers of differentiated and polarized cells as previously described (Nácher-Vázquez et al., 2017). Cell concentrations were determined as previously described (Garai-Ibabe et al., 2010). For adhesion assays, LAB grown in MRSG and MRSS to the middle of the exponential-phase cultures, were diluted to a final volume of 1 mL of DMEM (Invitrogen) supplemented with 0.5% of glucose or 0.5% sucrose, to give 1.25 × 10⁶ colony-forming units (cfu)/mL, and added to Caco-2 cells (ratio 10:1, bacteria:Caco-2 cells) in a final volume of 0.1 mL per well. After incubation for 1 h at 37 °C in a 5% CO₂ atmosphere, unattached bacteria were removed by washing three times with 0.2 mL of phosphate buffered saline (PBS) solution at pH 7.2 and then, Caco-2 cells were detached from the plastic surface by incubating for 5 min at 37 °C with 0.1 mL of 0.05% trypsin-EDTA per well. The detachment reaction was stopped by adding 0.1 mL of PBS pH 7.2. To determine the number of cell-associated bacteria, appropriate dilutions were plated onto MRSG-agar plates. All adhesion assays were conducted in triplicate, with two biological replicates in each.

2.7. Physicochemical characterization of the isolated dextrans

2.7.1. Determination of the molar mass distribution by SEC-MALLS

The molar mass distribution of the purified dextrans was analyzed

by means of size exclusion chromatography coupled with multiangle laser light scattering detection (SEC-MALLS) as previously described (Nikolic et al., 2012). In short, each lyophilized sample was re-suspended in 0.1 M NaNO₃ at a concentration of 5 mg/mL, kept overnight under gentle stirring and centrifuged (10,000 × g, 10 min) before analysis. The HPLC system (Waters, Milford, MA) consisted of a separation module Alliance 2695 connected with two detectors: a refractive index (RI 2414, Waters) to determine the amount of dextran using calibration curves obtained from standards of dextran (Fluka-Sigma, St. Louis, MO), ranging from 5 × 10³ to 4.9 × 10⁶ Da (Salazar et al., 2009), and the MALLS Dawn Heleos II (Wyatt Europe GmbH, Dembach). The quantification of dextrans was achieved with the Empower software (Waters) and the molar mass distribution analysis with the Astra 3.5 software (Wyatt Europe GmbH). Two SEC columns placed in series were used: TSK-Gel G3000 PW_{XL} + TSK-Gel G5000 PW_{XL} protected with a TSK-Gel guard column (Supelco-Sigma) and the separation was carried out at 40 °C with a flow rate of 0.45 mL/min using 0.1 M of NaNO₃ as mobile phase.

2.7.2. Thermal analysis

Thermogravimetric analysis (TGA) was carried out using a thermogravimeter Q-500 (TA Instruments), under dynamic nitrogen and air atmospheres (90 mL/min) at a heating rate of 10 °C/min, within the temperature interval from room temperature to 580 °C. Samples were weighted (between 8 and 14 mg) in a platinum pan.

2.7.3. Analysis by differential scanning calorimetry (DSC)

DSC curves were obtained from samples between 9 and 12 mg in aluminum crucibles under a nitrogen atmosphere flowing at 3 mL/min, in a differential scanning calorimeter DSC 3+ (Mettler Toledo). Samples were first maintained at −30 °C during 3 min. Then, two heating scans separated by a cooling stage at 10 °C/min were performed. The first heating scan was performed to erase the thermal history of the materials as reported previously (Fernández, Fernández, & Cobos, 2016; Icoz & Kokini, 2007), and was raised from −30 °C to 210 °C, maintaining the temperature for 5 min at the end. In the cooling stage, the temperature fell to −30 °C and was maintained for 3 min. Finally, in the second scan 300 °C were reached.

2.7.4. X-ray diffraction (XDR) analysis

The identification of the crystalline and/or amorphous structure of the purified dextrans was analyzed. The X-ray powder diffraction patterns were collected by using a PHILIPS X'PERT PRO automatic diffractometer operating at 40 kV and 40 mA, in theta-theta configuration, secondary monochromator with Cu-Kα radiation (λ = 1.5418 Å) and a PIXcel solid-state detector (active length in 2θ 3.347°). Data were collected from 5 to 60° 2θ (step size = 0.026 and time per step = 90 s) at room temperature, 0.04 rad sller slit and variable divergence slit giving a constant 5 mm area of sample illumination.

2.7.5. Atomic force microscopy (AFM) analysis

Aqueous solutions of the two dextrans were prepared at 1 mg/mL with filtered (0.45 μm) deionized water and kept ca. 16 h to assure solubilization. Then, serial dilutions were made to obtain a final concentration of 1 μg/mL. About 5 μL of this solution were dropped onto a cleaved mica substrate and allowed to dry at room temperature for 24 h in a desiccator. AFM images were obtained with a NanoScope V microscope (Digital Instruments) operating in tapping mode, with 512 × 512 pixels, and TESP 0.01–0.025 ohm-cm Antimony (n) doped Si tips (T = 3.8 μm, f₀ = 320 kHz) (Bruker). As a contrast enhancement technique (Corcuera et al., 2010), phase imaging extension was used. Scan rates ranged from 1 to 2 Hz.

2.8. Rheological analysis

The rheological behavior of the two dextrans was determined as

previously described (Zarour et al., 2017). Briefly, the lyophilized EPS were dissolved in ultrapure water at different concentrations, stirring at room temperature and then allowing them to settle overnight before each analysis. The viscoelastometer used was a Thermo-Haake Rheos-tress I (ThermoFisher Scientific), equipped with a cone-plate (60 mm diameter, 2° cone angle) geometry. Each solution (2 mL) was measured in two steps: the first one consisted on 3 min of resting without shear to maintain the temperature at 20 °C. Then, an interval shear-rate range was applied for 3 min between 1 and 500 s^{−1}. Each experiment was repeated at least three times. Haake Rheowin Data Manager was used for analyzing the continuous steady-state flow from the apparent viscosity and shear rate relationship. Viscosity at shear near zero (η₀) was extrapolated and regressed using the Cross model (Cross, 1965).

2.9. Statistical analysis

Adhesion data were analyzed by two-way analysis of variance (ANOVA) to determine the significant differences between the variables at p ≤ 0.05. The analysis was performed using the SAS 9.4 software (SAS Institute Inc).

3. Results and discussion

3.1. Elucidation of the type of EPS produced by *L. mali* CUPV271 and *Lc. carnosum* CUPV411

The EPS produced by the two LAB were purified from the supernatants of 48 h-cultures and analyzed to determine their composition and structure. Both EPS contained glucose as the sole monosaccharide, indicating that they produced a glucan-type HoPS.

Their FT-IR spectra were very similar (Fig. 1), with absorption bands typical of polysaccharides (Salazar, Ruas-Madiedo, Prieto, Calle, & de los Reyes-Gavilán, 2012). In the anomeric region, the bands at 917 and 844 cm^{−1}, characteristic of α-anomers (Heyn, 1974), and the absence of bands characteristic of β-linkages, indicated that they are α-glucans. The results from this analysis also confirmed the absence of non-glucidic components (phosphates, sulphates, protein) in the polysaccharides analyzed.

Methylation analysis (Table 1) showed the predominance of linear residues of (1,6)-glucopyranose in the structure of both polymers as well as the presence of 3,6-di-O-substituted glucopyranose (branching points) and terminal units of glucopyranose that amounted to 3.6% in the polysaccharide from *L. mali* and to 6.8% in that of *Lc. carnosum*. These data, together with the α-configuration of the linkages deduced from FT-IR, suggest that these polysaccharides are dextrans.

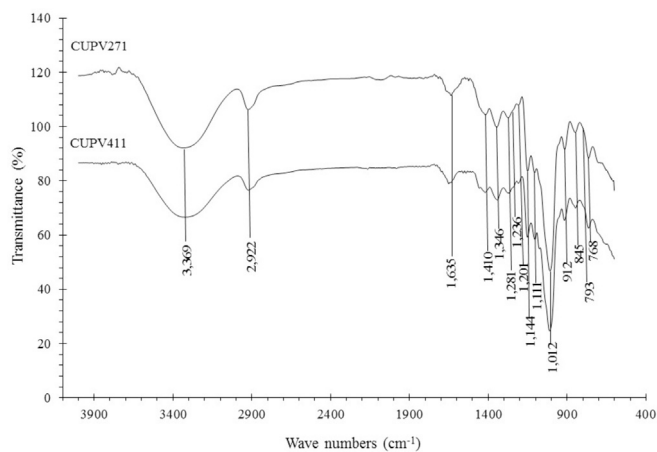


Fig. 1. FT-IR spectra of isolated dextrans. Up, spectrum of the HoPS from *L. mali* CUPV271 and down, the spectrum of the dextran isolated from *Lc. carnosum* CUPV411.

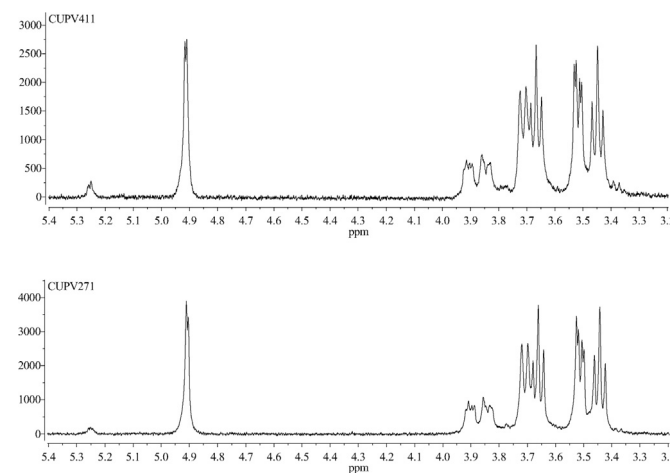
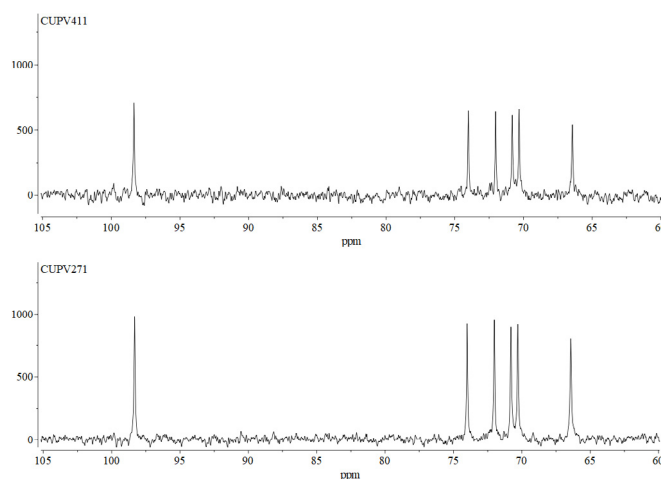
Table 1

Linkage types and their percentages deduced from methylation analysis of dextrans synthesized by *L. mali* CUPV271 and *Lc. carnosum* CUPV411.

Linkage type	Rt (min)	%	
		<i>L. mali</i> CUPV271	<i>Lc. carnosum</i> CUPV411
GlcP-(1→	6.9	3.6	6.8
→3)-GlcP-(1→	8.9	2.1	0.7
→6)-GlcP-(1→	9.9	84.8	81.1
→4,6)-GlcP-(1→	12.1	1.6	1.5
→3,6)-GlcP-(1→	12.4	7.9	9.9

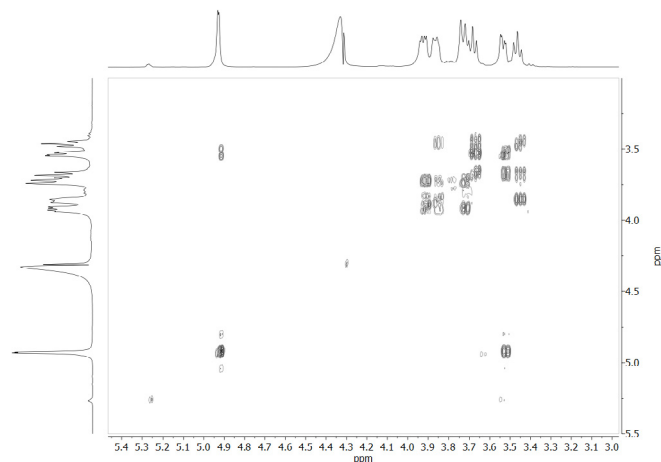
Commercial dextrans have branching degrees around 5%, and the side chains are mainly composed of single α -D-glucopyranosyl units (about 40%), or are two units long (about 45%), while only 15% of them contain more than 2 units (BeMiller, 2003). Therefore, the small percentage of linear units of glucose (1,3)-linked detected in the methylation analysis may belong to the short side-chains in the dextran structure. Around 1.5% of substitutions at positions O-4 were also detected in the two polysaccharides, which is more unusual, as this type of dextrans, branched at positions other than O-3, have been reported in few cases (Fraga Vidal, Moulis, Escalier, Remaud-Siméon, & Monsan, 2011).

For further confirmation of the methylation data, both polysaccharide samples were analyzed by NMR spectroscopy, revealing that their ^1H NMR and ^{13}C NMR spectra were very similar. The anomeric proton resonances for the ^1H NMR spectra (Fig. 2) of the polymers coincide with those reported for 1,3-branched dextrans as the B-1351 dextran (Cheetham, Fiala-Beer, & Walker, 1990). A main anomeric signal at 4.91 ppm (coupling constant $J = 3.7$ Hz) attributable to the α -(1→6)-glucopyranose linkages of the dextran backbone, and a small anomeric signal at 5.25 ppm, were observed in the anomeric region. Integration of the area of both peaks gave a ratio of 5.6/94.4, which also supports the data deduced from methylation analysis. The signals between 3.2 and 4.4 ppm correspond to the protons of the monosaccharides' backbone (Polak-Berecka et al., 2015). The ^{13}C NMR spectra of the polysaccharides (Fig. 3) showed a single anomeric signal from the α -(1→6)-glucopyranose backbone at 98.3 ppm (Miao et al., 2016), confirming that the EPS contained α -anomeric carbons instead of β -anomeric carbon atoms with resonances downfield from 102 ppm (Seymour, Knapp, Chen, Jeanes, & Bishop, 1979), as we deduced from the FT-IR analysis. However, the signals of the anomeric carbon of the α -glucose branches were not observed in the ^{13}C spectrum. The assignment of ^1H and ^{13}C resonances of the main monosaccharide (Table 2) was performed on the basis of homonuclear COSY (Fig. 4A) and heteronuclear HSQC (Fig. 4B) two-dimensional correlation NMR

**Fig. 2.** ^1H NMR spectra of CUPV411 strain (up) and CUPV271 strain (down).**Fig. 3.** ^{13}C NMR spectra of CUPV411 strain (up) and CUPV271 strain (down).**Table 2**

^1H and ^{13}C NMR chemical shifts (ppm) for the main monosaccharide α -(1→6)-glucopyranose.

	H-1	H-2	H-3	H-4	H-5	H-6	H-6'
^1H	4.91	3.51	3.61	3.44	3.85	3.90	3.72
^{13}C	98.3	72.0	74.0	70.3	70.8	66.5	66.5

**Fig. 4.** 2D-NMR analysis of dextran produced by CUPV411 strain. (A) ^1H - ^1H COSY spectrum and (B) ^1H - ^{13}C HSQC spectrum.

experiments. The system with ^1H anomeric signal at 5.25 ppm could not be assigned, although analysis of various dextrans has shown that this signal is characteristic of α -(1→3) branched dextrans, (Cheetham et al., 1990; Dertli, Colquhoun, Côté, Le, & Narbad, 2018; Miao et al., 2016; Seymour, Knapp, & Bishop, 1979), which also coincide with our methylation results.

The HMBC spectrum (Fig. 5) confirmed the α -(1,6) linkage through the correlation between H6 and H6' signals (3.90 ppm and 3.72 ppm, respectively) and C1 signal (98.3 ppm). In addition, the overlap of the HSQC and HMBC spectra (data not shown) only gave information on the (1→6) linkage through the correlation of H1–C1 signals (4.91–98.3 ppm) with the two protons of C6 (H6: 3.90 ppm and H6': 3.72), but signals from the minor components of the polysaccharide were not observable in any of the spectra analyzed. Thus, the presence of the α -glucopyranose side chains could not be confirmed with the experiments performed, although the ^1H NMR spectra (Fig. 2) showed a signal that, according to the literature, could be interpreted as corresponding to the O-3 branches.

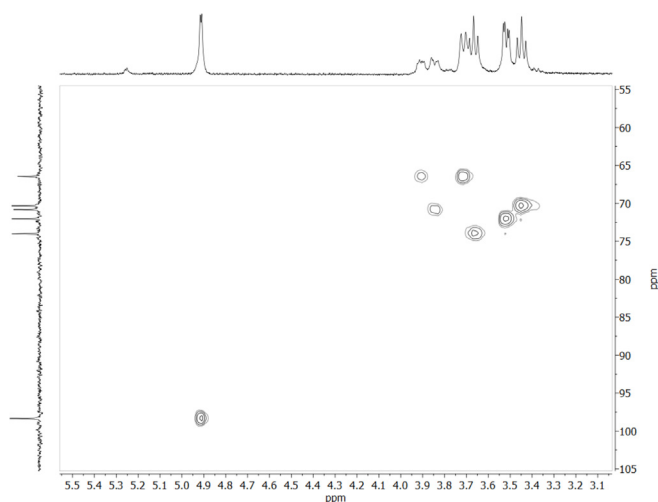
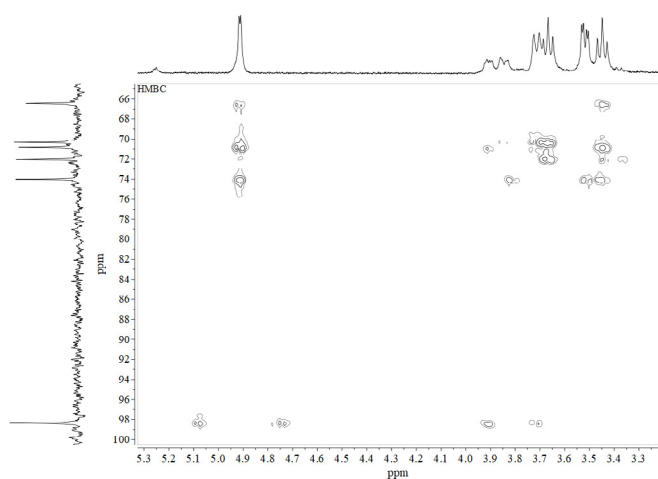
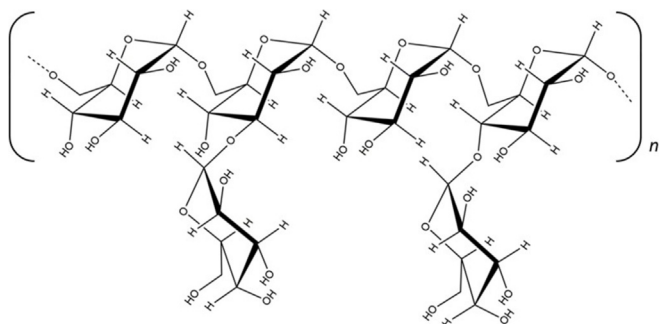


Fig. 4. (continued)

Fig. 5. HMBC spectrum of *Lc. carnosum* CUPV411.

Scheme 1. Representation of the main linkage types of the *Lc. carnosum* CUPV411 dextran. The total number of α -(1 \rightarrow 6)-glucopyranose units in the main backbone is represented by n , and according to the quantitative data from NMR, this value was 94.4%. Side chains (5.6%), mostly of a single α -glucopyranose unit, partially substitute the α (1 \rightarrow 6) backbone at O-3 and O-4.

The **Scheme 1** represents the main linkage types in the *Lc. carnosum* CUPV411 dextran.

3.2. Detection of dextran production by *L. mali* CUPV271 and *Lc. carnosum* CUPV411

Dextrans are synthesized by dextranases using sucrose as substrate (Kothari et al., 2014). Thus, for a macroscopic detection of the

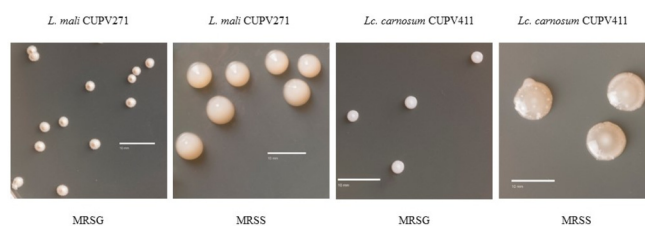


Fig. 6. Detection of EPS production by LAB on solid media. Bacterial colonies in MRSG and MRSS after 240 h of incubation.

dextrans synthesized by the two LAB, the bacteria were grown in MRSS-agar plates. In addition, plates containing MRSG-agar were also inoculated as negative controls. As expected, after growth for 48 h in the presence of sucrose the colonies of both strains were mucoid whereas the colonies generated in MRSG medium did not show this phenotype. Moreover, both LAB developed colonies with a larger size upon growth in MRSS medium (Fig. 5). Finally, comparing the colonies of both LAB grown in the presence of sucrose some differences were observed. The CUPV271 strain presented convex colonies firmly adhered to the agar even after 264 h of incubation. On the contrary, CUPV411 colonies were flatter and with less adherence to the agar. This difference in colonies' morphology has also been described for other dextran-producing LAB (Zarour et al., 2017).

Analysis of the two LAB by TEM (inset in Fig. 6) confirmed the presence of the EPS attached or surrounding the bacteria in cultures grown in MRSS and not MRSG.

3.3. Capacity of *L. mali* CUPV271 and *Lc. carnosum* CUPV411 to adhere to Caco-2 cells

As we have previously observed in some dextran-producing bacteria, the differences in the colonies' morphology correlate with different capacities to bind enterocytes in the presence or absence of EPS (Nácher-Vázquez et al., 2017; Zarour et al., 2017). Therefore, we tested the adhesion capacity of the LAB grown in media with or without sucrose (MRSS or MRSG) in an *in vitro* assay, measuring the binding of the bacteria to human epithelial Caco-2 cells (Fig. 6). The adhesion capacity of *Lc. carnosum* CUPV411 ($2.73 \pm 0.15\%$) did not change regardless of the presence or absence of dextran in the medium, which coincides with the results reported for several *Leuconostoc* strains. On the other hand, the adherence to eukaryotic cells of *L. mali* CUPV271 was significantly reduced from $2.85\% \pm 0.14\%$ to $0.86 \pm 0.07\%$ in conditions allowing dextran synthesis. These results are in accordance with those reported for the dextran-producing *L. sakei* MN1 (Nácher-Vázquez et al., 2017). However, it should be stated that sometimes the HoPS produced by LAB also enhance the bacterial binding capacity, as previously reported for the β -glucan produced by *Pediococcus parvulus* strains (Fernández de Palencia et al., 2009; Garai-Ibabe et al., 2010).

3.4. Physicochemical characterization of the dextrans

The results presented in sections 3.2 and 3.3 indicated differences between the dextrans synthesized by *L. mali* CUPV271 and *Lc. carnosum* CUPV411. However, the chemical analyses described in section 3.1 showed that both dextrans had similar primary structure and branching degrees. Therefore, with the aim of elucidating whether some significant differences existed between both dextrans, they were subjected to a deeper physicochemical characterization.

3.4.1. Molar mass distribution

The weight average molar mass (M_w), weight average radius of gyration (R_w), coefficient v ($\log R_w / \log M_w$) and polydispersity index (PDI, M_w/M_n) of the two isolated EPS were determined by SEC-MALLS. Chromatograms are depicted in Fig. 7 and parameters are summarized

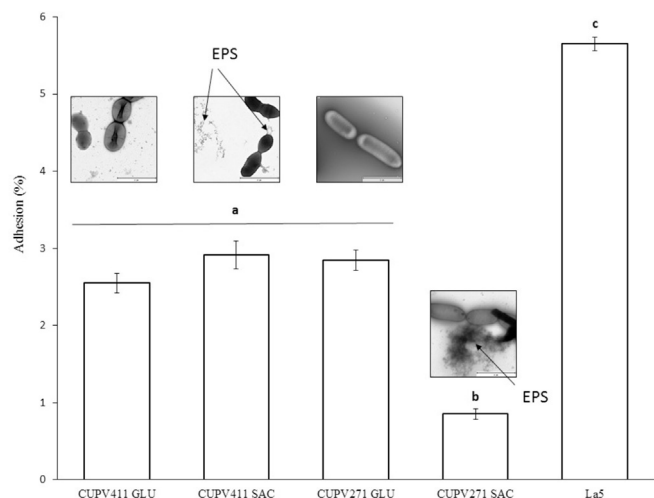


Fig. 7. Adhesion of LAB strains to Caco-2 cells. Adhesion levels are expressed as the percentage of cfu. Data were analyzed by ANOVA. Differences (a–c) were significant with a * $p \leq 0.05$.

Table 3

Physicochemical characteristics of the dextrans produced by *Lc. carnosum* CUPV411 and *L. mali* CUPV271.

	Mean \pm SD (n = 2)	
	CUPV271	CUPV411
Elution time (min)	25.6 \pm 0.04	24.9 \pm 0.04
Amount (mg/50 μ L)	223.4 \pm 24.4	106.9 \pm 6.7
M_w (g/mol)	1.23E+08 \pm 2.6E+06	3.58E+08 \pm 1.61E+07
Polydispersity (M_w/M_n)	1.05 \pm 0.08	1.25 \pm 0.02
R_w (nm)	63.55 \pm 0.64	163.65 \pm 2.19
ν (log R_w /log M_w)	0.22 \pm 2.62E-04	0.26 \pm 6.55E-05

M_w , weight average molar mass; R_w , weight average radius of gyration.

in Table 3. The chromatogram of the dextran produced by *L. mali* CUPV271 (Fig. 7A) showed a M_w of 1.23×10^8 g/mol, corresponding to a low polydispersity (1.05), very close to monodispersity. The M_w of the EPS of *Lc. carnosum* CUPV411 (Fig. 7B), was in the same log order, 3.58×10^8 g/mol, and showed a moderate polydispersity (1.25). This peak is being considered as a sole distribution of M_w . However, the presence of another slightly small distribution could have been assigned by the deformation at the left side of the peak. Moreover, it could be interpreted as a shoulder, which might be due to the mixture of aggregates and single molecular structures co-eluting under the same peak, as reported before (Maina et al., 2014). Nevertheless, this would not be clearly stated unless a column with more resolution at higher M_w levels is used.

3.4.2. Thermal degradation

The patterns of thermal degradation of the two dextrans in aerobic and anoxic atmospheres were analyzed by TGA. Table 4 shows the

Table 4

TGA data for the dextrans isolated from *Lc. carnosum* CUPV411 and *L. mali* CUPV271.

Sample	T_5 ($^{\circ}$ C)		T_{50} ($^{\circ}$ C)		T_{max} ($^{\circ}$ C)		Residue (%)		
	In N_2	In O_2	In N_2	In O_2	In N_2 ^a	In O_2	In N_2	In O_2	
CUPV411	80	83	301	305	287	288 ^a	497 ^b	21.1	1.1
CUPV271	90	85	311	310	305	304 ^a	489 ^b	14.1	0.6

^a Second or third stage for CUPV271 or CUPV411, respectively.

^b Third or fourth stage for CUPV271 or CUPV411, respectively.

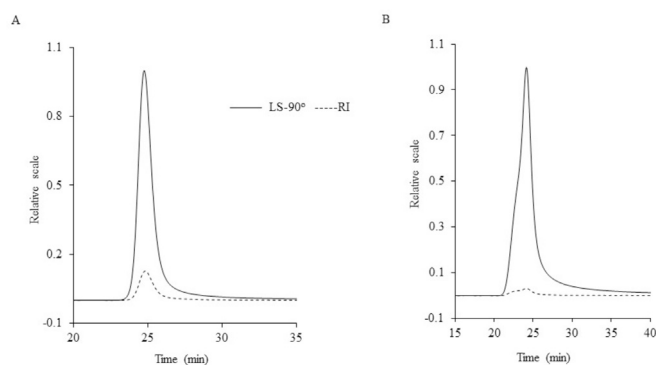


Fig. 8. Size exclusion chromatography (SEC) analysis of the EPS synthesized by the studied strains. (A) EPS produced by *Lc. carnosum* CUPV411 and (B) EPS isolated from *L. mali* CUPV271. The figure shows two chromatograms where the continuous line corresponds to the multi-angle laser light scattering (MALLS) detector, set at an angle of 90° , and the dashed line corresponds to the refractive index (RI) detector.

thermal decomposition temperatures for 5% and 50% weight loss ($T_{5\%}$ and $T_{50\%}$), the temperature of maximum loss rate (T_{max}) and the fraction of solid residue at 580° C of the thermograms obtained in nitrogen and air atmospheres.

The TGA curves presented in Fig. 8 indicate that degradation in anoxic conditions of the polymers of *Lc. carnosum* CUPV411 (Fig. 8A, black graph) and *L. mali* CUPV271 (Fig. 8B, black graph) took place in three and two steps, respectively. In the first stage, weight loss was observed at similar temperature range for both dextrans (between 25 and 115° C) and amounted to ca. 5%. This loss might be due to the evaporation of the water embedded in the polymers, which are very hygroscopic. However, it could also be due to the evaporation of the ethanol used for the precipitation of the dextrans, as previously reported (Zamora et al., 2002). The second degradation stage corresponded to the decomposition of the polymeric chain, accompanied by the rupture of C–C and C–O bonds, generating CO, CO₂ and water, as reported before (Kenari, Imani, & Nodehi, 2013; Miao et al., 2015). It was characterized by severe weight losses for both dextrans: 55% (from 226 to 333° C) for CUPV411, and 78% (from 229 to 441° C) for CUPV271. A third stage of degradation was observed for the dextran of CUPV411, which consisted of a 14% weight loss (from 333 to 465° C). In the end, a char residue from both dextrans was formed, corresponding to a carbonaceous or polynuclear aromatic structure.

The thermal degradation of both dextrans in aerobic conditions (Fig. 8A and B, grey graphs) was carried out in three and four steps for CUPV271 and CUPV411, respectively. The first stage was again characterized by a weight loss of 5% due to the evaporation of embedded water and remaining ethanol (below 105° C). A second stage where the majority of the depolymerization was carried out, was outlined by dramatic weight losses of 51% (from 219 to 322° C) for CUPV411 and 72% (from 221 to 401° C) for CUPV271. At the end of this degradation phase, a little shoulder was observed in the curve corresponding to the dextran from *L. mali*, which was not considered as a whole stage itself, and which implied a weight loss of around 8% (341 – 401° C). On the contrary, *Lc. carnosum* dextran experimented a third phase of thermal degradation in which a 14% weight loss occurred (between 322 and 389° C). Finally, the last phase of degradation for both dextrans, only present in the aerobic atmosphere, was due to the oxidative degradation of the carbonaceous structure formed in the previous stages. It caused 28% and 21% weight losses for CUPV411 and CUPV271 dextrans, respectively.

Therefore, the thermal degradation of the two dextrans was slightly different, since an additional step was observed for that of *Lc. carnosum* CUPV411 in both atmospheres which, according to the methylation data (Table 1), has more branching points in α -(1,3). However, this is

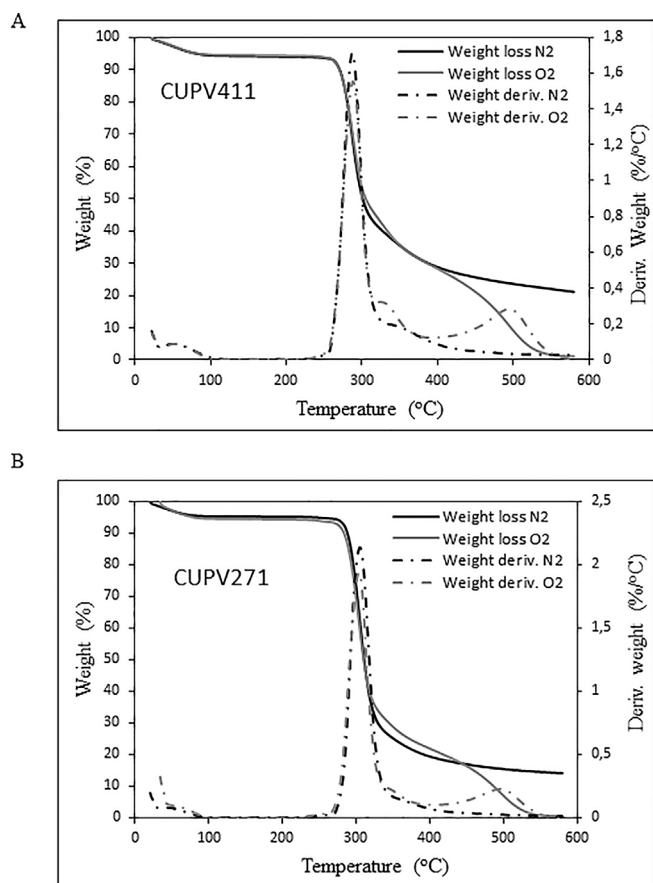


Fig. 9. TGA curves. Thermal degradation of the EPS of (A) *Lc. carnosum* CUPV411 and (B) *L. mali* CUPV271. Black lines correspond to nitrogen atmosphere and grey lines correspond the oxidative degradation. Continuous line refers to the weight loss expressed in percentage, and dashed line represents the weight derivative, expressed in %/°C.

not sufficient to explain the results obtained *in vivo* with the producing LAB. Nevertheless, the high degradation temperatures obtained for both dextrans, either in anoxia or in the presence of oxygen, would mean an advantage for application in the food industry.

3.4.3. Thermal properties

The degree of crystallinity of the dextrans was evaluated by differential scanning calorimetry. Fig. 9 depicts two heating scans of the samples. The first one (Fig. 9A), shows a broad endothermic peak around 115 °C for both dextrans, which is due to evaporation of the water embedded in the polymers, as described by other authors (Zhang & Chu, 2002). The glass transition temperature (T_g), measured in the last scan, was taken as the inflection point of the heat capacity change (Irague et al., 2012). The T_g values of the polysaccharides were 225.7 °C (CUPV411) and 226.8 °C (CUPV271), which are close to those reported for dextrans (Rosca et al., 2018). These high T_g are attributed to the presence of strong hydrogen bonds in these polymers (dos Santos Campos, Lopes Cassimiro, Spirandeli Crespi, Emília Almeida, & Daflon Gremião, 2013; Zhang & Chu, 2002).

No exothermic peaks have been observed with these dextrans, thus no melting temperature was obtained. In addition, no crystallization peaks were seen in the cooling stage. Therefore, these results suggest an amorphous behavior for the dextrans studied, as previously reported for other dextrans (dos Santos Campos et al., 2013; Zhang & Chu, 2002).

3.4.4. X-ray diffraction of dextrans

Despite the fact that in the DSC analysis no exothermic peaks were observed, there is a remote possibility for dextrans to form crystals in

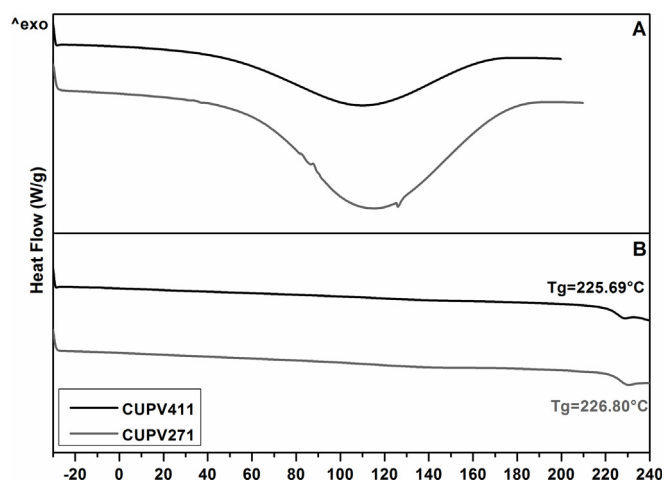


Fig. 10. DSC curves. Black lines for CUPV411 strain and grey ones for CUPV271 strain. (A) First heating scan from -30 °C to 210 °C. (B) Second heating scan in which the glass transition temperature (T_g) of each EPS is observed.

their structure. The degradation temperature under nitrogen atmosphere was ca. 220 °C for both dextrans, thus, if the melting temperature was higher than the degradation temperature, the exothermic peak indicating the melting of the crystals would not be observed by DSC. X-ray diffraction was carried out to check this possibility. Fig. 10 shows the diffraction profiles of dextrans produced by *L. mali* CUPV271 and *Lc. carnosum* CUPV411, confirming the amorphous structure of the polymers. However, a blunt peak appears in the profile of both dextrans in the 2θ range of 15–25°, indicating a small amount of the sample with some level of crystallinity, as reported previously (Yuan et al., 2009). Thus, no differences were found in the formation of crystals between the two dextrans under study.

3.4.5. Atomic force micrographs of dextrans

Finally, atomic force was used to see if differences in the spatial conformation of the dextrans existed. As also reported for the EPS produced by other *Lactobacillus* species (Ahmed, Wang, Anjum, Ahmad, & Khan, 2013; Wang et al., 2010), the AFM images (height and phase) of the dextran produced by *L. mali* (Fig. 11A) revealed a mixture of irregular rounded lumps with few random linear chains, which become visible when saturating to the maximum the image. These fibrillary structures were more evident in the phase micrograph, suggesting that they were thinner than the aggregates and composed of less material. The lumps were very different in shape and size, ranging from 0.13 to 0.54 μm , whereas the stretched material formed clusters of chains yielding $0.033 \pm 0.004 \mu\text{m}$ of width. On the contrary, irregular big aggregates ranging from 0.35 to 0.67 μm , and spherical small lumps with a diameter $< 0.1 \mu\text{m}$, were observed for the dextran isolated from *Lc. carnosum* (Fig. 11B), as previously described for the dextran produced by *Leuconostoc lactis* KC117496 (Saravanan & Shetty, 2016).

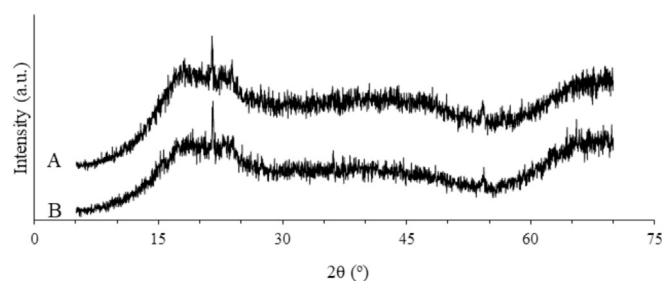


Fig. 11. X-ray diffraction diagrams of dextran produced by *L. mali* CUPV271 (A) and by *Lc. carnosum* CUPV411 (B).

Moreover, the molecules from both polymers seemed to be tightly packed, suggesting a pseudoplastic behavior with strong affinity for water molecules (Ahmed et al., 2013; Wang et al., 2010), which was further confirmed with rheology assays.

Taking together the results obtained in the different characterization assays, both dextrans present slight differences in their size or percentage of ramifications, although atomic force micrographs showed some differences at supramolecular level. Thus, the different spatial distribution of the dextrans might be on the basis of the different behaviors observed *in vivo*.

3.5. Rheological properties of dextrans produced by LAB

Since atomic force microscopy suggested the possible pseudoplastic behavior for the dextrans studied, we evaluated their flow behavior in solution, under shear at a constant temperature. The performance of the two dextrans was similar and coincided with that previously described for these type of polymers (Vuillemin et al., 2018; Zarour et al., 2017). Then, only the viscosity curves for the dextran of *L. carnosum* CUPV411 will be represented. An ideally viscous or Newtonian flow behavior was observed at low concentrations (up to a 0.5%), in which the viscosity remained constant over the entire shear rate range (Fig. 12). This viscosity was the same as in resting conditions (zero-shear viscosity, η_0). However, at higher concentrations, a shear-thinning or pseudoplastic flow behavior was observed, in which the viscosity decreased with increasing share rates. The hydrodynamic forces generated during the shear could have led to the breakdown of the structural units and the physical networks between the dextrans' chains, as reported before (Prasanna, Bell, Grandison, & Charalampopoulos, 2012; Zarour et al., 2017). Pseudoplastic characteristics of a polymer are not uniform in the whole range of shear rates. This behavior is characterized by showing a plateau value of the zero-shear viscosity η_0 at low shear rates below 1 s^{-1} . In this case, measures in the range of $0\text{--}1 \text{ s}^{-1}$ were limited by the characteristics of the instrument used. Therefore, an extrapolation by the Cross model was applied in order to obtain the η_0 value with the aim of comparing the viscosity of the two dextrans in a status near to the rest. At a given concentration of 5%, a higher plateau value of zero-shear viscosity was observed for dextran produced by *Lc. carnosum* CUPV411 (19.56 Pas) than that for the one produced by *L. mali* CUPV271 (0.09 Pas), indicating a higher average molar mass for the former dextran, as confirmed by SEC-MALLS.

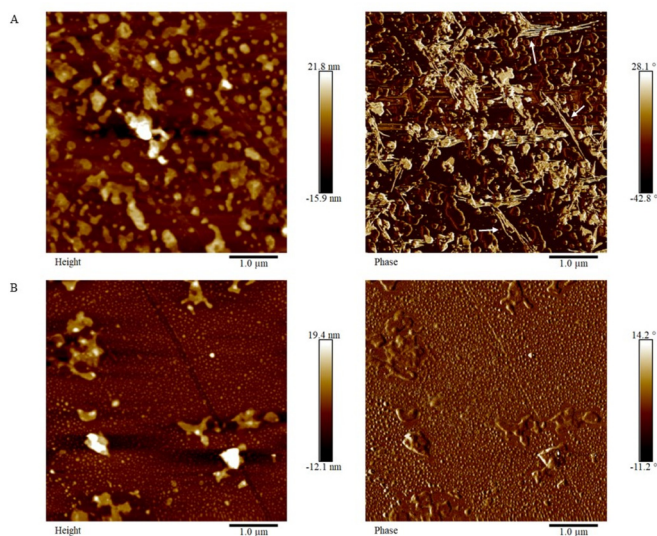


Fig. 12. Height (left) and phase (right) AFM planar images of dextrans synthesized by *L. mali* CUPV271 (A) and *Lc. carnosum* CUPV411 (B). White arrows in the phase micrograph of the dextran produced by CUPV271 indicates the fibrillary morphology.

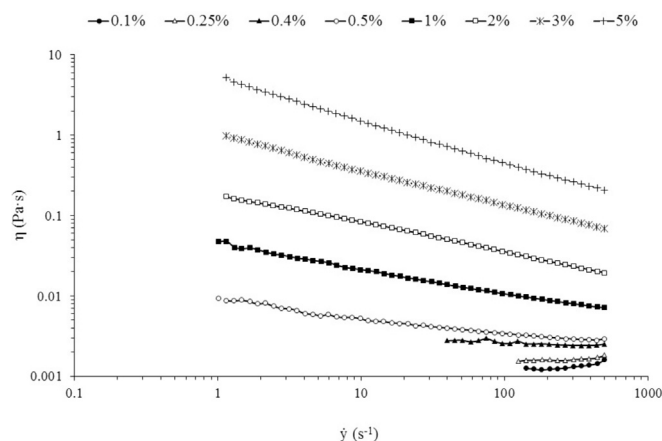


Fig. 13. Double logarithmic plot of viscosity curves of dextrans isolated from LAB. Viscosity curves for dextran isolated from *Leuconostoc carnosum* CUPV411 obtained by measuring aqueous solutions at different concentrations in a viscoelastometer.

The critical concentration, defined as the concentration of a polymer at which the equivalent sphere of a given polymer molecule just touches the equivalent spheres of all of its nearest neighbor molecules (Kulicke & Clasen, 2004), was calculated for both dextrans (Fig. 13). The data recorded suggested an increase in the Newtonian viscosity with the polymer's concentration. The critical concentration for the dextran from *L. mali* was 3.8%, while for that from *Lc. carnosum* it was 0.4%. These values are very related to the entanglements occurring both inside a single molecule and between different molecules. Therefore, the less-branched dextran produced by *L. mali* CUPV271 (Table 1) would require more molecules to reach the same number of entanglements than the polymer from *Lc. carnosum* CUPV411, which justifies its higher critical concentration (see Fig. 14).

The shear-thinning data presented above suggest that the dextrans studied would be very suitable to improve the texture or palatability of new fermented products.

3.6. Dextran yield

As far as our knowledge is concerned, it is the first time that EPS are isolated from *L. mali* and *Lc. carnosum* species. The isolation of the dextrans from the culture supernatants was only possible when sucrose and not glucose was present in the media, as it has been reported by other authors for dextran-producing LAB (Nácher-Vázquez et al., 2017; Zarour et al., 2017). The recovery of the EPS after 48 h of incubation in SMDS (2% sucrose), measured by the phenol-sulphuric acid method, was $3.65 \pm 0.21 \text{ g/L}$ for *Lc. carnosum* CUPV411, similar to the $1.25 \pm 0.04 \text{ g/L}$ described for *Lc. mesenteroides* RTF10 grown for 13 h in CDMS (0.8% sucrose) (Nácher-Vázquez et al., 2017). For *L. mali* CUPV271 the recovery was higher than for CUPV411 in the same conditions, yielding $11.65 \pm 1.15 \text{ g/L}$. This concentration exceeded the $2.20 \pm 0.09 \text{ g/L}$ produced by *L. sakei* MN1 after 13 h of incubation in CDMS (Nácher-Vázquez et al., 2017). Some species from *Oenococcus* have also been reported to produce EPS. In particular, the strain *O. oeni* S11, isolated from alcoholic beverages (sparkling white wine) in France, produced $3.87 \pm 0.02 \text{ g/L}$ of dextran in SMDS (1% sucrose) after a two-week incubation period (Dimopoulou et al., 2014). Thus, the overall results indicate a potential industrial use of the dextrans studied here, although their production levels are well below the 154 g/L reported for *Lc. mesenteroides* NRRL B-512F at optimized conditions for batch fermentation (Karthikeyan, Rakshit, & Baradarajan, 1996). Considering that neither the medium nor the culture conditions have been optimized in the current work, the perspective for production's improvement is high, supporting the potential use of the *L. mali*

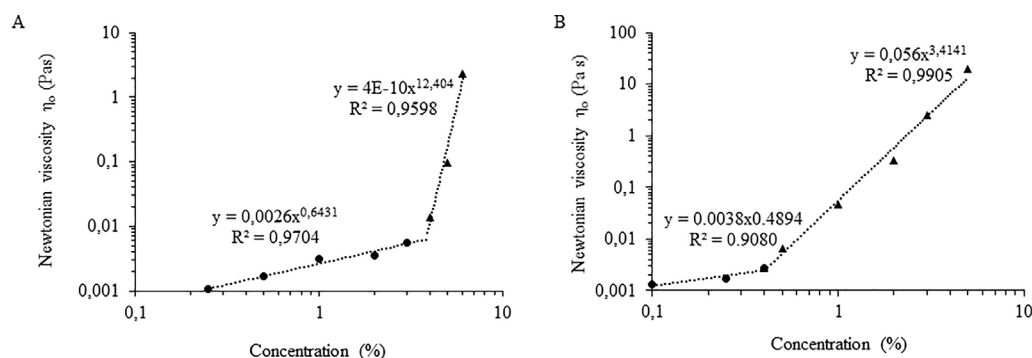


Fig. 14. Calculation of the critic concentration of the dextrans studied. Representation in a double logarithmic plot of the Newtonian viscosity versus the concentration expressed in percentage of (A) *L. mali* CUPV271 strain and (B) *L. carnosum* CUPV411 strain.

CUPV271 dextran for industrial purposes.

4. Conclusions

As far as we know, the EPSs produced by *Lc. carnosum* and *L. mali* strains have been purified and characterized for the first time. Chemical and spectroscopic analyses revealed that both polymers are O-3- and O-4-branched dextrans, whose presence affected differentially to the adhesion capacity of the producing LAB. This differential pattern could be due to differences in their supramolecular structures, as deduced from AFM. In addition, these dextrans are amorphous and presented a pseudoplastic behavior. This shear-thinning property may confer them an advantage in the food industry for improving sensory properties as mouth feel and flavor release. In addition, they would be very suitable for mixing, pouring or pumping, very common processes in the industry. Moreover, *L. mali* CUPV271 produces a considerably higher amount of polymer than *Lc. carnosum* CUPV411, thus, it might be a strong candidate for optimization aimed to the future development of a food, producing the dextran *in vivo*, or being included in the product as an additive.

Declaration of interest statement

None.

Funding

This work was supported by a grant from the Department of Environment, Territorial Planification, Agriculture and Fishing from the Basque Government, by the Provincial Council of Gipuzkoa (Exp. 77/17) and by the Spanish Ministry of Science and Innovation (AGL 2015-65010-C3-1-R).

Acknowledgements

We thank Dr. Guillermo Padilla Alonso for his valuable assistance in the bio-statistical analysis and Dr. Stephen Elson for the critical reading of the manuscript. Technical and human support by Dr. Aitor Larrañaga, (X-ray Facility) and Dr. Loli Martín (Materials and Surfaces – Macrobehavior Facility) from the general research service (SGIker) of the University of Basque Country (UPV/EHU) is also gratefully acknowledged. Finally, the valuable assistance of Dr. M^a Eugenia Muñoz (POLYMAT-Rheology group) is also acknowledged.

References

Ahmed, Z., Wang, Y., Anjum, N., Ahmad, A., & Khan, S. T. (2013). Characterization of exopolysaccharide produced by *Lactobacillus kefirifaciens* ZW3 isolated from Tibet kefir - Part II. *Food Hydrocolloids*, 30(1), 343–350. <https://doi.org/10.1016/j.foodhyd.2012.06.009>.

- BeMiller (2003). Dextran. In L. Trugo, & P. M. Finglas (Eds.). *Encyclopedia of food sciences and nutrition* (pp. 1772–1773). (2nd ed.). Cambridge Massachusetts: Academic Press. <https://doi.org/10.1016/B0-12-227055-X/00330-8>.
- Chang, R. L. S., Crawford, M. P., & West, M. D. (1980). An assessment of the potential use of anionic dextrans as a plasma substitute. *Journal of Biomedical Engineering*, 2(1), 41–44. [https://doi.org/10.1016/0141-5425\(80\)90090-4](https://doi.org/10.1016/0141-5425(80)90090-4).
- Cheetham, N. W. H., Fiala-Beer, E., & Walker, G. J. (1990). Dextran structural details from high-field proton NMR spectroscopy. *Carbohydrate Polymers*, 14(2), 149–158. [https://doi.org/10.1016/0144-8617\(90\)90027-P](https://doi.org/10.1016/0144-8617(90)90027-P).
- Ciucanu, I., & Kerek, F. (1984). A simple and rapid method for the permethylation of carbohydrates. *Carbohydrate Research*, 13, 209–217. [https://doi.org/10.1016/0008-6215\(84\)85242-8](https://doi.org/10.1016/0008-6215(84)85242-8).
- Corcuera, M. A., Rueda, L., Fernandez D'Arlas, B., Arbelaz, A., Marieta, C., Mondragon, I., et al. (2010). Microstructure and properties of polyurethanes derived from castor oil. *Polymer Degradation and Stability*, 95(11), 2175–2184. <https://doi.org/10.1016/j.polymdegradstab.2010.03.001>.
- Cross, M. M. (1965). Rheology of non-Newtonian fluids: A new flow equation for pseudoplastic systems. *Journal of Colloid Science*, 20(5), 417–437. [https://doi.org/10.1016/0095-8522\(65\)90022-X](https://doi.org/10.1016/0095-8522(65)90022-X).
- De Man, J. C., Rogosa, M., & Sharpe, M. E. (1960). A medium for the cultivation of lactobacilli. *Journal of Applied Bacteriology*, 23(1), 130–135. <https://doi.org/10.1111/j.1365-2672.1960.tb00188.x>.
- Dertli, E., Colquhoun, I. J., Côté, G. L., Le, G., & Narbad, A. (2018). Structural analysis of the α -D-glucan produced by the sourdough isolate *Lactobacillus brevis* E25. *Food Chemistry*, 242, 45–52. June 2017 <https://doi.org/10.1016/j.foodchem.2017.09.017>.
- Dimopoulou, M., Vuillemin, M., Campbell-Sills, H., Lucas, P. M., Ballestra, P., Miot-Sertier, C., et al. (2014). Exopolysaccharide (EPS) synthesis by *Oenococcus oeni*: From genes to phenotypes. *PLoS One*, 9(6), 1–15. <https://doi.org/10.1371/journal.pone.0098898>.
- Dubois, M., Gilles, K., Hamilton, J., Rebers, P., & Smith, F. (1956). Colorimetric method for determination of sugars and related substances. *Analytical Chemistry*, 28(3), 350–356. <https://doi.org/10.1021/ac60111a017>.
- Dueñas-Chasco, M. T., Rodríguez-Carvajal, M. A., Tejero Mateo, P., Franco-Rodríguez, G., Espartero, J. L., Irastorza-Iribas, A., et al. (1997). Structural analysis of the exopolysaccharide produced by *Pediococcus damnosus* 2.6. *Carbohydrate Research*, 303, 453–458. [https://doi.org/10.1016/S0008-6215\(97\)00192-4](https://doi.org/10.1016/S0008-6215(97)00192-4).
- Dueñas-Chasco, M. T., Rodríguez-Carvajal, M. A., Tejero-Mateo, P., Espartero, J. L., Irastorza-Iribas, A., & Gil-Serrano, A. M. (1998). Structural analysis of the exopolysaccharides produced by *Lactobacillus* spp. G-77. *Cancer Research*, 307, 125–133. [https://doi.org/10.1016/S0008-6215\(98\)00034-2](https://doi.org/10.1016/S0008-6215(98)00034-2).
- Fernández, M. D., Fernández, M. J., & Cobos, M. (2016). Effect of polyhedral oligomeric silsesquioxane (POSS) derivative on the morphology, thermal, mechanical and surface properties of poly(lactic acid)-based nanocomposites. *Journal of Materials Science*, 51(7), 3628–3642. <https://doi.org/10.1007/s10853-015-9686-5>.
- Fernández de Palencia, P., Werning, M. L., Sierra-Filardi, E., Dueñas, M. T., Irastorza, A., Corbí, A. L., et al. (2009). Probiotic properties of the 2-substituted (1,3)- β -D-glucan-producing bacterium *Pediococcus parvulus* 2.6. *Applied and Environmental Microbiology*, 75(14), 4887–4891. <https://doi.org/10.1128/AEM.00394-09>.
- Fraga Vidal, R., Moulis, C., Escalier, P., Remaud-Siméon, M., & Monsan, P. (2011). Isolation of a gene from *Leuconostoc citreum* B/110-1-2 encoding a novel dextranucrase enzyme. *Current Microbiology*, 62(4), 1260–1266. <https://doi.org/10.1007/s00284-010-9851-7>.
- Garai-Ibabe, G., Dueñas, M. T., Irastorza, A., Sierra-Filardi, E., Werning, M. L., López, P., et al. (2010). Naturally occurring 2-substituted (1,3)- β -D-glucan producing *Lactobacillus suebicus* and *Pediococcus parvulus* strains with potential utility in the production of functional foods. *Bioresource Technology*, 101(23), 9254–9263. <https://doi.org/10.1016/j.biortech.2010.07.050>.
- Heyn, A. N. J. (1974). The infrared absorption spectrum of dextran and its bound water. *Biopolymers*, 13(3), 475–506. <https://doi.org/10.1002/bip.1974.360130304>.
- Hu, Y., & Gänzle, M. G. (2018). Effect of temperature on production of oligosaccharides and dextran by *Weissella cibaria* 10 M. *International Journal of Food Microbiology*, 280(January), 27–34. <https://doi.org/10.1016/j.ijfoodmicro.2018.05.003>.
- Icoz, D. Z., & Kokini, J. L. (2007). Probing the boundaries of miscibility in model carbohydrates consisting of chemically derivatized dextrans using DSC and FTIR spectroscopy. *Carbohydrate Polymers*, 68(1), 68–76. <https://doi.org/10.1016/j.carbpol.>

- 2006.07.011.
- Irague, R., Rolland-Sabaté, A., Tarquis, L., Doublier, J. L., Moulis, C., Monsan, P., et al. (2012). Structure and property engineering of α -D-glucans synthesized by dextransucrase mutants. *Biomacromolecules*, 13(1), 187–195. <https://doi.org/10.1021/bm201453r>.
- Karthikeyan, R. S., Rakshit, S. K., & Baradarajan, A. (1996). Optimization of batch fermentation conditions for dextran production. *Bioprocess Engineering*, 15(5), 247–251. <https://doi.org/10.1007/BF02391585>.
- Kenari, H. S., Imani, M., & Nodehi, A. (2013). Full factorial design-of-experiments for preparation of crosslinked dextran microspheres. *Journal of Applied Polymer Science*, 127(5), 3712–3724. <https://doi.org/10.1002/app.37983>.
- Kothari, D., Das, D., Patel, S., & Goyal, A. (2014). Dextran and food application. In K. Gopal Ramawat, & J.-M. Mérillon (Eds.). *Polysaccharides* Switzerland: Springer International Publishing <https://doi.org/10.1007/978-3-319-03751-6>.
- Kulicke, W. M., & Clasen, C. (2004). In C. Clasen (Ed.). *Viscosimetry of polymers and polyelectrolytes*. Springer.
- Lakshmi Bhavani, A., & Nisha, J. (2010). Dextran - the polysaccharide with versatile uses. *International Journal of Pharma Bio Sciences*, 1(4), 569–573.
- Maina, N. H., Pitkänen, L., Heikkinen, S., Tuomainen, P., Virkki, L., & Tenkanen, M. (2014). Challenges in analysis of high-molar mass dextrans: Comparison of HPSEC, AsFIFFF and DOSY NMR spectroscopy. *Carbohydrate Polymers*, 99, 199–207. <https://doi.org/10.1016/j.carbpol.2013.08.021>.
- Meng, X., Gangöiti, J., Bai, Y., Pijning, T., Van Leeuwen, S. S., & Dijkhuizen, L. (2016). Structure–function relationships of family GH70 glucansucrase and 4,6- α -glucanotransferase enzymes, and their evolutionary relationships with family GH13 enzymes. *Cellular and Molecular Life Sciences*, 73(14), 2681–2706. <https://doi.org/10.1007/s00018-016-2245-7>.
- Miao, M., Huang, C., Jia, X., Cui, S. W., Jiang, B., & Zhang, T. (2015). Physicochemical characteristics of a high molecular weight bioengineered α -D-glucan from *Leuconostoc citreum* SK24.002. *Food Hydrocolloids*, 50, 37–43. <https://doi.org/10.1016/j.foodhyd.2015.04.009>.
- Miao, M., Jia, X., Jiang, B., Wu, S., Cui, S. W., & Li, X. (2016). Elucidating molecular structure and prebiotics properties of bioengineered α -D-glucan from *Leuconostoc citreum* SK24.002. *Food Hydrocolloids*, 54, 227–233. <https://doi.org/10.1016/j.foodhyd.2015.10.013>.
- Nácher-Vázquez, M., Ballesteros, N., Canales, Á., Rodríguez Saint-Jean, S., Pérez-Prieto, S. I., Prieto, A., et al. (2015). Dextrans produced by lactic acid bacteria exhibit antiviral and immunomodulatory activity against salmonid viruses. *Carbohydrate Polymers*, 124, 292–301. <https://doi.org/10.1016/j.carbpol.2015.02.020>.
- Nácher-Vázquez, M., Iturria, I., Zarour, K., Mohedano, M. L., Aznar, R., Pardo, M.Á., et al. (2017). Dextran production by *Lactobacillus sakei* MN1 coincides with reduced autoagglutination, biofilm formation and epithelial cell adhesion. *Carbohydrate Polymers*, 168, 22–31. <https://doi.org/10.1016/j.carbpol.2017.03.024>.
- Naessens, M., Cerdobbel, A., Soetaert, W., & Vandamme, E. J. (2005). *Leuconostoc* dextransucrase and dextran: Production, properties and applications. *Journal of Chemical Technology and Biotechnology*, 80(8), 845–860. <https://doi.org/10.1002/jctb.1322>.
- Nikolic, M., López, P., Strahinic, I., Suárez, A., Kojic, M., Fernández-García, M., et al. (2012). Characterisation of the exopolysaccharide (EPS)-producing *Lactobacillus paraplantarum* BGCG11 and its non-EPS producing derivative strains as potential probiotics. *International Journal of Food Microbiology*, 158(2), 155–162. <https://doi.org/10.1016/j.ijfoodmicro.2012.07.015>.
- Notararigo, S., Nácher-Vázquez, M., Ibarburu, I., Werning, M. L., Fernández de Palencia, P., Dueñas, M. T., et al. (2013). Comparative analysis of production and purification of homo- and hetero-polysaccharides produced by lactic acid bacteria. *Carbohydrate Polymers*, 94(1), 57–64. <https://doi.org/10.1016/j.carbpol.2012.05.016>.
- Pérez-Ramos, A., Nácher-Vázquez, M., Notararigo, S., López, P., & Mohedano, M. L. (2015). Current and future applications of bacterial extracellular polysaccharides. In V. R. Preedy, & R. R. Watson (Eds.). *Probiotics, prebiotics and synbiotics: Bioactive foods in health promotion* Oxford, UK: Elsevier <https://doi.org/10.1016/B978-0-12-802189-7.00022-8>.
- Polak-Berecka, M., Choma, A., Was'ko, A., Górská, S., Gamian, A., & Cybulska, J. (2015). Physicochemical characterization of exopolysaccharides produced by *Lactobacillus rhamnosus* on various carbon sources. *Carbohydrate Polymers*, 117, 501–509. <https://doi.org/10.1016/j.carbpol.2014.10.006>.
- Prasanna, P. H. P., Bell, A., Grandison, A. S., & Charalampopoulos, D. (2012). Emulsifying, rheological and physicochemical properties of exopolysaccharide produced by *Bifidobacterium longum* subsp. *infantis* CCUG 52486 and *Bifidobacterium infantis* NCIMB 702205. *Carbohydrate Polymers*, 90(1), 533–540. <https://doi.org/10.1016/j.carbpol.2012.05.075>.
- Rosca, I., Petrovici, A. R., Peptanariu, D., Nicolescu, A., Dodi, G., Avadanei, M., et al. (2018). Biosynthesis of dextran by *Weissella confusa* and its *In vitro* functional characteristics. *International Journal of Biological Macromolecules*, 107, 1765–1772. <https://doi.org/10.1016/j.ijbiomac.2017.10.048>.
- Salazar, N., Prieto, A., Leal, J. A., Mayo, B., Bada-Gancedo, J. C., de los Reyes-Gavilán, C. G., et al. (2009). Production of exopolysaccharides by *Lactobacillus* and *Bifidobacterium* strains of human origin, and metabolic activity of the producing bacteria in milk. *Journal of Dairy Science*, 92(9), 4158–4168. <https://doi.org/10.3168/jds.2009-2126>.
- Salazar, N., Ruas-Madiedo, P., Prieto, A., Calle, L. P., & de los Reyes-Gavilán, C. G. (2012). Characterization of exopolysaccharides produced by *Bifidobacterium longum* NB667 and its cholate-resistant derivative strain IPLA B667dCo. *Journal of Agricultural and Food Chemistry*, 60(4), 1028–1035. <https://doi.org/10.1021/jf204034n>.
- dos Santos Campos, F., Lopes Cassimiro, D., Spirandeli Crespi, M., Emília Almeida, A., & Daflon Gremião, M. P. (2013). Preparation and characterisation of Dextran-70 hydrogel for controlled release of praziquantel. *Brazilian Journal of Pharmaceutical Sciences*, 49(1), 75–83. <https://doi.org/10.1590/S1984-82502013000100009>.
- Saravanan, C., & Shetty, P. K. H. (2016). Isolation and characterization of exopolysaccharide from *Leuconostoc lactis* KC117496 isolated from idli batter. *International Journal of Biological Macromolecules*, 90, 100–106. <https://doi.org/10.1016/j.ijbiomac.2015.02.007>.
- Seymour, F. R., Knapp, R. D., & Bishop, S. H. (1979a). Correlation of the structure of dextrans to their $^1\text{H-N.M.R.}$ spectra*. *Carbohydrate Research*, 74, 77–92. [https://doi.org/10.1016/S0008-6215\(00\)86072-3](https://doi.org/10.1016/S0008-6215(00)86072-3).
- Seymour, F. R., Knapp, R. D., Chen, E. C. M., Jeanes, A., & Bishop, S. H. (1979b). Structural analysis of dextrans containing 2-O- α -D-glucosylated α -D-glucopyranosyl residues at the branch points, by use of ^{13}C -nuclear magnetic resonance spectroscopy and gas-liquid chromatography-mass spectrometry. *Carbohydrate Research*, 71(1), 231–250. [https://doi.org/10.1016/S0008-6215\(00\)84766-7](https://doi.org/10.1016/S0008-6215(00)84766-7).
- Torino, M. I., Font de Valdez, G., & Mozzi, F. (2015). Biopolymers from lactic acid bacteria. Novel applications in foods and beverages. *Frontiers in Microbiology*, 6, 1–16. <https://doi.org/10.3389/fmicb.2015.00834>.
- Vuillemin, M., Grimaud, F., Claverie, M., Rolland-Sabaté, A., Garnier, C., Lucas, P., et al. (2018). A dextran with unique rheological properties produced by the dextransucrase from *Oenococcus oeni* DSM 17330. *Carbohydrate Polymers*, 179(September 2017), 10–18. <https://doi.org/10.1016/j.carbpol.2017.09.056>.
- Wang, Y., Li, C., Liu, P., Ahmed, Z., Xiao, P., & Bai, X. (2010). Physical characterization of exopolysaccharide produced by *Lactobacillus plantarum* KF5 isolated from Tibet Kefir. *Carbohydrate Polymers*, 82(3), 895–903. <https://doi.org/10.1016/j.carbpol.2010.06.013>.
- Yuan, W., Geng, Y., Wu, F., Liu, Y., Guo, M., Zhao, H., et al. (2009). Preparation of polysaccharide glassy microparticles with stabilization of proteins. *International Journal of Pharmaceutics*, 366(1–2), 154–159. <https://doi.org/10.1016/j.ijpharm.2008.09.007>.
- Zamora, F., González, M. C., Dueñas, M. T., Irastorza, A., Velasco, S., & Ibarburu, I. (2002). Thermodegradation and thermal transitions of an exopolysaccharide produced by *Pediococcus damnosus* 2.6. *Journal of Macromolecular Science: Physics, A1 B* (3), 473–486. <https://doi.org/10.1081/MB-120004348>.
- Zarour, K., Llamas, M. G., Prieto, A., Ruas-Madiedo, P., Dueñas, M. T., Fernández de Palencia, P., et al. (2017). Rheology and bioactivity of high molecular weight dextrans synthesised by lactic acid bacteria. *Carbohydrate Polymers*, 174, 646–657. <https://doi.org/10.1016/j.carbpol.2017.06.113>.
- Zhang, Y., & Chu, C.-C. (2002). Thermal and mechanical properties of biodegradable hydrophilic-hydrophobic hydrogels based on dextran and poly (lactic acid). *Journal of Materials Science: Materials in Medicine*, 13(8), 773–781. <https://doi.org/10.1023/A:1016123125046>.

Las bacterias del ácido láctico son un grupo heterogéneo de bacterias que intervienen habitualmente en la elaboración de alimentos y bebidas fermentadas. Producen un gran número de metabolitos que resultan beneficiosos para la salud de los consumidores, como son las vitaminas, ácidos, enzimas, péptidos bioactivos o exopolisacáridos (EPS).

En esta tesis se ha estudiado la diversidad de las bacterias lácticas del género *Lactobacillus* productoras de EPS y que son responsables de la alteración del ahilado en la sidra natural del País Vasco. El estudio *in silico* de los genomas de las cepas *L. collinoides* CUPV237 y *L. sicerae* CUPV261^T reveló la presencia de genes relacionados con la ruta biosintética Wzy-dependiente, relacionada con la síntesis de heteropolisacárido (HePS). Los HePS producidos por estas estirpes están compuestos por glucosa y galactosa, además de ramnosa en el caso de *L. sicerae*, y de glucosamina en el de *L. collinoides*. Estos EPS al ser aplicados a un modelo de inflamación intestinal inducido por el agente químico DSS en larvas de pez cebra son capaces de disminuir significativamente la mortalidad larvaria.

Finalmente, se aisló un mutante espontáneo superproductor de riboflavina de la especie *Lactobacillus collinoides*, que produce hasta 3 mg mL⁻¹ de esta vitamina. El estudio genético mostró que este fenotipo estaba causado por una mutación localizada en el elemento regulador del operón *rib* responsable de la síntesis de esta vitamina.

eman ta zabal zazu



Universidad
del País Vasco

Euskal Herriko
Unibertsitatea